Chemical and Biological Studies on Human Oxygenases

A thesis submitted to the board of the faculty of physical sciences of the University of Oxford in partial fulfilment for the requirements of the degree of Doctor of Philosophy.

Cyrille C. Thinnes
Brasenose College

Michaelmas 2014

Abstract

Cyrille C. Thinnes, Brasenose College
DPhil Thesis, Michaelmas 2014

Chemical and Biological Studies on Human Oxygenases

As depitcted in Chapter I, 2-oxoglutarate- (2OG) dependent oxygenases are ubiquitous in living systems and display a wide range of cellular functions, spanning metabolism, transcription, and translation. Although functionally diverse, the 2OG oxygenases share a high degree of structural similarities between their catalytic sites. From a medicinal chemistry point of view, the combination of biological diversity and structural similarity presents a rather challenging task for the development of selective small molecules for functional studies *in vivo*.

The non-selective metal chelator 8-hydroxyquinoline (8HQ) was used as a template for the generation of tool compound **I** for the KDM4 subfamily of histone demethylases *via* application of the Betti reaction. Structural analogue **II** was used as the corresponding negative control (Figure A). These compounds were characterised *in vitro* against a range of 2OG oxygenases and subsequently used for studies in cells. **I** displays selectivity for KDM4 and increases the level of the H3K9me3 histone mark in cells. It has an effect on the post-translational modification pattern of histone H3, but not other histones, and reduces the viability of lung cancer cells, but not normal lung cells, derived from the same patient. **I** also stabilises hypoxia-inducable factor HIF in cells *via* a mechanism which seems to be independent from prolyl hydroxylase inhibition. This work is described in Chapters II and III.

The chemical biology research in epigenetics is complemented by qualitative analysis conducted in the social sciences at Saïd Business School. With a global view on how innovation occurs and may actively be fostered, Chapter IV focuses on the potential of epigenetics in drug discovery and how this process may actively be promoted within the framework of open innovation. Areas of focus include considerations of incremental and disruptive technology; how to claim, demarcate, and control the market; how knowledge brokering occurs; and insights about process, management, organisation, and culture of open innovation.

In contrast to the open-skies approach adopted for the development of a tool compound in Chapters II and III, a focused-library approach was taken for the generation of a tool compound for the OGFOD1 ribosomal prolyl hydroxylase. The development of a suitable *in vitro* activity assay for OGFOD1 in Chapter V enabled the development of lead compound **III** in Chapter VI (Figure A). **III** is selective for OGFOD1 against the structurally closely related prolyl hydroxylase PHD2.

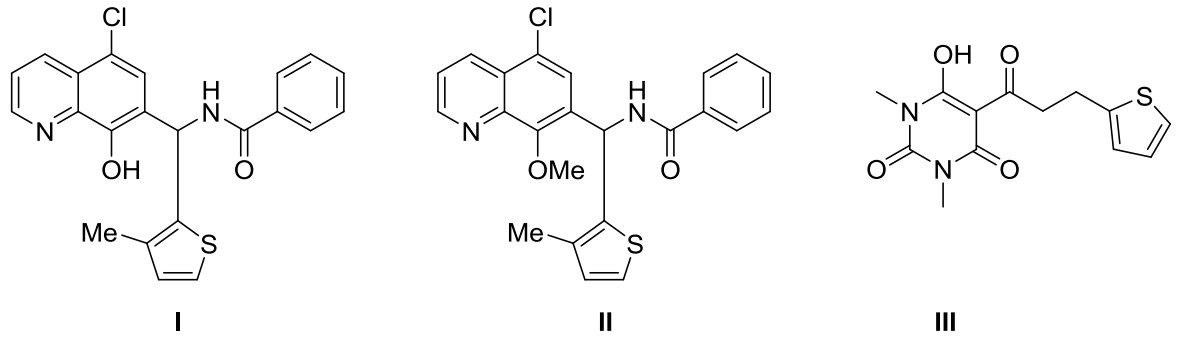

I **II** **III**

Figure A: Tool compounds generated during the course of this thesis. **I** is a tool compound for the KDM4 subfamily of histone demethylases, with the corresponding negative control **II**. **III** is a tool compound for the OGFOD1 ribosomal prolyl hydroxylase.

Acknowledgements

Thank you Chris, for being a mentor, not a supervisor. For guiding, not pushing. For suggesting, not commanding.

Thank you Duncan, Katherine, Jake, Marina, Greg, Rob, KD, Gareth, Clarisse, Sander and Martin for helping me in the synthesis lab. Why ask SciFinder when you can ask the postdocs? LG1 was a happy place.

Thank you Louise, Rich, Sarah, Joan, Olly, Jürgen, Emily, Adam, and Wendy for introducing me to the world of biological chemistry. I know you must have felt more like baby sitters, rather than coworkers, in the beginning.

Thank you Akane, Paul, Tony, and Clarence for helping me learn about the field of epigenetics, as well as being great people to work with in, what Chris called, a 5-person pharma company. Team awesome!

Thank you Sho, Mike, John, Christoph, and Wei for introducing me to the field of ribosomal oxygenases. It was a tough start, but that made the collaboration even better.

Thank you Madu for being a very supportive course mate, and great friend. I hope we will be able to work together again in the future.

Thank you everybody in the CJS lab for all the help, happiness, and sweets. It feels good to enjoy loads of beer and cake together. Until the jeans become a little tight.

Thank you Marc, Sarah, Jippy, Tim, the SIP cohort, and the MBA class of 2013 for all your help and motivation at SBS. There is more to science than science.

Thank you Cancer Research UK for providing the funding, and training, for my DPhil degree. You made me feel part of a cancer research community.

Thank you Brasenose College for all the support, socially and financially. I appreciate being part of a very supportive college community.

Thank you James, Wojciech, Martin, and the rest of the Sul Ki Do family for the friendly and high-energy environment to practice the martial arts in. Active meditation.

Thank you Eric, Daniel, James, Annabelle, Max, Pan, Pip, Lee, and Janice for being great friends in, and out of, Oxford.

Thank you mum, dad, and brother for all the love and support. It's good to talk to you on the weekends and put the Oxford lifestyle into perspective with the real world.

List of Experiments Carried out by Others

- X-ray crystallography experiments were carried out by Dr Rasheduzzuman Chowdhury (histone demethylases and PHD2) and Dr Shoishiro Horita (OGFOD1), Department of Chemistry, University of Oxford.
- AlphaScreen® experiments were carried out either by Drs Anthony Tumber and Giuseppe Scozzafava (histone demethylases) at the Structural Genomics Consortium at Oxford, or by Dr Tzu-Lan Yeh (PHD2) at the Wellcome Trust for Structural Genomics, University of Oxford.
- RapidFire™ experiments with histone demethylases were carried out by Dr Anthony Tumber at the Structural Genomics Consortium at Oxford.
- HeLa cell experiments with overexpressed KDM4A were carried out by Dr Clarence Yapp at the Structural Genomics Consortium at Oxford.
- Patient-matched lung cell experiments were carried out by Dr Anh Tran at UT Southwestern Medical Center.
- Experiments on whole histones were carried out by KuoFeng Hsu at the Department of Chemistry, University of Oxford.
- Western Blot experiments were carried out by Dr Andrew Chan at the Wellcome Trust for Human Genomics, University of Oxford.
- Non-denaturing mass spectrometry experiments were carried out by Hanna Tarhonskaya, Department of Chemistry, University of Oxford.
- Turbidimetric aqueous solubility, S9 liver microsome stability, and MDR1-MDCK efflux experiments were carried out by Cyprotex, Macclesfied.
- Recombinant protein production and purification was carried out by Gareth Elliott and Drs Shoishiro Horita and Armin Thalhammer (OGFOD1), Marta Dazzi (PHD2), or kindly provided by the Structural Genomics Consortium (histone demethylases).

Table of Contents

Abbreviations

2,4-PDCA	2,4-pyridinecarboxylic acid
2HG	2-hydroxyglutarate
2OG	2-oxoglutarate
8HQ	8-hydroxyquinoline
ADMET	administration, distribution, metabolism, excretion, toxicity
ATP	adenosine triphosphate
BBB	blood-brain barrier
BBOX1	γ-butyrobetaine hydroxylase
CAD	*C*-terminal transactivation domain
CHCA	α-cyano-4-hydroxycinnamic acid
CML	chronic myelogenous leukaemia
CNS	central nervous system
CODD	*C*-terminal oxygen-dependent degradation domain
C-P4H	collagen *trans*-4-prolyl hydroxylase
DAPI	4',6-diamidino-2-phenylindole
DIBAL-H	diisobutylaluminium hydride
DMAC	dimethylacetamide
DME	dimethoxyethane
DMF	dimethylformamide
DMOG	dimethyl *N*-oxalylglycine
DMSO	dimethylsulfoxide
DNA	deoxyribonucleic acid
DNMT	DNA methyltransferase
DNOC	*N*-oxalyl-D-cysteine
DSBH	double-stranded β-helix
DSF	differential scanning fluorimetry
DTT	dithiothreitol
EDCI	1-ethyl-3-(3-dimethylaminopropyl)carbodiimide
EDTA	ethylenediaminetetraacetic acid
EGF	epidermal growth factor
EGFH	epidermal growth factor hydroxylase
FAD	flavin adenine dinucleotide
FIH	factor inhibiting HIF
FTO	fat mass and obesity-associated protein
HDAC	histone deacetylase
HDTV	high-definition television
HIF	hypoxia-inducible factor
HOBt	hydroxybenzotriazole
HPPD	4-hydroxyphenylpyruvate
HRE	hypoxia-responsive element
HTS	high-throughput screening
IDH	isocitrate dehydrogenase
IF	immunofluorescence
IFA	intrinsic fluorescence assay
IP	intellectual property

JmjC	Jumonji domain-containing
KDM	histone lysine demethylase
LC	liquid chromatography
MALDI-TOF MS	matrix-assisted laser desorption ionisation time-of-flight mass spectrometry
MAO	monoamine oxidase
MePR	mesenchymal progenitor cells
MINA53	Myc-induced nuclear antigen
mRNA	messenger ribonucleic acid
MS	mass spectrometry
MW	microwave
NMR	nuclear magnetic resonance
NODD	*N*-terminal oxygen-dependent degradation domain
NOG	*N*-oxalylglycine
OGFOD1	2OG- and Fe(II)-dependent oxygenase domain-containing protein 1
PAGE	polyacrylamide gel electrophoresis
PAHX	phytanoyl coenzyme A hydroxylase
PCR	polymerase chain reaction
PDB	protein data bank
PG	protecting group
PHD2	prolyl hydroxylase domain-containing enzyme 2
PHD	plant homeobox domain
PTM	post-translational modification
R&D	research and development
rRNA	ribosomal RNA
RT	room temperature
SAM	*S*-adenosyl methionine
SAR	structure-activity relationships
SDS	sodium dodecyl sulphate
SGC	Structural Genomics Consortium
siRNA	small interfering RNA
snoRNA	small nucleolar ribosomal RNA
SREBP	sterol-response element-binding protein
SSR	structure-selectivity relationships
SUD1	Sudestada 1
TCA	tricarboxylic acid
TCEP	*tris*(2-carboxyethyl)phosphine
TFA	trfluoroacetic acid
THF	tetrahydrofuran
TMLH	N^{ε}-trimethyllysine hydroxylase
Tpa1p	termination and polyadenylation 1 protein
tRNA	aminoacyl-transfer RNA
Ts	tosyl
USP	unique selling proposition
VHL	von Hippel-Lindau
µSPE	micro-scale solid-phase extraction

Chapter I: Introduction

2-Oxoglutarate- (2OG) dependent oxygenases span the three pillars of molecular biology: metabolism, transcription, and translation (Figure 1). 2OG oxygenases catalyse a variety of reactions, most involving introduction of oxygen from dioxygen into their respective substrates. 2OG oxygenases are found in most aerobic organisms (with the exception of archaea) and carry out a wide variety of biological functions, ranging from involvement in the biosynthesis of morphine in poppy seeds to oxygen sensing in humans. In plants and microorganisms, 2OG oxygenase-mediated oxidations lead to reactions including halogenations, rearrangements, oxidative cyclisations, and desaturations. In higher animals, all 2OG oxygenases identified to date catalyse either hydroxylation or demethylation reactions.[1]

Figure 1: The *scutum fidei* of 2OG oxygenases. 2OG Oxygenases are ubiquitous in life. They are present in most cellular organisms in the prokaryotic, eukaryotic, and plant kingdoms. Their functions encompass the three pillars of molecular biology, namely metabolism, transcription, and translation.

Structure and Mechanism

The double-stranded β-helix (DSBH) fold, also known as 'jelly-roll' or 'cupin' fold, is characteristic of all 2OG oxygenases identified to date (Figure 2).[2] The oxygenase active site is located at the more open end of the 'barrel' formed by the eight strands of the DSBH. The DSBH core is always surrounded by two highly conserved *N*-terminal α-helices and, sometimes, a *C*-terminal helix. Inserts between the fourth and fifth strands of the DSBH are sometimes present, as exemplified by comparison of the asparaginyl hydroxylase Factor Inhibiting HIF (FIH), which has a long insert involved in substrate recognition, and the prolyl hydroxylase domain-containing enzyme PHD2, which has no such insert.[3] Additional elements surrounding the DSBH-containing active site are primarily involved in substrate recognition; evidence suggests that such elements are more flexible than those which are not involved with substrate recognition.[4,5] 2OG oxygenases are generally monomeric or dimeric, although higher order oligomers do exist, such as the collagen *trans*-4-prolyl hydroxylase (C-P4H) which exists as an $\alpha_2\beta_2$-heterotetramer.[6]

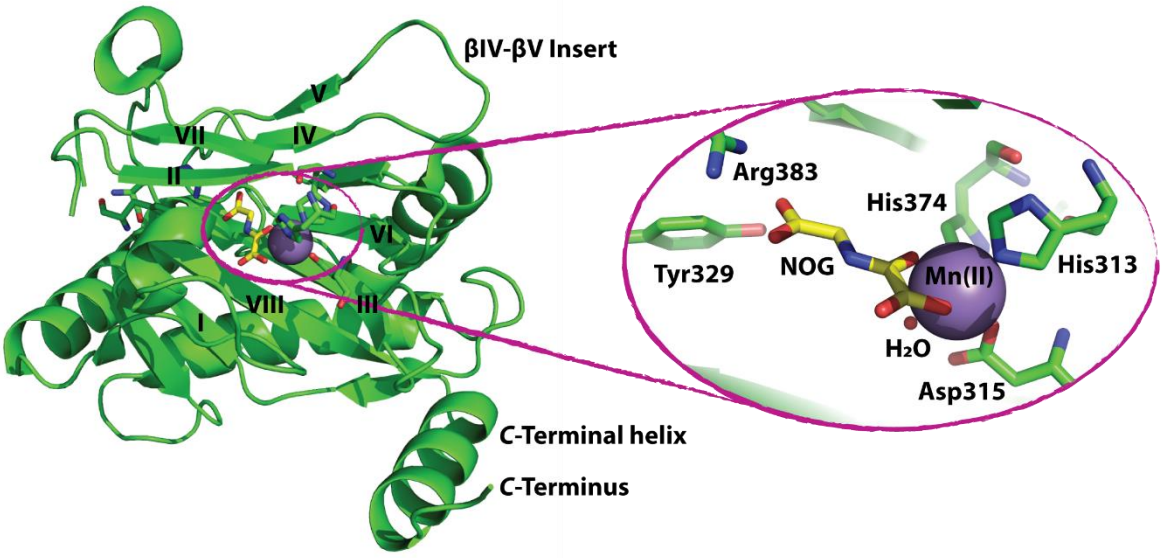

Figure 2: The catalytic domain of PHD2 (PDB ID: 3HQR) highlights the general structural features of 2OG oxygenases. The conserved double-stranded β-helix (DSBH) fold comprises eight strands, labelled I to VIII. The focus on the enzyme active site, with Mn(II) and *N*-oxalylglycine (NOG) substituting for Fe(II) and 2OG respectively, exemplifies the catalytic His-Asp-His triad which binds Fe(II). NOG interacts with the metal *via* bidentate chelation using its 1-carboxylate and 2-oxo groups. The 5-carboxylate engages in salt bridge and/or hydrogen bonding interactions.

Some 2OG oxygenases are multidomain proteins. In particular, some histone demethylases usually contain one or more non-catalytic histone binding domains which can have important functional roles.[7] PHD finger protein 8 (PHF8), for example, contains a plant homeobox domain (unhelpfully abbreviated PHD domain, not

to be confused with the prolyl hydroxylase domain) which is important for catalysis and targeting a particular histone state.[8,9] Other metal-binding domains may include plant homeodomain (PHD) fingers or, as in the case of the KDM4 subfamily, a Zn(II) binding motif within the 2OG oxygenase domain involved with substrate recognition.[10-12]

Detailed insights into the Fe(II) and substrate binding sites of 2OG oxygenases are based on extensive crystallographic and spectroscopic studies. The Fe(II) binding site is conserved and usually contains one aspartyl or glutamyl and two histidyl residues.[5,13,14] Fe(II) binding is relatively weak compared to the haem oxygenases: the metal may be removed by treatment with appropriate metal chelators such as ethylenediaminetetraacetic acid (EDTA) or desferrioxamine. The strength of Fe(II) binding varies considerably amongst different 2OG oxygenases and may have some functional relevance.[15] The binding of water molecules enables octahedral coordination around Fe(II), as observed in X-ray crystal structures (Figure 2).

A consensus mechanism is proposed for 2OG oxygenases (Figure 3). The first step involves binding of 2OG **1** to Fe(II) in a bidentate manner *via* its 1-carboxylate and 2-oxo groups. The 5-carboxylate interacts in salt bridge and/or hydrogen bond interactions and may flip from one side to the other. The prime substrate can then bind in the following step, leading to weakening of binding of the remaining water molecule to the metal, hereby triggering oxygen binding and subsequent reaction.[16] An Fe(IV) species is then generated by oxidative decarboxylation involving oxygen and the iron-bound 2OG with concomitant release of carbon dioxide and succinate **2**. The ferryl species has been characterised spectroscopically; it likely effects hydroxylation *via* a radical rebound mechanism, analogous to the haem oxygenases.[17-22] Evidence suggests that the respective rate-limiting steps change for different oxygenases; in some cases product release may be limiting.[23,24]

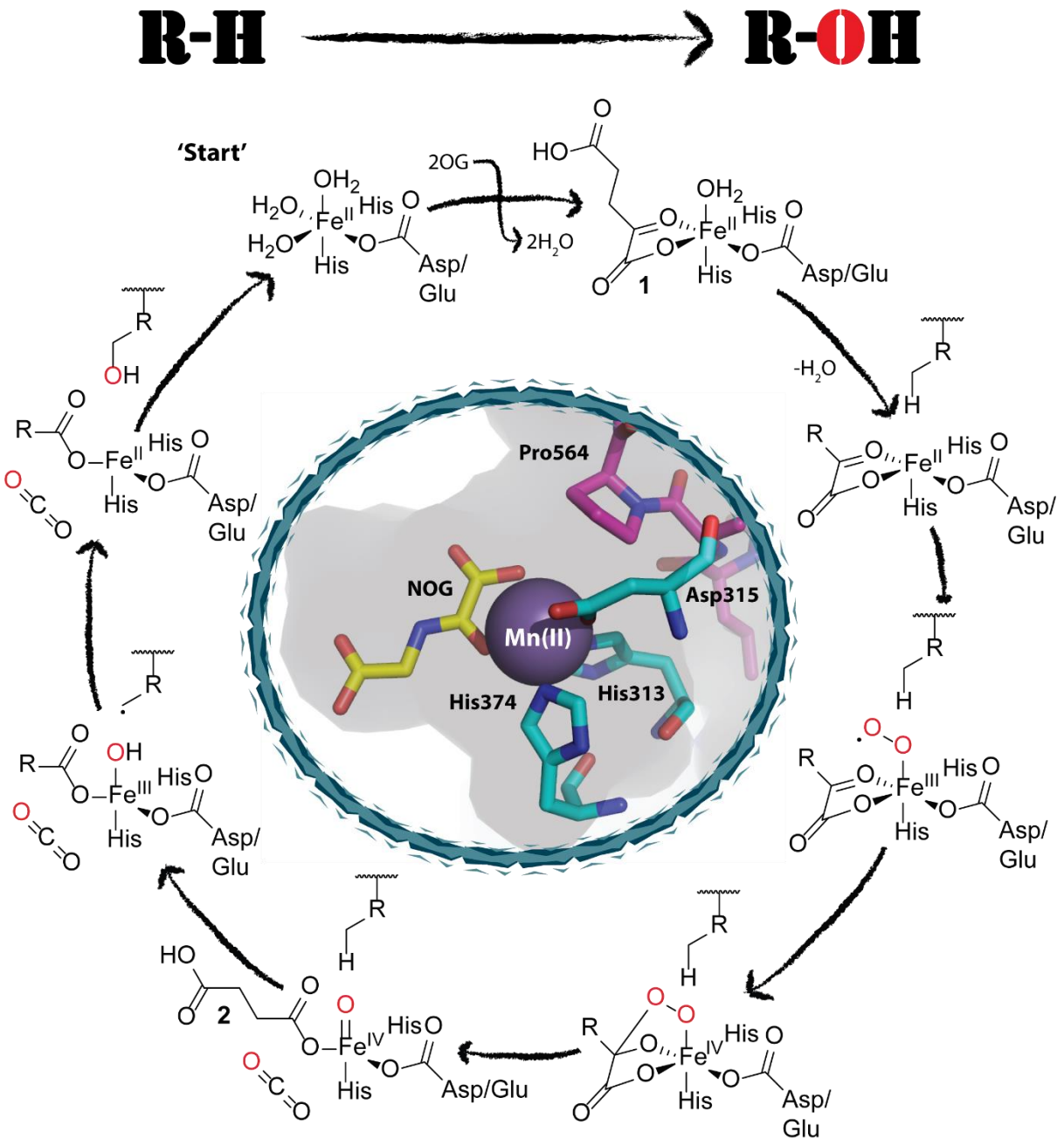

Figure 3: Outline of the consensus hydroxylation mechanism and metal coordination for the 2OG oxygenases based on the X-ray co-crystal structure with HIF-1α (PDB ID: 3HQR). Except for the O_2 complex and the Fe(III)-OH intermediate, there is spectroscopic evidence for all species shown, including the Fe(IV) ferryl species. Subsequent spontaneous reactions, such as demethylation, may occur after substrate hydroxylation.

Hydroxylation Reactions

Collagen Biosynthesis

The first 2OG oxygenases were identified as enzymes that play roles in prolyl and lysyl hydroxylations in collagen biosynthesis (Scheme 1).[25,26] Collagen prolyl hydroxylase C-P4H catalyses the *trans* prolyl-4-

hydroxylation which leads to stabilisation of the collagen triple helix, at least in part, *via* the stereoelectronic gauche effect.[27] Collagen may also be hydroxylated by the collagen C-3PH prolyl-3-hydroxylases called leprecans.[28] Contrary to hydroxylation at position 4, prolyl-3-hydroxylation leads to destabilisation of the collagen triple helix, possibly by allowing other reactions to occur. Lysine was found to be hydroxylated at position 5 by the corresponding procollagen lysyl hydroxylases (PLODs). This lysine modification was shown to act as a site for subsequent post-translational modification (PTM) in the form of glycosylation.[29] In fact, one of the human lysyl hydroxylases was found to be bifunctional by acting both as a lysyl hydroxylase and a glucosyltransferase. Mutations to collagen hydroxylase genes are related to connective tissue diseases, such as pathological fibrosis which is characterised by excessive accumulation of extracellular matrix.[29]

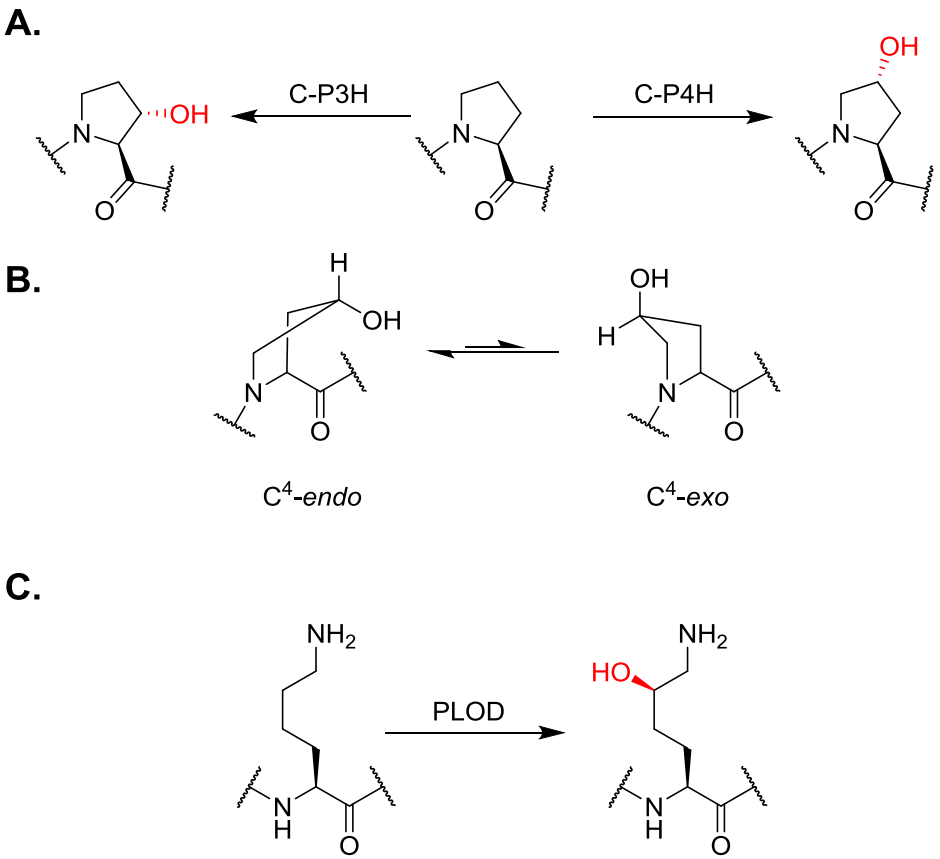

Scheme 1: A. Collagen prolyl hydroxylases contribute to either stabilisation or destabilisation of collagen. *trans*-Prolyl-4-hydroxylation leads to stabilisation of the *C*^{4}*-exo* conformation and hence of collagen *via* the gauche effect (**B.**). Prolyl-3-hydroxylation can lead to collagen destabilisation, possibly *via* subsequent post-translational modifications. **C.** Lysyl-4-hydroxylation provides an anchor point for further post-translational modifications, such as glucosylation.

Fatty Acid Metabolism

Two distinct pathways for fatty acid metabolism involve 2OG oxygenases: carnitine biosynthesis[30] and phytanic acid degradation.[31]

The first and the last steps of carnitine biosynthesis, from N^{ϵ}-trimethyllysine **3** into L-carnitine **5**, involve 2OG oxygenases (Scheme 2): N^{ϵ}-trimethyllysine hydroxylase (TMLH) and γ-butyrobetaine hydroxylase (BBOX1).[32-35] It is proposed that inhibition of carnitine biosynthesis reduces the production of reactive oxygen species *via* reduction of fatty acid oxidation. This may be of therapeutic benefit for patients after myocardial infarction or cardiac arrest.[36] This mechanism is exploited by the clinically used drug Mildronate **4**, which is proposed to act as a BBOX1 inhibitor in cells. Mildronate **4** is administered as a cardioprotective agent after myocardial infarction.[36,37]

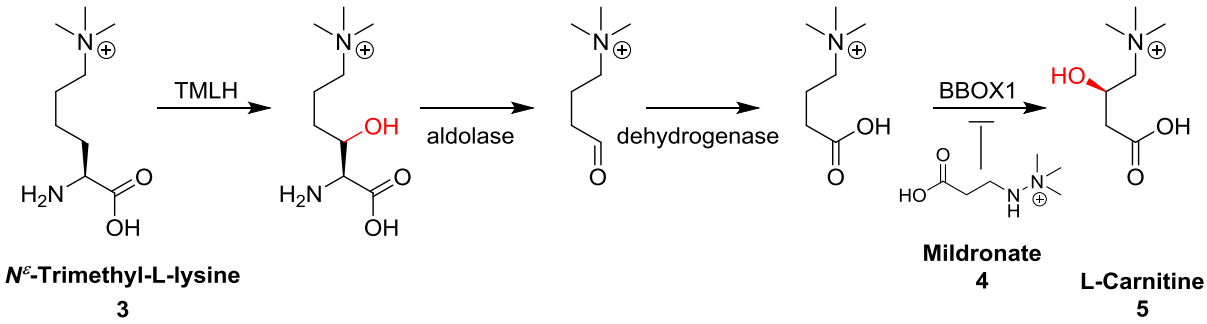

Scheme 2: Carnitine biosynthesis pathway. The 2OG oxygenases TMLH and BBOX1 catalyse the first and last steps respectively for the conversion of N^{ϵ}-trimethyl-L-lysine **3** into L-carnitine **5**.

Phytanoyl coenzyme A hydroxylase (PAHX) catalyses the α-oxidation step from phytanoyl-CoA **6** into 2-hydroxyphytanoyl-CoA **7** in the phytanic acid degradation pathway (Scheme 3).[31] The neurological disorder Refsum disease may arise from PAHX gene lesions leading to accumulation of phytanic acid.[38]

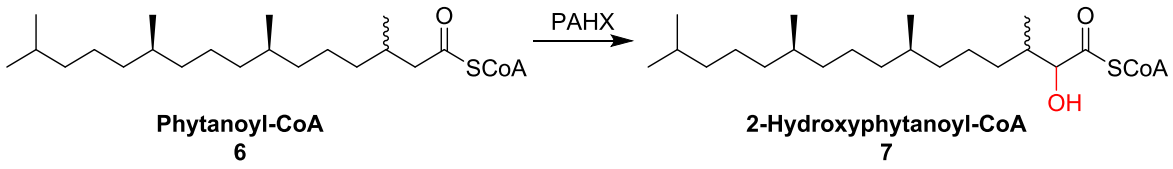

Scheme 3: The degradation pathway of phytanic acid involves α-oxidation of phytanoyl-CoA **6** into 2-hydroxyphytanoyl-CoA **7** by the 2OG oxygenase PAHX.

Oxygen Sensing

Most processes in the human body are fuelled by aerobic metabolism which relies on adequate tissue oxygenation. Hypoxia describes a state of inadequate tissue oxygenation which impedes normal cellular function. Hypoxia may arise from acute lack of oxygen, for example from breathing air of low oxygen content at high altitude, or from strenuous exercise.[39] However, hypoxia may also be a pathophysiological consequence commonly associated with cancer, anaemia, and heart disease.[40] In response to the dynamic

fluctuations of physiological oxygen concentrations, cells have evolved specialised mechanisms to sense oxygen gradients.[41]

Adaptation to cellular oxygen levels relies on hypoxia-inducible factors (HIFs) which are transcription factors mediating gene expression related to cell survival, erythropoiesis, angiogenesis, pH regulation, iron homeostasis, and metabolism.[42] HIFs are composed of one of the three known regulatory α subunits (HIF-1α, HIF-2α, HIF-3α) and a β subunit (HIF-β, ARNT).[43] HIF-1α is the most widely expressed α subunit in all tissues; HIF-2α and HIF-3α display greater tissue specificity with more specialised functions.

HIF-α levels are controlled *via* post-translational modifications; although steady-state mRNA levels of the product of the *HIF-α* genes are essentially independent of intracellular oxygen levels, HIF-α proteins are normally only detectable in cells under hypoxia, not normoxia. The post-translational regulation of HIF-α is primarily mediated *via* the 2OG-dependent prolyl hydroxylase PHD2, which hydroxylates the oxygen-dependent degradation domains of HIF-α. Under normoxia, hydroxylated HIF-α is susceptible to polyubiquitination and subsequent proteasomal degradation; this causes downregulation of hypoxia-dependent genes under normoxia. In contrast, the reduced activity of the HIF-α oxygenases under hypoxia results in an increase of the HIF-α half-life, allowing for its translocation into the nucleus and subsequent dimerisation with HIF-β to form a transcriptionally active α,β-heterodimer which binds to hypoxia-responsive elements (HREs) resulting in transcription of hypoxic-response genes. This negative feedback loop regulation of HIF activity ensures a rapid and dynamic response to hypoxic conditions. Besides hydroxylation by the PHDs for proteasomal degradation, hydroxylation by the asparaginyl hydroxylase FIH reduces interaction with the transcriptional coactivator p300 which is also required for hypoxic response gene transcription (Figure 4).[44]

Human HIF-α hydroxylation is catalysed by four 2OG oxygenases: the prolyl hydroxylase domain-containing PHD1, PHD2, PHD3 enzymes, and the asparaginyl hydroxylase factor inhibiting HIF (FIH). The ability of the HIF-α hydroxylases to act as oxygen sensors is reflected, and proposed to be based, in their relatively high K_m values for oxygen: 100-200 μM for the PHDs and 90 μM for FIH.[45] These values are slightly higher than the tissue O_2 tension levels under normoxia, which makes oxygen binding/reaction the rate-limiting step for

these processes; this allows for effective O_2 sensing and a dynamic response over the physiological range of O_2 concentration levels. A putative PHD4 expressed in the endoplasmic reticulum has been described, but no hydroxylation activity has been observed so far.[46] This isoform has nevertheless been related to tumour angiogenesis *via* interaction with HIF-2α.[47]

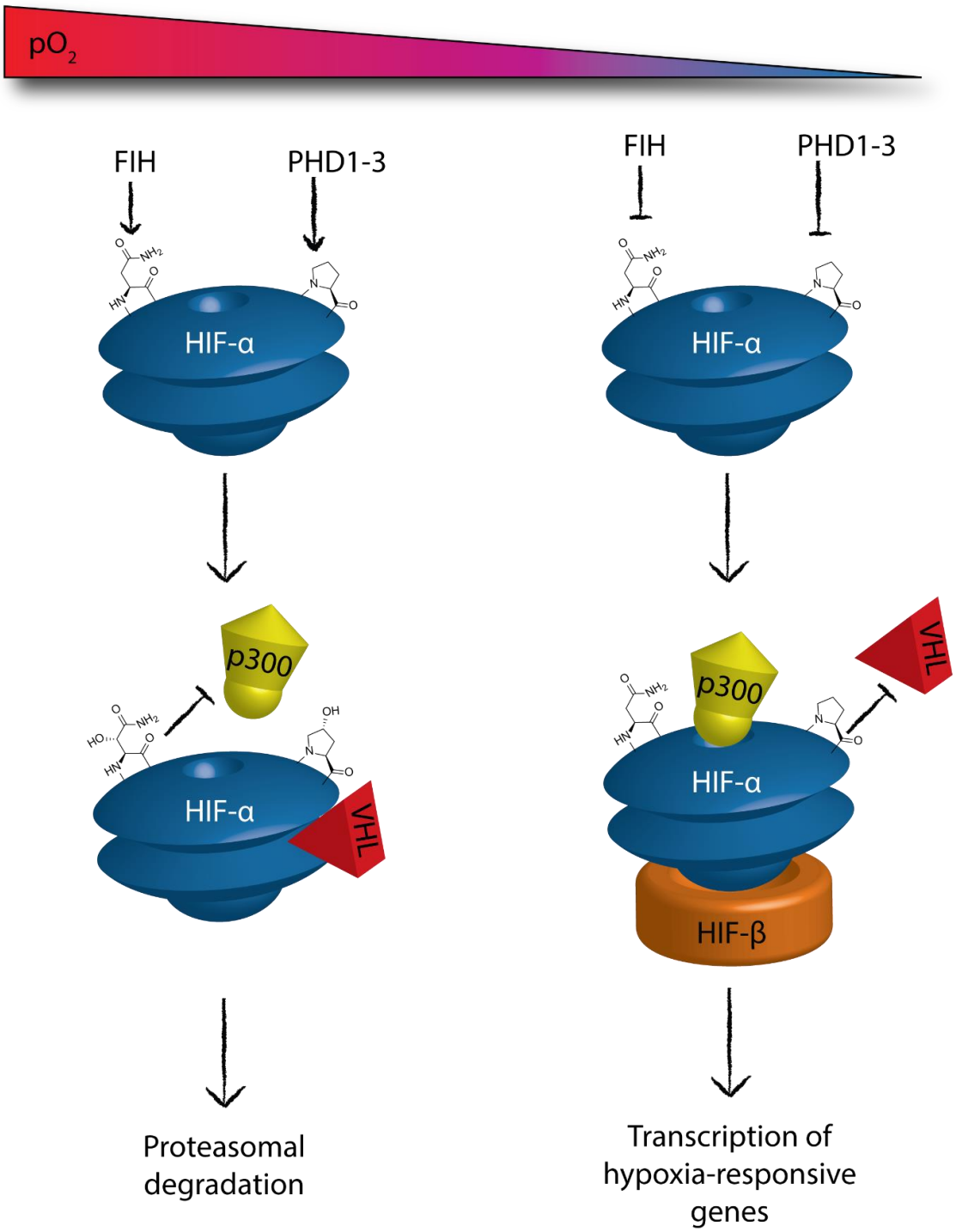

Figure 4: Under normoxic conditions the oxygen sensors prolyl hydroxylase domain-containing enzymes (PHDs) and the asparaginyl hydroxylase factor inhibiting HIF (FIH) ensure inactivity of the transcription factor hypoxia-inducible factor HIF. PHD-mediated prolyl hydroxylation of both *C*- and *N*-terminal oxygen-dependent degradation domains of HIF-α leads to ubiquitination by the von Hippel-Lindau (VHL) complex, ultimately leading to proteasomal degradation of HIF-α. Asparaginyl hydroxylation by FIH leads to inhibition of the HIF-α/p300 interaction required for transcriptional activity. Under hypoxic conditions, HIF-α is sufficiently stable to associate with the HIF-β subunit and with the transcriptional coactivator p300 for transcription of hypoxia-responsive target genes.

Under normoxia, the PHDs catalyse the *trans*-4-hydroxylation of conserved proline residues in the *C*-terminal (CODD) and *N*-terminal (NODD) oxygen-dependent degradation domains, of HIF-α. Conversely, the asparaginyl hydroxylase FIH acts on an asparaginyl residue in the *C*-terminal transactication domain (CAD) of HIF-α, which leads to inhibition of the protein-protein interaction between HIF-α and its transcriptional coactivator p300, ultimately leading to HRE gene silencing (Scheme 4). In contrast to the PHDs, FIH has many substrates other than HIF-α, such as the ankyrin repeat domains from NFκB and Notch signalling pathways.[48] As a first-line treatment for pathologies associated with HIF-responsive genes, the PHDs, especially PHD2, therefore appear to be more viable targets than FIH.

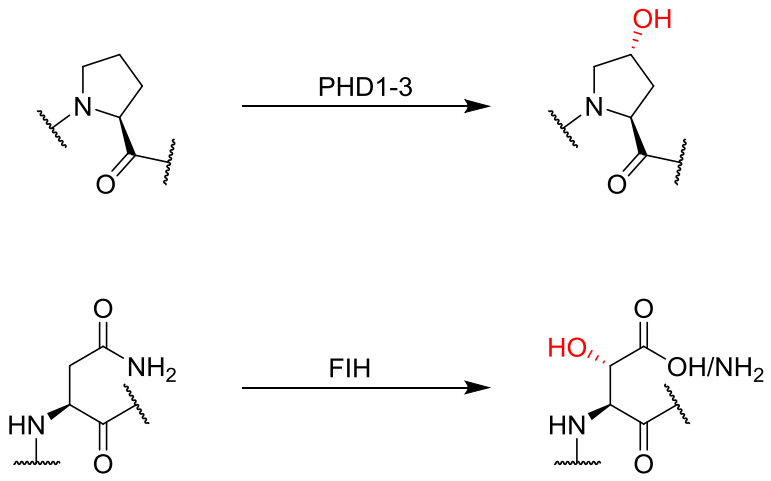

Scheme 4: The prolyl hydroxylase domain-containing PHD enzymes are oxygen sensors regulating HIF transcriptional activity by *trans*-4 hydroxylation of the *C*- and *N*-terminal oxygen-dependent degradation domains of the HIF-α subunit. Factor inhibiting HIF (FIH) regulates HIF transcriptional activity *via* asparaginyl hydroxylation leading to inhibition of association of HIF with the transcriptional coactivator p300. Other substrates of FIH include ankyrin repeat domains involved with NFκB and Notch signalling pathways.

Epidermal Growth Factor Hydroxylation

The identification of β-hydroxylated asparaginyl and aspartyl residues in epidermal growth factor (EGF) domains led to the discovery of the EGF hydroxylase AspH.[49] This EGF hydroxylase accepts both asparaginyl and aspartyl residues to effect *cis*-hydroxylation (Scheme 5), in contrast to FIH which effects *trans*-hydroxylation (Scheme 4). Loss of AspH in mice promotes developmental effects and tumour growth. The full biological function of this EGF hydroxylase, however, is currently unknown.

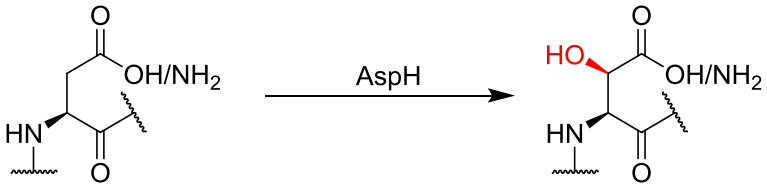

Scheme 5: The epidermal growth factor hydroxylase AspH hydroxylates both aspartyl and asparaginyl residues of EGF-like domains.

Demethylation Reactions

Histone Demethylases

The *N*-demethylation of lysine and arginine residues complements the corresponding methylation reactions to ensure dynamic responses to transcriptional regulation in eukaryotes. Two distinct subfamilies of histone N^{ϵ}-methyl lysine demethylases have been identified to date. The KDM2-7 2OG-dependent histone demethylases catalyse the demethylation of mono-, di-, and tri-methyl N^{ϵ}-methyllysines.[50] This selectivity is in contrast to the flavin-dependent KDM1 family, which has not been shown to catalyse demethylation of trimethyllysines.[51] Histone demethylases play crucial roles in epigenetic regulation and have substantial potential to offer novel drug targets for diseases including cancer and other genetic disorders.[52]

The context-dependent regulation of gene expression is substantially affected by the post-oligomerisation modifications of protein and nucleic acid components of chromatin. Methylation is a common modification of both nucleic acids and histones. Histones are further subjected to acetylation, phosphorylation, and ubiquitination, with the *N*-terminal tail of histone H3 being the most widely diversified chromatin component.[53-55] These post-translational modifications of chromatin have a direct consequence on the accessibility of DNA sequences for transcription; various modification patterns dynamically alter chromatin structure, lifetime, and binding interactions. Aberrant modification patterns have been linked to a variety of diseases, ranging from cancers to infectious disease and mental disorders.[56-58] Chromatin-modifying enzymes are consequently being pursued as potential drug targets, with four drugs already in clinical use, namely the histone methyltransferase inhibitors Azacitidine **8** and Decitabine **9**, as well as the histone deacetylase inhibitors Vorinostat **10** and Romidepsin **11** (Figure 5).[59-61]

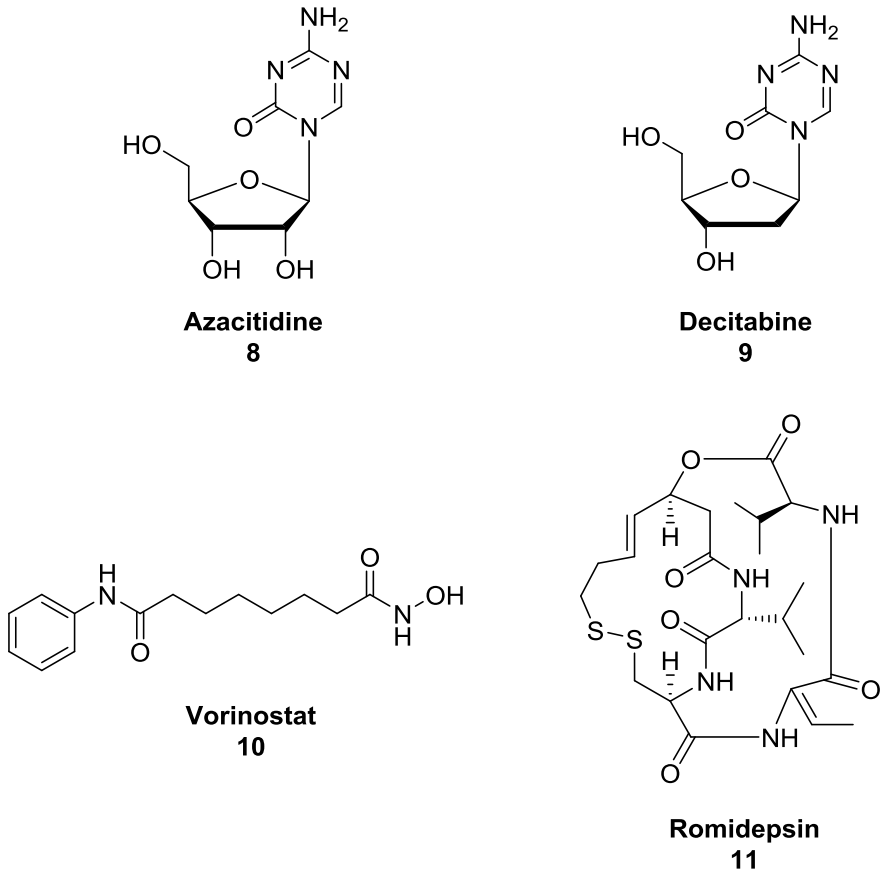

Figure 5: Structures of clinically used drugs modulating epigenetic mechanisms. DNA methyltransferase inhibitors Azacitidine **8** and Decitabine **9**; histone deacetylase inhibitors Vorinostat **10** and Romidepsin **11**.

The most modified amino acid residue in histone tails is probably lysine, which undergoes reactions including methylation, acetylation, crotonylation, ubiquitination, and hydroxylation.[62,63] The possibility of various methylation states on the same residue and in combination with other sites, in addition to other chromatin modifications, enables gene regulation at a very high level of complexity which currently poses an enormous challenge for current biological research, especially when considering that these modifications are largely dynamic, context-dependent, and some possibly even redundant (Figure 6). In this respect, one hopes that tangible therapeutic benefits do not rely on prior unravelling of detailed chemical mechanisms.

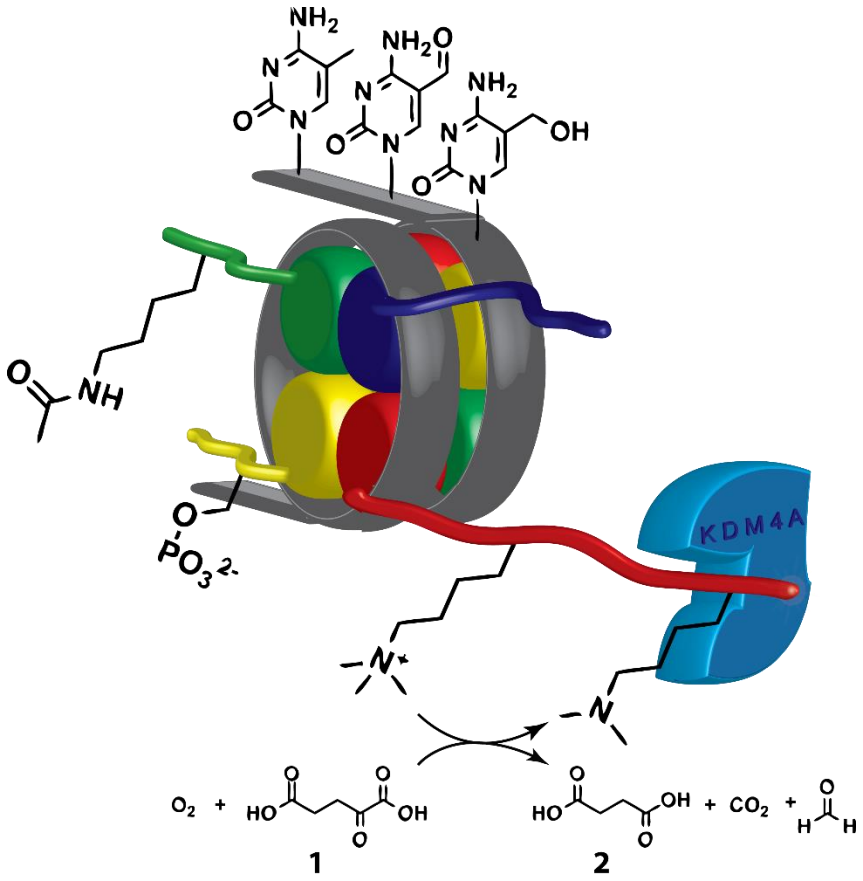

Figure 6: Common chromatin modifications include DNA base modifications such as methylation and hydroxylation. Histone tails are commonly acetylated, phosphorylated, and methylated. Some of these modifications are reversible. The work described in this thesis covers the 2OG histone demethylases, in particular the KDM4, or JMJD2, subfamily. This figure is adapted from a vector drawing by Dr Martin Münzel.

Over twenty histone lysine demethylases (KDMs) have been identified to date, many of which have been linked to disease, primarily cancer.[51,64] They are grouped into two families according to their sequence homologies and catalytic mechanisms: the KDM1, or lysine-specific demethylases (LSDs) and the JmjC domain-containing KDMs (KDM2-7 subfamilies). The KDM1 subfamily is related to the monoamine oxidases (MAOs) and relies on flavin adenine dinucleotide (FAD) as a cofactor. Demethylation is proposed to proceed *via* hydride transfer from the lysine N^{ϵ}-methyl group onto FAD to form an imine which is then hydrolysed to give the demethylated product (Figure 7).[64] This mechanism is incompatible with quaternary trimethylated lysines, which have been shown not to be substrates for the KDM1 subfamily.[65] The substrates of KDM1A are H3K4 and potentially H3K9 mono- and dimethylated lysine, whereas KDM1B is a H3K4-specific demethylase.[66] KDM1A has primarily been linked to cancer, including leukaemias and solid tumours.[67-69]

The JmjC domain-containing KDMs are 2OG oxygenases and represent the larger class of KDMs, with about twenty members grouped into five subfamilies: KDM2/7, KDM3, KDM4, KDM5, and KDM6.[7] The JmjC KDMs

are related to the *N*-methyl DNA and RNA demethylases such as AlkB and FTO, and to other nucleic acid oxygenases such as the ten-eleven translocation methylcytosine dioxygenases (TETs) (see next section).[70] Demethylation occurs *via* hydroxylation of the N^{ϵ}-methyl group to give a hemiaminal which then fragments into formaldehyde and the demethylated product. This mechanism allows for demethylation of mono-, di-, and trimethylated lysines (Figure 7).[66] As well as being overexpressed in several types of cancer, some JmjC KDMs are linked to pathologies of neural development and function, such as X-linked mental retardation, autism, and mid-line defects.[71-75] Development of small-molecule probes for the various KDMs is at a very early stage; their advent will be of high value in order to investigate their biological function as well as for the purpose of target validation.

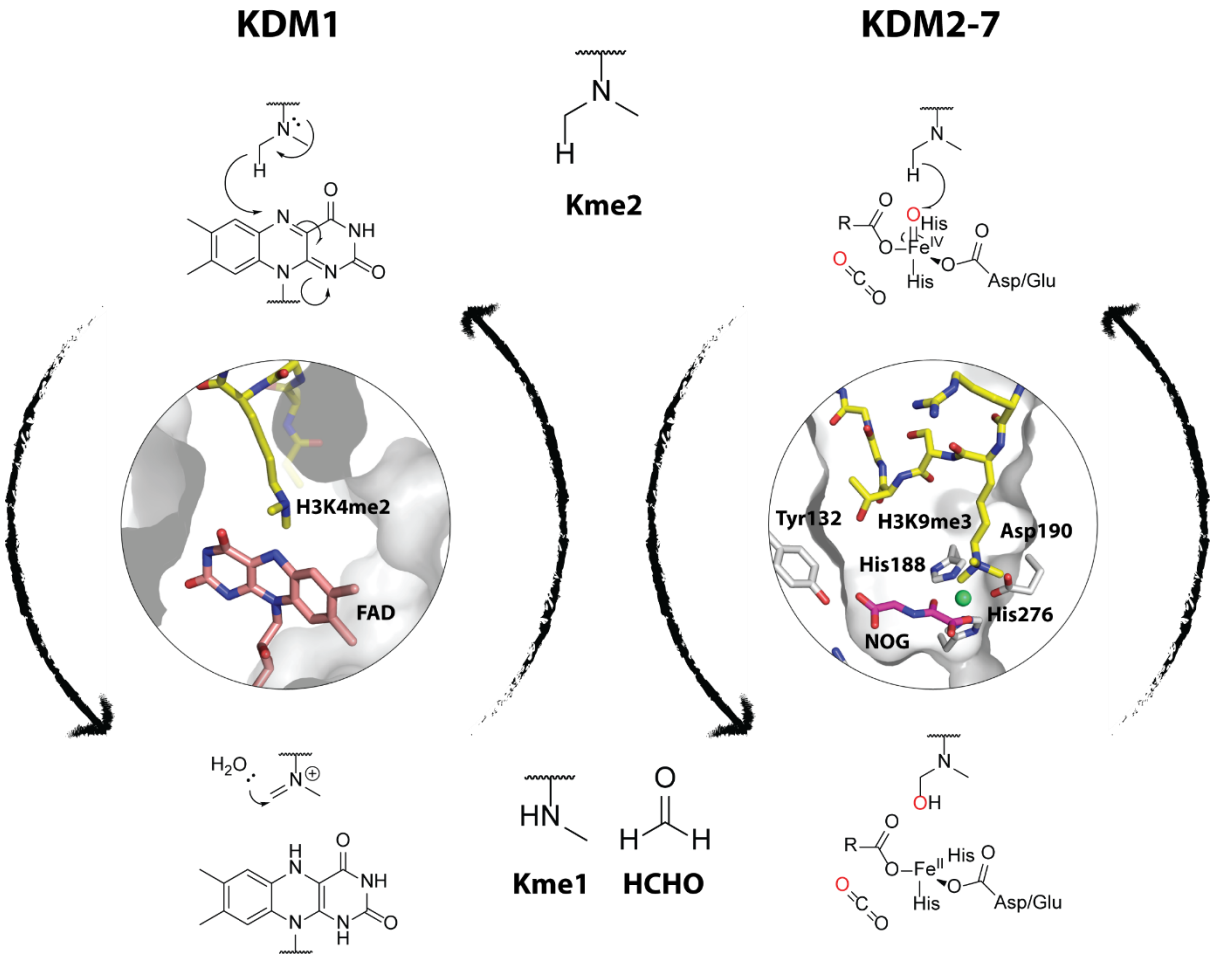

Figure 7: Histone demethylases catalyse the demethylation of histone lysyl residues. The FAD-dependent KDM1 subfamily demethylates mono- and dimethylated lysyl residues, whereas the 2OG KDM2-7 subfamilies can also demethylate trimethylated lysyl residues.

Nucleic Acid Modifications

In *E. coli*, the 2OG demethylase AlkB is involved in DNA damage repair by catalysing demethylation of single-stranded DNA methylated by alkylating agents.[76] AlkB primarily demethylates 1-methyladenine and 3-methylcytosine, with 1-methylguanine and 3-methylthymine being demethylated less efficiently.[77] There are eight AlkB homologues in humans named ABH1-8. Only ABH2 and ABH3 have, however, been reported to possess DNA demethylation activity (Scheme 6). ABH2 prefers double-stranded DNA as a substrate, whereas ABH3 prefers single-stranded DNA; both ABH2 and ABH3 have also been reported to catalyse RNA demethylation.[78,79]

The fat mass and obesity-associated protein (FTO) is related to the ABH demethylases and demethylates 3-methylthymine, as well as, to a lesser extent, 1-methyladenine and 3-methylcytosine (Scheme 6).[80] FTO mRNA levels are high in the brain and regulated by feeding and fasting. FTO has since been a putative target for the treatment of obesity.[81]

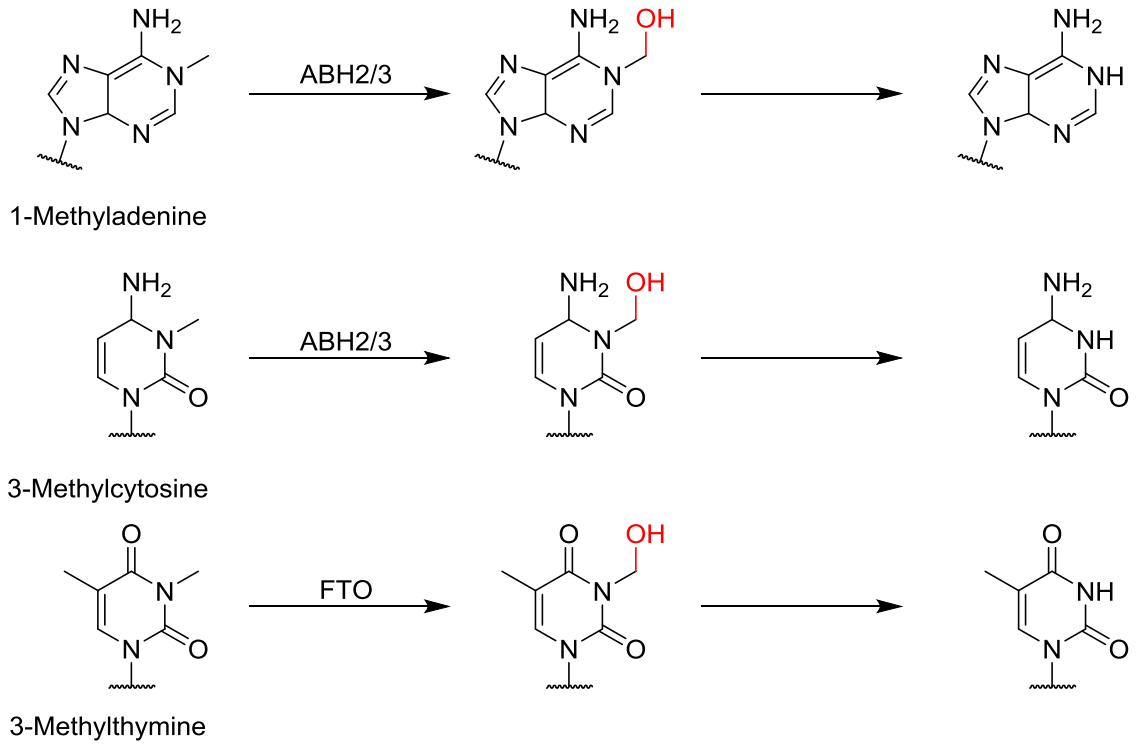

Scheme 6: An overview of 2OG-dependent nucleic acid demethylases. FTO is currently being investigated as a putative target for obesity.

Ribosome Hydroxylation

Protein Synthesis

Ribosomes are large ribonucleoprotein particles that synthesise proteins in all cells. Messenger RNAs (mRNAs) act as a template, and aminoacyl-transfer RNAs (tRNAs) act as substrates. A small 40S subunit and a large 60S subunit make up the fully assembled 80S ribosome in eukaryotes. In prokaryotes, the corresponding 50S large subunit and the 30S small subunit make up the fully assembled 70S ribosome. There are three distinct tRNA interaction sites: the A- (aminoacyl-tRNA) site, the P- (peptidyltransferase) site, and the E- (exit) site. Charged aminoacyl-tRNAs are delivered to the A-site where they form base pairs with the mRNA codons. Peptide bond formation happens at the P-site, after which tRNAs are released at the E-site. The three key steps of protein synthesis are initiation, elongation, and termination. Initiation involves association of ribosomal subunits, mRNA, initiation factors, and tRNA. Elongation describes the formation of the growing polypeptide chain according to codon-anticodon interactions between the mRNA and the corresponding charged aminoacyl-tRNAs. Finally, the termination step comprises finalisation of protein synthesis *via* recognition of stop codons by release factors and subsequent dissociation of the ribosome (Figure 8).[82]

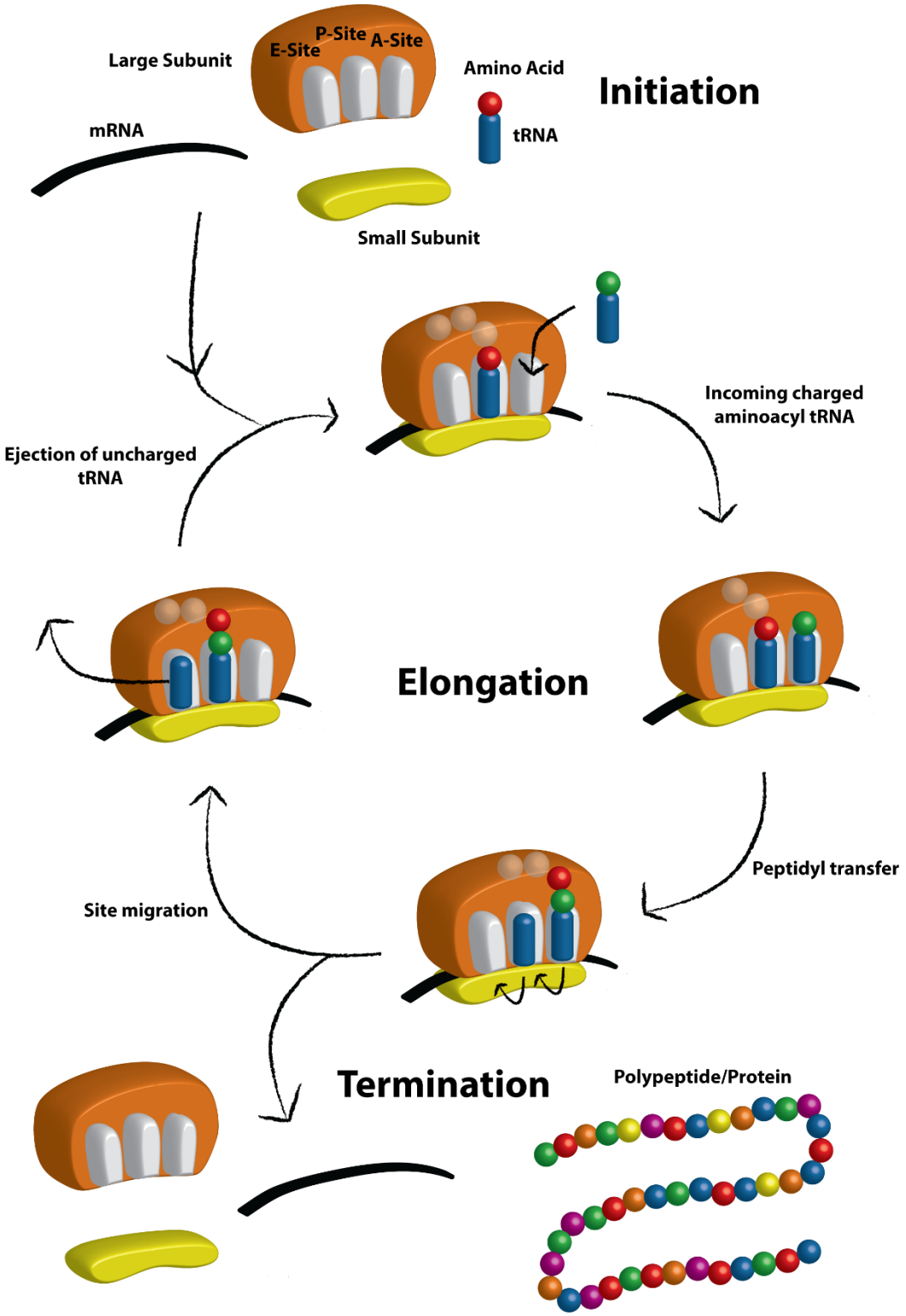

Figure 8: Overview of the steps involved in protein synthesis. Protein synthesis includes three main stages: initiation, elongation, and termination. Initiation involves assembly of the small and large ribosomal subunits with aminoacyl tRNA at the P-site and mRNA. During the elongation phase, the peptide chain is formed. The aminoacyl tRNAs defined by the mRNA codons bind to the A-site after which peptidyl transfer reaction occurs; the amino acid (chain) at the P-site is transferred to the amino acid at the A-site. Upon ratcheting of the mRNA through the ribosome, the empty tRNA is transferred from P-site to E-site for subsequent ejection from the ribosome, while the loaded tRNA moves from A-site to P-site for subsequent loading onto the newly accepted singly loaded tRNA at the A-site at the next elongation cycle. Elongation will continue until the so-called stop-codons are reached; termination occurs at this stage. The newly synthesised peptide chain is cleaved from the attached tRNA and the ribosome dissociates.

Post-Translational and Post-Oligomerisation Modifications to Ribosomes

Ribosomes may be modified, with the modifications targeting both ribosomal proteins and rRNA components (Figure 9).[83] Post-translational modifications in eukoryatic ribosomes comprise phosphorylation, acetylation, methylation, and ubiquitination. Ribosomes have been reported with entire ribosomal proteins missing, but still able to engage in translation.[84] The most well-characterised PTM is probably the phosphorylation of ribosomal protein S6 by the corresponding S6 kinases, S6K1 and S6K2, which phosphorylate five serine residues conserved in higher eukaryotes. This particular PTM likely has a role in initiation given its interaction with mRNA, tRNA, and initiation factors.[85] The determination of the effects of RPS6 phosphorylation in a cellular context, however, is complex because S6K1 and S6K2 have multiple substrates and are central regulators of cell metabolism, growth, and size.

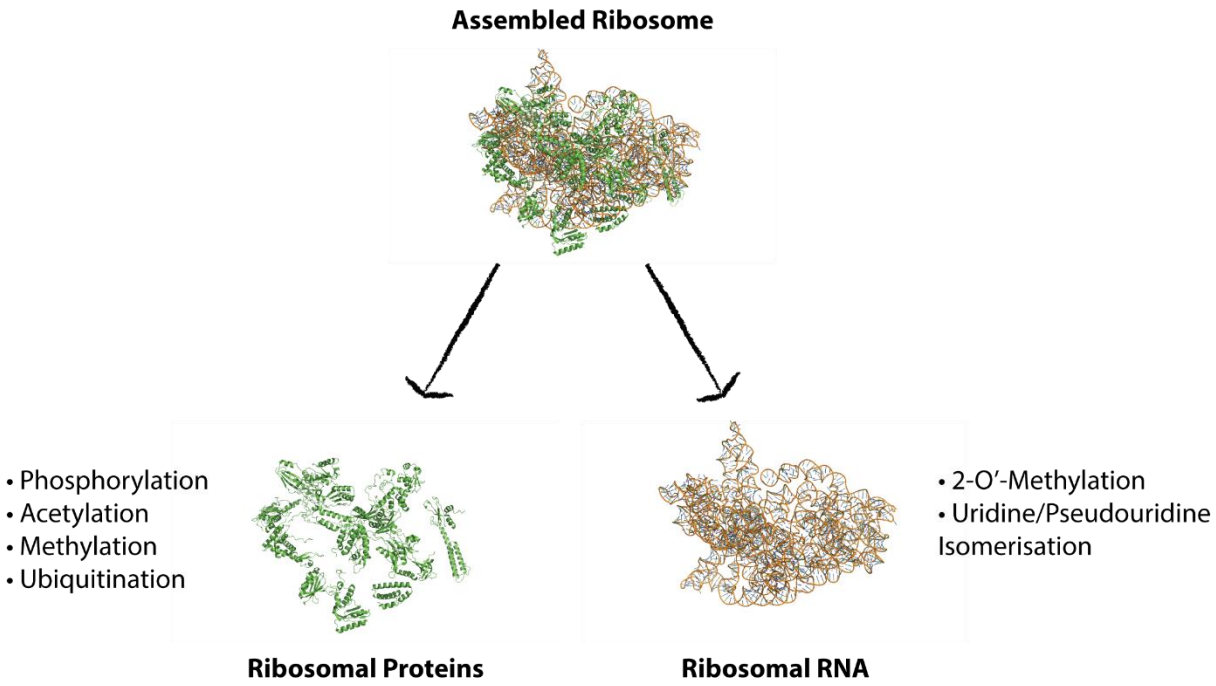

Figure 9: Overview of post-translational and post-oligomerisation modifications to ribosomes. Both protein and rRNA components may be modified.

The most common post-oligomerisation modifications of rRNAs are *S*-adenosylmethionine- (SAM) dependent ribose 2-*O*'-methylation and uridine-pseudouridine isomerisation (Scheme 7). These processes are enzyme-catalysed and in some cases guided by small nucleolar ribosomal RNAs (snoRNAs) which target ribosome-modifying enzymes to specific rRNA residues. In *S. cerevisiae*, about 60% of rRNA PTMs occur in functionally relevant ribosome regions. Deletion of individual modifications rarely lead to altered phenotype,

but double deletions tend to affect rates of cellular growth, amino acid incorporation, ribosomal assembly, and sensitivity to antibiotics.[86]

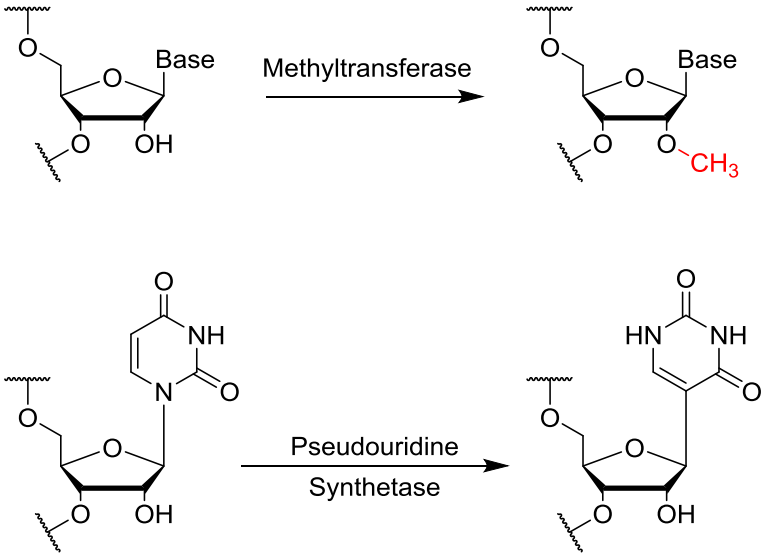

Scheme 7: The most common post-oligomerisation modifications of rRNA are 2-*O*'-methylation and uridine-pseudouridine isomerisation.

In general, the functional consequences of most PTMs to ribosomes are unclear. Any ribosome-dependent processes can, in principle, be affected, such as rate, accuracy, and selectivity. The so-called *ribosome filter hypothesis* suggests that the diversity of ribosome populations engendered by a variety of PTMs enables functional specialisation of the translation apparatus. It might therefore be possible that specific mRNA subsets may be preferentially translated by particular ribosome sub-populations.[87,88]

The previous section focused on 2OG oxygenases involved in mechanisms of metabolism and transcription. These 2OG oxygenases have been studied over the last couple of decades and are relatively well-characterised. A recent novel finding made during the course of work described in this thesis is the family of 2OG oxygenases acting on mechanisms of translation: the ribosomal hydroxylases. These proteins are found in both prokaryotes and eukaryotes. In *E. coli*, the growth-regulating 2OG hydroxylase ycfD catalyses hydroxylation of Arg81 of ribosomal protein Rpl16.[89] There are two human homologues of ycfD, namely Myc-induced nuclear antigen (MINA53) and bifunctional lysine-specific demethylase and histidyl hydroxylase (NO66) which catalyse hydroxylation of histidine residues of ribosomal proteins Rpl27a and Rpl8 respectively. Both MINA53 and NO66 are linked to cell proliferation, interact with the Myc oncogene pathway, and are highly expressed in several cancers and correlate with poor prognosis (Scheme 8).[90-93]

Ribosomal prolyl hydroxylases in prokaryotes have recently been described. In *Drosophila*, the Sudestada 1 (Sud1) ribosomal oxygenase catalyses prolyl hydroxylation of the small ribosomal subunit protein RPS23. Sud1 knockdown led to growth impairment related to reduction of both cell size and cell number as a result of impaired translation efficiency.[94] The fission yeast *S. pombe* homologue Ofd1 was shown to be implicated in the oxygen-dependent regulation of sterol-response genes *via* oxygen-sensitive degradation of the *N*-terminal region of the transcription factor Sre1, which is a homologue of the sterol-response element-binding protein SREBP. The SREBP pathway, however, is not conserved in budding yeast *S. cerevisiae* whose homologue termination and polyadenylation 1 protein (Tpa1p) catalyses hydroxylation of prolyl residue Pro62 of the 40S small ribosomal subunit protein Rps23p (Scheme 8).[95] This particular prolyl residue is the amino acid residue in closest proximity to the decoding centre (Figure 10). In fact, *Tpa1p* deletion led to 10-fold modulation of termination efficiency; Rps23p hydroxylation can result in either increase or decrease in translational accuracy in a stop codon context-dependent manner. This finding provides a molecular basis for the long-known association of RPS23, and its bacterial homologue S12, with translational accuracy.[96-98]

The human homologue of Tpa1p is the 2OG- and Fe(II)-dependent oxygenase domain-containing protein 1 (OGFOD1). OGFOD1 catalyses hydroxylation of Pro62 of the small ribosomal subunit protein RPS23 (Scheme 8).[99] Relative to other human prolyl hydroxylases, OGFOD1 demonstrates an unusually high affinity for the hydroxylated product of the RPS23 substrate with which it forms a stable complex. Knockdown, or inactivation, of OGFOD1 led to stress granule formation, translational arrest, and growth defects.[99]

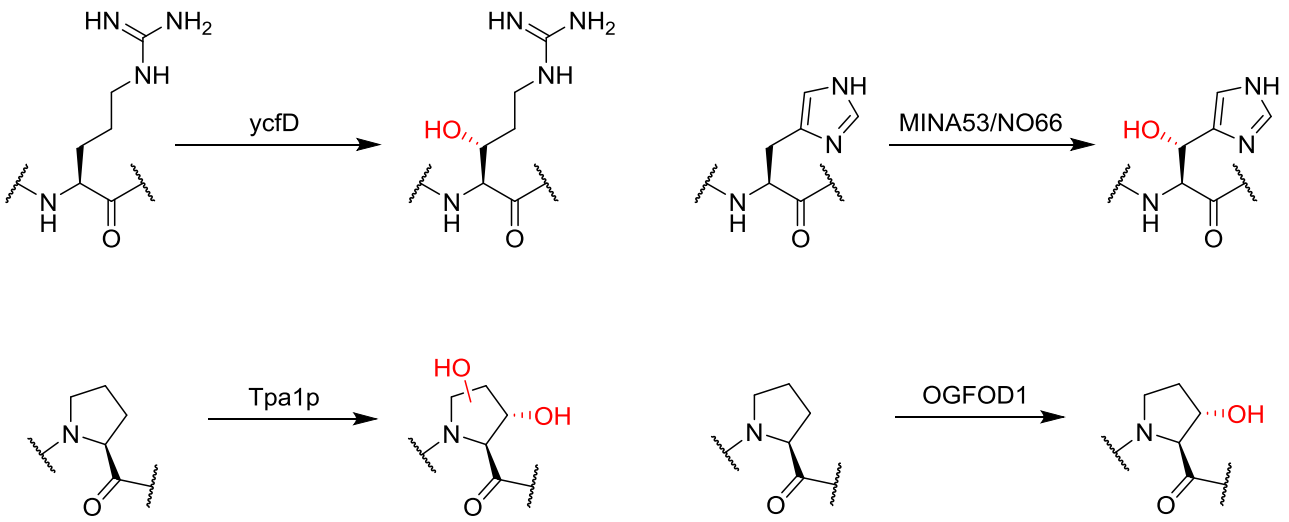

Scheme 8: Overview of 2OG ribosomal oxygenase reactions on ribosomal proteins. Eukaryotic ycfD hydroxylates an arginyl residue, whereas the human homologues MINA53 and NO66 are histidyl hydroxylases. The yeast prolyl hydroxylase Tpa1p may catalyse dihydroxylation, but the human homologue OGFOD1 has only been observed to catalyse monohydroxylation.

The conserved ribosomal prolyl hydroxylases are therefore implicated in translational accuracy related to cell growth.[94,95,99] One major difference, however, is that the human homologue OGFOD1 was shown to exclusively monohydroxylate RPS23, whereas the *S. cerevisiae* (Tpa1p), *S. pombe* (Ofd1), and green algae homologues were shown to be able to dihydroxylate the corresponding substrate prolyl residue. It is remarkable that a post-translational modification in the form of hydroxylation can either increase or decrease translational accuracy, depending on the sequence context. Besides the observation that the hydroxylated Pro62 is the amino acid closest to the ribosomal decoding center, this hydroxylation site is also close to the binding site of known antibiotics such as streptomycin and paramomycin (Figure 10). These results therefore suggest an opportunity for targeting hydroxylated, as opposed to unhydroxylated, ribosomes of hypoxic tissues.

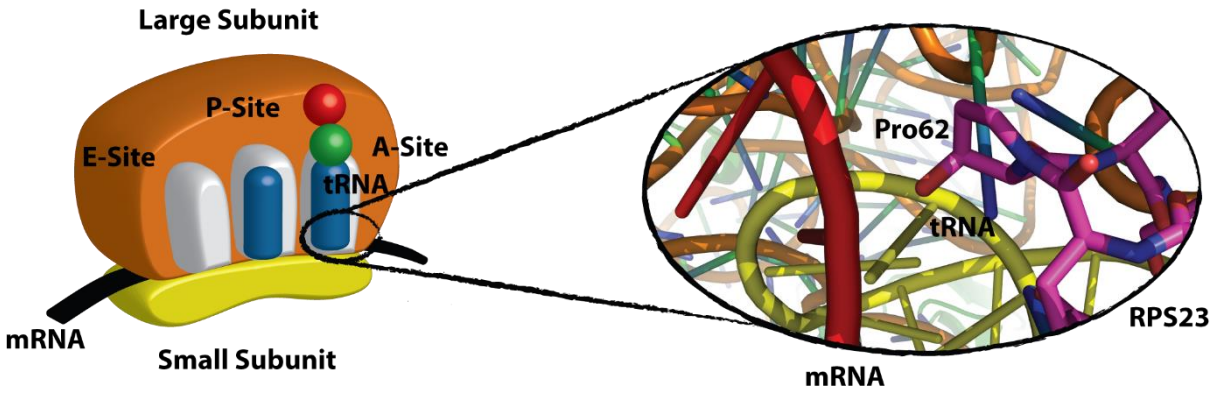

Figure 10: Hydroxylation of RPS23 by the corresponding prolyl hydroxylases has been associated with accuracy of stop-codon readthrough. The substrate prolyl residue Pro62 is the amino acid closest to the ribosomal decoding centre. In addition, this site is close to the binding sites of several antibiotics.

Overall, the superfamily of 2OG oxygenases presents a wide variety of biological functions while sharing a high degree of structural similarity. This structural similarity makes the development of selective small-molecule inhibitors a rather challenging task.

Inhibitors of 2OG Oxygenases

Small-molecule inhibitors of 2OG oxygenases are useful tools for the elucidation of biological function and may provide starting points for small-molecule drug discovery. In fact, the diversity of biological functions associated with 2OG oxygenases reflects the diversity of pathological conditions for which they present attractive putative drug targets. Historically, the first small molecules targeted against 2OG oxygenases emerged from pioneering work on the collagen prolyl hydroxylases and gibberrelin biosynthesis pathways and offered a diversity of chemotypes which offered a basis for the development of inhibitors against other 2OG oxygenases.[50] 2OG oxygenase inhibitors span a wide range of development stages, ranging from early-stage characterisation to compounds in patient clinical trials. The BBOX1 inhibitor Mildronate **4** is the only 2OG oxygenase inhibitor in clinical use, although its precise mechanism of action is unclear.[100] In the subsequent section, an introduction to 2OG oxygenase inhibitors of different types is given; many of the data were generated during the course of this work.[50]

Inhibition by Metal Ions

Divalent transition metal ions including Mn(II), Ni(II), Co(II), Cu(II), and Zn(II) have extensively been observed to inhibit 2OG oxygenases.[101-106] The 2OG oxygenase active site Fe(II) binds relatively weakly, therefore it is

postulated that inhibition by transition metals occurs *via* direct competition with Fe(II) binding inside the enzyme active site. Sometimes, binding of the metal to other locations than the active site may be relevant.[107] The varying extent of inhibition of 2OG oxygenases by transition metal ions may be reflected by the varying affinities for Fe(II) by the respective enzymes. Co(II) is commonly used to mimic hypoxia in cells, possibly *via* inhibition of the HIF prolyl hydroxylases. Similarly, various metals have been shown to affect global histone and DNA methylation levels, which may also be attributed, at least in part, through modulation of the corresponding 2OG demethylases.[108] Both Co(II) and Ni(II) have been shown to degrade ascorbate under certain conditions.[109] This alternative mechanism may lead to inactivation of ascorbate-dependent 2OG oxygenases and raises the possibility of 2OG oxygenase inhibition *via* depletion of cofactors, or possibly even substrate.

Various possible mechanisms of action, differing intracellular concentrations of enzyme, metals, and co-factors, as well as a multititude of metalloenzymes present in cells, make metal ion-mediated selective inhibition of 2OG oxygenases a challenging, if not impossible, task at present. Nevertheless, Co(II) has been used in the past as a treatment for anaemia because it induces erythropoiesis.[110] Another consideration should be the mechanisms of action of metal-containing drugs used in the clinic, in particular commonly used platinum-containing cancer chemotherapy agents such as *cis*-platin **12** or carboplatin **13** (Figure 11). It may be worthwhile examining their impact on epigenetic regulation and, if any, this knowledge may be of benefit with respect to off-target effects.[111]

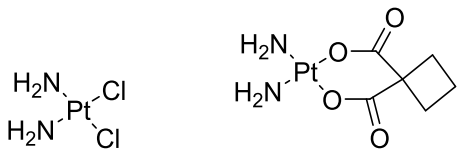

***cis*-Platin**
12

Carboplatin
13

Figure 11: Structures of platinum-containing anticancer drugs *cis*-platin **12** and carboplatin **13**.

Tricarboxylic Acid (TCA) Cycle Intermediates

Relatively little work has been reported on endogenous inhibitors of 2OG oxygenases. One exception, however, is inhibition of 2OG oxygenases by TCA cycle intermediates.[112] The endogenous source of 2OG **1**

itself is the TCA cycle, and therefore any alteration to the TCA cycle likely affects regulation of 2OG oxygenases. Furthermore, precursors and metabolites of 2OG are structurally closely related and are therefore likely to interact with 2OG oxygenases. This is proposed to be of particular importance in a pathophysiological context. Many cancers display mutations to TCA cycle enzymes which may lead to substantial increase in tissue concentrations of succinate **2**, fumarate **14**, and 2-hydroxyglutarate (2HG) **15** (Figure 12).[113-115] In glioma, mutations to isocitrate dehydrogenase 1 and 2 (IDH1/2) lead to gain of function: IDH1 and IDH2 convert 2OG **1** into 2HG **15**, and produce 2OG **1** from isocitrate as well. This increase in TCA cycle intermediates and 2HG **15** is pro-oncogenic, supposedly in part due to inhibition of 2OG oxygenases involved in transcriptional regulation.[116] Succinate **2**, fumarate **14**, and 2HG **15** all inhibit 2OG oxygenases *via* competition with 2OG, although rather weakly in the μM to mM range both *in vitro* and in cells (as their corresponding ester prodrug forms).[117-121]

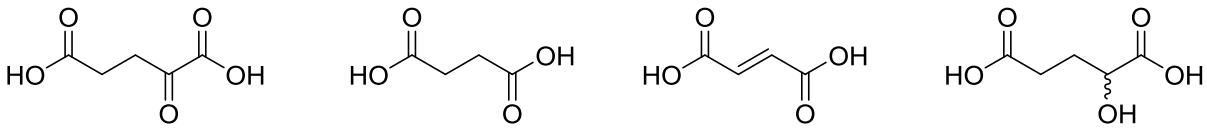

Figure 12: Structures of TCA cycle intermediates 2-Oxoglutarate (2OG) **1**, succinate **2**, fumarate **14**, and the cancer metabolite 2-hydroxyglutarate (2HG) **15**.

Natural Products

2OG oxygenases are involved in the biosynthesis of many natural products. Some natural products may therefore be useful sources of 2OG oxygenase inhibitors. These include the flavonoids which have been identified to be the largest family of natural products to inhibit 2OG oxygenases, including myricetin **16**, baicalein **17**, and epigallocatechin gallate **18**.[122,123] Another class of natural product 2OG oxygenase inhibitors are the flavonoid-related catechols, including dopamine **19**, haematoxylin **20** and caffeic acid **21** (Figure 13).[124-126] It is thought that the metal-chelating properties of both flavonoids and catechols are partly responsible for 2OG oxygenase inhibition. However, direct competition with 2OG has not been observed, and multiple factors may contribute to their mechanism of action. From a pharmaceutical perspective, these compounds are unlikely to be useful. Nevertheless, their effect on 2OG oxygenases raises the possibility of 2OG oxygenase regulation *via* natural product uptake through the diet.

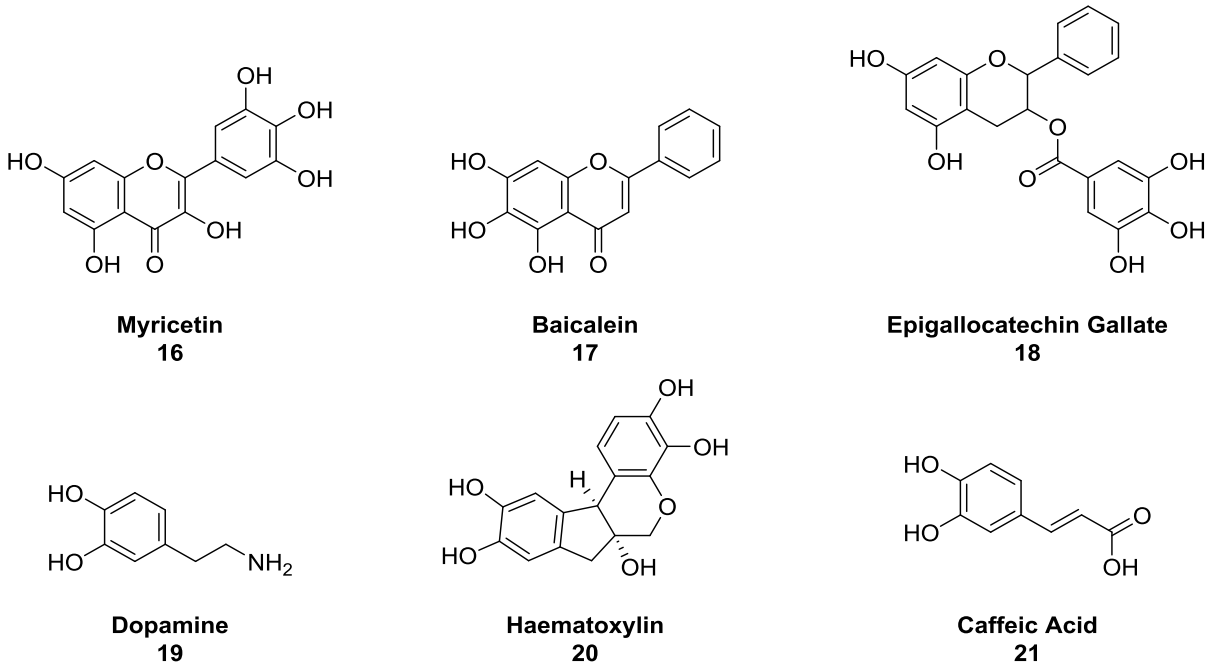

Figure 13: Structures of natural product 2OG oxygenase inhibitors. The flavonoids myricetin **16**, baicalein **17**, and epigallocatechin gallate **18**, and the catechols dopamine **19**, haematoxylin **20**, and caffeic acid **21**.

Generic Inhibitors

Several broad-spectrum 2OG oxygenase inhibitors have been identified to date.[127] The majority are 2OG mimetics and therefore bind in a similar manner. The most prominent generic inhibitors are *N*-oxalylglycine (NOG) **22**, and 2,4-pyridinedicarboxylic acid (2,4-PDCA) **23** (Figure 14). Multiple X-ray co-crystal structures reveal that they act as bidentate metal chelators inside the enzyme active sites and engage in carboxylate-mediated hydrogen bonding, with binding modes closely related to 2OG binding.

The *N*-oxalyl amide 2OG mimetic NOG **22** is likely to exert its inhibitory effect by competing with 2OG **1**. NOG **22** is a broad-spectrum inhibitor which displays a wide range of potencies against various 2OG oxygenases.[128] Given the poor cell permeability of the free NOG dicarboxylate, it is used as its dimethyl ester prodrug dimethyl *N*-oxalyl glycine (DMOG) in a cellular context. DMOG is a widely used hypoxia mimetic because it upregulates and activates the HIF system, supposedly *via* inhibition of both HIF prolyl and aparaginyl hydroxylases.[129-131] Concomitant inhibition of other 2OG oxygenases, such as histone demethylases, may also contribute to relatively good mimicry of hypoxia by DMOG.

Of the pyridine dicarboxylates, 2,4-PDCA **23** is the broadest-spectrum 2OG oxygenase inhibitor.[128] It is a more rigid 2OG analogue than acyclic NOG and is used as either dimethyl or diethyl ester prodrug for cellular studies.[118,132]

Other scaffolds able to mimic 2OG are hydroxamic acids (e.g. **25**) and 8-hydroxyquinolines (e.g. **24**) (Figure 14). Hydroxamic acids are well-established inhibitors of Zn(II) metalloenzymes and act *via* bidentate metal chelation. This observation also applies to their inhibition of 2OG oxygenases by analogous Fe(II) chelation.[133,134] The related *N*-hydroxythiazoles (e.g. **26**) are very potent inhibitors of PHD2.[135] 8-Hydroxyquinolines were primarily identified as KDM inhibitors, with IOX1 **47** (see Chapter II, Figure 24) being the most potent inhibitor *in vitro* and also active in cells.[136] IOX1 **47** seems to possess some inherent selectivity for histone demethylases as its *in vitro* potency is somewhat lower for the prolyl hydroxylases. IOX1 **47** binds in a way analogous to 2OG **1** with the notable difference that it induces a shift in the relative position of the active site metal (see Chapter III, Figure 29).[128]

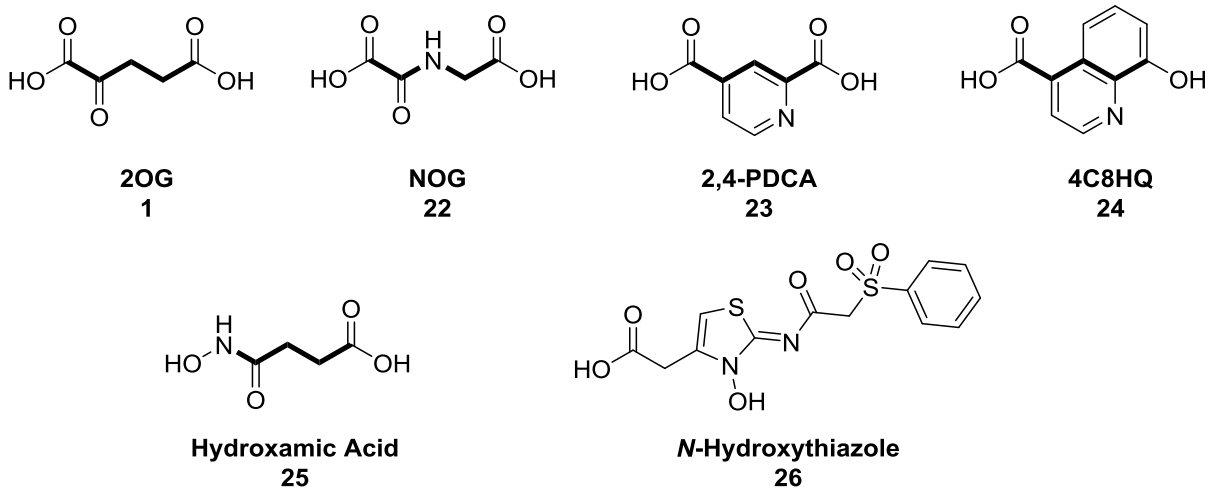

Figure 14: Structures of generic inhibitor classes mimicking the structure of 2OG **1**, including *N*-oxalylglycine **22**, pyridine carboylic acids **23**, 8-hydroxyquinolines **24**, hydroxamic acids **25**, and hydroxamic acid-related *N*-hydroxythiazoles **26**.

Overall, the generic inhibitors possess a bidentate metal chelating motif for anchorage inside the 2OG oxygenase active site by Fe(II) binding. They are structural analogues of 2OG and exhibit analogous binding modes inside the 2OG **1** binding pocket. Therefore, they are likely to inhibit 2OG oxygenases by competing with 2OG for binding. Although promiscuous on their own, the generic inhibitors offer attachment points for selective exploration of subfamily-specific inhibition of 2OG oxygenases. The generic inhibitors may hence

act as 2OG oxygenase inhibitor templates which may be diversified for the generation of subfamily-selective inhibitors (see Chapter II).

Selective Inhibitors of 2OG Oxygenases

PHD2 Inhibitors

PHD2 is probably the most validated 2OG oxygenase target for therapeutic small-molecule intervention.[41,137] Selective inhibition of PHD2 has therefore been studied extensively and various chemotypes have emerged from this field, some of which are in various stages of clinical trials. By virtue of being in clinical trials, these compounds have suitable drug-like properties in terms of both *in vitro* and *in vivo* profiles, including on-target therapeutic effects as well as pharmacological profile. Examples include the isoquinolines FG2216 **27** and FG4592 **28** from Fibrogen, the related chemical probe IOX2 **29** from the Structural Genomics Consortium, triazole **30** from Bayer, and triketone GSK1278863 **31** from GlaxoSmithKline, as reported during the course of work conducted in this thesis. FG4592 **28** is in Phase 3 clinical trials for anaemia and end stage kidney disease, GSK1278863 **31** is in Phase 1 clinical trials for anaemia in chronic kidney disease (Figure 15).[138]

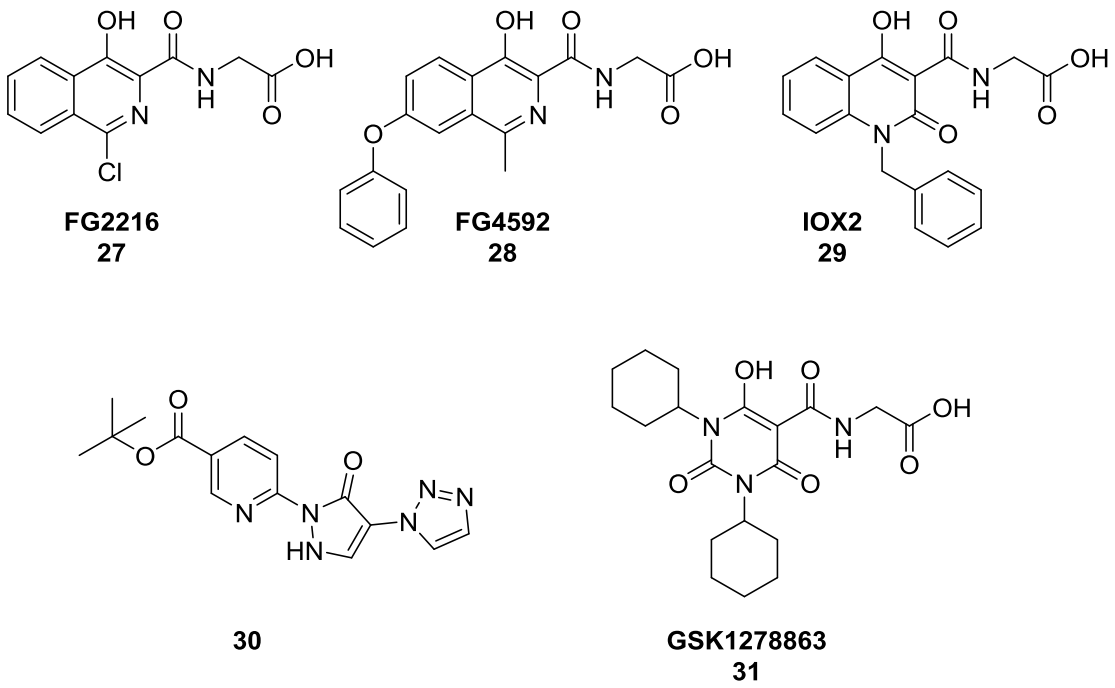

Figure 15: Examples of clinically relevant PHD2 inhibitors, including the isoquinolines FG2216 **27** and FG4592 **28** from Fibrogen, the SGC chemical probe IOX2 **29**, triazole **30** from Bayer, and GSK1278863 **31** from GlaxoSmithKline.

Histone Demethylase Inhibitors

Histone demethylase inhibitors are at relatively early stages of development compared to PHD2 inhibitors. So far, achieving both selectivity and activity in cells has been challenging. Nevertheless, a chemical probe for the KDM6 subfamily (KDM6A and KDM6B) has been developed by GSK, namely GSK-J1 **32**, and its corresponding cell-active ester prodrug GSK-J4 **33** (Figure 16).[139] The hope is to develop potent, selective, and cell-active chemical probes for investigating biological function and drive target validation for each 2OG oxygenase. GSK-J1/4, however, is the only histone demethylase chemical probe reported so far. The negative control compounds GSK-J2 **34** (acid) and GSK-J5 **35** (ester) are regioisomers which may not engage in metal chelation. This chemical probe has subsequently been shown to also inhibit the KDM5 subfamily *in vitro* with a potency about 20-fold less than for the KDM6 subfamily. This finding further illustrates the challenge of achieving selectivity for 2OG histone demethylases.

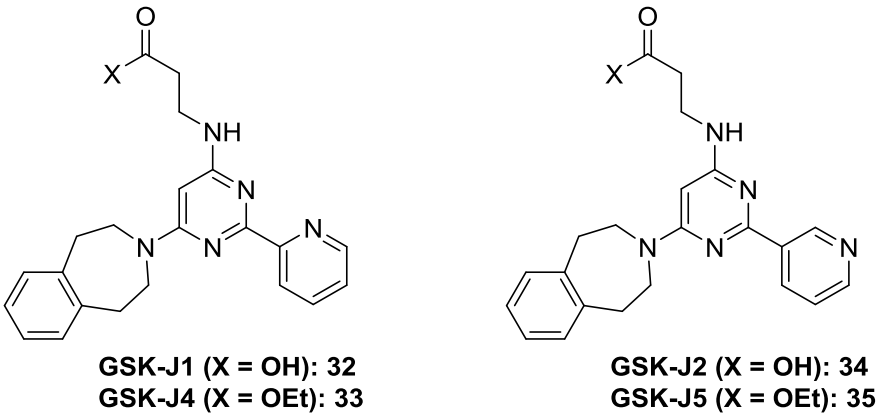

Figure 16: Structures of the chemical probe GSKJ1/J4 **32**/**33** and the corresponding control compounds GSKJ2/J5 **34**/**35**.

Targeting the Substrate Binding Pocket

The shared structural similarity of the enzyme active sites and the corresponding 2OG binding pockets between almost all 2OG oxygenases presents a well-known challenge for achieving selectivity by designing inhibitors solely based around the structure of 2OG **1**. An alternative approach is to base inhibitors around the substrate binding pockets of the enzyme in question by designing histone peptide substrate mimetics for specific KDMs. The JmjC KDMs can have either very distinct, or overlapping, histone H3 substrates. In one study, systematic truncation analysis yielded H3K9me3 truncated peptide sequences with varying degrees of selectivity for the corresponding demethylases. Conjugation of a demethylase-selective peptide to the

promiscuous iron chelator uracil yielded inhibitor **36** for demethylases recognising the same H3K9 methylation (Figure 17).[140]

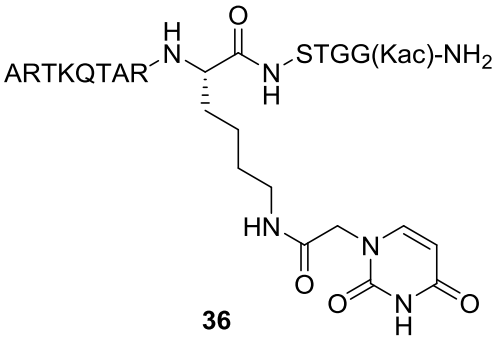

Figure 17: Example of an inhibitor, **36**, exploring both enzyme active site and substrate binding pocket of the KDM4 histone demethylase subfamily.

Another study used the generic inhibitor *N*-oxalyl-D-cysteine (DNOC) in conjunction with H3 peptide sequences which were systematically substituted with cysteine residues in a non-denaturing mass spectrometry-based screen for binding to the KDM4 subfamily.[141] Mixed disulfides that bound to the enzymes were used as a basis for the synthesis of stable analogues which led to KDM4 subfamily-selective inhibitor **37** (Figure 18). In addition, cross-linking to a H3K36-sequence peptide which binds to KDM4A-C, but not KDM4D/E, yielded inhibitor **38** which was shown to be intra-subfamily selective for KDM4A-C against KDM4D/E.

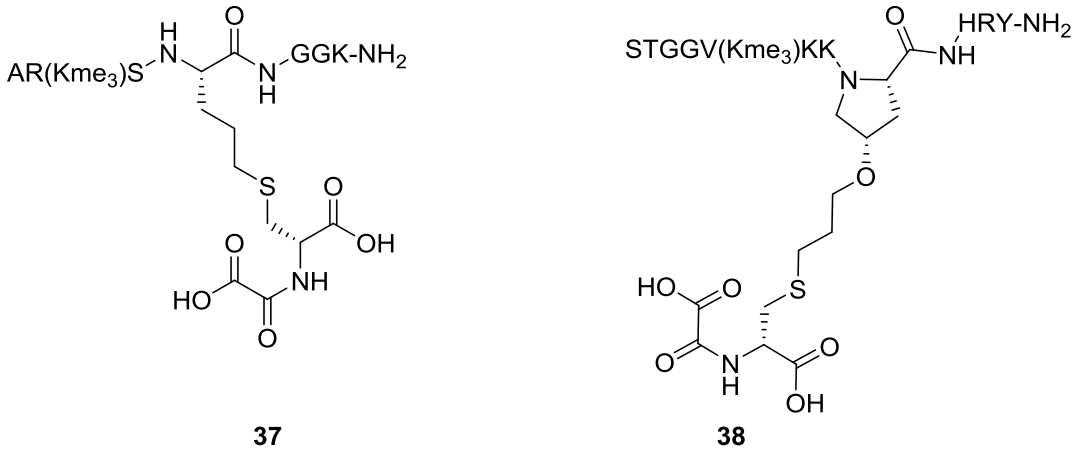

Figure 18: KDM4 subfamily-selective inhibitor **37** obtained by linking subfamily-specific histone mimetic peptide sequences to the general inhibitor NOG **22**. Compound **38** is intra-subfamily selective.

The methodology of linking 2OG binding pocket-targeting inhibitors to substrate binding pocket-targeting substrate mimetics led to the development of histone demethylase-targeting inhibitor Methylstat **39** (Figure

19). The carboxyhydroxamic acid moiety targets the 2OG binding pocket while the secondary amine acts as a protonated lysine mimetic. The free acid inhibits KDM4C in the micromolar range *in vitro*; the methyl ester prodrug is required for activity in cells.[142]

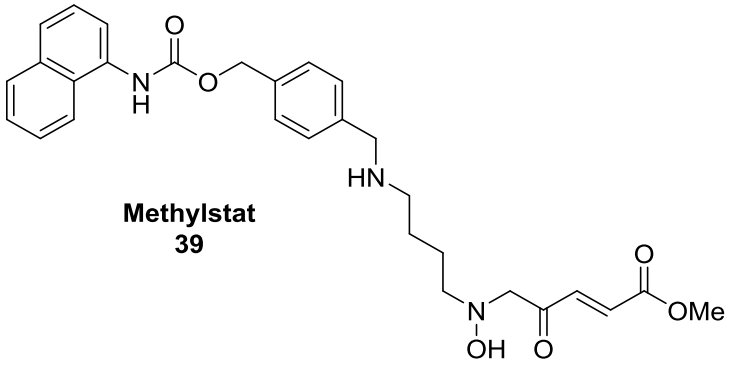

Figure 19: Structure of histone demethylase-specific compound Methylstat **39** which links a trimethyllysine-mimicking side chain to the corresponding 2OG-mimicking hydroxamic acid.

These studies provide a proof of principle demonstrating the possibility of achieving not only subfamily-, but also intra-subfamily-selective inhibitors by designing molecules which explore both 2OG and substrate binding pockets at the same time (see Chapter II).

The development of small molecules solely targeting the substrate binding pocket is at a very early stage. One example are the BIX-01294 **40** and E67 G9 and G9a-like methyltransferase inhibitors **41** and **42** which were shown to also inhibit KDM7A in the low-micromolar range (Figure 20).[143] It is proposed that these compounds mimic the H3 substrate, as suggested by X-ray co-crystal structure analysis of E67 **41** with KDM7A. This work led to the development of E67-2 **42** which retained potency against KDM7A while achieving over 30-fold selectivity against G9a-like methyltransferases. These results provide a proof of principle for the development of substrate-competing inhibitors.

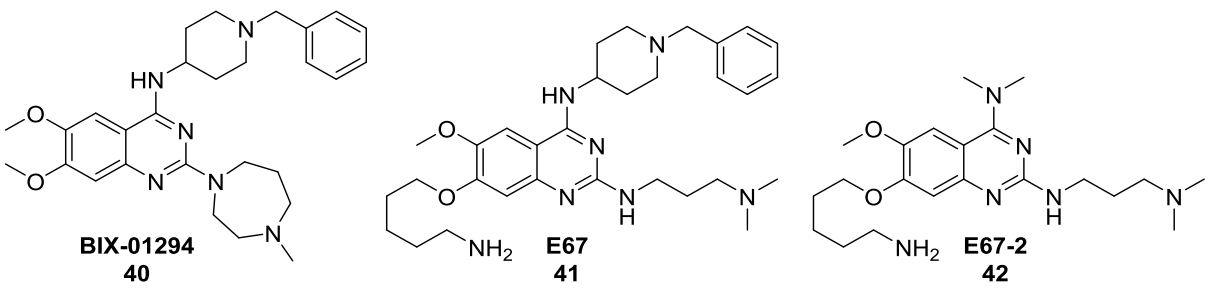

Figure 20: Structures of substrate-mimicking G9 and G9a-like methyltransferase inhibitors BIX-01294 **40** and related E67 compounds **41** and **42** which also inhibit the histone demethylase KDM7A. E67-2 **42** is selective for KDM7A over the G9a-like methylstransferase.

Inhibitors of Other Superfamilies

One may argue that the property of selectivity for small molecules is not well-defined. Selectivity criteria are usually somewhat arbitrary and based on *in vitro* considerations. For example, the chemical probe selectivity criteria set by the SGC are defined as 30-fold selectivity *in vitro* over related enzymes (www.thescgc.org). Here, the '30-fold' benchmark is arbitrary, whereas the term 'related enzymes' is open to interpretation. Selectivity may be easily quantifiable *in vitro*, but in a cellular context considerations of relative enzyme expression levels, as well as localisation and relative lifetimes, need to be taken into account. Furthermore, it would be challenging, if not impossible, to test a single molecule against every single enzyme in the human body. Therefore, it is likely that many small molecules, including drugs commonly used in the clinic, display off-target effects which are not necessarily known. Screening of commercially used small molecules initially unrelated to 2OG oxygenases has, therefore unsurprisingly, identified some of them to be inhibitors of 2OG oxygenases.

One example is the hydroxamic acid-based histone deacetylase (HDAC) inhibitor Vorinostat **10** (SAHA) which was shown to inhibit KDM4E.[118] Some of the epigenetic effects of SAHA may therefore stem from inhibition of histone demethylases, in conjunction with inhibition of histone deacetylases. An example of cross-species reactivity is the agrochemical Daminozide **43** which is an inhibitor of plant 2OG oxygenases involved in gibberellin biosynthesis.[144] Daminozide was later found to be a selective inhibitor for the KDM2/7 families over other JmjC KDMs following a screen of potential 2OG mimetics.[145] Crystallographic analysis suggests that the KDM2/7 selectivity may stem from a hydrophilic region present in KDM2/7 (next to Fe(II)) relative to the corresponding more hydrophobic region in other KDMs. Nevertheless, the KDM2/7 selectivity is remarkable given the small size of Daminozide. An agrochemical that acts on human enzymes raises obvious safety concerns. Another example of PHD inhibitors that lead to concomitant upregulation of HIF are several metabolites of Aspirin **44**.[146] This observation may be of interest considering the prophylactic properties of Aspirin for heart disease (Figure 21).[147]

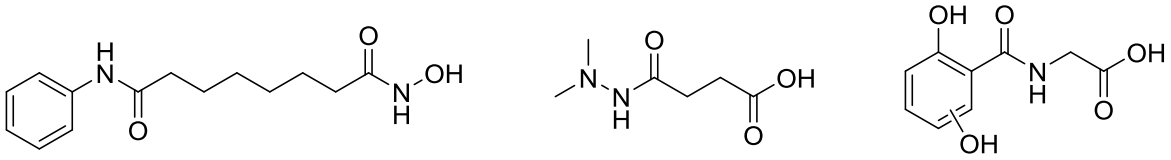

Vorinostat
10

Daminozide
43

Aspirin Metabolites
44

Figure 21: Structures of HDAC inhibitor Vorinostat **10**, plant growth inhibitor Daminozide **43**, and Aspirin metabolites **44**, all of which were shown to be inhibitors of 2OG oxygenases.

Finally, it may be worthwhile reconsidering the (nowadays) common dogma of the requirement for on-target selectivity for therapeutic effect. For example, DMOG leads to relatively good mimicry of hypoxia in cells, whereas selective PHD2 inhibitors do not.[148] Given the involvement of 2OG oxygenases in the transcriptional machinery, which is highly dynamic and context-dependent, it may be worthwhile developing inhibitors targeting specific sets of enzymes, rather than distinct, specific enzymes only, in order to achieve a therapeutic effect (see Chapter II, compound **86**). An example of this hypothesis is provided by development of pan-histone demethylase inhibitors, targeting both KDM1 and JmjC KDMs in an effort to address the observation that both KDM1 and KDM4 are coexpressed and colocalise with the androgen receptor in prostate cancer.[149] This was achieved by covalently linking the known KDM1 inhibitor tranylcypromine to the JmjC KDM inhibitors 4-carboxy-2,2'-bipyridine or IOX1 **47** (Figure 22).[150] These dual inhibitors **45** and **46** led to growth arrest and apoptosis in prostate and colon cancer cell lines. This effect was not observed with either single precursor inhibitors, or a mixture thereof. Little or no apoptosis was observed in non-cancerous mesenchymal progenitor (MePR) cells. Although at very early stages, there may be considerable scope for the development of cancer-selective inhibitors by targeting specific subsets of epigenetic regulator enzymes.

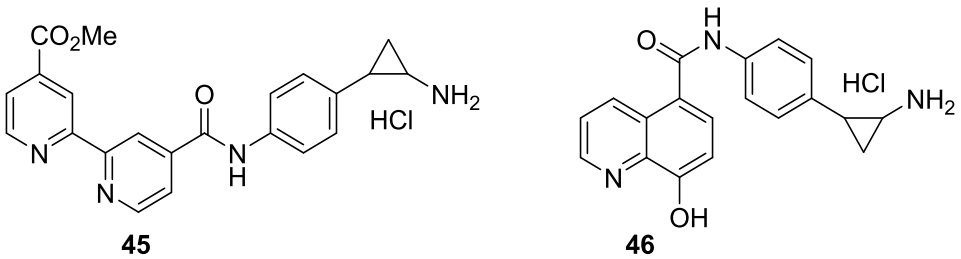

45

46

Figure 22: Structures of pan-demethylase inhibitors **45** and **46** which comprise KDM1 inhibitor tranylcypromine covalently linked to the JmjC KDM inhibitors 2,2'bipyridine-4,4' dicarboxylic acid and IOX1 **47**.

Thesis Objectives

The work described in this thesis is centered around small-molecule inhibition of 2OG oxygenases. The specific aims were to:

1. Validate the hypothesis of template-based inhibition for 2OG oxygenases.
2. Devise tool compounds for (sets of) KDM demethylases.
3. Set up an *in vitro* activity assay for the OGFOD1 ribosomal prolyl hydroxylase.
4. Develop a small-molecule inhibitor for OGFOD1 selective against PHD2.

From a social science perspective, the aims of the project were to:

A. Analyse open-innovation drug discovery in the area of epigenetics.

B. Formulate recommendations based on the insights gained during the above analysis.

Chapter II: Synthesis of Template-Based 2OG Oxygenase Inhibitors

Introduction

The link between KDM-mediated transcriptional regulation and the resulting physiological implications are of exponentially growing biomedical interest (see Figure 55, Chapter IV). Various pathophysiologies associated with cancer, infectious disease, and mental disorders have been linked to dysregulated histone methylation patterns.[56-58] The KDMs therefore offer an opportunity for the development of novel treatments and diagnostics. For example, overexpression of the KDM4 subfamily has been associated with several cancers, including breast, prostate, colorectal, and lung.[151,152] Current evidence suggests that these links rely on biological mechanisms of cell cycle progression and DNA damage response.[153-155]

The human KDM4 subfamily encompasses six members, namely KDM4A-F. KDM4A-C are the most studied KDM4 enzymes; KDM4D lacks both the PHD and Tudor domains present in KDM4A-C, and KDM4E/F appear to be 'encoded' from pseudogenes.[156] The subsequent discussions shall primarily focus on KDM4A-C. The substrates comprise H3K9 and H3K36 N^{ε}-trimethylated and dimethylated lysines, with H3K9me3 being demethylated most efficiently (the corresponding monomethylated lysines are only poor substrates).[157] In addition, KDM4A has been reported to demethylate H1.4K26me3.[158] Substrate selectivity, however, is far from clear.

Overall, there is a need for extensive functional and biochemical characterisation of the KDM4 subfamily with the ultimate goal of target validation for therapeutic or diagnostic use. Potent, selective, and cell-permeable small-molecule inhibitors are of particular interest with this respect because they offer a relatively fast, reversible, and cost-effective methodology compared to biological techniques based on, for example, gene knock-down or siRNAs.[159] No such tool compound has, however, been reported for the KDM4 subfamily. In fact, the only currently available KDM tool compound is GSK-J1/J4 **32**/**33** for the KDM6 subfamily (see Chapter I, Figure 16).[139] Subsequent results suggest this compound also, at least partially, inhibits the KDM5 subfamily. In the process of KDM tool compound development, the particular challenges include subfamily selectivity

and cell permeability. This chapter outlines a strategy adopted for the development of a tool compound for the KDM4 subfamily.

Chemotype Selection for Template Inhibition

The template inhibition strategy suggests an opportunity to develop a diverse set of small-molecule inhibitors for various 2OG oxygenases based on the same template chemotype. Template inhibition exploits the structural similarities between 2OG oxygenases for the development of small-molecule probes for elucidation of their functional diversity. Two key structural characteristics are apparent in 2OG oxygenases:

- A conserved (although varying in detail) and relatively rigid 2OG binding pocket
- A highly varied and more flexible substrate binding site

In terms of inhibitor design strategy, the 2OG binding site offers an attractive site to which generic inhibitors, or templates, can be targeted, whereas the latter offers enzyme-specific areas into which side chains can be built off the template into the substrate binding pockets. The template can be viewed as an anchor which hooks into the enzyme active site, whereas the side chains act as the corresponding exploration boat which selectively probes the substrate binding pocket.

Viable template candidates are fragment-like small molecules which can be conveniently diversified with a variety of side chains. Several template scaffolds have been extensively studied in-house and are generally based on 2OG **1**, involving a bidentate Fe(II)-chelating motif, as in *N*-oxalylglycine (NOG) **22**, 2,4-pyridinedicarboxylic acid (2,4-PDCA) **23**, or 8-hydroxyquinoline-4-carboxylic acid (4C8HQ) **24** (Figure 23).[118]

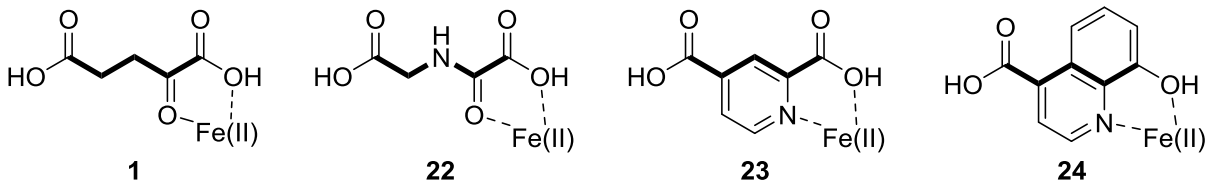

Figure 23: Generic 2OG oxygenase inhibitors based on the core structure of cofactor 2-oxoglutarate **1**: *N*-oxalylglycine (NOG) **22**, 2,4-pyridinedicarboxylic acid (2,4-PDCA) **23**, and 8-hydroxyquinoline-4-carboxylic acid (4C8HQ) **24**.

8-Hydroxyquinoline-5-carboxylic acid (IOX1) **47** was shown to be a potent *in vitro* pan-demethylase inhibitor which retains moderate potency in cells.[136] In addition, several 7-substituted 8HQs including **48** and **49** were

identified as putative PHD2 inhibitors in a cell-based reporter assay (Figure 24).[160] Subsequent *in silico* modelling studies suggest that 7-substituted 8HQs offer an opportunity for template-based inhibition: the 8HQ motif may act as an Fe(II) chelator, whereas the side chains at position 7 may reach towards the entrance of the respective substrate binding pockets (Figure 25). Given the beneficial profile both *in vitro* and in cells, alongside *in silico* structural considerations, 7-substituted 8HQs were judged to be a suitable starting point for template-based inhibitor design (Figure 24).

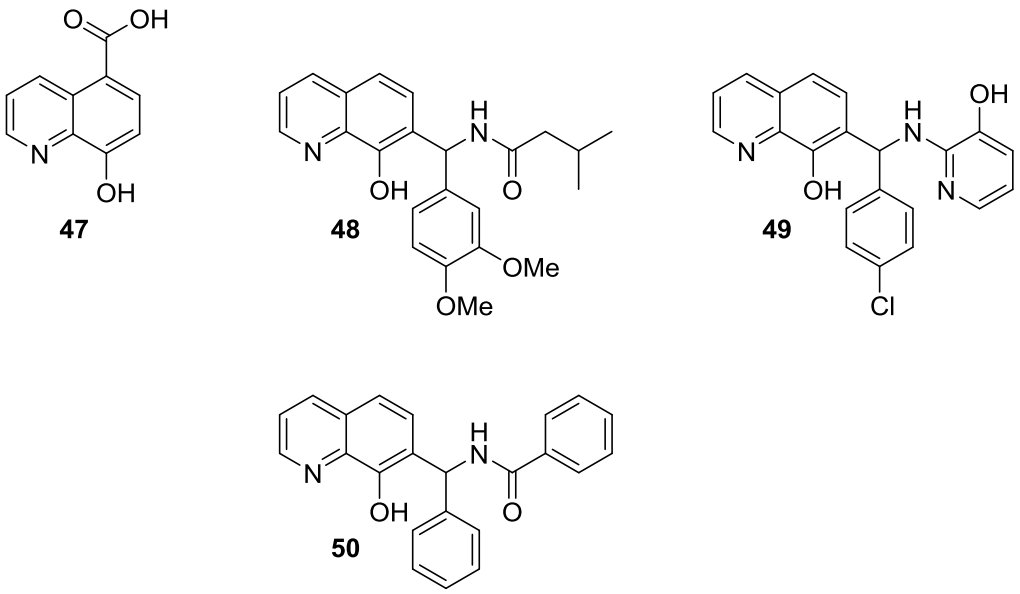

Figure 24: Structures of pan-demethylase inhibitor IOX1 **47**, and cell-active modulators of the hypoxic response **48** and **49**. 7-Substituted 8-hydroxyquinoline **50** was chosen as a starting point for inhibitor development.

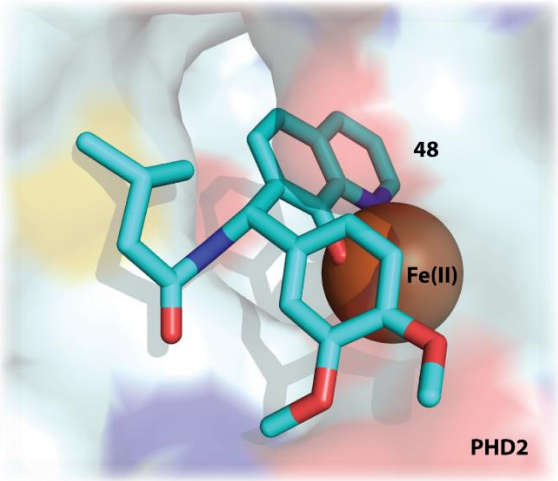

Figure 25: *In silico* docking model of **48** into PHD2 (PDB ID: 4BQY).

Methodology Development for 7-Substituted 8HQs

Identification of Reaction and Purification Conditions

Given the precedented work on HIF prolyl hydroxylases,[160] an initial focused library based on the benzylic amide side chain for 7-susbtitution of 8HQs was proposed and **50** was defined to be the target molecule for initial synthetic development (Figure 24). Considering the novelty of the template-based inhibition strategy for 2OG oxygenases, as well as the lack of any X-ray co-crystal structure with any structural analogues of 7-substituted 8HQs, an open-skies approach was judged to be most likely to furnish a proof of principle. The required workflow would require systematic diversification of the respective moieties around the target molecule **50** and concomitant biochemical testing for guiding subsequent inhibitor development. This strategy of iterative medicinal chemistry required the synthetic procedures to be rapid, versatile, and medium- to high-throughput compatible.

Initial retrosynthetic analysis of **50** suggested Mannich-type amination of 8HQ and subsequent amidation of primary benzylic amine **51** (Scheme 9).[161] A microwave- (MW) assisted Mannich reaction which involves *in situ* generation of ammonia from ammonium bicarbonate and subsequent formation of intermediate **54** to yield **55** after acid hydrolysis has previously been reported.[162] The authors describe a characteristic pressure increase upon ammonia gas formation followed by a pressure decrease as the reaction proceeds. However, such pressure changes were not observed, and NMR analysis revealed only protonated starting material **53** after the same-pot acid hydrolysis step of supposed intermediate **54**. Similar reaction procedures using ammonia in methanol under reflux conditions proved equally unsuccessful.

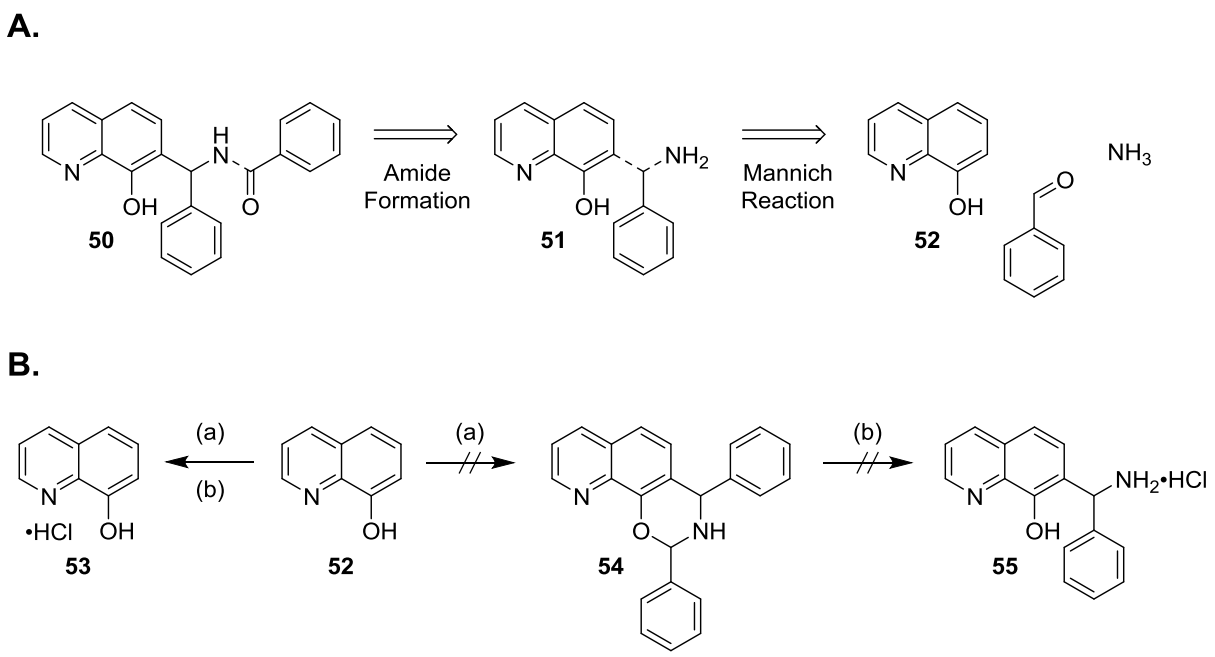

Scheme 9: A. Initial retrosynthetic analysis for compound **50**. **B.** Reagents and conditions: (a) Sodium bicarbonate, EtOH, MW irradiation, 130 °C, 45 min. (b) HCl 10 % aq., 90 °C, 60 min.

An alternative strategy was based on a Betti-type reaction using aromatic amides (as opposed to amines) as nucleophiles under high-temperature and solvent-free conditions.[163,164] Heating 8HQ **52**, benzamide, and benzaldehyde at 180 °C for 3 h afforded a crude reaction mixture that contained **50**, as judged by NMR analysis (Scheme 10).

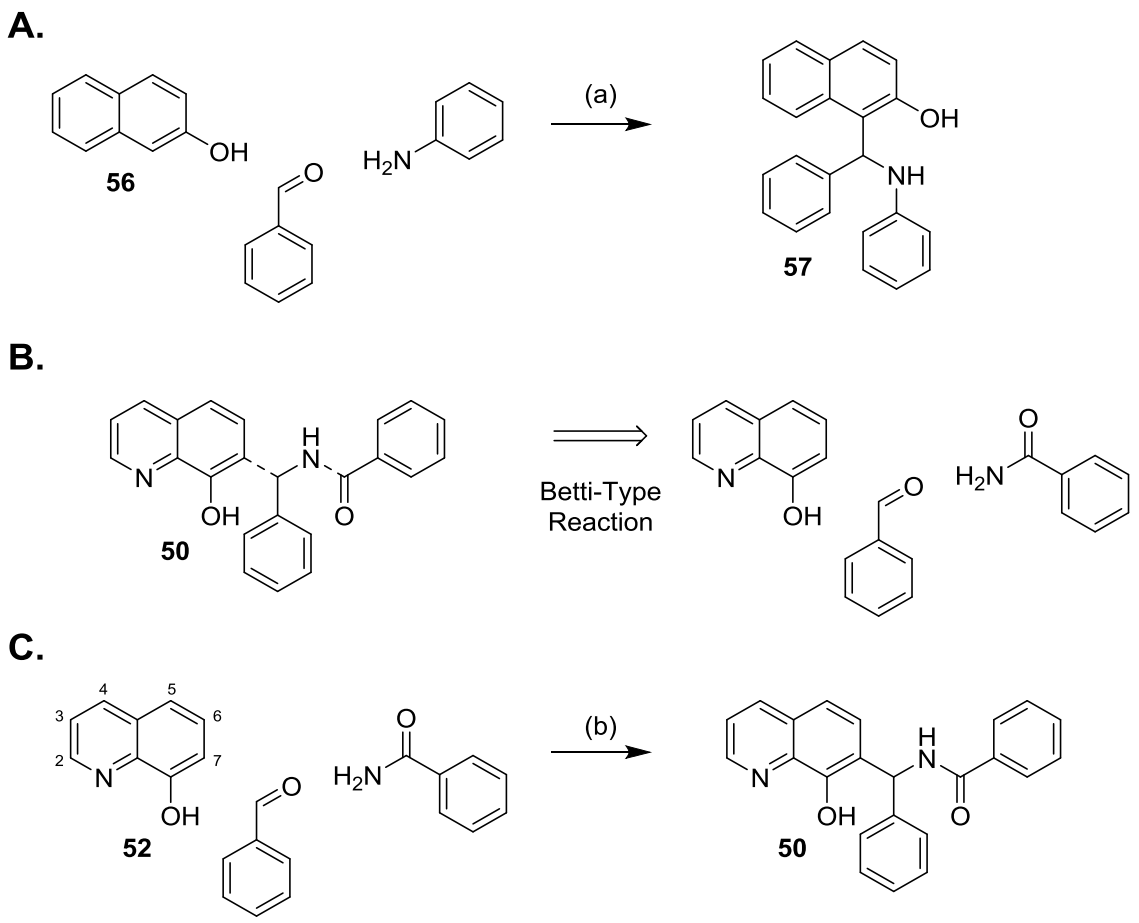

Scheme 10: A. Original Betti reaction between 2-naphthol **56**, benzaldehyde, and aniline. Reagents and conditions: (a) EtOH, RT, 72 h. **B.** Retrosynthetic analysis for **50** employing a Betti-type reaction methodology. **C.** Reagents and conditions: (b) Neat, 180 °C, 3 h.

After successful identification of reaction conditions able to yield scaffold **50**, the focus shifted towards optimisation of purification conditions. Various strategies were considered, including aqueous workup, flash column chromatography, recrystallisation, and trituration. Trituration seemed particularly attractive in terms of the chosen synthetic procedure: treatment of the hot reaction mixture with toluene was stipulated to precipitate out the target molecule upon cooling down, whereas unreacted starting materials should stay in solution. Given the high reaction temperature of 180 °C, this strategy can be considered as '*in situ* recrystallisation'. Indeed, quenching of the reaction mixture with toluene and subsequent trituration of the resulting precipitate with toluene and diethyl ether gave racemic **50** in 42 % yield and >95 % purity as judged by integration of the liquid chromatography-mass spectrometry (LC-MS) UV trace.

This three-component one-pot Betti-type reaction, involving both synthesis and purification in one step, hereby gave convenient access to model compound **50** in sufficient quantity and purity for biochemical testing. The synthetic procedure was judged worthwhile for pursuing the creation of a focused library of 8HQ

template-based inhibitors given the potential to fulfil the requirements of rapid access to, and diversification of, 7-substituted 8HQs.

Regioselectivity of the Three-Component Reaction

Inspection of previous work on the classic Betti reaction suggested that reaction probably occurs at *C*-7 of 8HQ (Scheme 11).[164] Stereoelectronic considerations preclude substitution of both the pyridine ring as well as position 6; substitution at position 5, however, seemed a viable alternative to substitution at position 7. Integration of the characteristic 8HQ resonances in the crude NMR spectrum revealed a regioselectivity of approximately 2:1 for the major 7-substituted 8HQ **50** versus the minor 5-substituted regioisomer **58**. This finding was confirmed by LC-MS analysis, which, in addition to the two monosubstituted products, also revealed a trace amount of 5,7-disubstituted 8HQ **59**.

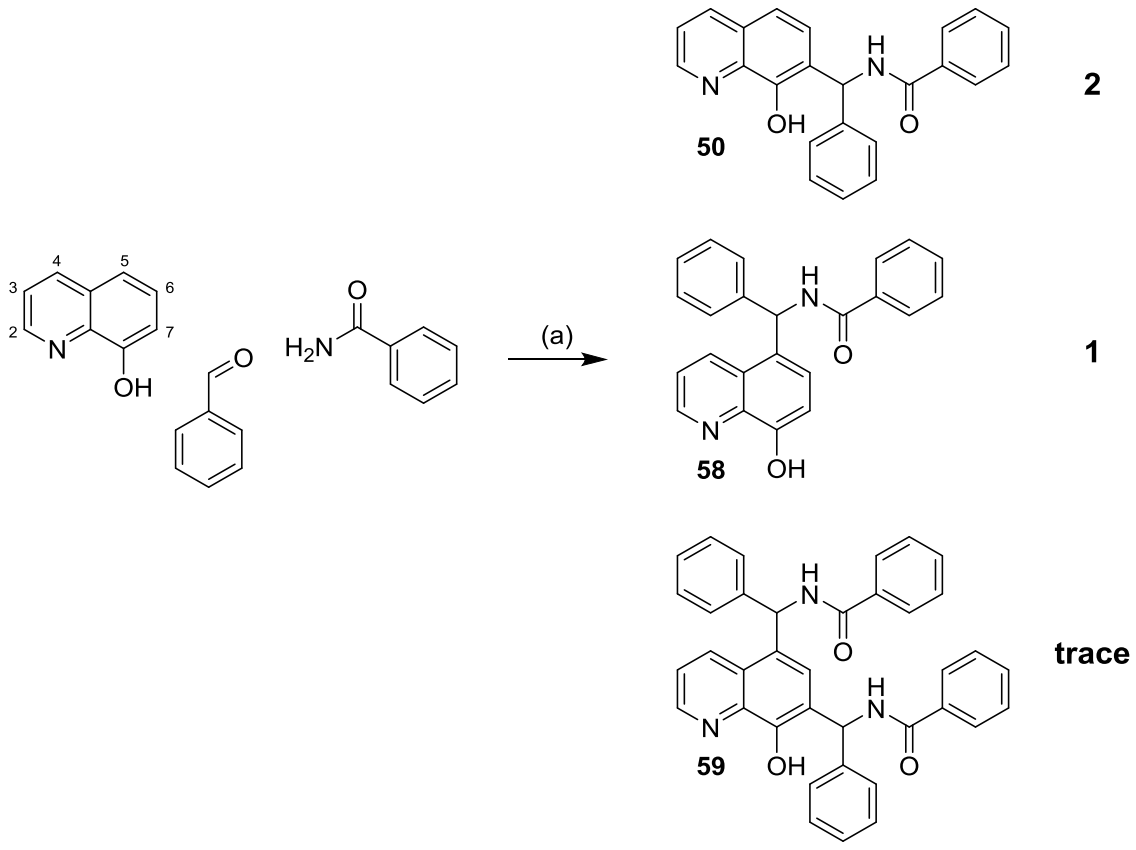

Scheme 11: Reagents and conditions: (a) Neat, 180 °C, 3 h.

In contrast, reactions with 5-substituted 8HQ starting materials yielded single 7-substituted products; no formation of alternative regioisomers was detected. It is noteworthy that the yields with 5-chlorosubstituted analogues were comparatively higher than with their unsubstituted counterparts: this likely correlates with

the relatively high melting points (> 200 °C) of the 7-substituted products. In contrast, the 5-unsubtituted 8HQ products (mp < 200 °C) remain liquid at the given reaction temperature; the 5-substituted products will precipitate from the reaction melt as soon as they are formed. This precipitation may shift thermodynamic reaction equilibrium toward product formation, in analogy to a classic Finkelstein reaction, and hence a general increase in yield is observed with these compounds (Scheme 12).[165]

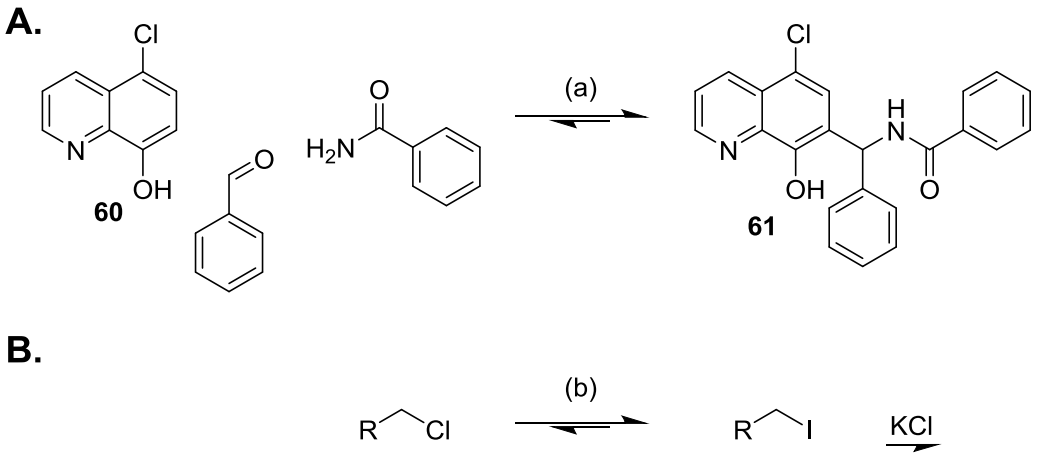

Scheme 12: A. Reagents and conditions: (a) Neat, 180 °C, 3 h. **B.** Finkelstein reaction. Reagents and conditions: (b) KI, acetone, reflux.

Reaction Substrate Scope

In order to maximise diversification of the 8HQ template library, it was desirable to explore the reaction scope with respect to each component of the three-component Betti-type reaction, i.e. the corresponding aldehyde, 8HQ, and amide starting materials.

Aldehydes

An extensive variety of aldehydes is commercially available at reasonable price. An initial focused selection of aldehydes was purchased in order to explore the substrate scope of the Betti-type reaction. Preliminary selection criteria were based on the chemical properties of the aldehydes, including representative compounds generally classified as aromatic, aliphatic, heterocyclic, electron-rich, electron-poor, and bulky.

Benzaldehyde and many of its *ortho*-, *meta*-, and *para*-substituted analogues (toluenes, halogens and anisoles) gave access to the corresponding 7-substituted 8HQs at 180 °C under solvent-free conditions (Scheme 13). Unsubstituted aliphatic cyclohexylaldehyde did not yield the desired product under the given conditions, possibly because of increased steric hindrance compared to the aromatic benzaldehyde.

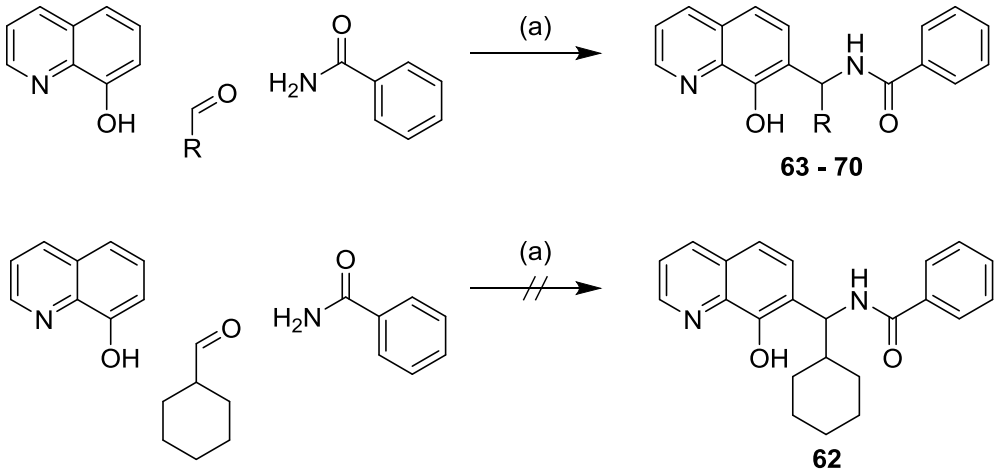

Compound	R =	Yield	Compound	R =	Yield
63	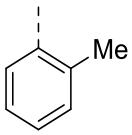	88 %	**67**	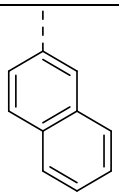	40 %
64	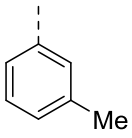	27 %	**68**	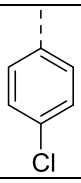	88 %
65	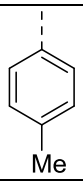	16 %	**69**	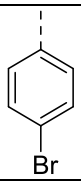	100 %
66	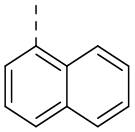	37 %	**70**	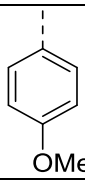	79 %

Scheme 13: Reagents and conditions: (a) Neat, 180 °C, 3 h. A selection of representative structures is displayed with the corresponding isolated yields.

Heterocyclic aldehydes did not yield the desired product under the above reaction conditions: the heterocycles disintegrated under the high-temperature conditions. It was hence desirable to optimise the reaction conditions for reaction temperature to ensure optimal substrate scope. A range of model reactions were set up at various temperatures ranging from 90 °C to 170 °C. The minimum temperature for the reaction to proceed was found to be 130 °C, temperature below which no product formation was observed after 6 h maximal reaction time. Heterocyclic aldehydes, including furans, thiophenes and pyridines, underwent reaction at 130 °C to give the corresponding 7-substituted 8HQs without decomposition (Scheme 14).

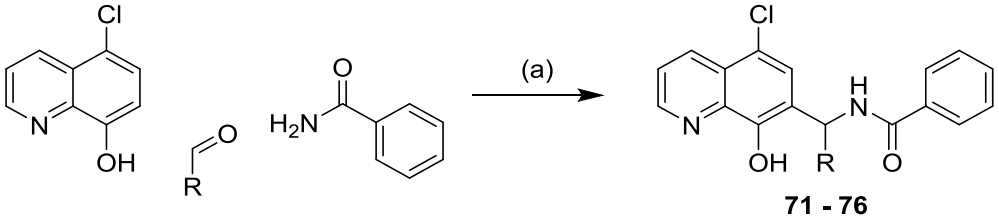

Compound	R =	Yield	Compound	R =	Yield
71	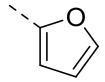	34 %	**74**	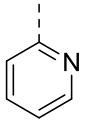	30 %
72	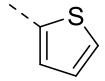	26 %	**75**	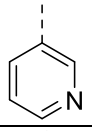	63 %
73	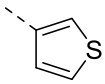	51 %	**76**	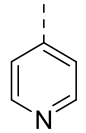	10 %

Scheme 14: Reagents and conditions: (a) Neat, 130 °C, 3 h. A selection of representative structures is displayed with the corresponding isolated yields.

It was found that starting materials containing nucleophilic groups, such as alcohols or amines, were not tolerated; reactions led to polymerisation under the given reaction conditions. Even tertiary amines, which are considered non-nucleophilic in classical terms, led to polymerisation (Scheme 15). This observation is in fact not surprising: the high-temperature, solvent-free conditions force amides to act as nucleophiles. These reaction conditions supposedly require a fine equilibrium between reactivities of all reaction partners to drive the equilibrium toward Betti-type reaction rather than non-specific polymerisation.

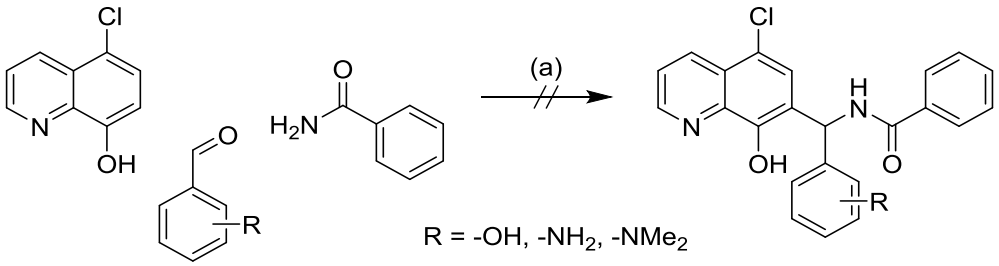

Scheme 15: Reagents and conditions: (a) Neat, 130 °C, 3 h.

Non-nucleophilic functional groups were well-tolerated: alkyl, aromatic, nitrile, halogen, ether, ketone, and ester groups all led to the corresponding 7-substituted 8HQs; even the free carboxylic acid **84** led to the desired product (Scheme 16).

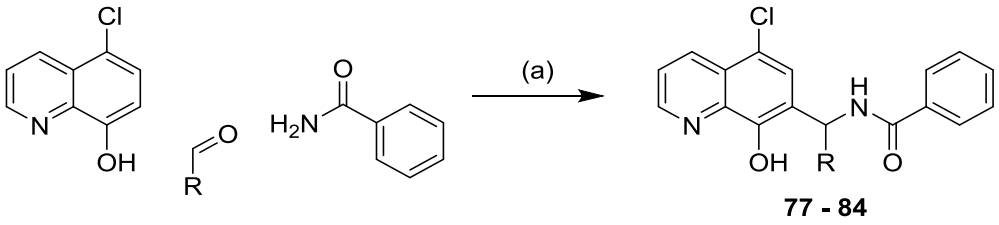

Compound	R =	Yield	Compound	R =	Yield
77	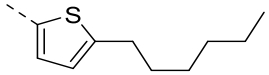	35 %	**81**	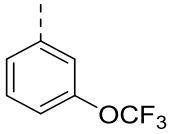	72 %
78	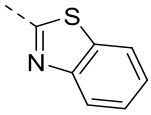	20 %	**82**	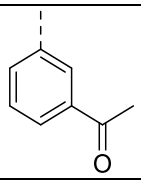	55 %
79	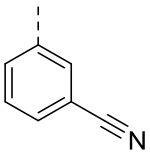	66 %	**83**	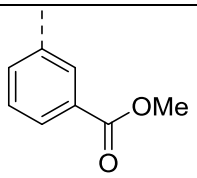	63 %
80	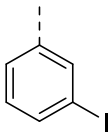	64 %	**84**	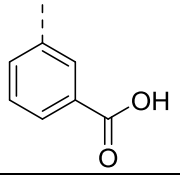	94 %

Scheme 16: Reagents and conditions: (a) Neat, 130 °C, 3 h. A selection of representative structures is displayed with the corresponding isolated yields.

The carboxylic acid functionality of **84** offered a convenient handle for introduction of polar groups *via* amide bond coupling after the Betti reaction. This methodology proved particularly useful for the introduction of solubilising moieties such as morpholines (**87** - **91)** (Scheme 17). In addition, free acid **84** offered an opportunity for the synthesis of potential dual target inhibitors such as **86** by covalently linking the 8HQ-based inhibitor **84** to another inhibitor for a different enzyme. This is of therapeutic interest given the hypothesis of 'single target – single disease' is, at least in the case of epigenetic target proteins, a simplistic concept of medicinal chemistry.[166] Especially in the field of epigenetics, dynamic and context-dependent polypharmacologies determine complex phenotypes. The recent proof-of-principle compounds **45** and **46** illustrate that dual KDM1/KDM4 inhibitors may have the potential for cancer-selective applications (see Chapter I, Figure 22). To exemplify this strategy, the selective bromodomain inhibitor **85**, synthesised by Dr Duncan Hay, was covalently linked to the 7-substituted 8HQ scaffold **84** to yield **86** which may potentially inhibit both KDM4 histone demethylases and the bromodomain CBP/p300 interaction (Scheme 17).[167]

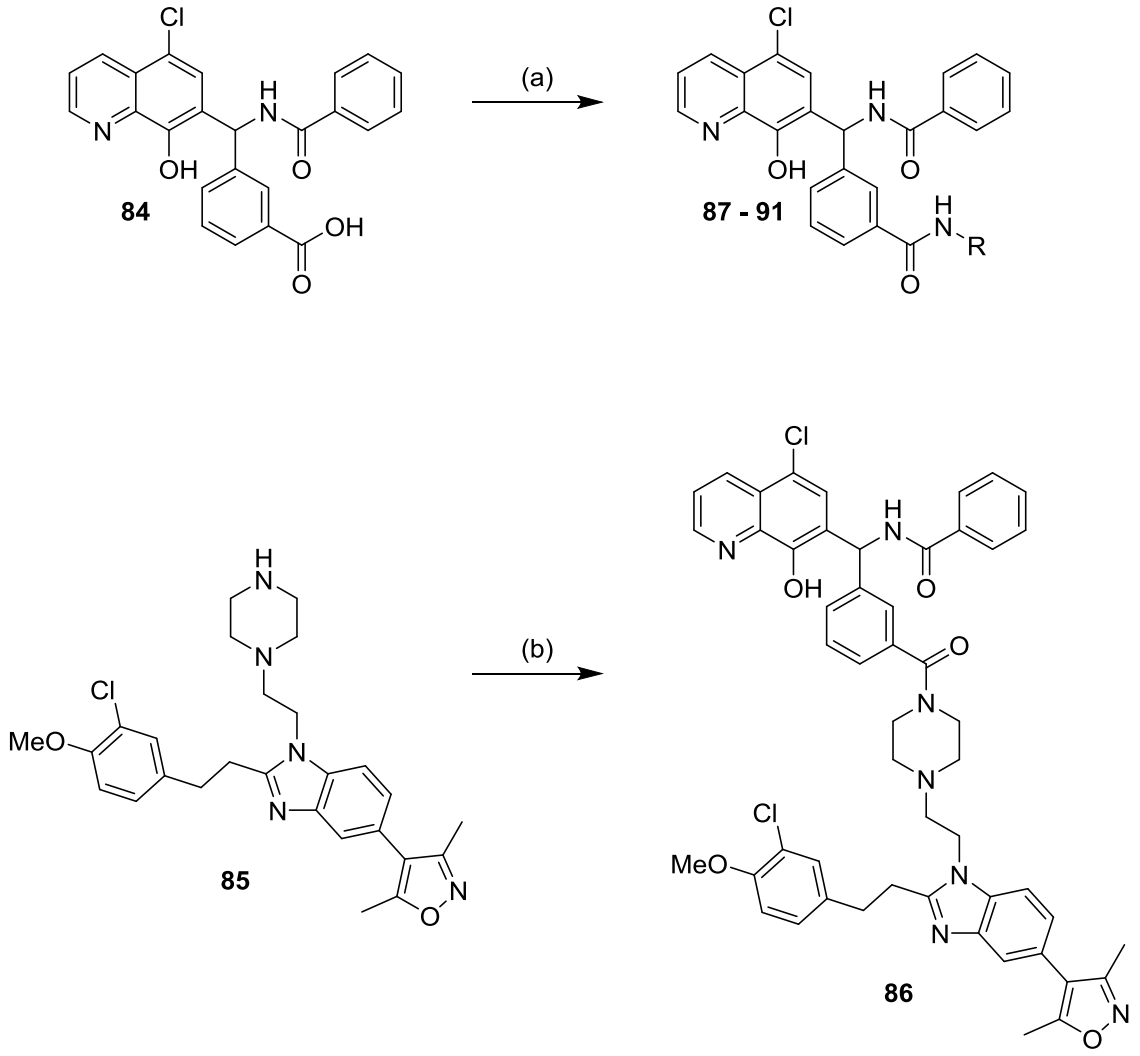

Compound	R =	Yield	Compound	R =	Yield
87	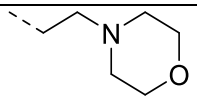	59 %	**90**	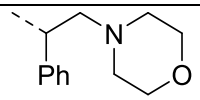	86 %
88	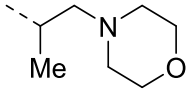	69 %	**91**	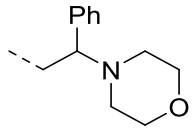	100 %
89	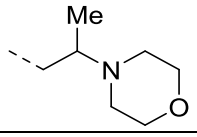	75 %			

Scheme 17: Reagents and conditions: (a) EDCI, HOBt, DMF, CH_2Cl_2, 50 °C, 18 h. (b) **84**, EDCI, HOBt, DMF, CH_2Cl_2, 50 °C, 18 h.

In a similar fashion, 8HQ-based inhibitor **84** can be converted into biotinylated analogue **94** for streptavidin-mediated affinity purification.[168] Biotin and streptavidin bind rapidly, and very tightly, to each other. By linking a small-molecule inhibitor to biotin, the small molecule may bind to the enzyme of interest, and the biotin will bind to a streptavidin-coated device, such as magnetic beads, or a solid support. Ultimately, by

using a selective small-molecule inhibitor, it may therefore be possible to specifically remove one particular enzyme of interest out of a system, for example cell lysate. For a synthetic proof of principle, 7-substituted 8HQ **84** was linked to azide-containing linker **92** in order to attach biotin *via* copper-free click chemistry to give **94** (Scheme 18).[169] The requirement for copper-free click chemistry emerged from the incompatibility of copper ions with 8HQs because the metal ions are scavenged by the 8HQ chelating motif.

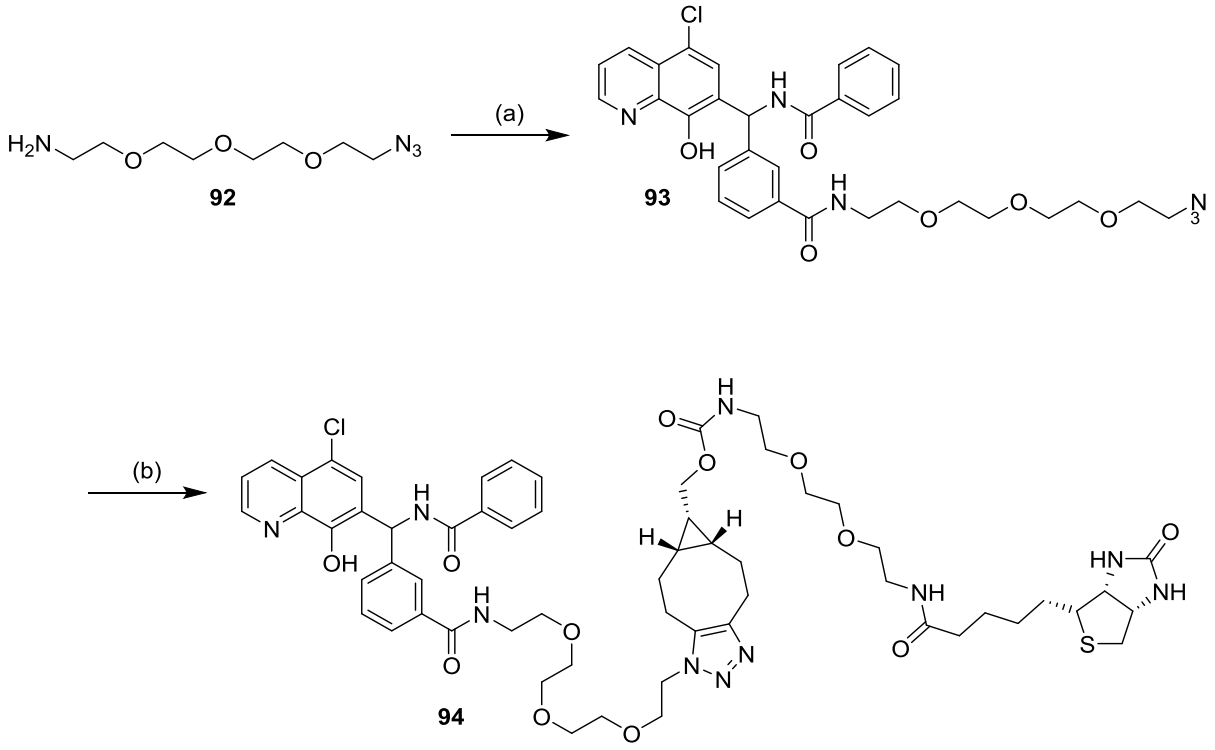

Scheme 18: Reagents and conditions: (a) **84**, EDCI, HOBt, DMF, CH_2Cl_2, 50 °C, 18 h. (b) SX-A1029 (Synaffix), acetonitrile, RT, 18 h.

A variety of commercially unavailable aldehydes were synthesised in-house. Palladium cross-coupling reactions between 3-formylboronic acid and the corresponding bromide offered a convenient way for accessing aldehydes based on the biphenyl motif (Scheme 19). No prior protection of the aldehyde was required for the cross-coupling reaction. The corresponding benzyl-linked aldehydes were commercially unavailable, and procedures for their synthesis seemed unattractive for the given cost/benefit ratio; the corresponding biphenyl ethers, such as **100**, were judged to present viable isosteric alternatives (Scheme 19).

In the case of 3-methylthiophenecarboxaldehyde **97**, the purity of the commercially available aldehyde was only 90 %, as stated on the product packaging. As judged by NMR analysis, the main contaminant was the 5-methylthiophenecarboxaldehyde regioisomer which could not be removed by flash column chromatography. The resulting regioisomer contamination in the 7-substituted 8HQ final product **193** was similarly inseparable

by either flash column chromatography or recrystallisation. In an attempt to maximise purity for extensive biochemical characterisation (see Chapter III), the 3-methylthiophenecarboxaldehyde **97** was synthesised in high purity (> 99 %) from the 3-methylthiophenecarbonitrile **96** *via* partial reduction to the corresponding aldehyde using diisobutylaluminium hydride (DIBAL-H); no regioisomer contaminant was identified. This enabled the synthesis of the corresponding highly pure 7-substituted 8HQ final product **193** (Scheme 19).

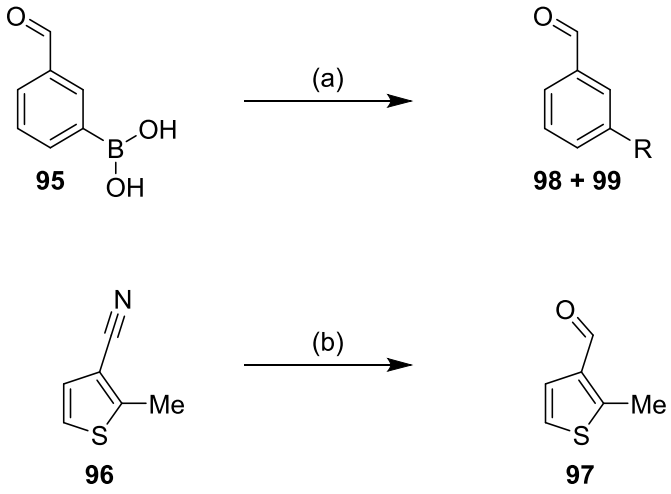

Compound	R =	Yield	Compound	R =	Yield
98	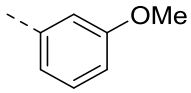	52 %	**99**	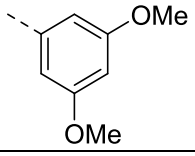	73 %

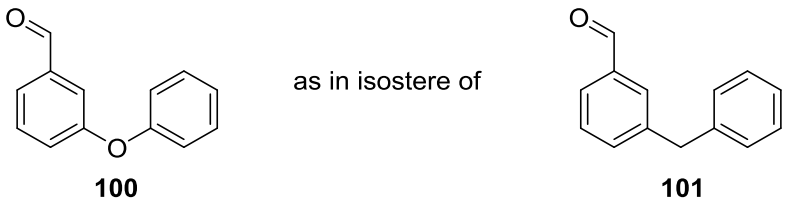

Scheme 19: Reagents and conditions: (a) Aryl bromide, tetrakistriphenylphosphinepalladium (0), Na_2CO_3, dimethoxyethane (DME), MW irradiation, 110 °C, 2 h. (b) DIBAL-H, chlorobenzene, 0 °C, 1 h. On the left is the commercially available, impure, 3-methyl-2-thiophenecarboxaldehyde **97**; on the right is the pure aldehyde synthesised in-house.

Modified 8-Hydroxyquinolines

The commercial availability of 8HQs is relatively limited compared to aldehydes and primary amides, and is biased towards 5- and 7-substituted, as well as 5,7-disubstituted compounds, reflecting their chemical reactivity. It was hence desirable to explore the chemistry of 8HQs for enabling diversification of the 8HQ core of the target compounds.

One convenient way for accessing various 8HQ substitution patterns is *via* Skraup-type chemistry using 2-aminophenol and acrolein **102** (Scheme 20).[170] Although known and explored for many decades, this reaction required optimisation for our specific purposes of 8HQ diversification. Order and speed of addition, as well as reaction temperature, proved crucial for enabling clean reaction progression and reasonable yields. First, the requisite 2-aminophenol was heated to reflux in 6N aqueous HCl before the required acrolein was slowly added, drop by drop. Failure to adopt this methodology always led to very low yields associated with polymerisation side reactions. This methodology allowed substitution of the 8HQ pyridine core with various alkyl chains at positions 2, 3, and 4. An attempt to synthesise 2-phenyl-8-hydroxyquinoline **108** from cinnamaldehyde **107** was unsuccessful. A variety of 5- and 6-substituted 8HQs were synthesised from the corresponding 2-aminophenols (Scheme 20). This methodology proved particularly useful for the one-step synthesis of IOX1 **47** from acrolein **102** and 5-carboxy-2-aminophenol: IOX1 **47** was hitherto synthesised in a multistep synthesis requiring protection/deprotection chemistry and carbonylation reaction with carbon monoxide by our collaborator. We suspect this multistep procedure was adopted because, until then, the temperature and addition components of the Skraup method remained unoptimised (Scheme 20).

The Skraup method was also applicable to the synthesis of the symmetric [6,6'-biquinoline]-8,8'-diol **110** from 3,3’-dihydroxybenzidine **109** in 34 % yield.

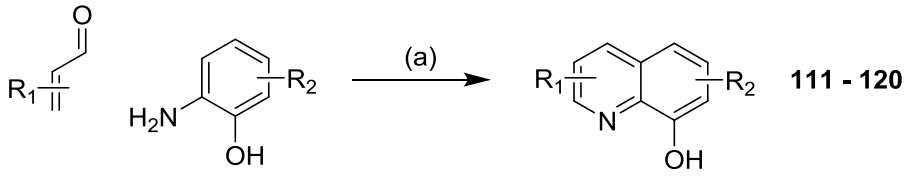
(a)
111 - 120

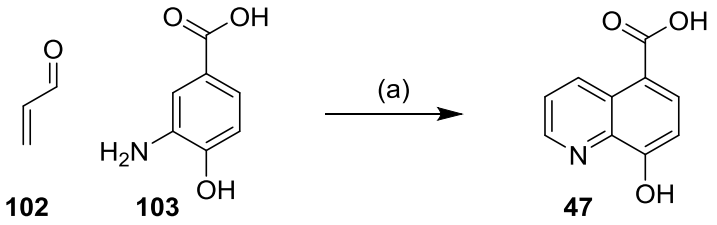
(a)
102
103
47

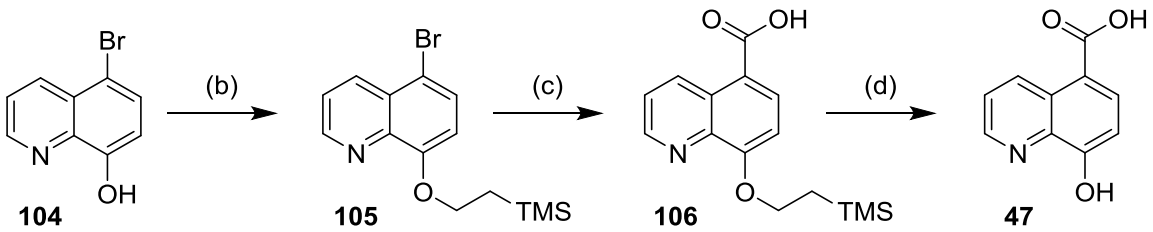
(b)
(c)
(d)
104
105
106
47
TMS

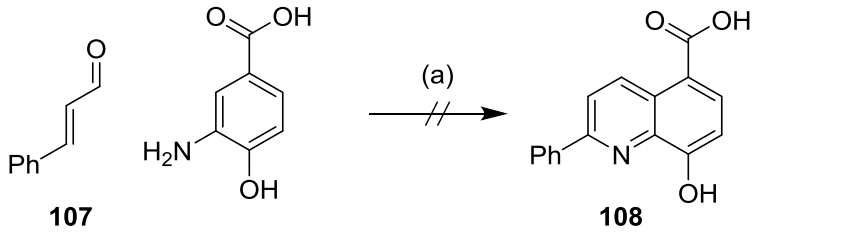
(a)
107
108

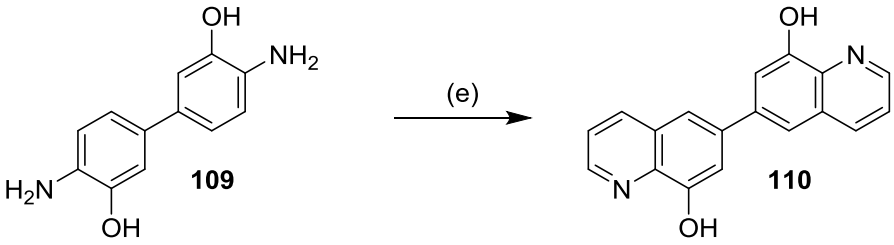
(e)
109
110

Compound	Structure	Yield	Compound	Structure	Yield
111	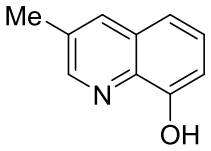	43 %	**116**	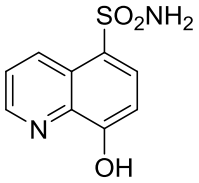	42 %
112	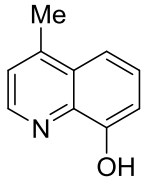	59 %	**117**	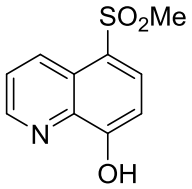	57 %
113	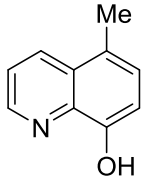	78 %	**118**	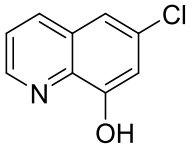	73 %
114	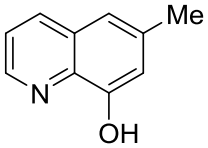	39 %	**119**	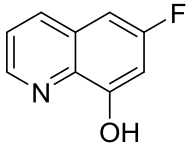	61 %
115	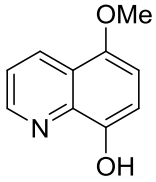	65 %	**120**	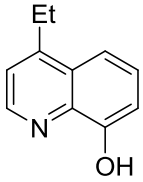	71 %

Scheme 20: Reagents and conditions: (a) 6 M HCl aq., reflux. (b) 2-Trimethylsilyl ethanol, DIEA, PPh_3, THF, toluene, RT, 18 h. (c) Tetrakistriphenylphosphinepalladium (0), CO (g), Na_2CO_3, DME, reflux, 2h. (d) Bu_4NF, THF, RT, 6 h. (e) Acrolein, 6 M HCl aq., reflux. A selection of representative compounds is listed in the table with the corresponding isolated yields.

An attempt to synthesise 7-substituted 8HQ target molecules from 8HQ-2-carboxylic acid **121** failed (Scheme 21). The model reaction consistently yielded the decarboxylated 7-substituted product **50**. The reaction conditions are incompatible with 2-carboxylic acid-substituted 8HQs with respect to pyrolytic decarboxylation.

This decarboxylation reaction can be exploited for accessing 4-substituted 8HQs from the natural product xanthurenic acid **122** (Scheme 21).[171] After pyrolytic decarboxylation, the alcohol at position 4 can be alkylated with the requisite alkyl halide, or converted into the corresponding halide with phosphorus oxychloride/oxybromide for subsequent palladium cross coupling or aromatic addition-elimination reaction (Scheme 21).[172] In line with the results from various aldehydes, the Betti-type reaction proceeded well with non-nucelophylic substituents at position 4. Xanthurenic acid **122** itself, the free 4-alcohol **124**, and any 4-amine substituted derivatives decomposed upon attempting 7-substitution. In addition, the 4-chloro- **125** and 4-bromo-substituted 8HQs decomposed, likely because of the relatively high reactivity at position 4.

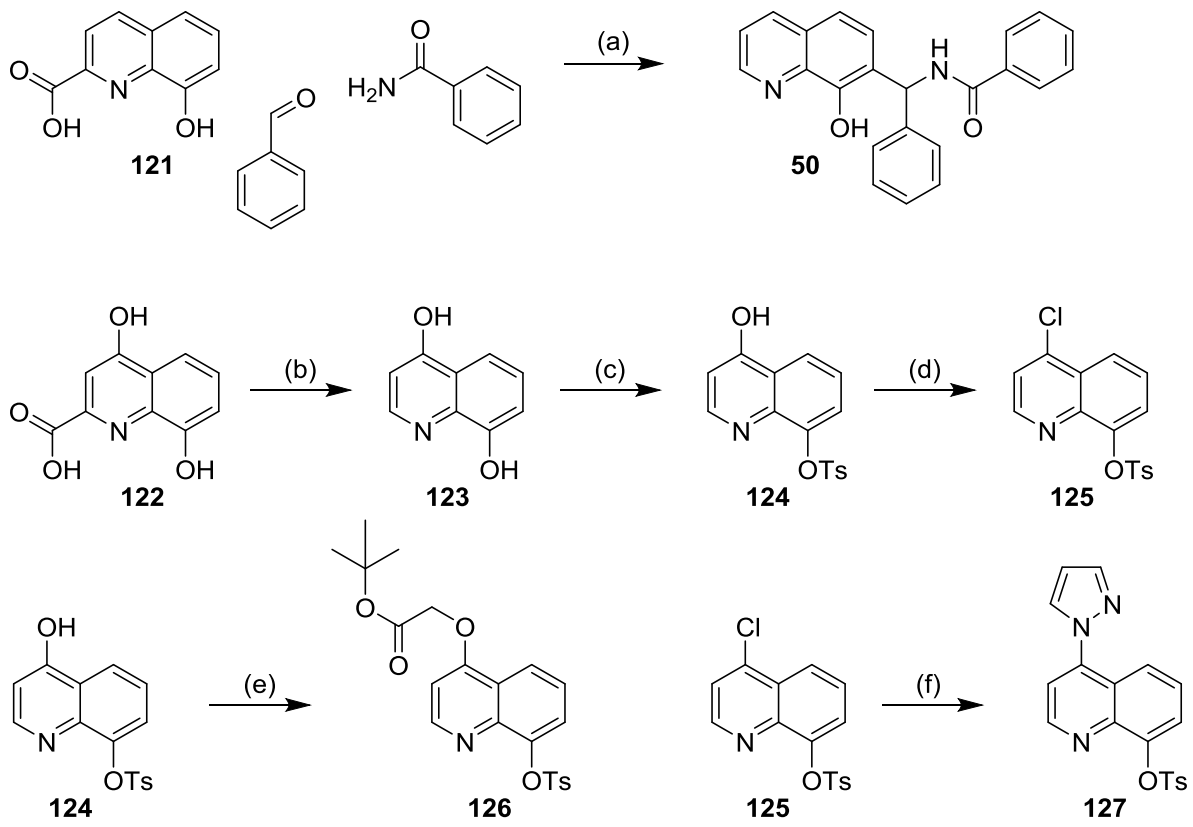

Scheme 21: Reagents and conditions: (a) Neat, 150 °C, 3 h. (b) Diphenyl ether, 240 °C, 3 h. (c) TsCl, NaOH 1 M, acetone, RT, 3 h. (d) Phosphorus oxychloride, reflux, 1 h. (e) NaH, DMF, then *tert*-butylbromoacetate, RT, 2 h. (f) Pyrazole, toluene, reflux, 5 h.

Protein-ligand *in silico* modelling studies using a KDM4A X-ray crystal structure (see Figure 29, Chapter III) suggested that the 7-substituted 8HQ-4-carboxylic acid would be of interest because of potential polar interactions with Tyr132 and Lys206 in analogy to IOX1 **47** binding (see Chapter III, Figure 28). In order to prepare 8-hydroxyquinoline-4-carboxylic acid **24**, quinoline-4-carboxylic acid **128** was heated to 200 ^{o}C in a sand-embedded sealed glass tube in the presence of 80 % fuming sulphuric acid and phosphorus pentoxide.[173] Addition of water to the dark-brown, cool reaction melt and subsequent scratching gave pure, white quinoline-4-carboxylic-8-sulphonic acid **129** as a white powder in 61 % yield. This product was subsequently slurried with a concentrated solution of potassium hydroxide and dried *in vacuo*. This solid mixture was then heated to > 300 ° C with an electric heat gun until the mixture turned bright yellow. This colour change indicated the displacement of sulphur trioxide by hydroxide ion to form 8-hydroxquinoline-4-carboxylic acid **24**, which was obtained as a single pure compound after acidification (Scheme 22). Subsequent attempts at 7-substitution of this compound, however, led to decomposition of the reagents. This decomposition was also observed when trying to substitute the 8HQ-5-carboxylic acid counterpart IOX1 **47**. The decomposition is likely due to reaction with the aldehyde and/or amide components upon Betti-type

reaction conditions. Considering the harsh reaction conditions for the synthesis of 8HQ-4-carboxylic acid **24**, the stability of the 4-acid is remarkable given the high propensity for decarboxylation of its 8HQ-2-carboxylic acid counterpart **121** (see Scheme 21). Attempts to perform the Betti reaction on the ester-protected 8HQ carboxylic acids were similarly unsuccessful: both methyl and ethyl esters decomposed. Only the isopropyl ester was stable under the reaction conditions. Substitution at *C*-7, however, did not occur and the reaction only returned starting materials. It is possible that the carboxylic acid substituent renders the 8HQ component too electron-poor to perform a Betti-type reaction. Nevertheless, the comparison of both 4- and 5-carboxylic acids was of interest from a crystallographic point of view (see Chapter III).

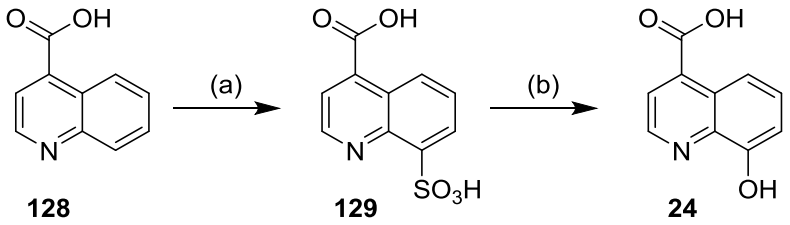

128 **129** **24**

Scheme 22: Reagents and conditions: (a) Fuming H_2SO_4, 65 % SO_3, phosphorus pentoxide, sealed tube, 200 °C, 2 h. (b) KOH, 300 °C, 10 min.

One recurring theme during my odyssey of 8HQ chemistry was the incompatibility of the 8HQ chemotype with any metal-mediated reactions. Initially it seemed viable to access free amine 7-substituted 8HQs from their parent nitro-substituted derivatives *via* reduction chemistry employing hydrogenation over Pd on charcoal. Various attempts with different hydrogenation conditions were unsuccessful, including the use of acetic acid as a solvent in order to protonate the pyridine, and supposedly preventing metal chelation. Similarly, any attempts to reduce nitro to amine with elemental Fe or Zn in hydrochloric acid failed. Finally, by using sodium dithionite as a reducing agent, reaction of the 7-substituted 5-nitro-8HQ **131** succeeded to give the 5-amino derivative **130** (Scheme 23). It was later found, however, that the 7-substituted-5-amino 8HQ **130** was unstable in DMSO stock solution over prolonged time: it turned from bright-yellow into a dark-brown solution within days at room temperature.

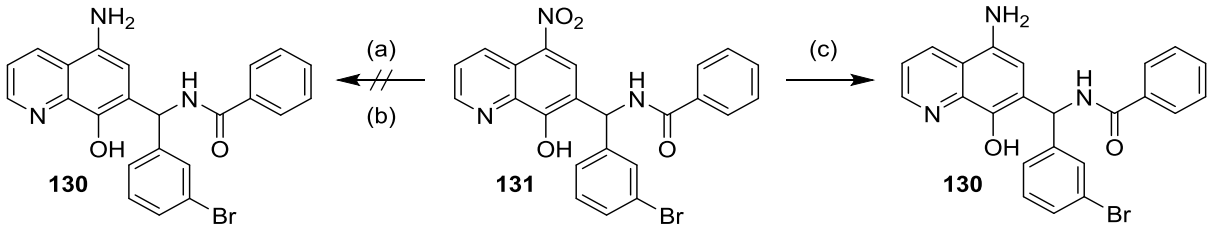

Scheme 23: Reagents and conditions: (a) Pd/C, H_2, EtOAc or MeOH or AcOH, RT, 3 h. (b) Zn or Fe, HCl (6 N, aq.). (c) Sodium dithionite, EtOH, reflux, 18 h.

Palladium-Catalysed Coupling Reactions with 8HQs

The incompatibility of 8HQs with any transition metals, likely due to, at least in part, catalyst inactivation by chelation, demanded a suitable protecting group (PG) strategy for enabling palladium-catalysed coupling reactions for diversification of the 8HQ core from the corresponding chlorides or bromides respectively. Previous screening results indicated that the 8HQ *N*-oxide was able to act as an Fe(II) chelator; protection of the 8HQ hydroxyl was hence deemed the site of choice for protection.

Initial efforts focused on silylation of the free 8HQ alcohol. However, it was found that the resulting 8HQ silyl ethers were intrinsically unstable with respect to hydrolysis. TMS-derived 8HQ could not be isolated as it hydrolysed back into the free 8HQ under aqueous work-up conditions. The relatively more stable TBDMS-derived 8HQ **133** could be isolated and purified, but subsequently proved unstable with respect to desilylation under palladium cross-coupling reaction conditions. Direct *O*-silylation strategies for 8HQ protection were therefore abandoned. One silicon-derived protecting group did, however, prove suitable for 8HQ protection: trimethylsilylethanol. Mitsunobu-type conditions yielded the protected 8HQ **105** in 78 % yield; this compound proved stable under palladium cross-coupling reaction conditions (Scheme 24).[170]

Protecting group strategies other than silicon-based PGs were explored at the same time. A common means of phenol protection is methylation to give the corresponding anisole. Subsequent deprotection is usually halide-mediated, most commonly using boron tribromide, hydrobromic or hydroiodic acid. 8HQ methylation succeded in quantitative yield using iodomethane in the presence of potassium carbonate in DMF; deprotection using standard demethylation conditions, however, were sluggish. Treatment with hydrobromic acid solution merely formed the corresponding 8HQ hydrobromide salt, whereas a supposedly mild method using *in situ* generation of hydroiodic acid from refluxing iodocyclohexane led to decomposition of reaction components.[174] Deprotection using boron tribromide solution was unsuitable for convenient

inhibitor generation: isolated yields were very low, possibly because of complex formation between 8HQ and the boron species. Methylation was hence considered unsuitable for 8HQ protection (Scheme 24).

Eventually, the most convenient way for 8HQ protection was found to be tosylation. The desired 8HQ **104** was stirred with one equivalent of 1M aqueous NaOH before one equivalent of a solution of TsCl in acetone was added dropwise. After 1h, the product was collected by filtration as a white powder without further purification. The resulting tosyl-protected 8HQ **135** was stable with respect to palladium cross-coupling reaction conditions and could be deprotected in quantitative yield by treating with aqueous NaOH in ethanol under reflux. Given the ease of protection and deprotection conditions, as well as the stability under cross-coupling conditions, tosylation was chosen to be the method of choice for 8HQ protection (Scheme 24).

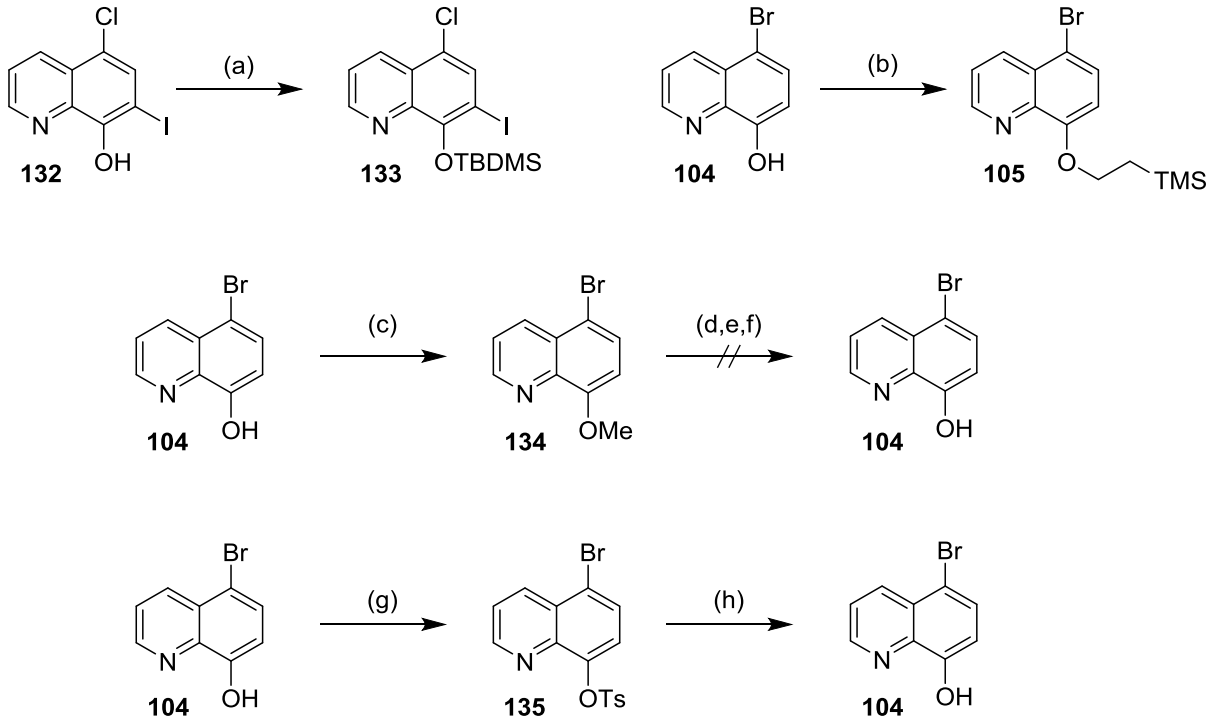

Scheme 24: Reagents and conditions: (a) TBDMS-Cl, imidazole, CH_2Cl_2, RT, 18 h. (b) 2-Trimethylsilyl ethanol, DIEA, PPh_3, THF, toluene, RT, 18 h. (c) MeI, K_2CO_3, DMF, 60 °C, 18 h. (d) BBr_3, CH_2Cl_2, RT, 24 h. (e) Iodocyclohexane, DMF, reflux, 18 h. (f) HBr in dioxane, dioxane, reflux, 18 h. (g) TsCl, NaOH 1 M, acetone, RT, 3 h. (h) NaOH 1 M aq., EtOH, reflux, 1 h.

Tosyl protection of 8HQs did indeed prevent catalyst inactivation *via* 8HQ palladium complex formation. Initial reaction trials with tetrakistriphenylphosphinepalladium (0) catalyst **140**, 5-bromo-8HQ **135**, and phenylboronic acid, however, only returned starting materials. No improvement was achieved by variation of solvent composition, halide substituent, as well as reaction time and temperature. The focus of methodology improvement consequently shifted towards the palladium catalyst.

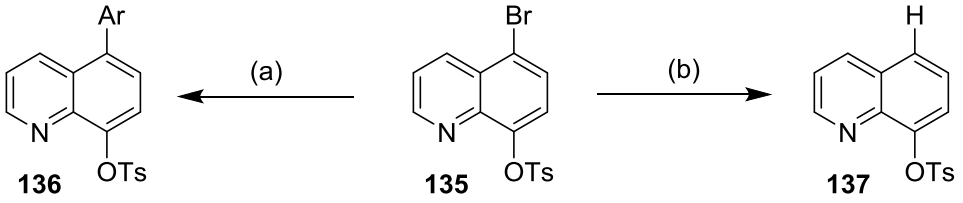

Scheme 25: Reagents and conditions: (a) Pd source, ligand, arylboronic acid, dimethoxyethane, sodium bicarbonate, MW irradiation.

An initial selection of both Pd metal sources, as well as ligands, were investigated (Table 1). No reaction was observed when $Pd(OAc)_2$ was used as a metal source. Eventually, $Pd_2(dba)_3$ **144** was found to enable reaction of the starting materials: however, not into the desired cross-coupled product, but into the dehalogenated 8HQ **137** (Scheme 25). In fact, the dehalogenated product **137** was found to be the only product when reaction occurred under initial catalyst screening.

Previous work on palladium cross-coupling methodology suggested that the use of bulky electron-rich catalysts may be beneficial for promoting cross-coupling product formation when the substrates are prone to dehalogenation side reactions.[175] Screening of various catalysts including 2,2'-bis(diphenylphosphino)-1,1'-binaphthyl (BINAP) **142**, and a selection of substituted bi-aryl species identified 1,1'-bis(di-*tert*-butylphosphino)ferrocene **145** as the best catalyst ligand for cross-coupling product formation, with 100 % conversion of starting material and only 33 % of dehalogenated product detected, with 67 % of the desired cross-coupled product (Table 1). As one possible reaction mechanism for dehalogenation may be metal-halogen exchange-mediated protonation, it was stipulated that side product formation may be further minimised by performing the reaction under anhydrous conditions. Screening of various conditions by LC-MS analysis suggested a reaction mixture containing dimethylacetamide (DMAC) and solid potassium carbonate as the best solvent and base combination: reaction conversion was 100% using both 5-chloro- and 5-bromo-substituted 8HQs, without any dehalogenated byproducts detected.

Entry	Pd Source	Ligand	Reaction	Dehalogenation	Cross-Coupling
1	$Pd(OAc)_2$	XPhos	No	/	/
2	$Pd_2(dba)_3$	XPhos	Yes	25 %	none
3	CAS 1028206-56-5 XPhos Precat.		No	/	/
4	Tetrakis(triphenylphosphine)palladium(0)		No	/	/
5	$Pd_2(dba)_3$	BINAP	Yes	100 %	none
6	[1,1'-Bis(di-isopropylphosphino)ferrocene]dichloropalladium(II)		No	/	/
7	[1,1'-Bis(di-cyclohexylphosphino)ferrocene]dichloropalladium(II)		No	/	/
8	[1,1'-Bis(di-*tert*-butylphosphino)ferrocene]dichloropalladium(II)		Yes	33 %	67 %
9	[1,1'-Bis(di-*tert*-butylphosphino)ferrocene]dichloropalladium(II)*		Yes	none	100 %

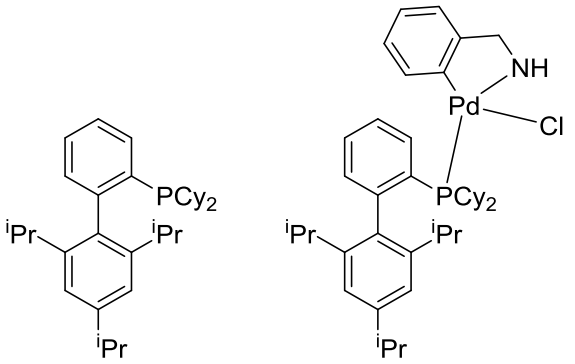

138

139

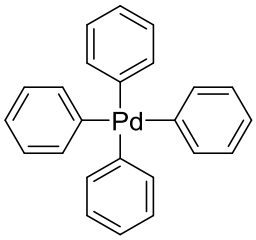

140

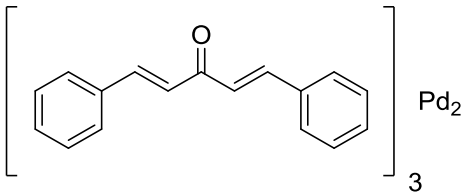

141

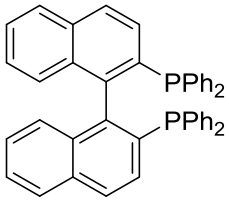

142

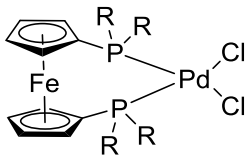

R = isopropyl **143**
cyclohexyl **144**
tert-butyl **145**

Table 1: Reagents and conditions: 5-Bromo-8-tosylhydroxyquinoline **135**, phenylboronic acid, 5 mol % Pd, 10 mol % ligand, DME, $NaHCO_3$ (sat. aq.).* 5-Bromo-8-tosylhydroxyquinoline **135**, phenylboronic acid, 5 mol % Pd, 10 mol % ligand, DMAC, K_2CO_3.

Coupling reactions between 4- and 5-chloro-8HQ and phenylboronic and 2-furanylboronic acids respectively yielded the corresponding 4- and 5-substituted target compounds **146**, **148**, **149**, and **150** (Scheme 26): for example, the final reaction conditions gave **148** in 22 % yield. The relatively low yield may be attributed to the low solubility of the resulting product which interfered with aqueous workup. However, no systematic optimisation of purification conditions was undertaken.

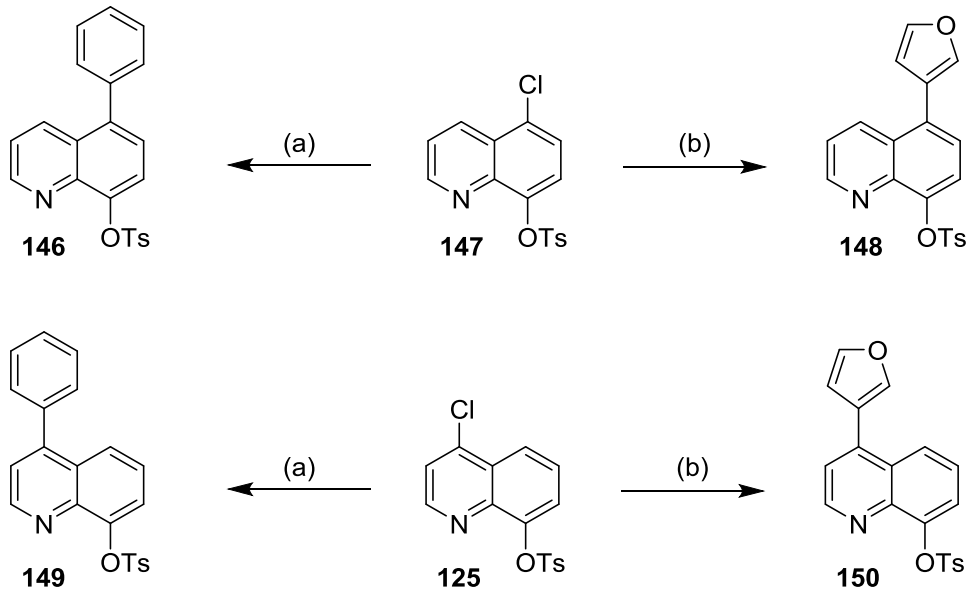

Scheme 26: Reagents and conditions: (a) Phenylboronic acid, [1,1'-bis(di-*tert*-butylphosphino)ferrocene]dichloropalladium(II) **145** (5 mol %), K_2CO_3, DMAC, 180 °C, 30 min, MW irradiation. (b) 3-Furanylboronic acid, [1,1'-bis(di-*tert*-butylphosphino)ferrocene]dichloropalladium(II) **145** (5 mol %), K_2CO_3, DMAC, 180 °C, 30 min, MW irradiation.

The insights into protecting group chemistry and catalyst choice from palladium-catalysed cross-coupling reaction conditions with boronic acids were directly adaptable to the analogous cyanation reactions using zinc cyanide and bulky electron-rich palladium catalyst XPhos **138** to yield the corresponding cyanide from the respective 8HQ chloride (Scheme 27).[176] Zinc cyanide was the cyanide donor of choice because its low solubility in the DMAC reaction solvent ensures that only a very low concentration of cyanide is present in the reaction mixture at any point of time. Other inorganic cyanide salts, such as potassium cyanide, have relatively high solubility in DMAC, which leads to catalyst poisoning because of the strong σ-donor capabilities of the cyanide ion.

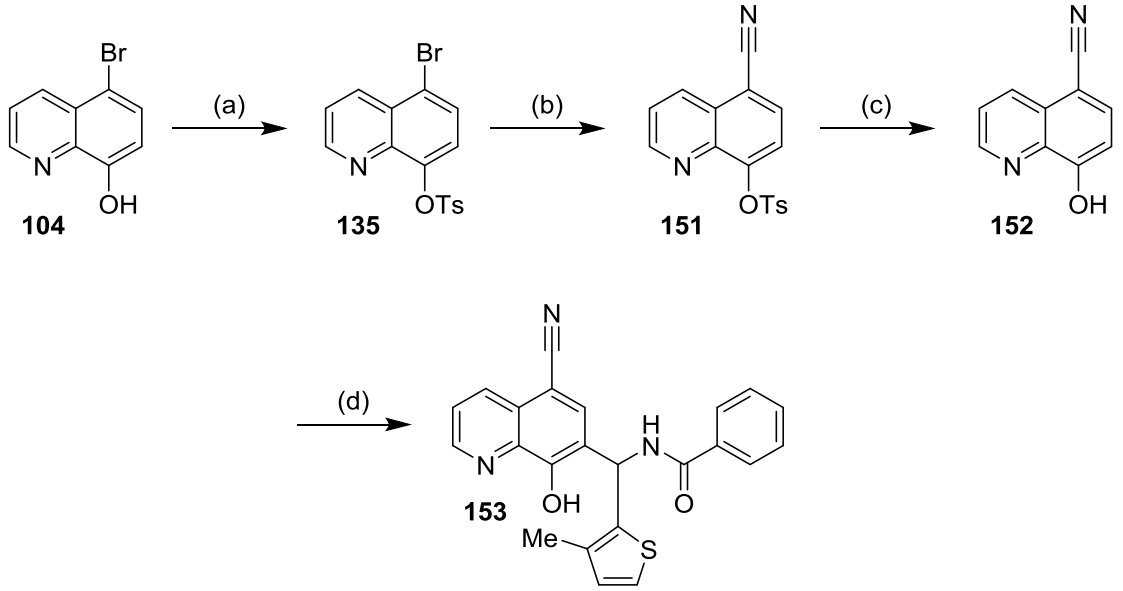

Scheme 27: (a) TsCl, NaOH 1 M, acetone, RT, 3 h. (b) 2 mol % $Pd(OAc)_2$, 4 mol % XPhos **138**, $Zn(CN)_2$, Zn dust, H_2SO_4, DMAC, 140 °C, 2 h, MW irradiation. (c) NaOH 1 M aq., EtOH, reflux, 1 h. (d) 3-Methyl-2-thiophenecarboxaldehyde **97**, benzamide, neat, 130 °C, 3 h.

Both the 4- and 5-nitrile-substited 8HQs underwent 7-substitution to give the respective products, such as reaction of **152** to give **153** (Scheme 27). The attempt to convert the nitriles into the corresponding carboxylic acids by refluxing in either hydrochloric acid or sodium hydroxide solution, however, only yielded a complex mixture of components.

Amides

Fewer suitable amides than aldehydes were commercially available. In order to systematically diversify the chemical library, several amides required in-house synthesis. The method of choice was microwave-assisted reduction of nitriles into the corresponding amides using sodium perborate tetrahydrate.[177] This reduction selectively yielded the amide without overreducing to the carboxylic acid. Availability of nitrile starting materials, chemoselectivity, and ease of purification made it the method of choice for accessing a variety of amides. As a representative example, the synthesis of 3-thiophenecarboxamide **155** from 3-thiophenecarbonitrile **154** is exemplified below (Scheme 28).

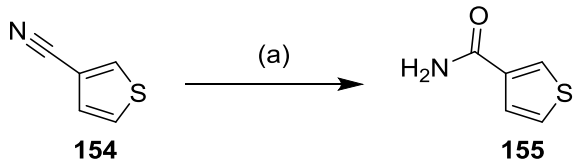

Scheme 28: Reagents and conditions: (a) $NaBO_3 \bullet 4H_2O$, H_2O, EtOH, MW irradiation, 100 °C, 10 min.

As outlined in Figure 26, aromatic, heterocyclic, electron-rich, electron-poor, and bulky amides were all found to be substrates for the one-pot three-component Betti-type reaction, in line with the findings for the aldehyde components. Contrary to the aldehydes, aliphatic amides, including purely aliphatic as well as benzylic amides, were found to undergo reaction. Rather unsurprisingly, 7-substituted 8HQs with aliphatic components were more soluble than their aromatic counterparts. Also carbamates and ureas were found to undergo reaction. One convenient way for accessing the free benzylic amine product **160** was to use carbamate **158** for 7-substitution under standard conditions, and to subsequently treat product **159** with trifluoroacetic acid (TFA).

A.

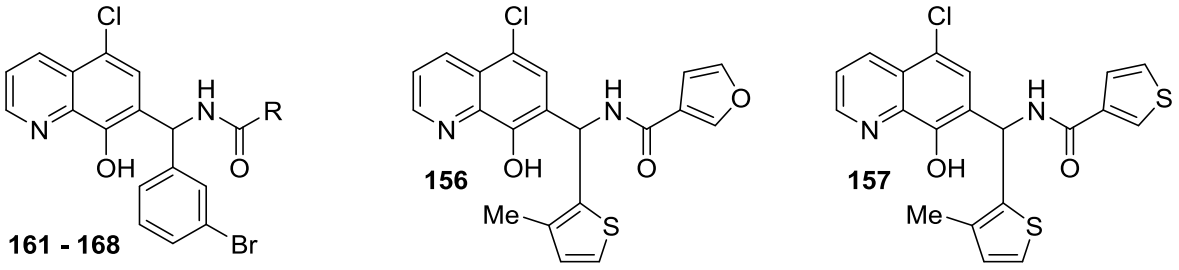

B.

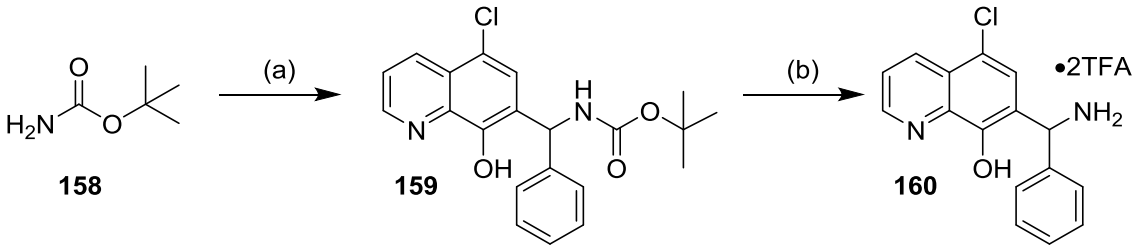

Compound	R =	Yield	Compound	R =	Yield
161	Me	55 %	**165**	NO_2	46 %
162		47 %	**166**		66 %
163	OMe	67 %	**167**	NH_2	88 %
164	Cl	55 %	**168**	O	54 %

Figure 26: A. Scope of amide substituents encompassing primary aliphatic, electron-rich, electron-poor, bulky, and heterocyclic amides, as well as ureas and carbamates. **B.** Reagents and conditions: (a) 5-Chloro-8-hydroxyquinoline, benzaldehyde, neat, 130 °C, 3 h. (b) TFA, CH_2Cl_2.

It was hypothesised that secondary amides might undergo reaction more readily than their primary counterparts because of increased electron-density on the nitrogen atom. No reaction, however, was observed with *N*-methylbenzamide **169** instead of benzamide, possibly because of steric hindrance on the amide nitrogen atom. In contrast to both nicotinamide and isonicotinamide, the *ortho* isomer **171** did not undergo reaction, possibly because of reduced electron density on the nitrogen atom (Scheme 29).

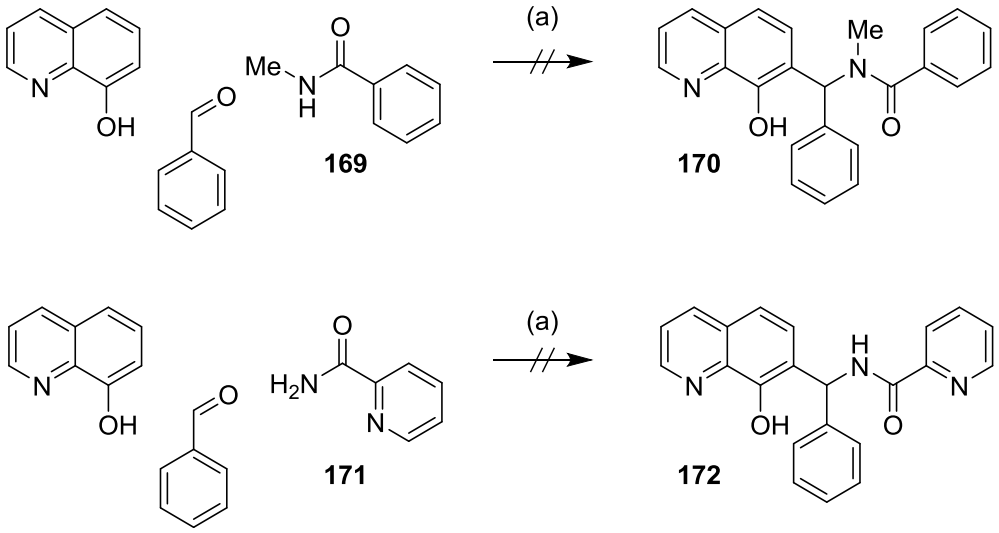

Scheme 29: Reagents and conditions: (a) Neat, 130 °C, 3 h.

2-Substituted 8HQs

The 2-substituted regioisomer **175** of 7-substituted 8HQ **50** was of interest for elucidation of its binding mode, in analogy to comparison of both IOX1 **47** and 8HQ-4-carboylic acid **24** (see Chapter III). One way of accessing the 2-benzylamine-substituted 8HQ **174** was *via* the corresponding 8HQ-2-carbonitrile **173** by reaction with phenyllithium solution at -78 °C and subsequent reductive amination of the resulting imine with sodium borohydride. Trial amidation reactions with either benzyl chloride or benzoic acid and Mukayiama's coupling reagent did, however, not give the desired benzamide **175** (Scheme 30).

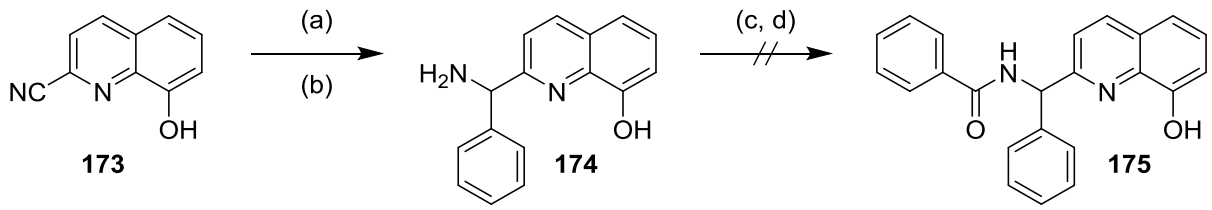

Scheme 30: Reagents and conditions: (a) Phenyllithium, THF, - 78 °C, 2 h. (b) $NaBH_4$, EtOH. (c) Benzoyl chloride, CH_2Cl_2, RT, 3 h. (d) Benzoic acid, Mukayiama's reagent, CH_2Cl_2, reflux, 3 h.

Multicomponent Reaction Scope

With the aim of exploring the reaction scope in terms of the number of reaction partners, it was considered possible to turn the three-component one-pot reaction into a five-component one-pot reaction by using either bifunctional aldehydes or amides (Scheme 31). The simplest bifunctional amide is urea: reaction with urea yielded the corresponding symmetric molecule **176**. Similarly, reaction with both isophthalaldehyde **177** and terephthalaldehyde **179** yielded the corresponding macromolecules **178** and **180**. It should be noted that the reaction conditions yield the racemic products, hereby giving a mixture of three molecules: two diastereoisomers and the corresponding enantiomers (one of which is the *meso* form). Separation of stereoisomers was not attempted. A general drawback of these macrocyclic molecules was, unsurprisingly, their solubility. Some were so insoluble, even in DMSO, that their NMR spectra could not be obtained, which renders these types of molecules obsolete for inhibitor-driven applications. Given the electronic properties of 8HQs, exploration of this rapid means of macrocycle formation may, however, be useful for more materials-focused, supramolecular, or asymmetric catalyst syntheses.

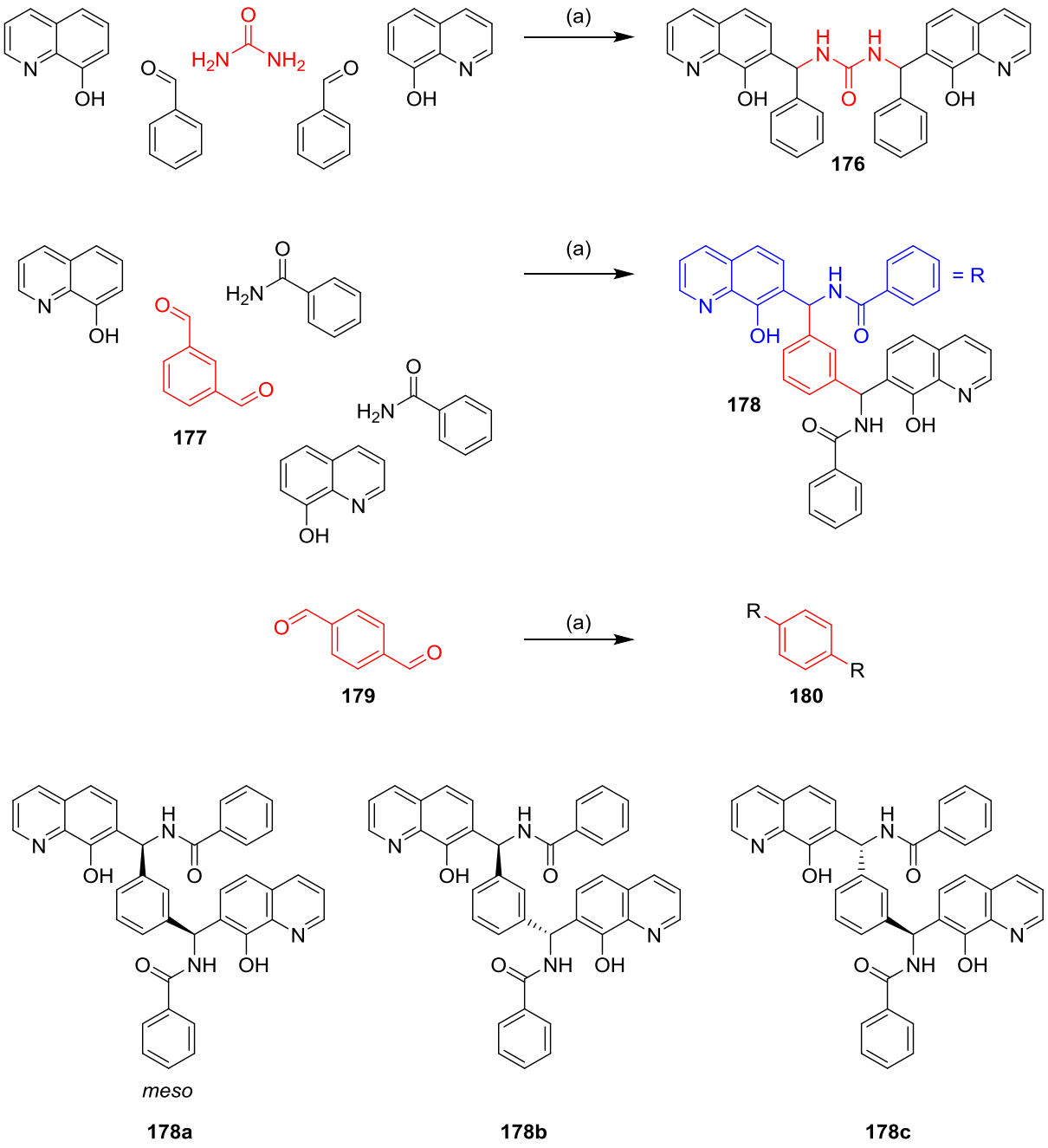

Scheme 31: Reagents and conditions: (a) Neat, 180 °C, 3 h. The reaction will give rise to three products: two diastereoisomers and the corresponding enantiomers as a racemic mixture.

With an analogous approach, it was possible to turn the three-component one-pot reaction into a two-component one-pot reaction by tying both aldehyde and amide functionalities into molecule **182**. Bifunctional **182** was synthesised from the corresponding nitrile **181** using the previously described microwave-assisted reduction with sodium perborate tetrahydrate (Scheme 28) to give the exclusively cyclised form of **182**.[177] Reaction of **182** with 8HQ led to the corresponding 7-substituted product **183** (Scheme 32).

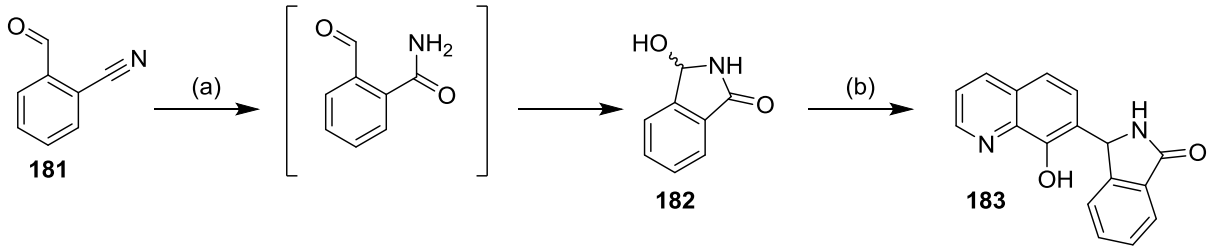

Scheme 32: Reagents and conditions: (a) $NaBO_3 \bullet 4H_2O$, H_2O, EtOH, MW irradiation, 100 °C, 10 min. (b) 8HQ, neat, 180 °C, 3 h.

Amine Side Chains

The synthesis of amine-based, instead of amide-based, side chains was also explored. The original Betti reaction requires stirring natphthalen-2-ol **156**, benzaldehyde, and aniline in ethanol at room temperature for several days (Scheme 10).[164] Substitution of the significantly more electron-poor 8HQs would potentially be more difficult.

An attempt to reduce reaction time by using reflux or microwave-assisted superheating, instead of room temperature, did not give any product at all: the rate of imine formation and instant hydrolysis possibly outweighs the rate of nucleophilic attack by 8HQ. Previous work on the Betti reaction explored the use of Lewis catalysts, usually based on transition or lanthanide metals, for enhancement of reaction conditions: most of these were incompatible with the strong metal-chelating properties of 8HQs.[164] Trying to adopt the amide-based reaction conditions, solvent-free and high-temperature, did either not yield the desired reaction products, or led to decomposition. Facing a multitude of various potentially counterbalancing factors, the original Betti reaction conditions were used: in fact, the old-fashioned methodology was successful. As a representative example, 5-chloro-8HQ was stirred with 3-methyl-2-thiophenecarboxaldehyde **97** and pyrrolidine in ethanol at room temperature for 3 days to yield **184** as a light-brown precipitate in 18 % yield. This synthetic route was also viable for the resynthesis of **49** identified from the high-throughput cell-based reporter assay for modulation of the hypoxic response (Scheme 33).[160]

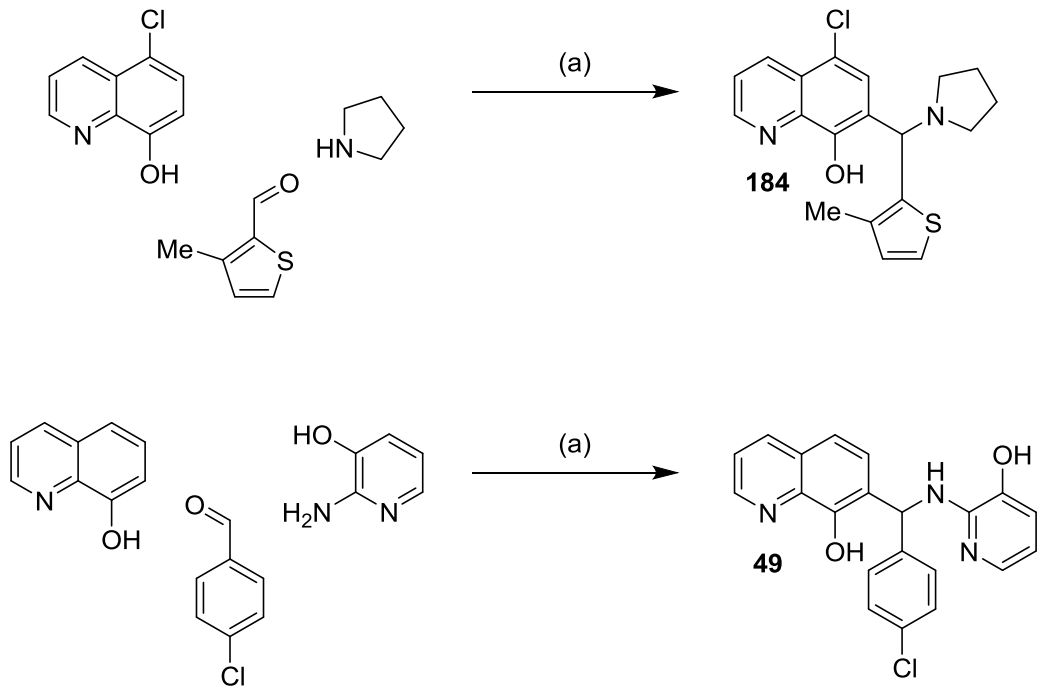

Scheme 33: Reagents and conditions: (a) EtOH, RT, 72 h.

Exploration of Alternatives to the Betti-Type Reaction

The unusual conditions for the adopted one-pot three-component reaction presented the question as to the reaction mechanism of the Betti-type reaction. The aldehyde component is probably the most reactive reaction partner: the question would be if the reaction mechanism first involves condensation between the aldehyde and the amide to form an imine-type species which is then attacked by the 8HQ, i.e. a more Mannich-type reaction, or if the first step involves formation of a benzylic alcohol by condensation between the 8HQ and the aldehyde, which is then intercepted by the amide, i.e. a more Ritter-type reaction (Scheme 34).[178] Attempts to isolate potential condensation products between both aldehyde and amide **185**, as well as aldehyde and 8HQ **186**, under the Betti-type conditions, were, however unsuccessful. The reaction mechanism relating to the 7-substitution of 8HQs remains unclear.

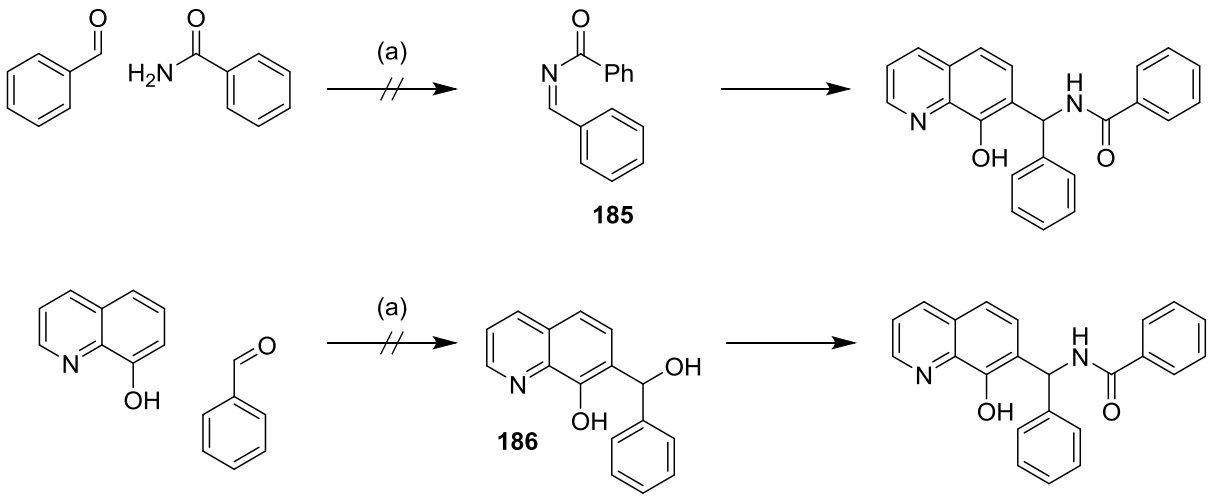

Scheme 34: Reagents and conditions: (a) Neat, 180 °C, 3 h.

A preliminary attempt to make the 7-substituted 8HQ **50** *via* a different three-component one-pot reaction, namely the Ritter reaction, was successful (Scheme 35). The final product **50**, identical to the product obtained *via* Betti-type reaction, was isolated using the Ritter reaction. The relative yield, however, was lower: 24 % *via* Ritter, 85 % *via* Betti-type reaction. The Ritter reaction did not yield any advantages over the Betti reaction at this stage. Given the substantial amount of progress made *via* the Betti reaction, as well as other time constraints, no further investigations into adapting the Ritter reaction for substitution of 8HQs were pursued. This digression merely gives a pointer for additional reaction development in the future. However, the success of the Ritter reaction towards the 7-substitution of 8HQs, together with the inability to perform 7-substitution with *N*-methylbenzamide (Scheme 29), might indicate the possibility of a Ritter reaction upon performing the Betti conditions: under the given high-temperature conditions, it may be possible that the primary amide undergoes pyrolytic dehydration to form the corresponding nitrile, which then performs a Ritter reaction.[179]

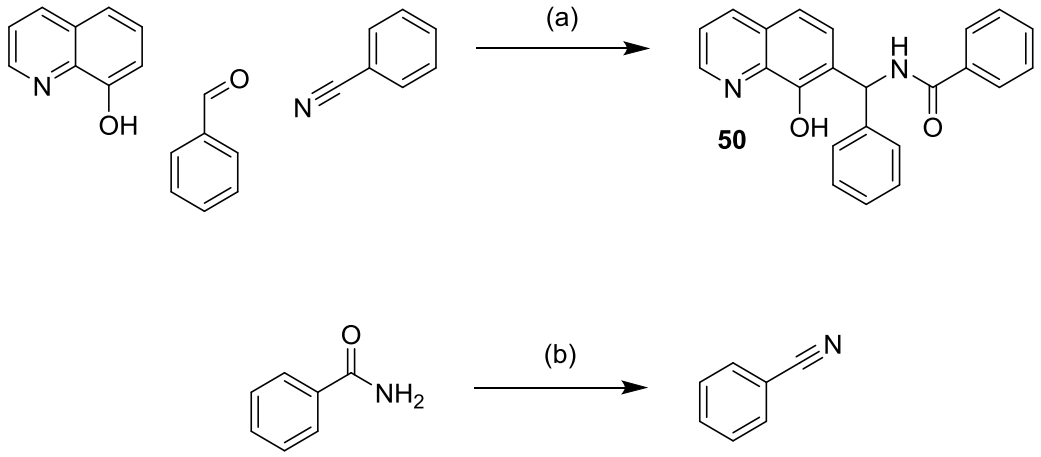

Scheme 35: Reagents and conditions: (a) Benzonitrile (solvent), TfOH, 150 °C, 18 h. (b) Neat, 180 °C, 3 h.

Summary

Optimisation of reaction conditions of a variation of the Betti reaction led to the development of a robust general procedure for accessing 7-substituted 8-hydroxyquinolines with the following advantages: single-step synthesis and purification of target compounds in one pot, tolerance of a diverse range of readily accessible 8HQs, amides, and aldehydes, and scope for high-throughput synthesis. Additionally, the reaction is compatible with green chemistry principles because of high atom efficiency and solvent-free synthesis conditions. At the same time, various methodologies were explored for the diversification of 8HQ, aldehyde, and amide starting materials.

Besides their primary use as template-based inhibitors, synthetic strategies for other potential uses of 7-substituted 8HQs were explored, such as: dual inhibitors for the simultaneous inhibition of multiple targets, biotin-linked probes for affinity purification, and macromolecules for materials-based or supramolecular applications.

The subsequent chapter will focus on work towards the primary aim of using 7-substituted 8HQs as template-based inhibitors for 2OG oxygenase inhibition.

Chapter III: 8HQs as 2OG Oxygenase Inhibitors

8HQ Binding Studies

Some 4-, 5-, and 7-substituted 8HQs have previously been identified as KDM4E inhibitors in a fluorescence-based high-throughput screen.[180] The 5-substituted 8HQs displayed highest potency and were further validated in a secondary assay employing mass spectrometry. The most potent compound identified was 5-carboxy-8HQ (IOX1) **47** with an IC_{50} of 200 nM *in vitro* and an EC_{50} of 87 µM in cells. IOX1 **47** was shown to be a broad-spectrum 2OG oxygenase inhibitor with sub-micromolar *in vitro* IC_{50} values against KDM4A/C/E, KDM3A and KDM6B, low-micromolar IC_{50} values against KDM2A, KDM5C, KDM6A, PHF8, PHD2, and FIH, and high-micromolar IC_{50} against BBOX1 (Figure 27).[128]

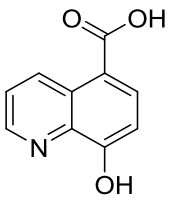

47

Enzyme	IC_{50} in µM
KDM6B	0.12
KDM3A	0.17
KDM4A	0.2
KDM4E	0.3
KDM4C	0.6
KDM6A	1
KDM2A	10.3
PHD2	14.3
FIH	20.5
KDM5C	25
PHF8	37
BBOX1	196

Figure 27: Structure of broad-spectrum demethylase inhibitor IOX1 **47** and associated potencies against 2OG oxygenases.

IOX1 **47** binds to the KDM enzymes *via* bidentate Fe(II) chelation inside the KDM4 enzyme active site using its pyridine nitrogen and phenol oxygen.[128] Similar to the 2OG mimetic NOG **22**, the 5-carboxylate engages in hydrogen bonding and electrostatic interactions with Tyr132 and Lys206. An additional π-π stacking interaction occurs between the quinoline ring and Phe185 (Figure 28). Overall, the inhibitory activity of IOX1 **47** likely stems, at least in part, from active site binding competition with 2OG **1** by mimicking both metal chelation and carboxylate interactions; solution phase studies support this hypothesis.[136] In some cases, it

may be possible that chelation of IOX1 **47** to Fe(II) in solution contributes to the observed 2OG oxygenase inhibition.

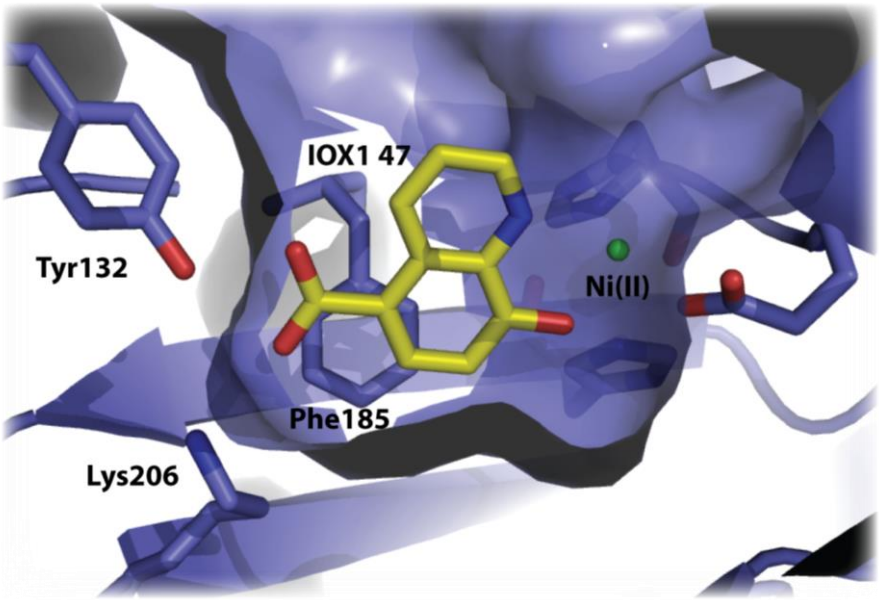

Figure 28: View from an X-ray crystal structure of KDM4A (PDB ID: 3NJY) in complex with IOX1 **47** (yellow). Key interactions include hydrogen bonding interactions between the IOX1 **47** carboxylate and Tyr132 and Lys206, π-stacking interaction with Phe185, and bidentate active-site metal chelation.

A striking difference in the relative position of the active site metal is observed when comparing IOX1 **47**-2OG oxygenase co-crystal structures with 2OG oxygenase co-crystal structures obtained with other small-molecule inhibitors. Relative to the KDM4A, KDM6B, and FIH structures with NOG **22** or 2,4-PDCA **23**, the position of the active site metal is shifted with IOX1 **47**. This translocation is independent of the metal as this observation persists for IOX1 **47**-protein co-crystals using Fe(II), Ni(II), Zn(II), and Mn(II) (Figure 29).

In order to investigate the structural basis of metal translocation, the structural homologue of IOX1 **47**, 4-carboxy-8-hydroxyquinoline (4C8HQ) **24**, was synthesised (see Scheme 22, Chapter II) and subsequently co-crystallised with KDM4A (PDB ID: 4BIS). This structure reveals that overall, 4C8HQ **24** binds in a similar mode to IOX1 **47**. However, no metal translocation is evident with 4C8HQ (Figure 29).[128]

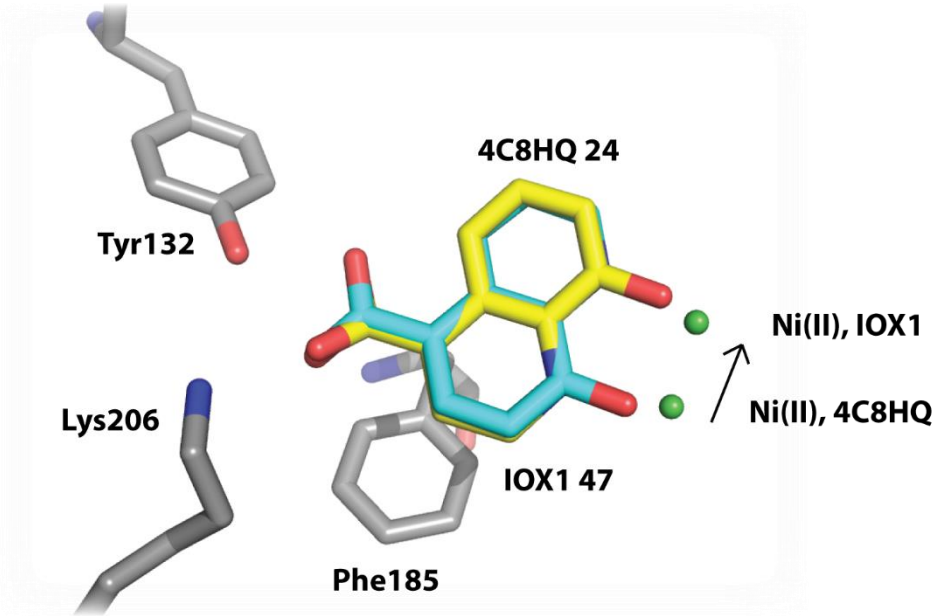

Figure 29: View from an overlay of X-ray crystal structures of KDM4A in complex with IOX1 **47** (cyan) (PDB ID: 3NJY) and 4-carboxy-8-hydroxyquinoline **24** (yellow) (PDB ID: 4BIS). It is notable that IOX1 **47** causes the active site metal to translocate upon binding, whereas 4C8HQ **24**, and other known inhibitors, do not induce this metal movement.

Furthermore, metal displacement correlates with inhibitory potency of 8HQs against KDM4A. The *in vitro* IC_{50} values for 4C8HQ **24** against KDM4A and KDM6B are 4 µM and 9 µM respectively; these values are significantly higher than the corresponding values for IOX1 **47**, which are 300 nM and 140 nM respectively. In addition, potential energy calculations on 4C8HQ **24** and IOX1 **47** complexes with KDM4A reveal a lower energy conformation for IOX1 **47** over 4C8HQ **24** (ΔE = -7.8 kcal mol^{-1}). These results suggest that metal translocation may potentially be exploited as a strategy for the identification of potent KDM4 inhibitors.

In vitro Screening

The *in vitro* screening data were acquired by Drs Anthony Tumber and Giuseppe Scozzafava at the epigenetics section of the Structural Genomics Consortium (SGC) in Oxford. The primary screening platform was an antibody-based fluorescence technique called AlphaScreen®.[181] Some of the data were obtained *via* mass spectrometry-based RapidFire™.[182]

AlphaScreen® uses so-called donor and acceptor beads. Upon irradiation at 680 nm, the donor bead generates singlet oxygen which is able to excite the acceptor bead to emit light at 600 nm if the acceptor bead is located within a distance below the 200 nm diffusion limit of singlet oxygen. The currently used assay system uses streptavidin-linked donor beads which bind to the biotin-labelled histone peptide substrate. The

acceptor beads are linked to H3K9me2-specific antibodies which bind to H3K9me2 of demethylated peptide. The histone substrate peptide therefore acts as a linker for both donor and acceptor beads to be held within the singlet oxygen diffusion limit if the peptide is demethylated. The relative amounts of demethylation can therefore be quantified by measuring fluorescence at 600 nM of the acceptor bead (Figure 30).

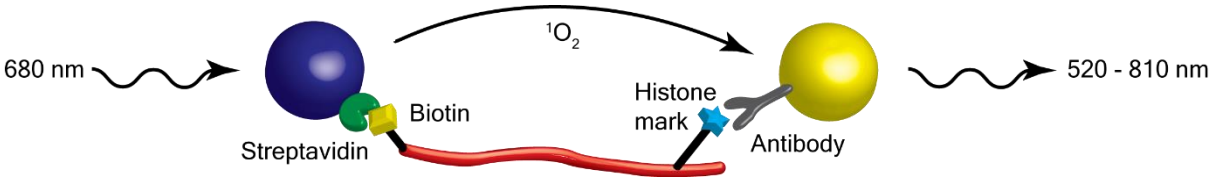

Figure 30: AlphaScreen® assay for KDM *in vitro* screening. Generation of singlet oxygen by irradiation of the donor bead leads to emission of light at 600 nm from the acceptor bead if the system accommodates both beads below the 200 nm diffusion limit of singlet oxygen. This occurs if the H3K9me2-specific antibody on the acceptor bead binds to the demethylated H3K9me2 histone mark of the substrate peptide, which is linked to the donor bead *via* a biotin-streptavidin interaction.

RapidFire™ combines automation capabilities of a plate reader with LC-MS capabilities for concomitant reagent separation and mass analysis.[182] This method enables direct detection of histone substrate peptide demethylation while ensuring high-throughput-compatible speed of analysis. RapidFire™ has therefore evolved to be the method of choice for KDM inhibitor screening during the course of this thesis. The majority of data, however, were obtained *via* AlphaScreen® because the RapidFire™ KDM assay was at a developmental stage during the phase of *in vitro* testing of the majority of 7-substituted 8HQs.

Preliminary single point screening results from a focused library of 7-substituted 8HQs against both KDM4E and KDM6B suggested potencies in the mid- to low-micromolar range. Most notably, the 5-chloro-8HQs displayed higher potencies against KDM4E than KDM6B, suggesting the potential of this particular scaffold for the development of selective KDM4 inhibitors (Figure 34). These results provided the basis of the majority of subsequent investigations toward KDM4-selective inhibitors.

The primary counterscreen enzyme of choice was KDM6B. Given IOX1 **47** has some minor inherent selectivity for the KDM4 and KDM6B subfamilies against other 2OG oxygenases, it was judged that an 8HQ-based inhibitor selective for KDM4 over KDM6B would add most value to small-molecule approaches for functional elucidation of 2OG-dependent histone demethylases.

An iterative medicinal chemistry approach, based on a combination of structure-activity relationships (SAR) and structure-selectivity relationships (SSR), yielded a diverse library of 7-substituted 8HQs which display a

wide range of both potencies and selectivities. The data are visualised in Figures 31 - 33 where potency for each compound is plotted against selectivity: the general compound distribution reflects the evolution towards potent and selective compounds for KDM4. This evolution is even more pronounced when comparing the compound distribution for KDM4E and KDM4C. Initially, every compound was screened against KDM4E, which is more amenable to recombinant protein production and purification compared to KDM4C. *KDM4E*, however, is considered a pseudogene and therefore less biologically relevant. After optimisation of KDM4C production and purification, the KDM4 *in vitro* screening was then primarily conducted with KDM4C. The early-stage compounds tested against KDM4E therefore display greater distribution with respect to both potency and selectivity than the later-stage compounds screened against KDM4C, which, in general, tend to be more potent and more selective. Below is an overview of the general bias of the library towards KDM4 subfamily inhibition. For a full data set, please see Appendix B.

Against KDM4E:

- 178 compounds were tested in a single point assay at 100 µM final concentration: 107 compounds (60 % of the total tested library) showed ≥ 95 % inhibition.
- 39 compounds were tested in a single point assay at 20 µM final concentration: 25 compounds (64 % of the total tested library) showed ≥ 70% inhibition.
- 198 compounds were then selected for the determination of dose response:
    - 78 compounds (39 % of total tested library) manifested an $IC_{50} \leq 10$ µM.
    - 142 compounds (72 % of total tested library) manifested an $IC_{50} \leq 25$ µM.
    - 36 compounds (18 % of total tested library) manifested an $IC_{50} \geq 100$ µM.

Against KDM4C:

- 95 compounds were selected for the determination of dose response:
    - 61 compounds (64 % of total tested library) manifested an $IC_{50} \leq 10$ µM.
    - 80 compounds (84 % of total tested library) manifested an $IC_{50} \leq 25$ µM.
    - 13 compounds (13 % of total tested library) manifested an $IC_{50} \geq 100$ µM.

Against KDM6B:

- 105 compounds were tested in a single point assay at 100 µM final concentration: 42 compounds (40 % of the total tested library) showed ≥ 95 % inhibition.
- 142 Compounds were then selected for the determination of dose response:
  - 11 compounds (8 % of total tested library) manifested an IC_{50} ≤ 10 µM.
  - 45 compounds (32 % of total tested library) manifested an IC_{50} ≤ 25 µM.
  - 54 compounds (38 % of total tested library) manifested an IC_{50} ≥ 100 µM.

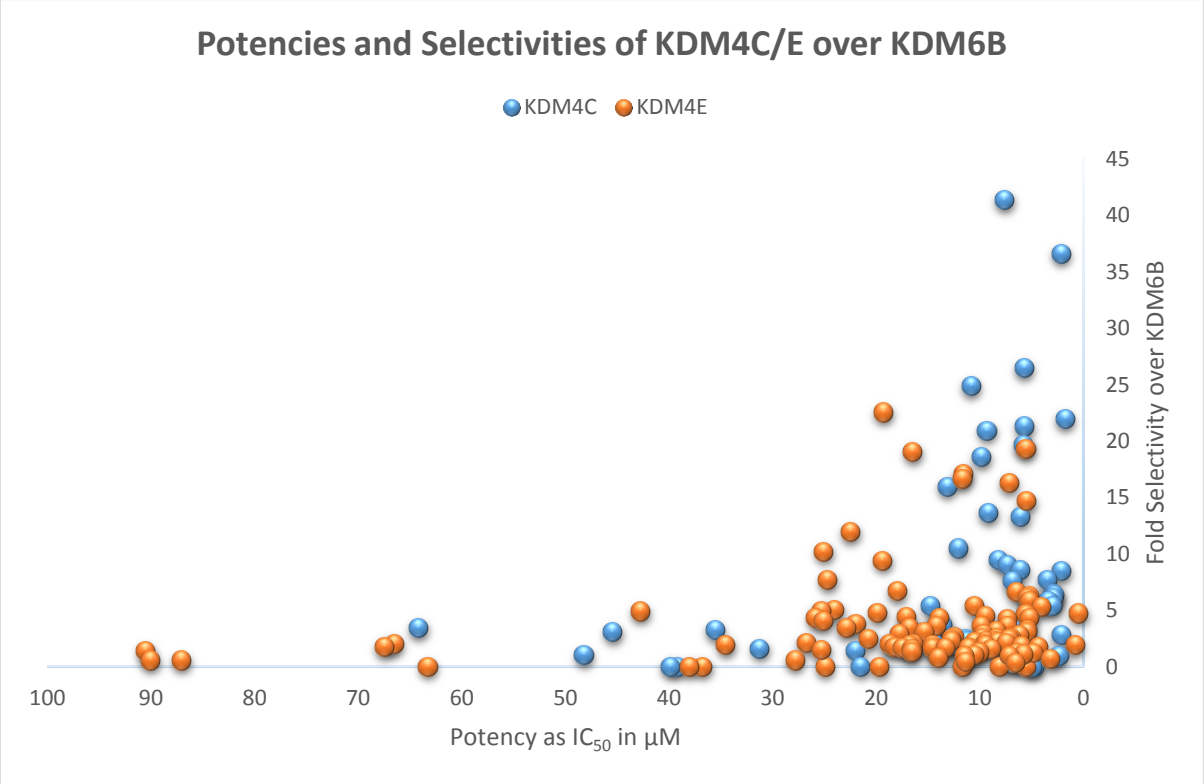

Figure 31: Plot of potency for KDM4C/E as IC_{50} in µM *versus* selectivity against KDM6B calculated as the ratio of IC_{50} for KDM6B and the respective IC_{50} for KDM4C/E.

A comparatively small number of compounds were also screened against KDM2A: a variety of potencies and selectivities is still apparent, but to a significantly lesser extent when compared to KDM6B.

- 32 compounds were tested in a single point assay at 100 µM final concentration: 13 compounds (41 % of the total tested library) showed ≥ 95 % inhibition.

- 41 compounds were tested in a single point assay at 90 µM final concentration: 21 compounds (41 % of the total tested library) showed ≥ 95 % inhibition.
- 73 compounds were then selected for the determination of dose response:
  - 8 compounds (11 % of total tested library) manifested an IC_{50} ≤ 10 µM.
  - 18 compounds (25 % of total tested library) manifested an IC_{50} ≤ 25 µM.
  - 33 compounds (45 % of total tested library) manifested an IC_{50} ≥ 100 µM.

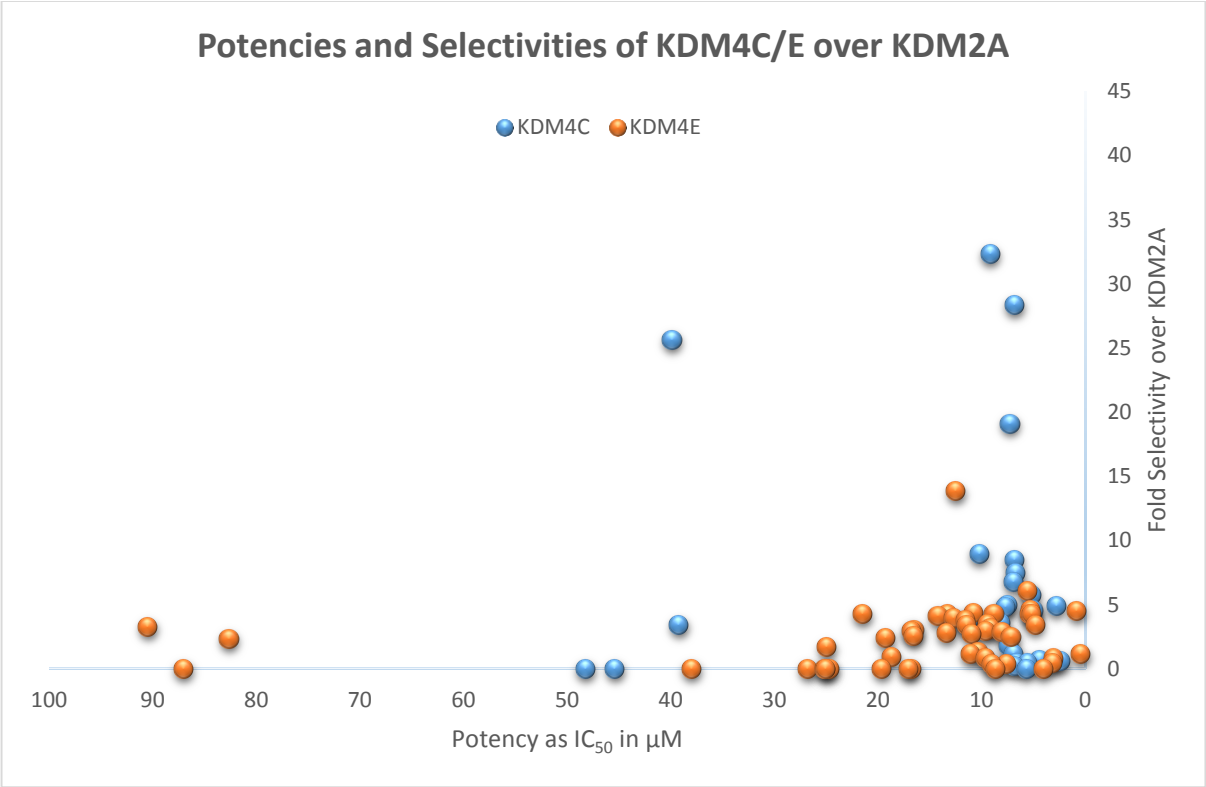

Figure 32: Plot of potency for KDM4C/E as IC_{50} in µM *versus* selectivity against KDM2A calculated as the ratio of IC_{50} for KDM2A and the respective IC_{50} for KDM4C/E.

Another counterscreen employed KDM5C, but primarily at 20 µM single point compound concentration (data not shown).

The generated library of 7-substituted 8HQs offers a wide variety of potencies and selectivities, but tends towards potent and selective KDM4 inhibitors. The library even offers a diverse range of potencies and selectivities within the KDM4 subfamily of KDM4C and KDM4E, which are structurally very similar.

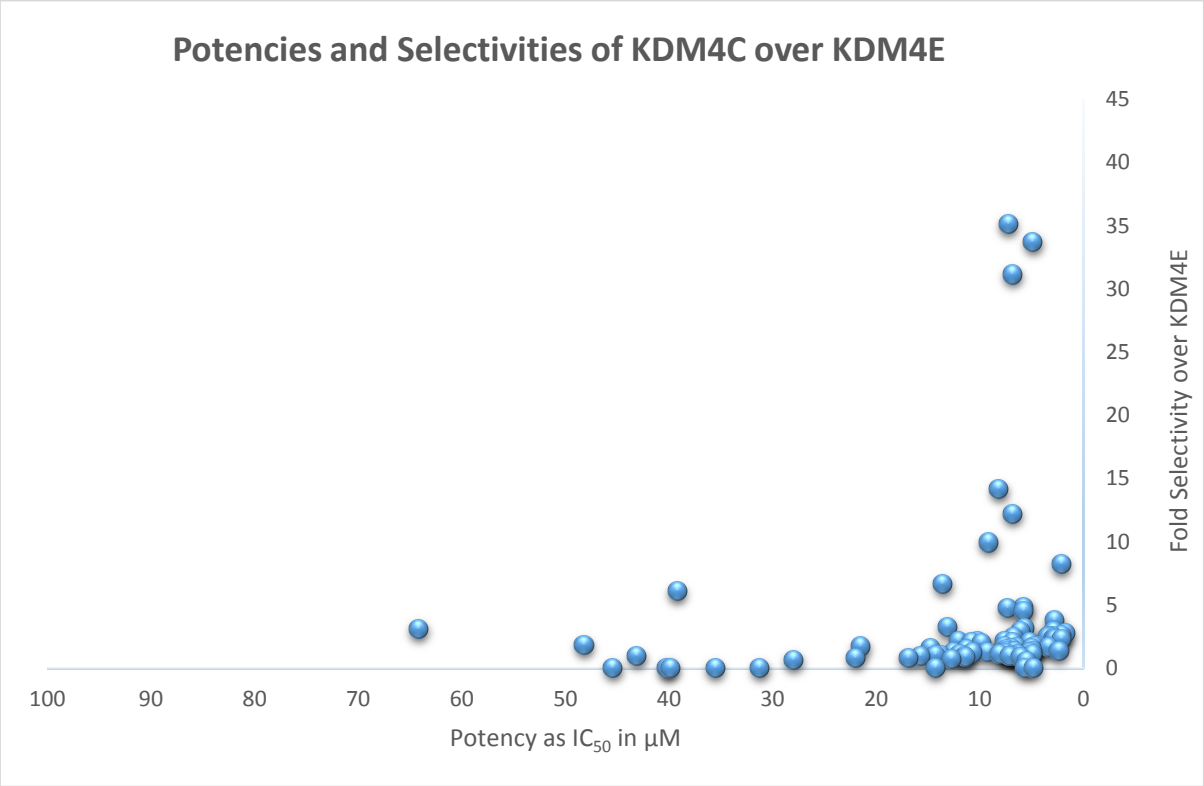

Figure 33: Plot of potency for KDM4C as IC_{50} in µM *versus* selectivity against KDM4E calculated as the ratio of IC_{50} for KDM4E and the respective IC_{50} for KDM4C.

Overall, these results validate the approach of a template-based inhibition strategy for achieving selectivity by tuning substitution patterns attached to a generic, initially non-selective, inhibitor. Not only has selectivity been achieved within the superfamily of 2OG oxygenases, not only within 2OG-dependent KDMs, but also within one subfamily of KDM4 histone demethylases with both very well-conserved enzyme active sites and substrate binding pockets.

Structure-Guided Library design

Aldehyde-Derived Substituents

A first glimpse at the potential of KDM4 selectivity emerged from single point inhibition data from aldehyde-derived *ortho*- and *meta*-substituted methyl **186**, **188**, and bromo **189** 5-chloro-8HQ derivatives which were potent inhibitors of KDM4E, but not KDM6B, at 20 µM final concentration.

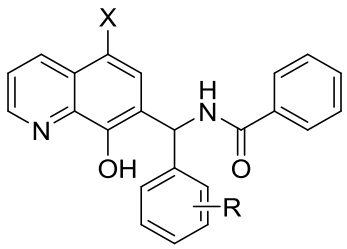

Compound	X =	R =	% Inhibition at 20 µM (KDM4E)	% Inhibition at 20 µM (KDM6B)
64	H	3-CH_3	100	45
186	Cl	3-CH_3	70	0
63	H	2-CH_3	100	60
188	Cl	2-CH_3	100	9
189	Cl	3-Br	100	0

Figure 34: A selection of 7-substituted 8HQs illustrating structure-activity and structure-selectivity relationships of early-stage compounds. Red designates ≥ 75 % inhibition, yellow designates between 25 % and 75 % inhibition, and green designates ≤ 25 % inhibition at 20 µM final compound single point assay.

Selectivity seemed to emerge from a combination of 5-substitution of the 8HQ core and derivatisation of the *meta*-position of the aldehyde-derived moiety as may be inferred from comparison of **64** and **186**, or **63** and **188** (Figure 34).

This led to the exploration of a series of 5-chloro *meta*-substituted analogues, including trifluoromethoxy **81**, trifluoromethyl **190**, fluoro **191**, iodo **80**, nitrile **79**, acetyl **82**, carboxyl **84**, and methyl ester **83** functionalities. Indeed, all of these compounds displayed some selectivity, with the most selective compound being methyl ester-substituted **83**. These results further supported the hypothesis that building from the aldehyde-derived *meta*-position may be beneficial for the development of KDM4-selective compounds.

Compound	X =	R =	IC_{50} in µM (KDM4E)	IC_{50} in µM (KDM6B)
81	Cl	3-OCF_3	22	82
190	Cl	3-CF_3	20	95
191	Cl	3-F	25	38
80	Cl	3-I	10	56

79	Cl	3-CN	8	21
82	Cl	3-C=OCH_3	7	31
84	Cl	3-CO_2H	17	30
83	Cl	3-CO_2CH_3	6	42

Table 2: Overview of the effect of *meta*-substitution of the aldehyde-derived moiety of 7-substituted 8HQs relating to the general structure of Figure 34. Red designates potencies ≤ 25 μM, yellow potencies between 25 μM and 75 μM, and green potencies ≥ 75 μM.

In addition to varying substitution patterns of the aldehyde-derived moiety, explorations into the effects of varying the amide-derived core were undertaken (see Chapter II). Initially, structural variations were systematically gradual, closely following structural variations of the aldehyde-derived core. Several small libraries focused around variations of the amide moiety led to a diverse range of potencies and selectivities, but it proved challenging to relate alterations in structure to clear-cut patterns of either SAR or SSR.

Initial attempts to create an *in silico* binding model of 7-substituted 8HQs with KDM4 enzymes to guide further synthesis were unsuccessful. Conventional molecular docking software uses algorithms which are generally poor predictors of binding contributions from metal chelation. In fact, this approach only yielded binding models based on non-specific binding and poor ranking: energy differences were hardly distinguishable. The adopted open-skies synthesis approach, however, led to SAR and SSR which could be used as a basis of a manual *in silico* docking model. The position of the 8HQ moiety was guided by the co-crystal structure of IOX1 **47** with KDM4A and locked to engage in Fe(II) chelation (Figure 35). Both enantiomers of the, in principle, racemic compound mixture, were modelled into the enzyme active site *in silico*. Inspection of the model between the inhibitors and the enzyme active site suggested that the *S*-enantiomer benefits from a better fit without any steric constraints. The *R*-enantiomer, however, revealed potential steric clashes with the protein, which could not be removed by simple bond rotations. Accounting for the observation that large *meta*-substitution on the aldehyde-derived moiety is tolerated for KDM4 inhibition, but not KDM6B, led to a model where this moiety reaches into the large open channel towards the substrate binding pocket of KDM4 which is absent in KDM6B. The manual *in silico* docking model hence reflects the SSR of 7-substituted 8HQs and offers a plausible explanation for the empirically observed data. This model was then used to guide future inhibitor design (Figure 35).

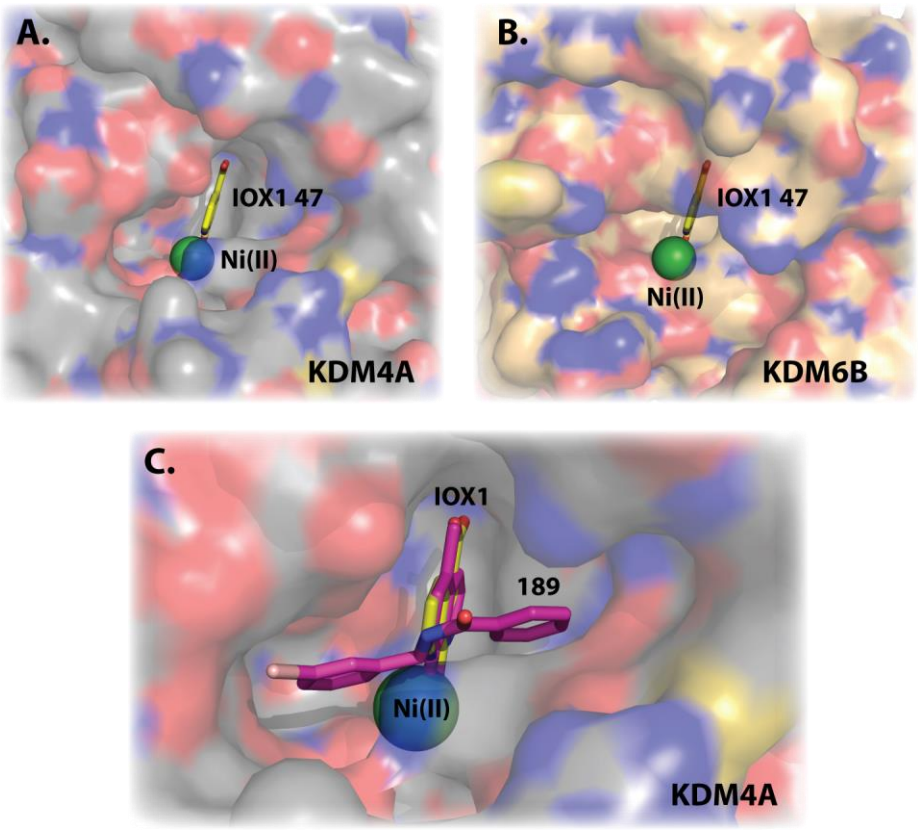

Figure 35: Views from X-ray crystal structures of KDM4A (PDB ID: 3NJY) and KDM6B (PDB ID: 2XXZ) in complex with IOX1 **47**. **A.** The substrate binding pocket leading to the enzyme active site forms a well-defined channel in KDM4A. **B.** In contrast to the well-defined channel in KDM4A, the substrate binding pocket of KDM6B leading to the enzyme active site is wide open to one side and does not form a channel. **C.** Manual docking model of the (*S*)-enantiomer of **189** into KDM4A.

Given the relatively high lipophilicity of the 7-substituted 8HQs, substituents with heterocyclic substitution patterns were particularly attractive to maintain favourable physical properties for ultimate use as a tool compound *in vivo*. Initially, it was thought that an increase in potency may be achieved by increasing the Fe(II)-chelating properties by incorporating the heteroatom at positions 2 or 3 of the aldehyde-derived moiety, hence potentially enabling tridentate chelation (Figure 36). Such an increase in potency was not observed. The 3-methylthiophene-substituted **193**, however, showed both favourable low-micromolar IC_{50} of 5 µM for KDM4E and selectivity against KDM6B, while maintaining acceptable physicochemical properties for use as a small-molecule tool compound (Figure 37).

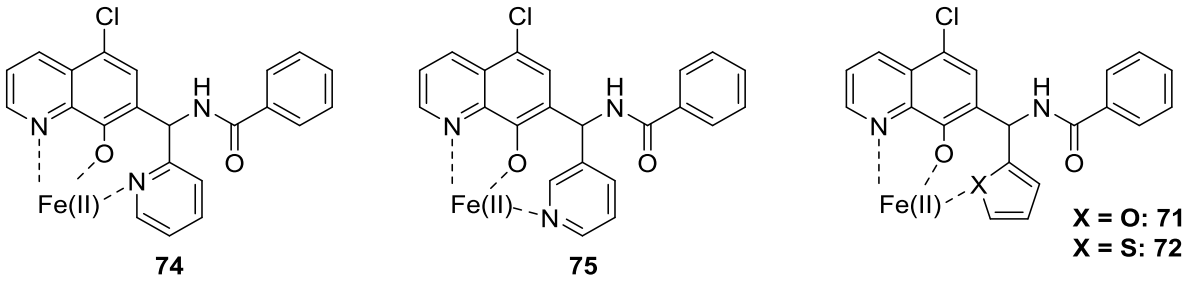

Figure 36: In addition to reducing the lipophilic character of 7-substituted 8HQs, heterocyclic substitution patterns were investigated as a strategy to increase the hapticity of active-site metal chelation.

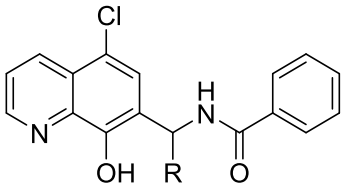

Compound	R =	IC_{50} in µM (KDM4E)	IC_{50} in µM (KDM6B)
74	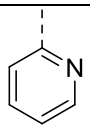	7	7
75	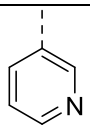	6	8
76	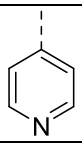	4	7
71	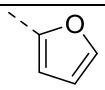	21	51
72		11	23
192	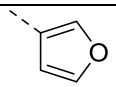	22	No Inhibition
73	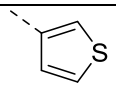	14	9
193	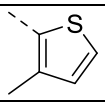	5	106

Figure 37: Overview of the effect of a variety of heterocyclic aldehyde-derived moieties of 7-substituted 8HQs. Red designates potencies ≤ 25 µM, yellow potencies between 25 µM and 75 µM, and green potencies ≥ 75 µM.

It is rather striking that simple methyl substitution of unselective **72** generates selective **193**. Nevertheless, this observation is in line with respect to previous data highlighting the necessity for both 5-chloro substitution and substitution of the aldehyde-derived aromatic ring in order to achieve selectivity. The

recurring theme of 'small chemical changes induce a large biological change' can be further illustrated by comparing compounds **193**, **194**, **195**, and **196**: these structurally closely related compounds not only maintain selectivity over KDM6B, but also, apparently, display subtype selectivity for KDM4C over KDM4E (Table 3).

Compound	R =	IC_{50} in µM (KDM4C)	IC_{50} in µM (KDM4E)	IC_{50} in µM (KDM6B)
194	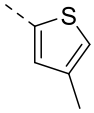	7	14	52
195	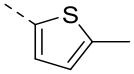	9	90	124
196	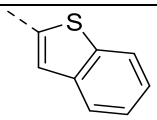	40	No Inhibition	No Inhibition

Table 3: Overview of various thiophene-based heterocyclic moieties of 7-substituted 8HQs relating to the general structure of Figure 37. Migration of the methyl group leads to a different selectivity profile: small chemical changes may induce a large biochemical effect. Red designates potencies ≤ 25 µM, yellow potencies between 25 µM and 75 µM, and green potencies ≥ 75 µM.

Although a selection of various compounds had been obtained with a satisfactory selectivity profile for KDM4 over KDM6B, as well as preliminary SSR which was consistent with an *in silico* model, further studies were conducted to achieve an increase in potency, while maintaining selectivity. Based on the *in silico* model, initial efforts were geared towards an increase in potency by enabling hydrogen bonding from substituents from the bulky aldehyde-derived biphenyl-type *meta*-position. The relatively lipophilic binding pocket, however, did not seem particularly amenable to hydrogen bonding interactions. Based on the model, several target molecules with large side chains were synthesised. Rather than gradually increasing the size of *meta*-substituents, a more radical approach was adopted by substantially increasing bulk in the form of biphenyl-based functionalities. This led to biphenyl compounds such as **197**, as well as the benzyl ethers such as **199** (Figure 38). The corresponding 4-substituted compound **198** was, indeed, less potent and less selective than 3-substituted **197**, in accordance with the *in silico* model. The *para*-substituted compounds also suffered from considerable reduced solubility compared to their *meta*-substituted analogues. The combination of 5-chloro (and 5-bromo) substitution and large *meta*-substituents did indeed lead to inhibitors selective for KDM4 over KDM6B. Switching the substituent at position 5 to a nitro group in **202** reduced selectivity relative to 5-chloro-substituted **199**. Pairing large *meta*-substitution with a larger amide group was not tolerated for KDM4 inhibition. In summary, the data largely validate the *in silico* model for guiding inhibitor design in terms

of selectivity: large aldehyde-derived *meta*-substituents, in combination with a halogen at position 5, leads to selective inhibitors. Nevertheless, the potency of these inhibitors reached a plateau at low-micromolar IC_{50} values (Figure 38).

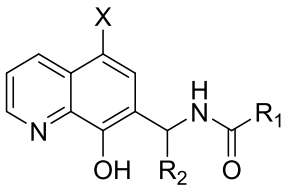

Compound	X =	R_1 =	R_2 =	IC_{50} in µM (KDM4C)	IC_{50} in µM (KDM4E)	IC_{50} in µM (KDM6B)
197	Cl	Ph	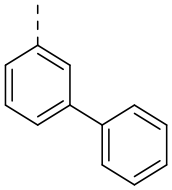	6	18	120
198	Cl	Ph	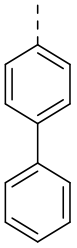	39	No Inhibition	238
199	Cl	Ph	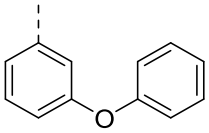	5	No Inhibition	424
200	Cl	Ph	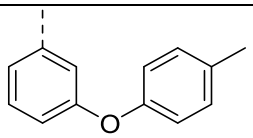	35	No Inhibition	116
201	Cl	Ph	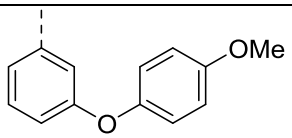	6	No Inhibition	149
202	NO_2	Ph	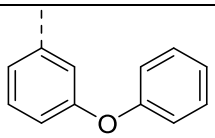	6	11	18
203	Br	Ph	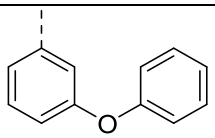	5	No Inhibition	8
204	Br	Bn	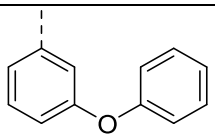	182	No Inhibition	No Inhibition
205	Cl	Ph	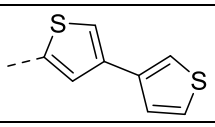	6	26	112

206	Cl	Ph	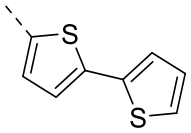	7	34	66

Figure 38: Overview of the effect of various substitution patterns of 7-substituted 8HQs on the potency and selectivity against KDM4C/E and KDM6B. Red designates potencies ≤ 25 µM, yellow potencies between 25 µM and 75 µM, and green potencies ≥ 75 µM.

Another exploration into increasing potency emerged from inspection of a co-crystal structure of KDM4A with a peptide fragment of the H3K9me3 substrate (PDB ID: 2OQ6) (Figure 39). The positively charged trimethyllysine residue sits in an electron-rich hydrophilic binding pocket which, after manual docking, is in close proximity to the amide-derived part of 7-substituted 8HQs. It was hence desirable to mimic the trimethyllysine substrate residue as a part of the small-molecule scaffold. Common trimethyllysine mimics are tertiary amines such as trimethylamine-derived moieties and *N*-substituted pyrrolidines.[183] By analogy with trimethyllysine, these mimics likely target a negatively charged binding pocket as they are primarily protonated under physiological pH. At the same time, the reversibility of protonation allows for desirable profiles of cell permeability and pharmacokinetics. Contemplations of molecular modelling and synthetic tractability led to the use of amine-, instead of amide-substituted 8HQs. While these compounds showed comparable potencies to the amide-derived inhibitors, they did not display any selectivity against KDM6B; the desired increase in potency was not observed (Figure 40).

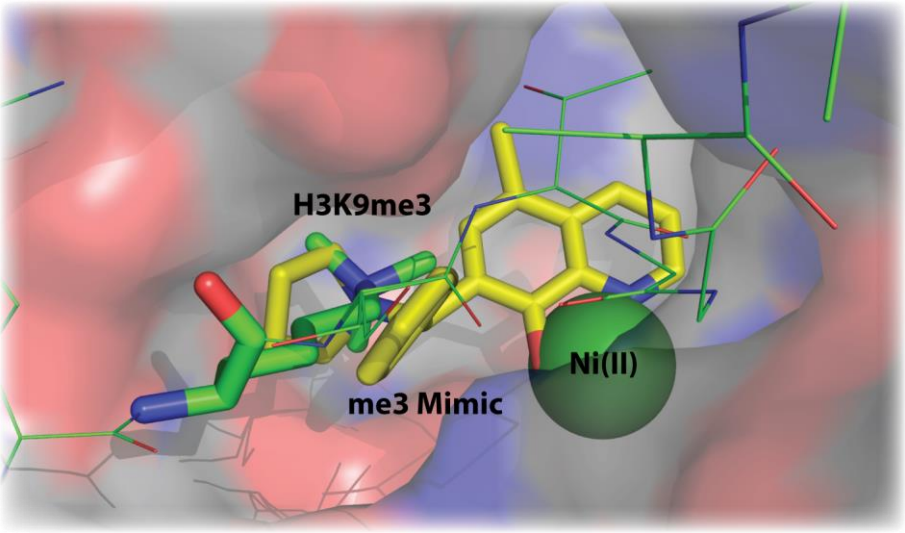

Figure 39: View from an X-ray crystal structure of KDM4A in complex with histone trimethyllysine peptide substrate (PDB ID: 2OQ6). The 7-substituted 8HQ was manually modelled into the active site and reveals that substitution with tertiary amines, instead of amides, may give an opportunity to target the positive charge of the protonated trimethyllysine mimic into the negatively charged KDM4 binding pocket which usually accommodates the substrate trimethyllysine residue.

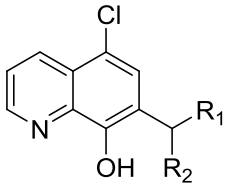

Compound	R_1 =	R_2 =	IC_{50} in µM (KDM4E)	IC_{50} in µM (KDM6B)
183	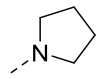		11	5
207	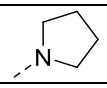	H	6	11
208	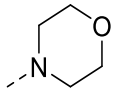	H	10	12
209	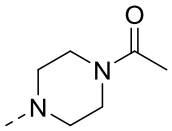	H	11	18
210	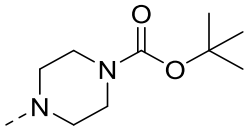	H	6	6

Figure 40: Overview of the effect of various tertiary amines intended to mimic trimethyllysine inside the substrate binding pocket. Red designates potencies ≤ 25 µM, yellow potencies between 25 µM and 75 µM, and green potencies ≥ 75 µM.

Further exploration of amide- and aldehyde-derived moieties did not result in increased potency (Table 4). Continuous extension of substitution patterns would unavoidably lead to compounds with borderline, if not unacceptable, physical properties for use as tool compounds. It was hence decided to shift subsequent synthetic efforts towards variation of the 8HQ-derived core.

Compound	R_1 =	R_2 =	IC_{50} in µM (KDM4C)	IC_{50} in µM (KDM4E)	IC_{50} in µM (KDM6B)
160	NH_2	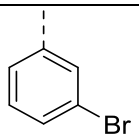	Not determined	10	11
161	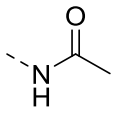	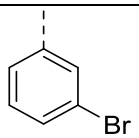	Not determined	25	255
166	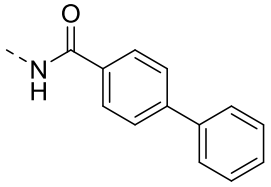	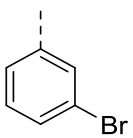	Not determined	38	No Inhibition
162	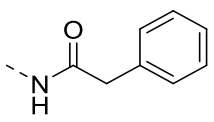	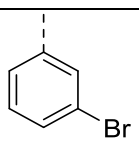	Not determined	24	120

211	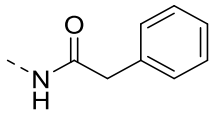		40	No inhibition	No inhibition
212	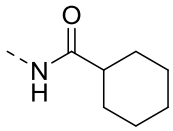		7	Not determined	253
213	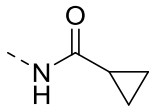		7	82	Not determined

Table 4: Overview of the effect of a selection of amide substitution patterns on the activity of 7-substituted 8HQs. Red designates potencies ≤ 25 µM, yellow potencies between 25 µM and 75 µM, and green potencies ≥ 75 µM.

Variation of the 8HQ Core

Substitution at positions 2-6 of the 8HQ core was tolerated for 7-substituted 8HQs. Simple methyl substitution of the 8HQ core even led to a slight increase in potency compared to previously synthesised compounds (Figure 41).

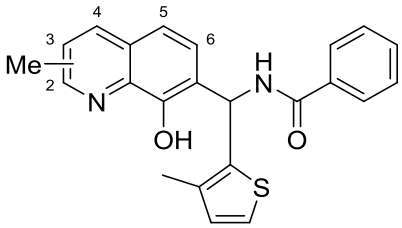

Compound	Position	IC_{50} in µM (KDM4C)	IC_{50} in µM (KDM4E)	IC_{50} in µM (KDM6B)
214	2	3	8	26
215	3	2	6	27
216	4	2	7	17
217	5	3	8	18
218	6	3	7	15

Figure 41: Overview of the effect of variation of the 8HQ core on the activity of 7-substituted 8HQs. Red designates potencies ≤ 25 µM, yellow potencies between 25 µM and 75 µM, and green potencies ≥ 75 µM.

The *in silico* docking model suggested that substitutions at either position 4 or 5 may be most beneficial for engaging in additional hydrogen bonding with Tyr132 and Lys206 in KDM4A, similar to the binding observed for IOX1 **47** (Figure 29). The 5-amino-8HQ **130** did only display a negligible increase in potency at the expense of selectivity against KDM6B. Furthermore, this compound proved relatively unstable with respect to degradation, possibly because of the high electron density of the 8HQ core. The 5-methoxy-substituted compound **219** also has the potential to engage in hydrogen bonding; again, the desired increase in potency was not detected, and selectivity against KDM6B was lost (Table 5). The 4- and 5-carboxy-substituted target

compounds, based on considerations of IOX1 **47** binding, were of considerable potential biochemical value, but their synthesis was unsuccessful (see Chapter II).

Compound	Structure	IC_{50} in µM (KDM4C)	IC_{50} in µM (KDM4E)	IC_{50} in µM (KDM6B)
130	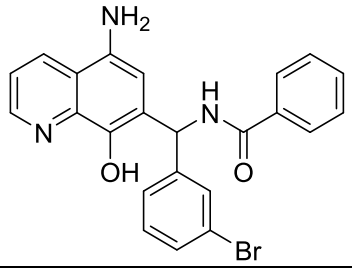	2	3	3
219	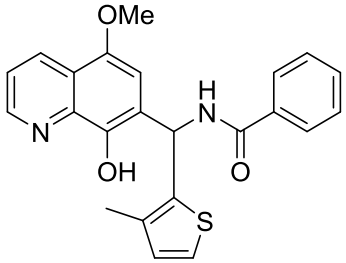	2	5	17

Table 5: Overview of the activity of 7-substituted 8HQs which possess heteroatoms at position 5 of the 8HQ core. Red designates potencies ≤ 25 µM, yellow potencies between 25 µM and 75 µM, and green potencies ≥ 75 µM.

Parallel investigations into co-crystallisation of **193** with KDM4A were largely unsuccessful. However, a low-resolution electron density map was obtained for one of the crystals and suggested movement of Phe185 relative to the corresponding structure of IOX1 **47** with KDM4A (Figure 29). This movement would give rise to an increase in size of the active site binding pocket and allow for substitution of the 8HQ moiety with larger substituents. In fact, 4-ethyl-substituted **220**, as well as 5-furanyl substituted **221**, showed inhibition of KDM4C. Ethyl substitution and 5-furanyl substitutions do not appear to be tolerated by inspection of the *in silico* docking model, but are tolerated when Phe185 is rotated accordingly because this movement results in an enlargement of the active site binding pocket. Therefore, it is possible that the Phe185 movement suggested from the low-resolution crystal structure may offer additional scope for compound optimisation by derivatisation of the 8HQ moiety, for example *via* the previously optimised palladium-catalysed cross-coupling reactions (see Chapter II).

Compound	Structure	IC_{50} in µM (KDM4C)	IC_{50} in µM (KDM4E)
220	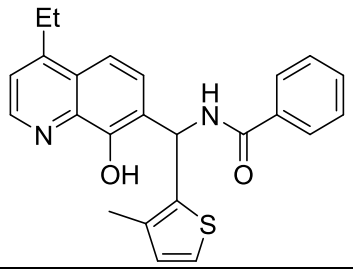	5	5
221	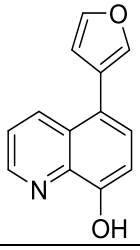	4	Not determined

Table 6: Overview of the activity of 4-ethyl-substituted 8HQ **220** and 5-substituted **221** on the KDM4 demethylases.

Cellular Characterisation

The biological effect of 7-substituted 8HQs in cells was assessed by antibody-based immunofluorescence (IF).[136] Indirect detection was used by which fluorophore-linked secondary antibodies were targeted towards the H3K9me3-specific primary antibodies. Higher fluorescence therefore correlates with higher degrees of KDM inhibition.

A random selection of early-stage compounds which showed reasonable *in vitro* activity against KDM4E was tested in HeLa cells with overexpressed KDM4A (experiment performed by Dr Clarence Yapp) (Figure 42). Each of the selected compounds showed activity in cells by stabilising the H3K9me3 mark with EC_{50} values in the micromolar range. Overall, the compounds are more potent than the IOX1 **47** control compound. It is notable that the potencies in cells are of the same order of magnitude as the corresponding *in vitro* potencies.

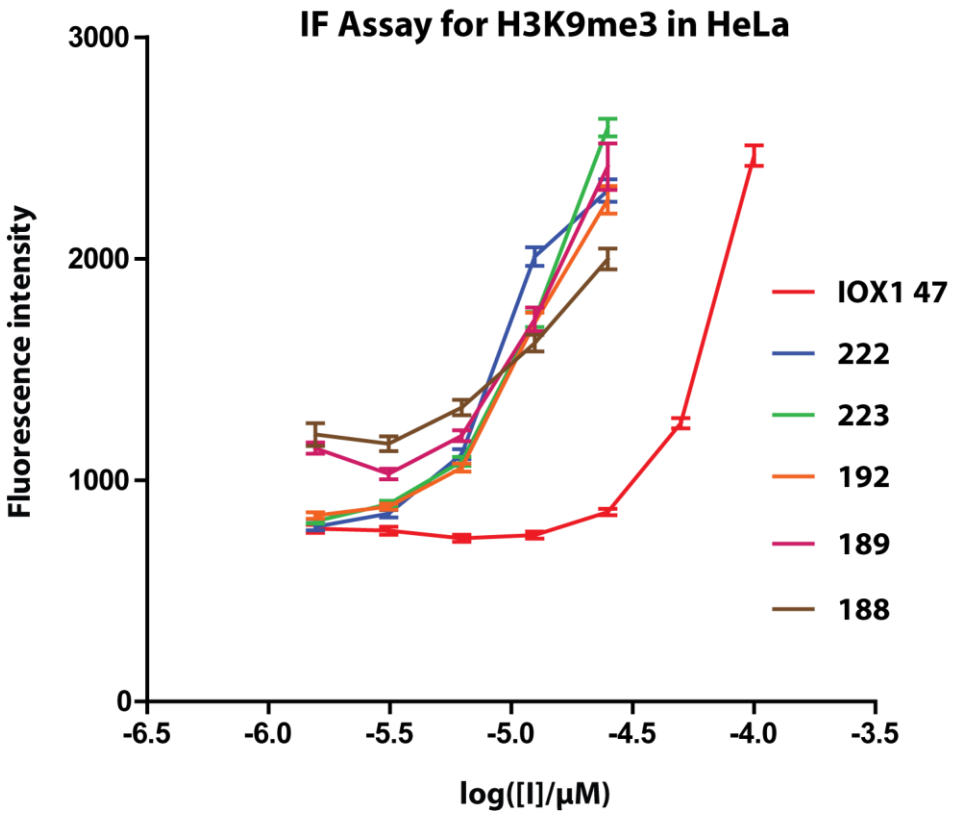

Compound	Structure	*In vitro* IC_{50} in µM (KDM4)	Cellular EC_{50} in µM (KDM4A)	*In vitro* IC_{50} in µM (KDM6B)
222	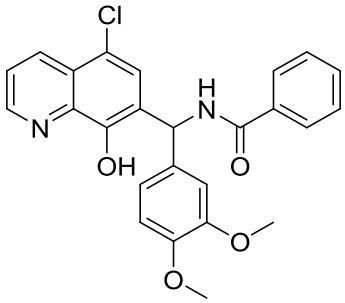	5 (KDM4E)	11	No inhibition
223	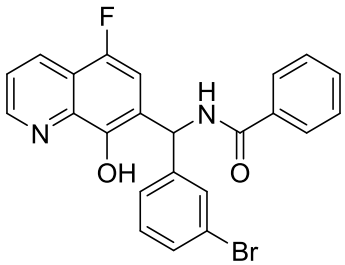	9 (KDM4E)	12	No inhibition
192	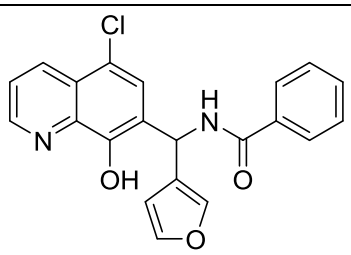	22 (KDM4E)	16	No inhibition

189	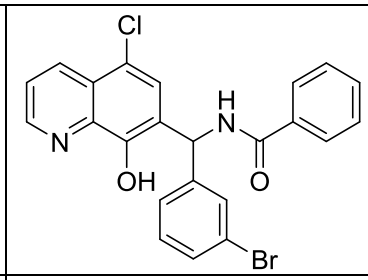	19 (KDM4E)	17	433
188	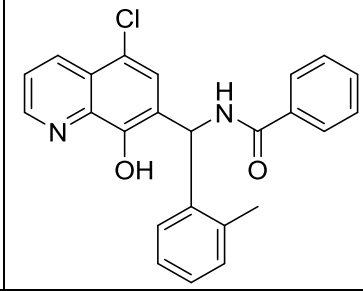	9 (KDM4C)	33	123
47	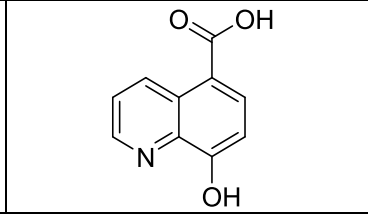	0.29 (KDM4A)	86	0.12

Figure 42: Summary of activity in HeLa cells of a selection of 7-substituted 8HQs as determined by immunofluorescence. Quantitation of H3K9me3 levels was assessed in biological triplicates. Data points represent the arithmetic average for each triplicate with the corresponding standard deviation plotted as error bar. Red designates potencies ≤ 25 µM, yellow potencies between 25 µM and 75 µM, and green potencies ≥ 75 µM.

Given both good *in vitro* potency (IC_{50} = 5 µM) and selectivity profiles, in addition to the favourable activity in cells (EC_{50} = 9 µM), as well as reasonable physicochemical properties, **193** was selected as a lead compound. The IF experiment with overexpressed KDM4A in HeLa cells was repeated and confirmed the EC_{50} value of 9 µM, one order of magnitude more potent than IOX1 **47**, which displays an EC_{50} of 86 µM (Figure 43). One prominent feature of the dose-response curve is the sudden drop of fluorescence intensity at high compound concentration, which was initially attributed to cytotoxicity. To assess whether this cytotoxicity was an on-target effect or merely an idiosynchratic effect of the selected chemotype, **224** was synthesised as a negative control compound. **224** is structurally very similar to lead compound **193**, and should likely show very similar physical properties to **193**, but its metal-chelating properties are disrupted by methylation of the phenol oxygen: Fe(II) binding inside the KDM4 active site should therefore not occur and the compound should be inactive. This lack of activity is in indeed observed *in vitro*. In cells, as well, this compound had no effect on the H3K9me3 mark, and it did not affect cell proliferation. These results suggest that cytotoxicity may be due to an on-target effect of KDM4 inhibition (Figure 43).

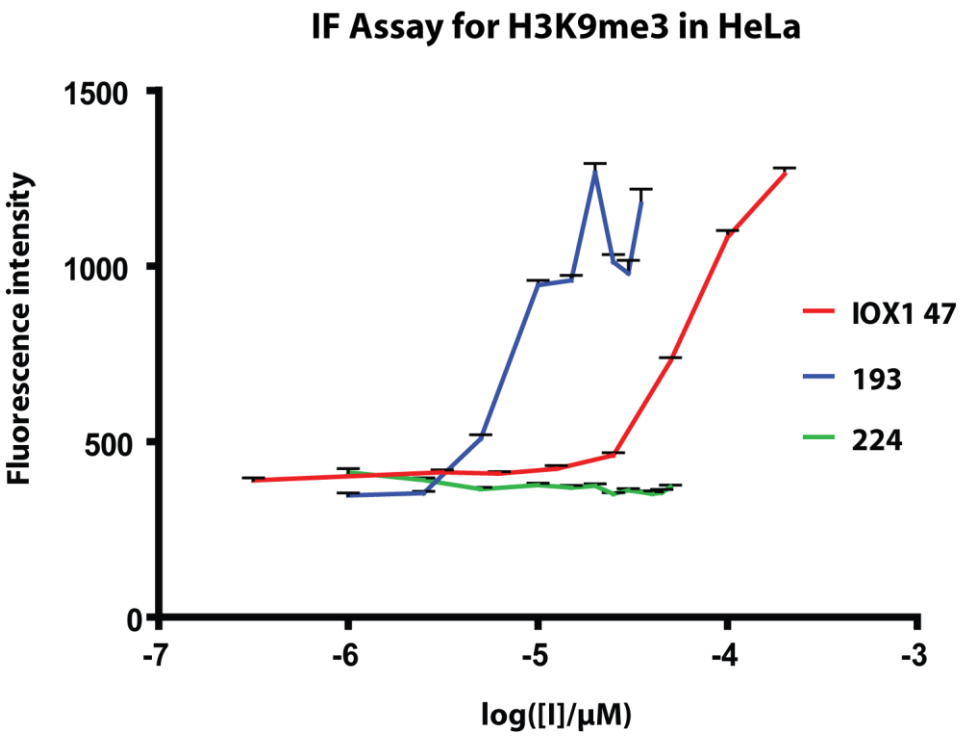

Compound	Structure	*In vitro* IC_{50} in µM (KDM4)	Cellular EC_{50} in µM (KDM4A)	*In vitro* IC_{50} in µM (KDM6B)
193	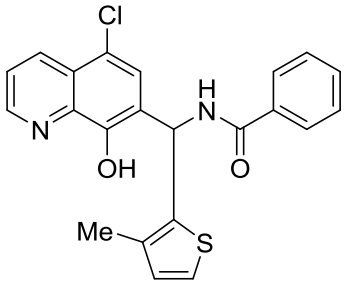	5 (KDM4E)	9	106
224	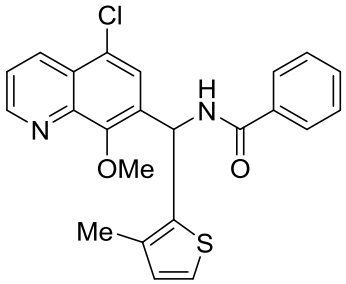	No inhibition	No inhibition	No inhibition

Figure 43: Summary of activity in HeLa cells of lead compound **193** and the corresponding negative control compound **224** alongside IOX1 **47** as determined by immunofluorescence. Quantitation of H3K9me3 levels was assessed in biological triplicates. Data points represent the arithmetic average for each triplicate with the corresponding standard deviation plotted as error bar. Red designates potencies ≤ 25 µM, yellow potencies between 25 µM and 75 µM, and green potencies ≥ 75 µM.

A cell proliferation assay in HeLa cells (performed by Dr Clarence Yapp) revealed an EC_{50} of 25 µM for **193**, and no effect for **224** (Figure 44).[184] Inspection of the cells inside the IF assay plate revealed cell growth arrest, rather than cell death, at high concentrations of **193** (Figure 45). Cell growth arrest is hence considered to be at the basis of the reduced fluorescence intensity at high compound concentration for the IF dose-response curves.

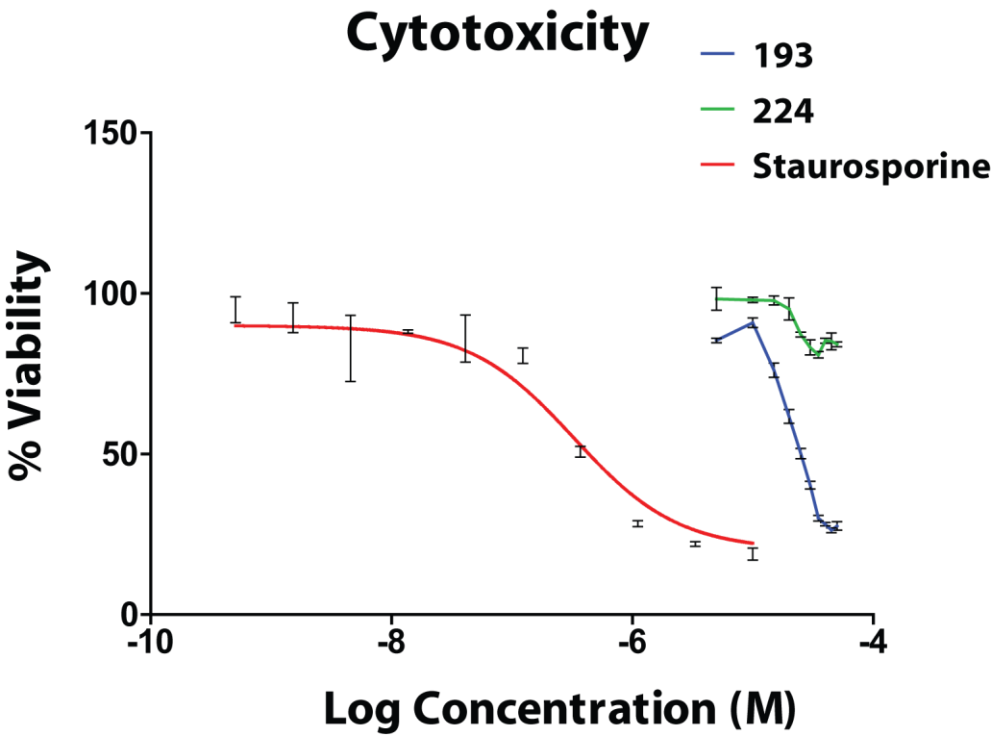

Figure 44: Cytotoxicity of lead compound **193** and the corresponding negative control compound **224** alongside staurosporine as assessed by CellTiter (Promega) cell proliferation assay in HeLa cells. Quantitation of cell number was assessed in biological triplicates. Data points represent the arithmetic average for each triplicate with the corresponding standard deviation plotted as error bar.

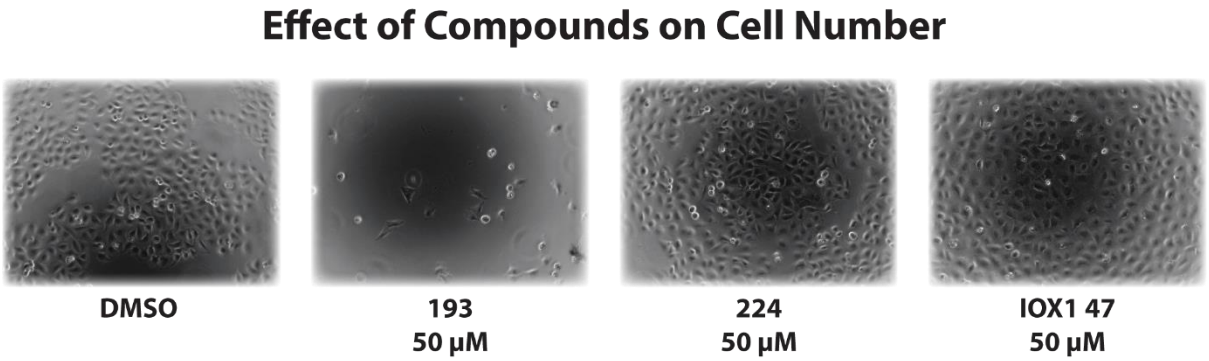

Figure 45: Pictures of HeLa cells used for IF assay after treatment with various compounds. **224** and IOX1 **47** have little effect on cell proliferation relative to the DMSO control under the given conditions. Cells treated with **193** are viable: it seems as if **193** does not induce cell death, but inhibits cell proliferation.

Given the increased KDM4 levels in breast cancer, the effect of **193** was investigated in the MCF7 breast cancer cell line at endogenous levels of KDM4. The cell proliferation assay gave an EC_{50} of 22 µM (Figure 46). Inspection of the IF assay plates indicated that **193**, but not **224**, inhibits cell proliferation (Figure 47). Again in line with the HeLa experiments, **193** had an EC_{50} of 12 µM, whereas **224** showed no effect (Figure 48). Overall, the biological effect of **193** is about ten-fold more pronounced than that of control compound IOX1 **47**.

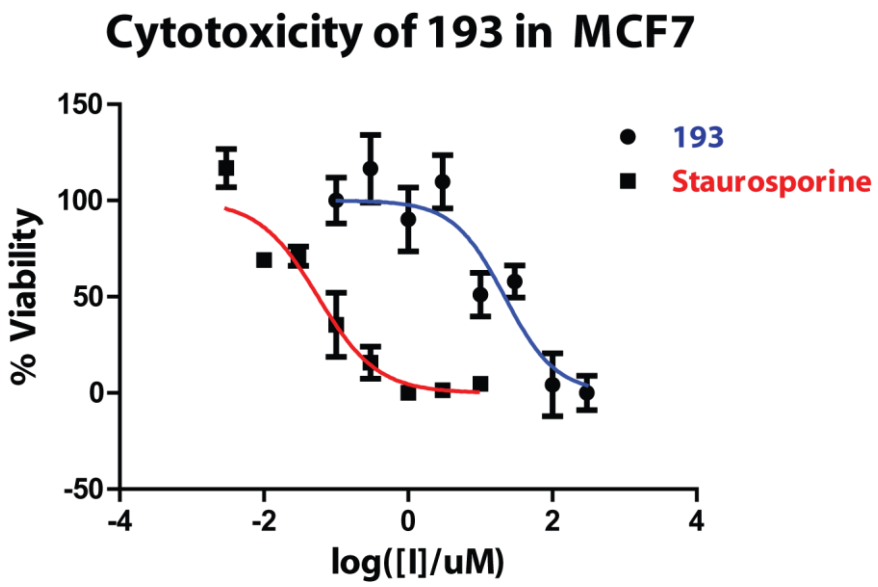

Figure 46: Cytotoxicity of lead compound **193** alongside staurosporine as assessed by CellTiter (Promega) cell proliferation assay in MCF7 cells. Quantitation of cell number was assessed in biological triplicates. Data points represent the arithmetic average for each triplicate with the corresponding standard deviation plotted as error bar.

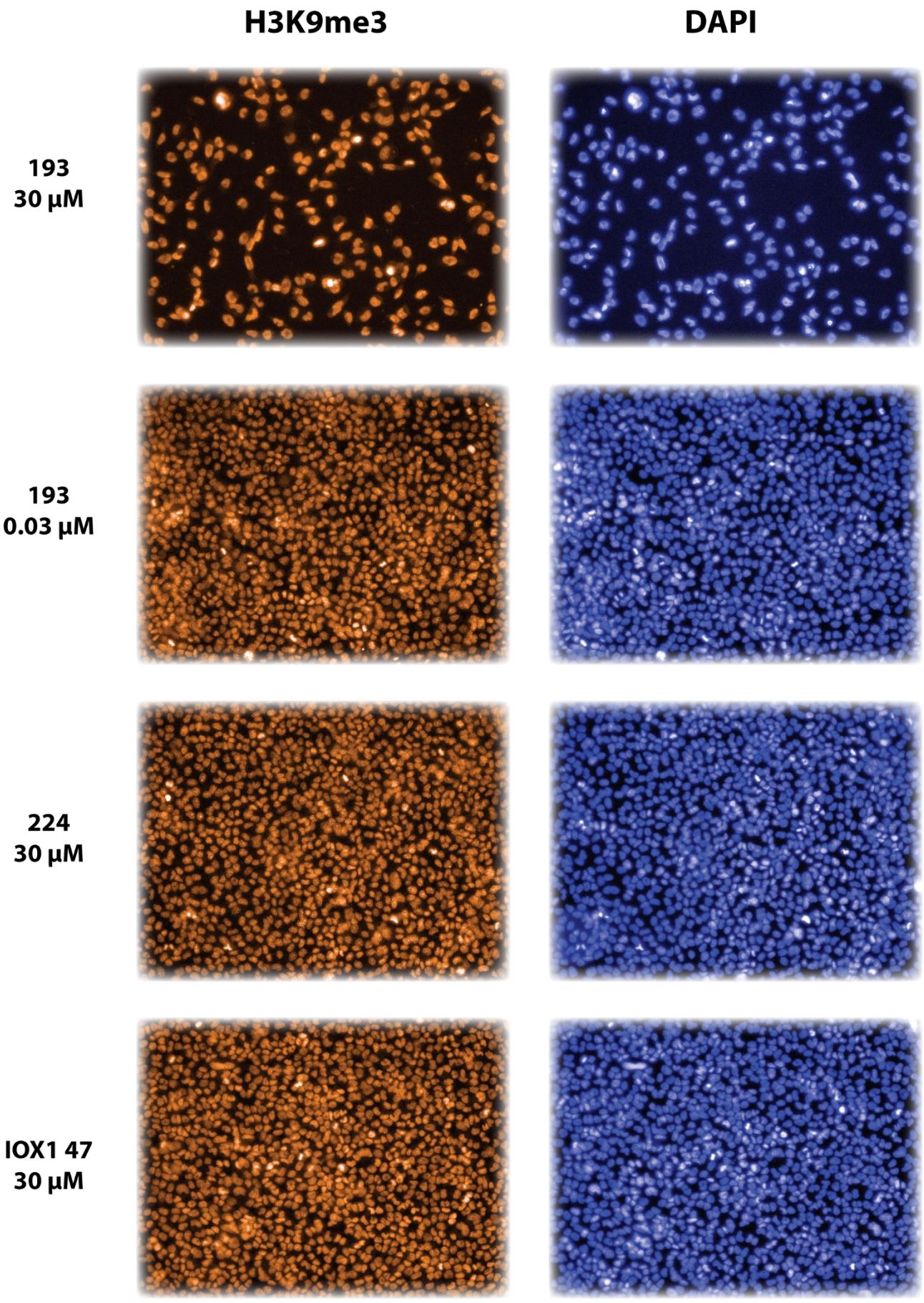

Figure 47: Snapshots of MCF7 cells grown in the presence of the stated small molecules for 3 days. Rabbit anti-H3K9me3 antibody (AB8898) was monitored with Alexafluor 568 goat anti-rabbit IgG.

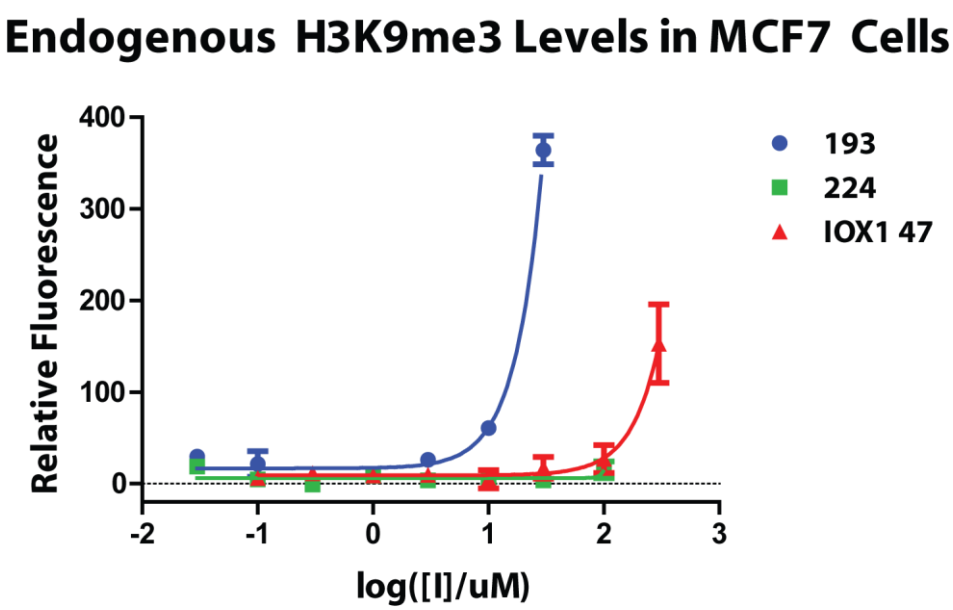

Figure 48: Activity in MCF7 cells of lead compound **193** and the corresponding negative control compound **224** alongside IOX1 **47** as determined by immunofluorescence. Quantitation of H3K9me3 levels was assessed in biological triplicates at endogenous KDM4 expression levels. Data points represent the arithmetic average for each triplicate with the corresponding standard deviation plotted as error bar.

Evidence that KDM4 histone demethylases are overexpressed in lung cancers led to the comparison of the effect of **193** in patient-matched cell lines, one derived from cancerous, the other derived from normal lung of the same patient: non-tumorigenic human bronchial epithelial cells (HBECT30KT) and human carcinoma cells (HCC4017) (experiment performed by Dr Anh Tran, Martinez group, UT Southwester Medical Center, Texas).[185] Strikingly, **193** had a marked effect on the viability of HCC4017 cancer cells only, with an EC_{50} of 6 µM, whereas the non-cancer cells were relatively unaffected. Control compound **224** had little effect on either cell line (Figure 49).

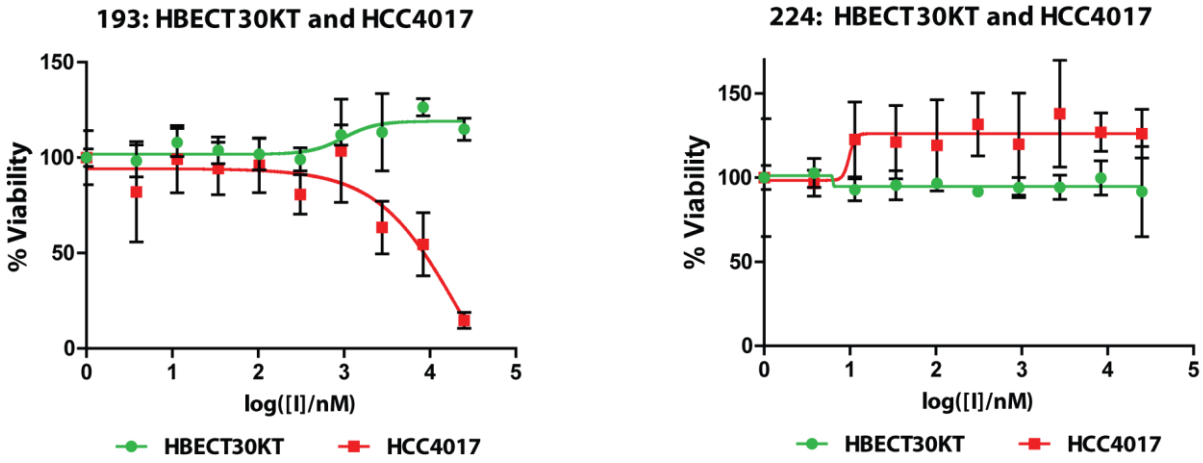

Figure 49: Cell viability dose response curves for patient-matched lines from normal and cancerous lungs treated with **193** and inactive control compound **224** over four days suggest cancer specificity of **193**. Error bars represent standard deviation across eight replicates.

Global Effect on Histone Modification

Methodologies for isolation, separation, and mass analysis of whole histones were developed and optimised in our group by Kuo-Feng Hsu and created an opportunity to test the effect of lead compound **193** on global histone modifications (experiment performed by Kuo-Feng Hsu).

Histones H3.1 and H3.2 from HEK293T cells treated with **193** showed significantly reduced amounts of global histone modification than the corresponding histones from untreated cells (Figure 50). The compound appeared to have no effect on histones H2A, H2B, and H4. These observations are in line with the assumption that **193** is a KDM4 inhibitor, and the current knowledge that KDM4s are demethylases specific for H3, but not other histones.

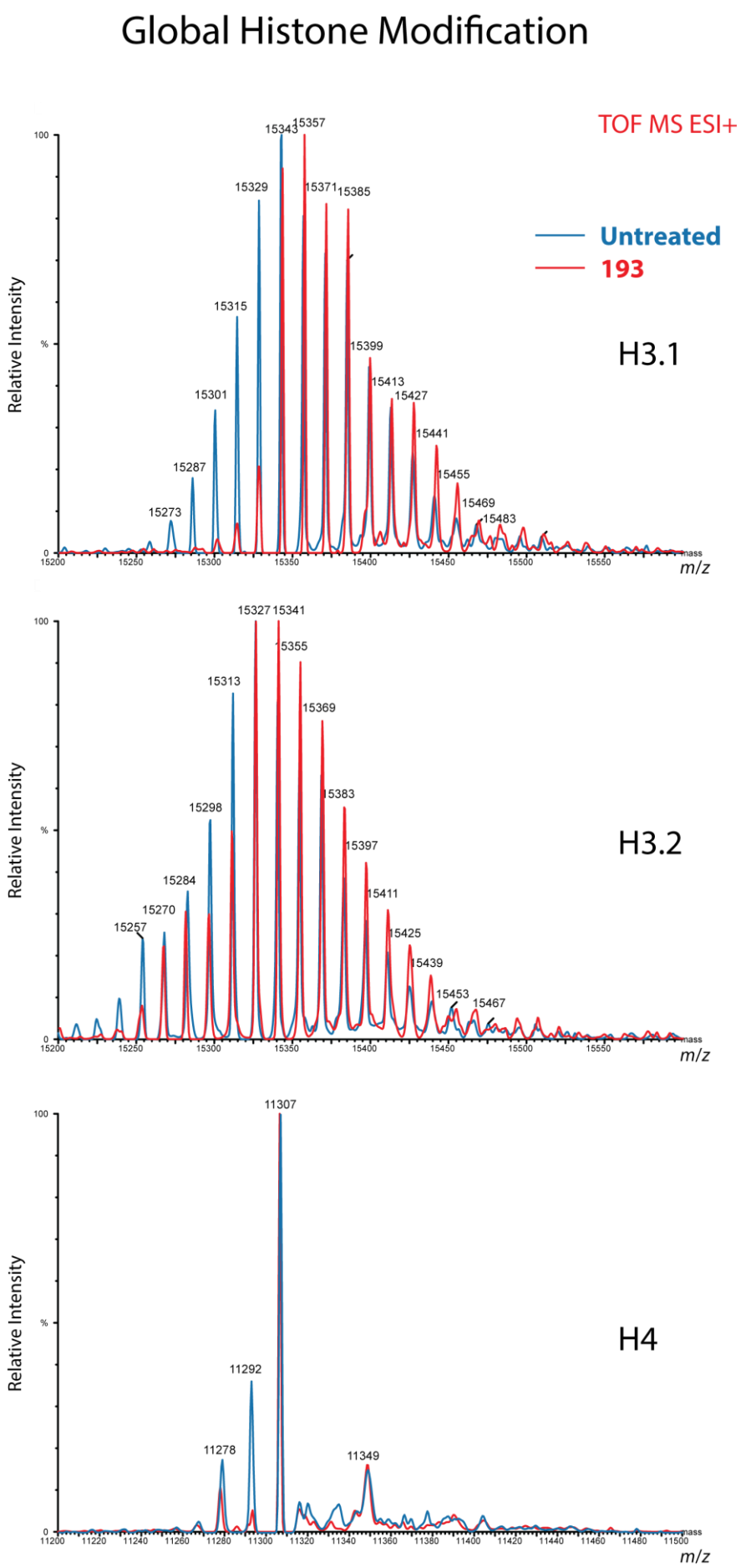

Figure 50: LC-MS analysis of histones extracted from HEK293T cells after treatment with 30 µM of **193** for 24 h under normoxic conditions.

Modulation of the Hypoxic Response Pathway

The inhibitory effect of 7-substituted 8HQs on the 2OG-dependent prolyl hydroxylase PHD2 was of interest given the precedented work linking 7-substituted 8HQs to the hypoxic response in cells.[186] One of the first focused libraries of 7-substituted 8HQs was therefore screened against PHD2, but none of the initially screened compounds inhibited PHD2 *in vitro*.

Subsequent studies with KDM4-selective **193** and **199**, as well as unselective **225**, in RCC4 cells, however, indicated strong stabilisation of HIF, comparable to the effect of the PHD2-specific inhibitor IOX2 **29** (see Chapters I and VI), by treating the cells with a final inhibitor concentration of 5 µM and 10 µM. It seems that CODD, NODD, and CAD hydroxylation is inhibited in the presence of these compounds (experiment performed by Dr Andrew Chan) (Figure 51). Intracellular PHD2 levels seem unaffected by the inhibitors. The effect of these compounds on the PHD2 prolyl hydroxylase was therefore reconsidered.

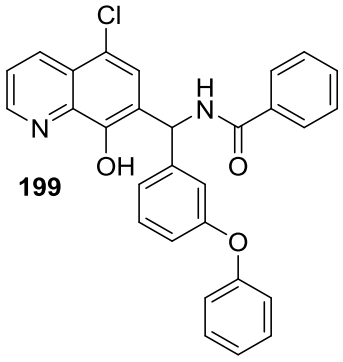

199

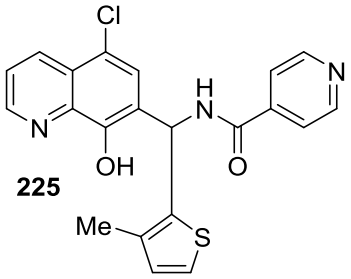

225

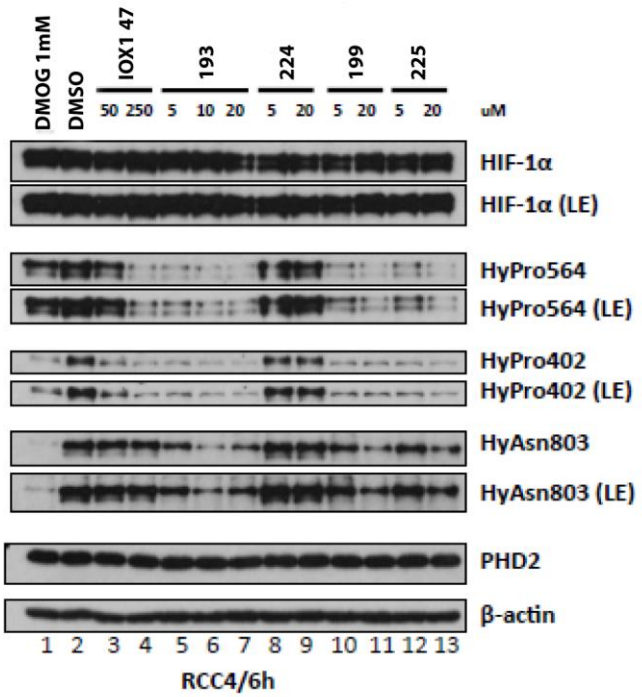

Figure 51: WesternBlot analysis of the effects of **193**, **224**, **199**, and **225** on HIF-1α, CODD, NODD, and CAD, as well as PHD2 expression levels after treatment of RCC4 cells for 6 h.

In line with previously obtained results, **193** displayed negligible potency against PHD2 *in vitro* by MALDI-TOF MS activity assay. AlphaScreen® indicated an IC_{50} of 96 µM (dose response obtained by Dr Tzu-Lan Yeh), potency which does not correlate with the strong stabilisation of HIF in cells with 5, 10, or 20 µM final compound concentration (Figure 52). 2OG displacement studies by NMR also indicated an IC_{50} > 100 µM against recombinant PHD2 (dose response obtained by Dr Ivanhoe Leung, results not shown). Non-denaturing mass spectrometry of PHD2, too, did not indicate binding of **193** to PHD2, neither did it indicate an alternative mechanism of PHD2 inhibition by which **193** was postulated to induce ejection of the active site Fe(II) (experiment performed by Hanna Tarhonskaya) (Figure 52). Stabilisation of HIF *via* direct inhibition of PHD2 hence seems unlikely. Alternative explanations for stabilisation of HIF may be chelation of Fe(II), induction of a stress response, or an alternative mechanism, potentially *via* a KDM4-mediated pathway.

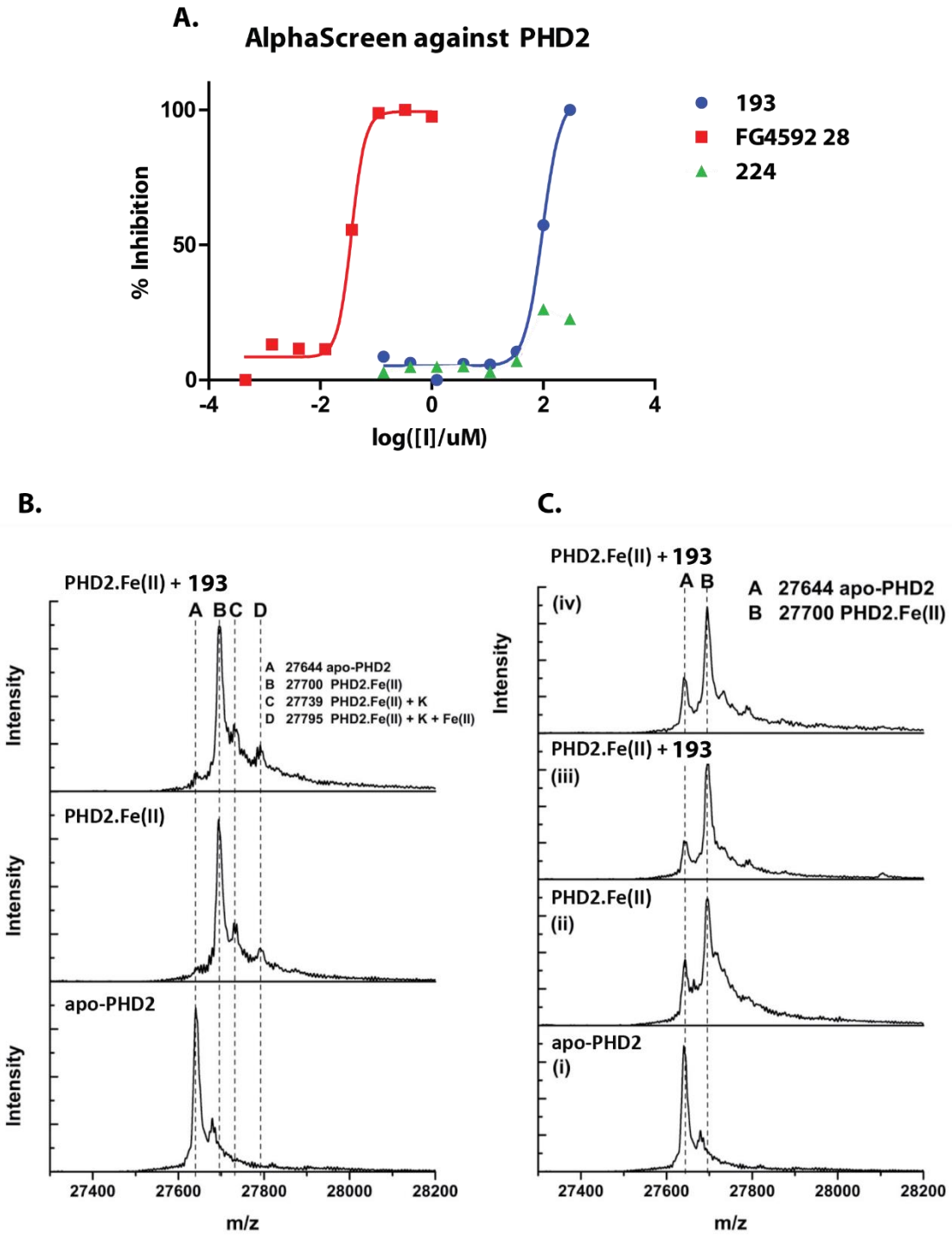

Figure 52: A. Activity of **193**, **224**, and FG4592 **28** against PHD2 as measured by AlphaScreen® assay. **B.** Native mass spectrometry analysis of equimolar amounts (15 µM each) of PHD2, Fe(II) and **193** in ammonium acetate buffer, 15 mM, pH 7.5. **C.** (i) apo-PHD2 (15 µM); (ii) apo-PHD2 (15 µM), Fe(II) (7 µM); (iii) apo-PHD2 (15 µM), Fe(II) (7 µM), **193** (15 µM); (iv) apo-PHD2 (15 µM), Fe(II) (7 µM), **193** (78 µM).

Summary

The template-based inhibition strategy was validated by adopting a blue-skies approach for the generation of KDM4-selective inhibitors. Iterative medicinal chemistry generated a library of small molecules which cover a wide range of potencies and selectivities, ultimately leading to a bias of the library towards potent

and selective inhibitors for the KDM4 subfamily. Systematic diversification of inhibitors and concomitant testing led to an *in silico* model based on both structure-activity and structure-selectivity relationships which was used as a guide for subsequent inhibitor design.

The attractiveness of selected promising 7-substituted 8HQs lies in their respective potencies in cells. It is remarkable that their apparent potencies in cells are of the same order of magnitude as their potencies *in vitro*.

The 3-methylthiophene derivative **193** was selected as a lead compound based on its favourable potency and selectivity profile *in vitro* (Figure 53). The compound has an EC_{50} of 9 µM for KDM4A and is not only more selective than the 'gold-standard' IOX1 **47**, but also more potent in cells by one order of magnitude. The structurally closely related negative control compound **224** was synthesised by methylation of the **193** phenol moiety, hereby preventing the ability of the compound to engage in metal chelation and consequently rendering it inactive.

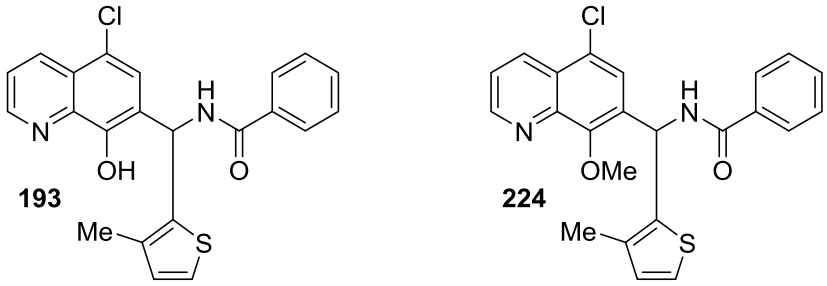

Compound	KDM4C	KDM4E	KDM2A	KDM3A	KDM5C	KDM6B	PHD2
193	5 µM	5 µM	34 µM	191 µM	178 µM	106 µM	96 µM
224	No effect	No effect	No effect	No effect	No effect	No effect	No effect

Figure 53: Summary of the effect of lead compound **193**, and negative control **224**, on a selection of 2OG oxygenases *in vitro*. The values are given as IC_{50}.

Lead compound **193** stabilises the H3K9me3 mark at endogenous KDM levels in MCF7 cells, where it also exerts a cytostatic effect. In patient-matched cell lines, one from lung cancer, one from healthy lung of the same patient, **193** appears to selectively reduce the viability of the lung cancer cells. Compound **193** also has an effect on the global profile of post-translational histone modification on H3, but not H2A, H2B, or H4, in line with the findings that the KDM4 subfamily acts on H3.

Recent findings display a strong HIF stabilisation effect of **193** in cells at low compound concentrations. The compound is a weak inhibitor of PHD2 *in vitro*, and has not been shown to bind to the catalytic domain of PHD2. Possible explanations for this effect may relate to a generic stress response, metal chelation, or a PHD2-indepent pathway for HIF stabilisation. Further research into the mechanism of HIF stabilisation *via* **193** is ongoing.

Compound Characterisation

General Procedure 1 for Betti-Type Amidoalkylation Reactions

The requisite 8HQ (1.0 eq.), amide (1.0 eq.), and aldehyde (2.0 eq.) were stirred between 130 °C and 180 °C for 3 h. Toluene (5 mL) was added and the reaction mixture allowed to cool to RT. The resulting precipitate was washed with toluene (3 × 5 mL), Et_2O (3 × 5 mL), and MeOH (3 x 5 mL) before being dried under reduced pressure to give the target compounds, typically without requirement for further purification, unless specified otherwise.

General Procedure 2 for the Synthesis of 8-Hydroxyquinolines

A solution of the required 2-aminophenol (1 eq.) in HCl (6 N aq.) was stirred under reflux. The specified acrolein (1.5 eq.) was then slowly added, drop by drop, and the resulting reaction mixture was stirred for another 2 h under reflux. After cooling to room temperature, the pH was adjusted to 7 with a solution of NaOH (6 N aq.). The aqueous reaction mixture was extracted three times with EtOAc. The combined organic layers were washed with brine, dried over anhydrous $MgSO_4$, and concentrated *in vacuo*. The crude product was purified *via* flash column chromatography (5 % - 20 % EtOAc, cyclohexane) to give the desired compound.

8-Hydroxyquinoline-4-carboxylic acid **24**[173]

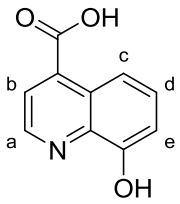

129 (1 g, 3.95 mmol) was dissolved in a solution of potassium hydroxide (5 g, 89.3 mmol) in water. The solvent was evaporated under reduced pressure. The residue was heated to above 300 °C with a heat gun until a colour change from off-white to dark yellow occurred. The residue was left to cool to room temperature and dissolved in water (200 mL). The pH was adjusted to 4.5 with aqueous hydrochloric acid and the solution was extracted with ethyl acetate (500 mL) three times. The combined organic layers were combined and dried over anhydrous Na_2SO_4 and the solvent was evaporated to give **24** (542 mg, 73 %) as a yellow solid.

mp 259 °C; ν_{max}/cm^{-1} 2539 (O-H); δ_H (400 MHz, DMSO-d_6) 8.96 (1 H, d, *J*=4.5 Hz, H_a), 8.07 (1 H, d, *J*=8.0 Hz, H_e), 7.93 (1 H, d, *J*=4.5 Hz, H_b), 7.54 (1 H, t, *J*=8.0 Hz, H_d), 7.15 (1 H, d, *J*=8.0 Hz, H_c); δ_C (100 MHz, DMSO-d_6) 168.6 (*C*=O), 154.5, 148.6, 140.2, 137.3, 129.8, 126.2, 123.2, 116.2, 112.4; *m*/*z* (ESI$^-$) 188 ([M-H]$^-$); HRMS (ESI$^+$) $C_{10}H_8NO_3$, ([M+H]$^+$) requires 190.0499; found 190.0501.

N-((3,4-Dimethoxyphenyl)(8-hydroxyquinolin-7-yl)methyl)-3-methylbutanamide **48**

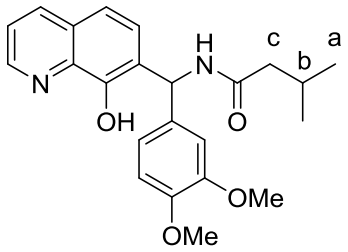

Following general procedure 1, 8-hydroxyquinoline (290 mg, 2.0 mmol), isovaleramide (202 mg, 2.0 mmol) and 3,4-dimethoxybenzaldehyde (644 mg, 4.0 mmol) gave **48** (103 mg, 13 %) as a beige powder.

mp 193 °C; ν_{max}/cm^{-1} 3270 (NH), 2861 (OH), 1633 (C=O); δ_H (400 MHz, $CDCl_3$) 8.69 - 8.80 (1 H, m, quinoline-*Ar*), 8.10 - 8.20 (1 H, m, quinoline-*Ar*), 7.40 - 7.50 (2 H, m, *Ar*), 7.32 - 7.38 (1 H, m, *Ar*), 7.18 - 7.23 (1 H, m, *Ar*), 6.96 - 7.01 (1 H, m, *Ar*), 6.77 - 6.83 (1 H, m, *Ar*), 6.72 - 6.77 (1 H, m, *Ar*), 6.55 (1 H, d, *J*=9.0 Hz, benzyl-*H*), 3.82 (3 H, s, OCH_3), 3.81 (3 H, s, OCH_3), 2.05 - 2.27 (3 H, m, $H_{b/c}$), 0.96 (6 H, dd, *J*=12.0, 6.0 Hz, CH_{3a}); δ_C (100 MHz, $CDCl_3$) 171.6 (*C*=O), 149.1, 149.0148.2, 138.3, 136.1, 134.3, 128.4, 127.7, 122.6, 121.9, 118.9, 118.0, 110.8, 110.5, 55.8 (OCH_3), 55.8 (OCH_3), 54.3 (benzyl-*C*), 46.3 (C_c), 26.3 (C_b), 22.5 (C_a); *m*/*z* (ESI$^-$) 393 ([M-H]$^-$); HRMS (ESI$^+$) $C_{23}H_{27}N_2O_4$, ([M+H]$^+$) requires 395.1965; found 395.1969.

7-((4-Chlorophenyl)((3-hydroxypyridin-2-yl)amino)methyl)quinolin-8-ol **49**[186]

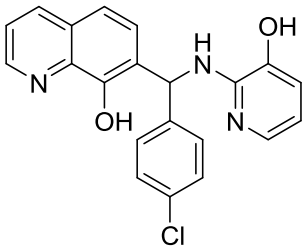

A solution of 8-hydroxyquinoline (2.9 g, 20 mmol), 4-chlorobenzaldehyde (2.8 g, 20 mmol), and 2-amino-4-hydroxypyridine (2.2 g, 20 mmol) in ethanol (50 mL) was stirred for 72 h at room temperature. The resulting precipitate was filtered, washed with EtOH, H_2O, and dried to give **49** (2.6 g, 34 %) as an off-white powder.

mp 189 °C; ν_{max}/cm^{-1} 3338 (OH); δ_H (400 MHz, DMSO-d_6) 8.80 - 8.91 (1 H, m, quinoline-*Ar*), 8.20 - 8.41 (1 H, m, quinoline-*Ar*), 7.64 - 7.72 (1 H, m, quinoline-*Ar*), 7.51 - 7.57 (1 H, m, *Ar*), 7.46 - 7.50 (1 H, m, *Ar*), 7.30 - 7.44 (5 H, m, *Ar*), 6.81 - 6.93 (2 H, m, *Ar*), 6.39 - 6.48 (2 H, m, *Ar*); δ_C (100 MHz, DMSO-d_6) 150.3, 148.8, 148.8, 143.3, 140.1, 138.7, 137.6, 136.5, 131.4, 129.2, 128.5, 128.1, 127.8, 125.6, 122.2, 118.5, 118.0, 112.9, 53.0 (benzyl-*C*); *m*/*z* (ESI$^-$) 376 ([M-H]$^-$); HRMS (ESI$^+$) $C_{21}H_{17}O_2N_3Cl$, ([M+H]$^+$) requires 378.1004; found 378.0999.

N-((8-Hydroxyquinolin-7-yl)(phenyl)methyl)benzamide **50**

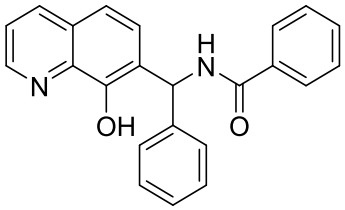

Following general procedure 1, 8-hydroxyquinoline (290 mg, 2.0 mmol), benzamide (242 mg, 2.0 mmol) and benzaldehyde (406 µL, 4.0 mmol) gave **50** (295 mg, 42 %) as an off-white powder.

mp 190-192 °C; ν_{max}/cm^{-1} 3328 (NH), 3058 (OH), 1640 (C=O); δ_H (400 MHz, DMSO-d_6) 10.04 (1 H, br. s., N-*H*), 9.17 - 9.33 (1 H, m, quinoline-*Ar*), 8.79 - 8.94 (1 H, m, quinoline-*Ar*), 8.24 - 8.38 (1 H, m, quinoline-*Ar*), 7.88 - 8.03 (2 H, m, quinoline-*Ar*), 7.66 - 7.77 (1 H, m, *Ar*), 7.51 - 7.61 (2 H, m, *Ar*), 7.39 - 7.51 (3 H, m, *Ar*), 7.28 - 7.38 (4 H, m, *Ar*), 7.24 (1 H, br. s., O-*H*), 7.02 (1 H, d, *J*=8.0 Hz, benzyl-*H*); δ_C (100 MHz, DMSO-d_6) 166.8 (*C*=O), 150.6, 149.2, 143.0, 138.9, 136.9, 135.3, 132.1, 129.1, 129.0, 128.5, 128.1, 127.8, 127.7, 125.2, 122.7, 118.2, 51.4 (benzyl-*C*); *m*/*z* (ESI$^-$) 353 ([M-H]$^-$, 100 %); HRMS (ESI$^+$) $C_{23}H_{19}N_2O_2$, ([M+H]$^+$) requires 355.1441; found 355.1434.

50 *via* Ritter Reaction

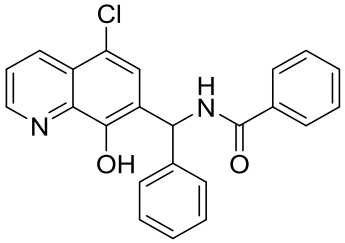

A solution of 5-chloro-8-hydroxyquinoline (180 mg, 1 mmol), benzaldehyde (102 µL, 1 mmol), and trifluoromethanesulfonic acid (178 µL, 2 mmol) in benzonitrile (5 mL) was stirred at 150 °C for 16 h. The

reaction mixture was then allowed to cool to room temperature, after which H_2O was added. The resulting precipitate was collected by filtration and dried *in vacuo* to give **50** (93 mg, 24 %) as an off-white solid.

Experimental analysis consistent with **50** obtained *via* Betti-type reaction.

N-((5-Chloro-8-hydroxyquinolin-7-yl)(phenyl)methyl)benzamide **61**

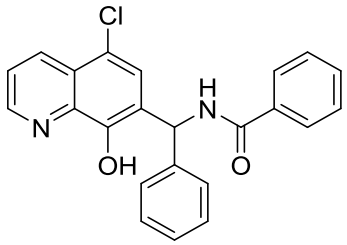

Following general procedure 1, 5-chloro-8-hydroxyquinoline (359 mg, 2.0 mmol), benzamide (242 mg, 2.0 mmol) and benzaldehyde (406 µL, 4.0 mmol) gave **61** (662 mg, 85 %) as a white powder.

mp 244 °C; ν_{max}/cm^{-1} 3330 (NH), 3063 (OH), 1636 (C=O); δ_H (400 MHz, DMSO-d_6) 10.42 (1 H, br. s., N-*H*), 9.19 - 9.33 (1 H, m, quinoline-*Ar*), 8.92 - 9.04 (1 H, m, quinoline-*Ar*), 8.42 - 8.54 (1 H, m, quinoline-*Ar*), 7.90 - 8.01 (2 H, m, *Ar*), 7.87 (1 H, s, *Ar*), 7.68 - 7.78 (1 H, m, *Ar*), 7.52 - 7.59 (1 H, m, *Ar*), 7.45 - 7.52 (2 H, m, *Ar*), 7.31 - 7.37 (4 H, m, *Ar*), 7.22 - 7.30 (1 H, m, *Ar*), 7.03 (1 H, d, *J*=8.5 Hz, benzyl-*H*); δ_C (100 MHz, DMSO-d_6) 166.9 (*C*=O), 150.4, 150.1, 142.5, 139.5, 135.1, 133.4, 132.3, 129.3, 129.1, 128.5, 128.0, 127.9, 127.7, 125.9, 125.8, 123.9, 119.4, 50.9 (benzyl-*C*); *m/z* (ESI$^-$) 387 ([M-H]$^-$, 100 %); HRMS (ESI$^+$) $C_{23}H_{17}ClN_2NaO_2$, ([M+Na]$^+$) requires 411.0871; found 411.0861.

N-((8-Hydroxyquinolin-7-yl)(*o*-tolyl)methyl)benzamide **63**

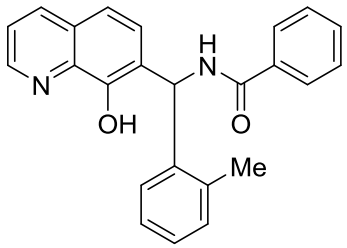

Following general procedure 1, 8-hydroxyquinoline (290 mg, 2.0 mmol), benzamide (242 mg, 2.0 mmol) and *o*-tolualdehyde (463 µL, 4.0 mmol) gave **63** (324 mg, 88 %) as an off-white powder.

mp 196 °C; ν_{max}/cm^{-1} 3302 (NH), 3057 (OH), 1638 (C=O); δ_H (400 MHz, DMSO-d_6) 9.99 (1 H, br. s., N-*H*), 9.05 - 9.21 (1 H, m, quinoline-*Ar*), 8.78 - 8.93 (1 H, m, quinoline-*Ar*), 8.22 - 8.39 (1 H, m, quinoline-*Ar*), 7.87 - 8.03 (2 H, m, quinoline-*Ar*), 7.49 - 7.60 (2 H, m, *Ar*), 7.36 - 7.49 (4 H, m, *Ar*), 7.08 - 7.29 (4 H, m, *Ar*), 7.04 (1 H, d, *J*=8.5 Hz, benzyl-*H*), 2.30 (3 H, s, CH_3); δ_C (100 MHz, DMSO-d_6) 166.4 (*C*=O), 150.9, 149.1, 141.1, 138.8, 137.0, 136.9, 135.2, 132.1, 131.1, 129.0, 128.5, 128.4, 128.0, 127.8, 126.5, 124.5, 122.6, 117.8, 49.1 (benzyl-*C*), 19.7 (*C*H$_3$); *m/z* (ESI$^-$) 367 ([M-H]$^-$, 100 %); HRMS (ESI$^+$) $C_{24}H_{20}N_2NaO_2$, ([M+Na]$^+$) requires 391.1417; found 391.1412.

N-((8-Hydroxyquinolin-7-yl)(*m*-tolyl)methyl)benzamide **64**

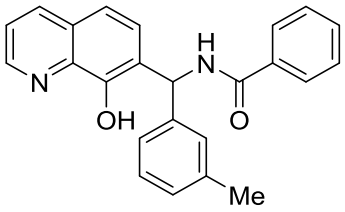

Following general procedure 1, 8-hydroxyquinoline (145 mg, 1.0 mmol), benzamide (121 mg, 1.0 mmol) and *m*-tolualdehyde (236 µL, 2.0 mmol) gave **64** (99 mg, 27 %) as a white powder.

mp 190 °C; ν_{max}/cm^{-1} 3321 (NH), 3056 (OH), 1639 (C=O); δ_H (400 MHz, DMSO-d_6) 10.00 (1 H, br. s, N-*H*), 9.12 - 9.31 (1 H, m, quinoline-*Ar*), 8.79 - 8.93 (1 H, m, quinoline-*Ar*), 8.24 - 8.37 (1 H, m, quinoline-*Ar*), 7.87 - 8.02 (2 H, m, quinoline-*Ar*), 7.65 - 7.79 (1 H, m, *Ar*), 7.50 - 7.58 (2 H, m, *Ar*), 7.41 - 7.50 (3 H, m, *Ar*), 7.10 - 7.23 (3 H, m, *Ar*), 7.04 (1 H, m, *Ar*), 6.99 (1 H, d, *J*=8.5 Hz, benzyl-*H*), 2.25 (3 H, s, CH_3); δ_C (100 MHz, DMSO-d_6) 166.8 (*C*=O), 150.6, 149.2, 143.0, 138.9, 138.2, 136.9, 135.3, 132.1, 129.8, 129.1, 129.0, 128.7, 128.5, 128.3, 127.9, 125.3, 125.3, 122.6, 118.2, 51.3 (benzyl-*C*), 22.0 (*C*H$_3$); *m/z* (ESI$^-$) 367 ([M-H]$^-$, 100 %); HRMS (ESI$^+$) $C_{24}H_{20}N_2NaO_2$, ([M+Na]$^+$) requires 391.1417; found 391.1401.

N-((8-Hydroxyquinolin-7-yl)(*p*-tolyl)methyl)benzamide **65**

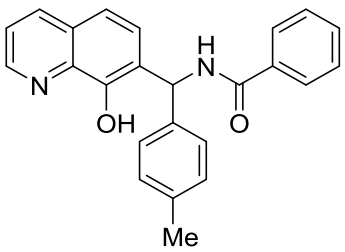

Following general procedure 1, 8-hydroxyquinoline (145 mg, 1.0 mmol), benzamide (121 mg, 1.0 mmol) and *p*-tolualdehyde (236 µL, 2.0 mmol) gave **65** (60 mg, 16 %) as a white powder.

mp 173 °C; ν_{max}/cm^{-1} 3308 (NH), 3048 (OH), 1640 (C=O); δ_H (400 MHz, DMSO-d_6) 9.97 (1 H, br. s, N-*H*), 9.16 - 9.22 (1 H, m, quinoline-*Ar*), 8.85 - 8.88 (1 H, m, quinoline-*Ar*), 8.29 - 8.33 (1 H, m, quinoline-*Ar*), 7.90 - 7.97 (2 H, m, quinoline-*Ar*), 7.66 - 7.75 (1 H, m, *Ar*), 7.51 - 7.58 (2 H, m, *Ar*), 7.41 - 7.49 (3 H, m, *Ar*), 7.18 - 7.24 (1 H, m, *Ar*), 7.08 - 7.15 (3 H, m, *Ar*), 6.96 (1 H, d, *J*=8.5 Hz, benzyl-*H*), 2.25 (3 H, s, CH_3); δ_C (100 MHz, DMSO-d_6) 166.7 (*C*=O), 150.6, 149.2, 140.1, 138.9, 136.9, 136.7, 135.4, 132.1, 129.6, 129.1, 128.9, 128.5, 128.1, 127.8, 125.4, 122.6, 118.1, 51.1 (benzyl-*C*), 21.5 (*C*H$_3$); *m*/*z* (ESI$^-$) 367 ([M-H]$^-$, 100 %); HRMS (ESI$^+$) $C_{24}H_{20}N_2NaO_2$, ([M+Na]$^+$) requires 391.1417; found 391.1420.

N-((8-Hydroxyquinolin-7-yl)(naphthalen-1-yl)methyl)benzamide **66**

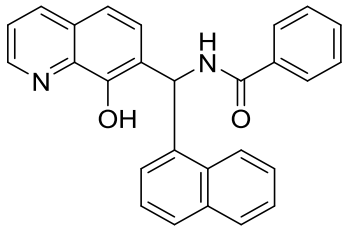

Following general procedure 1, 8-hydroxyquinoline (145 mg, 1.0 mmol), benzamide (121 mg, 1.0 mmol) and 1-naphthaldehyde (272 µL, 2.0 mmol) gave **66** (150 mg, 37 %) as an off-white powder.

mp 208-210 °C; ν_{max}/cm^{-1} 3388 (NH), 3057 (OH), 1633 (C=O); δ_H (400 MHz, DMSO-d_6) 10.12 (1 H, br. s., N-*H*), 9.28 - 9.42 (1 H, m, quinoline-*Ar*), 8.79 - 8.93 (1 H, m, quinoline-*Ar*), 8.24 - 8.37 (1 H, m, quinoline-*Ar*), 8.08 - 8.20 (1 H, m, quinoline-*Ar*), 7.91 - 8.01 (3 H, m, *Ar*), 7.84 - 7.90 (1 H, m, *Ar*), 7.67 (1 H, d, *J*=8.5 Hz, benzyl-*H*), 7.58 - 7.63 (1 H, m, *Ar*), 7.48 - 7.58 (4 H, m, *Ar*), 7.40 - 7.48 (4 H, m, *Ar*), 7.34 - 7.39 (1 H, m, *Ar*); δ_C (100 MHz, DMSO-d_6) 166.5 (*C*=O), 150.7, 149.2, 138.9, 138.7, 136.9, 135.1, 134.4, 132.1, 132.0, 129.6, 129.0, 128.6, 128.6, 128.5, 128.2, 127.3, 126.6, 126.2, 125.7, 124.7, 124.1, 122.7, 117.9, 48.5 (benzyl-*C*); *m*/*z* (ESI$^-$) 403 ([M-H]$^-$, 100 %); HRMS (ESI$^+$) $C_{27}H_{20}N_2NaO_2$, ([M+Na]$^+$) requires 427.1417; found 427.1408.

N-((8-Hydroxyquinolin-7-yl)(naphthalen-2-yl)methyl)benzamide **67**

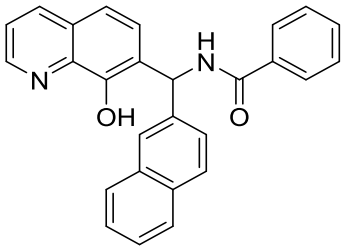

Following general procedure 1, 8-hydroxyquinoline (145 mg, 1.0 mmol), benzamide (121 mg, 1.0 mmol) and 2-naphthaldehyde (312 mg, 2.0 mmol) gave **67** (162 mg, 40 %) as a white powder.

mp 165 ^{o}C; ν_{max}/cm^{-1} 3305 (NH), 1636 (C=O); δ_H (400 MHz, $CDCl_3$) 8.68 - 8.78 (1 H, m, quinoline-*Ar*), 8.21 - 8.29 (1 H, m, quinoline-*Ar*), 8.14 - 8.20 (1 H, m, quinoline-*Ar*), 7.88 - 7.98 (2 H, m, quinoline-*Ar*), 7.72 - 7.84 (4 H, m, *Ar*), 7.57 - 7.65 (2 H, m, *Ar*), 7.49 - 7.56 (1 H, m, *Ar*), 7.37 - 7.48 (6 H, m, *Ar*), 6.94 (1 H, d, *J*=8.5 Hz, benzyl-*H*); δ_C (100 MHz, DMSO-d_6) 166.5 (*C*=O), 154.2, 149.3, 148.3, 138.9, 138.4, 136.2, 134.5, 133.6, 132.7, 131.6, 128.8, 128.6, 128.4, 128.1, 127.8, 127.6, 127.2, 126.1, 125.9, 125.4, 122.3, 122.0, 118.3, 55.6 (benzyl-*C*); *m/z* (ESI$^-$) 403 ([M-H]$^-$, 100 %); HRMS (ESI$^+$) $C_{27}H_{21}N_2O_2$, ([M+H]$^+$) requires 405.1598; found 405.1582.

N-((5-Chloro-8-hydroxyquinolin-7-yl)(4-chlorophenyl)methyl)benzamide **68**

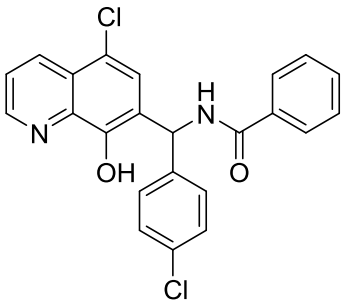

Following general procedure 1, 5-chloro-8-hydroxyquinoline (359 mg, 2.0 mmol), benzamide (242 mg, 2.0 mmol) and 4-chlorobenzaldehyde (560 mg, 4.0 mmol) gave **68** (743 mg, 88 %) as a white powder.

mp 267 - 269 ^{o}C; ν_{max}/cm^{-1} 3308 (NH), 2361 (OH), 1631 (C=O); 691 (C-Cl); δ_H (400 MHz, DMSO-d_6) 10.49 (1 H, br. s. , N-*H*), 9.23 - 9.36 (1 H, m, quinoline-*Ar*), 8.91 - 9.04 (1 H, m, quinoline-*Ar*), 8.42 - 8.56 (1 H, m, quinoline-*Ar*), 7.91 - 7.98 (2 H, m, *Ar*), 7.85 (1 H, s, *Ar*), 7.70 - 7.77 (1 H, m, *Ar*), 7.52 - 7.59 (1 H, m, *Ar*), 7.45 - 7.52 (2 H, m, *Ar*), 7.38 - 7.43 (2 H, m, *Ar*), 7.30 - 7.37 (2 H, m, *Ar*), 6.99 (1 H, d, *J*=8.5 Hz, benzyl-*H*); δ_C (100 MHz, DMSO-d_6) 166.9 (*C*=O), 150.5, 150.1, 141.4, 139.5, 135.0, 133.4, 132.5, 132.3, 130.0, 129.3, 129.2, 128.5, 127.4,

125.9, 125.4, 124.0, 119.5, 50.5 (benzyl-*C*); *m/z* (ESI^+) 867 ($[2M+Na]^+$); HRMS (ESI^-) $C_{23}H_{15}Cl_2N_2O_2$, ($[M-H]^-$) requires 421.0516; found 421.

N-((4-Bromophenyl)(5-chloro-8-hydroxyquinolin-7-yl)methyl)benzamide **69**

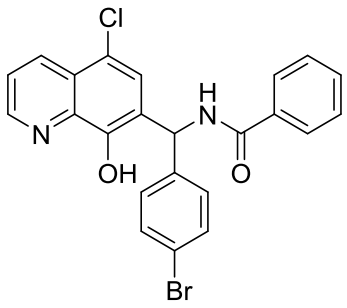

Following general procedure 1, 5-chloro-8-hydroxyquinoline (359 mg, 2.0 mmol), benzamide (242 mg, 2.0 mmol) and 4-bromobenzaldehyde (740 mg, 4.0 mmol) gave **69** (931 mg, 100 %) as an off-white powder.

mp 276 °C; ν_{max}/cm^{-1} 3316 (NH), 2946 (OH), 1630 (C=O); 691 (C-Br); δ_H (400 MHz, DMSO-d_6) 10.49 (1 H, br. s. , br. s., N-*H*), 8.91 - 9.05 (1 H, m, quinoline-*Ar*), 8.42 - 8.56 (1 H, m, quinoline-*Ar*), 7.89 - 7.98 (2 H, m, *Ar*), 7.84 (1 H, s, m, *Ar*), 7.68 - 7.78 (1 H, m, *Ar*), 7.52 - 7.62 (3 H, m, *Ar*), 7.44 - 7.51 (2 H, m, *Ar*), 7.22 - 7.34 (2 H, m, *Ar*), 6.97 (1 H, d, *J*=8.5 Hz, benzyl-*H*); δ_C (100 MHz, DMSO-d_6) 166.9 (*C*=O), 150.5, 150.1, 141.9, 139.5, 135.0, 133.4, 132.3, 132.2, 130.3, 129.2, 128.5, 127.4, 125.9, 125.4, 124.0, 121.0, 119.5, 50.6 (benzyl-*C*); *m/z* (ESI^-) 467 ($[M-H]^-$); HRMS (ESI^+) $C_{23}H_{16}BrClN_2NaO_2$, ($[M+Na]^+$) requires 490.9955; found 490.9944.

N-((5-Chloro-8-hydroxyquinolin-7-yl)(4-methoxyphenyl)methyl)benzamide **70**

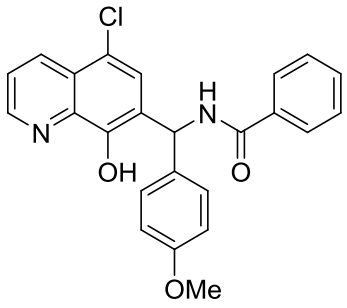

Following general procedure 1, 5-chloro-8-hydroxyquinoline (359 mg, 2.0 mmol), benzamide (242 mg, 2.0 mmol) and 4-methoxybenzaldehyde (486 µL, 4.0 mmol) gave **70** (662 mg, 79 %) as a white powder.

mp 242 - 243 °C; ν_{max}/cm^{-1} 3314 (NH), 1631 (C=O); δ_H (400 MHz, DMSO-d_6) 10.36 (1 H, br. s., N-*H*), 9.15 - 9.25 (1 H, m, quinoline-*Ar*), 8.90 - 9.02 (1 H, m, quinoline-*Ar*), 8.39 - 8.55 (1 H, m, quinoline-*Ar*), 7.90 - 7.97 (2 H,

m, *Ar*), 7.85 - 7.89 (1 H, m, *Ar*), 7.68 - 7.76 (1 H, m, *Ar*), 7.51 - 7.58 (1 H, m, *Ar*), 7.45 - 7.51 (2 H, m, *Ar*), 7.20 - 7.29 (2 H, m, *Ar*), 6.94 (1 H, d, *J*=8.5 Hz, benzyl-*H*) 6.88 - 6.92 (2 H, m, *Ar*), 3.72 (3 H, s, O-CH_3); δ_C (100 MHz, DMSO-d_6) 166.8 (*C*=O), 159.2, 150.2, 150.0, 139.5, 135.2, 134.4, 133.4, 132.2, 129.2, 129.1, 128.4, 127.6, 126.3, 125.7, 123.8, 119.4, 114.7, 56.0 (O-*C*H_3), 50.5 (benzyl-*C*); *m*/*z* (ESI$^-$) 417 ([M-H]$^-$, 100%); HRMS (ESI$^-$) $C_{24}H_{19}ClN_2NaO_3$, ([M+Na]$^+$) requires 441.0976; found 441.0963.

N-((5-Chloro-8-hydroxyquinolin-7-yl)(furan-2-yl)methyl)benzamide **71**

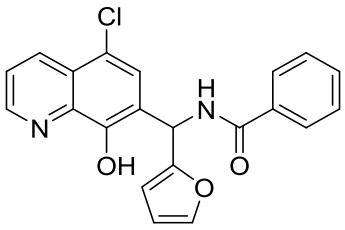

Following general procedure 1, 5-chloro-8-hydroxyquinoline (359 mg, 2.0 mmol), benzamide (242 mg, 2.0 mmol) and furfural (331µL, 4.0 mmol) gave **71** (255 mg, 34 %) as an off-white powder.

mp 245 ^{o}C; ν_{max}/cm^{-1} 3309 (NH), 1639 (C=O), 691 (C-Cl); δ_H (400 MHz, DMSO-d_6) 10.49 (1 H, br. s., N-*H*), 9.32 - 9.42 (1 H, m, quinoline-*Ar*), 8.94 - 9.01 (1 H, m, quinoline-*Ar*), 8.45 - 8.53 (1 H, m, quinoline-*Ar*), 7.86 - 7.99 (3 H, m, *Ar*), 7.69 - 7.77 (1 H, m, *Ar*), 7.64 (1 H, s, *Ar*), 7.52 - 7.58 (1 H, m, *Ar*), 7.44 - 7.51 (2 H, m, *Ar*), 7.02 (1 H, d, *J*=8.5 Hz, benzyl-*H*), 6.37 - 6.44 (1 H, m, *Ar*), 6.08 - 6.15 (1 H, m, *Ar*); δ_C (100 MHz, DMSO-d_6) 166.7 (*C*=O), 154.5, 150.6, 150.0, 143.6, 139.5, 134.8, 133.4, 132.4, 129.2, 128.5, 127.5, 126.1, 124.0, 123.7, 119.4, 111.4, 108.4, 45.6 (benzyl-*C*); *m*/*z* (ESI$^-$) 377 ([M-H]$^-$); HRMS (ESI$^+$) $C_{21}H_{15}ClIN_2NaO_3$, ([M+Na]$^+$) requires 401.0652; found 401.0663.

N-((5-Chloro-8-hydroxyquinolin-7-yl)(thiophen-2-yl)methyl)benzamide **72**

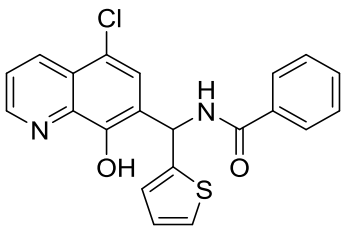

Following general procedure 1, 5-chloro-8-hydroxyquinoline (359 mg, 2.0 mmol), benzamide (242 mg, 2.0 mmol) and 2-thiophenecarboxaldehyde (373 µL, 4.0 mmol) gave **72** (205 mg, 26 %) as a white powder.

mp 237 °C; ν_{max}/cm^{-1} 3325 (NH), 1640 (C=O), 700 (C-Cl); δ_H (400 MHz, DMSO-d_6) 10.53 (1 H, br. s., N-*H*), 9.44 - 9.53 (1 H, m, quinoline-*Ar*), 8.96 - 9.01 (1 H, m, quinoline-*Ar*), 8.45 - 8.54 (1 H, m, quinoline-*Ar*), 8.00 (1 H, s, *Ar*), 7.91 - 7.97 (2 H, m, *Ar*), 7.70 - 7.78 (1 H, m, *Ar*), 7.53 - 7.59 (1 H, m, *Ar*), 7.42 - 7.53 (3 H, m, *Ar*), 7.20 (1 H, d, *J*=8.5 Hz, benzyl-*H*), 6.92 - 6.99 (1 H, m, *Ar*), 6.79 - 6.85 (1 H, m, *Ar*); δ_C (100 MHz, DMSO-d_6) 166.7 (*C*=O), 150.3, 150.1, 146.5, 139.5, 134.9, 133.4, 132.4, 129.2, 128.5, 127.8, 127.3, 126.2, 126.1, 126.1, 125.6, 124.0, 119.5, 47.0 (benzyl-*C*); *m*/*z* (ESI$^-$) 393 ([M-H]$^-$); HRMS (ESI$^+$) $C_{21}H_{15}ClIN_2NaO_2S$, ([M+Na]$^+$) requires 417.0435; found 417.0423.

N-((5-Chloro-8-hydroxyquinolin-7-yl)(thiophen-3-yl)methyl)benzamide **73**

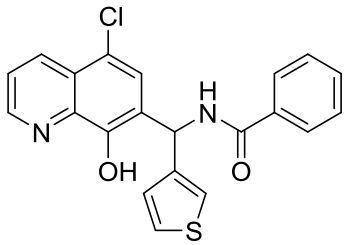

Following general procedure 1, 5-chloro-8-hydroxyquinoline (359 mg, 2.0 mmol), benzamide (242 mg, 2.0 mmol) and 3-thiophenecarboxaldehyde (373 µL, 4.0 mmol) gave **73** (400 mg, 51 %) as an off-white powder.

mp 247 °C; ν_{max}/cm^{-1} 3309 (NH), 1636 (C=O), 710 (C-Cl); δ_H (400 MHz, DMSO-d_6) 10.42 (1 H, br. s., N-*H*), 9.24 - 9.36 (1 H, m, quinoline-*Ar*), 8.93 - 9.03 (1 H, m, quinoline-*Ar*), 8.39 - 8.55 (1 H, m, quinoline-*Ar*), 7.89 - 7.97 (3 H, m, *Ar*), 7.67 - 7.76 (1 H, m, *Ar*), 7.44 - 7.58 (4 H, m, *Ar*), 7.20 - 7.26 (1 H, m, *Ar*), 7.06 - 7.12 (1 H, m, *Ar*), 7.03 (1 H, d, *J*=9.0 Hz, benzyl-*H*); δ_C (100 MHz, DMSO-d_6) 166.7 (*C*=O), 150.1, 150.0, 143.5, 139.6, 135.1, 133.4, 132.2, 129.1, 128.5, 128.1, 127.5, 127.4, 126.2, 125.8, 123.8, 122.9, 119.4, 47.5 (benzyl-*C*); *m*/*z* (ESI$^-$) 393 ([M-H]$^-$); HRMS (ESI$^+$) $C_{21}H_{15}ClIN_2NaO_2S$, ([M+Na]$^+$) requires 417.0435; found 417.0423.

N-((5-Chloro-8-hydroxyquinolin-7-yl)(pyridin-2-yl)methyl)benzamide **74**

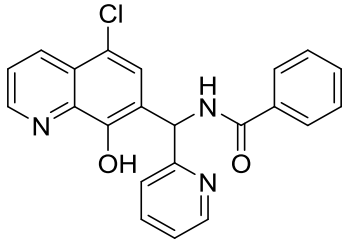

Following general procedure 1, 5-chloro-8-hydroxyquinoline (359 mg, 2.0 mmol), benzamide (242 mg, 2.0 mmol) and 2-pyridinecarboxaldehyde (380 µL, 4.0 mmol) gave **74** (235 mg, 30 %) as an off-white powder.

mp 196 - 198 °C; ν_{max}/cm^{-1} 3306 (NH), 1646 (C=O); δ_H (400 MHz, DMSO-d_6) 10.46 (1 H, br. s., N-*H*), 9.26 - 9.33 (1 H, m, quinoline-*Ar*), 8.94 - 8.99 (1 H, m, quinoline-*Ar*), 8.52 - 8.56 (1 H, m, quinoline-*Ar*), 8.44 - 8.49 (1 H, m, quinoline-*Ar*), 7.94 - 7.99 (2 H, m, *Ar*), 7.78 - 7.81 (1 H, m, *Ar*), 7.69 - 7.75 (1 H, m, *Ar*), 7.52 - 7.57 (1 H, m, *Ar*), 7.42 - 7.52 (3 H, m, *Ar*), 7.26 - 7.32 (1 H, m, *Ar*), 7.02 (1 H, d, *J*=8.0 Hz, benzyl-*H*); δ_C (100 MHz, DMSO-d_6) 166.8 (*C*=O), 160.7, 150.7, 149.9, 139.6, 137.9, 135.0, 133.3, 132.3, 129.2, 128.5, 128.3, 128.0, 125.9, 125.3, 123.9, 123.3, 122.8, 119.2, 52.8 (benzyl-*C*); *m*/*z* (ESI$^-$) 388 ([M-H]$^-$); HRMS (ESI$^+$) $C_{22}H_{17}ClIN_3O_2$, ([M+H]$^+$) requires 390.1004; found 390.0997.

N-((5-Chloro-8-hydroxyquinolin-7-yl)(pyridin-3-yl)methyl)benzamide **75**

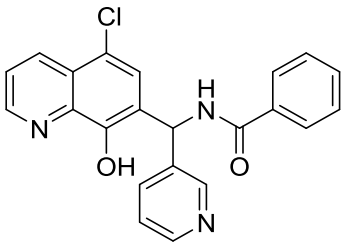

Following general procedure 1, 5-chloro-8-hydroxyquinoline (359 mg, 2.0 mmol), benzamide (242 mg, 2.0 mmol) and 3-pyridinecarboxaldehyde (366 µL, 4.0 mmol) gave **75** (495 mg, 63 %) as a white powder.

mp 266 - 227 °C; ν_{max}/cm^{-1} 3309 (NH), 1638 (C=O), 700 (C-Cl); δ_H (400 MHz, DMSO-d_6) 10.57 (1 H, br. s., N-*H*), 9.28 - 9.45 (1 H, m, quinoline-*Ar*), 8.88 - 9.02 (1 H, m, quinoline-*Ar*), 8.58 (1 H, s, quinoline-*Ar*), 8.43 - 8.53 (2 H, m, *Ar*), 7.85 - 8.02 (3 H, m, *Ar*), 7.65 - 7.81 (2 H, m, *Ar*), 7.44 - 7.62 (3 H, m, *Ar*), 7.29 - 7.41 (1 H, m, *Ar*), 7.02 (1 H, d, *J*=8.5 Hz, benzyl-*H*); δ_C (100 MHz, DMSO-d_6) 167.0 (*C*=O), 150.5, 150.2, 149.5, 149.1, 139.5, 137.8, 135.9, 134.9, 133.4, 132.4, 129.2, 128.5, 127.1, 126.0, 125.0, 124.5, 124.0, 119.7, 49.5 (benzyl-*C*); *m*/*z* (ESI$^-$) 388 ([M-H]$^-$); HRMS (ESI$^+$) $C_{22}H_{16}ClN_3NaO_2$, ([M+Na]$^+$) requires 412.0823; found 412.0816.

N-((5-Chloro-8-hydroxyquinolin-7-yl)(pyridin-4-yl)methyl)benzamide **76**

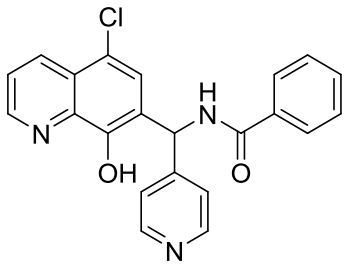

Following general procedure 1, 5-chloro-8-hydroxyquinoline (359 mg, 2.0 mmol), benzamide (242 mg, 2.0 mmol) and 4-pyridinecarboxaldehyde (376µL, 4.0 mmol) gave **76** (76 mg, 10 %) as a white powder.

mp 265 °C; ν_{max}/cm^{-1} 3286 (NH), 1634 (C=O), 700 (C-Cl); δ_H (400 MHz, DMSO-d_6) 10.64 (1 H, br. s., N-*H*), 9.31 - 9.41 (1 H, m, quinoline-*Ar*), 8.96 - 9.01 (1 H, m, quinoline-*Ar*), 8.52 - 8.56 (2 H, m, *Ar*), 8.46 - 8.51 (1 H, m, *Ar*), 7.92 - 7.99 (2 H, m, *Ar*), 7.81 (1 H, s) 7.71 - 7.78 (1 H, m, *Ar*), 7.54 - 7.60 (1 H, m, *Ar*), 7.44 - 7.53 (2 H, m, *Ar*), 7.30 - 7.35 (2 H, m, *Ar*), 7.01 (1 H, d, *J*=8.5 Hz, benzyl-*H*); δ_C (100 MHz, DMSO-d_6) 167.2 (*C*=O), 151.1, 150.8, 150.7, 150.2, 139.6, 134.8, 133.4, 132.4, 129.2, 128.5, 127.4, 126.1, 124.4, 124.1, 123.1, 119.6, 50.3 (benzyl-*C*); *m*/*z* (FI$^+$) 389 ([M]$^+$); HRMS (FI$^+$) $C_{22}H_{16}ClN_3O_2$, ([M]$^+$) requires 389.0931; found 389.0926.

N-((5-Chloro-8-hydroxyquinolin-7-yl)(5-hexylthiophen-2-yl)methyl)benzamide **77**

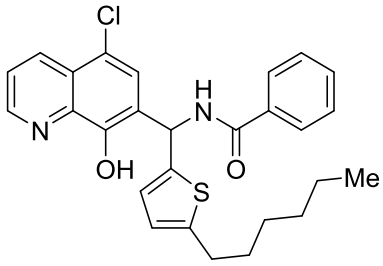

Following general procedure 1, 5-chloro-8-hydroxyquinoline (359 mg, 2.0 mmol), benzamide (242 mg, 2.0 mmol) and 5-hexylthiophene-2-carboxaldehyde (771 µL, 4.0 mmol) gave **77** (331 mg, 35 %) as an off-white powder.

mp 145 °C; ν_{max}/cm^{-1} 3291 (NH), 1636 (C=O); δ_H (400 MHz, DMSO-d_6) 10.50 (1 H, br. s., N*H*), 9.36 - 9.51 (1 H, m, quinoline-*Ar*), 8.92 - 9.02 (1 H, m, quinoline-*Ar*), 8.44 - 8.53 (1 H, m, quinoline-*Ar*), 8.00 (1 H, s, quinoline-*Ar*), 7.91 - 7.96 (1 H, m, *Ar*), 7.84 - 7.90 (1 H, m, *Ar*), 7.69 - 7.78 (1 H, m, *Ar*), 7.52 - 7.60 (1 H, m, *Ar*), 7.41 - 7.52 (2 H, m, *Ar*), 7.12 (1 H, d, *J*=8.5 Hz, benzyl-*H*), 6.52 - 6.68 (2 H, m, *Ar*), 2.61 - 2.75 (2 H, m, C*H*$_2$), 1.43 -

1.62 (2 H, m, CH_2), 1.10 - 1.37 (6 H, m), 0.73 - 0.90 (3 H, m, CH_3); δ_C (100 MHz, DMSO-d_6) 166.6 (*C*=O), 150.3, 150.1, 145.4, 134.6, 139.5, 134.9, 133.4, 132.4, 132.1, 129.2, 128.5, 127.4, 126.0, 125.6, 124.7, 124.0, 119.5, 47.1 (benzyl-*C*), 32.0, 31.8, 30.2, 29.0, 22.9, 14.8; *m*/*z* (FI) 478 ([M]$^+$); HRMS (FI) $C_{27}H_{27}ClN_2O_2S$, ([M]$^+$) requires 478.1482; found 478.1486.

N-(Benzo[d]thiazol-2-yl(5-chloro-8-hydroxyquinolin-7-yl)methyl)benzamide **78**

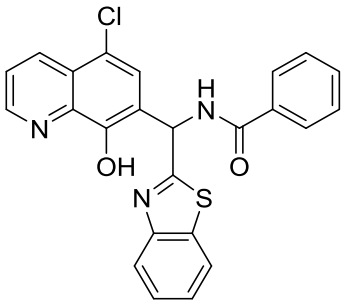

Following general procedure 1, 5-chloro-8-hydroxyquinoline (359 mg, 2.0 mmol), benzamide (242 mg, 2.0 mmol) and benzothiazole-2-carboxaldehyde (653 mg, 4.0 mmol) gave **78** (177 mg, 20 %) as an off-white powder.

mp 212 ^oC; ν_{max}/cm^{-1} 3255 (NH), 1640 (amide C=O); δ_H (400 MHz, DMSO-d_6) 10.79 (1 H, br. s., N*H*), 9.70 - 9.82 (1 H, m, quinoline-*Ar*), 9.46 - 9.57 (1 H, m, quinoline-*Ar*), 8.93 - 9.09 (1 H, m, quinoline-*Ar*), 8.47 - 8.58 (1 H, m, quinoline-*Ar*), 7.89 - 8.02 (4 H, m, *Ar*), 7.57 - 7.64 (1 H, m, *Ar*), 7.34 - 7.55 (5 H, m, *Ar*); δ_C (100 MHz, DMSO-d_6) 153.7 (*C*=O), 151.2, 150.3, 139.6, 135.7, 134.5, 134.1, 133.5, 132.8, 129.3, 128.6, 127.7, 127.2, 126.4, 124.3, 123.6, 123.2, 119.5, 50.3 (benzyl-*C*); *m*/*z* (ESI$^-$) 444 ([M-H]$^-$); HRMS (ESI$^+$) $C_{24}H_{16}ClIN_3NaO_2S$, ([M+Na]$^+$) requires 468.0544; found 468.0636.

N-((5-Chloro-8-hydroxyquinolin-7-yl)(3-cyanophenyl)methyl)benzamide **79**

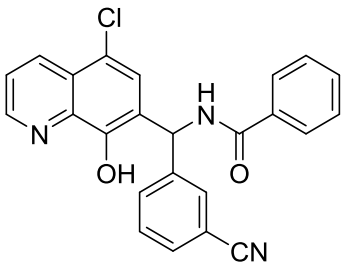

Following general procedure 1, 5-chloro-8-hydroxyquinoline (359 mg, 2.0 mmol), benzamide (242 mg, 2.0 mmol) and 3-formylbenzonitrile (524 mg, 4.0 mmol) gave **79** (548 mg, 66 %) as a white powder.

mp 226 - 228 °C; ν_{max}/cm^{-1} 3298 (NH), 1633 (C=O), 691 (C-Cl); δ_H (400 MHz, DMSO-d_6) 10.59 (1 H, br. s., N-*H*), 9.28 - 9.38 (1 H, m, quinoline-*Ar*), 8.94 - 9.01 (1 H, m, quinoline-*Ar*), 8.45 - 8.52 (1 H, m, quinoline-*Ar*), 7.93 - 7.99 (2 H, m, *Ar*), 7.85 (1 H, s, *Ar*), 7.80 (1 H, s, *Ar*), 7.67 - 7.78 (3 H, m, *Ar*), 7.53 - 7.60 (2 H, m, *Ar*), 7.45 - 7.53 (2 H, m, *Ar*), 7.02 (1 H, d, *J*=8.5 Hz, benzyl-*H*); δ_C (100 MHz, DMSO-d_6) 167.0 (*C*=O), 150.6, 150.2, 144.0, 139.6, 134.8, 133.4, 133.2, 132.4, 131.9, 131.4, 130.7, 129.2, 128.5, 127.1, 126.1, 124.9 124.0, 119.7, 119.6, 112.3, 50.8 (benzyl-*C*); *m*/*z* (ESI$^+$) 414 ([M+H]$^+$); HRMS (ESI$^+$) $C_{24}H_{16}ClIN_3NaO_2$, ([M+Na]$^+$) requires 436.0823; found 436.0815.

N-((5-Chloro-8-hydroxyquinolin-7-yl)(3-iodophenyl)methyl)benzamide **80**

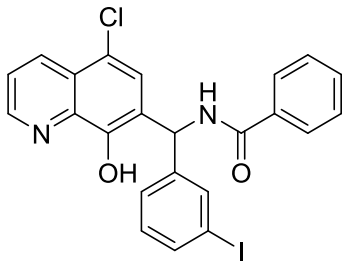

Following general procedure 1, 5-chloro-8-hydroxyquinoline (359 mg, 2.0 mmol), benzamide (242 mg, 2.0 mmol) and 3-iodobenzaldehyde (928 mg, 4.0 mmol) gave **80** (659 mg, 64 %) as a white powder.

mp 226 - 228 °C; ν_{max}/cm^{-1} 3300 (NH), 1632 (C=O), 692 (C-Cl); δ_H (400 MHz, DMSO-d_6) 10.54 (1 H, br. s., N-*H*), 9.26 - 9.33 (1 H, m, quinoline-*Ar*), 8.94 - 8.99 (1 H, m, quinoline-*Ar*), 8.45 - 8.51 (1 H, m, quinoline-*Ar*), 7.90 - 7.97 (2 H, m, *Ar*), 7.87 (1 H, s, *Ar*), 7.68 - 7.76 (2 H, m, *Ar*), 7.61 - 7.66 (1 H, m, *Ar*), 7.53 - 7.59 (1 H, m, *Ar*), 7.46 - 7.52 (2 H, m, *Ar*), 7.35 - 7.40 (1 H, m, *Ar*), 7.13 - 7.19 (1 H, m, *Ar*), 6.96 (1 H, d, *J*=9.0 Hz, benzyl-*H*); δ_C (100 MHz, DMSO-d_6) 166.9 (*C*=O), 150.4, 150.2, 145.1, 139.5, 136.7, 136.4, 134.9, 133.4, 132.4, 131.6, 129.2, 128.5, 127.7, 127.3, 125.9, 125.3, 124.0, 119.6, 95.9, 50.5 (benzyl-*C*); *m*/*z* (ESI$^-$) 512 ([M-H]$^-$); HRMS (ESI$^+$) $C_{23}H_{16}ClIN_2NaO_2$, ([M+Na]$^+$) requires 536.9837; found 536.9825.

N-((5-Chloro-8-hydroxyquinolin-7-yl)(3-(trifluoromethoxy)phenyl)methyl)benzamide **81**

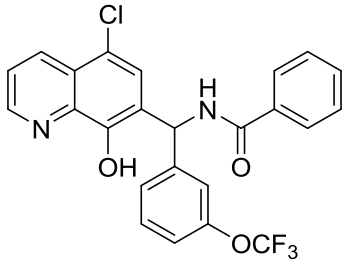

Following general procedure 1, 5-chloro-8-hydroxyquinoline (359 mg, 2.0 mmol), benzamide (242 mg, 2.0 mmol) and 3-trifluoromethoxybenzaldehyde (535 µL, 4.0 mmol) gave **81** (682 mg, 72 %) as a white powder.

mp 210 °C; ν_{max}/cm^{-1} 3297 (NH), 1634 (C=O), 680 (C-Cl); δ_H (400 MHz, DMSO-d_6) 10.56 (1 H, br. s., N-*H*), 9.29 - 9.40 (1 H, m, quinoline-*Ar*), 8.93 - 9.00 (1 H, m, quinoline-*Ar*), 8.42 - 8.53 (1 H, m, quinoline-*Ar*), 7.91 - 7.98 (2 H, m, *Ar*), 7.86 (1 H, s, *Ar*), 7.70 - 7.77 (1 H, m, *Ar*), 7.53 - 7.59 (1 H, m, *Ar*), 7.45 - 7.52 (3 H, m, *Ar*), 7.35 - 7.40 (1 H, m, *Ar*), 7.32 (1 H, s, *Ar*), 7.25 - 7.30 (1 H, m, *Ar*), 7.05 (1 H, d, *J*=9.0 Hz, benzyl-*H*); δ_C (100 MHz, DMSO-d_6) 167.0 (*C*=O), 150.6, 150.2, 149.4, 145.3, 139.5, 134.9, 133.4, 132.4, 131.3, 129.2, 128.5, 127.3, 127.2, 126.0, 125.1, 124.0, 120.3, 119.6, 50.6 (benzyl-*C*); δ_F (377 MHz, DMSO-d_6) -56.7 (CF_3); *m*/*z* (ESI$^-$) 495 ([M-H]$^-$); HRMS (ESI$^+$) $C_{24}H_{16}ClF_3N_2NaO_3$, ([M+Na]$^+$) requires 495.0694; found 495.0683.

N-((3-Acetylphenyl)(5-chloro-8-hydroxyquinolin-7-yl)methyl)benzamide **82**

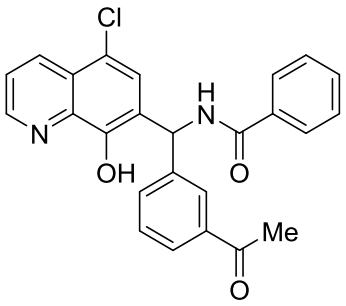

Following general procedure 1, 5-chloro-8-hydroxyquinoline (359 mg, 2.0 mmol), benzamide (242 mg, 2.0 mmol) and 3-acetylbenzaldehyde (524 mg, 4.0 mmol) gave **82** (476 mg, 55 %) as a white powder.

mp 192 °C; ν_{max}/cm^{-1} 3301 (NH), 1689 (acetyl C=O), 1633 (amide C=O), 692 (C-Cl); δ_H (400 MHz, DMSO-d_6) 10.53 (1 H, br. s., N-*H*), 9.33 - 9.39 (1 H, m, quinoline-*Ar*), 8.94 - 8.99 (1 H, m, quinoline-*Ar*), 8.44 - 8.51 (1 H, m, quinoline-*Ar*), 7.92 - 7.98 (3 H, m, *Ar*), 7.87 - 7.91 (2 H, m, *Ar*), 7.69 - 7.76 (1 H, m, *Ar*), 7.60 - 7.66 (1 H, m, *Ar*), 7.45 - 7.57 (4 H, m, *Ar*), 7.08 (1 H, d, *J*=8.5 Hz, benzyl-*H*), 2.55 (3 H, s, CH_3); δ_C (100 MHz, DMSO-d_6) 198.7 (acetyl *C*=O), 167.0 (amide *C*=O),150.5, 150.1, 143.1, 139.5, 137.8, 135.0, 133.4, 132.9, 132.4, 129.8, 129.2, 128.5, 128.4, 127.4, 127.1, 125.9, 125.5, 124.0, 119.5, 51.0 (benzyl-*C*), 27.7 (*C*H$_3$); *m*/*z* (ESI$^-$) 429 ([M-H]$^-$); HRMS (ESI$^+$) $C_{25}H_{19}ClIN_2NaO_3$, ([M+Na]$^+$) requires 453.0976; found 453.0975.

Methyl 3-(benzamido(5-chloro-8-hydroxyquinolin-7-yl)methyl)benzoate **83**

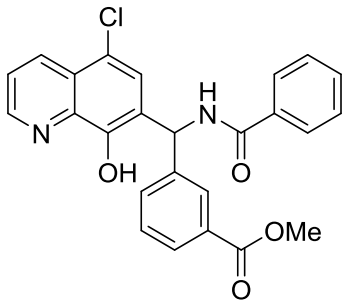

Following general procedure 1, 5-chloro-8-hydroxyquinoline (359 mg, 2.0 mmol), benzamide (242 mg, 2.0 mmol) and methyl 3-formylbenzoate (656 mg, 4.0 mmol) gave **83** (549 mg, 63 %) as a white powder.

mp 224 ^{o}C; ν_{max}/cm^{-1} 3303 (NH), 1724 (esther C=O), 1636 (amide C=O), 696 (C-Cl); δ_H (400 MHz, DMSO-d_6) 10.54 (1 H, br. s., N*H*), 9.34 - 9.43 (1 H, m, quinoline-*Ar*), 8.92 - 9.01 (1 H, m, quinoline-*Ar*), 8.43 - 8.54 (1 H, m, quinoline-*Ar*), 7.93 - 7.97 (3 H, m, *Ar*), 7.84 - 7.90 (2 H, m, *Ar*), 7.70 - 7.76 (1 H, m, *Ar*), 7.62 - 7.66 (1 H, m, *Ar*), 7.46 - 7.60 (4 H, m, *Ar*), 7.08 (1 H, d, *J*=9.0 Hz, benzyl-*H*), 3.81 (3 H, s, C*H*$_3$); δ_C (100 MHz, DMSO-d_6) 167.0 (acid *C*=O), 167.0 (amide *C*=O),150.5, 150.2, 143.3, 139.5, 134.9, 133.4, 133.1, 132.4, 130.6, 129.9, 129.2, 128.8, 128.6, 128.5, 127.4, 126.0, 125.3, 124.0, 119.6 (benzyl-*C*), 53.1 (O*C*H$_3$), 50.9 (benzyl-*C*); *m*/*z* (ESI$^+$) 469 ([M+Na]$^+$); HRMS (ESI$^+$) $C_{25}H_{19}ClIN_2NaO_4$, ([M+Na]$^+$) requires 469.0926; found 469.0909.

3-(Benzamido(5-chloro-8-hydroxyquinolin-7-yl)methyl)benzoic acid **84**

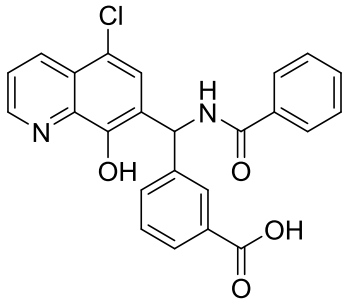

Following general procedure 1, 5-chloro-8-hydroxyquinoline (359 mg, 2.0 mmol), benzamide (242 mg, 2.0 mmol) and 3-formylbenzoic acid (600 mg, 4.0 mmol) gave **84** (814 mg, 94 %) as a white powder.

mp 280 ^{o}C; ν_{max}/cm^{-1} 3324 (NH), 1693 (acid C=O), 1635 (amide C=O), 695 (C-Cl); δ_H (400 MHz, DMSO-d_6) 13.04 (1 H, br. s., CO_2H), 10.53 (1 H, br. s., N-*H*), 9.34 - 9.42 (1 H, m, quinoline-*Ar*), 8.94 - 9.00 (1 H, m, quinoline-*Ar*), 8.45 - 8.52 (1 H, m, quinoline-*Ar*), 7.94 - 7.99 (2 H, m, *Ar*), 7.89 - 7.93 (2 H, m, *Ar*), 7.83 - 7.88 (1 H, m, *Ar*), 7.69

- 7.76 (1 H, m, *Ar*), 7.59 - 7.63 (1 H, m, *Ar*), 7.53 - 7.58 (1 H, m, *Ar*), 7.46 - 7.53 (3 H, m, *Ar*), 7.08 (1 H, d, *J*=8.5 Hz, benzyl-*H*); δ_C (100 MHz, DMSO-d_6) 168.1 (acid *C*=O), 166.9 (amide *C*=O),150.5, 150.1, 143.0, 139.5, 134.9, 133.4, 132.7, 132.4, 131.7, 129.7, 129.2, 129.0, 128.8, 128.5, 127.4, 125.9, 125.4, 124.0, 119.5, 50.8 (benzyl-*C*); *m/z* (ESI$^-$) 431 ([M-H]$^-$); HRMS (ESI$^+$) $C_{25}H_{19}ClIN_2NaO_3$, ([M+Na]$^+$) requires 455.0769; found 455.0753.

N-((3-(4-(2-(2-(3-Chloro-4-methoxyphenethyl)-5-(3,5-dimethylisoxazol-4-yl)-1*H*-benzo[d]imidazol-1-yl)ethyl)piperazine-1-carbonyl)phenyl)(5-chloro-8-hydroxyquinolin-7-yl)methyl)benzamide **86**

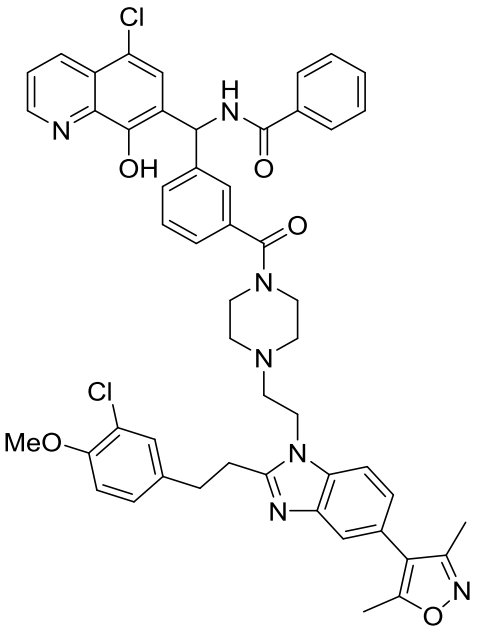

To a solution of **84** (23 mg, 0.05 mmol), 1-ethyl-3-(3-dimethylaminopropyl)carbodiimide (10 mg, 0.05 mmol), hydroxybenzotriazole (9 mg, 0.06 mmol), and diisopropylethylamine (271 µL, 15 mmol) in DMF (1 mL) was added DH fragment (26 mg, 0.05 mmol). The reaction mixture was stirred for 16 h at 50 °C. The reaction mixture was then concentrated *in vacuo* and the resulting residue purified *via* SCX ion exchange column to give **86** (37 mg, 82 %) as an orange solid.

mp 195 °C; ν_{max}/cm^{-1} 1717 (C=O), 1629 (C=O); δ_H (400 MHz, $CDCl_3$) 8.68 - 8.76 (1 H, m, quinoline-*Ar*), 8.37 - 8.45 (1 H, m, quinoline-*Ar*), 7.86 - 7.95 (1 H, m, quinoline-*Ar*), 7.73 - 7.82 (2 H, m, *Ar*), 7.51 - 7.59 (2 H, m, *Ar*), 7.45 - 7.50 (1 H, m, *Ar*), 7.32 - 7.45 (5 H, m, *Ar*), 7.23 - 7.31 (3 H, m, *Ar*), 7.15 - 7.22 (3 H, m, *Ar*), 7.04 - 7.09 (1 H, m, 6.97 - 7.03 (1 H, m) 6.74 - 6.79 (1 H, m) 6.64 - 6.69 (1 H, m) 3.98 - 4.10 (2 H, m) 3.79 (3 H, s) 3.40 (3 H, s) 3.01 - 3.19 (5 H, m) 2.48 - 2.55 (2 H, m) 2.35 (3 H, s) 2.20 - 2.24 (4 H, m); δ_C (100 MHz, DMSO-d_6) 169.2, 166.5, 165.1, 158.9, 155.7, 153.3, 150.1, 149.7, 142.3, 139.2, 136.0, 135.0, 134.9, 134.6, 133.0, 132.0, 130.2,

129.2, 129.0, 128.8, 128.7, 128.1, 127.1, 126.2, 126.2, 125.5, 125.1, 123.6, 123.4, 123.3, 121.2, 119.2, 117.1, 113.2, 110.9, 56.5, 50.4, 31.6, 28.7, 11.8, 11.0; *m/z* (ESI$^+$) 908 ([M+H]$^+$); HRMS (ESI$^+$) $C_{51}H_{48}O_5N_7Cl_2$, ([M+Na]$^+$) requires 908.3089; found 908.3073.

3-(Benzamido(5-chloro-8-hydroxyquinolin-7-yl)methyl)-N-(2-morpholinoethyl)benzamide **87**

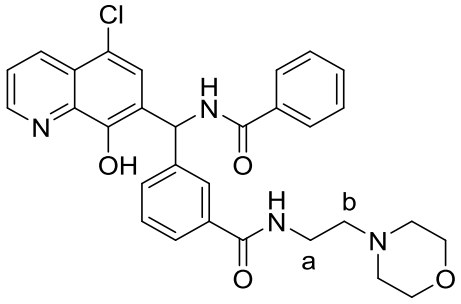

To a solution of **84** (217 mg, 0.5 mmol), 1-ethyl-3-(3-dimethylaminopropyl)carbodiimide (96 mg, 0.5 mmol), hydroxybenzotriazole (81 mg, 0.6 mmol), and diisopropylethylamine (261 µL, 15 mmol) in DMF (10 mL) was added 4-(2-aminoethyl)morpholine (130 mg, 0.5 mmol). The reaction mixture was stirred for 16 h at 50 °C. The reaction mixture was then concentrated *in vacuo* and the resulting residue purified *via* flash column chromatography (0 % - 10 % MeOH, CH_2Cl_2, 1 % NH_4OH) to give **87** (160 mg, 59 %) as a white solid.

mp 144 ^{o}C; ν_{max}/cm^{-1} 3268 (NH), 1638 (C=O); δ_H (400 MHz, $CDCl_3$) 8.66 - 8.70 (1 H, m, quinoline-*Ar*), 8.34 - 8.41 (1 H, m, quinoline-*Ar*), 7.99 - 8.06 (1 H, m, quinoline-*Ar*), 7.75 - 7.83 (3 H, m, *Ar*), 7.51 - 7.58 (2 H, m, *Ar*), 7.37 - 7.50 (3 H, m, *Ar*), 7.30 - 7.36 (2 H, m, *Ar*), 7.24 - 7.30 (1 H, m, *Ar*), 7.19 (1 H, s, *Ar*), 6.81 - 6.94 (1 H, m, *Ar*), 6.68 (1 H, d, *J*=8.5 Hz, benzyl-*H*), 3.48 - 3.56 (4 H, m), 3.39 (2 H, q, *J*=6.0 Hz, H_a), 2.46 (2 H, t, *J*=6.0 Hz, H_b), 2.30 - 2.40 (4 H, m); δ_C (100 MHz, DMSO-d_6) 167.3, 166.6, 148.5, 141.5, 138.7, 135.1, 134.0, 133.4, 131.8, 130.1, 128.9, 128.6, 127.7, 127.2, 126.1, 125.8, 122.8, 122.5, 121.1, 86.8, 55.9, 54.6, 53.2, 36.0; *m/z* (ESI$^+$) 545 ([M+H]$^+$); HRMS (ESI$^+$) $C_{30}H_{30}O_4N_4Cl$, ([M+H]$^+$) requires 545.1950; found 545.1945.

3-(Benzamido(5-chloro-8-hydroxyquinolin-7-yl)methyl)-N-(1-morpholinopropan-2-yl)benzamide **88**

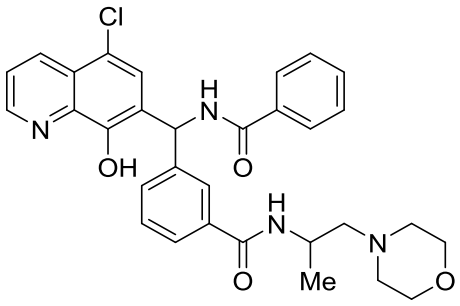

To a solution of **84** (217 mg, 0.5 mmol), 1-ethyl-3-(3-dimethylaminopropyl)carbodiimide (96 mg, 0.5 mmol), hydroxybenzotriazole (81 mg, 0.6 mmol), and diisopropylethylamine (261 µL, 15 mmol) in DMF (10 mL) was added 1-(morpholin-4-yl)propan-2-amine (72 mg, 0.5 mmol). The reaction mixture was stirred for 16 h at 50 °C. The reaction mixture was then concentrated *in vacuo* and the resulting residue purified *via* flash column chromatography (0 % - 10 % MeOH, CH_2Cl_2, 1 % NH_4OH) to give **88** (193 mg, 69 %) as a white solid.

mp 216 °C; ν_{max}/cm^{-1} 3393 (NH), 1638 (C=O); δ_H (400 MHz, DMSO-d_6) 10.48 (1 H, br. s., N*H*), 9.25 - 9.41 (1 H, m, quinoline-*Ar*), 8.91 - 9.05 (1 H, m, quinoline-*Ar*), 8.43 - 8.59 (1 H, m, quinoline-*Ar*), 8.11 - 8.27 (1 H, m, quinoline-*Ar*), 7.94 - 7.99 (2 H, m, *Ar*), 7.81 - 7.88 (2 H, m, *Ar*), 7.70 - 7.78 (2 H, m, *Ar*), 7.41 - 7.61 (4 H, m, *Ar*), 7.07 (1 H, d, *J*=8.5 Hz, benzyl-*H*), 4.12 - 4.23 (1 H, m, C*H*), 3.45 - 3.53 (4 H, m, OCH_2), 2.33 - 2.43 (4 H, m, NCH_2), 2.22 - 2.32 (2 H, m, CH_2), 1.13 (3 H, d, *J*=6.5 Hz, C*H*3); δ_C (100 MHz, DMSO-d_6) 166.5 (*C*=O), 166.0 (*C*=O), 150.1, 149.7, 142.3, 142.3, 139.1, 135.6, 134.6, 133.0, 131.9, 130.3, 128.8, 128.1, 127.2, 127.0, 126.2, 125.6, 125.2, 123.5, 119.0, 66.7, 63.9, 53.9, 50.6, 42.6, 19.4 (*C*H$_3$);

m/z (ESI$^+$) 559 ([M+H]$^+$); HRMS (ESI$^+$) $C_{31}H_{32}O_4N_4Cl$, ([M+H]$^+$) requires 559.2107; found 559.2100.

3-(Benzamido(5-chloro-8-hydroxyquinolin-7-yl)methyl)-N-(2-morpholinopropyl)benzamide **89**

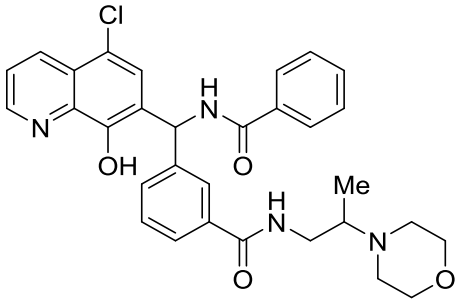

To a solution of **84** (217 mg, 0.5 mmol), 1-ethyl-3-(3-dimethylaminopropyl)carbodiimide (96 mg, 0.5 mmol), hydroxybenzotriazole (81 mg, 0.6 mmol), and diisopropylethylamine (261 µL, 15 mmol) in DMF (10 mL) was added 2-(morpholin-4-yl)propanamine (72 mg, 0.5 mmol). The reaction mixture was stirred for 16 h at 50 °C. The reaction mixture was then concentrated *in vacuo* and the resulting residue purified *via* flash column chromatography (0 % - 10 % MeOH, CH_2Cl_2, 1 % NH_4OH) to give **89** (211 mg, 75 %) as a white solid.

mp 196 °C; ν_{max}/cm^{-1} 3293 (NH), 1653 (C=O), 1635 (C=O); δ_H (400 MHz, DMSO-d_6) 10.50 (1 H, br. s., N*H*), 9.28 - 9.42 (1 H, m, quinoline-*Ar*), 8.92 - 9.07 (1 H, m, quinoline-*Ar*), 8.44 - 8.56 (1 H, m, quinoline-*Ar*), 8.23 - 8.36 (1 H, m, quinoline-*Ar*), 7.93 - 8.00 (2 H, m, *Ar*), 7.85 - 7.89 (1 H, m, *Ar*), 7.82 (1 H, s, *Ar*), 7.70 - 7.77 (2 H, m, *Ar*), 7.39 - 7.61 (4 H, m, *Ar*), 7.08 (1 H, d, *J*=8.5 Hz, benzyl-*H*), 3.43 - 3.52 (4 H, m, OCH_2), 3.29 - 3.42 (4 H, m, NCH_2), 2.71 - 2.77 (1 H, m, C*H*), 2.36 - 2.48 (2 H, m, CH_2), 0.90 - 0.95 (3 H, m, CH_3); δ_C (100 MHz, DMSO-d_6) 166.5 (*C*=O), 166.5 (*C*=O), 150.1, 149.7, 142.2, 139.1, 135.4, 134.6, 133.0, 131.9, 130.4, 128.9, 128.8, 128.1, 127.2, 126.7, 126.1, 125.5, 125.2, 123.5, 119.1, 67.1, 58.6, 50.6, 49.0, 42.2, 12.8 (*C*H_3); *m/z* (ESI$^+$) 559 ([M+H]$^+$); HRMS (ESI$^+$) $C_{31}H_{32}O_4N_4Cl$, ([M+H]$^+$) requires 559.2107; found 559.2103.

3-(Benzamido(5-chloro-8-hydroxyquinolin-7-yl)methyl)-N-(2-morpholino-1-phenylethyl)benzamide 90

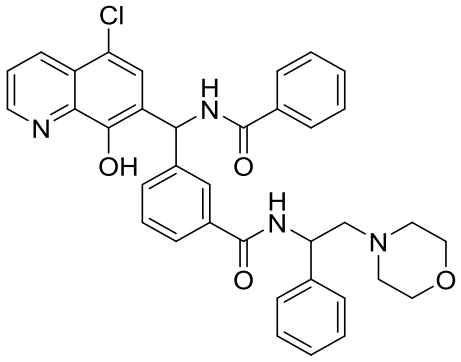

To a solution of **84** (217 mg, 0.5 mmol), 1-ethyl-3-(3-dimethylaminopropyl)carbodiimide (96 mg, 0.5 mmol), hydroxybenzotriazole (81 mg, 0.6 mmol), and diisopropylethylamine (261 µL, 15 mmol) in DMF (10 mL) was added 2-(morpholin-4-yl)-1-phenylethan-1-amine (103 mg, 0.5 mmol). The reaction mixture was stirred for 16 h at 50 °C. The reaction mixture was then concentrated *in vacuo* and the resulting residue purified *via* flash column chromatography (0 % - 10 % MeOH, CH_2Cl_2, 1 % NH_4OH) to give **90** (267 mg, 86 %) as a white solid.

mp 217 °C; ν_{max}/cm^{-1} 3271 (NH), 1637 (C=O); δ_H (400 MHz, DMSO-d_6) 10.49 (1 H, br. s., N*H*), 9.27 - 9.42 (1 H, m, quinoline-*Ar*), 8.93 - 9.04 (1 H, m, quinoline-*Ar*), 8.73 - 8.86 (1 H, m, quinoline-*Ar*), 8.45 - 8.57 (1 H, m, quinoline-*Ar*), 7.93 - 8.01 (2 H, m, *Ar*), 7.80 - 7.89 (4 H, m, *Ar*), 7.70 - 7.77 (1 H, m, *Ar*), 7.54 - 7.62 (1 H, m, *Ar*), 7.44 - 7.53 (4 H, m, *Ar*), 7.36 - 7.43 (2 H, m, *Ar*), 7.27 - 7.34 (2 H, m, *Ar*), 7.19 - 7.26 (1 H, m, *Ar*), 7.08 (1 H, d, *J*=8.5 Hz, benzyl-*H*), 3.42 - 3.57 (4 H, m, OCH_2), 2.90 (1 H, s, C*H*), 2.32 - 2.49 (4 H, m, NCH_2); δ_C (100 MHz, DMSO-d_6) 166.5 (*C*=O), 166.4 (*C*=O), 162.8, 150.1, 149.7, 142.9, 142.3, 139.1, 135.4, 134.7, 133.0, 131.9, 130.5, 128.8, 128.7, 128.1, 127.9, 127.3, 127.2, 127.0, 126.3, 125.5, 125.2, 123.5, 119.1, 66.7, 63.8, 53.6, 50.7, 50.6; *m*/*z* (ESI$^+$) 621 ([M+H]$^+$); HRMS (ESI$^+$) $C_{36}H_{34}O_4N_4Cl$, ([M+H]$^+$) requires 621.2263; found 621.2258.

3-(Benzamido(5-chloro-8-hydroxyquinolin-7-yl)methyl)-N-(2-morpholino-2-phenylethyl)benzamide **91**

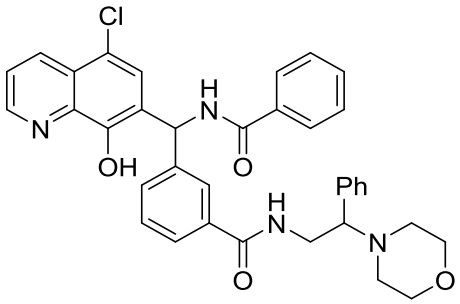

To a solution of **84** (217 mg, 0.5 mmol), 1-ethyl-3-(3-dimethylaminopropyl)carbodiimide (96 mg, 0.5 mmol), hydroxybenzotriazole (81 mg, 0.6 mmol), and diisopropylethylamine (261 µL, 15 mmol) in DMF (10 mL) was added 2-(morpholin-4-yl)-2-phenylethan-1-amine (103 mg, 0.5 mmol). The reaction mixture was stirred for 16 h at 50 °C. The reaction mixture was then concentrated *in vacuo* and the resulting residue purified *via* flash column chromatography (0 % - 10 % MeOH, CH_2Cl_2, 1 % NH_4OH) to give **91** (310 mg, 100 %) as a white solid.

mp 201 °C; ν_{max}/cm^{-1} 3297 (NH), 1640 (C=O); δ_H (200 MHz, $CDCl_3$) 8.75 - 8.86 (1 H, m, quinoline-*Ar*), 8.41 - 8.56 (1 H, m, quinoline-*Ar*), 8.02 - 8.11 (1 H, m, quinoline-*Ar*), 8.00 (2 H, s, *Ar*), 7.84 - 7.94 (2 H, m, *Ar*), 7.76 - 7.82 (1 H, m, *Ar*), 7.34 - 7.67 (8 H, m, *Ar*), 7.16 - 7.33 (4 H, m, *Ar*), 6.77 (1 H, d, *J*=8.5 Hz, benzyl-*H*), 3.60 (2 H, m, CH_2), 2.94 (4 H, m), 2.87 (4 H, m); *m*/*z* (ESI$^+$) 621 ([M+H]$^+$); HRMS (ESI$^+$) $C_{36}H_{34}O_4N_4Cl$, ([M+H]$^+$) requires 621.2263; found 621.2257.

N-(2-(2-(2-(2-Azidoethoxy)ethoxy)ethoxy)ethyl)-3-(benzamido(5-chloro-8-hydroxyquinolin-7-yl)methyl)benzamide **93**

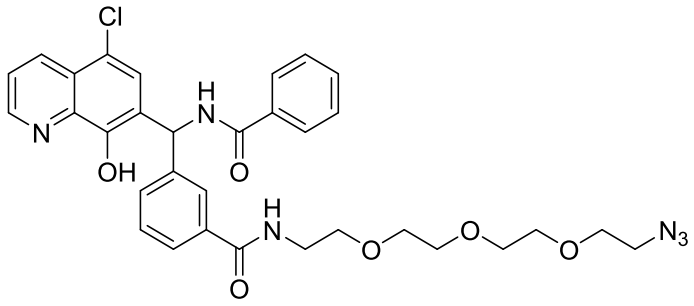

To a solution of **84** (433 mg, 1 mmol), 1-ethyl-3-(3-dimethylaminopropyl)carbodiimide (192 mg, 1 mmol), hydroxybenzotriazole (162 mg, 1 mmol), and diisopropylethylamine (174 µL, 2 mmol) in DMF (10 mL) was added 11-azido-3,6,9-trioxoundecan-1-amine (198 µL, 1 mmol). The reaction mixture is stirred for 16 h at 50 °C. The reaction mixture is concentrated *in vacuo* and the resulting residue purified *via* flash column chromatography (15 % - 50 % EtOAc, cyclohexane) to give **93** (473 mg, 75%) as a light-green solid.

mp 242 °C; ν_{max}/cm^{-1} 2098 (azide); δ_H (400 MHz, $CDCl_3$) 8.58 - 8.77 (1 H, m, quinoline-*Ar*), 8.26 - 8.45 (1 H, m, quinoline-*Ar*), 7.97 - 8.06 (1 H, m, *Ar*), 7.91 (1 H, s, *Ar*), 7.75 - 7.86 (2 H, m, *Ar*), 7.53 - 7.61 (2 H, m, *Ar*), 7.42 - 7.51 (2 H, m, *Ar*), 7.37 - 7.42 (1 H, m, *Ar*), 7.25 - 7.36 (3 H, m, *Ar*), 6.81 - 6.90 (1 H, m, *Ar*), 6.69 (1 H, d, *J*=8.5 Hz, benzyl-*H*), 3.45 - 3.57 (11 H, m), 2.70 - 2.92 (6 H, m); δ_C (100 MHz, $CDCl_3$) 167.4, 166.6, 162.6, 148.8, 148.4, 141.5, 138.6, 135.2, 134.1, 133.5, 131.7, 130.1, 128.8, 128.6, 127.7, 127.2, 126.1, 125.8, 125.8, 122.7, 122.7, 121.1, 70.2, 70.0, 69.7, 54.5, 50.6, 39.8, 36.5, 31.4; *m/z* (ESI$^+$) 633 ([M+H]$^+$); HRMS (ESI$^+$) $C_{32}H_{33}O_6N_6ClNa$, ([M+Na]$^+$) requires 655.2042; found 655.2032.

Biotin-tagged 7-substituted 8HQ as a probe for affinity purification **94**

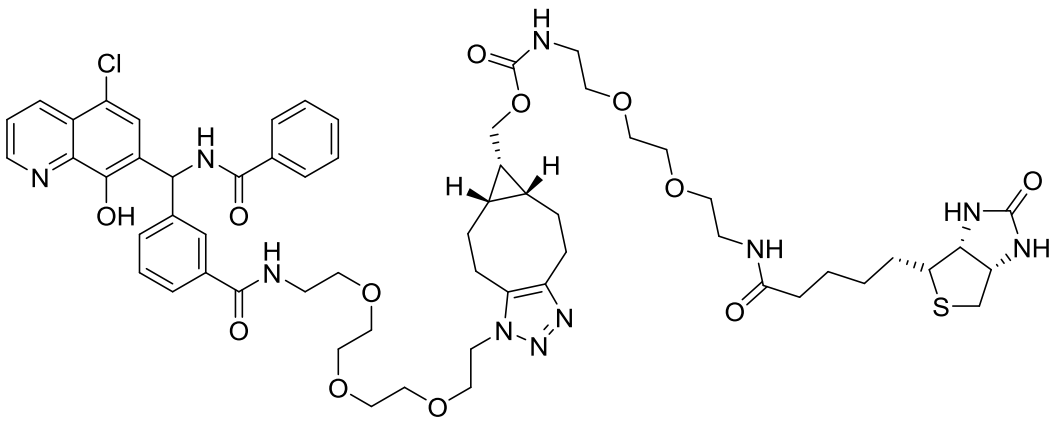

A solution of **93** (0.6 mg, 1 µmol) and SX-Ala29 (Synaffix) (0.6 mg, 1 µmol) in acetonitrile (1 mL) was stirred at room temperature for 16 h. The solvent was evaporated *in vacuo* to give **94** (1.2 mg, 100 %) as a white solid. LC-MS was the only means of analysis for this compound. Integration of the UV trace revealed 100 % conversion into the desired product.

m/z (ESI^+) 592 ($[M+2H]^{2+}$).

3-Methyl-2-thiophenecarboxaldehyde 97

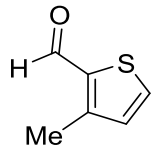

A solution of diisobutylaluminium hydride (1M in hexanes, 29.2 mL, 29.2 mmol) was added dropwise to a stirring solution of 3-methylthiophene-2-carbonitrile (2.4 mL, 20.3 mmol) in chlorobenzene (60 mL) at 0 °C over a period of 20 min. The resulting mixture was stirred for one further hour at 0 °C and then diluted with $CHCl_3$ (100 mL). The mixture was shaken with 10 % HCl aq. for about 10 min and then extracted with $CHCl_3$. The combined organic layers were dried over anhydrous $MgSO_4$ and concentrated *in vacuo*. The crude product was purified *via* flash column chromatography (5 % EtOAc, 95 % cyclohexane) to give **97** as a light-yellow oil (4.55 g, 75 %).

δ_H (400 MHz, $CDCl_3$) 10.04 (1 H, s, C*H*O), 7.63 (1 H, d, *J*=5.0 Hz), 6.97 (1 H, d, *J*=5.0 Hz), 2.58 (3 H, s, CH_3); δ_C (100 MHz, $CDCl_3$) 182.4 (*C*HO), 147.4, 137.6, 134.3, 131.8, 14.2 (*C*H_3); *m/z* (ESI^+) 127 ($[M+H]^+$).

3',5'-Dimethoxy-[1,1'-biphenyl]-3-carbaldehyde 98

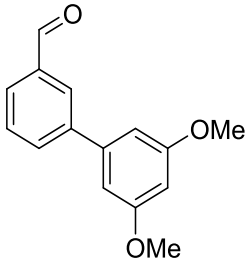

3-Formylphenylboronic acid (900 mg, 6 mmol), 1-bromo-3,5-dimethoxybenzene (1.09 g, 5 mmol), tetrakis(triphenylphosphine)palladium (0) (171 mg, 1.5 µmol) were mixed in dimethoxyethane (10 mL) inside a sealed vial. A 2 M aqueous solution of sodium carbonate (5 mL) was added, and the vial was purged with

N_2 three times. The mixture was stirred at 100 °C for 2.5 h under microwave irradiation. The reaction mixture was cooled to room temperature and diluted with EtOAc (200 mL). The organic layer was washed with water, a saturated aqueous solution of NH_4Cl, brine, and dried over anhydrous $MgSO_4$. The solvent was removed under reduced pressure. The residue was subjected to flash column chromatography on silica gel using EtOAc/cyclohexane (20:8) as eluent to give **98** as a clear oil (634 mg, 52 %).

δ_H (400 MHz, $CDCl_3$) 10.05 (1 H, s, C*H*O), 8.06 (1 H, s, *Ar*), 7.76 - 7.88 (2 H, m, *Ar*), 7.50 - 7.62 (1 H, m, *Ar*), 6.68 - 6.78 (2 H, m, *Ar*), 6.43 - 6.55 (1 H, m, *Ar*), 3.84 (6 H, s, CH_3); δ_C (100 MHz, $CDCl_3$) 192.3 (*C*HO), 161.2 (*C*OCH_3), 142.0, 141.2, 136.8, 133.1, 129.4, 128.9, 128.1, 105.4, 99.9, 55.4 (O*C*H_3); *m/z* (ESI$^+$) 243 ([M+H]$^+$); HRMS (ESI$^+$) $C_{15}H_{15}O_3$, ([M+H]$^+$) requires 243.1016; found 243.1011.

3'-Methoxy-[1,1'-biphenyl]-3-carbaldehyde **99**[187]

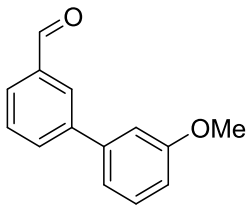

3-Formylphenylboronic acid (900 mg, 6 mmol), 3-bromoanisole (633µL, 5 mmol), tetrakis(triphenylphosphine)palladium (0) (171 mg, 1.5 µmol) were mixed in dimethoxyethane (10 mL) inside a sealed vial. A 2 M aqueous solution of sodium carbonate (5 mL) was added, and the vial was purged with N_2 three times. The mixture was stirred at 100 °C for 2.5 h under microwave irradiation. The reaction mixture was cooled to room temperature and diluted with EtOAc (200 mL). The organic layer was washed with water, a saturated aqueous solution of NH_4Cl, brine, and dried over anhydrous $MgSO_4$. The solvent was removed under reduced pressure. The residue was subjected to flash column chromatography on silica gel using EtOAc/cyclohexane (20 % / 80 %) as eluent to give **99** (770 mg, 73 %) as a clear oil.

δ_H (400 MHz, $CDCl_3$) 10.06 (1 H, s, C*H*O), 8.05 - 8.10 (1 H, m, *Ar*), 7.79 - 7.88 (2 H, m, *Ar*), 7.54 - 7.62 (1 H, m, *Ar*), 7.33 - 7.43 (1 H, m, *Ar*), 7.17 - 7.22 (1 H, m, *Ar*), 7.12 - 7.17 (1 H, m, *Ar*), 6.91 - 6.97 (1 H, m, *Ar*), 3.86 (3 H, s, OCH_3); δ_C (100 MHz, $CDCl_3$) 192.3 (*C*HO), 160.1 (*C*OCH_3), 141.9, 141.1, 136.9, 133.1, 130.1, 129.5, 128.7, 128.2, 119.6, 113.4, 112.9, 55.3 (O*C*H_3); *m/z* (ESI$^+$) 213 ([M+H]$^+$).

5-Bromo-8-(2-(trimethylsilyl)ethoxy)quinolone **105**[136]

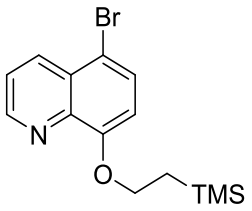

Diisopropylazodicarboxylate (740 µL, 3.6 mmol) was added dropwise to a stirring solution of 5-bromo-8-hydroxyquinoline (400 mg, 1.8 mmol), 2-trimethylsilylethanol (380 µL, 2.7 mmol), and triphenylphosphine (940 mg, 3.6 mmol) in tetrahydrofuran (4 mL) and toluene (4 mL) at 0 °C. The reaction mixture was warmed to room temperature and stirred for 16 h. The reaction mixture was concentrated *in vacuo*. The crude product was purified *via* flash column chromatography (5 % - 50 % EtOAc, cyclohexane) to give **105** (455 mg, 78 %) as a light-yellow oil.

δ_H (400 MHz, $CDCl_3$) 8.74 - 8.91 (1 H, m, quinoline-*Ar*), 8.24 - 8.46 (1 H, m, quinoline-*Ar*), 7.47 - 7.71 (1 H, m, quinoline-*Ar*), 7.32 - 7.49 (1 H, m, quinoline-*Ar*), 6.63 - 6.91 (1 H, m, quinoline-*Ar*), 4.05 - 4.36 (2 H, m, CH_2), 1.24 - 1.37 (2 H, m, CH_2), -0.01 (9 H, s, Si(CH_3)$_3$; δ_C (100 MHz, $CDCl_3$) 156.0, 151.2, 142.7, 136.9, 131.5, 129.8, 124.0, 112.9, 110.6, 68.0, 23.5, 19.0, 0.0 (Si(*C*H_3)$_3$); *m/z* (ESI$^+$) 324 ([M+H]$^+$);

[6,6'-Biquinoline]-8,8'-diol **110**

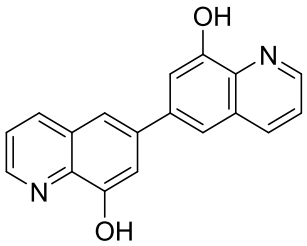

Following general procedure 2, 3,3'-dihydroxybenzidine (2.2 g, 10 mmol) and acrolein (2 mL, 30 mmol) gave **110** (979 mg, 34 %) as a light-brown powder.

mp > 250 °C; δ_H (400 MHz, DMSO-d_6) 10.32 (2 H, br. s., O*H*), 8.70 - 9.01 (2 H, m), 8.27 - 8.63 (2 H, m), 7.87 (2 H, s), 7.46 - 7.73 (4 H, m); δ_C (100 MHz, DMSO-d_6) 154.0, 148.6, 139.2, 137.7, 129.6, 122.9, 122.7, 116.5, 111.2; *m/z* (ESI$^+$) 289 ([M+H]$^+$); HRMS (ESI$^+$) $C_{18}H_{13}O_2N_2$, ([M+H]$^+$) requires 289.0972; found 289.0966.

3-Methylquinolin-8-ol **111**

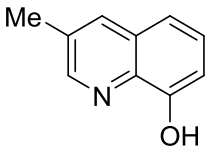

Following general procedure 2, 2-aminophenol (1.1 g, 10 mmol) and methacrolein (1.2 mL, 15 mmol) gave **111** (684 mg, 43 %) as a light-brown powder.

mp 108 °C; ν_{max}/cm^{-1} 3294 (OH); δ_H (400 MHz, DMSO-d_6) 8.65 - 8.81 (1 H, m), 8.02 - 8.13 (1 H, m), 7.35 - 7.44 (1 H, m), 7.22 - 7.33 (1 H, m), 6.93 - 7.05 (1 H, m), 2.48 (3 H, s, CH_3); δ_C (100 MHz, DMSO-d_6) 153.8, 150.3, 137.3, 135.0, 131.4, 129.2, 128.0, 117.5, 110.9, 18.6 (*C*H$_3$); *m/z* (ESI$^+$) 160 ([M+H]$^+$); HRMS (ESI$^+$) $C_{10}H_{10}ON$, ([M+H]$^+$) requires 160.0757; found 160.0754.

4-Methylquinolin-8-ol **112**

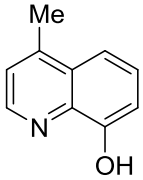

Following general procedure 2, 2-aminophenol (1.1 g, 10 mmol) and but-3-ene-2-one (1.2 mL, 15 mmol) gave **112** (938 mg, 59 %) as an off-white powder.

mp 140 °C; δ_H (400 MHz, DMSO-d_6) 8.52 - 8.82 (1 H, m), 7.43 - 7.52 (2 H, m), 7.37 - 7.42 (1 H, m), 7.02 - 7.14 (1 H, m), 2.65 (3 H, s, CH_3); δ_C (100 MHz, DMSO-d_6) 154.0, 148.1, 144.8, 138.6, 129.0, 127.7, 122.9, 114.4, 111.3, 18.9 (*C*H$_3$); *m/z* (ESI$^+$) 160 ([M+H]$^+$); HRMS (ESI$^+$) $C_{10}H_{10}ON$, ([M+H]$^+$) requires 160.0757; found 160.0754.

5-Methylquinolin-8-ol **113**

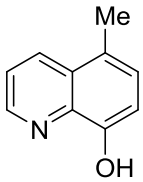

Following general procedure 2, 2-amino-4-methylphenol (1.0 g, 8.1 mmol) and acrolein (814 µL, 12.2 mmol) gave **113** (1.00 g, 78 %) as a light-orange powder.

mp 119 °C; ν_{max}/cm^{-1} 3198 (OH); δ_H (400 MHz, methanol-d_4) 8.54 - 8.74 (1 H, m), 8.11 - 8.30 (1 H, m), 7.29 - 7.42 (1 H, m), 7.03 - 7.15 (1 H, m), 6.78 - 6.94 (1 H, m), 2.42 (3 H, s, CH_3); δ_C (100 MHz, methanol-d_4) 151.1, 147.3, 138.8, 132.8, 128.0, 127.1, 124.2, 121.0, 109.9, 16.5 (CH_3); *m/z* (ESI$^+$) 160 ([M+H]$^+$); HRMS (ESI$^+$) $C_{10}H_{10}NO$, ([M+H]$^+$) requires 160.0757; found 160.0755.

6-Methylquinolin-8-ol **114**

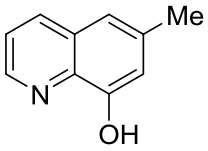

Following general procedure 2, 2-amino-5-methylphenol (1.23 g, 10 mmol) and acrolein (1.0 mL, 15 mmol) gave **114** (620 mg, 39 %) as an orange powder.

mp 88 °C; δ_H (400 MHz, methanol-d_4) 8.62 - 8.73 (1 H, m), 8.03 - 8.20 (1 H, m), 7.32 - 7.50 (1 H, m), 7.12 (1 H, s), 6.88 - 7.03 (1 H, m), 2.45 (3 H, s, CH_3); δ_C (100 MHz, methanol-d_6) 152.4, 146.9, 137.6, 137.3, 135.4, 129.2, 121.4, 116.8, 112.6, 20.6 (*C*H$_3$); *m/z* (ESI$^+$) 160 ([M+H]$^+$); HRMS (ESI$^+$) $C_{10}H_{10}ON$, ([M+H]$^+$) requires 160.0757; found 160.0756.

5-Methoxyquinolin-8-ol **115**

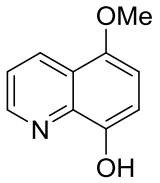

Following general procedure 2, 2-amino-4-methoxyphenol (1.0 g, 7.2 mmol) and acrolein (720 µL, 10.8 mmol) gave **115** (819 mg, 65 %) as a light-brown powder.

mp 102 °C; ν_{max}/cm^{-1} 3325 (OH); δ_H (400 MHz, methanol-d_4) 8.72 - 8.86 (1 H, m), 8.44 - 8.59 (1 H, m), 7.30 - 7.58 (1 H, m), 6.95 - 7.08 (1 H, m), 6.76 - 6.89 (1 H, m), 3.94 (3 H, s, OCH_3); δ_C (100 MHz, methanol-d_4) 148.2, 147.6, 146.3, 138.8, 130.8, 121.0, 120.4, 109.7, 104.6, 54.9 (O*C*H$_3$); *m/z* (ESI$^+$) 176 ([M+H]$^+$);

8-Hydroxyquinoline-5-sulfonamide 116

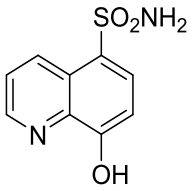

Following general procedure 2, 2-aminophenol-4-sulfonamide (1.0 g, 5.3 mmol) and acrolein (534 µL, 8.0 mmol) gave **116** (499 mg, 42 %) as a light-brown powder.

mp 232 °C; ν_{max}/cm^{-1} 1350 (S=O); δ_H (400 MHz, DMSO-d_6) 8.87 - 9.06 (2 H, m), 7.89 - 8.27 (1 H, m), 7.66 - 7.80 (1 H, m), 7.55 (2 H, br. s., SO_2NH_2), 7.06 - 7.22 (1 H, m); δ_C (100 MHz, DMSO-d_6) 158.0, 149.1, 139.0, 134.1, 129.7, 129.1, 124.9, 123.4, 109.8; *m/z* (ESI$^+$) 225 ([M+H]$^+$); HRMS (ESI$^-$) $C_9H_7O_3N_2S$, ([M-H]$^-$) requires 223.0183; found 223.0182. HRMS (ESI$^+$) $C_{10}H_{10}NO_2$, ([M+H]$^+$) requires 176.0706; found 176.0703.

5-(Methylsulfonyl)quinolin-8-ol 117

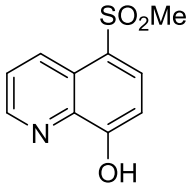

Following general procedure 2, 3-amino-4-hydroxyphenylmethylsulfonate (1.0 g, 5.3 mmol) and acrolein (534 µL, 8.0 mmol) gave **117** (673 mg, 57 %) as a light-brown powder.

mp 203 °C; ν_{max}/cm^{-1} 2920 (OH); δ_H (400 MHz, DMSO-d_6) 8.89 - 9.11 (2 H, m), 8.10 - 8.23 (1 H, m), 7.63 - 7.94 (1 H, m), 7.09 - 7.34 (1 H, m), 3.30 (3 H, s, SO_2CH_3); δ_C (100 MHz, DMSO-d_6) 159.5, 149.5, 138.7, 133.2, 132.3, 125.6, 125.6, 124.3, 110.4, 45.0 (SO_2CH_3); *m/z* (ESI$^+$) 224 ([M+H]$^+$); HRMS (ESI$^-$) $C_{10}H_8O_3NS$, ([M-H]$^-$) requires 222.0230; found 222.0229.

6-Chloroquinolin-8-ol 118

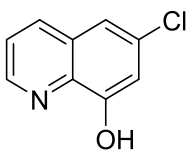

Following general procedure 2, 2-amino-5-chlorophenol (1.43 g, 10 mmol) and acrolein (1 mL, 15 mmol) gave **118** (1.3 g, 73 %) as an off-white powder.

mp 154 °C; ν_{max}/cm^{-1} 3324 (OH); δ_H (400 MHz, DMSO-d_6) 8.80 - 8.93 (1 H, m), 8.24 - 8.37 (1 H, m), 7.55 - 7.69 (1 H, m), 7.52 (1 H, s), 7.04 - 7.16 (1 H, m); δ_C (100 MHz, DMSO-d_6) 155.2, 149.0, 137.8, 136.1, 132.0, 129.7, 123.4, 116.9, 112.5; *m/z* (ESI$^+$) 180 ([M+H]$^+$); HRMS (ESI$^-$) C_9H_5ONCl, ([M-H]$^-$) requires 178.0065; found 178.0063.

6-Fluoroquinolin-8-ol 119

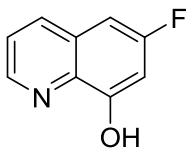

Following general procedure 2, 2-amino-5-fluorophenol (1.0 g, 7.9 mmol) and acrolein (788 µL, 11.8 mmol) gave **119** (785 mg, 61 %) as an orange-brown powder.

mp 135 °C; ν_{max}/cm^{-1} 3063 (OH); δ_H (400 MHz, methanol-d_4) 8.47 - 8.78 (1 H, m), 7.91 - 8.22 (1 H, m), 7.21 - 7.52 (1 H, m), 6.85 - 6.96 (1 H, m), 6.71 - 6.85 (1 H, m); δ_C (100 MHz, methanol-d_4) 162.5, 160.0, 155.2, 147.1, 136.2, 135.6, 129.5, 129.3, 122.4; *m/z* (ESI$^+$) 164 ([M+H]$^+$); HRMS (ESI$^-$) C_9H_5ONF, ([M-H]$^-$) requires 162.0361; found 162.0358.

4-Ethylquinolin-8-ol 120

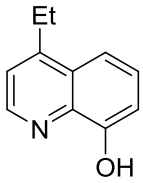

Following general procedure 2, 2-aminophenol (1.1 g, 10 mmol) and 1-penten-3-one (1.5 mL, 15 mmol) gave **120** (1.23 g, 71 %) as a light-brown powder.

mp 102 °C; ν_{max}/cm^{-1} 3297 (OH); δ_H (400 MHz, DMSO-d_6) 8.46 - 8.53 (1 H, m), 7.26 - 7.32 (1 H, m), 7.18 - 7.24 (1 H, m), 7.12 - 7.18 (1 H, m), 6.77 - 6.88 (1 H, m), 2.82 (2 H, q, *J*=7.5 Hz, CH_2), 1.06 (3 H, t, *J*=7.5 Hz, CH_3); δ_C

(100 MHz, DMSO-d_6) 154.3, 150.2, 148.3, 138.9, 128.2, 127.7, 120.8, 113.8, 111.2, 25.0 (CH_2), 14.4 (CH_3); *m/z* (ESI$^-$) 172 ([M-H]$^-$); HRMS (ESI$^+$) $C_{11}H_{11}NO$, ([M+H]$^+$) requires 174.0913; found 174.0917.

Quinoline-4,8-diol **123**[171]

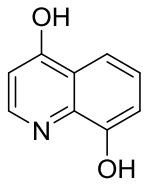

Xanthurenic acid **122** (5 g, 24.4 mmol) was suspended in diphenyl ether (50 mL) and stirred at 250 °C for 2.5 h. After the reaction mixture had cooled to room temperature, cyclohexane (250 mL) was added and the suspension was filtered. The precipitate was dried under reduced pressure to give **123** as a brown solid (3.9 g, 100 %).

mp 311 °C; δ_H (400 MHz, DMSO-d_6) 11.39 (1 H, br. s., O*H*), 10.74 (1 H, br. s., O*H*), 7.71 - 7.83 (1 H, m, *Ar*), 7.49 - 7.56 (1 H, m, *Ar*), 7.09 - 7.17 (1 H, m, *Ar*), 7.03 - 7.09 (1 H, m, *Ar*), 6.01 - 6.09 (1 H, m, *Ar*); δ_C (100 MHz, DMSO-d_6) 177.5, 147.6, 139.8, 131.4, 127.6, 124.0, 115.5, 115.1, 109.4; *m/z* (ESI$^-$) 160 ([M-H]$^-$);

4-Hydroxyquinolin-8-yl 4-methylbenzenesulfonate **124**[171]

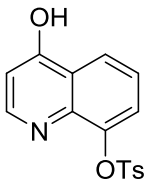

123 (3.94 g, 24.5 mmol) was dissolved in a 1M aqueous sodium hydroxide solution (25.7 mL). A solution of *p*-toluenesulfonyl chloride (4.67 g, 24.5 mmol) in acetone (7 mL) was added dropwise. The reaction mixture was stirred at room temperature for 3 h. Water (30 mL) was added and the precipitate was filtered and washed with water (40 mL) and acetone (40 mL) to give **124** as a light-brown powder (5.379 g, 70 %).

mp 255 °C; δ_H (400 MHz, DMSO-d_6) 11.47 (1 H, br. s., O*H*), 7.91 - 8.01 (1 H, m, *Ar*), 7.74 - 7.84 (2 H, m, *Ar*), 7.65 - 7.73 (1 H, m, *Ar*), 7.34 - 7.45 (3 H, m, *Ar*), 7.20 - 7.30 (1 H, m, *Ar*), 5.97 - 6.09 (1 H, m, *Ar*), 2.36 (3 H, s, *Ar*); δ_C (100 MHz, DMSO-d_6) 147.2, 140.6, 138.8, 133.8, 131.4, 130.9, 129.6, 128.1, 124.8, 124.7, 123.3, 110.2, 22.0 (CH_3); *m/z* (ESI$^-$) 314 ([M-H]$^-$);

4-Chloroquinolin-8-yl 4-methylbenzenesulfonate **125**[171]

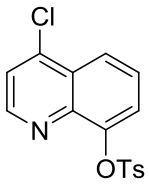

124 (3.15 g, 10 mmol) and phosphorus oxychloride (25 mL, solvent) were stirred under reflux for 1 h. After cooling to room temperature, the reaction mixture was poured into a stirring mixture of ammonium hydroxide and ice. The precipitate was collected by filtration and washed with water to give **125** as a brown solid (2.98 g, 89 %).

mp 139 °C; δ_H (400 MHz, DMSO-d_6) 8.71 - 8.79 (1 H, m, *Ar*), 8.11 - 8.21 (1 H, m, *Ar*), 7.72 - 7.85 (4 H, m, *Ar*), 7.58 - 7.64 (1 H, m, *Ar*), 7.38 - 7.44 (2 H, m, *Ar*), 2.38 (3 H, s, CH_3); δ_C (100 MHz, DMSO-d_6) 151.7, 146.5, 145.8, 142.7, 142.1, 132.9, 130.8, 129.2, 128.7, 127.9, 124.2, 124.0, 123.4, 22.0 (*C*H_3); *m/z* (FI^+) 333 ($[M]^+$);

tert-Butyl 2-((8-(Tosyloxy)quinolin-4-yl)oxy)acetate **126**

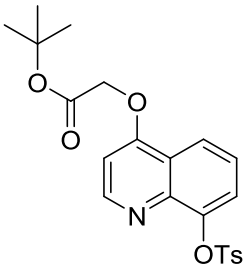

A 60 % dispersion of sodium hydride in oil (47 mg, 7.8 mmol) was slowly added to a stirring solution of **124** (750 mg, 2.38 mmol) in DMF (15 mL) at room temperature. When hydrogen evolution had ceased, *tert*-butylbromoacetate was added to the solution and the reaction mixture was stirred for an additional 2 h at room temperature before being diluted with EtOAc and extracted with H_2O and brine. The organic layer was dried over anhydrous $MgSO_4$ and concentrated *in vacuo*. The crude product was purified *via* flash column chromatography (25 % - 50 % EtOAc, cyclohexane) to give **126** (745 mg, 73 %) as an off-white powder.

mp 153 °C; δ_H (400 MHz, $CDCl_3$) 8.49 - 8.56 (1 H, m, quinoline-*Ar*), 8.05 - 8.14 (1 H, m, quinoline-*Ar*), 7.68 - 7.79 (2 H, m, *Ar*), 7.44 - 7.51 (1 H, m, *Ar*), 7.28 - 7.40 (1 H, m, *Ar*), 7.06 - 7.16 (2 H, m) 6.44 - 6.54 (1 H, m, *Ar*), 4.62 (2 H, s, CH_2), 2.27 (3 H, s, CH_3), 1.39 (9 H, s, C(CH_3)$_3$); δ_C (100 MHz, $CDCl_3$) 166.5 (*C*=O), 160.5, 151.3,

145.1, 142.4, 133.0, 129.4, 128.8, 125.2, 123.0, 122.7, 121.3, 101.5, 83.1, 66.7 (CH_2), 28.0 ($C(CH_3)_3$), 21.6 (CH_3); *m/z* (ESI^+) 430 ($[M+H]^+$); HRMS (ESI^+) $C_{22}H_{24}NO_6S$, ($[M+H]^+$) requires 430.1319; found 430.1323.

4-(1H-Pyrazol-1-yl)quinolin-8-yl 4-methylbenzenesulfonate **127**[172]

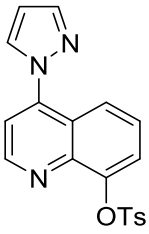

Pyrazole (336 mg, 5 mmol) and **125** (333 mg, 1 mmol) were stirred in toluene under reflux for 5 h. The reaction volume was reduced *in vacuo* and the mixture was left at room temperature. The crystals formed were collected by filtration to give **127** (226 mg, 62 %) as light-brown crystals.

mp 141 °C; δ_H (400 MHz, $CDCl_3$) 8.76 - 8.86 (1 H, m), 8.07 - 8.22 (1 H, m), 7.82 - 7.87 (2 H, m), 7.77 - 7.81 (2 H, m), 7.54 - 7.63 (1 H, m), 7.43 - 7.52 (1 H, m), 7.34 - 7.39 (1 H, m), 7.15 - 7.23 (2 H, m), 6.50 - 6.57 (1 H, m), 2.34 (3 H, s, CH_3); δ_C (100 MHz, $CDCl_3$) 150.6, 145.6, 145.3, 144.2, 143.2, 142.7, 132.9, 131.3, 129.6, 128.8, 127.0, 124.1, 123.4, 123.2, 116.1, 108.4, 21.7 (CH_3); *m/z* (ESI^+) 366 ($[M+H]^+$);

8-Sulfoquinoline-4-carboxylic acid **129**[173]

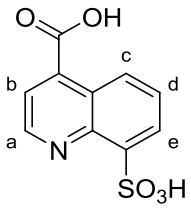

Fuming sulphuric acid (65 % SO_3, 1 mL) was added dropwise to 4-quinolinecarboxylic acid (1 g, 5.68 mmol) inside a 10 mL microwave vial. The vial was sealed and the reaction mixture heated at 200 °C in a sand bath for 2 h. The mixture was left to cool down to room temperature and water (5 mL) was added dropwise. The black residue was triturated with water until formation of a homogenous white powder occurred. The powder was collected by filtration and dried under reduced pressure to give **129** (886 mg, 61 %) as a white powder.

mp > 300 °C; ν_{max}/cm^{-1} 1721 (C=O); δ_H (400 MHz, DMSO-d_6) 9.50 (1 H, d, *J*=5.5 Hz, H_a), 8.82 (1 H, d, *J*=8.5 Hz, H_e), 8.49 (1 H, d, *J*=7.5 Hz, H_c), 8.43 (1 H, d, *J*=5.5 Hz, H_b) 8.05 (1 H, dd, *J*=8.5, 7.5 Hz, H_e); δ_C (100 MHz, DMSO-d_6) 166.5 (*C*=O), 148.5, 146.9, 138.8, 135.2, 133.3, 130.9, 129.1, 126.7, 123.5; *m/z* (ESI$^-$) 252 ([M-H]$^-$); HRMS (ESI$^+$) $C_{10}H_7NNaO_2S$, ([M+Na]$^+$) requires 275.9937; found 275.9940.

N-((5-Amino-8-hydroxyquinolin-7-yl)(3-bromophenyl)methyl)benzamide **130**

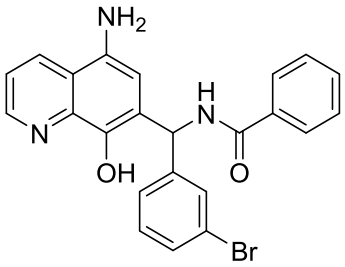

131 (256 mg, 0.54 mmol) was suspended in ethanol (10 mL) and a 1M aqueous solution of sodium dithionite (5 mL) was added. The mixture was stirred under reflux for 16 h, cooled to room temperature and concentrated under reduced pressure. The residue was redissolved in CH_2Cl_2 and extracted with sodium bicarbonate. The organic layer was washed with brine and concentrated under reduced pressure to give **130** as a yellow powder (197 mg, 81 %).

mp 202 - 203 °C; ν_{max}/cm^{-1} 3338 (NH), 1633 (C=O); δ_H (400 MHz, DMSO-d_6) 9.15 - 9.25 (1 H, m, quinoline-*Ar*), 8.95 (1 H, br. s., N*H*), 8.76 - 8.83 (1 H, m, quinoline-*Ar*), 8.43 - 8.56 (1 H, m, quinoline-*Ar*), 7.88 - 8.00 (2 H, m, *Ar*), 7.52 - 7.59 (1 H, m, *Ar*), 7.41 - 7.51 (5 H, m, *Ar*), 7.25 - 7.38 (2 H, m, *Ar*), 6.85 (1 H, d, *J*=8.0 Hz, benzyl-*H*), 6.76 (1 H, s, *Ar*), 5.33 (2 H, br. s., NH_2); δ_C (100 MHz, DMSO-d_6) 165.9 (*C*=O), 148.0, 145.2, 140.6, 138.3, 136.3, 134.3, 131.6, 131.3, 130.5, 129.8, 129.6, 128.2, 127.7, 126.6, 123.9, 121.6, 119.5, 117.9, 107.7, 50.8 (benzyl-*C*); *m/z* (ESI$^-$) 446 ([M-H]$^-$); HRMS (ESI$^-$) $C_{23}H_{17}BrN_3O_2$, ([M-H]$^-$) requires 446.0474; found 446.0499.

N-((3-Bromophenyl)(8-hydroxy-5-nitroquinolin-7-yl)methyl)benzamide **131**

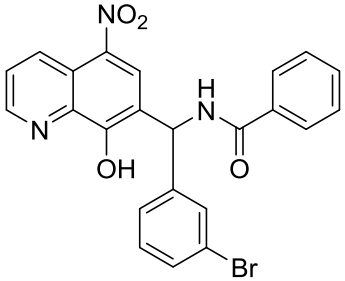

Following general procedure 1, 8-hydroxy-5-nitroquinoline (380 mg, 2.0 mmol), benzamide (242 mg, 2.0 mmol) and 3-bromobenzaldehyde (468 µL, 4.0 mmol) gave **131** (625 mg, 65 %) as a light-orange powder.

mp 264 °C; ν_{max}/cm^{-1} 3287 (NH), 1635 (C=O); δ_H (400 MHz, DMSO-d_6) 9.38 - 9.55 (1 H, m, quinoline-*Ar*), 9.15 - 9.27 (1 H, m, quinoline-*Ar*), 8.94 - 9.06 (1 H, m, quinoline-*Ar*), 8.80 (1 H, s, quinoline-*Ar*), 7.83 - 8.00 (3 H, m, *Ar*), 7.53 - 7.60 (2 H, m, *Ar*), 7.46 - 7.53 (3 H, m, *Ar*), 7.38 - 7.43 (1 H, m, *Ar*), 7.30 - 7.37 (1 H, m, *Ar*), 6.97 (1 H, d, *J*=8.5 Hz, benzyl-*H*); δ_C (100 MHz, DMSO-d_6) 166.9 (*C*=O), 158.9, 149.7, 144.6, 137.6, 135.0, 134.8, 134.1, 132.4, 131.6, 131.1, 130.8, 129.2, 128.8, 128.5, 127.5, 126.2, 123.9, 122.8, 122.7, 50.8 (benzyl-*C*); *m*/*z* (ESI$^-$) 476 ([M-H]$^-$); HRMS (ESI$^-$) $C_{23}H_{15}BrN_3O_4$, ([M-H]$^-$) requires 476.0251; found 476.0259.

8-((*tert*-Butyldimethylsilyl)oxy)-5-chloro-7-iodoquinoline 133

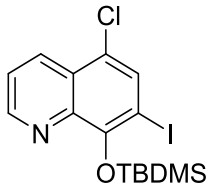

tert-Butyldimethylsilyl chloride (3.32 g, 22 mmol) was slowly added to a stirring solution of clioquinol (6.11 g, 20 mmol) and imidazole (1.43 g, 21 mmol) in CH_2Cl_2 (50 mL) at room temperature. The reaction mixture was stirred for 12 h, diluted with Et_2O (500 mL), washed with a 0.1 M aqueous solution of HCl (50 mL), water (100 mL), brine (100 mL) and dried over anhydrous $MgSO_4$. The solvent was subsequently evaporated under reduced pressure to give **133** (7.91 g, 94 %) as an off-white powder.

mp 81 °C; ν_{max}/cm^{-1} 1096 (Si-O); δ_H (400 MHz, $CDCl_3$) 8.69 - 8.94 (1 H, m, *Ar*), 8.32 - 8.59 (1 H, m, *Ar*), 7.95 (1 H, s, *Ar*), 7.40 - 7.59 (1 H, m, *Ar*), 1.14 (9 H, s, Si(CH$_3$)$_2$C(C*H*$_3$)$_3$), 0.38 (6 H, s, Si(C*H*$_3$)$_2$C(CH$_3$)$_3$)); δ_C (100 MHz, $CDCl_3$)153.2, 147.9, 139.8, 135.7, 133.1, 126.8, 122.2, 121.9, 85.2, 26.3 Si(CH$_3$)$_2$C(*C*H$_3$)$_3$), 19.6 Si(CH$_3$)$_2$*C*(CH$_3$)$_3$), -2.1 Si(*C*H$_3$)$_2$C(CH$_3$)$_3$); *m*/*z* (ESI$^+$) 420 ([M+H]$^+$); HRMS (ESI$^+$) $C_{15}H_{20}ClINOSi$, ([M+H]$^+$) requires 420.0042; found 420.0043.

5-Bromoquinolin-8-yl 4-methylbenzenesulfonate **135**

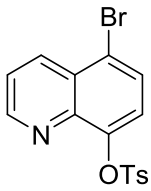

5-Bromo-8-hydroxyquinoline (2.23 g, 10.0 mmol) was dissolved in a 1M aqueous sodium hydroxide solution (11.0 mL). A solution of *p*-toluenesulfonyl chloride (1.91 g, 11.0 mmol) in acetone (7 mL) was added dropwise. The reaction mixture was stirred at room temperature for 3 h. Water (30 mL) was added and the precipitate was filtered and washed with water (40 mL) and acetone (40 mL) to give **135** as an off-white powder (3.08 g, 81 %).

mp 134 °C; ν_{max}/cm^{-1} 3305 (NH), 1369 (S=O); δ_H (400 MHz, DMSO-d_6) 8.77 - 8.99 (1 H, m, *Ar*), 8.40 - 8.59 (1 H, m, *Ar*), 7.90 - 8.06 (1 H, m, *Ar*), 7.76 - 7.82 (2 H, m, *Ar*), 7.69 - 7.75 (1 H, m, *Ar*), 7.43 - 7.47 (1 H, m, *Ar*), 7.38 - 7.42 (2 H, m, *Ar*), 2.38 (3 H, s, C*H*$_3$); δ_C (100 MHz, DMSO-d_6) 152.7, 146.5, 145.5, 142.4, 135.9, 132.9, 130.9, 130.8, 129.3, 128.9, 124.8, 123.8, 120.5, 22.0 (*C*H$_3$); *m/z* (ESI$^+$) 378 ([M+H]$^+$); HRMS (ESI$^+$) $C_{16}H_{12}BrNNaO_3S$, ([M+Na]$^+$) requires 399.9613; found 399.9606.

5-Phenylquinolin-8-yl 4-methylbenzenesulfonate **146**

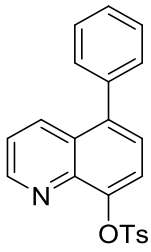

A microwave vial was charged with **147** (33 mg, 0.1 mmol), phenylboronic acid (15 mg, 0.12 mmol), [1,1'-bis(di-*tert*-butylphosphino)ferrocene]dichloropalladium(II) **145** (4 mg, 0.005 mmol), potassium carbonate (44 mg, 0.32 mmol), and dimethylacetamide (1 mL). The vial was sealed and the mixture was thoroughly degassed and subjected to an atmosphere of nitrogen gas. The reaction mixture was then stirred at 180 °C for 30 min under microwave irradiation before being diluted with EtOAc (10 mL) and extracted with H_2O and brine. The organic layer was dried over anhydrous $MgSO_4$ and concentrated *in vacuo*. The crude product was purified *via* flash column chromatography to give **146** (6 mg, 17 %) as an off-white solid.

mp 145 °C; ν_{max}/cm^{-1} 1351 (S=O); δ_H (400 MHz, DMSO-d_6) 8.91 - 8.96 (1 H, m, *Ar*), 8.87 - 8.90 (1 H, m, *Ar*), 8.53 - 8.61 (1 H, m, *Ar*), 8.15 - 8.23 (1 H, m, *Ar*), 7.86 - 7.92 (2 H, m, *Ar*), 7.78 - 7.83 (2 H, m, *Ar*), 7.71 - 7.78 (1 H, m, *Ar*), 7.36 - 7.62 (5 H, m, *Ar*), 2.42 (3 H, s, CH_3); δ_C (100 MHz, DMSO-d_6) 152.3, 151.3, 146.0, 144.7, 139.0, 138.3, 134.4, 133.1, 130.4, 130.3, 129.2, 128.8, 127.2, 127.0, 124.1, 123.1, 122.0, 21.6 (*C*H$_3$); *m*/*z* (ESI$^+$) 376 ([M+H]$^+$); HRMS (ESI$^+$) $C_{22}H_{18}O_3NS$, ([M+H]$^+$) requires 376.1002; found 376.0996.

5-Chloroquinolin-8-yl 4-methylbenzenesulfonate **147**[188]

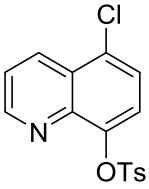

5-Chloro-8-hydroxyquinoline (1.8 g, 10 mmol) was dissolved in a 1M aqueous sodium hydroxide solution (10.5 mL). A solution of *p*-toluenesulfonyl chloride (1.91 g, 24.5 mmol) in acetone (4 mL) was added dropwise. The reaction mixture was stirred at room temperature for 3 h. Water (20 mL) was added and the precipitate was filtered and washed with water (20 mL) and acetone (20 mL) to give **147** as an off-white powder (2.76 g, 83 %).

mp 133 °C; δ_H (200 MHz, DMSO-d_6) 8.70 - 8.80 (1 H, m, quinoline-*Ar*), 8.10 - 8.29 (1 H, m, quinoline-*Ar*), 7.70 - 7.92 (4 H, m, *Ar*), 7.53 - 7.69 (1 H, m, *Ar*), 7.30 - 7.50 (2 H, m, *Ar*), 2.42 (3 H, s, CH_3); *m*/*z* (ESI$^+$) 334 ([M+H]$^+$).

5-(Furan-3-yl)quinolin-8-yl 4-methylbenzenesulfonate **148**

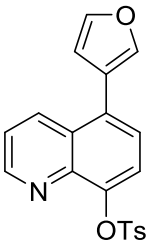

A microwave vial was charged with **147** (33 mg, 0.1 mmol), 3-furanylboronic acid (13 mg, 0.12 mmol), [1,1'-bis(di-*tert*-butylphosphino)ferrocene]dichloropalladium(II) **145** (4 mg, 0.005 mmol), potassium carbonate (44 mg, 0.32 mmol), and dimethylacetamide (1 mL). The vial was sealed and the mixture was thoroughly degassed and subjected to an atmosphere of nitrogen gas. The reaction mixture was then stirred at 180 °C for 30 min under microwave irradiation before being diluted with EtOAc (10 mL) and extracted with H_2O and

brine. The organic layer was dried over anhydrous $MgSO_4$ and concentrated *in vacuo*. The crude product was purified *via* flash column chromatography to give **148** (8 mg, 22 %) as an off-white solid.

mp 132 °C; ν_{max}/cm^{-1} 1347 (S=O); δ_H (400 MHz, $CDCl_3$) 8.66 - 8.91 (1 H, m, *Ar*), 8.25 - 8.43 (1 H, m, *Ar*), 7.79 - 7.90 (2 H, m, *Ar*), 7.48 - 7.60 (3 H, m, *Ar*), 7.38 - 7.44 (1 H, m, *Ar*), 7.30 - 7.37 (1 H, m, *Ar*), 7.14 - 7.25 (2 H, m, *Ar*), 6.52 - 6.60 (1 H, m, *Ar*), 2.35 (3 H, s, C*H*$_3$); δ_C (100 MHz, $CDCl_3$) 150.4, 145.2, 144.6, 143.5, 141.3, 140.8, 134.5, 133.2, 130.5, 129.6, 128.9, 128.2, 126.6, 122.9, 122.3, 121.9, 112.0, 21.7 (*C*H$_3$); *m/z* (ESI$^+$) 366 ([M+H]$^+$); HRMS (ESI$^+$) $C_{20}H_{16}O_4NS$, ([M+H]$^+$) requires 366.0795; found 366.0789.

4-Phenylquinolin-8-yl 4-methylbenzenesulfonate 149

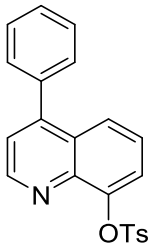

A microwave vial was charged with **125** (33 mg, 0.1 mmol), phenylboronic acid (15 mg, 0.12 mmol), [1,1'-bis(di-*tert*-butylphosphino)ferrocene]dichloropalladium(II) **145** (4 mg, 0.005 mmol), potassium carbonate (44 mg, 0.32 mmol), and dimethylacetamide (1 mL). The vial was sealed and the mixture was thoroughly degassed and subjected to an atmosphere of nitrogen gas. The reaction mixture was then stirred at 180 °C for 30 min under microwave irradiation before being diluted with EtOAc (10 mL) and extracted with H_2O and brine. The organic layer was dried over anhydrous $MgSO_4$ and concentrated *in vacuo*. The crude product was purified *via* flash column chromatography to give **149** (4 mg, 11 %) as an off-white solid.

mp 168 °C; ν_{max}/cm^{-1} 1375 (S=O); *m/z* (ESI$^+$) 376 ([M+H]$^+$); HRMS (ESI$^+$) $C_{22}H_{18}O_3NS$, ([M+H]$^+$) requires 376.1002; found 376.0997.

4-(Furan-3-yl)quinolin-8-yl 4-methylbenzenesulfonate 150

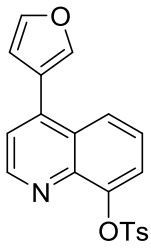

A microwave vial was charged with **125** (33 mg, 0.1 mmol), 3-furanylboronic acid (13 mg, 0.12 mmol), [1,1'-bis(di-*tert*-butylphosphino)ferrocene]dichloropalladium(II) **145** (4 mg, 0.005 mmol), potassium carbonate (44 mg, 0.32 mmol), and dimethylacetamide (1 mL). The vial was sealed and the mixture was thoroughly degassed and subjected to an atmosphere of nitrogen gas. The reaction mixture was then stirred at 180 °C for 30 min under microwave irradiation before being diluted with EtOAc (10 mL) and extracted with H_2O and brine. The organic layer was dried over anhydrous $MgSO_4$ and concentrated *in vacuo*. The crude product was purified *via* flash column chromatography to give **150** (6 mg, 16 %) as an off-white solid.

mp 107 °C; ν_{max}/cm^{-1} 1364 (S=O); δ_H (400 MHz, $CDCl_3$) 8.72 - 8.80 (1 H, m, *Ar*), 7.95 - 8.07 (1 H, m, *Ar*), 7.81 - 7.90 (2 H, m, *Ar*), 7.69 (1 H, s, *Ar*), 7.51 - 7.57 (2 H, m, *Ar*), 7.40 - 7.48 (1 H, m, *Ar*), 7.27 - 7.36 (1 H, m, *Ar*), 7.17 - 7.24 (2 H, m, *Ar*), 6.60 - 6.70 (1 H, m, *Ar*), 2.35 (3 H, s, C*H*$_3$); δ_C (100 MHz, $CDCl_3$) 150.2, 145.6, 145.2, 143.9, 141.6, 140.0, 133.2, 129.6, 128.9, 128.1, 126.2, 124.6, 122.7, 122.4, 121.6, 111.5, 21.8 (*C*H$_3$); *m*/*z* (ESI$^+$) 366 ([M+H]$^+$); HRMS (ESI$^+$) $C_{20}H_{16}O_4NS$, ([M+H]$^+$) requires 366.0795; found 366.0789.

5-Cyanoquinolin-8-yl 4-methylbenzenesulfonate **151**

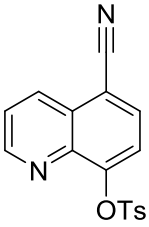

Prior to use, anhydrous dimethylacetamide was sparged with a gentle stream of nitrogen gas for 30 min. A 50 mM solution of sulphuric acid was prepared with 10 mL dimethylacetamide and 26.8 µL of concentrated H_2SO_4 and sparged with N_2 for 10 min. A microwave vial equipped with a magnetic follower was charged with palladium acetate (56 mg, 0.1 mmol) and XPhos **138** (238 mg, 0.5 mmol). The vial was then sealed, subjected to an atmosphere of N_2 and filled with H_2SO_4 (2 mL, 50 mM in dimethyl acetamide). The catalyst mixture was then stirred at 80 °C for 30 min under microwave irradiation.

In parallel, a microwave vial equipped with a magnetic follower was charged with zinc dust (13.1 mg, 0.2 mmol), zinc cyanide (352 mg, 3 mmol) and **147** (1.67 g, 5 mmol). The vial was sealed and subjected to an atmosphere of N_2 and 15 mL of dimethylacetamide were added. Then, the previously prepared catalyst

solution was added (1 mL) and the reaction mixture was stirred for 45 min at 160 °C under microwave irradiation. The mixture was then diluted with EtOAc and extracted with H_2O and brine. The combined organic layers were dried over anhydrous $MgSO_4$ and concentrated *in vacuo*. The crude product was purified *via* flash column chromatography (15 % - 30 % EtOAc, cyclohexane) to give **151** (1.09 g, 67 %) as an off-white powder.

mp 119 °C; ν_{max}/cm^{-1} 2224 (nitrile); δ_H (400 MHz, $CDCl_3$) 8.83 - 8.91 (1 H, m, *Ar*), 8.39 - 8.46 (1 H, m, *Ar*), 7.86 - 7.92 (1 H, m, *Ar*), 7.78 - 7.83 (2 H, m, *Ar*), 7.58 - 7.65 (1 H, m, *Ar*), 7.52 - 7.57 (1 H, m, *Ar*), 7.20 - 7.26 (2 H, m, *Ar*), 2.35 (3 H, s, C*H*$_3$); δ_C (100 MHz, $CDCl_3$) 152.2, 149.4, 145.8, 141.3, 133.9, 133.3, 133.0, 132.7, 131.8, 129.8, 129.6, 128.8, 124.0, 121.8, 21.8 (*C*H$_3$); *m/z* (ESI$^+$) 325 ([M+H]$^+$); HRMS (ESI$^+$) $C_{17}H_{12}O_3N_2NaS$, ([M+Na]$^+$) requires 347.0461; found 347.0455.

8-Hydroxyquinoline-5-carbonitrile 152

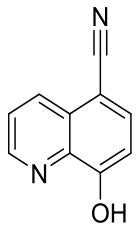

A solution of **151** (162 mg, 0.5 mmol) in sodium hydroxide (1M aq., 0.5 mL), ethanol (3 mL) and H_2O (3 mL) was stirred under reflux for 1 h. The ethanol was removed *in vacuo* and the pH adjusted to 5. The precipitate was filtered and dried to give **152** (76 mg, 89 %) as a white solid.

mp 174 °C; ν_{max}/cm^{-1} 3066 (OH), 2222 (nitrile); δ_H (400 MHz, DMSO-d_6) 8.91 - 9.08 (1 H, m) 8.35 - 8.50 (1 H, m) 7.95 - 8.19 (1 H, m) 7.73 - 7.86 (1 H, m) 7.02 - 7.31 (1 H, m); δ_C (100 MHz, DMSO-d_6) 159.3, 150.2, 138.5, 136.1, 133.5, 129.3, 124.9, 118.0, 112.3, 98.3; *m/z* (ESI$^+$) 171 ([M+H]$^+$); HRMS (ESI$^-$) $C_{10}H_5ON_2$, ([M-H]$^-$) requires 169.0407; found 169.0405.

N-((5-Cyano-8-hydroxyquinolin-7-yl)(3-methylthiophen-2-yl)methyl)benzamide **153**

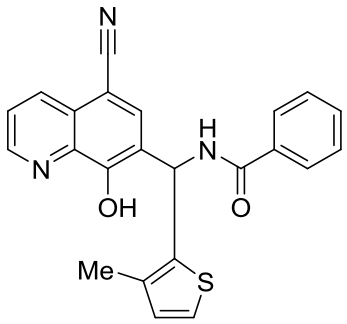

Following general procedure 1, **152** (64 mg, 0.38 mmol), benzamide (46 mg, 0,38 mmol) and 3-methyl-2-thiophenecarboxaldehyde (81 µL, 0.76 mmol) gave **153** (130 mg, 86 %) as a light-brown powder after purification *via* flash column chromatography (40 % - 60 % EtOAc, cyclohexane).

mp 202 °C; ν_{max}/cm^{-1} 3231 (NH), 2218 (nitrile), 1630 (C=O); δ_H (400 MHz, DMSO-d_6) 9.30 - 9.41 (1 H, m, quinoline-*Ar*), 8.99 - 9.09 (1 H, m, quinoline-*Ar*), 8.43 - 8.51 (1 H, m, quinoline-*Ar*), 8.35 (1 H, s, quinoline-*Ar*), 7.90 - 7.98 (2 H, m, *Ar*), 7.82 - 7.87 (1 H, m, *Ar*), 7.53 - 7.61 (1 H, m, *Ar*), 7.45 - 7.52 (2 H, m, *Ar*), 7.28 - 7.32 (1 H, m, *Ar*), 7.17 (1 H, d, *J*=8.0 Hz, benzyl-*H*), 6.90 - 6.96 (1 H, m, *Ar*), 2.18 (3 H, s, C*H*$_3$); δ_C (100 MHz, DMSO-d_6) 166.2 (*C*=O), 155.9, 150.5, 139.1, 138.0, 134.9, 134.5, 134.4, 133.7, 132.0, 131.1, 128.8, 128.2, 128.1, 125.6, 125.0, 123.8, 118.0, 97.9 (nitrile), 45.2 (benzyl-*C*), 14.0 (*C*H$_3$); *m/z* (ESI$^+$) 400 ([M+H]$^+$); HRMS (ESI$^+$) $C_{23}H_{18}O_2N_3S$, ([M+H]$^+$) requires 400.1114; found 400.1110.

N-((5-Chloro-8-hydroxyquinolin-7-yl)(3-methylthiophen-2-yl)methyl)nicotinamide **155**

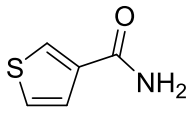

3-Thiophenecarbonitrile (274 µL, 3 mmol) and sodium perborate tetrahydrate (1845 mg, 12 mmol) were suspended in a mixture of water (10 mL) and ethanol (5 mL) inside a sealed vial and stirred at 100 °C for 10 minutes. The aqueous solution was extracted with Et_2O three times and the combined organic fractions were concentrated under reduced pressure to afford **155** as a white powder (299 mg, 78 %).

mp 185 °C; δ_H (400 MHz, DMSO-d_6) 8.08 - 8.16 (1 H, m, *Ar*) 7.52 - 7.57 (1 H, m, *Ar*) 7.45 - 7.50 (1 H, m, *Ar*); δ_C (100 MHz, DMSO-d_6) 164.6 (*C*=O), 138.9, 129.9, 128.0, 127.4; *m/z* (ESI$^-$) 126 ([M-H]$^{+-}$).

N-((5-Chloro-8-hydroxyquinolin-7-yl)(3-methylthiophen-2-yl)methyl)furan-2-carboxamide **156**

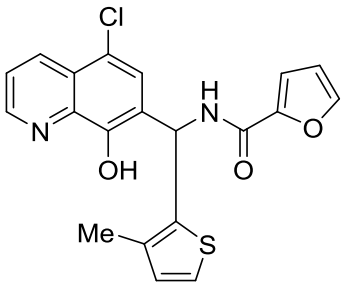

Following general procedure 1, 5-chloro-8-hydroxyquinoline (359 mg, 2.0 mmol), 2-furancarboxamide (222 mg, 2.0 mmol) and 3-methyl-2-thiophenecarboxaldehyde (431µL, 4.0 mmol) gave **156** (208 mg, 26 %) as an off-white powder.

mp 157 ^{o}C; ν_{max}/cm^{-1} 3305 (NH), 1658 (amide C=O); δ_H (400 MHz, DMSO-d_6) 10.51 (1 H, br. s., N*H*), 9.24 - 9.31 (1 H, m, quinoline-*Ar*), 8.92 - 9.00 (1 H, m, quinoline-*Ar*), 8.44 - 8.54 (1 H, m, quinoline-*Ar*), 7.83 - 7.93 (2 H, m, *Ar*), 7.67 - 7.78 (1 H, m, *Ar*), 7.24 - 7.30 (2 H, m, *Ar*), 7.09 (1 H, d, *J*=8.5 Hz, benzyl-*H*), 6.86 - 6.92 (1 H, m, *Ar*), 6.60 - 6.67 (1 H, m, *Ar*), 2.14 (3 H, s, C*H*$_3$); δ_C (100 MHz, DMSO-d_6) 157.8 (*C*=O), 150.4, 150.1, 148.1, 146.3, 139.5, 135.1, 133.4, 131.3, 129.8, 129.1, 127.3, 126.0, 125.4, 124.0, 119.2, 115.0, 112.7, 45.1 (benzyl-*C*), 14.4 (*C*H$_3$); *m/z* (ESI$^+$) 399 ([M+H]$^+$); HRMS (ESI$^+$) $C_{20}H_{15}ClIN_2NaO_3S$, ([M+Na]$^+$) requires 421.0384; found 421.0370.

N-((5-Chloro-8-hydroxyquinolin-7-yl)(3-methylthiophen-2-yl)methyl)thiophene-3-carboxamide **157**

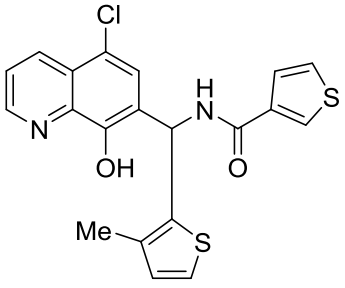

Following general procedure 1, 5-chloro-8-hydroxyquinoline (359 mg, 2.0 mmol), **155** (254 mg, 2.0 mmol) and 3-methyl-2-thiophenecarboxaldehyde (431µL, 4.0 mmol) gave **157** (231 mg, 28 %) as an off-white powder.

mp 188 ^{o}C; ν_{max}/cm^{-1} 3303 (NH), 1638 (C=O); δ_H (400 MHz, DMSO-d_6) 10.48 (1 H, br. s., N*H*), 9.08 - 9.20 (1 H, m, quinoline-*Ar*), 8.97 (1 H, s , quinoline-*Ar*), 8.42 - 8.56 (1 H, m, *Ar*), 8.31 (1 H, s, *Ar*), 7.87 (1 H, s, *Ar*), 7.69 - 7.78 (1 H, m, *Ar*), 7.59 (2 H, s, *Ar*), 7.23 - 7.30 (1 H, m, *Ar*), 7.11 (1 H, d, *J*=8.0 Hz, benzyl-*H*), 6.84 - 6.95 (1 H,

m, *Ar*), 2.14 (3 H, s, C*H*$_3$); δ_C (100 MHz, DMSO-d_6) 162.0 (*C*=O), 150.5, 150.1, 139.8, 139.4, 137.9, 135.1, 133.4, 131.4, 130.3, 128.1, 127.5, 127.2, 126.0, 125.7, 124.0, 119.2, 45.4 (benzyl-*C*), 14.4 (*C*H$_3$); *m*/*z* (ESI$^+$) 415 ([M+H]$^+$); HRMS (ESI$^+$) $C_{20}H_{15}ClIN_2NaO_2S_2$, ([M+Na]$^+$) requires 437.0156; found 437.0141.

tert-Butyl ((3-bromophenyl)(5-chloro-8-hydroxyquinolin-7-yl)methyl)carbamate 159

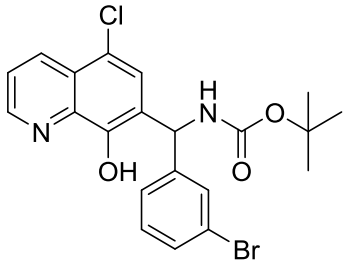

Following general procedure 1, 5-chloro-8-hydroxyquinoline (359 mg, 2.0 mmol), *tert*-butyl carbamate (234 mg, 2.0 mmol) and 3-bromobenzaldehyde (468 µL, 4.0 mmol) gave **159** (239 mg, 26 %) as a white powder.

mp 177 °C; ν_{max}/cm^{-1} 3298 (NH), 1684 (C=O); δ_H (400 MHz, DMSO-d_6) 10.49 (1 H, br. s., N-*H*), 8.87 - 9.00 (1 H, m, quinoline-*Ar*), 8.38 - 8.53 (1 H, m, quinoline-*Ar*), 8.04 - 8.18 (1 H, m, quinoline-*Ar*), 7.84 (1 H, s, *Ar*), 7.62 - 7.75 (1 H, m, *Ar*), 7.49 (1 H, s, *Ar*), 7.37 - 7.45 (1 H, m, *Ar*), 7.22 - 7.35 (2 H, m, *Ar*), 6.46 (1 H, d, *J*=9.5 Hz, benzyl-*H*), 1.39 (9 H, s, C(C*H*$_3$)$_3$); δ_C (100 MHz, DMSO-d_6) 171.5 (*C*=O), 150.1, 149.8, 146.0, 129.5, 133.4, 131.5, 130.7, 130.1, 126.9, 126.7, 126.0, 125.8, 123.9, 122.5, 119.7, 79.4 (*C*(CH$_3$)$_3$), 51.5 (benzyl-*C*), 29.0 (C(*C*H$_3$)$_3$); *m*/*z* (FI$^+$) 462 ([M]$^+$); HRMS (FI$^+$) $C_{21}H_{20}BrClN_2O_3$, ([M]$^+$) requires 462.0346; found 462.0340.

7-(Amino(3-bromophenyl)methyl)-5-chloroquinolin-8-ol bis(2,2,2-trifluoroacetate) 160

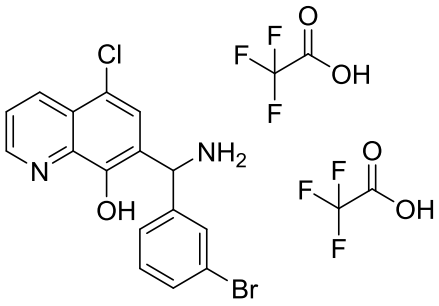

Trifluoroacetic acid (83 µL, 1 mmol) was added dropwise to a stirring suspension of **159** (100 mg, 0.22 mmol) in CH_2Cl_2 (10 mL). After 30 min, the solvent was removed under reduced pressure. The residue was dried under vacuum to give **160** (118 mg, 100%) as a bright-yellow solid.

mp 107 °C; ν_{max}/cm^{-1} 1666 (C=O); δ_H (400 MHz, DMSO-d_6) 9.02 (3 H, br. s) 8.48 - 8.57 (1 H, m, NH_3^+), 7.88 (1 H, s, *Ar*), 7.77 - 7.83 (1 H, m, *Ar*), 7.73 - 7.76 (1 H, m, *Ar*), 7.54 - 7.61 (1 H, m, *Ar*), 7.35 - 7.47 (2 H, m, *Ar*), 7.11 - 7.28 (3 H, m, *Ar*), 6.06 (1 H, s, benzyl-*H*); δ_C (100 MHz, DMSO-d_6) 151.1, 150.6, 140.6, 139.6, 133.6, 132.3, 131.9, 130.8, 129.8, 129.1, 127.3, 126.2, 124.7, 122.8, 120.8, 120.0, 52.2 (benzyl-*C*), 21.9 (*C*F_3); *m*/*z* (FI^+) 362 ($[M]^+$); HRMS (FI^+) $C_{16}H_{12}BrClIN_2O$, ($[M]^+$) requires 361.9822; found 361.9809.

N-((3-Bromophenyl)(5-chloro-8-hydroxyquinolin-7-yl)methyl)acetamide **161**

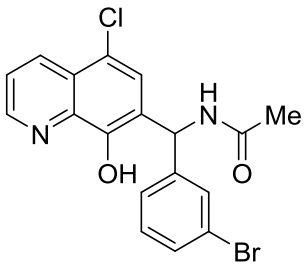

Following general procedure 1, 5-chloro-8-hydroxyquinoline (359 mg, 2.0 mmol), acetamide (118 mg, 2.0 mmol) and 3-bromobenzaldehyde (468 µL, 4.0 mmol) gave **161** (449 mg, 55 %) as a white powder.

mp 200 - 202 °C; ν_{max}/cm^{-1} 3286 (NH), 1640 (C=O); δ_H (400 MHz, DMSO-d_6) 10.48 (1 H, br. s., N*H*), 8.92 - 8.98 (1 H, m, quinoline-*Ar*), 8.84 - 8.90 (1 H, m, quinoline-*Ar*), 8.45 - 8.50 (1 H, m, quinoline-*Ar*), 7.66 - 7.77 (2 H, m, *Ar*), 7.39 - 7.47 (2 H, m, *Ar*), 7.24 - 7.32 (2 H, m, *Ar*), 6.69 (1 H, d, *J*=9.0 Hz, benzyl-*H*), 1.93 - 1.99 (3 H, m, C*H*$_3$); δ_C (100 MHz, DMSO-d_6) 169.6 (*C*=O), 150.2, 150.2, 145.6, 139.5, 133.4, 131.6, 130.8, 130.2, 127.0, 126.8, 125.9, 125.6, 124.0, 122.6, 119.7, 50.1 (benzyl-*C*), 23.5 (*C*H$_3$); *m*/*z* (ESI^-) 402 ($[M-H]^-$); HRMS (ESI^+) $C_{18}H_{14}BrClIN_2NaO_2$, ($[M+Na]^+$) requires 426.9819; found 426.9810.

N-((3-Bromophenyl)(5-chloro-8-hydroxyquinolin-7-yl)methyl)-2-phenylacetamide **162**

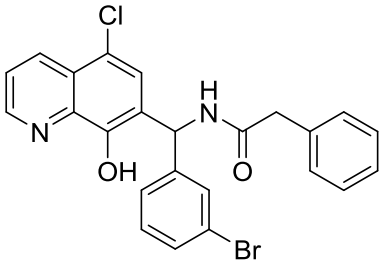

Following general procedure 1, 5-chloro-8-hydroxyquinoline (359 mg, 2.0 mmol), 2-phenylacetamide (270 mg, 2.0 mmol) and 3-bromobenzaldehyde (468 µL, 4.0 mmol) gave **162** (456 mg, 47 %) as a white powder.

mp 169 °C; ν_{max}/cm^{-1} 3273 (NH), 1638 (C=O), 694 (C-Cl); δ_H (400 MHz, DMSO-d_6) 10.48 (1 H, br. s., N-*H*), 9.04 - 9.16 (1 H, m, quinoline-*Ar*), 8.91 - 9.00 (1 H, m, quinoline-*Ar*), 8.41 - 8.51 (1 H, m, quinoline-*Ar*), 7.65 - 7.76 (2 H, m, *Ar*), 7.39 - 7.53 (3 H, m, *Ar*), 7.16 - 7.35 (6 H, m, *Ar*), 6.65 (1 H, d, *J*=8.5 Hz, benzyl-*H*), 3.37 (2 H, s, CH_2); δ_C (100 MHz, DMSO-d_6) 170.5 (*C*=O), 150.2, 145.3, 137.4, 137.1, 133.4, 131.6, 130.8, 130.3, 129.9, 129.0, 127.3, 127.1, 127.0, 126.8, 125.9, 125.3, 124.0, 122.6, 119.7, 50.3 (benzyl-*C*), 43.1 (*C*H$_2$); *m*/*z* (ESI$^-$) 481 ([M-H]$^-$); HRMS (ESI$^-$) $C_{21}H_{17}BrClN_2O_2$, ([M-H]$^-$) requires 479.0167; found 479.0157.

N-((3-Bromophenyl)(5-chloro-8-hydroxyquinolin-7-yl)methyl)-3-methoxybenzamide **163**

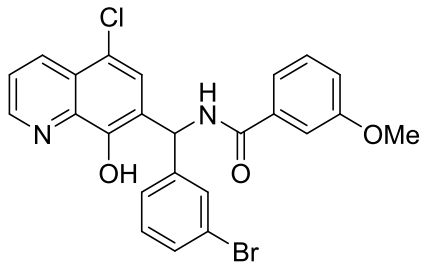

Following general procedure 1, 5-chloro-8-hydroxyquinoline (359 mg, 2.0 mmol), 3-methoxybenzamide (302 mg, 2.0 mmol) and 3-bromobenzaldehyde (468 µL, 4.0 mmol) gave **163** (668 mg, 67 %) as a white powder.

mp 178 °C; ν_{max}/cm^{-1} 3306 (NH), 1634 (C=O); δ_H (400 MHz, DMSO-d_6) 10.55 (1 H, br. s., N-*H*), 9.22 - 9.35 (1 H, m, quinoline-*Ar*), 8.92 - 9.03 (1 H, m, quinoline-*Ar*), 8.40 - 8.56 (1 H, m, quinoline-*Ar*), 7.85 (1 H, s, quinoline-*Ar*), 7.69 - 7.78 (1 H, m, *Ar*), 7.45 - 7.56 (4 H, m, *Ar*), 7.38 - 7.44 (1 H, m, *Ar*), 7.29 - 7.38 (2 H, m, *Ar*), 7.09 - 7.16 (1 H, m, *Ar*), 6.99 (1 H, d, *J*=8.5 Hz, benzyl-*H*), 3.81 (3 H, s, OCH_3); δ_C (100 MHz, DMSO-d_6) 166.6 (*C*=O), 160.0, 150.5, 150.2, 145.2, 139.5, 136.3, 133.4, 131.6, 130.9, 130.5, 130.4, 127.3, 127.3, 126.0, 125.1, 124.0, 122.6, 120.7, 119.6, 118.1, 113.8, 56.2 (O*C*H$_3$), 50.2 (benzyl-*C*); *m*/*z* (ESI$^+$) 497 ([M+H]$^+$); HRMS (ESI$^+$) $C_{24}H_{19}BrClIN_2O_3$, ([M+H]$^+$) requires 497.0262; found 497.0249.

N-((3-Bromophenyl)(5-chloro-8-hydroxyquinolin-7-yl)methyl)-4-chlorobenzamide **164**

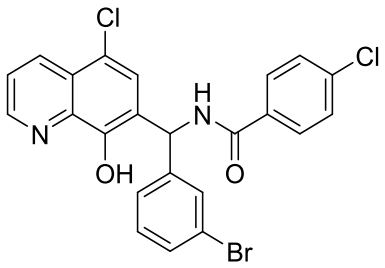

Following general procedure 1, 5-chloro-8-hydroxyquinoline (359 mg, 2.0 mmol), 4-chlorobenzamide (311 mg, 2.0 mmol) and 3-bromobenzaldehyde (468µL, 4.0 mmol) gave **164** (552 mg, 55 %) as a white powder. **164** was then stirred in a 4M HCl solution in dioxane for 1 h. The solvent was removed under reduced pressure to give the hydrochloride salt of **164** as a bright-yellow powder in quantitative yield.

mp 271 °C; ν_{max}/cm^{-1} 3302 (NH), 1635 (C=O); δ_H (400 MHz, DMSO-d_6) 9.36 - 9.48 (1 H, m, quinoline-*Ar*), 8.94 - 9.02 (1 H, m, quinoline-*Ar*), 8.44 - 8.57 (1 H, m, quinoline-*Ar*), 7.94 - 8.00 (2 H, m, *Ar*), 7.83 - 7.93 (1 H, m, *Ar*), 7.69 - 7.81 (1 H, m, *Ar*), 7.53 - 7.60 (2 H, m, *Ar*), 7.49 - 7.53 (1 H, m, *Ar*), 7.44 - 7.48 (1 H, m, *Ar*), 7.26 - 7.40 (2 H, m, *Ar*), 6.98 (1 H, d, *J*=8.5 Hz, benzyl-*H*); δ_C (100 MHz, DMSO-d_6) 165.9 (*C*=O), 150.2, 145.0, 139.1, 137.2, 134.1, 133.5, 131.6, 130.1, 130.6, 130.5, 130.3, 129.3, 129.1, 127.4, 126.1, 125.5, 124.1, 122.6, 119.8, 50.8 (benzyl-*C*); *m/z* (ESI$^+$) 501 ([M+H]$^+$); HRMS (ESI$^+$) $C_{23}H_{15}BrCl_2N_2NaO_2$, ([M+Na]$^+$) requires 522.9586; found 522.9575.

N-((3-Bromophenyl)(5-chloro-8-hydroxyquinolin-7-yl)methyl)-4-nitrobenzamide 165

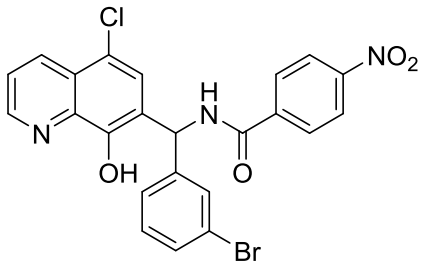

Following general procedure 1, 5-chloro-8-hydroxyquinoline (359 mg, 2.0 mmol), 4-nitrobenzamide (332 mg, 2.0 mmol) and 3-bromobenzaldehyde (468µL, 4.0 mmol) gave **165** (476 mg, 46 %) as a white powder.

mp 206 °C; ν_{max}/cm^{-1} 3315 (NH), 1640 (C=O); δ_H (400 MHz, DMSO-d_6) 10.60 (1 H, br. s., N*H*), 9.50 - 9.71 (1 H, m, quinoline-*Ar*), 8.89 - 9.05 (1 H, m, quinoline-*Ar*), 8.42 - 8.55 (1 H, m, quinoline-*Ar*), 8.34 (2 H, d, *J*=8.5 Hz, *α*-*H*-NO$_2$), 8.17 (2 H, d, *J*=8.5 Hz, *β*-*H*-NO$_2$), 7.81 (1 H, s, *Ar*), 7.69 - 7.77 (1 H, m, *Ar*), 7.53 (1 H, s, *Ar*), 7.46 - 7.51 (1 H, m, *Ar*), 7.25 - 7.44 (2 H, m, *Ar*), 6.98 (1 H, d, *J*=8.5 Hz, benzyl-*H*); δ_C (100 MHz, DMSO-d_6) 165.4 (*C*=O), 150.6, 150.2, 150.0, 144.8, 140.5, 139.5, 133.4, 131.7, 131.1, 130.6, 130.1, 127.3, 127.1, 126.0, 124.8, 124.4, 124.1, 122.7, 119.6, 51.0 (benzyl-*C*); *m/z* (ESI$^+$) 512 ([M+H$^+$); HRMS (ESI$^+$) $C_{23}H_{15}BrClN_3NaO_4$, ([M+Na]$^+$) requires 533.9827; found 533.9815.

N-((3-Bromophenyl)(5-chloro-8-hydroxyquinolin-7-yl)methyl)-[1,1'-biphenyl]-4-carboxamide **166**

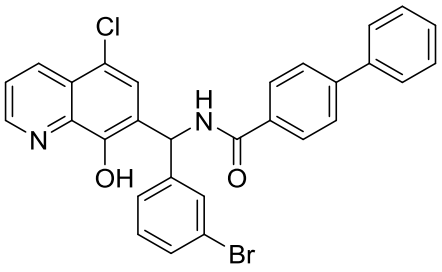

Following general procedure 1, 5-chloro-8-hydroxyquinoline (359 mg, 2.0 mmol), biphenyl-4-carboxamide (394 mg, 2.0 mmol) and 3-bromobenzaldehyde (468µL, 4.0 mmol) gave **166** (718 mg, 66 %) as a white powder.

mp 236 °C; ν_{max}/cm^{-1} 3305 (NH), 1627 (C=O); δ_H (400 MHz, DMSO-d_6) 10.57 (1 H, br. s., N*H*), 9.31 - 9.43 (1 H, m, quinoline-*Ar*), 8.93 - 9.01 (1 H, m, quinoline-*Ar*), 8.44 - 8.52 (1 H, m, quinoline-*Ar*), 8.01 - 8.09 (2 H, m, *Ar*), 7.89 (1 H, s, *Ar*), 7.78 - 7.84 (2 H, m, *Ar*), 7.68 - 7.76 (3 H, m, *Ar*), 7.54 (1 H, s, *Ar*), 7.45 - 7.52 (3 H, m, *Ar*), 7.36 - 7.43 (2 H, m, *Ar*), 7.28 - 7.35 (1 H, m, *Ar*), 7.03 (1 H, d, *J*=9.0 Hz, benzyl-*H*); δ_C (100 MHz, DMSO-d_6) 165.6 (*C*=O), 150.1, 150.2, 145.3, 144.0, 140.0, 139.5, 133.6, 133.4, 133.3, 131.6, 130.9, 130.6, 129.9, 129.2, 129.0, 127.8, 127.5, 127.3, 126.0, 125.2, 124.0, 122.6, 119.6, 50.7 (benzyl-*C*); *m/z* (ESI$^+$) 445 ([M+H$^+$); HRMS (ESI$^+$) $C_{29}H_{20}BrClN_2NaO_2$, ([M+Na]$^+$) requires 565.0289; found 565.0277.

1-((3-Bromophenyl)(5-chloro-8-hydroxyquinolin-7-yl)methyl)urea **167**

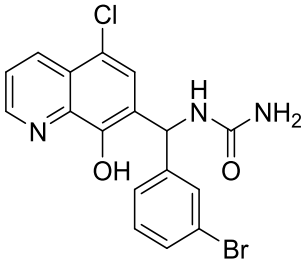

Following general procedure 1, 5-chloro-8-hydroxyquinoline (359 mg, 2.0 mmol), urea (120 mg, 2.0 mmol) and 3-bromobenzaldehyde (234 µL, 2.0 mmol) gave **167** (470 mg, 58 %) as an off-white powder.

mp 183 °C; ν_{max}/cm^{-1} 3339 (NH), 1636 (C=O); δ_H (400 MHz, DMSO-d_6) 10.47 (1 H, br. s., N-*H*), 8.78 - 9.14 (1 H, m, quinoline-*Ar*), 8.35 - 8.61 (1 H, m, quinoline-*Ar*), 7.60 - 7.87 (2 H, m, *Ar*), 7.09 - 7.57 (6 H, m, *Ar*), 6.28 - 6.56 (1 H, m, benzyl-*H*), 5.55 - 5.87 (1 H, m, *Ar*); δ_C (100 MHz, DMSO-d_6) 157.2 (*C*=O), 150.1, 139.6, 133.4, 131.5,

131.4, 130.6, 130.0, 127.0, 126.6, 126.2, 125.9, 123.9, 122.6, 119.7, 52.3 (benzyl-*C*); *m/z* (FI^+) 404 ($[M]^+$); HRMS (FI^+) $C_{17}H_{13}BrClIN_3O_2$, ($[M]^+$) requires 404.9880; found 404.0892.

Benzyl((3-bromophenyl)(5-chloro-8-hydroxyquinolin-7-yl)methyl)carbamate 168

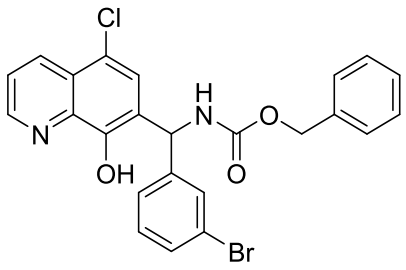

Following general procedure 1, 5-chloro-8-hydroxyquinoline (359 mg, 2.0 mmol), benzyl carbamate (302 mg, 2.0 mmol) and 3-bromobenzaldehyde (468 µL, 4.0 mmol) gave **168** (537 mg, 54 %) as a white powder.

mp 180 °C; v_{max}/cm^{-1} 3305 (NH), 1684 (C=O); δ_H (400 MHz, DMSO-d_6) 10.55 (1 H, br. s. , N-*H*), 8.91 - 8.99 (1 H, m, quinoline-*Ar*), 8.49 - 8.57 (1 H, m, quinoline-*Ar*), 8.42 - 8.50 (1 H, m, quinoline-*Ar*), 7.80 (1 H, s, *Ar*), 7.67 - 7.75 (1 H, m, *Ar*), 7.51 (1 H, s, *Ar*), 7.41 - 7.47 (1 H, m, *Ar*), 7.25 - 7.39 (6 H, m, *Ar*), 6.51 (1 H, d, *J*=9.5 Hz, benzyl-*H*), 5.08 (2 H, s, CH_2); δ_C (100 MHz, DMSO-d_6) 156.6 (*C*=O), 150.2, 149.9, 145.5, 139.5, 137.7, 133.4, 131.6, 130.9, 130.1, 129.2, 128.8, 128.7, 126.8, 126.7, 125.9, 125.6, 124.0, 122.6, 119.8, 66.7 (*C*H_2), 52.2 (benzyl-*C*); *m/z* (FI^+) 496 ($[M]^+$); HRMS (FI^+) $C_{24}H_{18}BrClN_2O_3$, ($[M]^+$) requires 496.0189; found 496.0206.

2-(Amino(phenyl)methyl)quinolin-8-ol 174

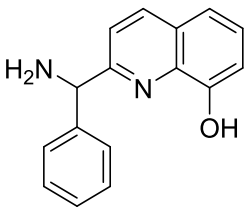

Phenyllithium (1.8 M in nBu_2O, 2.72 mL, 4.9 mmol) was slowly added to a stirring solution of 8-hydroxyquinoline-2-carbonitrile (446 mg, 2.45 mmol) in THF at -78 °C. The reaction was allowed to warm to RT over 2 h. After recooling the reaction mixture to -78 °C, EtOH (7 mL) was added dropwise followed by the addition of $NaBH_4$ (110 mg, 2.9 mmol). The reaction mixture was allowed to warm to RT over 3 h. A solution of HCl (1 N in H_2O) was added dropwise until hydrogen evolution ceased. The mixture was treated with saturated aqueous $NaHCO_3$ and then extracted three times with $CHCl_3$. Combined organic layers were dried

over anhydrous $MgSO_4$, filtered and reduced to dryness. The organic residue was then recrystallised from toluene to give **174** as a bright-yellow solid (276 mg, 45 %).

mp 149-151 °C; ν_{max}/cm^{-1} 1244 (NH_2); δ_H (400 MHz, Acetone-d_6) 8.23 (1 H, d, *J*=8.5 Hz, 4-quinolinyl-*H*), 7.76 (1 H, d, *J*=8.5 Hz, 3-quinolinyl-*H*), 7.54 - 7.60 (2 H, m, *Ar*), 7.38 - 7.47 (2 H, m, *Ar*), 7.32 - 7.37 (2 H, m, *Ar*), 7.23 - 7.33 (4 H, m, *Ar*), 7.07 - 7.14 (1 H, m, *Ar*), 6.07 (1 H, s), benzyl-*H*); δ_C (100 MHz, Acetone-d_6) 137.1, 128.7, 128.5, 128.1, 127.7, 127.6, 127.2, 126.7, 121.6, 118.3, 117.9, 110.4, 70.6 (benzyl-*C*); *m*/*z* (ESI$^+$) 251 ([M+H]$^+$, 100 %); HRMS (ESI) $C_{16}H_{14}N_2O$, requires 250.1106; found 250.1110.

1,3-bis((8-Hydroxyquinolin-7-yl)(phenyl)methyl)urea dihydrochloride 176

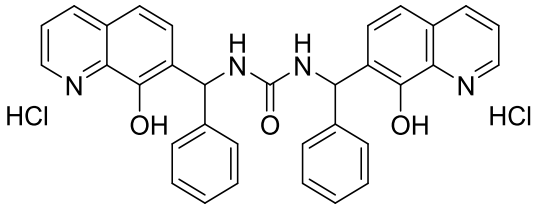

Following general procedure 1, 8-hydroxyquinoline (290 mg, 2.0 mmol), urea (60 mg, 1.0 mmol) and benzaldehyde (406 µL, 4.0 mmol) gave **176** (127 mg, 12 %) as an off-white powder. The solid was then stirred in a 4M HCl solution in dioxane for 1 h. The solvent was removed under reduced pressure to give the hydrochloride salt of **176** as an off-white powder in quantitative yield.

mp 154 °C; ν_{max}/cm^{-1} 1748 (C=O); δ_H (400 MHz, DMSO-d_6) 8.88 - 9.02 (2 H, m, quinoline-*Ar*), 8.70 - 8.84 (2 H, m, quinoline-*Ar*), 8.18 - 8.47 (2 H, m, quinoline-*Ar*), 7.65 - 7.72 (2 H, m, *Ar*), 7.58 - 7.64 (2 H, m, *Ar*), 7.37 - 7.42 (8 H, m, *Ar*), 7.27 - 7.34 (4 H, m, *Ar*), 5.85 - 5.91 (2 H, m, benzyl-*H*); δ_C (100 MHz, DMSO-d_6) 151.5 (*C*=O), 150.2, 144.4, 144.0, 142.8, 138.1, 136.9, 129.8, 129.0, 127.7, 125.5, 124.4, 123.2, 121.0, 57.1 (benzyl-*C*); A molecular ion could not be identified *via* the mass spectrometry techniques of ESI, EI or FI.

N-((3-(benzamido(1-hydroxynaphthalen-2-yl)methyl)phenyl)(8-hydroxyquinolin-7-yl)methyl)benzamide **178**

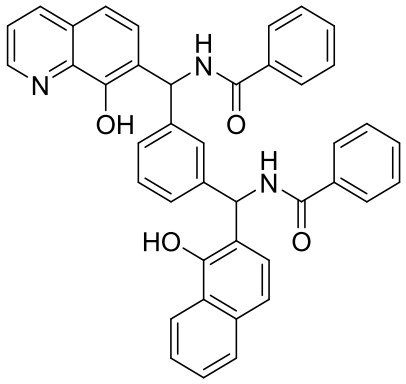

Following general procedure 1, 8-hydroxyquinoline (290 mg, 2.0 mmol), benzamide (242 mg, 2.0 mmol) and isotherephthalaldehyde (134 mg, 1.0 mmol) gave **178** (312 mg, 42 %) as an off-white powder. The compound was tested as a mixture of isomers.

δ_H (400 MHz, DMSO-d_6) 9.98 (1 H, br. s, N*H*), 9.13 - 9.35 (1 H, m, quinoline-*Ar*), 8.91 - 9.10 (2 H, m, *Ar*), 8.66 - 8.91 (2 H, m, *Ar*), 8.15 - 8.36 (1 H, m, *Ar*), 7.74 - 7.93 (6 H, m, *Ar*), 7.60 - 7.75 (2 H, m, *Ar*), 7.17 - 7.60 (14 H, m, *Ar*), 6.86 - 7.16 (2 H, m, benzyl-*H*); *m/z* (ESI^+) 316 ($[M+2H]^{2+}$).

N,N'-(1,4-phenylenebis((8-hydroxyquinolin-7-yl)methylene))dibenzamide **180**

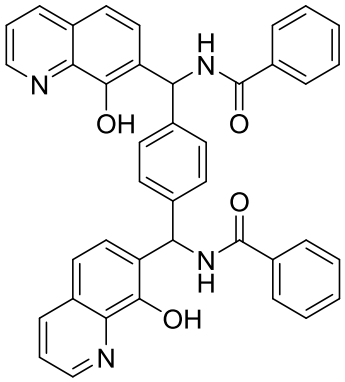

Following general procedure, 8-hydroxyquinoline (290 mg, 2.0 mmol), benzamide (242 mg, 2.0 mmol) and therephthalaldehyde (134 mg, 1.0 mmol) gave **180** (312 mg, 42 %) as an off-white powder. The compound was highly insoluble and was analysed by LC-MS only.

m/z (ESI^+) 316 ($[M+2H]^{2+}$).

3-Hydroxyisoindolin-1-one **182**

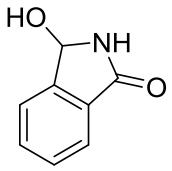

2-Cyanobenzaldehyde (131 mg, 1 mmol) and sodium perborate tetrahydrate (615 mg, 4 mmol) were suspended in a mixture of water (10 mL) and ethanol (5 mL) inside a sealed vial and stirred at 100 °C for 10 minutes. The aqueous solution was extracted with Et_2O three times and the combined organic fractions were concentrated under reduced pressure to give **182** as a white powder (115 mg, 77 %).

mp 171 °C; ν_{max}/cm^{-1} 3339 (NH), 1697 (C=O); δ_H (400 MHz, DMSO-d_6) 8.87 (1 H, s, O*H*), 7.38 - 7.73 (4 H, m, *Ar*), 6.33 (1 H, d, *J*=9.0 Hz, N*H*), 5.87 (1 H, d, *J*=9.0 Hz, C*H*(OH)); δ_C (100 MHz, DMSO-d_6) 169.3 (*C*=O), 147.8, 132.9, 130.0, 124.5, 123.2, 78.9 (*C*H(OH)); *m*/*z* (ESI$^-$) 148 ([M-H]$^-$); HRMS (ESI$^+$) $C_8H_7NNaO_2$, ([M+Na]$^+$) requires 172.0369; found 172.0374.

3-(5-Chloro-8-hydroxyquinolin-7-yl)isoindolin-1-one hydrochloride **183**

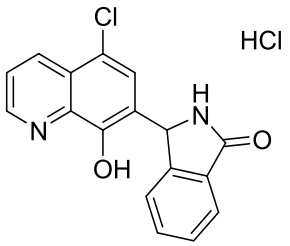

Following general procedure 1, 5-chloro-8-hydroxyquinoline (144 mg, 1.0 mmol), and **182** (149 mg, 1.0 mmol) gave **183** (123 mg, 40 %) as a white powder. **183** was then stirred in a 4M HCl solution in dioxane for 1 h. The solvent was removed under reduced pressure to give the hydrochloride salt of **183** as a light-yellow powder in quantitative yield.

mp 267 - 268 °C; ν_{max}/cm^{-1} 3177 (NH), 1657 (C=O); δ_H (400 MHz, DMSO-d_6) 8.96 - 9.11 (2 H, m, quinoline-*Ar*), 8.37 - 8.61 (1 H, m, quinoline-*Ar*), 7.68 - 7.83 (2 H, m, *Ar*), 7.37 - 7.58 (3 H, m, *Ar*), 7.14 (1 H, s, *Ar*), 6.32 (1 H, s, benzyl-*H*), 3.56 (1 H, s, O*H*); δ_C (100 MHz, DMSO-d_6) 170.8 (*C*=O), 151.0, 150.1, 148.7, 139.5, 134.1, 133.0, 132.5, 129.2, 126.2, 125.5, 124.3, 124.2, 123.9, 123.6, 119.9, 54.4 (benzyl-*C*); *m*/*z* (ESI$^-$) 309 ([M-H]$^-$); HRMS (ESI$^+$) $C_{17}H_{11}ClN_2NaO_2$, ([M+Na]$^+$) requires 333.0401; found 333.0391.

5-Chloro-7-((3-methylthiophen-2-yl)(pyrrolidin-1-yl)methyl)quinolin-8-ol **184**

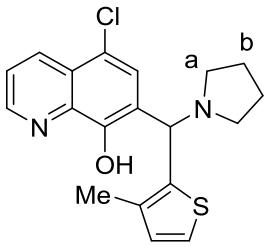

A mixture of 5-chloro-8-hydroxyquinoline (180 mg, 1 mmol), 3-methyl-2-thiophenecarboxaldehyde (108 µL, 1 mmol), pyrrolidine (83 µL, 1 mmol), and triethylamine (140 µL, 1 mmol) was stirred in ethanol (15 mL) for 72 h at room temperature. The volume of the reaction mixture was reduced and the precipitate was filtered, washed with EtOH, H_2O, and dried to give **184** (65 mg, 18 %) as a light-brown powder.

mp 148 °C; ν_{max}/cm^{-1} 3333 (OH); δ_H (400 MHz, DMSO-d_6) 10.47 (1 H, br. s., O*H*), 8.90 - 9.02 (1 H, m, quinoline-*Ar*), 8.37 - 8.56 (1 H, m, quinoline-*Ar*), 7.86 (1 H, s, *Ar*), 7.67 - 7.79 (1 H, m, *Ar*), 7.21 - 7.44 (1 H, m, *Ar*), 6.77 (1 H, m, *Ar*), 5.37 (1 H, s, benzyl-*H*), 2.38 - 2.52 (4 H, m, H_a), 2.33 (3 H, s, CH_3), 1.70 - 1.86 (4 H, m, H_b); δ_C (100 MHz, DMSO-d_6) 149.7, 149.5, 141.0, 139.5, 133.6, 132.9, 129.9, 126.9, 126.3, 125.1, 124.5, 123.4, 119.2, 60.2 (C_a), 53.4 (benzyl-*C*), 23.6 (C_b), 14.5 (thiophene-*C*H_3); *m/z* (ESI$^+$) 359 ([M+H]$^+$); HRMS (ESI$^+$) $C_{19}H_{20}ON_2ClS$, ([M+H]$^+$) requires 359.0979; found 359.0969.

N-((5-Chloro-8-hydroxyquinolin-7-yl)(m-tolyl)methyl)benzamide **187**

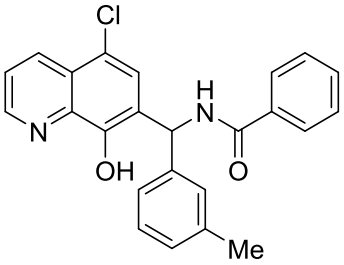

Following general procedure 1, 5-chloro-8-quinolinol (359 mg, 2.0 mmol), benzamide (242 mg, 2.0 mmol) and *m*-tolualdehyde (472 µL, 4.0 mmol) gave **187** (664 mg, 83 %) as a white powder.

mp 239-240 °C; ν_{max}/cm^{-1} 3306 (NH), 1635 (C=O); δ_H (400 MHz, DMSO-d_6) 10.40 (1 H, br. s., N-*H*), 9.14 - 9.32 (1 H, m, quinoline-*Ar*), 8.91 - 9.02 (1 H, m, quinoline-*Ar*), 8.40 - 8.55 (1 H, m, quinoline-*Ar*), 7.90 - 8.00 (2 H, m, *Ar*), 7.87 (1 H, s, *Ar*), 7.66 - 7.77 (1 H, m, *Ar*), 7.52 - 7.60 (1 H, m, *Ar*), 7.45 - 7.51 (2 H, m, *Ar*), 7.19 - 7.26 (1

H, m, *Ar*), 7.10 - 7.18 (2 H, m, *Ar*), 7.04 - 7.10 (1 H, m, *Ar*), 6.99 (1 H, d, *J*=9.0 Hz, benzyl-*H*), 2.26 (3 H, s, CH_3); δ_C (100 MHz, DMSO-d_6) 166.8 (*C*=O), 150.4, 150.0, 142.5, 139.5, 138.4, 135.1, 133.4, 132.2, 129.2, 129.1, 128.6, 128.6, 128.5, 127.7, 126.0, 125.8, 125.2, 123.8, 119.4, 50.9 (benzyl-*C*), 22.0 (*C*H_3); *m/z* (ESI$^-$) 401 ([M-H]$^-$, 100 %); HRMS (ESI$^-$) $C_{24}H_{18}ClN_2O_2$, ([M-H]$^-$) requires 401.1062; found 401.1061.

N-((5-Chloro-8-hydroxyquinolin-7-yl)(o-tolyl)methyl)benzamide **188**

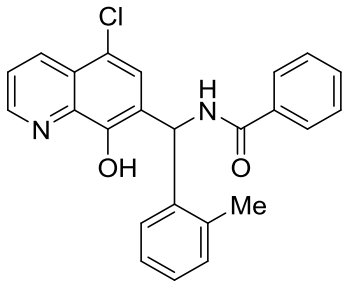

Following general procedure 1, 5-chloro-8-quinolinol (359 mg, 2.0 mmol), benzamide (242 mg, 2.0 mmol) and *o*-tolualdehyde (463 µL, 4.0 mmol) gave **188** (627 mg, 64 %) as an off-white powder.

mp 217-218 °C; ν_{max}/cm^{-1} 3289 (NH), 1637 (C=O); δ_H (400 MHz, DMSO-d_6) 10.40 (1 H, br. s., N-*H*), 9.09 - 9.24 (1 H, m, quinoline-*Ar*), 8.88 - 9.01 (1 H, m, quinoline-*Ar*), 8.40 - 8.53 (1 H, m, quinoline-*Ar*), 7.90 - 7.97 (2 H, m, *Ar*), 7.68 - 7.75 (1 H, m, *Ar*), 7.64 (1 H, s, *Ar*), 7.50 - 7.56 (1 H, m, *Ar*), 7.42 - 7.49 (2 H, m, *Ar*), 7.12 - 7.27 (4 H, m, *Ar*), 7.04 (1 H, d, *J*=8.5 Hz, benzyl-*H*), 2.29 (3 H, s, CH_3); δ_C (100 MHz, DMSO-d_6) 166.5 (*C*=O), 150.7, 150.0, 140.5, 139.4, 136.9, 135.0, 133.4, 132.2, 131.2, 129.8, 128.4, 128.0, 127.9, 127.4, 126.7, 125.8, 125.2, 123.9, 119.0, 48.8 (benzyl-*C*), 19.6 (*C*H_3); *m/z* (ESI$^-$) 401 ([M-H]$^-$, 100 %); HRMS (ESI$^-$) $C_{24}H_{18}ClN_2O_2$, ([M-H]$^-$) requires 401.1062; found 401.1062.

N-((5-Chloro-8-hydroxyquinolin-7-yl)(3-nitrophenyl)methyl)benzamide **189**

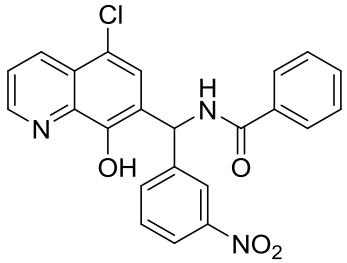

Following general procedure 1, 5-chloro-8-hydroxyquinoline (359 mg, 2.0 mmol), benzamide (242 mg, 2.0 mmol) and 3-nitrobenzaldehyde (604 mg, 4.0 mmol) gave **189** (276 mg, 31 %) as a white powder.

mp 195 - 198 °C; ν_{max}/cm^{-1} 3300 (NH), 1633 (C=O); δ_H (400 MHz, DMSO-d_6) 10.62 (1 H, br. s., N-*H*), 9.38 - 9.50 (1 H, m, quinoline-*Ar*), 8.94 - 9.02 (1 H, m, quinoline-*Ar*), 8.44 - 8.53 (1 H, m, quinoline-*Ar*), 8.18 - 8.22 (1 H, m, *Ar*), 8.12 - 8.17 (1 H, m, *Ar*), 7.92 - 7.98 (2 H, m, *Ar*), 7.90 (1 H, s, *Ar*), 7.81 - 7.86 (1 H, m, *Ar*), 7.71 - 7.77 (1 H, m, *Ar*), 7.63 - 7.69 (1 H, m, *Ar*), 7.54 - 7.58 (1 H, m, *Ar*), 7.46 - 7.53 (2 H, m, *Ar*), 7.11 (1 H, d, *J*=9.0 Hz, benzyl-*H*); δ_C (100 MHz, DMSO-d_6) 167.1 (*C*=O), 150.6, 150.2, 148.8, 144.7, 139.5, 135.0, 134.8, 133.5, 132.5, 131.0, 129.2, 128.5, 127.2, 126.1, 124.7, 124.1, 123.1, 122.4, 119.7, 50.8 (benzyl-*C*); *m*/*z* (ESI$^-$) 432 ([M-H]$^-$); HRMS (ESI$^+$) $C_{23}H_{16}ClN_3NaO_4$, ([M+Na]$^+$) requires 456.0722; found 456.0712.

N-((5-Chloro-8-hydroxyquinolin-7-yl)(3-(trifluoromethyl)phenyl)methyl)benzamide **190**

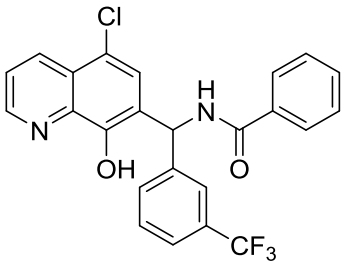

Following general procedure 1, 5-chloro-8-hydroxyquinoline (359 mg, 2.0 mmol), benzamide (242 mg, 2.0 mmol) and 3-trifluoromethylbenzaldehyde (571 µL, 4.0 mmol) gave **190** (645 mg, 71 %) as a white powder.

mp 219 - 222 °C; ν_{max}/cm^{-1} 3294 (NH), 1634 (C=O), 692 (C-Cl); δ_H (400 MHz, DMSO-d_6) 10.58 (1 H, br. s., N-*H*), 9.31 - 9.46 (1 H, m, quinoline-*Ar*), 8.94 - 9.01 (1 H, m, quinoline-*Ar*), 8.44 - 8.52 (1 H, m, quinoline-*Ar*), 7.91 - 7.99 (2 H, m, *Ar*), 7.88 (1 H, s, *Ar*), 7.45 - 7.77 (8 H, m, *Ar*), 7.09 (1 H, d, *J*=8.5 Hz, benzyl-*H*); δ_C (100 MHz, DMSO-d_6) 167.0 (*C*=O), 150.6, 150.2, 143.9, 139.5, 134.9, 133.4, 132.4, 132.4, 130.5, 130.2, 129.2, 128.5, 127.2, 126.0, 125.1, 124.8, 124.3, 124.0, 123.7, 119.7, 50.9 (benzyl-*C*); δ_F (377 MHz, DMSO-d_6) -61.0 (C*F*$_3$); *m*/*z* (ESI$^-$) 455 ([M-H]$^-$); HRMS (ESI$^+$) $C_{24}H_{16}ClF_3N_2NaO_2$, ([M+Na]$^+$) requires 479.0745; found 479.0740.

N-((5-Chloro-8-hydroxyquinolin-7-yl)(3-fluorophenyl)methyl)benzamide **191**

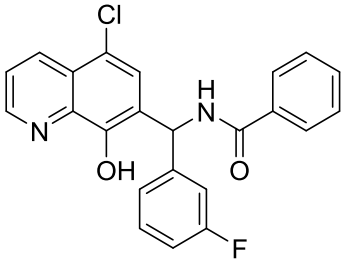

Following general procedure 1, 5-chloro-8-hydroxyquinoline (359 mg, 2.0 mmol), benzamide (242 mg, 2.0 mmol) and 3-fluorobenzaldehyde (424 µL, 4.0 mmol) gave **191** (631 mg, 78 %) as a white powder.

mp 234 °C; ν_{max}/cm^{-1} 3311 (NH), 1631 (C=O), 692 (C-Cl); δ_H (400 MHz, DMSO-d_6) 10.53 (1 H, br. s., N-*H*), 9.24 - 9.37 (1 H, m, quinoline-*Ar*), 8.91 - 9.02 (1 H, m, quinoline-*Ar*), 8.41 - 8.54 (1 H, m, quinoline-*Ar*), 7.90 - 8.00 (2 H, m, *Ar*), 7.86 (1 H, s, *Ar*), 7.65 - 7.78 (1 H, m, *Ar*), 7.45 - 7.61 (3 H, m, *Ar*), 7.34 - 7.44 (1 H, m, *Ar*), 7.07 - 7.24 (3 H, m, *Ar*), 7.03 (1 H, d, *J*=8.5 Hz, benzyl-*H*); δ_C (100 MHz, DMSO-d_6) 167.0 (*C*=O), 150.5, 150.1, 139.5, 135.0, 133.4, 132.4, 131.4, 131.3, 129.2, 128.5, 127.4, 125.9, 125.4, 124.2, 124.0, 119.6, 114.8, 114.7, 144.6, 50.7 (benzyl-*C*); δ_F (377 MHz, DMSO-d_6) -113.0 (C*F*); *m*/*z* (ESI$^-$) 405 ([M-H]$^-$); HRMS (ESI$^+$) $C_{23}H_{16}ClFN_2NaO_2$, ([M+Na]$^+$) requires 429.0777; found 429.0770.

N-((5-Chloro-8-hydroxyquinolin-7-yl)(furan-3-yl)methyl)benzamide 192

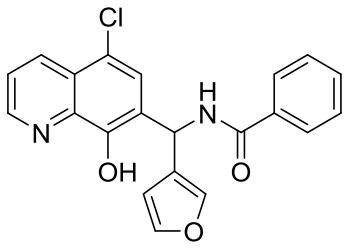

Following general procedure 1, 5-chloro-8-hydroxyquinoline (359 mg, 2.0 mmol), benzamide (242 mg, 2.0 mmol) and 3-furancarboxaldehyde (346 µL, 4.0 mmol) gave **192** (181 mg, 24 %) as a white powder.

mp 218 °C; ν_{max}/cm^{-1} 3323 (NH), 1638 (C=O); δ_H (400 MHz, DMSO-d_6) 10.39 (1 H, br. s., N-*H*), 9.12 - 9.27 (1 H, m, quinoline-*Ar*), 8.92 - 9.03 (1 H, m, quinoline-*Ar*), 8.43 - 8.54 (1 H, m, quinoline-*Ar*), 7.85 - 7.99 (3 H, m, *Ar*), 7.68 - 7.77 (1 H, m, *Ar*), 7.61 - 7.65 (1 H, m, *Ar*), 7.54 (1 H, m, *Ar*), 7.40 - 7.50 (2 H, m, *Ar*), 6.88 (1 H, d, *J*=8.5 Hz, benzyl-*H*), 6.50 (1 H, s, *Ar*); δ_C (100 MHz, DMSO-d_6) 166.7 (*C*=O), 150.1, 150.0, 144.5, 140.8, 139.6, 135.1, 133.4, 132.2, 129.1, 128.5, 127.4, 126.0, 125.8, 123.8, 119.4, 111.2, 43.9 (benzyl-*C*); *m*/*z* (ESI$^+$) 379 ([M+H]$^+$); HRMS (ESI$^+$) $C_{24}H_{15}ClIN_2NaO_3$, ([M+Na]$^+$) requires 401.0663; found 401.0652.

N-((5-chloro-8-hydroxyquinolin-7-yl)(3-methylthiophen-2-yl)methyl)benzamide **193**

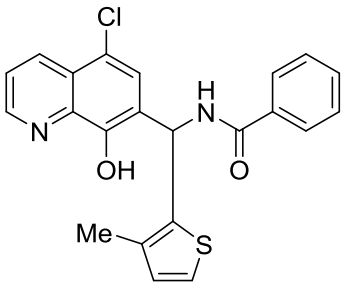

Following general procedure 1, 5-chloro-8-hydroxyquinoline (359 mg, 2.0 mmol), benzamide (242 mg, 2.0 mmol) and 3-methyl-2-thiophenecarboxaldehyde (431µL, 4.0 mmol) gave **193** (584 mg, 71 %) as a white powder.

mp 223 ^{o}C; ν_{max}/cm^{-1} 3274 (NH), 1638 (C=O); δ_H (400 MHz, DMSO-d_6) 10.49 (1 H, br. s., N*H*), 9.28 - 9.39 (1 H, m, quinoline-*Ar*), 8.87 - 9.03 (1 H, m, quinoline-*Ar*), 8.42 - 8.56 (1 H, m, quinoline-*Ar*), 7.86 - 7.97 (3 H, m, *Ar*), 7.68 - 7.79 (1 H, m, *Ar*), 7.41 - 7.60 (3 H, m, *Ar*), 7.24 - 7.29 (1 H, m, *Ar*), 7.17 (1 H, d, *J*=8.0 Hz, benzyl-*H*), 6.90 (1 H, m, *Ar*), 2.15 (3 H, s, C*H*$_3$); δ_C (100 MHz, DMSO-d_6) 166.5 (*C*=O), 150.5, 150.1, 139.9, 139.4, 135.0, 134.9, 133.4, 132.3, 131.4, 129.2, 129.1, 128.5, 127.3, 126.0, 125.6, 124.0, 119.2, 45.7 (benzyl-*C*), 14.4 (*C*H$_3$); *m/z* (ESI$^-$) 407 ([M-H]$^-$); HRMS (ESI$^-$) $C_{22}H_{16}ClN_2O_2S$, ([M-H]$^-$) requires 407.0626; found 407.0613.

N-((5-Chloro-8-hydroxyquinolin-7-yl)(4-methylthiophen-2-yl)methyl)benzamide **194**

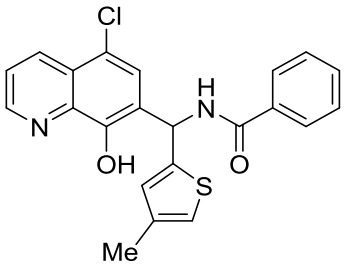

Following general procedure 1, 5-chloro-8-hydroxyquinoline (359 mg, 2.0 mmol), benzamide (242 mg, 2.0 mmol) and 4-methylthiophene-2-carboxaldehyde (492 µL, 4.0 mmol) gave **194** (382 mg, 47 %) as a white powder.

mp 206 ^{o}C; ν_{max}/cm^{-1} 3313 (NH), 1632 (C=O); δ_H (400 MHz, DMSO-d_6) 10.50 (1 H, br. s., N-*H*), 9.25 - 9.59 (1 H, m, quinoline-*Ar*), 8.89 - 9.03 (1 H, m, quinoline-*Ar*), 8.40 - 8.57 (1 H, m, quinoline-*Ar*), 8.00 (1 H, s, *Ar*), 7.91 - 7.97 (2 H, m, *Ar*), 7.70 - 7.77 (1 H, m, *Ar*), 7.52 - 7.59 (1 H, m, *Ar*), 7.45 - 7.52 (2 H, m, *Ar*), 7.14 (1 H, d, *J*=9.0

Hz, benzyl-*H*), 7.01 (1 H, s, *Ar*), 6.62 (1 H, s, *Ar*), 2.11 (3 H, s, CH_3); δ_C (100 MHz, DMSO-d_6) 166.6 (*C*=O), 150.3, 150.1, 146.3, 139.5, 137.6, 134.9, 133.4, 132.4, 129.2, 128.5, 128.2, 127.4, 126.0, 125.6, 124.0, 121.1, 119.5, 47.1 (benzyl-*C*), 16.3 (*C*H_3); *m/z* (ESI$^+$) 431 ([M+Na]$^+$); HRMS (ESI$^+$) $C_{22}H_{17}ClIN_2NaO_2S$, ([M+Na]$^+$) requires 431.0591; found 430.9132.

N-((5-chloro-8-hydroxyquinolin-7-yl)(5-methylthiophen-2-yl)methyl)benzamide **195**

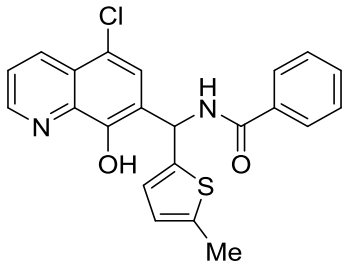

Following general procedure 1, 5-chloro-8-hydroxyquinoline (359 mg, 2.0 mmol), benzamide (242 mg, 2.0 mmol) and 5-methylthiophene-2-carboxaldehyde (431 µL, 4.0 mmol) gave **195** (264 mg, 32 %) as a white powder.

mp 213 ^{o}C; ν_{max}/cm^{-1} 3302 (NH), 1634 (C=O); δ_H (400 MHz, DMSO-d_6) 10.49 (1 H, br. s. , N*H*), 9.30 - 9.48 (1 H, m, quinoline-*Ar*), 8.90 - 9.07 (1 H, m, quinoline-*Ar*), 8.41 - 8.57 (1 H, m, quinoline-*Ar*), 7.99 (1 H, s, *Ar*), 7.89 - 7.95 (2 H, m, *Ar*), 7.68 - 7.78 (1 H, m, *Ar*), 7.52 - 7.59 (1 H, m, *Ar*), 7.44 - 7.51 (2 H, m, *Ar*), 7.10 (1 H, d, *J*=9.0 Hz, benzyl-*H*), 6.49 - 6.67 (2 H, m, *Ar*), 2.37 (3 H, s, CH_3); δ_C (100 MHz, DMSO-d_6) 166.6 (*C*=O), 150.3, 150.1, 143.8, 139.5, 139.5, 134.9, 133.4, 132.3, 129.2, 128.5, 127.4, 126.0, 125.8, 125.8, 125.6, 124.0, 119.5, 47.1 (benzyl-*C*), 15.8 (*C*H_3); *m/z* (ESI$^-$) 431 ([M+Na]$^+$); HRMS (ESI$^+$) $C_{22}H_{17}ClIN_2NaO_2S$, ([M+Na]$^+$) requires 431.0591; found 431.0587.

N-(Benzo[b]thiophen-2-yl(5-chloro-8-hydroxyquinolin-7-yl)methyl)benzamide **196**

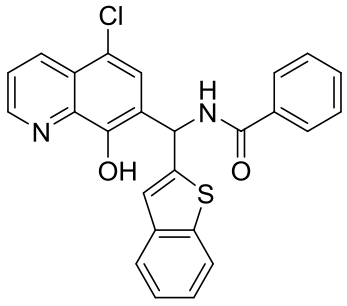

Following general procedure 1, 5-chloro-8-hydroxyquinoline (359 mg, 2.0 mmol), benzamide (242 mg, 2.0 mmol) and benzo[b]thiohene-2-carboxaldehyde (649 mg, 4.0 mmol) gave **196** (273 mg, 31 %) as a white powder.

mp 267 - 268 °C; ν_{max}/cm^{-1} 3296 (NH), 1634 (C=O); δ_H (400 MHz, DMSO-d_6) 10.65 (1 H, br. s., N*H*), 9.55 - 9.68 (1 H, m, quinoline-*Ar*), 8.94 - 9.05 (1 H, m, quinoline-*Ar*), 8.47 - 8.60 (1 H, m, quinoline-*Ar*), 8.04 (1 H, s, *Ar*), 7.94 - 8.01 (3 H, m, *Ar*), 7.86 - 7.92 (1 H, m, *Ar*), 7.72 - 7.80 (2 H, m, *Ar*), 7.55 - 7.62 (1 H, m, *Ar*), 7.47 - 7.55 (2 H, m, *Ar*), 7.25 - 7.37 (2 H, m, *Ar* and benzyl-*H*), 7.10 (1 H, s, *Ar*); δ_C (100 MHz, DMSO-d_6) 166.8 (*C*=O), 150.6, 150.2, 147.4, 141.1, 139.9, 134.8, 133.5, 132.5, 129.3, 129.2, 128.6, 128.4, 127.4, 125.3, 125.1, 124.8, 124.4, 124.1, 123.2, 122.6, 119.7, 47.6 (benzyl-*C*); *m*/*z* (ESI$^-$) 443 ([M-H]$^-$); HRMS (ESI$^-$) $C_{25}H_{16}ClIN_2O_2S$, ([M-H]$^-$) requires 443.0626; found 443.0621.

N-([1,1'-Biphenyl]-3-yl(5-chloro-8-hydroxyquinolin-7-yl)methyl)benzamide **197**

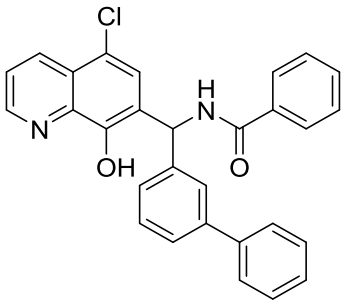

Following general procedure 1, 5-chloro-8-hydroxyquinoline (359 mg, 2.0 mmol), benzamide (242 mg, 2.0 mmol) and biphenyl-3-carboxaldehyde (651 µL, 2.0 mmol) gave **197** (611 mg, 66 %) as a white powder.

mp 211 °C; ν_{max}/cm^{-1} 3299 (NH), 1633 (C=O); δ_H (400 MHz, DMSO-d_6) 10.48 (1 H, br. s., N-*H*), 9.29 - 9.41 (1 H, m, quinoline-*Ar*), 8.93 - 9.00 (1 H, m, quinoline-*Ar*), 8.43 - 8.51 (1 H, m, quinoline-*Ar*), 7.91 - 8.01 (3 H, m, *Ar*), 7.66 - 7.74 (2 H, m, *Ar*), 7.53 - 7.62 (4 H, m, *Ar*), 7.40 - 7.52 (5 H, m, *Ar*), 7.29 - 7.40 (2 H, m, *Ar*), 7.10 (1 H, d, *J*=9.0 Hz, benzyl-*H*); δ_C (100 MHz, DMSO-d_6) 167.0 (*C*=O), 150.4, 150.1, 143.2, 141.3, 141.0, 139.6, 135.1, 133.4, 132.3, 130.0, 129.8, 129.2, 128.5, 128.4, 127.6, 127.4, 127.3, 126.4, 126.4, 126.0, 125.8, 123.9, 119.5, 51.2 (benzyl-*C*); *m*/*z* (FI$^+$) 464 ([M]$^+$); HRMS (FI$^+$) $C_{29}H_{21}ClN_2O_2$, ([M]$^+$) requires 464.1292; found 464.1292.

N-([1,1'-Biphenyl]-4-yl(5-chloro-8-hydroxyquinolin-7-yl)methyl)benzamide hydrochloride **198**

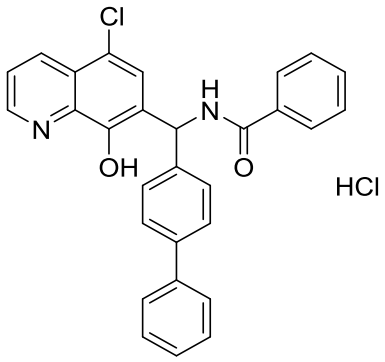

Following general procedure 1, 5-chloro-8-hydroxyquinoline (359 mg, 2.0 mmol), benzamide (242 mg, 2.0 mmol) and biphenyl-4-carboxaldehyde (729 mg, 4.0 mmol) gave **198** (604 mg, 65 %) as a white powder. **198** was then stirred in a 4M HCl solution in dioxane for 1 h. The solvent was removed under reduced pressure to give the hydrochloride salt of **198** as a bright-yellow powder in quantitative yield.

mp 262 - 263 ^{o}C; ν_{max}/cm^{-1} 3305 (NH), 1634 (C=O); δ_H (400 MHz, DMSO-d_6) 9.32 - 9.40 (1 H, m, quinoline-*Ar*), 8.97 - 9.04 (1 H, m, quinoline-*Ar*), 8.51 - 8.61 (1 H, m, quinoline-*Ar*), 7.94 - 8.00 (3 H, m, *Ar*), 7.75 - 7.81 (1 H, m, *Ar*), 7.59 - 7.67 (4 H, m, *Ar*), 7.53 - 7.58 (1 H, m, *Ar*), 7.47 - 7.52 (2 H, m, *Ar*), 7.40 - 7.46 (4 H, m, *Ar*), 7.29 - 7.37 (1 H, m, *Ar*), 7.08 (1 H, d, *J*=8.5 Hz, benzyl-*H*); δ_C (100 MHz, DMSO-d_6) 166.9 (*C*=O), 149.9, 149.7, 141.5, 140.7, 139.9, 138.8, 135.0, 134.4, 132.3, 129.8, 129.2, 128.7, 128.5, 128.3, 127.9, 127.7, 127.5, 126.6, 126.0, 124.0, 119.8, 50.8 (benzyl-*C*); *m/z* (ESI$^-$) 463 ([M-H]$^-$); HRMS (ESI$^+$) $C_{29}H_{21}ClN_2NaO_{42}$, ([M+Na]$^+$) requires 487.1184; found 487.1187.

N-((5-Chloro-8-hydroxyquinolin-7-yl)(3-phenoxyphenyl)methyl)benzamide **199**

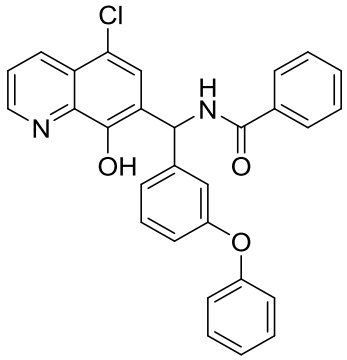

Following general procedure 1, 5-chloro-8-hydroxyquinoline (359 mg, 2.0 mmol), benzamide (242 mg, 2.0 mmol) and 3-phenoxybenzaldehyde (690 µL, 4.0 mmol) gave **199** (548 mg, 57 %) as an off-white powder.

mp 225 °C; ν_{max}/cm^{-1} 3307 (NH), 1638 (C=O); δ_H (400 MHz, DMSO-d_6) 10.49 (1 H, br. s., N*H*), 9.21 - 9.35 (1 H, m, quinoline-*Ar*), 8.89 - 9.03 (1 H, m, quinoline-*Ar*), 8.40 - 8.54 (1 H, m, quinoline-*Ar*), 7.87 - 7.93 (2 H, m, *Ar*), 7.86 (1 H, s, *Ar*), 7.68 - 7.76 (1 H, m, *Ar*), 7.51 - 7.59 (1 H, m, *Ar*), 7.44 - 7.51 (2 H, m, *Ar*), 7.30 - 7.38 (3 H, m, *Ar*), 7.08 - 7.13 (2 H, m, *Ar*), 6.96 - 7.06 (4 H, m, *Ar*), 6.82 - 6.89 (1 H, m, *Ar*); δ_C (100 MHz, DMSO-d_6) 167.0 (*C*=O), 157.6, 157.1, 150.5, 150.1, 144.9, 139.5, 135.1, 133.4, 132.3, 130.9, 130.9, 129.2, 128.5, 128.4, 127.6, 125.9, 125.4, 124.4, 123.9, 123.1, 119.5, 118.0, 117.6, 50.7 (benzyl-*C*); *m/z* (ESI$^-$) 479 ([M-H]$^-$); HRMS (ESI$^+$) $C_{30}H_{21}ClN_2NaO_3$, ([M+Na]$^+$) requires 503.1133; found 503.1131.

N-((5-Chloro-8-hydroxyquinolin-7-yl)(3-(p-tolyloxy)phenyl)methyl)benzamide **200**

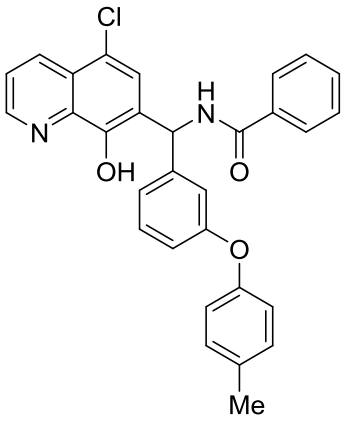

Following general procedure 1, 5-chloro-8-hydroxyquinoline (359 mg, 2.0 mmol), benzamide (242 mg, 2.0 mmol) and 3-(4-methylphenoxy)benzaldehyde (770 µL, 4.0 mmol) gave **200** (546 mg, 55 %) as a white powder.

mp 212 °C; ν_{max}/cm^{-1} 3306 (NH), 1634 (C=O); δ_H (400 MHz, DMSO-d_6) 10.49 (1 H, br. s., N*H*), 9.17 - 9.35 (1 H, m, quinoline-*Ar*), 8.89 - 9.01 (1 H, m, quinoline-*Ar*), 8.37 - 8.58 (1 H, m, quinoline-*Ar*), 7.86 - 7.93 (2 H, m, *Ar*), 7.85 (1 H, s, *Ar*), 7.67 - 7.76 (1 H, m, *Ar*), 7.51 - 7.59 (1 H, m, *Ar*), 7.43 - 7.51 (2 H, m, *Ar*), 7.27 - 7.36 (1 H, m, *Ar*), 7.11 - 7.16 (2 H, m, *Ar*), 7.03 - 7.09 (1 H, m, *Ar*), 6.96 - 7.02 (2 H, m, *Ar*), 6.86 - 6.91 (2 H, m, *Ar*), 6.76 - 6.84 (1 H, m, *Ar*), 2.24 (3 H, s, C*H*$_3$); δ_C (100 MHz, DMSO-d_6) 167.0 (*C*=O), 158.2, 154.6, 150.4, 150.1, 144.7, 139.5, 135.1, 133.6, 133.4, 132.3, 131.2, 129.1, 128.5, 127.6, 125.9, 125.6, 123.9, 122.6, 119.8, 119.5, 117.5, 117.0, 50.6 (benzyl-*C*), 21.1 (*C*H$_3$); *m/z* (ESI$^-$) 493 ([M-H]$^-$); HRMS (ESI$^+$) $C_{30}H_{23}ClN_2NaO_3$, ([M+Na]$^+$) requires 517.1289; found 517.1276.

N-((5-chloro-8-hydroxyquinolin-7-yl)(3-(4-methoxyphenoxy)phenyl)methyl)benzamide 201

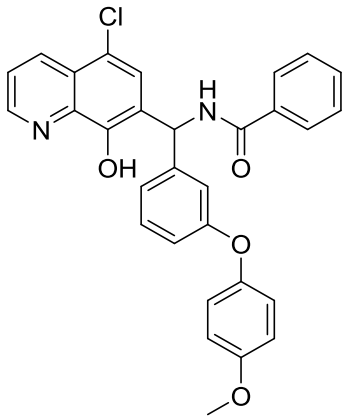

Following general procedure 1, 5-chloro-8-hydroxyquinoline (359 mg, 2.0 mmol), benzamide (242 mg, 2.0 mmol) and 3-(4-methoxy)phenoxybenzaldehyde (837 µL, 4.0 mmol) gave **201** (576 mg, 56 %) as a white powder.

mp 200-202 °C; ν_{max}/cm^{-1} 3274 (NH), 1633 (C=O); δ_H (400 MHz, DMSO-d_6) 10.47 (1 H, br. s., N*H*), 9.21 - 9.32 (1 H, m, quinoline-*Ar*), 8.91 - 9.01 (1 H, m, quinoline-*Ar*), 8.42 - 8.52 (1 H, m, quinoline-*Ar*), 7.87 - 7.93 (2 H, m, *Ar*), 7.85 (1 H, s, *Ar*), 7.68 - 7.78 (1 H, m, *Ar*), 7.52 - 7.59 (1 H, m, *Ar*), 7.42 - 7.51 (2 H, m, *Ar*), 7.21 - 7.36 (1 H, m, *Ar*), 6.94 - 7.06 (5 H, m, *Ar*), 6.86 - 6.94 (2 H, m, *Ar*), 6.67 - 6.80 (1 H, m) 3.71 (3 H, s, C*H*$_3$); δ_C (100 MHz, $CDCl_3$) 167.0 (*C*=O), 159.0, 156.4, 150.4, 150.1, 149.8, 144.7, 139.5, 135.1, 133.4, 132.3, 130.8, 129.1, 128.4, 127.6, 125.9, 125.6, 123.9, 122.2, 121.7, 119.5, 116.7, 116.2, 115.9, 56.2 (*C*H$_3$), 50.6 (benzyl-*C*); *m/z* (ESI$^-$) 509 ([M-H]$^-$); HRMS (ESI$^+$) $C_{30}H_{23}ClN_2NaO_4$, ([M+Na]$^+$) requires 533.1239; found 533.1239.

N-((8-Hydroxy-5-nitroquinolin-7-yl)(3-phenoxyphenyl)methyl)benzamide 202

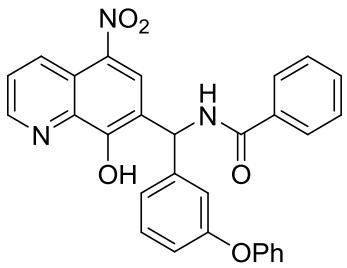

Following general procedure 1, 5-nitro-8-hydroxyquinoline (380 mg, 2.0 mmol), benzamide (242 mg, 2.0 mmol) and 3-phenoxybenzaldehyde (690 µL, 4.0 mmol) gave **202** (669 mg, 68 %) as a light-yellow powder.

mp 222 °C; ν_{max}/cm^{-1} 3294 (NH), 1634 (C=O); δ_H (400 MHz, DMSO-d_6) 9.41 - 9.51 (1 H, m, quinoline-*Ar*), 9.15 - 9.23 (1 H, m, quinoline-*Ar*), 8.97 - 9.06 (1 H, m, quinoline-*Ar*), 8.78 (1 H, s, *Ar*), 7.85 - 7.98 (3 H, m, *Ar*), 7.53 - 7.59 (1 H, m, *Ar*), 7.46 - 7.53 (2 H, m, *Ar*), 7.31 - 7.42 (3 H, m, *Ar*), 7.07 - 7.18 (3 H, m, *Ar*), 6.97 - 7.03 (3 H, m, *Ar*), 6.85 - 6.94 (1 H, m, *Ar*); δ_C (100 MHz, DMSO-d_6) 166.6 (*C*=O), 158.4, 157.2, 156.8, 149.4, 143.8, 137.2, 134.7, 134.6, 133.6, 132.0, 130.7, 130.5, 128.8, 128.7, 128.1, 125.8, 124.0, 123.8, 122.9, 122.2, 119.1, 117.9, 117.6, 50.4 (benzyl-*C*); *m/z* (FI) 491 ([M]); HRMS (FI) $C_{29}H_{21}N_3O_5$, ([M]) requires 491.1481; found 491.1247.

N-((5-Bromo-8-hydroxyquinolin-7-yl)(3-phenoxyphenyl)methyl)benzamide **203**

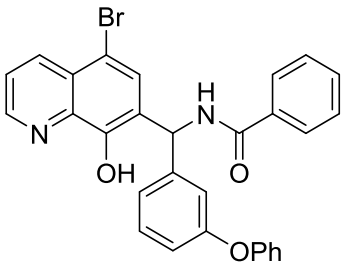

Following general procedure 1, 5-bromo-8-hydroxyquinoline (448 mg, 2.0 mmol), benzamide (242 mg, 2.0 mmol) and 3-phenoxybenzaldehyde (690 µL, 4.0 mmol) gave **203** (872 mg, 79 %) as a white powder.

mp 214 °C; ν_{max}/cm^{-1} 3294 (NH), 1636 (C=O); δ_H (400 MHz, DMSO-d_6) 10.54 (1 H, br. s., N*H*), 9.24 - 9.38 (1 H, m, quinoline-*Ar*), 8.89 - 9.02 (1 H, m, quinoline-*Ar*), 8.35 - 8.49 (1 H, m, quinoline-*Ar*), 8.03 (1 H, s, *Ar*), 7.85 - 7.95 (2 H, m, *Ar*), 7.71 - 7.78 (1 H, m, *Ar*), 7.45 - 7.60 (4 H, m, *Ar*), 7.31 - 7.42 (2 H, m, *Ar*), 7.09 - 7.18 (2 H, m, *Ar*), 6.97 - 7.07 (3 H, m, *Ar*), 6.88 (1 H, d, *J*=8.0 Hz, benzyl-*H*); δ_C (100 MHz, DMSO-d_6) 166.6 (*C*=O), 157.2, 156.8, 150.7, 149.7, 144.5, 139.4, 135.5, 134.7, 132.1, 131.9, 130.7, 130.6, 130.5, 128.8, 128.1, 128.0, 126.8, 125.8, 124.0, 122.7, 119.2, 119.1, 109.0, 50.2 (benzyl-*C*); *m/z* (ESI$^+$) 525 ([M+H]$^+$); HRMS (ESI$^+$) $C_{29}H_{21}O_3N_2BrNa$, ([M+Na]$^+$) requires 547.0628; found 547.0606.

N-((5-Bromo-8-hydroxyquinolin-7-yl)(3-phenoxyphenyl)methyl)-2-phenylacetamide **204**

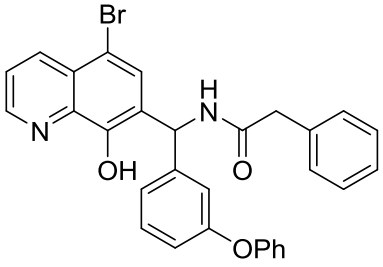

Following general procedure 1, 5-bromo-8-hydroxyquinoline (448 mg, 2.0 mmol), 2-phenylacetamide (270 mg, 2.0 mmol) and 3-phenoxybenzaldehyde (690 µL, 4.0 mmol) gave **204** (873 mg, 81 %) as a white powder.

mp 212 °C; ν_{max}/cm^{-1} 3270 (NH), 1639 (C=O); δ_H (400 MHz, DMSO-d_6) 10.48 (1 H, br. s., N*H*), 9.08 - 9.15 (1 H, m, quinoline-*Ar*), 8.92 - 8.97 (1 H, m, quinoline-*Ar*), 8.38 - 8.44 (1 H, m, quinoline-*Ar*), 7.87 (1 H, s, quinoline-*Ar*), 7.66 - 7.79 (1 H, m, *Ar*), 7.18 - 7.43 (7 H, m, *Ar*), 7.09 - 7.18 (1 H, m, *Ar*), 6.95 - 7.06 (4 H, m, *Ar*), 6.79 - 6.90 (1 H, m, *Ar*), 6.68 (1 H, d, *J*=8.5 Hz, benzyl-*H*), 3.57 (2 H, s, CH_2); δ_C (100 MHz, DMSO-d_6) 170.0 (*C*=O), 157.1, 156.8, 150.4, 149.7, 144.5, 139.4, 136.7, 135.5, 130.6, 130.5, 130.0, 129.4, 128.7, 126.8, 126.7, 126.0, 124.0, 123.9, 122.5, 119.0, 117.6, 117.3, 109.1, 49.9 (*C*H$_2$), 42.7 (benzyl-*C*); *m*/*z* (ESI$^+$) 539 ([M+H]$^+$); HRMS (ESI$^+$) $C_{30}H_{23}O_3N_2BrNa$, ([M+Na]$^+$) requires 561.0784; found 561.0759.

N-([3,3'-Bithiophen]-5-yl(5-chloro-8-hydroxyquinolin-7-yl)methyl)benzamide 205

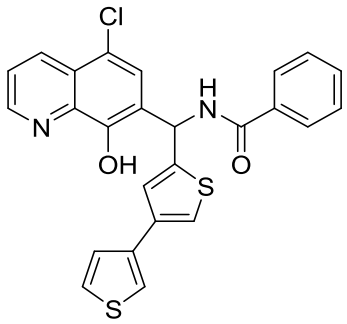

Following general procedure 1, 5-chloro-8-hydroxyquinoline (359 mg, 2.0 mmol), benzamide (242 mg, 2.0 mmol) and 3,3'-bithiophen-5-carboxaldehyde (777 mg, 4.0 mmol) gave **205** (373 mg, 39 %) as an off-white powder.

mp 213 °C; ν_{max}/cm^{-1} 3287 (NH), 1641 (C=O); δ_H (400 MHz, DMSO-d_6) 10.57 (1 H, br. s., N*H*), 9.41 - 9.60 (1 H, m, quinoline-*Ar*), 8.96 - 9.03 (1 H, m, quinoline-*Ar*), 8.46 - 8.55 (1 H, m, quinoline-*Ar*), 8.01 (1 H, s, *Ar*), 7.92 - 7.99 (2 H, m, *Ar*), 7.72 - 7.78 (1 H, m, *Ar*), 7.65 - 7.72 (2 H, m, *Ar*), 7.47 - 7.61 (4 H, m, *Ar*), 7.42 - 7.47 (1 H, m, *Ar*), 7.26 (1 H, s, *Ar*), 7.20 (1 H, d, *J*=8.5 Hz, benzyl-*H*); δ_C (100 MHz, DMSO-d_6) 166.7 (*C*=O), 150.5, 150.1, 147.4, 139.6, 137.6, 137.3, 134.9, 133.4, 132.4, 129.2, 128.5, 127.6, 127.3, 127.2, 126.2, 125.4, 125.2, 124.0, 121.3, 120.4, 119.6, 47.2 (benzyl-*C*); *m*/*z* (ESI$^+$) 499 ([M+Na]$^+$); HRMS (ESI$^+$) $C_{25}H_{17}ClIN_2NaO_2S_2$, ([M+Na]$^+$) requires 499.0312; found 499.0294.

N-([2,2'-Bithiophen]-5-yl(5-chloro-8-hydroxyquinolin-7-yl)methyl)benzamide **206**

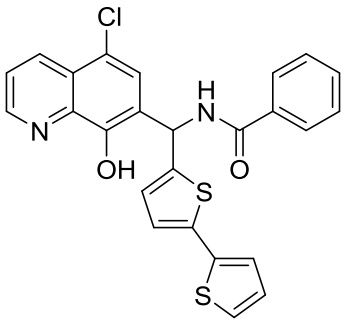

Following general procedure 1, 5-chloro-8-hydroxyquinoline (359 mg, 2.0 mmol), benzamide (242 mg, 2.0 mmol) and 2,2'-bithiophen-5-carboxaldehyde (777 mg, 4.0 mmol) gave **206** (345 mg, 36 %) as a green-brown powder.

mp 154 °C; ν_{max}/cm^{-1} 3291 (NH), 1635 (C=O); δ_H (400 MHz, DMSO-d_6) 10.62 (1 H, br. s., N*H*), 9.50 - 9.57 (1 H, m, quinoline-*Ar*), 8.95 - 9.03 (1 H, m, quinoline-*Ar*), 8.46 - 8.55 (1 H, m, quinoline-*Ar*), 8.02 (1 H, s, *Ar*), 7.91 - 7.98 (2 H, m, *Ar*), 7.70 - 7.80 (1 H, m, *Ar*), 7.54 - 7.60 (1 H, m, benzyl-*H*), 7.42 - 7.53 (3 H, m, *Ar*), 7.21 - 7.25 (1 H, m, *Ar*), 7.15 - 7.20 (1 H, m, *Ar*), 7.09 - 7.14 (1 H, m, *Ar*), 7.00 - 7.07 (1 H, m, *Ar*), 6.75 - 6.79 (1 H, m, *Ar*); δ_C (100 MHz, DMSO-d_6) 166.7 (*C*=O), 150.4, 150.2, 145.6, 139.6, 137.2, 136.7, 134.8, 133.5, 132.5, 120.2, 129.2, 128.5, 127.2, 126.2, 126.2, 125.1, 124.8, 124.4, 124.1, 119.6, 47.1 (benzyl-*C*); *m/z* (ESI$^+$) 499 ([M+Na]$^+$); HRMS (ESI$^+$) $C_{25}H_{17}ClIN_2NaO_2S_2$, ([M+Na]$^+$) requires 499.0312; found 499.0300.

5-Chloro-7-(pyrrolidin-1-ylmethyl)quinolin-8-ol **207**

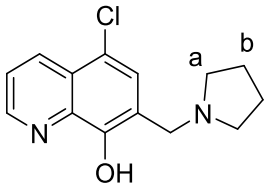

A mixture of 5-chloro-8-hydroxyquinoline (180 mg, 1 mmol), paraformaldehyde (36.2 mg, 1.2 mmol), pyrrolidine (100 µL, 1.2 mmol), and triethylamine (170 µL, 1.2 mmol) was stirred in ethanol (15 mL) for 16 h under reflux. The volume of the reaction mixture was reduced and the precipitate was filtered, washed with EtOH, H_2O, and dried to give **207** (60 mg, 23 %) as a light-brown powder.

mp 125 °C; δ_H (400 MHz, DMSO-d_6) 8.83 - 9.03 (1 H, m, quinoline-*Ar*), 8.30 - 8.64 (1 H, m, quinoline-*Ar*), 7.64 - 7.74 (1 H, m, quinoline-*Ar*), 7.62 (1 H, s, quinoline-*Ar*), 3.83 (2 H, s, benzyl-CH_2), 2.46 - 2.57 (4 H, m, H_b), 1.67 - 1.77 (4 H, m, H_a); δ_C (100 MHz, DMSO-d_6) 151.3, 149.4, 139.3, 132.7, 128.6, 125.2, 123.0, 122.1, 118.4, 54.2, 53.9, 23.7 (C_a); *m/z* (ESI$^+$) 263 ([M+H]$^+$); HRMS (ESI$^+$) $C_{14}H_{16}ON_2Cl$, ([M+H]$^+$) requires 263.0946; found 263.0942.

5-Chloro-7-(morpholinomethyl)quinolin-8-ol **208**

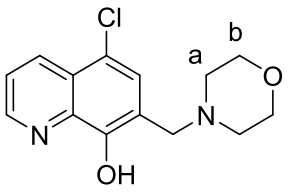

A mixture of 5-chloro-8-hydroxyquinoline (180 mg, 1 mmol), paraformaldehyde (36.2 mg, 1.2 mmol), morpholine (103 µL, 1.2 mmol), and triethylamine (170 µL, 1.2 mmol) was stirred in ethanol (15 mL) for 16 h under reflux. The volume of the reaction mixture was reduced and the precipitate was filtered, washed with EtOH, H_2O, and dried to give **208** (42 mg, 15 %) as an off-white powder.

mp 112 °C; ν_{max}/cm^{-1} 3313 (OH); δ_H (400 MHz, DMSO-d_6) 8.73 - 9.06 (1 H, m, quinoline-*Ar*), 8.35 - 8.55 (1 H, m, quinoline-*Ar*), 7.67 - 7.73 (1 H, m, quinoline-*Ar*), 7.65 (1 H, s, quinoline-*Ar*), 3.70 (2 H, s, benzyl-CH_2), 3.55 - 3.64 (4 H, m, H_b), 2.41 - 2.48 (4 H, m, H_a); δ_C (100 MHz, DMSO-d_6) 151.4, 149.4, 139.2, 132.9, 129.1, 125.4, 123.2, 120.9, 118.6, 66.7 , (H_a), 56.4, 53.6; *m/z* (ESI$^+$) 279 ([M+H]$^+$); HRMS (ESI$^+$) $C_{14}H_{16}O_2N_2Cl$, ([M+H]$^+$) requires 279.0895; found 279.0891.

1-(4-((5-Chloro-8-hydroxyquinolin-7-yl)methyl)piperazin-1-yl)ethan-1-one **209**

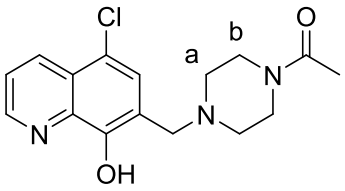

A mixture of 5-chloro-8-hydroxyquinoline (180 mg, 1 mmol), paraformaldehyde (36.2 mg, 1.2 mmol), 1-acetylpiperazine (171 µL, 1.2 mmol), and triethylamine (170 µL, 1.2 mmol) was stirred in ethanol (15 mL) for

16 h under reflux. The volume of the reaction mixture was reduced and the precipitate was filtered, washed with EtOH, H_2O, and dried to give **209** (45 mg, 14 %) as a light-brown powder.

mp > 250 °C; ν_{max}/cm^{-1} 1621 (C=O); δ_H (400 MHz, DMSO-d_6) 8.98 - 9.10 (1 H, m, quinoline-*Ar*), 8.52 - 8.69 (1 H, m, quinoline-*Ar*), 8.03 - 8.16 (1 H, m, quinoline-*Ar*), 7.80 - 7.92 (1 H, m, quinoline-*Ar*), 4.48 - 4.63 (2 H, m, benzyl-CH_2), 3.45 - 3.74 (4 H, m, H_b), 2.91 - 3.24 (4 H, m, H_a), 2.03 (3 H, s, CH_3); δ_C (100 MHz, DMSO-d_6) 169.0 (*C*=O), 153.4, 153.1, 149.4, 134.2, 131.3, 127.2, 124.6, 119.1, 113.3, 53.1 (C_b), 50.6 (C_a), 47.7 (benzyl-*C*), 21.5 (*C*H_3); *m/z* (ESI$^+$) 320 ([M+H]$^+$); HRMS (ESI$^+$) $C_{16}H_{19}O_2N_3Cl$, ([M+H]$^+$) requires 320.1160; found 320.1156.

tert-Butyl 4-((5-Chloro-8-hydroxyquinolin-7-yl)methyl)piperazine-1-carboxylate 210

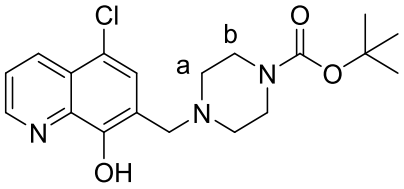

A mixture of 5-chloro-8-hydroxyquinoline (180 mg, 1 mmol), paraformaldehyde (36.2 mg, 1.2 mmol), 1-*tert*-butylpiperazine (224 mg, 1.2 mmol), and triethylamine (170 µL, 1.2 mmol) was stirred in ethanol (15 mL) for 16 h under reflux. The volume of the reaction mixture was reduced and the precipitate was filtered, washed with EtOH, H_2O, and dried to give **210** (79 mg, 21 %) as a light-brown powder.

mp 201 °C; ν_{max}/cm^{-1} 1701 (C=O); δ_H (400 MHz, DMSO-d_6) 8.83 - 9.06 (1 H, m, quinoline-*Ar*), 8.36 - 8.58 (1 H, m, quinoline-*Ar*), 7.67 - 7.77 (1 H, m, quinoline-*Ar*), 7.65 (1 H, s, quinoline-*Ar*), 3.71 (2 H, s, benzyl-CH_2), 3.27 - 3.38 (4 H, m, H_b), 2.33 - 2.45 (4 H, m, H_a), 1.39 (9 H, s, C(CH_3)$_3$); δ_C (100 MHz, DMSO-d_6) 154.2 (*C*=O), 151.3, 149.4, 139.2, 132.9, 129.1, 125.4, 123.2, 121.0, 118.7, 79.2 (C_b), 55.9 (benzyl-*C*H$_2$), 52.9 (C_a), 28.5 (C(*C*H$_3$)$_3$); *m/z* (ESI$^+$) 378 ([M+H]$^+$); HRMS (ESI$^+$) $C_{19}H_{25}O_3N_3Cl$, ([M+H]$^+$) requires 378.1579; found 378.1574.

N-((5-Chloro-8-hydroxyquinolin-7-yl)(3-methylthiophen-2-yl)methyl)-2-phenylacetamide 211

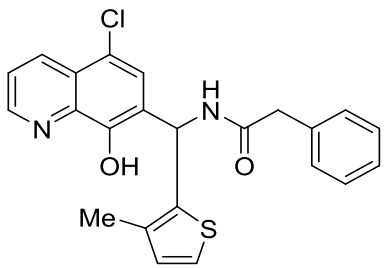

Following general procedure 1, 5-chloro-8-hydroxyquinoline (359 mg, 2.0 mmol), 2-phenylacetamide (270 mg, 2.0 mmol) and 3-methyl-2-thiophenecarboxaldehyde (431 µL, 4.0 mmol) gave **211** (567 mg, 67 %) as a white powder.

mp 181 °C; ν_{max}/cm^{-1} 3237 (NH), 1667 (C=O); δ_H (400 MHz, DMSO-d_6) 10.44 (1 H, br. s., N*H*), 9.07 - 9.16 (1 H, m, quinoline-*Ar*), 8.89 - 9.02 (1 H, m, quinoline-*Ar*), 8.39 - 8.55 (1 H, m, quinoline-*Ar*), 7.68 - 7.77 (2 H, m, *Ar*), 7.18 - 7.35 (5 H, m, *Ar*), 6.87 - 6.90 (1 H, m, *Ar*), 6.84 (1 H, d, *J*=8.5 Hz, benzyl-*H*), 3.55 (2 H, s, CH_2), 2.11 (3 H, s, CH_3); δ_C (100 MHz, DMSO-d_6) 169.7 (*C*=N), 149.9, 149.7, 139.4, 139.0, 136.8, 134.6, 133.0, 130.9, 129.4, 128.7, 126.8, 126.2, 125.5, 125.4, 123.6, 123.5, 118.9, 44.8 (benzyl-*C*), 42.5 (*C*H$_2$), 13.9 (*C*H$_3$); *m/z* (ESI$^-$) 421 ([M-H]$^-$); HRMS (ESI$^+$) $C_{23}H_{19}ClN_2NaO_2S$, ([M+Na]$^+$) requires 445.0748; found 445.0731.

N-((5-Chloro-8-hydroxyquinolin-7-yl)(3-methylthiophen-2-yl)methyl)cyclohexanecarboxamide 212

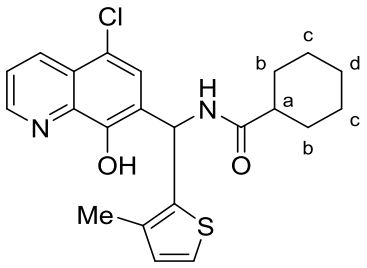

Following general procedure 1, 5-chloro-8-hydroxyquinoline (359 mg, 2.0 mmol), cyclohexanecarboxamide (254 mg, 2.0 mmol) and 3-methyl-2-thiophenecarboxaldehyde (431 µL, 4.0 mmol) gave **212** (390 mg, 47 %) as an off-white powder.

mp 164 °C; ν_{max}/cm^{-1} 3297 (NH), 1640 (C=O); δ_H (400 MHz, DMSO-d_6) 10.34 (1 H, br. s., N*H*), 8.90 - 8.99 (1 H, m, quinoline-*Ar*), 8.65 - 8.74 (1 H, m, quinoline-*Ar*), 8.43 - 8.52 (1 H, m, quinoline-*Ar*), 7.72 - 7.76 (2 H, m, *Ar*), 7.19 - 7.25 (1 H, m, *Ar*), 6.79 - 6.90 (2 H, m, *Ar* and benzyl-*H*), 2.21 - 2.32 (1 H, m, H_a), 2.11 (3 H, s, CH_3), 1.57 - 1.76 (4 H, m, H_b), 1.05 - 1.42 (6 H, m, $H_{c/d}$); δ_C (100 MHz, DMSO-d_6) 175.1 (*C*=O), 150.2, 150.1, 140.5, 139.4, 134.6, 133.4, 131.3, 126.9, 125.9, 123.9, 123.7, 119.2, 44.5 (benzyl-*C*), 30.4 (C_a), 29.8 (C_b), 26.2 (C_c), 26.1 (C_d), 14.3 (*C*H$_3$); *m/z* (ESI$^-$) 413 ([M-H]$^-$); HRMS (ESI$^+$) $C_{22}H_{23}ClN_2NaO_2S$, ([M+Na]$^+$) requires 437.1061; found 437.1051.

N-((5-chloro-8-hydroxyquinolin-7-yl)(3-methylthiophen-2-yl)methyl)cyclopropanecarboxamide **213**

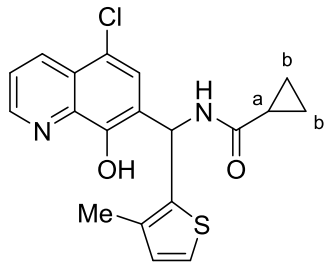

Following general procedure 1, 5-chloro-8-hydroxyquinoline (359 mg, 2.0 mmol), cyclopropanecarboxamide (170 mg, 2.0 mmol) and 3-methyl-2-thiophenecarboxaldehyde (431µL, 4.0 mmol) gave **213** (312 mg, 42 %) as an off-white powder.

mp 202 °C; ν_{max}/cm^{-1} 3272 (NH), 1644 (C=O); δ_H (400 MHz, DMSO-d_6) 10.41 (1 H, br. s., N*H*), 9.02 - 9.10 (1 H, m, quinoline-*Ar*), 8.91 - 8.99 (1 H, m, quinoline-*Ar*), 8.44 - 8.55 (1 H, m, quinoline-*Ar*), 7.77 (1 H, s, *Ar*), 7.68 - 7.75 (1 H, m, *Ar*), 7.19 - 7.28 (1 H, m, *Ar*), 6.92 (1 H, d, *J*=8.5 Hz) 6.82 - 6.88 (1 H, m, *Ar*), 2.13 (3 H, s, C*H*$_3$), 1.65 - 1.80 (1 H, m, H_a), 0.56 - 0.81 (4 H, m, H_b); δ_C (100 MHz, DMSO-d_6) 172.6 (*C*=O), 150.1, 150.1, 140.3, 139.4, 134.7, 133.4, 131.3, 127.9, 126.7, 125.9, 123.9, 123.9, 119.3, 45.0 (benzyl-*C*), 14.4 (*C*H$_3$), 14.2 (C_a), 7.4 (C_b); *m/z* (ESI$^-$) 371 ([M-H]$^-$); HRMS (ESI$^-$) $C_{19}H_{17}ClN_2O_2S$, ([M-H]$^-$) requires 371.0626; found 371.0625.

N-((8-Hydroxy-2-methylquinolin-7-yl)(3-methylthiophen-2-yl)methyl)benzamide **214**

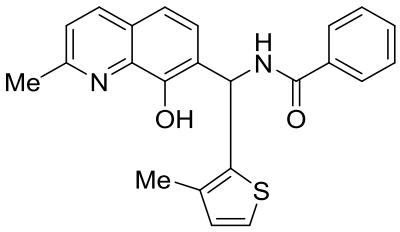

Following general procedure 1, 8-hydroxyquinaldine (318 mg, 2 mmol), benzamide (242 mg, 2 mmol) and 3-methyl-2-thiophenecarboxaldehyde (431 µL, 4 mmol) gave **214** (264 mg, 34 %) as a light brown powder after purification *via* flash column chromatography (10 % - 20 % EtOAc, cyclohexane).

mp 189 °C; ν_{max}/cm^{-1} 3289 (NH), 1631 (C=O); δ_H (400 MHz, DMSO-d_6) 9.27 - 9.38 (1 H, m, quinoline-*Ar*), 8.16 - 8.22 (1 H, m, quinoline-*Ar*), 7.89 - 7.96 (3 H, m, *Ar*), 7.64 - 7.72 (1 H, m, *Ar*), 7.50 - 7.60 (1 H, m, *Ar*), 7.42 - 7.49 (2 H, m, *Ar*), 7.36 - 7.41 (1 H, m, *Ar*), 7.22 - 7.27 (1 H, m, *Ar*), 7.11 - 7.19 (1 H, m, benzyl-*H*), 6.82 - 6.94 (1 H, m, *Ar*), 2.71 (3 H, s, quinoline-C*H*$_3$), 2.17 (3 H, s, thiophene-C*H*$_3$); δ_C (100 MHz, DMSO-d_6) 166.1 (*C*=O),

157.5, 149.5, 140.4, 137.7, 136.6, 134.7, 134.3, 131.7, 130.8, 128.6, 128.1, 126.4, 125.9, 124.3, 123.3, 123.2, 117.4, 45.7 (benzyl-*C*), 25.2 (quinoline-*C*H_3), 14.1 (thiophene-*C*H_3); *m*/*z* (ESI$^+$) 389 ([M+H]$^+$); HRMS (ESI$^+$) $C_{23}H_{21}O_2N_2S$, ([M+H]$^+$) requires 389.1318; found 389.1310.

N-((8-Hydroxy-3-methylquinolin-7-yl)(3-methylthiophen-2-yl)methyl)benzamide **215**

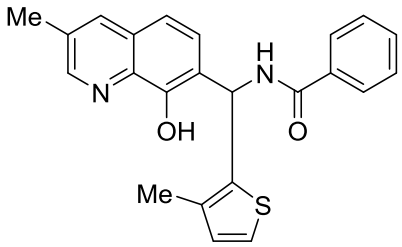

Following general procedure 1, **111** (318 mg, 2.0 mmol), benzamide (242 mg, 2.0 mmol) and 3-methyl-2-thiophenecarboxaldehyde (431 µL, 4.0 mmol) gave **215** (519 mg, 67 %) as a light-brown powder after purification *via* flash column chromatography (10 % - 20 % EtOAc, cyclohexane).

mp 160 ^{o}C; ν_{max}/cm^{-1} 3274 (NH), 1636 (C=O); δ_H (400 MHz, DMSO-d_6) 10.05 (1 H, br. s, N*H*), 9.26 - 9.38 (1 H, m, quinoline-*Ar*), 8.67 - 8.80 (1 H, m, quinoline-*Ar*), 8.04 - 8.11 (1 H, m, quinoline-*Ar*), 7.88 - 7.96 (2 H, m, *Ar*), 7.68 - 7.76 (1 H, m, *Ar*), 7.51 - 7.56 (1 H, m, *Ar*), 7.43 - 7.50 (2 H, m, *Ar*), 7.31 - 7.37 (1 H, m, *Ar*), 7.20 - 7.27 (1 H, m, *Ar*), 7.11 - 7.18 (1 H, m, benzyl-*H*), 6.86 - 6.91 (1 H, m, *Ar*), 2.51 (3 H, s, quinoline-CH_3), 2.16 (3 H, s, thiophene-CH_3); δ_C (100 MHz, DMSO-d_6) 166.0 (*C*=O), 150.5, 150.3, 140.5, 136.8, 135.0, 134.7, 134.3, 131.7, 131.5, 130.8, 128.7, 128.6, 128.1, 127.1, 123.7, 123.3, 116.9, 45.6 (benzyl-*C*), 18.7 (quinoline-*C*H_3), 14.1 (thiophene-*C*H_3); *m*/*z* (ESI$^-$) 387 ([M-H]$^-$); HRMS (ESI$^+$) $C_{23}H_{20}N_2NaO_2S$, ([M+Na]$^+$) requires 411.1138; found 411.1137.

N-((8-Hydroxy-4-methylquinolin-7-yl)(3-methylthiophen-2-yl)methyl)benzamide **216**

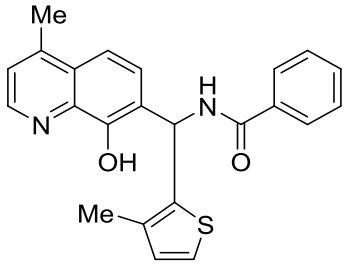

Following general procedure 1, **112** (114 mg, 0.72 mmol), benzamide (87 mg, 0.72 mmol) and 3-methyl-2-thiophenecarboxaldehyde (155 µL, 4.0 mmol) gave **216** (142 mg, 51 %) as a light-brown powder after purification *via* flash column chromatography (10 % - 20 % EtOAc, cyclohexane).

mp 174 °C; ν_{max}/cm^{-1} 3294 (NH), 1637 (C=O); δ_H (400 MHz, DMSO-d_6) 10.03 (1 H, br. s, N*H*), 9.27 - 9.42 (1 H, m, quinoline-*Ar*), 8.69 - 8.76 (1 H, m, quinoline-*Ar*), 7.90 - 7.98 (2 H, m, quinoline-*Ar*), 7.75 - 7.82 (1 H, m, *Ar*), 7.51 - 7.59 (2 H, m, *Ar*), 7.45 - 7.50 (2 H, m, *Ar*), 7.40 - 7.44 (1 H, m, *Ar*), 7.22 - 7.27 (1 H, m, *Ar*), 7.10 - 7.20 (1 H, m, benzyl-*H*), 6.87 - 6.93 (1 H, m, *Ar*), 2.67 (3 H, s, quinoline-CH_3), 2.18 (3 H, s, thiophene-CH_3); δ_C (100 MHz, DMSO-d_6) 166.1 (*C*=O), 150.6, 148.3, 145.0, 140.2, 138.1, 134.7, 134.4, 131.7, 130.8, 129.4, 128.6, 128.1, 126.6, 124.3, 123.4, 122.8, 114.0, 45.6 (benzyl-*C*), 18.8 (quinoline-*C*H$_3$), 14.1 (thiophene-*C*H$_3$); *m*/*z* (ESI$^-$) 387 ([M-H]$^-$); HRMS (ESI$^+$) $C_{23}H_{20}N_2NaO_2S$, ([M+Na]$^+$) requires 411.1138; found 411.1142.

N-((8-Hydroxy-5-methylquinolin-7-yl)(3-methylthiophen-2-yl)methyl)benzamide 217

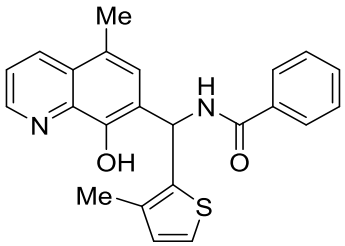

Following general procedure 1, **113** (159 mg, 1 mmol), benzamide (121 mg, 1 mmol) and 3-methyl-2-thiophenecarboxaldehyde (215 µL, 2.0 mmol) gave **217** (190 mg, 49 %) as an off-white powder after purification *via* flash column chromatography (10 % - 20 % EtOAc, cyclohexane).

mp 170 °C; ν_{max}/cm^{-1} 3299 (NH), 1638 (C=O); δ_H (400 MHz, DMSO-d_6) 9.84 (1 H, br. s., N*H*), 9.24 - 9.34 (1 H, m, quinoline-*Ar*), 8.81 - 8.95 (1 H, m, quinoline-*Ar*), 8.31 - 8.48 (1 H, m, quinoline-*Ar*), 7.85 - 8.02 (2 H, m, *Ar*), 7.58 - 7.64 (2 H, m, *Ar*), 7.51 - 7.57 (1 H, m, *Ar*), 7.43 - 7.50 (2 H, m, *Ar*), 7.21 - 7.27 (1 H, m, *Ar*), 7.11 - 7.18 (1 H, m, benzyl-*H*), 6.84 - 6.93 (1 H, m, *Ar*), 2.56 (3 H, s, quinoline-CH_3), 2.17 (3 H, s, thiophene-CH_3); δ_C (100 MHz, DMSO-d_6) 166.1 (*C*=O), 148.3, 140.3, 138.7, 134.7, 133.5, 131.7, 130.8, 128.7, 128.7, 128.1, 127.2, 127.0, 123.6, 123.3, 122.0, 45.6 (benzyl-*C*), 18.4 (quinoline-*C*H$_3$), 14.1 (thiophene-*C*H$_3$); *m*/*z* (ESI$^+$) 389 ([M+H]$^+$); HRMS (ESI$^+$) $C_{23}H_{20}N_2NaO_2S$, ([M+Na]$^+$) requires 411.1138; found 411.1131.

N-((8-Hydroxy-6-methylquinolin-7-yl)(3-methylthiophen-2-yl)methyl)benzamide **218**

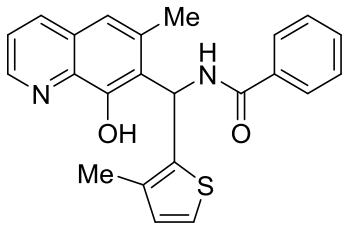

Following general procedure 1, **114** (289 mg, 1.82 mmol), benzamide (220 mg, 1.82 mmol) and 3-methyl-2-thiophenecarboxaldehyde (392 µL, 3.64 mmol) gave **218** (403 mg, 57 %) as a light-brown powder after purification *via* flash column chromatography (10 % - 20 % EtOAc, cyclohexane).

mp 211 °C; ν_{max}/cm^{-1} 2980 (NH), 1660 (C=O); δ_H (400 MHz, DMSO-d_6) 8.96 - 9.03 (1 H, m, quinoline-*Ar*), 8.88 - 8.94 (1 H, m, quinoline-*Ar*), 8.26 - 8.38 (1 H, m, quinoline-*Ar*), 7.80 - 7.90 (2 H, m, *Ar*), 7.61 - 7.68 (2 H, m, *Ar*), 7.52 - 7.58 (1 H, m, *Ar*), 7.43 - 7.51 (2 H, m, *Ar*), 7.29 - 7.37 (1 H, m, *Ar*), 7.23 - 7.28 (1 H, m, benzyl-*H*), 6.81 - 6.90 (1 H, m, *Ar*), 3.18 (3 H, s, quinoline-C*H*$_3$), 2.29 (3 H, s, thiophene-C*H*$_3$); δ_C (100 MHz, DMSO-d_6) 165.4 (*C*=O), 153.2, 149.4, 137.8, 137.5, 135.9, 135.0, 134.4, 132.1, 132.0, 130.7, 129.0, 128.3, 127.7, 124.0, 123.7, 122.3, 118.0, 47.3 (benzyl-*C*), 15.9 (quinoline-*C*H$_3$), 14.3 (thiophene-*C*H$_3$); *m*/*z* (ESI$^+$) 389 ([M+H]$^+$); HRMS (ESI$^+$) $C_{23}H_{21}O_2N_2S$, ([M+H]$^+$) requires 389.1318; found 389.1310.

N-((8-Hydroxy-5-methoxyquinolin-7-yl)(3-methylthiophen-2-yl)methyl)benzamide **219**

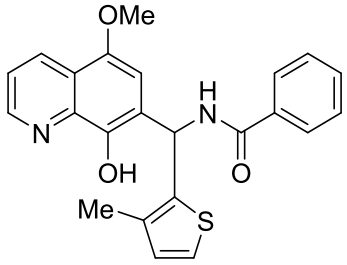

Following general procedure, **115** (146 mg, 0.83 mmol), benzamide (100 mg, 0.83 mmol) and 3-methyl-2-thiophenecarboxaldehyde (180 µL, 1.7 mmol) gave **219** (211 mg, 63 %) as an off-white powder after purification *via* flash column chromatography (10 % - 20 % EtOAc, cyclohexane).

mp 254 °C; ν_{max}/cm^{-1} 3325 (NH), 1636 (C=O); δ_H (400 MHz, DMSO-d_6) 9.53 (1 H, br. s., N*H*), 9.30 - 9.38 (1 H, m, quinoline-*Ar*), 8.82 - 8.95 (1 H, m, quinoline-*Ar*), 8.44 - 8.54 (1 H, m, quinoline-*Ar*), 7.89 - 7.96 (2 H, m, *Ar*), 7.53 - 7.61 (2 H, m, *Ar*), 7.45 - 7.52 (2 H, m, *Ar*), 7.39 (1 H, s, *Ar*), 7.22 - 7.27 (2 H, m, *Ar*), 6.85 - 6.92 (1 H, m,

Ar), 3.92 (3 H, s, OC*H*$_3$), 2.20 (3 H, s, C*H*$_3$); δ_C (100 MHz, DMSO-d_6) 166.1 (*C*=O), 149.3, 146.9, 143.8, 140.2, 138.7, 134.8, 134.5, 131.7, 130.9, 130.8, 128.7, 128.1, 123.8, 123.4, 121.6, 120.0, 105.6, 56.4 (O*C*H$_3$), 45.5 (benzyl-*C*), 14.1 (*C*H$_3$); *m*/*z* (ESI$^+$) 405 ([M+H]$^+$); HRMS (ESI$^+$) $C_{23}H_{20}N_2NaO_3S$, ([M+Na]$^+$) requires 427.1087; found 427.1082.

N-((4-Ethyl-8-hydroxyquinolin-7-yl)(3-methylthiophen-2-yl)methyl)benzamide **220**

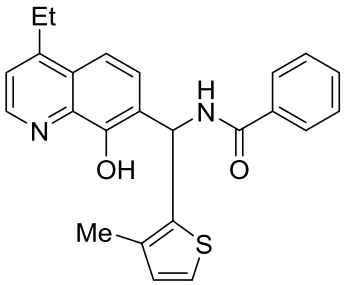

Following general procedure, **120** (277 mg, 1.6 mmol), benzamide (194 mg, 1.6 mmol) and 3-methyl-2-thiophenecarboxaldehyde (345 µL, 3.2 mmol) gave **220** (367 mg, 57 %) as a light-brown powder after purification *via* flash column chromatography (10 % - 20 % EtOAc, cyclohexane).

mp 178 °C; ν_{max}/cm^{-1} 3280 (NH), 1638 (C=O); δ_H (400 MHz, DMSO-d_6) 9.98 (1 H, br. s., N*H*), 9.26 - 9.40 (1 H, m, quinoline-*Ar*), 8.71 - 8.83 (1 H, m, quinoline-*Ar*), 7.90 - 7.98 (2 H, m, *Ar*), 7.73 - 7.80 (1 H, m, *Ar*), 7.58 - 7.64 (1 H, m, *Ar*), 7.51 - 7.57 (1 H, m, *Ar*), 7.40 - 7.50 (2 H, m, *Ar*), 7.23 - 7.29 (1 H, m, *Ar*), 7.15 (1 H, d, *J*=8.0 Hz, benzyl-*H*), 6.87 - 6.94 (1 H, m, *Ar*), 3.09 (2 H, q, *J*=7.5 Hz, C*H*$_2$CH$_3$), 2.18 (3 H, s, C*H*$_3$), 1.32 (3 H, t, *J*=7.5 Hz, CH$_2$C*H*$_3$); δ_C (100 MHz, DMSO-d_6) 166.1 (*C*=O), 150.7, 150.4, 148.5, 140.2, 138.3, 134.7, 134.4, 131.7, 130.8, 128.6, 128.1, 127.2, 126.7, 124.0, 123.4, 120.9, 113.6, 45.6 (benzyl-*C*), 24.9 (*C*H$_2$CH$_3$), 14.5 (*C*H$_3$), 14.1 (CH$_2$*C*H$_3$); *m*/*z* (ESI$^-$) 401 ([M-H]$^-$); HRMS (ESI$^+$) $C_{24}H_{23}O_2N_2S$, ([M+H]$^+$) requires 403.1475; found 403.1469.

5-(Furan-3-yl)quinolin-8-ol **221**

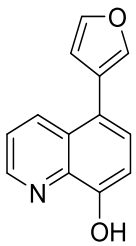

A solution of **148** (445 mg, 1.2 mmol) in sodium hydroxide (1M aq., 3.66 mL), ethanol (7.5 mL) and H_2O (7.5 mL) was stirred under reflux for 2 h. The ethanol was removed *in vacuo* and the pH adjusted to 6.5. The precipitate was filtered and dried to give **221** (252 mg, 98 %) as an off-white solid.

mp 79 °C; ν_{max}/cm^{-1} 3189 (OH); δ_H (400 MHz, $CDCl_3$) 8.71 - 8.81 (2 H, m, *Ar*), 8.41 - 8.50 (1 H, m, *Ar*), 8.22 - 8.35 (1 H, m, *Ar*), 7.42 - 7.52 (3 H, m, *Ar*), 7.25 - 7.32 (1 H, m, *Ar*), 6.97 - 7.09 (1 H, m, *Ar*); δ_C (100 MHz, $CDCl_3$) 151.4, 151.2, 148.3, 133.6, 131.0, 130.1, 128.9, 127.6, 127.4, 122.6, 121.8, 110.1; *m*/*z* (ESI$^+$) 212 ([M+H]$^+$); HRMS (ESI$^+$) $C_{13}H_{10}NO_2$, ([M+H]$^+$) requires 212.0706; found 212.0712.

N-((5-Chloro-8-hydroxyquinolin-7-yl)(3,4-dimethoxyphenyl)methyl)benzamide 222

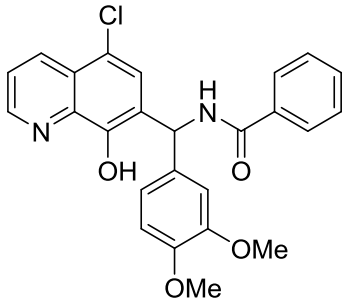

Following general procedure 1, 5-chloro-8-hydroxyquinoline (359 mg, 2.0 mmol), benzamide (242 mg, 2.0 mmol) and 3,4-dimethoxybenzaldehyde (444 mg, 4.0 mmol) gave **222** (690 mg, 77 %) as a white powder.

mp 234 °C; ν_{max}/cm^{-1} 3294 (NH), 1632 (C=O), 697 (C-Cl); δ_H (400 MHz, DMSO-d_6) 10.37 (1 H, br. s., N-*H*), 9.10 - 9.27 (1 H, m, quinoline-*Ar*), 8.88 - 9.02 (1 H, m, quinoline-*Ar*), 8.41 - 8.53 (1 H, m, quinoline-*Ar*), 7.88 - 7.95 (2 H, m, *Ar*), 7.86 (1 H, s, *Ar*), 7.65 - 7.76 (1 H, m, *Ar*), 7.51 - 7.58 (1 H, m, *Ar*), 7.44 - 7.51 (2 H, m, *Ar*), 7.02 (1 H, d, *J*=8.5 Hz, benzyl-*H*) 6.88 - 6.96 (2 H, m, *Ar*), 6.80 - 6.86 (1 H, m, *Ar*), 3.71 (3 H, s, OC*H*$_3$), 3.70 (3 H, s, OC*H*$_3$); δ_C (100 MHz, DMSO-d_6) 166.8 (*C*=O), 150.2, 150.0, 149.5, 148.8, 139.5, 135.3, 134.9, 133.4, 132.2, 129.1, 128.4, 127.6, 126.3, 125.7, 123.8, 120.2, 119.3, 112.6, 112.1, 56.4 (2x O*C*H$_3$), 50.8 (benzyl-*C*); *m*/*z* (ESI$^-$) 447 ([M-H]$^-$); HRMS (ESI$^-$) $C_{25}H_{21}ClN_2NaO_2$, ([M+Na]$^+$) requires 471.1082; found 471.1076.

N-((3-Bromophenyl)(5-fluoro-8-hydroxyquinolin-7-yl)methyl)benzamide **223**

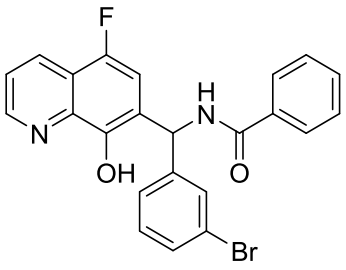

Following general procedure 1, 5-fluoro-8-hydroxyquinoline (326 mg, 2.0 mmol), benzamide (242 mg, 2.0 mmol) and 3-bromobenzaldehyde (468 µL, 4.0 mmol) gave **223** (543 mg, 61 %) as a white powder.

mp 208 °C; ν_{max}/cm^{-1} 3309 (NH), 1634 (C=O); δ_H (400 MHz, DMSO-d_6) 10.21 (1 H, br. s., N-*H*), 9.25 - 9.31 (1 H, m, quinoline-*Ar*), 8.93 - 8.99 (1 H, m, quinoline-*Ar*), 8.41 - 8.46 (1 H, m, quinoline-*Ar*), 7.90 - 7.97 (3 H, m, *Ar*), 7.64 - 7.70 (1 H, m, *Ar*), 7.53 - 7.62 (2 H, m, *Ar*), 7.46 - 7.52 (3 H, m, *Ar*), 7.35 - 7.39 (1 H, m, *Ar*), 7.28 - 7.34 (1 H, m, *Ar*), 7.02 (1 H, d, *J*=9.0 Hz, benzyl-*H*); δ_C (100 MHz, DMSO-d_6) 167.0 (*C*=O), 150.4, 145.4, 134.9, 134.5, 132.5, 132.4, 131.6, 131.5, 131.4, 130.8, 130.6, 130.2, 130.1, 129.2, 128.5, 128.5, 127.3, 126.8, 122.6, 50.8 (benzyl-*C*); δ_F (377 MHz, DMSO-d_6) -133.9 (C*F*); *m/z* (ESI$^+$) 451 ([M+H]$^+$); HRMS (ESI$^+$) $C_{23}H_{16}BrFN_2NaO_2$, ([M+Na]$^+$) requires 473.0271; found 473.0254.

N-((5-Chloro-8-methoxyquinolin-7-yl)(3-methylthiophen-2-yl)methyl)benzamide **224**

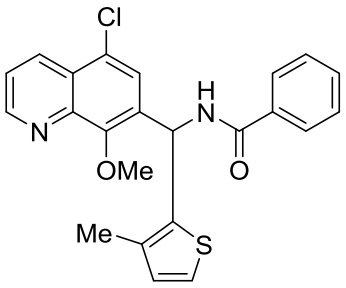

A solution of **193** (102 mg, 0.25 mmol), iodomethane (17 µL, 0.27 mmol), and potassium carbonate (69 mg, 0.5 mmol) in DMF (2 mL) was stirred for 16 h at room temperature. The reaction mixture was diluted with EtOAc (25 mL) and extracted with H_2O and brine. The organic layer was concentrated *in vacuo* and the crude product was purified *via* flash column chromatography to give **224** (51 mg, 97 %) as an off-white powder.

mp 129 °C; ν_{max}/cm^{-1} 3275 (NH), 1632 (C=O); δ_H (400 MHz, $CDCl_3$) 8.73 - 8.93 (1 H, m, quinoline-*Ar*), 8.33 - 8.45 (1 H, m, quinoline-*Ar*), 7.70 - 7.80 (2 H, m, quinoline-*Ar*), 7.63 (1 H, s, *Ar*), 7.35 - 7.43 (2 H, m, *Ar*), 7.27 -

7.34 (2 H, m, *Ar*), 7.21 - 7.26 (1 H, m, *Ar*), 6.92 - 7.03 (2 H, m, *Ar*), 6.68 - 6.76 (1 H, m, *Ar*), 4.07 (3 H, s, OCH_3) 2.19 (3 H, s, CH_3); δ_C (100 MHz, $CDCl_3$) 166.4 (*C*=O), 152.6, 150.1, 143.3, 137.8, 135.0, 133.8, 133.7, 133.3, 131.9, 130.8, 128.7, 127.1, 126.2, 125.6, 123.2, 122.0, 62.8 (O*C*H_3), 48.4 (benzyl-*C*), 14.2 (*C*H_3); *m/z* (ESI^+) 423 ($[M+H]^+$); HRMS (ESI^+) $C_{23}H_{19}ClN_2NaO_2S$, ($[M+Na]^+$) requires 445.0748; found 445.0828.

N-((5-Chloro-8-hydroxyquinolin-7-yl)(3-methylthiophen-2-yl)methyl)isonicotinamide **225**

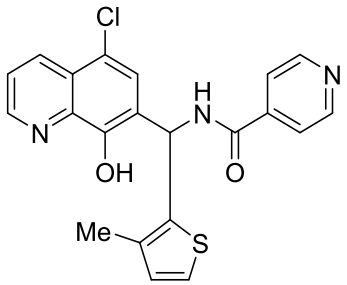

Following general procedure 1, 5-chloro-8-hydroxyquinoline (359 mg, 2.0 mmol), isonicotinamide (244 mg, 2.0 mmol) and 3-methyl-2-thiophenecarboxaldehyde (431 µL, 4.0 mmol) gave **225** (415 mg, 51 %) as an off-white powder.

mp 120 °C; ν_{max}/cm^{-1} 3242 (NH), 1642 (C=O); δ_H (400 MHz, DMSO-d_6) 10.55 (1 H, br. s., N*H*), 9.59 - 9.70 (1 H, m, quinoline-*Ar*), 8.91 - 9.03 (1 H, m, quinoline-*Ar*), 8.66 - 8.78 (1 H, m, *Ar*), 8.43 - 8.56 (1 H, m, *Ar*), 7.81 - 7.88 (2 H, m, *Ar*), 7.69 - 7.80 (3 H, m, *Ar*), 7.25 - 7.32 (1 H, m, *Ar*), 7.15 (1 H, d, *J*=8.0 Hz, benzyl-*H*), 6.84 - 6.96 (1 H, m, *Ar*), 2.15 (3 H, s, CH_3); δ_C (100 MHz, DMSO-d_6) 165.1 (*C*=O), 151.0, 150.6, 150.2, 142.2, 141.8, 139.4, 139.3, 135.3, 133.4, 131.4, 127.1, 126.1, 125.0, 124.2, 124.1, 122.3, 119.3, 45.9 (benzyl-*C*), 14.4 (*C*H_3); *m/z* (ESI^-) 817 ($[2M-H]^-$); HRMS (ESI^+) $C_{21}H_{16}ClIN_3NaO_2S$, ($[M+Na]^+$) requires 432.0544; found 432.0531.

N-((8-Hydroxyquinolin-7-yl)(phenyl)methyl)-3-methylbenzamide **226**

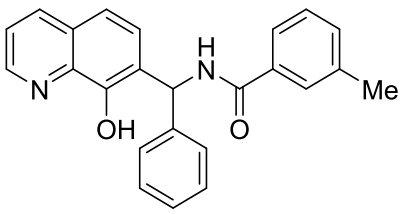

Following general procedure 1, 8-hydroxyquinoline (145 mg, 1.0 mmol), *m*-toluamide (135 mg, 1.0 mmol) and benzaldehyde (203 µL, 2.0 mmol) gave **226** (80 mg, 22 %) as a white powder.

mp 165 °C; ν_{max}/cm^{-1} 3306 (NH), 3058 (OH), 1638 (C=O); δ_H (400 MHz, DMSO-d_6) 10.02 (1 H, br. s., N-*H*), 9.12 - 9.25 (1 H, m, quinoline-*Ar*), 8.78 - 8.93 (1 H, m, quinoline-*Ar*), 8.18 - 8.44 (1 H, m, quinoline-*Ar*), 7.78 (1 H, s, quinoline-*Ar*), 7.68 - 7.75 (2 H, m, *Ar*), 7.52 - 7.58 (1 H, m, *Ar*), 7.41 - 7.46 (1 H, m, *Ar*), 7.30 - 7.36 (6 H, m, *Ar*), 7.24 (1 H, br. s, O-*H*), 7.01 (1 H, d, *J*=9.0 Hz, benzyl-*H*), 2.30 - 2.42 (3 H, m, *Me*); δ_C (100 MHz, DMSO-d_6) 166.9 (*C*=O), 150.7, 149.2, 143.1, 138.9, 138.4, 136.9, 135.3, 132.7, 129.1, 129.0, 128.9, 128.5, 128.1, 127.9, 127.6, 125.7, 125.2, 122.7, 118.2, 51.4 (benzyl-*C*), 21.8 (*C*H$_3$); *m*/*z* (ESI$^-$) 367 ([M-H]$^-$, 100 %); HRMS (ESI$^+$) $C_{24}H_{20}N_2NaO_2$, ([M+Na]$^+$) requires 391.1417; found 391.1403.

N-((8-Hydroxyquinolin-7-yl)(phenyl)methyl)-2-methylbenzamide **227**

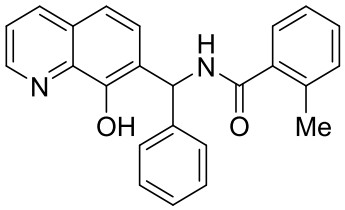

Following general procedure 1, 8-hydroxyquinoline (145 mg, 1.0 mmol), *o*-toluamide (135 mg, 1.0 mmol) and benzaldehyde (203 µL, 2.0 mmol) gave **227** (206 mg, 56 %) as a white powder.

mp 170 °C; ν_{max}/cm^{-1} 3292 (NH), 3060 (OH), 1643 (C=O); δ_H (400 MHz, DMSO-d_6) 10.04 (1 H, br. s, N-*H*), 9.15 - 9.32 (1 H, m, quinoline-*Ar*), 8.83 - 8.91 (1 H, m quinoline-*Ar*), 8.24 - 8.37 (1 H, m quinoline-*Ar*), 7.66 - 7.72 (1 H, m quinoline-*Ar*), 7.53 - 7.59 (1 H, m quinoline-*Ar*), 7.42 - 7.47 (1 H, m, *Ar*), 7.35 - 7.40 (3 H, m, *Ar*), 7.29 - 7.35 (3 H, m, *Ar*), 7.20 - 7.27 (3 H, m, *Ar*), 7.00 (1 H, d, *J*=9.0 Hz, benzyl-*H*), 2.29 (3 H, s, C*H*$_3$); δ_C (100 MHz, DMSO-d_6) 169.4 (*C*=O), 150.5, 149.2, 143.2, 138.9, 136.9, 136.0, 131.1, 130.1, 129.2, 128.4, 128.0, 127.9, 127.7, 127.6, 126.3, 125.4, 122.7, 118.2, 50.9 (benzyl-*C*), 20.2 (*C*H$_3$); *m*/*z* (ESI$^-$) 367 ([M-H]$^-$, 100 %); HRMS (ESI$^+$) $C_{24}H_{20}N_2NaO_2$, ([M+Na]$^+$) requires 391.1417; found 391.1404.

N-((8-Hydroxyquinolin-7-yl)(phenyl)methyl)-4-methylbenzamide **228**

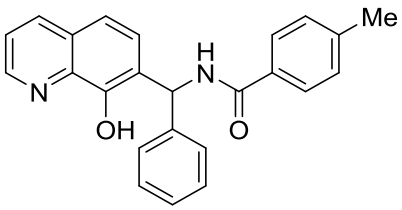

Following general procedure 1, 8-hydroxyquinoline (145 mg, 1.0 mmol), *p*-toluamide (135 mg, 1.0 mmol) and benzaldehyde (203 µL, 2.0 mmol) gave **228** (203 mg, 22 %) as a white powder.

mp 214-216 °C; ν_{max}/cm^{-1} 3305 (NH), 3047 (OH), 1632 (C=O); δ_H (400 MHz, DMSO-d_6) 10.04 (1 H, br. s, N-*H*), 9.11 - 9.22 (1 H, m, quinoline-*Ar*), 8.82 - 8.89 (1 H, m, quinoline-*Ar*), 8.25 - 8.35 (1 H, m, quinoline-*Ar*), 7.83 - 7.88 (2 H, m, quinoline-*Ar*), 7.68 - 7.74 (1 H, m, *Ar*), 7.52 - 7.59 (1 H, m, *Ar*), 7.41 - 7.46 (1 H, m, *Ar*), 7.32 (2 H, s, *Ar*), 7.30 - 7.32 (2 H, m, *Ar*), 7.25 - 7.30 (2 H, m, *Ar*), 7.23 (1 H, br. s, O-*H*), 7.01 (1 H, d, *J*=9.0 Hz, benzyl-*H*), 2.35 (3 H, s, CH_3); δ_C (100 MHz, DMSO-d_6) 166.65 (*C*=O), 150.6, 149.2, 143.1, 142.0, 138.9, 136.9, 132.5, 129.8, 129.6, 129.1, 128.5, 128.1, 127.9, 127.6, 125.3, 122.6, 118.2, 51.3 (benzyl-*C*), 21.8 (*C*H$_3$); *m*/*z* (ESI$^-$) 367 ([M-H]$^-$, 100 %); HRMS (ESI$^+$) $C_{24}H_{20}N_2NaO_2$, ([M+Na]$^+$) requires 391.1417; found 391.1400.

8-Hydroxyquinoline-*N*-oxide 229

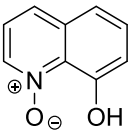

A stirred solution of 8-hydroxyquinoline (2.5 g, 17.2 mmol) in CH_2Cl_2 was cooled to 0 °C and *m*-chloroperbenzoic acid (4 g, 18.5 mmol) was added slowly over 3 minutes. The solution was kept at 0 °C and stirred for 3 h. The reaction mixture was extracted with saturated aqueous $NaHCO_3$ and reduced to dryness to give **229** (1.737g, 63 %) as orange needles.

mp 132 °C (135 °C lit.); δ_H (400 MHz, $CDCl_3$) 8.18 - 8.26 (1 H, m, *Ar*), 7.71 - 7.84 (1 H, m, *Ar*), 7.42 - 7.51 (1 H, m, *Ar*), 7.16 - 7.26 (2 H, m, *Ar*), 6.98 - 7.09 (1 H, m, *Ar*); δ_C (100 MHz, $CDCl_3$) 154.0, 134.4, 132.3, 130.6, 129.9, 129.6, 120.4, 116.8, 114.8; *m*/*z* (ESI$^+$) 184 ([M+Na]$^+$, 100 %);

N-((8-Hydroxy-5-nitroquinolin-7-yl)(phenyl)methyl)benzamide 230

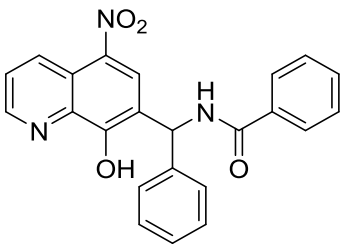

Following general procedure 1, 5-nitroquinolin-8-ol (380 mg, 2.0 mmol), benzamide (242 mg, 2.0 mmol) and benzaldehyde (406 µL, 4.0 mmol) gave **230** (680 mg, 98 %) as an orange powder.

mp 259 - 261 °C; ν_{max}/cm^{-1} 3288 (NH), 1641 (C=O); δ_H (400 MHz, DMSO-d_6) 9.39 - 9.51 (1 H, m, quinoline-*Ar*), 9.12 - 9.23 (1 H, m, quinoline-*Ar*), 8.95 - 9.06 (1 H, m, quinoline-*Ar*), 8.80 (1 H, s, *Ar*), 7.91 - 7.98 (2 H, m, *Ar*), 7.84 - 7.91 (1 H, m, *Ar*), 7.52 - 7.59 (1 H, m, *Ar*), 7.45 - 7.52 (2 H, m, *Ar*), 7.33 - 7.41 (4 H, m, *Ar*), 7.23 - 7.33 (1 H, m, *Ar*), 7.01 (1 H, d, *J*=8.5 Hz, benzyl-*H*); δ_C (100 MHz, DMSO-d_6) 166.9 (*C*=O), 158.6, 149.9, 141.8, 137.7, 135.2, 135.0, 133.9, 132.3, 129.4, 129.2, 129.1, 128.5, 128.2, 128.1, 126.1, 124.6, 122.5, 51.0 (benzyl-*C*); *m*/*z* (ESI$^-$) 398 ([M-H]$^-$, 100%); HRMS (ESI$^-$) $C_{23}H_{17}N_3NaO_4$, ([M+Na]$^+$) requires 422.1111; found 422.1101.

N-((5-Chloro-8-hydroxyquinolin-7-yl)(phenyl)methyl)-2-methylbenzamide **231**

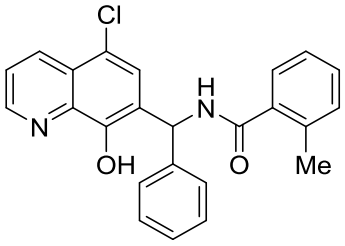

Following general procedure 1, 5-chloro-8-quinolinol (359 mg, 2.0 mmol), *o*-toluamide (170 mg, 2.0 mmol) and benzaldehyde (406 µL, 4.0 mmol) gave **231** (445 mg, 55 %) as a white powder.

mp 213-215 °C; ν_{max}/cm^{-1} 3284 (NH), 1637 (C=O), 730 (C-Cl); δ_H (400 MHz, DMSO-d_6) 10.44 (1 H, br. s., N-*H*), 9.15 - 9.36 (1 H, m, quinoline-*Ar*), 8.90 - 9.03 (1 H, m, quinoline-*Ar*), 8.38 - 8.55 (1 H, m, quinoline-*Ar*), 7.86 (1 H, s, *Ar*), 7.68 - 7.77 (1 H, m, *Ar*), 7.29 - 7.42 (6 H, m, *Ar*), 7.20 - 7.29 (3 H, m, *Ar*), 6.99 (1 H, d, *J*=9.0 Hz, benzyl-*H*), 2.28 (3 H, s, C*H*$_3$); δ_C (100 MHz, DMSO-d_6) 169.4 (*C*=O), 150.2, 150.1, 142.6, 139.6, 137.9, 136.0, 133.4, 131.2, 130.2, 129.3, 127.9, 127.9, 127.4, 126.4, 126.1, 125.8, 123.9, 119.5, 50.6 (benzyl-*C*), 20.2 (*C*H$_3$); *m*/*z* (ESI$^-$) 401 ([M-H]$^-$, 100 %); HRMS (ESI$^-$) $C_{24}H_{18}ClN_2O_2$, ([M-H]$^-$) requires 401.1062; found 401.1067.

N-((5-Chloro-8-hydroxyquinolin-7-yl)(phenyl)methyl)-3-methylbenzamide **232**

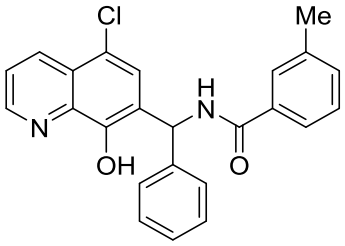

Following general procedure 1, 5-chloro-8-quinolinol (359 mg, 2.0 mmol), *m*-toluamide (170 mg, 2.0 mmol) and benzaldehyde (406 µL, 4.0 mmol) gave **232** (439 mg, 55 %) as a white powder.

mp 222-225 °C; ν_{max}/cm^{-1} 3300 (NH), 1634 (C=O); δ_H (400 MHz, DMSO-d_6) ^{1}H NMR 10.42 (1 H, br. s., N-*H*), 9.15 - 9.27 (1 H, m, quinoline-*Ar*), 8.94 - 9.02 (1 H, m, quinoline-*Ar*), 8.43 - 8.53 (1 H, m, quinoline-*Ar*), 7.86 (1 H, s, *Ar*), 7.77 (1 H, s, *Ar*), 7.70 - 7.75 (2 H, m, *Ar*), 7.31 - 7.38 (6 H, m, *Ar*), 7.21 - 7.29 (1 H, m, *Ar*), 7.01 (1 H, d, *J*=8.5 Hz, benzyl-*H*), 2.23 - 2.43 (3 H, m, C*H*$_3$); δ_C (100 MHz, DMSO-d_6) 166.9 (*C*=O), 150.4, 150.0, 142.5, 139.5, 138.4, 135.1, 133.4, 132.8, 129.3, 129.0, 128.9, 128.0, 127.9, 127.7, 126.0, 125.8, 125.7, 123.9, 119.4, 50.9 (benzyl-*C*), 21.8 (*C*H$_3$); *m/z* (ESI$^-$) 401 ([M-H]$^-$, 100 %); HRMS (ESI$^-$) $C_{24}H_{18}ClN_2O_2$, ([M-H]$^-$) requires 401.1062; found 401.1068.

N-((5-Chloro-8-hydroxyquinolin-7-yl)(phenyl)methyl)-4-methylbenzamide **233**

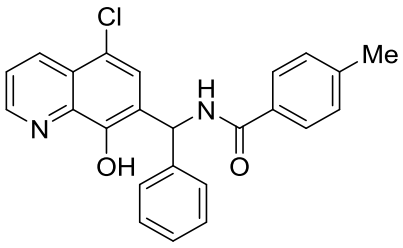

Following general procedure 1, 5-chloro-8-quinolinol (359 mg, 2.0 mmol), *p*-toluamide (170 mg, 2.0 mmol) and benzaldehyde (406 µL, 4.0 mmol) gave **233** (513 mg, 64 %) as white powder.

mp 237-240 °C; ν_{max}/cm^{-1} 3321 (NH), 1634 (C=O); δ_H (400 MHz, DMSO-d_6) 10.41 (1 H, br. s., N-*H*), 9.12 - 9.25 (1 H, m, quinoline-*Ar*), 8.90 - 9.00 (1 H, m, quinoline-*Ar*), 8.40 - 8.55 (1 H, m, quinoline-*Ar*), 7.80 - 7.93 (3 H, m, *Ar*), 7.65 - 7.77 (1 H, m, *Ar*), 7.31 - 7.35 (4 H, m, *Ar*), 7.23 - 7.31 (3 H, m, *Ar*), 7.02 (1 H, d, *J*=8.5 Hz, benzyl-*H*), 2.35 (3 H, s, C*H*$_3$); δ_C (100 MHz, DMSO-d_6) 166.7 (*C*=O), 150.4, 150.0, 142.6, 142.4, 139.5, 133.4, 132.3, 129.7, 129.3, 128.5, 128.0, 127.9, 127.7, 126.0, 125.8, 123.9, 119.4, 50.9 (benzyl-*C*), 21.8 (*C*H$_3$); *m/z* (ESI$^-$) 401 ([M-H]$^-$, 100 %); HRMS (ESI$^-$) $C_{24}H_{18}ClN_2O_2$, ([M-H]$^-$) requires 401.1062; found 401.1062.

N-((5-Chloro-8-hydroxyquinolin-7-yl)(p-tolyl)methyl)benzamide **234**

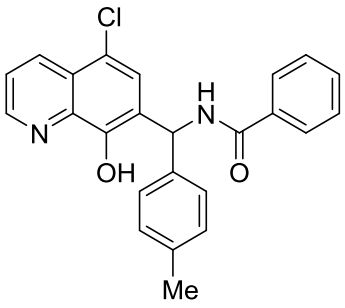

Following general procedure 1, 5-chloro-8-quinolinol (359 mg, 2.0 mmol), benzamide (242 mg, 2.0 mmol) and *p*-tolualdehyde (472 µL, 4.0 mmol) gave **234** (686 mg, 85 %) as white powder.

mp 248-249 °C; ν_{max}/cm^{-1} 3310 (NH), 1634 (C=O); δ_H (400 MHz, DMSO-d_6) 10.39 (1 H, br. s., N-*H*), 9.15 - 9.28 (1 H, m, quinoline-*Ar*), 8.91 - 9.01 (1 H, m, quinoline-*Ar*), 8.41 - 8.55 (1 H, m, quinoline-*Ar*), 7.90 - 7.97 (2 H, m, *Ar*), 7.86 (1 H, s, *Ar*), 7.68 - 7.75 (1 H, m, *Ar*), 7.51 - 7.58 (1 H, m, *Ar*), 7.44 - 7.51 (2 H, m, *Ar*), 7.19 - 7.26 (2 H, m, *Ar*), 7.10 - 7.17 (2 H, m, *Ar*), 6.98 (1 H, d, *J*=9.0 Hz, benzyl-*H*), 2.26 (3 H, s, C*H*$_3$); δ_C (100 MHz, DMSO-d_6) 166.8 (*C*=O), 150.3, 150.0, 139.5, 137.0, 135.2, 133.4, 132.2, 129.8, 129.1, 128.5, 128.0, 127.7, 126.2, 125.8, 123.8, 119.4, 50.7 (benzyl-*C*), 21.5 (*C*H$_3$); *m*/*z* (ESI$^-$) 401 ([M-H]$^-$, 100 %); HRMS (ESI$^-$) $C_{24}H_{18}ClN_2O_2$, ([M-H]$^-$) requires 401.1062; found 401.1061.

N-((5-Chloro-8-hydroxyquinolin-7-yl)(naphthalen-1-yl)methyl)benzamide **235**

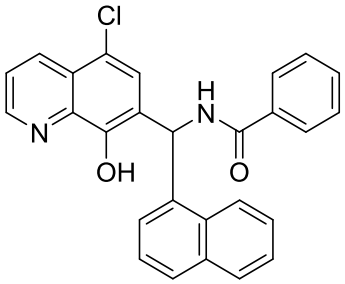

Following general procedure 1, 5-chloro-8-quinolinol (359 mg, 2.0 mmol), benzamide (242 mg, 2.0 mmol) and 1-naphthaldehyde (544 µL, 4.0 mmol) gave **235** (541 mg, 62 %) as a white powder.

mp 229-230 °C; ν_{max}/cm^{-1} 3234 (NH), 1630 (C=O); δ_H (400 MHz, DMSO-d_6) 10.54 (1 H, br. s., N-*H*), 9.33 - 9.42 (1 H, m, quinoline-*Ar*), 8.94 - 9.01 (1 H, m, quinoline-*Ar*), 8.45 - 8.51 (1 H, m, quinoline-*Ar*), 8.06 - 8.16 (1 H, m, *Ar*), 7.92 - 8.00 (3 H, m, *Ar*), 7.86 - 7.91 (1 H, m, *Ar*), 7.71 - 7.76 (1 H, m, *Ar*), 7.70 (1 H, s) 7.65 (1 H, d, *J*=8.5

Hz) 7.49 - 7.58 (3 H, m, *Ar*), 7.43 - 7.49 (3 H, m, *Ar*), 7.39 (1 H, m, *Ar*); δ_C (100 MHz, DMSO-d_6) 166.5 (*C*=O), 150.5, 150.1, 139.5, 138.1, 134.9, 134.4, 133.4, 132.3, 131.8, 129.6, 129.1, 128.8, 128.5, 128.0, 127.4, 126.7, 126.2, 126.0, 125.6, 125.3, 123.9, 119.2, 48.3 (benzyl-*C*); *m*/*z* (ESI$^-$) 437 ([M-H]$^-$, 100 %); HRMS (ESI$^-$) $C_{27}H_{18}ClN_2O_2$, ([M-H]$^-$) requires 437.1062; found 437.1050.

N-((5-Chloro-8-hydroxyquinolin-7-yl)(naphthalen-2-yl)methyl)benzamide **236**

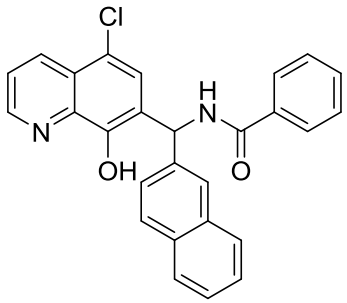

Following general procedure 1, 5-chloro-8-quinolinol (359 mg, 2.0 mmol), benzamide (242 mg, 2.0 mmol) and 2-naphthaldehyde (312 mg, 4.0 mmol) gave **236** (654 mg, 75 %) as a white powder.

mp 263-266 ^oC; ν_{max}/cm^{-1} 3367 (NH), 1654 (C=O); δ_H (400 MHz, DMSO-d_6) 10.49 (1 H, br. s. ,N-*H*), 9.31 - 9.45 (1 H, m, quinoline-*Ar*), 8.91 - 9.04 (1 H, m, quinoline-*Ar*), 8.42 - 8.56 (1 H, m, quinoline-*Ar*), 7.96 - 8.02 (2 H, m, *Ar*), 7.84 - 7.93 (4 H, m, *Ar*), 7.80 (1 H, s, *Ar*), 7.69 - 7.76 (1 H, m, *Ar*), 7.43 - 7.61 (6 H, m, *Ar*), 7.19 (1 H, d, *J*=8.5 Hz, benzyl-*H*); δ_C (100 MHz, DMSO-d_6) 166.9 (*C*=O), 150.6, 150.1, 140.0, 139.6, 135.1, 133.6, 133.4, 133.0, 132.3, 129.2, 129.0, 128.7, 128.5, 128.3, 127.8, 127.2, 126.8, 126.7, 126.1, 125.9, 125.8, 123.9, 119.5, 51.2 (benzyl-*C*); *m*/*z* (ESI$^-$) 437 ([M-H]$^-$, 100 %); HRMS (ESI$^-$) $C_{27}H_{18}ClN_2O_2$, ([M-H]$^-$) requires 437.1062; found 437.1061.

N-((8-Hydroxy-5-nitroquinolin-7-yl)(o-tolyl)methyl)benzamide **237**

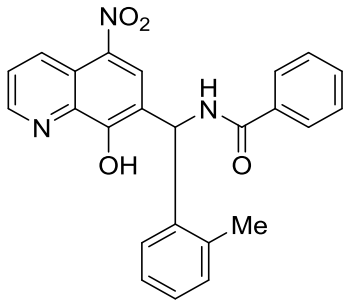

Following general procedure 1, 8-hydroxy-5-nitroquinoline (380 mg, 2.0 mmol), benzamide (242 mg, 2.0 mmol) and *o*-tolualdehyde (463 µL, 4.0 mmol) gave **237** (173 mg, 21 %) as a brown powder.

mp 213 °C; ν_{max}/cm^{-1} 3302 (NH), 1639 (C=O); δ_H (400 MHz, DMSO-d_6) 9.26 - 9.33 (1 H, m, quinoline-*Ar*), 9.15 - 9.23 (1 H, m, quinoline-*Ar*), 8.95 - 9.04 (1 H, m, quinoline-*Ar*), 8.62 (1 H, s, quinoline-*Ar*), 7.92 - 7.98 (2 H, m, *Ar*), 7.85 - 7.91 (1 H, m, *Ar*), 7.50 - 7.58 (1 H, m, *Ar*), 7.43 - 7.50 (2 H, m, *Ar*), 7.12 - 7.28 (4 H, m, *Ar*), 7.05 (1 H, d, *J*=8.5 Hz, benzyl-*H*), 2.31 (3 H, s, C*H*$_3$); δ_C (100 MHz, DMSO-d_6) 166.6 (*C*=O), 158.8, 149.9, 139.8, 137.6, 136.9, 134.9, 134.9, 133.9, 132.3, 131.3, 129.1, 128.5, 128.3, 128.2, 127.9, 126.8, 126.1, 123.9, 122.6, 48.8 (benzyl-*C*), 19.6 (*C*H$_3$); *m*/*z* (ESI$^-$) 412 ([M-H]$^-$); HRMS (ESI$^+$) $C_{24}H_{19}N_3NaO_4$, ([M+Na]$^+$) requires 436.1268; found 436.1253.

N-((8-Hydroxy-5-nitroquinolin-7-yl)(*m*-tolyl)methyl)benzamide 238

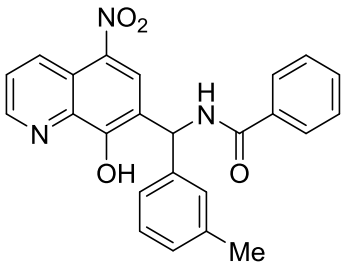

Following general procedure 1, 8-hydroxy-5-nitroquinoline (380 mg, 2.0 mmol), benzamide (242 mg, 2.0 mmol) and *m*-tolualdehyde (472 µL, 4.0 mmol) gave **238** (556 mg, 67 %) as a light-orange powder.

mp 217 °C; ν_{max}/cm^{-1} 3271 (NH), 1636 (C=O); δ_H (400 MHz, DMSO-d_6) 9.31 - 9.47 (1 H, m, quinoline-*Ar*), 9.09 - 9.25 (1 H, m, quinoline-*Ar*), 8.94 - 9.05 (1 H, m, quinoline-*Ar*), 8.81 (1 H, s, quinoline-*Ar*), 7.91 - 7.99 (2 H, m, *Ar*), 7.85 - 7.91 (1 H, m, *Ar*), 7.52 - 7.58 (1 H, m, *Ar*), 7.45 - 7.52 (2 H, m, *Ar*), 7.22 - 7.28 (1 H, m, *Ar*), 7.14 - 7.21 (2 H, m, *Ar*), 7.06 - 7.12 (1 H, m, *Ar*), 6.98 (1 H, d, *J*=8.5 Hz, benzyl-*H*), 2.29 (3 H, s, C*H*$_3$); δ_C (100 MHz, DMSO-d_6) 166.9 (*C*=O), 158.5, 153.2, 149.9, 141.8, 138.5, 137.7, 135.2, 135.0, 133.9, 132.3, 129.3, 129.2, 129.1, 128.8, 128.5, 126.1, 125.4, 124.7, 122.5, 51.0 (benzyl-*C*), 22.0 (*C*H$_3$); *m*/*z* (ESI$^-$) 412 ([M-H]$^-$); HRMS (ESI$^-$) $C_{24}H_{18}N_3O_4$, ([M-H]$^-$) requires 412.1303; found 412.1307.

N-((8-Hydroxy-5-nitroquinolin-7-yl)(*p*-tolyl)methyl)benzamide **239**

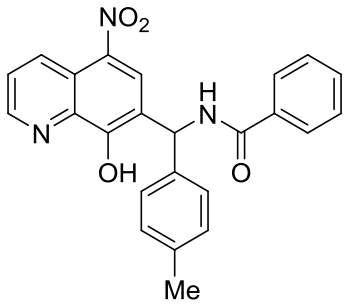

Following general procedure 1, 8-hydroxy-5-nitroquinoline (380 mg, 2.0 mmol), benzamide (242 mg, 2.0 mmol) and *p*-tolualdehyde (472 µL, 4.0 mmol) gave **239** (684 mg, 83 %) as a light-orange powder.

mp 248 - 250 °C; ν_{max}/cm^{-1} 3302 (NH), 1636 (C=O); δ_H (400 MHz, DMSO-d_6) 9.36 - 9.43 (1 H, m, quinoline-*Ar*), 9.13 - 9.20 (1 H, m, quinoline-*Ar*), 8.98 - 9.03 (1 H, m, quinoline-*Ar*), 8.79 (1 H, s, quinoline-*Ar*), 7.91 - 7.97 (2 H, m, *Ar*), 7.85 - 7.90 (1 H, m, *Ar*), 7.52 - 7.58 (1 H, m, *Ar*), 7.45 - 7.51 (2 H, m, *Ar*), 7.22 - 7.28 (2 H, m, *Ar*), 7.12 - 7.19 (2 H, m, *Ar*), 6.96 (1 H, d, *J*=8.5 Hz, benzyl-*H*), 2.27 (3 H, s, CH_3); δ_C (100 MHz, DMSO-d_6) 166.9 (*C*=O), 158.5, 149.9, 138.8, 137.7, 137.3, 135.2, 135.1, 133.8, 132.3, 129.9, 129.1, 129.0, 128.5, 128.2, 126.1, 124.8, 122.5, 50.8 (benzyl-*C*), 21.5 (*C*H$_3$); *m*/*z* (ESI$^-$) 412 ([M-H]$^-$); HRMS (ESI$^-$) $C_{24}H_{18}N_3O_4$, ([M-H]$^-$) requires 412.1303; found 412.1309.

N-((8-Hydroxy-5-nitroquinolin-7-yl)(phenyl)methyl)-2-methylbenzamide **240**

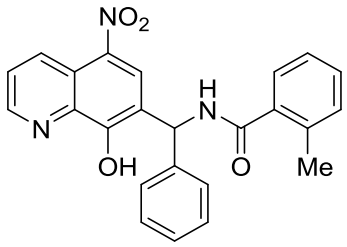

Following general procedure 1, 8-hydroxy-5-nitroquinoline (380 mg, 2.0 mmol), *o*-toluamide (270 mg, 2.0 mmol) and benzaldehyde (406 µL, 4.0 mmol) gave **240** (669 mg, 81 %) as a light-brown powder.

mp 244 - 246 °C; ν_{max}/cm^{-1} 3278 (NH), 1636 (C=O); δ_H (400 MHz, DMSO-d_6) 9.39 - 9.47 (1 H, m, quinoline-*Ar*), 9.15 - 9.21 (1 H, m, quinoline-*Ar*), 8.99 - 9.05 (1 H, m, quinoline-*Ar*), 8.82 (1 H, s, quinoline-*Ar*), 7.84 - 7.92 (1 H, m, *Ar*), 7.31 - 7.43 (6 H, m, *Ar*), 7.22 - 7.30 (3 H, m, *Ar*), 6.95 (1 H, d, *J*=8.5 Hz, benzyl-*H*), 2.29 (3 H, s, CH_3); δ_C (100 MHz, DMSO-d_6) 169.5 (*C*=O), 158.4, 149.9, 141.8, 137.8, 137.7, 136.0, 135.2, 133.9, 131.2, 130.2,

129.4, 128.7, 128.1, 128.1, 128.0, 126.4, 126.1, 124.8, 122.5, 50.8 (benzyl-*C*), 20.15 (*C*H_3); *m*/*z* (ESI$^-$) 412 ([M-H]$^-$); HRMS (ESI$^-$) $C_{24}H_{18}N_3O_4$, ([M-H]$^-$) requires 412.1303; found 412.1303.

N-((8-Hydroxy-5-nitroquinolin-7-yl)(phenyl)methyl)-3-methylbenzamide **241**

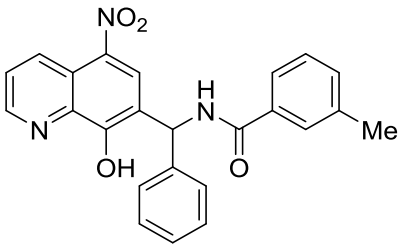

Following general procedure 1, 8-hydroxy-5-nitroquinoline (380 mg, 2.0 mmol), *m*-toluamide (270 mg, 2.0 mmol) and benzaldehyde (406 µL, 4.0 mmol) gave **241** (261 mg, 32 %) as an orange powder.

mp 222 ^{o}C; ν_{max}/cm^{-1} 3293 (NH), 1636 (C=O); δ_H (400 MHz, DMSO-d_6) 9.35 - 9.41 (1 H, m, quinoline-*Ar*), 9.15 - 9.20 (1 H, m, quinoline-*Ar*), 8.99 - 9.03 (1 H, m, quinoline-*Ar*), 8.78 (1 H, s, quinoline-*Ar*), 7.85 - 7.92 (1 H, m, *Ar*), 7.76 (1 H, s, *Ar*), 7.70 - 7.75 (1 H, m, *Ar*), 7.33 - 7.40 (6 H, m, *Ar*), 7.26 - 7.32 (1 H, m, *Ar*), 6.99 (1 H, d, *J*=8.5 Hz, benzyl-*H*), 2.36 (3 H, s, CH_3); δ_C (100 MHz, DMSO-d_6) 167.0 (*C*=O), 158.6, 149.9, 141.8, 138.4, 137.7, 135.2, 135.0, 133.9, 132.9, 129.4, 129.1, 128.9, 128.2, 128.1, 126.1, 125.7, 124.7, 122.5, 51.0 (benzyl-*C*), 21.8 (*C*H_3); *m*/*z* (ESI$^-$) 412 ([M-H]$^-$); HRMS (ESI$^+$) $C_{24}H_{19}N_3NaO_4$, ([M+Na]$^+$) requires 436.1268; found 436.1259.

N-((8-Hydroxy-5-nitroquinolin-7-yl)(phenyl)methyl)-4-methylbenzamide **242**

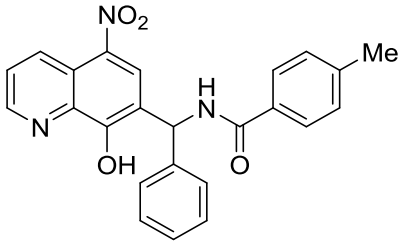

Following general procedure 1, 8-hydroxy-5-nitroquinoline (380 mg, 2.0 mmol), *p*-toluamide (270 mg, 2.0 mmol) and benzaldehyde (406 µL, 4.0 mmol) gave **242** (563 mg, 68 %) as an orange powder.

mp 259 ^{o}C; ν_{max}/cm^{-1} 3229 (NH), 1638 (C=O); δ_H (400 MHz, DMSO-d_6) 9.32 - 9.40 (1 H, m, quinoline-*Ar*), 9.13 - 9.21 (1 H, m, quinoline-*Ar*), 8.96 - 9.04 (1 H, m, quinoline-*Ar*), 8.80 (1 H, s, quinoline-*Ar*), 7.83 - 7.90 (3 H, m, *Ar*), 7.33 - 7.40 (4 H, m, *Ar*), 7.25 - 7.32 (3 H, m, *Ar*), 7.01 (1 H, d, *J*=8.5 Hz, benzyl-*H*), 2.31 - 2.38 (3 H, m, CH_3);

δ_C (100 MHz, DMSO-d_6) 166.8 (*C*=O), 158.6, 149.9, 142.2, 141.9, 137.7, 135.2, 133.9, 132.2, 129.7, 129.4, 129.1, 128.5, 128.2, 128.1, 126.1, 124.7, 122.5, 51.0 (benzyl-*C*), 21.8 (*C*H_3); *m*/*z* (ESI$^-$) 412 ([M-H]$^-$); HRMS (ESI$^+$) $C_{24}H_{19}N_3NaO_4$, ([M+Na]$^+$) requires 436.1268; found 436.1254.

N-((8-Hydroxy-5-nitroquinolin-7-yl)(naphthalen-1-yl)methyl)benzamide **243**

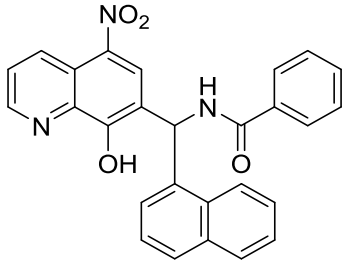

Following general procedure 1, 8-hydroxy-5-nitroquinoline (380 mg, 2.0 mmol), benzamide (242 mg, 2.0 mmol), and 1-naphthaldehyde (544 µL, 4.0 mmol) gave **243** (532 mg, 59 %) as an off-white powder.

mp 237 °C; ν_{max}/cm^{-1} 3386 (NH), 1635 (C=O); δ_H (400 MHz, DMSO-d_6) 9.47 - 9.55 (1 H, m, quinoline-*Ar*), 9.19 - 9.24 (1 H, m, quinoline-*Ar*), 9.01 - 9.05 (1 H, m, quinoline-*Ar*), 8.71 (1 H, s, quinoline-*Ar*), 8.08 - 8.13 (1 H, m, *Ar*), 7.98 - 8.02 (1 H, m, *Ar*), 7.88 - 7.97 (4 H, m, *Ar*), 7.67 (1 H, d, *J*=8.5 Hz, benzyl-*H*), 7.51 - 7.60 (4 H, m, *Ar*), 7.45 - 7.51 (3 H, m, *Ar*), 7.39 - 7.43 (1 H, m, *Ar*); δ_C (100 MHz, DMSO-d_6) 165.8 (*C*=O), 157.8, 149.0, 136.8, 136.5, 134.1, 133.9, 133.6, 133.1, 131.5, 131.0, 128.9, 128.4, 128.3, 128.2, 127.6, 126.7, 125.9, 125.4, 125.3, 124.9, 123.1, 122.9, 121.9, 47.3 (benzyl-*C*); *m*/*z* (ESI$^-$) 448 ([M-H]$^-$); HRMS (ESI$^-$) $C_{27}H_{18}N_3O_4$, ([M-H]$^-$) requires 448.1303; found 448.1301.

N-((8-Hydroxy-5-nitroquinolin-7-yl)(naphthalen-2-yl)methyl)benzamide **244**

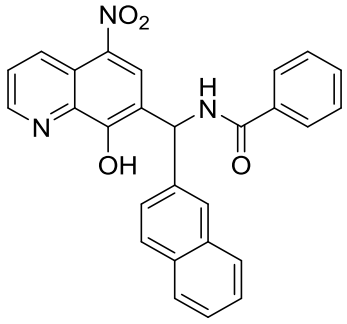

Following general procedure 1, 8-hydroxy-5-nitroquinoline (380 mg, 2.0 mmol), benzamide (242 mg, 2.0 mmol), and 2-naphthaldehyde (312 mg, 4.0 mmol) gave **244** (608 mg, 68 %) as an orange powder.

mp 216 - 217 °C; ν_{max}/cm^{-1} 3284 (NH), 1630 (C=O); δ_H (400 MHz, DMSO-d_6) 9.53 - 9.59 (1 H, m, quinoline-*Ar*), 9.19 - 9.23 (1 H, m, quinoline-*Ar*), 9.00 - 9.06 (1 H, m, quinoline-*Ar*), 8.86 (1 H, s, quinoline-*Ar*), 7.87 - 8.04 (6 H, m, *Ar*), 7.85 (1 H, s, *Ar*), 7.54 - 7.61 (2 H, m, *Ar*), 7.46 - 7.53 (5 H, m, *Ar*), 7.18 (1 H, d, *J*=8.5 Hz, benzyl-*H*); δ_C (100 MHz, DMSO-d_6) 166.1 (*C*=O), 158.0, 149.0, 138.5, 136.8, 134.1, 133.1, 132.8, 132.2, 131.5, 128.3, 128.3, 128.2, 127.9, 127.8, 127.6, 127.5, 126.3, 126.1, 126.0, 125.6, 125.3, 123.6, 121.8, 50.5 (benzyl-*C*); *m*/*z* (ESI$^-$) 448 ([M-H]$^-$); HRMS (ESI$^-$) $C_{27}H_{18}N_3O_4$, ([M-H]$^-$) requires 448.1303; found 448.1302.

N-((4-Bromophenyl)(8-hydroxy-5-nitroquinolin-7-yl)methyl)benzamide **245**

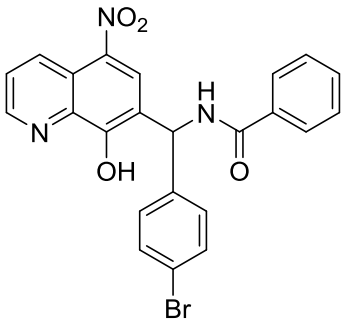

Following general procedure 1, 8-hydroxy-5-nitroquinoline (380 mg, 2.0 mmol), benzamide (242 mg, 2.0 mmol) and 4-bromobenzaldehyde (740 mg, 4.0 mmol) gave **245** (643 mg, 67 %) as a light-yellow powder.

mp 248 - 250 °C; ν_{max}/cm^{-1} 3222 (NH), 1637 (C=O); δ_H (400 MHz, DMSO-d_6) 9.39 - 9.52 (1 H, m, quinoline-*Ar*), 9.15 - 9.23 (1 H, m, quinoline-*Ar*), 8.98 - 9.04 (1 H, m, quinoline-*Ar*), 8.77 (1 H, s, quinoline-*Ar*), 7.86 - 7.98 (3 H, m, *Ar*), 7.53 - 7.59 (3 H, m, *Ar*), 7.45 - 7.52 (2 H, m, *Ar*), 7.29 - 7.36 (2 H, m, *Ar*), 6.95 (1 H, d, *J*=8.5 Hz, benzyl-*H*); δ_C (100 MHz, DMSO-d_6) 167.0 (*C*=O), 158.8, 149.8, 141.2, 137.6, 135.1, 134.9, 134.0, 132.4, 132.3, 130.5, 129.2, 128.9, 128.5, 126.2, 124.1, 122.7, 121.3, 50.7 (benzyl-*C*); *m*/*z* (ESI$^-$) 476 ([M-H]$^-$); HRMS (ESI$^-$) $C_{23}H_{15}BrN_3O_4$, ([M-H]$^-$) requires 476.0251; found 476.0247.

N-((4-Chlorophenyl)(8-hydroxy-5-nitroquinolin-7-yl)methyl)benzamide **246**

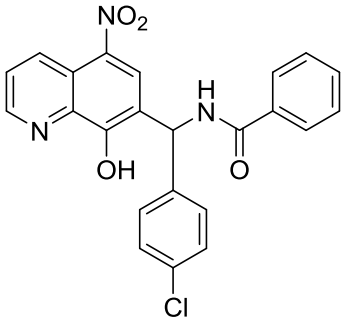

Following general procedure 1, 8-hydroxy-5-nitroquinoline (380 mg, 2.0 mmol), benzamide (242 mg, 2.0 mmol) and 4-chlorobenzaldehyde (560 mg, 4.0 mmol) gave **246** (690 mg, 80 %) as a light-yellow powder.

mp 246 - 249 °C; ν_{max}/cm^{-1} 3271 (NH), 1640 (C=O); δ_H (400 MHz, DMSO-d_6) 9.38 - 9.52 (1 H, m, quinoline-*Ar*), 9.14 - 9.24 (1 H, m, quinoline-*Ar*), 8.94 - 9.05 (1 H, m, quinoline-*Ar*), 8.78 (1 H, s, quinoline-*Ar*), 7.85 - 7.98 (3 H, m, *Ar*), 7.53 - 7.60 (1 H, m, *Ar*), 7.46 - 7.52 (2 H, m, *Ar*), 7.36 - 7.45 (4 H, m, *Ar*), 6.97 (1 H, d, *J*=8.5 Hz, benzyl-*H*); δ_C (100 MHz, DMSO-d_6) 167.0 (*C*=O), 158.8, 149.8, 140.8, 137.6, 135.1, 134.9, 134.0, 132.8, 132.4, 130.2, 129.3, 129.2, 128.9, 128.5, 126.2, 124.1, 122.7, 50.6 (benzyl-*C*); *m/z* (ESI$^-$) 432 ([M-H]$^-$); HRMS (ESI$^-$) $C_{23}H_{15}ClN_3O_4$, ([M-H]$^-$) requires 432.0757; found 476.0751.

N-((8-Hydroxy-5-nitroquinolin-7-yl)(4-methoxyphenyl)methyl)benzamide **247**

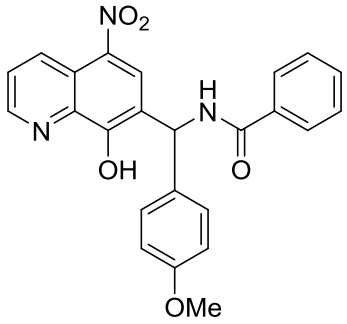

Following general procedure 1, 8-hydroxy-5-nitroquinoline (380 mg, 2.0 mmol), benzamide (242 mg, 2.0 mmol) and 4-methoxybenzaldehyde (486 µL, 4.0 mmol) gave **247** (459 mg, 53 %) as an orange powder.

mp 204 °C; ν_{max}/cm^{-1} 3250 (NH), 1637 (C=O); δ_H (400 MHz, DMSO-d_6) 9.31 - 9.45 (1 H, m, quinoline-*Ar*), 9.08 - 9.23 (1 H, m, quinoline-*Ar*), 8.92 - 9.06 (1 H, m, quinoline-*Ar*), 8.81 (1 H, s, quinoline-*Ar*), 7.91 - 7.97 (2 H, m, *Ar*), 7.84 - 7.90 (1 H, m, *Ar*), 7.51 - 7.57 (1 H, m, *Ar*), 7.45 - 7.51 (2 H, m, *Ar*), 7.25 - 7.33 (2 H, m, *Ar*), 6.88 - 6.96 (3 H, m, benzyl-*H* and *Ar* overlap), 3.72 (3 H, s, OCH_3); δ_C (100 MHz, DMSO-d_6) 166.8 (*C*=O), 159.3, 158.4, 154.6, 149.9, 137.7, 135.1, 133.8, 133.7, 132.3, 129.5, 129.1, 128.9, 128.5, 126.1, 125.0, 122.4, 114.7, 56.0 (O*C*H$_3$), 50.6 (benzyl-*C*); *m/z* (ESI$^-$) 428 ([M-H]$^-$); HRMS (ESI$^+$) $C_{24}H_{19}N_3NaO_5$, ([M+Na]$^+$) requires 452.1217; found 452.1212.

N-((3,4-Dimethoxyphenyl)(8-hydroxyquinolin-7-yl)methyl)benzamide **248**

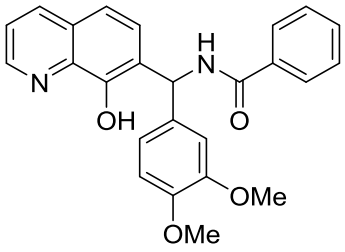

Following general procedure 1, 8-hydroxyquinoline (290 mg, 2.0 mmol), benzamide (242 mg, 2.0 mmol) and 3,4-dimethoxybenzaldehyde (664 mg, 4.0 mmol) gave **248** (176 mg, 21 %) as a white powder.

mp 174 °C; ν_{max}/cm^{-1} 3312 (NH), 1633 (C=O); δ_H (400 MHz, DMSO-d_6) 9.12 - 9.19 (1 H, m, quinoline-*Ar*), 8.81 - 8.90 (1 H, m, quinoline-*Ar*), 8.26 - 8.34 (1 H, m, quinoline-*Ar*), 7.88 - 7.96 (2 H, m, quinoline-*Ar*), 7.69 - 7.74 (1 H, m, *Ar*), 7.50 - 7.57 (2 H, m, *Ar*), 7.41 - 7.50 (3 H, m, *Ar*), 7.00 - 7.02 (1 H, m, benzyl-*H*), 6.87 - 6.94 (2 H, m, *Ar*), 6.79 - 6.85 (1 H, m, *Ar*), 3.71 (3 H, s, CH_3), 3.69 (3 H, s, CH_3); δ_C (100 MHz, DMSO-d_6) 166.7 (*C*=O), 150.5, 149.5, 149.1, 148.7, 138.9, 136.9, 135.5, 135.5, 132.6, 129.8, 129.1, 128.4, 128.4, 127.7, 125.6, 120.4, 118.1, 112.5, 112.3, 56.4 (O*C*H$_3$), 56.4 (O*C*H$_3$), 51.3 (benzyl-*C*); *m/z* (ESI$^+$) 437 ([M+Na]$^+$); HRMS (ESI$^+$) $C_{25}H_{22}N_2NaO_4$, ([M+Na]$^+$) requires 437.1472; found 437.1467.

N-((5-Bromo-8-hydroxyquinolin-7-yl)(phenyl)methyl)benzamide **249**

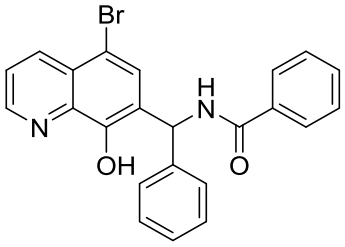

Following general procedure 1, 5-bromo-8-hydroxyquinoline (448 mg, 2.0 mmol), benzamide (242 mg, 2.0 mmol) and benzaldehyde (406 µL, 4.0 mmol) gave **249** (620 mg, 72 %) as a white powder.

mp 246 - 247 °C; ν_{max}/cm^{-1} 3263 (NH), 1638 (C=O); δ_H (400 MHz, DMSO-d_6) 10.46 (1 H, br. s., N*H*), 9.21 - 9.34 (1 H, m, quinoline-*Ar*), 8.89 - 8.98 (1 H, m, quinoline-*Ar*), 8.35 - 8.45 (1 H, m, quinoline-*Ar*), 8.03 (1 H, s, quinoline-*Ar*), 7.89 - 7.98 (2 H, m, *Ar*), 7.68 - 7.75 (1 H, m, *Ar*), 7.52 - 7.59 (1 H, m, *Ar*), 7.46 - 7.52 (2 H, m, *Ar*), 7.31 - 7.37 (4 H, m, *Ar*), 7.22 - 7.29 (1 H, m, *Ar*), 7.03 (1 H, d, *J*=8.5 Hz, benzyl-*H*); δ_C (100 MHz, DMSO-d_6) 166.9 (*C*=O), 151.0, 150.0, 142.5, 139.8, 135.8, 135.1, 132.3, 131.2, 129.3, 129.2, 128.5, 128.0, 127.9, 127.1, 126.6,

124.2, 109.3, 50.9 (benzyl-*C*); *m/z* (ESI$^-$) 431 ([M-H]$^-$); HRMS (ESI$^-$) $C_{23}H_{16}BrN_2O_2$, ([M-H]$^-$) requires 431.0401; found 431.0399.

N-((8-Hydroxyquinolin-7-yl)(phenyl)methyl)-2-phenylacetamide **250**

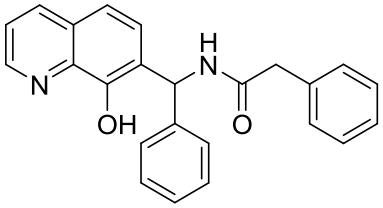

Following general procedure 1, 8-hydroxyquinoline (290 mg, 2.0 mmol), 2-phenylacetamide (270 mg, 2.0 mmol) and benzaldehyde (406 µL, 4.0 mmol) gave **250** (420 mg, 57 %) as a white powder.

mp 207 °C; ν_{max}/cm^{-1} 3307 (NH), 1634 (C=O); δ_H (400 MHz, DMSO-d_6) 9.95 (1 H, br. s, N*H*), 8.95 - 9.06 (1 H, m, quinoline-*Ar*), 8.81 - 8.88 (1 H, m, quinoline-*Ar*), 8.22 - 8.36 (1 H, m, quinoline-*Ar*), 7.50 - 7.59 (2 H, m, *Ar*), 7.39 - 7.45 (1 H, m, *Ar*), 7.14 - 7.35 (10 H, m, *Ar*), 6.70 (1 H, d, *J*=8.5 Hz, benzyl-*H*) 3.58 (2 H, s, CH_2); δ_C (100 MHz, DMSO-d_6) 170.3 (*C*=O), 150.4, 149.2, 143.2, 138.9, 137.3, 136.9, 129.9, 129.1, 129.0, 128.4, 127.9, 127.6, 127.2, 127.2, 125.3, 122.6, 118.2, 50.9 (benzyl-*C*), 43.1 (*C*H$_2$); *m/z* (ESI$^-$) 367 ([M-H]$^-$); HRMS (ESI$^-$) $C_{24}H_{19}N_2O_2$, ([M-H]$^-$) requires 367.1452; found 367.1444.

N-((8-Hydroxyquinolin-7-yl)(phenyl)methyl)pentanamide **251**

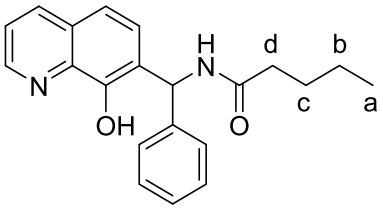

Following general procedure 1, 8-hydroxyquinoline (290 mg, 2.0 mmol), valeramide (202 mg, 2.0 mmol) and benzaldehyde (406 µL, 4.0 mmol) gave **251** (245 mg, 37 %) as a beige powder.

mp 178 - 179 °C; ν_{max}/cm^{-1} (DCM) 3334 (NH), 2957 (OH), 1645 (C=O); δ_H (400 MHz, DMSO-d_6) 9.94 (1 H, br. s., N*H*), 8.81 - 8.88 (1 H, m, quinoline-*Ar*), 8.66 - 8.76 (1 H, m, quinoline-*Ar*), 8.26 - 8.33 (1 H, m, quinoline-*Ar*), 7.50 - 7.59 (2 H, m, *Ar*), 7.39 - 7.47 (1 H, m, *Ar*), 7.15 - 7.34 (5 H, m, *Ar*), 6.73 (1 H, d, *J*=9.0 Hz, benzyl-*H*), 2.18 - 2.28 (2 H, m, CH_{2d}), 1.51 (2 H, quin, *J*=7.5 Hz CH_{2c}), 1.26 (2 H, sxt, *J*=7.5 Hz CH_{2b}), 0.85 (3 H, t, *J*=7.5 Hz, CH_{3a}); δ_C (100 MHz, DMSO-d_6) 172.4 (*C*=O), 150.3, 149.2, 143.5, 138.9, 136.9, 129.1, 128.3, 127.9, 127.5, 127.3,

125.6, 118.2, 50.6 (benzyl-*C*), 35.9 (C_d), 28.4 (C_c), 22.7 (C_b), 14.6 (C_a); *m/z* (ESI$^-$) 333 ([M-H]$^-$); HRMS (ESI$^+$) $C_{22}H_{21}N_2NaO_2$, ([M+Na]$^+$) requires 357.1573; found 357.1565.

N-((8-Hydroxyquinolin-7-yl)(phenyl)methyl)-3-methylbutanamide **252**

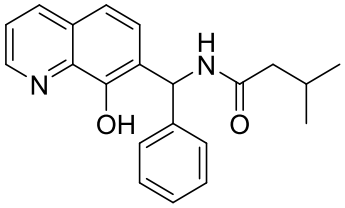

Following general procedure 1, 5-chloro-8-quinolinol (359 mg, 2.0 mmol), benzamide (242 mg, 2.0 mmol) and *o*-tolualdehyde (463 µL, 4.0 mmol) gave **252** (627 mg, 64 %) as an off-white powder.

mp 217-218 °C; ν_{max}/cm^{-1} 3274 (NH), 1636 (C=O); δ_H (400 MHz, DMSO-d_6) 10.40 (1 H, br. s., N-*H*), 9.09 - 9.24 (1 H, m, quinoline-*Ar*), 8.88 - 9.01 (1 H, m, quinoline-*Ar*), 8.40 - 8.53 (1 H, m, quinoline-*Ar*), 7.90 - 7.97 (2 H, m, *Ar*), 7.68 - 7.75 (1 H, m, *Ar*), 7.64 (1 H, s, *Ar*), 7.50 - 7.56 (1 H, m, *Ar*), 7.42 - 7.49 (2 H, m, *Ar*), 7.12 - 7.27 (4 H, m, *Ar*), 7.04 (1 H, d, *J*=8.5 Hz, benzyl-*H*), 2.29 (3 H, s, C*H*$_3$); δ_C (100 MHz, DMSO-d_6) 166.5 (*C*=O), 150.7, 150.0, 140.5, 139.4, 136.9, 135.0, 133.4, 132.2, 131.2, 129.8, 128.4, 128.0, 127.9, 127.4, 126.7, 125.8, 125.2, 123.9, 119.0, 48.8 (benzyl-*C*), 19.6 (*C*H$_3$); *m/z* (ESI$^-$) 401 ([M-H]$^-$, 100 %); HRMS (ESI$^-$) $C_{24}H_{18}ClN_2O_2$, ([M-H]$^-$) requires 401.1062; found 401.1062.

N-((3,4-Dimethoxyphenyl)(8-hydroxyquinolin-7-yl)methyl)-2-phenylacetamide **253**

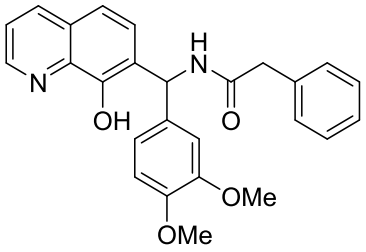

Following general procedure 1, 8-hydroxyquinoline (290 mg, 2.0 mmol), 2-phenylacetamide (270 mg, 2.0 mmol) and 3,4-dimethoxybenzaldehyde (644 mg, 4.0 mmol) gave **253** (445 mg, 52 %) as a white powder.

mp 182 °C; ν_{max}/cm^{-1} 3292 (NH), 1638 (C=O); δ_H (400 MHz, DMSO-d_6) 9.93 (1 H, br. s, N*H*), 8.90 - 8.97 (1 H, m, quinoline-*Ar*), 8.81 - 8.88 (1 H, m, quinoline-*Ar*), 8.27 - 8.33 (1 H, m, quinoline-*Ar*), 7.50 - 7.57 (2 H, m, *Ar*), 7.39 - 7.43 (1 H, m, *Ar*), 7.25 - 7.32 (4 H, m, *Ar*), 6.86 - 6.91 (2 H, m, *Ar*), 6.80 - 6.85 (1 H, m, *Ar*), 6.66 - 6.70 (1

H, m, *Ar*), 6.64 (1 H, d, *J*=8.5 Hz, benzyl-*H*), 3.68 (3 H, s, OCH_3), 3.63 (3 H, s, OCH_3), 3.37 (2 H, s, CH_2); δ_C (100 MHz, DMSO-d_6) 173.1 (*C*=O), 170.2, 150.3, 149.5, 149.2, 148.6, 138.9, 137.4, 136.9, 135.7, 129.9, 129.0, 128.3, 127.2, 125.6, 122.6, 119.9, 118.1, 112.5, 111.7, 56.4 (O*C*H_3), 56.2 (O*C*H_3), 50.5 (benzyl-*C*); *m*/*z* (ESI$^+$) 429 ([M+H]$^+$); HRMS (ESI$^+$) $C_{26}H_{24}N_2NaO_4$, ([M+Na]$^+$) requires 451.1628; found 451.1624.

N-((3,4-Dimethoxyphenyl)(8-hydroxyquinolin-7-yl)methyl)pentanamide **254**

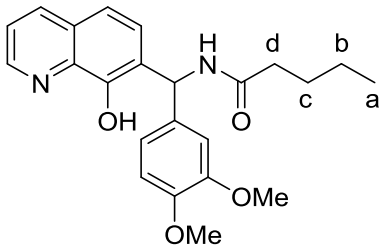

Following general procedure 1, 8-hydroxyquinoline (290 mg, 2.0 mmol), valeramide (202 mg, 2.0 mmol) and 3,4-dimethoxybenzaldehyde (644 mg, 4.0 mmol) gave **254** (92 mg, 12 %) as an off-white powder.

mp 150 - 152 °C; ν_{max}/cm^{-1} 3250 (NH), 2868 (OH), 1635 (C=O); δ_H (400 MHz, $CDCl_3$) 8.71 - 8.85 (1 H, m, quinoline-*Ar*), 8.06 - 8.24 (1 H, m, quinoline-*Ar*), 7.40 - 7.50 (2 H, m, quinoline-*Ar*), 7.32 - 7.38 (1 H, m, *Ar*), 7.16 - 7.25 (1 H, m, *Ar*), 6.93 - 7.01 (1 H, m, *Ar*), 6.67 - 6.86 (2 H, m, *Ar*), 6.53 (1 H, d, *J*=9.0 Hz, benzyl-*H*), 3.83 (3 H, s, OCH_3), 3.82 (3 H, s, OCH_3), 2.30 (2 H, t, *J*=7.5 Hz, CH_{2d}), 1.67 (2 H, quin, *J*=7.5 Hz, CH_{2c}), 1.37 (2 H, sxt, *J*=7.5 Hz, CH_{2b}), 0.91 (3 H, t, *J*=7.5 Hz, CH_{3a}); δ_C (100 MHz, $CDCl_3$) 172.3 (*C*=O), 149.0, 149.0, 148.2, 138.3, 136.1, 134.3, 128.5, 127.6, 122.5, 121.9, 118.9, 118.0, 110.9, 110.5, 55.9 (O*C*H_3), 55.8 (O*C*H_3), 54.4 (benzyl-*C*), 36.7 (C_d), 27.8 (C_c), 22.4 (C_b), 13.8 (C_a); *m*/*z* (ESI$^-$) 393 ([M-H]$^-$); HRMS (ESI$^+$) $C_{23}H_{27}N_2O_4$, ([M+H]$^+$) requires 395.1965; found 395.1973.

N-((5-Chloro-8-hydroxyquinolin-7-yl)(3-methoxyphenyl)methyl)benzamide **255**

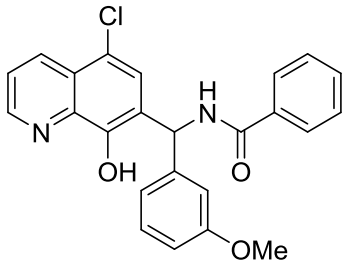

Following general procedure 1, 5-chloro-8-hydroxyquinoline (359 mg, 2.0 mmol), benzamide (242 mg, 2.0 mmol) and 3-methoxybenzaldehyde (487 µL, 4.0 mmol) gave **255** (635 mg, 76 %) as white powder. **255** was then stirred in a 4M HCl solution in dioxane for 1 h. The solvent was removed under reduced pressure to give the hydrochloride salt of **255** as a bright-yellow powder in quantitative yield.

mp 250 °C; ν_{max}/cm^{-1} 3288 (NH), 1641 (C=O); δ_H (400 MHz, DMSO-d_6) 10.13 (1 H, br. s, N*H*), 9.21 - 9.33 (1 H, m, quinoline-*Ar*), 8.95 - 9.03 (1 H, m, quinoline-*Ar*), 8.50 - 8.58 (1 H, m, quinoline-*Ar*), 7.91 - 7.98 (2 H, m, *Ar*), 7.90 (1 H, s, *Ar*), 7.72 - 7.81 (1 H, m, *Ar*), 7.51 - 7.58 (1 H, m, *Ar*), 7.44 - 7.50 (2 H, m, *Ar*), 7.21 - 7.31 (1 H, m, *Ar*), 7.00 (1 H, d, *J*=9.0 Hz, benzyl-*H*), 6.89 - 6.96 (2 H, m, *Ar*), 6.79 - 6.87 (1 H, m, *Ar*), 3.70 (3 H, s, OC*H*$_3$); δ_C (100 MHz, DMSO-d_6) 166.9 (*C*=O), 160.2, 149.8, 149.6, 144.0, 138.7, 135.1, 134.5, 132.3, 130.4, 129.2, 128.5, 128.0, 126.7, 126.0, 123.9, 120.3, 119.7, 114.2, 112.8, 55.9 (O*C*H$_3$), 50.9 (benzyl-*C*); *m*/*z* (ESI$^+$) 419 ([M+H]$^+$); HRMS (ESI$^+$) $C_{24}H_{20}ClN_2O_3$, ([M+H]$^+$) requires 419.1157; found 419.1160.

N-((5-Chloro-8-hydroxyquinolin-7-yl)(phenyl)methyl)pentanamide 256

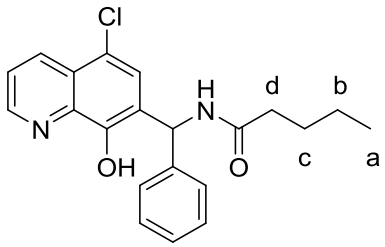

Following general procedure 1, 5-chloro-8-hydroxyquinoline (359 mg, 2.0 mmol), valeramide (202 mg, 2.0 mmol) and benzaldehyde (406 µL, 4.0 mmol) gave **256** (636 mg, 84 %) as a white powder.

mp 205 °C; ν_{max}/cm^{-1} 3262 (NH), 1637 (C=O), 700 (C-Cl); δ_H (400 MHz, DMSO-d_6) 10.34 (1 H, br. s., N-*H*), 8.89 - 9.00 (1 H, m, quinoline-*Ar*), 8.71 - 8.83 (1 H, m, quinoline-*Ar*), 8.39 - 8.53 (1 H, m, quinoline-*Ar*), 7.65 - 7.75 (2 H, m, *Ar*), 7.28 - 7.35 (2 H, m, *Ar*), 7.17 - 7.27 (3 H, m, *Ar*), 6.72 (1 H, d, *J*=9.0 Hz, benzyl-*H*), 2.23 (2 H, t, *J*=7.0 Hz, C*H*$_{2/d}$), 1.51 (2 H, quin, *J*=7.0 Hz, C*H*$_{2/c}$), 1.26 (2 H, sxt, *J*=7.0 Hz, C*H*$_{2/b}$), 0.86 (3 H, t, *J*=7.0 Hz, C*H*$_{2/a}$); δ_C (100 MHz, DMSO-d_6) 172.5 (*C*=O), 150.1, 142.8, 139.5, 133.4, 129.3, 2x 127.8, 127.1, 126.4, 125.7, 123.8, 119.5, 50.3 (benzyl-*C*), 35.9 (C_d), 28.4 (C_c), 22.6 (C_b), 14.6 (C_a); *m*/*z* (ESI$^-$) 367 ([M-H]$^-$); HRMS (ESI$^-$) $C_{21}H_{21}ClN_2NaO_2$, ([M+Na]$^+$) requires 391.1184; found 391.1180.

N-((5-Chloro-8-hydroxyquinolin-7-yl)(phenyl)methyl)-2-phenylacetamide **257**

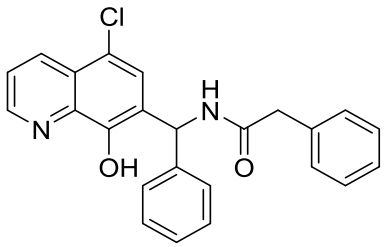

Following general procedure 1, 5-chloro-8-hydroxyquinoline (359 mg, 2.0 mmol), 2-phenylacetamide (270 mg, 2.0 mmol) and benzaldehyde (406 µL, 4.0 mmol) gave **257** (485 mg, 60 %) as a white powder.

mp 217 - 218 °C; ν_{max}/cm^{-1} 3299 (NH), 1645 (C=O), 696 (C-Cl); δ_H (400 MHz, DMSO-d_6) 10.35 (1 H, br. s., N-*H*), 9.00 - 9.13 (1 H, m, quinoline-*Ar*), 8.89 - 8.99 (1 H, m, quinoline-*Ar*), 8.40 - 8.52 (1 H, m, quinoline-*Ar*), 7.64 - 7.76 (2 H, m, *Ar*), 7.15 - 7.37 (10 H, m, *Ar*), 6.68 (1 H, d, *J*=8.5 Hz, benzyl-*H*), 3.58 (2 H, s, CH_2); δ_C (100 MHz, DMSO-d_6) 170.4 (*C*=O), 150.1, 142.5, 139.5, 137.2, 133.4, 129.9, 129.3, 129.1, 129.0, 127.9, 127.2, 127.1, 127.0, 126.1, 125.7, 123.8, 119.5, 50.7 (benzyl-*C*), 43.1 (*C*H$_2$); *m*/*z* (ESI$^-$) 401 ([M-H]$^-$); HRMS (ESI$^-$) $C_{24}H_{19}ClN_2NaO_2$, ([M+Na]$^+$) requires 425.1027; found 425.1024.

N-((5-Chloro-8-hydroxyquinolin-7-yl)(phenyl)methyl)-3-methylbutanamide **258**

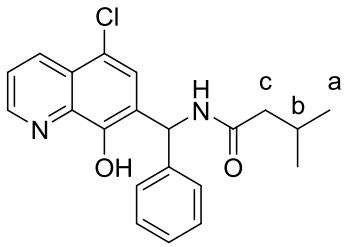

Following general procedure 1, 5-chloro-8-hydroxyquinoline (359 mg, 2.0 mmol), isovaleramide (202 mg, 2.0 mmol) and benzaldehyde (406 µL, 4.0 mmol) gave **258** (534 mg, 73 %) as a white powder.

mp 199 °C; ν_{max}/cm^{-1} 3235 (NH), 1633 (C=O), 700 (C-Cl); δ_H (400 MHz, DMSO-d_6) 10.34 (1 H, br. s., N-*H*), 8.89 - 8.99 (1 H, m, quinoline-*Ar*), 8.72 - 8.83 (1 H, m, quinoline-*Ar*), 8.41 - 8.51 (1 H, m, quinoline-*Ar*), 7.62 - 7.79 (2 H, m, *Ar*), 7.17 - 7.36 (5 H, m, *Ar*), 6.72 (1 H, d, *J*=8.5 Hz, benzyl-*H*), 2.09 - 2.13 (2 H, m, C$H_{2/c}$), 2.01 (1 H, m, CH_b), 0.87 (6 H, dd, *J*=8.0, 7.0 Hz, 2xC$H_{3/a}$); δ_C (100 MHz, DMSO-d_6) 171.9 (*C*=O), 150.1, 142.8, 139.5, 133.4, 129.2, 127.8, 127.8, 127.1, 126.4, 125.7, 123.8, 119.4, 50.3 (benzyl-*C*), 45.4 (*C*H$_{2/c}$), 26.6 (*C*H$_b$), 23.2 (*C*H$_{3/a}$); *m*/*z* (ESI$^-$) 367 ([M-H]$^-$); HRMS (ESI$^-$) $C_{21}H_{21}ClN_2NaO_2$, ([M+Na]$^+$) requires 391.1184; found 391.1180.

N-((3-Bromophenyl)(5-chloro-8-hydroxyquinolin-7-yl)methyl)pentanamide **259**

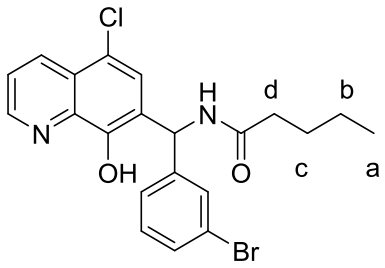

Following general procedure 1, 5-chloro-8-hydroxyquinoline (359 mg, 2.0 mmol), Valeramide (202 mg, 2.0 mmol) and 3-bromobenzaldehyde (468 µL, 4.0 mmol) gave **259** (786 mg, 88 %) as an off-white powder.

mp 211 °C; ν_{max}/cm^{-1} 3250 (NH), 1639 (C=O), 688 (C-Cl); δ_H (400 MHz, DMSO-d_6) 10.46 (1 H, br. s., N-*H*), 8.90 - 9.01 (1 H, m, quinoline-*Ar*), 8.76 - 8.87 (1 H, m, quinoline-*Ar*), 8.39 - 8.54 (1 H, m, quinoline-*Ar*), 7.65 - 7.77 (2 H, m, *Ar*), 7.38 - 7.49 (2 H, m, *Ar*), 7.19 - 7.34 (2 H, m, *Ar*), 6.69 (1 H, d, *J*=8.5 Hz, benzyl-*H*), 2.24 (2 H, t, *J*=7.0 Hz, C$H_{2/d}$), 1.51 (2 H, quin, *J*=7.0 Hz C$H_{2/c}$), 1.26 (2 H, sxt, *J*=7.0 Hz C$H_{2/b}$), 0.86 (3 H, t, *J*=7.0 Hz C$H_{3/a}$); δ_C (100 MHz, DMSO-d_6) 172.6 (*C*=O), 150.2, 145.6, 139.5, 133.4, 131.6, 130.7, 130.3, 127.0, 126.8, 125.8, 125.6, 123.9, 122.6, 119.6, 50.0 (benzyl-*C*), 35.8 (*C*H$_{2/d}$), 28.3 (*C*H$_{2/c}$), 22.6 (*C*H$_{2/b}$), 14.5 (*C*H$_{3/a}$); *m*/*z* (ESI$^-$) 445 ([M-H]$^-$); HRMS (ESI$^-$) $C_{21}H_{19}BrClN_2O_2$, ([M-H]$^-$) requires 445.0324; found 445.0318.

N-((3-Bromophenyl)(5-chloro-8-hydroxyquinolin-7-yl)methyl)-3-methylbutanamide **260**

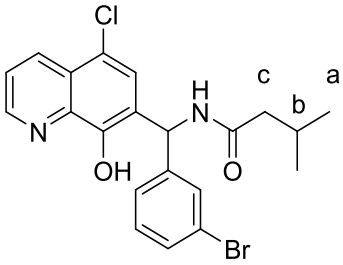

Following general procedure 1, 5-chloro-8-hydroxyquinoline (359 mg, 2.0 mmol), isovaleramide (202 mg, 2.0 mmol) and 3-bromobenzaldehyde (468 µL, 4.0 mmol) gave **260** (722 mg, 81 %) as a white powder.

mp 212 °C; ν_{max}/cm^{-1} 3206 (NH), 1658 (C=O), 684 (C-Cl); δ_H (400 MHz, DMSO-d_6) 10.45 (1 H, br. s., N-*H*), 8.91 - 8.98 (1 H, m, quinoline-*Ar*), 8.78 - 8.87 (1 H, m, quinoline-*Ar*), 8.43 - 8.50 (1 H, m, quinoline-*Ar*), 7.65 - 7.76 (2 H, m, *Ar*), 7.40 - 7.46 (2 H, m, *Ar*), 7.21 - 7.33 (2 H, m, *Ar*), 6.70 (1 H, d, *J*=9.0 Hz, benzyl-*H*), 2.09 - 2.15 (2 H, m, C$H_{2/c}$), 1.94 - 2.06 (1 H, m CH_b), 0.87 (6 H, m,); δ_C (100 MHz, DMSO-d_6) 172.0 (*C*=O), 150.2, 145.6, 139.5,

133.4, 131.6, 130.7, 130.3, 127.0, 126.9, 125.8, 125.6, 124.0, 122.6, 119.6, 50.0 (benzyl-*C*), 45.4 ($CH_{2/c}$), 26.6 (CH_b), 23.1 ($CH_{3/a}$); *m/z* (ESI^+) 447 ($[M+H]^+$); HRMS (ESI^-) $C_{21}H_{19}BrClN_2O_2$, ($[M-H]^-$) requires 445.0324; found 445.0313.

N-((5-Chloro-8-hydroxyquinolin-7-yl)(5-nitrothiophen-3-yl)methyl)benzamide **261**

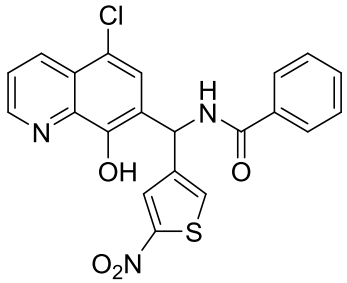

Following general procedure 1, 5-chloro-8-hydroxyquinoline (359 mg, 2.0 mmol), benzamide (242 mg, 2.0 mmol) and 2-nitrothiophene-4-carboxaldehyde (628 µL, 4.0 mmol) gave **261** (218 mg, 25 %) as an off-white powder.

mp 155 - 158 °C; ν_{max}/cm^{-1} 3305 (NH), 1638 (C=O), 692 (C-Cl); δ_H (400 MHz, DMSO-d_6) 10.68 (1 H, br. s., N-*H*), 9.38 - 9.48 (1 H, m, quinoline-*Ar*), 8.98 - 9.05 (1 H, m, quinoline-*Ar*), 8.49 - 8.55 (1 H, m, quinoline-*Ar*), 8.07 - 8.14 (1 H, m, *Ar*), 7.93 - 8.02 (3 H, m, *Ar*), 7.83 - 7.86 (1 H, m, *Ar*), 7.74 - 7.81 (1 H, m, *Ar*), 7.48 - 7.56 (3 H, m, *Ar*), 7.00 (1 H, d, *J*=9.0 Hz, benzyl-*H*); δ_C (100 MHz, DMSO-d_6) 166.9 (*C*=O), 152.2, 150.4, 150.2, 143.2, 139.6, 134.8, 132.5, 132.3, 129.9, 129.2, 129.2, 128.5, 126.8, 126.1, 124.9, 124.1, 119.8, 47.8 (benzyl-*C*); *m/z* (ESI^-) 438 ($[M-H]^-$); HRMS (ESI^-) $C_{21}H_{13}ClIN_3O_4S$, ($[M-H]^-$) requires 438.0321; found 438.0313.

N-((5-Chloro-8-hydroxyquinolin-7-yl)(2,4-dimethoxyphenyl)methyl)benzamide **262**

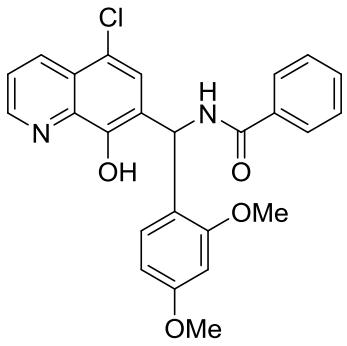

Following general procedure 1, 5-chloro-8-hydroxyquinoline (359 mg, 2.0 mmol), benzamide (242 mg, 2.0 mmol) and 2,4-dimethoxybenzaldehyde (664 mg, 4.0 mmol) gave **262** (464 mg, 52 %) as a white powder.

mp 186 - 187 °C; ν_{max}/cm^{-1} 3306 (NH), 1636 (C=O); δ_H (400 MHz, DMSO-d_6) 10.18 (1 H, br. s., N-*H*), 8.92 - 8.96 (1 H, m, quinoline-*Ar*), 8.87 - 8.92 (1 H, m, quinoline-*Ar*), 8.43 - 8.51 (1 H, m, quinoline-*Ar*), 7.87 - 7.93 (2 H, m, *Ar*), 7.66 - 7.73 (1 H, m, *Ar*), 7.55 (1 H, s, *Ar*), 7.48 - 7.53 (1 H, m, *Ar*), 7.41 - 7.47 (2 H, m, *Ar*), 7.07 - 7.12 (1 H, m, *Ar*), 7.01 (1 H, d, *J*=8.0 Hz, benzyl-*H*), 6.56 - 6.61 (1 H, m, *Ar*), 6.47 - 6.54 (1 H, m, *Ar*), 3.75 (3 H, s, OC*H*$_3$), 3.73 (3 H, s, OC*H*$_3$); δ_C (100 MHz, DMSO-d_6) 166.2 (*C*=O), 160.8, 158.7, 150.6, 149.8, 139.4, 135.3, 133.3, 132.0, 129.5, 129.0, 128.4, 127.9, 126.0, 125.6, 123.7, 122.3, 118.6, 105.2, 99.4, 56.5 (O*C*H$_3$), 56.1 (O*C*H$_3$), 46.6 (benzyl-*C*); *m*/*z* (ESI$^-$) 895 ([2M-H]$^-$); HRMS (ESI$^+$) $C_{25}H_{21}ClIN_2NaO_4$, ([M+Na]$^+$) requires 471.1082; found 471.1079.

N-((8-Hydroxyquinolin-7-yl)(phenyl)methyl)acetamide **263**

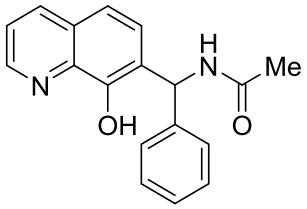

Following general procedure 1, 8-hydroxyquinoline (290 mg, 2.0 mmol), acetamide (118 mg, 2.0 mmol) and benzaldehyde (406 µL, 4.0 mmol) gave **263** (316 mg, 54 %) as a white powder.

mp 197 °C; ν_{max}/cm^{-1} 3305 (NH), 1644 (C=O); δ_H (400 MHz, DMSO-d_6) 9.97 (1 H, br. s. , N-*H*), 8.82 - 8.89 (1 H, m, quinoline-*Ar*), 8.74 - 8.81 (1 H, m, quinoline-*Ar*), 8.26 - 8.34 (1 H, m, quinoline-*Ar*), 7.50 - 7.58 (2 H, m, *Ar*), 7.39 - 7.45 (1 H, m, *Ar*), 7.24 - 7.31 (4 H, m, *Ar*), 7.16 - 7.23 (1 H, m, *Ar*), 6.72 (1 H, d, *J*=8.5 Hz, benzyl-*H*), 1.95 (3 H, s, C*H*$_3$); δ_C (100 MHz, DMSO-d_6) 169.4 (*C*=O), 150.3, 149.2, 143.4, 138.9, 136.9, 129.1, 128.4, 127.9, 127.6, 127.3, 125.6, 122.6, 118.2, 50.7 (benzyl-*C*), 23.5 (*C*H$_3$); *m*/*z* (ESI$^-$) 291 ([M-H]$^-$); HRMS (ESI$^+$) $C_{18}H_{16}IN_2NaO_2$, ([M+Na]$^+$) requires 315.1104; found 315.1093.

N-((3-Bromophenyl)(5-chloro-8-hydroxyquinolin-7-yl)methyl)-3-fluorobenzamide **264**

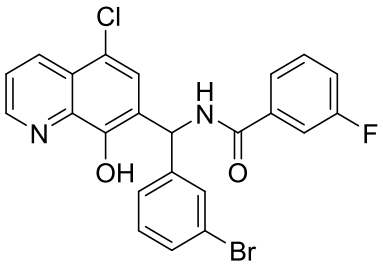

Following general procedure 1, 5-chloro-8-hydroxyquinoline (359 mg, 2.0 mmol), 3-fluorobenzamide (278 mg, 2.0 mmol) and 3-bromobenzaldehyde (468µL, 4.0 mmol) gave **264** (407 mg, 42 %) as a white powder.

mp 219 °C; ν_{max}/cm^{-1} 3290 (NH), 1635 (C=O); δ_H (400 MHz, DMSO-d_6) 10.57 (1 H, br. s., N*H*), 9.32 - 9.43 (1 H, m, quinoline-*Ar*), 8.93 - 9.02 (1 H, m, quinoline-*Ar*), 8.43 - 8.55 (1 H, m, quinoline-*Ar*), 7.80 - 7.84 (1 H, m, *Ar*), 7.70 - 7.80 (3 H, m, *Ar*), 7.50 - 7.59 (2 H, m, *Ar*), 7.46 - 7.50 (1 H, m, *Ar*), 7.28 - 7.45 (3 H, m, *Ar*), 6.97 (1 H, d, *J*=8.5 Hz, benzyl-*H*); δ_C (100 MHz, DMSO-d_6) 165.6 (*C*=O), 164.0 (*C*-F), 150.5, 150.2, 145.0, 139.5, 137.2, 133.4, 131.6, 131.5, 131.4, 131.0, 130.6, 127.3, 127.2, 126.0, 125.0, 124.7, 124.0, 122.6, 119.6, 115.4, 41.0 (benzyl-*C*); *m*/*z* (ESI$^-$) 483 ([M-H]$^-$); HRMS (ESI$^+$) $C_{23}H_{15}BrClFN_2NaO_2$, ([M+Na]$^+$) requires 506.9882; found 506.9876.

N-((5-Chloro-8-hydroxyquinolin-7-yl)(3-methylthiophen-2-yl)methyl)-3-nitrobenzamide 265

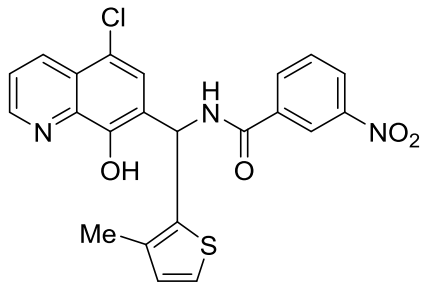

Following general procedure 1, 5-chloro-8-hydroxyquinoline (359 mg, 2.0 mmol), 3-nitrobenzamide (332 mg, 2.0 mmol) and 3-methyl-2-thiohenecarboxaldehyde (431 µL, 4.0 mmol) gave **265** (326 mg, 36 %) as an off-white powder.

mp 143 °C; ν_{max}/cm^{-1} 3278 (NH), 1646 (C=O); δ_H (400 MHz, DMSO-d_6) 10.55 (1 H, br. s., N*H*), 9.69 - 9.79 (1 H, m, quinoline-*Ar*), 8.92 - 9.01 (1 H, m, quinoline-*Ar*), 8.74 - 8.82 (1 H, m, quinoline-*Ar*), 8.46 - 8.54 (1 H, m, *Ar*), 8.29 - 8.44 (2 H, m, *Ar*), 7.86 (1 H, s, *Ar*), 7.77 - 7.83 (1 H, m, *Ar*), 7.68 - 7.76 (1 H, m, *Ar*), 7.26 - 7.33 (1 H, m, *Ar*), 7.17 (1 H, d, *J*=8.0 Hz, benzyl-*H*), 6.86 - 6.98 (1 H, m, *Ar*), 2.16 (3 H, s, C*H*$_3$); δ_C (100 MHz, DMSO-d_6) 164.4 (*C*=O), 150.6, 150.2, 148.6, 139.4, 139.3, 136.0, 135.3, 135.1, 133.4, 131.4, 131.0, 127.1, 126.1, 125.2, 124.2, 124.1, 123.1, 119.3, 46.1 (benzyl-*C*), 14.4 (*C*H$_3$); *m*/*z* (ESI$^-$) 929 ([2M+Na]$^+$); HRMS (ESI$^+$) $C_{22}H_{16}ClIN_3O_4S$, ([M+Na]$^+$) requires 476.0442; found 476.0434.

2-Chloro-*N*-((5-chloro-8-hydroxyquinolin-7-yl)(3-methylthiophen-2-yl)methyl)benzamide 266

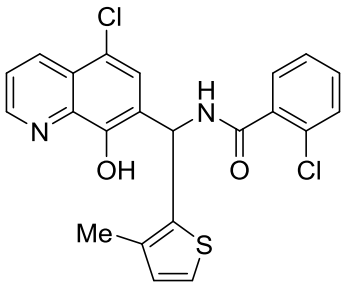

Following general procedure 1, 5-chloro-8-hydroxyquinoline (359 mg, 2.0 mmol), 2-chlorobenzamide (311 mg, 2.0 mmol) and methyl 3-methyl-2-thiophenecarboxaldehyde (656 mg, 4.0 mmol) gave **266** (290 mg, 33 %) as off-white powder.

mp 148 ^{o}C; ν_{max}/cm^{-1} 3297 (NH), 1647 (C=O); δ_H (400 MHz, DMSO-d_6) 10.51 (1 H, br. s., N*H*), 9.49 - 9.57 (1 H, m, quinoline-*Ar*), 8.91 - 9.01 (1 H, m, quinoline-*Ar*), 8.45 - 8.54 (1 H, m, quinoline-*Ar*), 7.87 - 7.91 (1 H, m, *Ar*), 7.69 - 7.78 (1 H, m, *Ar*), 7.36 - 7.52 (4 H, m, *Ar*), 7.23 - 7.28 (1 H, m, *Ar*), 7.08 (1 H, d, *J*=8.0 Hz, benzyl-*H*), 6.85 - 6.93 (1 H, m, *Ar*), 2.25 (3 H, s, C*H*$_3$); δ_C (100 MHz, DMSO-d_6) 166.3 (*C*=O), 150.3, 150.1, 139.4, 137.5, 135.2, 133.4, 131.7, 131.2, 130.8, 130.4, 129.8, 129.7, 129.1, 127.9, 127.0, 126.0, 125.4, 124.2, 124.0, 119.3, 45.4 (benzyl-*C*), 14.5 (*C*H$_3$); *m/z* (ESI$^-$) 441 ([M-H]$^-$); HRMS (ESI$^-$) $C_{22}H_{15}Cl_2N_2O_2S$, ([M-H]$^-$) requires 441.0237; found 441.0233.

3-Chloro-*N*-((5-chloro-8-hydroxyquinolin-7-yl)(3-methylthiophen-2-yl)methyl)benzamide 267

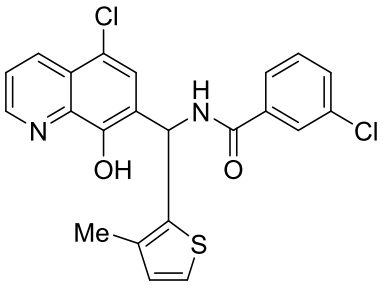

Following general procedure 1, 5-chloro-8-hydroxyquinoline (359 mg, 2.0 mmol), 3-chlorobenzamide (311 mg, 2.0 mmol) and methyl 3-methyl-2-thiophenecarboxaldehyde (656 mg, 4.0 mmol) gave **267** (266 mg, 30 %) as an off-white powder.

mp 172 ^{o}C; ν_{max}/cm^{-1} 3300 (NH), 1642 (C=O); δ_H (400 MHz, DMSO-d_6) 10.51 (1 H, br. s., N*H*), 9.42 - 9.50 (1 H, m, quinoline-*Ar*), 8.92 - 9.02 (1 H, m, quinoline-*Ar*), 8.46 - 8.53 (1 H, m, quinoline-*Ar*), 7.99 (1 H, s, *Ar*), 7.86 -

7.92 (1 H, m, *Ar*), 7.83 - 7.86 (1 H, m, *Ar*), 7.70 - 7.77 (1 H, m, *Ar*), 7.58 - 7.66 (1 H, m, *Ar*), 7.46 - 7.56 (1 H, m, *Ar*), 7.25 - 7.31 (1 H, m, *Ar*), 7.14 (1 H, d, *J*=8.0 Hz, benzyl-*H*), 6.87 - 6.93 (1 H, m, *Ar*), 2.14 (3 H, s, CH_3); δ_C (100 MHz, DMSO-d_6) 169.4 (*C*=O), 154.9, 154.4, 143.9, 143.8, 141.0, 139.5, 138.3, 137.8, 136.5, 135.7, 135.5, 132.5, 131.7, 131.5, 130.4, 129.6, 128.4, 128.4, 123.6, 50.2 (benzyl-*C*), 18.7 (*C*H_3); *m*/*z* (ESI$^-$) 441 ([M-H]$^-$); HRMS (ESI$^-$) $C_{22}H_{15}Cl_2N_2O_4S$, ([M-H]$^-$) requires 441.0237; found 441.0241.

N-((5-Chloro-8-hydroxyquinolin-7-yl)(3-methylthiophen-2-yl)methyl)-4-methoxybenzamide **268**

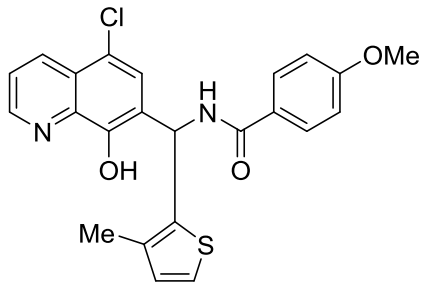

Following general procedure 1, 5-chloro-8-hydroxyquinoline (359 mg, 2.0 mmol), 4-methoxybenzamide (302 mg, 2.0 mmol) and methyl 3-methyl-2-thiophenecarboxaldehyde (431 µL, 4.0 mmol) gave **268** (339 mg, 39 %) as an off-white powder.

mp 163 - 164 °C; ν_{max}/cm^{-1} 3305 (NH), 1637 (C=O); δ_H (400 MHz, DMSO-d_6) 10.45 (1 H, br. s., N*H*), 9.14 - 9.19 (1 H, m, quinoline-*Ar*), 8.91 - 9.00 (1 H, m, quinoline-*Ar*), 8.45 - 8.53 (1 H, m, quinoline-*Ar*), 7.90 - 7.95 (2 H, m, *Ar*), 7.89 (1 H, s, *Ar*), 7.69 - 7.76 (1 H, m, *Ar*), 7.23 - 7.28 (1 H, m, *Ar*), 7.15 (1 H, d, *J*=8.0 Hz, benzyl-*H*), 6.97 - 7.02 (2 H, m, *Ar*), 6.87 - 6.91 (1 H, m, *Ar*), 3.77 - 3.82 (3 H, m, thiophene-CH_3), 2.14 (3 H, s, OCH_3); δ_C (100 MHz, DMSO-d_6) 165.9 (*C*=O), 162.6 (*C*OCH$_3$), 150.4, 150.0, 140.1, 139.4, 134.9, 133.4, 131.3, 130.4, 127.4, 127.0, 126.0, 125.8, 123.9, 123.9, 119.2, 114.3, 114.2, 56.2 (benzyl-*C*), 14.4 (*C*H_3); *m*/*z* (ESI$^+$) 899 ([2M+Na]$^+$); HRMS (ESI$^+$) $C_{23}H_{20}ClIN_2O_3S$, ([M+H]$^+$) requires 439.0878; found 439.0241.

N-((5-Chloro-8-hydroxyquinolin-7-yl)(3-methylthiophen-2-yl)methyl)thiophene-2-carboxamide **269**

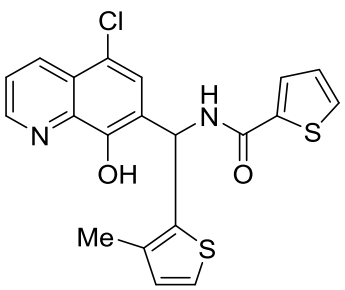

Following general procedure 1, 5-chloro-8-hydroxyquinoline (359 mg, 2.0 mmol), thiophene-2-carboxamide (254 mg, 2.0 mmol) and methyl 3-methyl-2-thiophenecarboxaldehyde (431 µL, 4.0 mmol) gave **269** (179 mg, 22 %) as a white powder.

mp 172 °C; ν_{max}/cm^{-1} 3302 (NH), 1634 (C=O); δ_H (400 MHz, DMSO-d_6) 10.51 (1 H, br. s., N*H*), 9.31 - 9.40 (1 H, m, quinoline-*Ar*), 8.92 - 9.00 (1 H, m, quinoline-*Ar*), 8.43 - 8.56 (1 H, m, quinoline-*Ar*), 7.98 - 8.03 (1 H, m, *Ar*), 7.86 (1 H, s, *Ar*), 7.75 - 7.82 (1 H, m, *Ar*), 7.69 - 7.76 (1 H, m, *Ar*), 7.24 - 7.32 (1 H, m, *Ar*), 7.13 - 7.20 (1 H, m, *Ar*), 7.07 - 7.12 (1 H, m, *Ar*), 6.85 - 6.95 (1 H, m, *Ar*), 2.14 (3 H, s, C*H*$_3$); δ_C (100 MHz, DMSO-d_6) 161.2 (*C*=O), 150.5, 150.1, 140.1, 139.5, 139.4, 135.2, 133.4, 132.2, 131.4, 129.7, 128.8, 127.2, 126.0, 125.5, 124.1, 124.0, 119.2, 45.6 (benzyl-*C*), 14.4 (*C*H$_3$); *m*/*z* (ESI$^+$) 415 ([M+H]$^+$); HRMS (ESI$^+$) $C_{20}H_{16}ClIN_2O_2S_2$, ([M+H]$^+$) requires 415.0336; found 415.0330.

N-((5-Chloro-8-hydroxyquinolin-7-yl)(3-methylthiophen-2-yl)methyl)nicotinamide 270

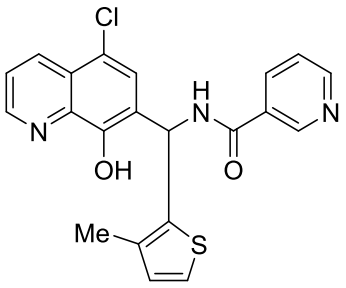

Following general procedure 1, 5-chloro-8-hydroxyquinoline (359 mg, 2.0 mmol), nicotinamide (244 mg, 2.0 mmol) and 3-methyl-2-thiophenecarboxaldehyde (431 µL, 4.0 mmol) gave **270** (303 mg, 37 %) as an off-white powder.

mp 210 °C; ν_{max}/cm^{-1} 3173 (NH), 1667 (C=O); δ_H (400 MHz, DMSO-d_6) 10.54 (1 H, br. s., N*H*), 9.50 - 9.61 (1 H, m, quinoline-*Ar*), 9.04 - 9.07 (1 H, m, *Ar*), 8.94 - 9.00 (1 H, m, *Ar*), 8.69 - 8.74 (1 H, m, *Ar*), 8.45 - 8.55 (1 H, m, *Ar*), 8.20 - 8.30 (1 H, m, *Ar*), 7.86 (1 H, s, *Ar*), 7.69 - 7.79 (1 H, m, *Ar*), 7.46 - 7.58 (1 H, m, *Ar*), 7.26 - 7.32 (1 H, m, *Ar*), 7.16 (1 H, d, *J*=8.0 Hz, benzyl-*H*), 6.88 - 6.94 (1 H, m, *Ar*), 2.16 (3 H, s, C*H*$_3$); δ_C (100 MHz, DMSO-d_6) 165.1 (*C*=O), 152.3, 150.5, 150.1, 149.5, 139.5, 139.4, 136.2, 135.2, 133.4, 131.4, 130.4, 127.1, 126.1, 125.2, 124.3, 124.1, 124.0, 119.3, 45.8 (benzyl-*C*), 14.4 (*C*H$_3$); *m*/*z* (ESI$^+$) 410 ([M+H]$^+$); HRMS (ESI$^+$) $C_{21}H_{16}ClIN_3NaO_2S$, ([M+Na]$^+$) requires 321.0554; found 432.0527.

4-Methoxyquinolin-8-yl 4-methylbenzenesulfonate 271

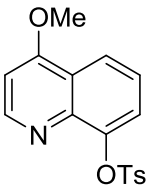

Sodium hydride (60 % in oil, 190 mg, 4.76 mmol) was stirred with **124** (1000 mg, 3.17 mmol) in DMF (20 mL) at room temperature until H_2 evolution ceased. Methyl trifluoromethylsulfonate (347 µL) was slowly added under N_2. After 2 h, the reaction mixture was poured into water (140 mL) and allowed to stand at room temperature overnight. The precipitate was collected by filtration and washed with water to give **271** as a white powder (298 mg, 29 %).

mp 147 °C; δ_H (400 MHz, DMSO-d_6) 8.09 - 8.19 (1 H, m, *Ar*), 7.79 - 7.84 (1 H, m, *Ar*), 7.72 - 7.77 (2 H, m, *Ar*), 7.45 - 7.52 (2 H, m, *Ar*), 7.27 - 7.33 (1 H, m, *Ar*), 7.17 - 7.23 (1 H, m, *Ar*), 6.03 - 6.08 (1 H, m, *Ar*), 3.90 (3 H, s, OC*H*$_3$) 2.42 (3 H, s, C*H*$_3$); δ_C (100 MHz, DMSO-d_6) 175.9 (*C*OCH$_3$), 148.7, 147.5, 131.7, 131.3, 130.9, 130.1, 129.6, 129.3, 127.5, 126.1, 124.0, 110.1, 45.7 (CO*C*H$_3$), 22.1 (*C*H$_3$); *m/z* (ESI$^+$) 352 ([M+Na]$^+$).

4-Chloroquinolin-8-ol 272

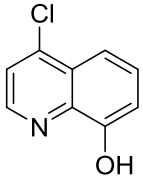

125 (1 g, 3 mmol) was stirred in an aqueous solution of sodium hydroxide (2M, 7.5 mL, 15 mmol) and ethanol (10 mL) under reflux for 1 h. The reaction mixture was diluted with water (50 mL) and neutralised with aqueous HCl to pH 7. The precipitate was collected by filtration to give **272** as a light-brown powder (374 mg, 69 %).

mp 144 °C; ν_{max}/cm^{-1} 3154 (OH); δ_H (400 MHz, DMSO-d_6) 10.14 (1 H, br. s., O*H*), 8.67 - 8.87 (1 H, m, *Ar*), 7.67 - 7.82 (1 H, m, *Ar*), 7.49 - 7.65 (2 H, m, *Ar*), 7.07 - 7.31 (1 H, m, *Ar*); δ_C (100 MHz, DMSO-d_6) 154.8, 148.7, 142.1, 140.3, 129.9, 127.4, 122.9, 114.1, 113.6 ; *m/z* (FI$^+$) 179 ([M]$^+$).

5-Chloro-7-iodoquinolin-8-yl 4-methylbenzenesulfonate **273**

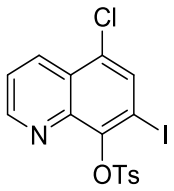

Clioquinol (6.11 g, 20.0 mmol) was dissolved in 1M aqueous sodium hydroxide solution (21.0 mL). A solution of *p*-toluenesulfonyl chloride (3.81 g, 21.0 mmol) in acetone (7 mL) was added dropwise. The reaction mixture was stirred at room temperature for 3 h. Water (30 mL) was added and the precipitate was collected by filtration, and washed with water (40 mL) and acetone (40 mL) to give **273** as an off-white powder (8.0 g, 87 %).

mp 136 ^{o}C; ν_{max}/cm^{-1} 1376 (S=O); δ_H (400 MHz, DMSO-d_6) 8.65 - 8.76 (1 H, m, *Ar*), 8.48 - 8.56 (1 H, m, *Ar*), 8.25 (1 H, s, *Ar*), 7.85 (2 H, d, *J*=8.0 Hz, SC*H*CH), 7.66 - 7.77 (1 H, m, *Ar*), 7.47 (2 H, d, *J*=8.0 Hz, SCHC*H*), 2.45 (3 H, s, CH_3); δ_C (100 MHz, DMSO-d_6) 152.5, 150.5, 148.3, 146.3, 142.3, 136.1, 135.2, 133.6, 130.6, 130.1, 129.4, 127.1, 124.5, 94.5, 22.1 (*C*H$_3$); *m/z* (ESI$^-$) 457 ([M-H]$^-$); HRMS (ESI$^+$) $C_{16}H_{11}ClINNaO_3S$, ([M+Na]$^+$) requires 481.9085; found 481.9074.

N-((5-Chloro-8-hydroxyquinolin-7-yl)(2,3-dihydrobenzo[b][1,4]dioxin-6-yl)methyl)benzamide **274**

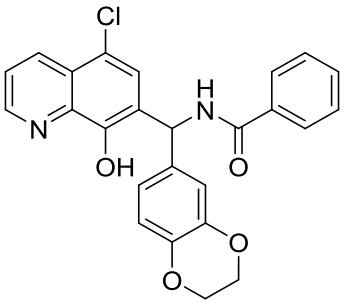

Following general procedure 1, 5-chloro-8-hydroxyquinoline (359 mg, 2.0 mmol), benzamide (242 mg, 2.0 mmol) and 1,4-benzodioxan-6-carboxaldehyde (657 mg, 4.0 mmol) gave **274** (549 mg, 63 %) as a white powder.

mp 226 ^{o}C; ν_{max}/cm^{-1} 3282 (NH), 1631 (C=O); δ_H (400 MHz, DMSO-d_6) 10.40 (1 H, br. s., N*H*), 9.08 - 9.25 (1 H, m, quinoline-*Ar*), 8.84 - 9.04 (1 H, m, quinoline-*Ar*), 8.34 - 8.59 (1 H, m, quinoline-*Ar*), 7.82 - 8.04 (3 H, m, *Ar*), 7.64 - 7.78 (1 H, m, *Ar*), 7.39 - 7.60 (3 H, m, *Ar*), 6.90 (1 H, d, *J*=8.5 Hz, benzyl-*H*), 6.72 - 6.86 (3 H, m, *Ar*), 4.19

(4 H, s, CH_2); δ_C (100 MHz, DMSO-d_6) 166.8 (*C*=O), 150.2, 150.0, 144.0, 143.3, 139.5, 135.6, 135.1, 133.4, 132.2, 129.1, 128.4, 127.5, 126.1, 125.7, 123.8, 120.9, 119.4, 117.8, 116.6, 64.9 (*C*H_2), 50.4 (benzyl-*C*); *m*/*z* (ESI$^-$) 445 ([M+H]$^-$); HRMS (ESI$^+$) $C_{25}H_{19}ClIN_2NaO_4$, ([M+Na]$^+$) requires 469.0926; found 469.0917.

(*E*)-*N*-(1-(5-Chloro-8-hydroxyquinolin-7-yl)-3-phenylallyl)benzamide 275

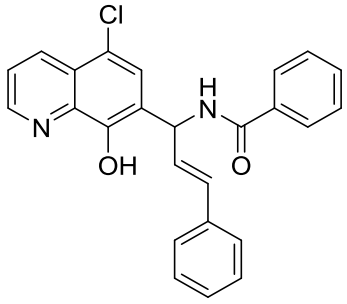

Following general procedure 1, 5-chloro-8-hydroxyquinoline (359 mg, 2.0 mmol), benzamide (242 mg, 2.0 mmol) and *trans*-cinnamaldehyde (504 µL, 4.0 mmol) gave **275** (545 mg, 67 %) as a white powder.

mp 227 °C; ν_{max}/cm^{-1} 3290 (NH), 1630 (C=O); δ_H (400 MHz, DMSO-d_6) 10.40 (1 H, br. s., N*H*), 9.07 - 9.25 (1 H, m, quinoline-*Ar*), 8.89 - 9.02 (1 H, m, quinoline-*Ar*), 8.37 - 8.56 (1 H, m, quinoline-*Ar*), 7.92 - 8.00 (2 H, m, *Ar*), 7.90 (1 H, s, *Ar*), 7.67 - 7.75 (1 H, m, *Ar*), 7.52 - 7.59 (1 H, m, *Ar*), 7.46 - 7.52 (2 H, m, *Ar*), 7.40 - 7.45 (2 H, m, *Ar*), 7.26 - 7.34 (2 H, m, *Ar*), 7.17 - 7.25 (1 H, m, *Ar*), 6.54 - 6.60 (2 H, m, *Ar*), 6.45 - 6.51 (1 H, m, benzyl-*H*); δ_C (100 MHz, DMSO-d_6) 166.5 (*C*=O), 150.3, 150.0, 139.6, 137.2, 135.1, 133.4, 132.2, 130.9, 130.0, 129.5, 129.2, 128.5, 128.4, 127.2, 125.8, 125.7, 123.8, 119.4, 50.0 (benzyl-*C*); *m*/*z* (ESI$^+$) 437 ([M+Na]$^+$); HRMS (ESI$^+$) $C_{25}H_{19}ClN_2NaO_2$, ([M+Na]$^+$) requires 437.1027; found 437.1019.

4-Bromoquinolin-8-yl 4-methylbenzenesulfonate 276

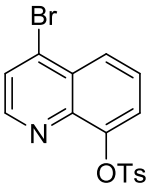

124 (3.07 g, 9.7 mmol) was added portionwise to a stirring solution of phosphorus oxybromide (8.39 g, 29.2 mmol) in $CHCl_3$ (15 mL). The mixture was heated under reflux for 4 h and poured into an ice/water slurry to decompose the excess phosphorus oxybromide. The $CHCl_3$ layer was separated and the aqueous layer adjusted to pH 6-7 with ammonium hydroxide and extracted with additional $CHCl_3$. The combined organic

layers were washed with water and brine. The solvent was evaporated under reduced pressure to give **276** (2.53 g, 69 %) as a brown solid.

mp 138 °C; δ_H (400 MHz, $CDCl_3$) 8.47 - 8.66 (1 H, m, *Ar*), 7.97 - 8.26 (1 H, m, *Ar*), 7.78 - 7.92 (2 H, m, *Ar*), 7.46 - 7.74 (3 H, m, *Ar*), 7.07 - 7.35 (2 H, m, *Ar*), 2.41 (3 H, s, CH_3); δ_C (100 MHz, DMSO-d_6)150.1, 145.5, 145.2, 142.5, 133.8, 133.0, 129.5, 129.2, 128.7, 127.1, 126.0, 125.9, 123.3, 21.7 (*C*H_3); *m*/*z* (ESI^+) 378 ($[M+H]^+$); HRMS (ESI^+) $C_{16}H_{13}BrNO_3S$, ($[M+H]^+$) requires 377.9794; found 377.9786.

N-((5-Chloro-8-hydroxyquinolin-7-yl)(6-(thiophen-2-yl)pyridin-2-yl)methyl)benzamide **277**

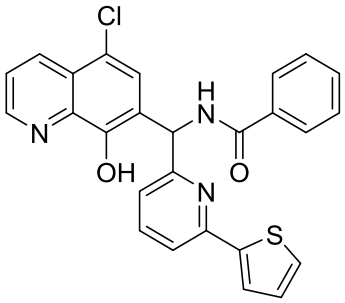

Following general procedure 1, 5-chloro-8-hydroxyquinoline (359 mg, 2.0 mmol), benzamide (242 mg, 2.0 mmol) and 6-(2-thienyl)-2-pyridinecarboxaldehyde (757 mg, 4.0 mmol) gave **277** (494 mg, 52 %) as an off-white powder.

mp 218 °C; ν_{max}/cm^{-1} 3294 (NH), 1650 (amide C=O); δ_H (400 MHz, DMSO-d_6) 10.50 (1 H, br. s., N*H*), 9.22 - 9.36 (1 H, m, quinoline-*Ar*), 9.06 - 9.16 (1 H, m, quinoline-*Ar*), 8.92 - 9.02 (1 H, m, quinoline-*Ar*), 8.40 - 8.56 (1 H, m, quinoline-*Ar*), 7.91 - 8.00 (2 H, m, *Ar*), 7.88 (1 H, m, *Ar*), 7.77 - 7.85 (2 H, m, *Ar*), 7.68 - 7.75 (1 H, m, *Ar*), 7.47 - 7.67 (2 H, m, *Ar*), 7.24 - 7.32 (1 H, m, *Ar*), 7.09 - 7.21 (2 H, m, *Ar*), 6.93 - 7.04 (1 H, m, *Ar*); δ_C (100 MHz, DMSO-d_6) 160.2 (*C*=O), 158.6, 152.1, 150.8, 150.0, 145.2, 145.1, 139.6, 139.1, 138.9, 135.1, 134.7, 133.4, 132.5, 132.3, 129.5, 129.3, 128.3, 126.4, 125.9, 123.9, 121.2, 119.2, 52.7 (benzyl-*C*); *m*/*z* (EI^+) 471 ($[M]^+$); HRMS (EI^+) $C_{26}H_{18}N_3O_2SCl$, ($[M]^+$) requires 471..0808; found 471.0800.

N-((5-Chloro-8-hydroxyquinolin-7-yl)(6-(thiophen-3-yl)pyridin-2-yl)methyl)benzamide **278**

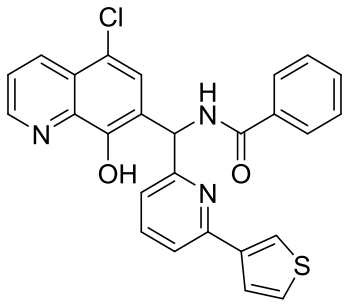

Following general procedure 1, 5-chloro-8-hydroxyquinoline (359 mg, 2.0 mmol), benzamide (242 mg, 2.0 mmol) and 6-(3-thienyl)pyridine-2-carboxaldehyde (757 mg, 4.0 mmol) gave **278** (508 mg, 54 %) as an off-white powder.

mp 230 °C; ν_{max}/cm^{-1} 3299 (NH), 1634 (C=O); δ_H (400 MHz, DMSO-d_6) 10.60 (1 H, br. s., N*H*), 9.49 - 9.59 (1 H, m, quinoline-*Ar*), 8.89 - 9.10 (1 H, m, quinoline-*Ar*), 8.44 - 8.55 (1 H, m, quinoline-*Ar*), 8.03 (1 H, s, *Ar*), 7.92 - 8.00 (2 H, m, *Ar*), 7.71 - 7.77 (1 H, m, *Ar*), 7.54 - 7.61 (3 H, m, *Ar*), 7.47 - 7.53 (2 H, m, *Ar*), 7.31 - 7.39 (2 H, m, *Ar*), 7.24 - 7.30 (1 H, m, *Ar*), 7.21 (1 H, d, *J*=8.5 Hz, benzyl-*H*), 6.78 - 6.86 (1 H, m, *Ar*); δ_C (100 MHz, DMSO-d_6) 166.8 (*C*=O), 150.4, 150.1, 146.0, 143.4, 139.6, 134.8, 134.5, 133.5, 132.4, 130.0, 129.2, 128.5, 128.4, 127.4, 127.3, 126.1, 126.0, 125.2, 124.2, 124.1, 119.6, 47.2 (benzyl-*C*); *m/z* (EI$^+$) 471 ([M]$^+$); HRMS (EI$^+$) $C_{26}H_{18}ClN_3O_2S$, ([M]$^+$) requires 471.0808; found 471.0811.

N-((5-Chloro-8-hydroxyquinolin-7-yl)(5-phenylisoxazol-3-yl)methyl)benzamide **279**

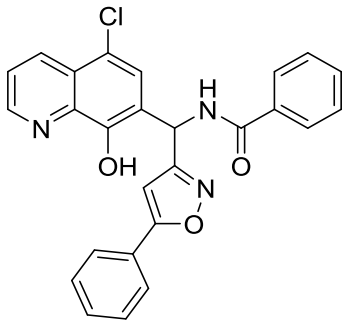

Following general procedure 1, 5-chloro-8-hydroxyquinoline (359 mg, 2.0 mmol), benzamide (242 mg, 2.0 mmol) and 5-phenylisoxazole-3-carboxaldehyde (693 mg, 4.0 mmol) gave **279** (473 mg, 52 %) as a white powder.

mp 235 °C; ν_{max}/cm^{-1} 3278 (NH), 1652 (C=O); δ_H (400 MHz, DMSO-d_6) 10.62 (1 H, br. s., N*H*), 9.47 - 9.59 (1 H, m, quinoline-*Ar*), 9.24 - 9.32 (1 H, m, quinoline-*Ar*), 8.96 - 9.03 (1 H, m, quinoline-*Ar*), 8.45 - 8.56 (1 H, m, *Ar*), 7.92 - 7.99 (2 H, m, *Ar*), 7.82 - 7.89 (2 H, m, *Ar*), 7.71 - 7.80 (1 H, m, *Ar*), 7.54 - 7.61 (1 H, m, *Ar*), 7.46 - 7.54 (5 H, m, *Ar*), 7.12 (1 H, d, *J*=8.5 Hz, benzyl-*H*), 7.07 (1 H, s, *Ar*); δ_C (100 MHz, DMSO-d_6) 170.1 (*C*=O), 166.9, 166.7, 165.7, 150.8, 150.1, 139.6, 134.7, 132.6, 131.3, 130.1, 129.2, 128.6, 128.5, 127.5, 126.5, 126.2, 124.1, 123.2, 119.5, 100.5, 45.0 (benzyl-*C*); *m/z* (ESI$^-$) 454 ([M-H]$^-$); HRMS (ESI$^+$) $C_{26}H_{18}ClN_3NaO_3$, ([M+Na]$^+$) requires 478.0929; found 478.0924.

N-((5-Chloro-8-hydroxyquinolin-7-yl)(4-phenylthiophen-2-yl)methyl)benzamide **280**

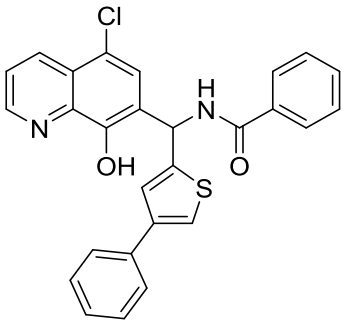

Following general procedure 1, 5-chloro-8-hydroxyquinoline (359 mg, 2.0 mmol), benzamide (242 mg, 2.0 mmol) and 4-phenylthiophene-2-carboxaldehyde (753 mg, 4.0 mmol) gave **280** (481 mg, 51 %) as an off-white powder.

mp 237 °C; ν_{max}/cm^{-1} 3271 (NH), 1638 (C=O); δ_H (400 MHz, DMSO-d_6) 10.59 (1 H, br. s., N*H*), 9.42 - 9.62 (1 H, m, quinoline-*Ar*), 8.89 - 9.08 (1 H, m, quinoline-*Ar*), 8.39 - 8.55 (1 H, m, quinoline-*Ar*), 8.03 (1 H, s, *Ar*), 7.93 - 8.00 (2 H, m, *Ar*), 7.70 - 7.80 (2 H, m, *Ar*), 7.58 - 7.64 (2 H, m, *Ar*), 7.54 - 7.57 (1 H, m, *Ar*), 7.47 - 7.53 (2 H, m, *Ar*), 7.32 - 7.38 (2 H, m, *Ar*), 7.29 (1 H, s, *Ar*), 7.18 - 7.27 (2 H, m, *Ar*); δ_C (100 MHz, DMSO-d_6) 166.7 (*C*=O), 150.4, 150.1, 147.6, 141.8, 139.6, 135.9, 134.8, 133.4, 132.4, 129.7, 129.2, 128.5, 128.0, 127.2, 126.7, 126.1, 125.5, 124.8, 124.0, 121.0, 119.6, 47.3 (benzyl-*C*); *m/z* (EI$^+$) 470 ([M]$^+$); HRMS (EI$^+$) $C_{27}H_{19}ClN_2O_2S$, ([M]$^+$) requires 470.0856; found 470.0863.

N-((5-Chloro-8-hydroxyquinolin-7-yl)(5-phenylthiophen-2-yl)methyl)benzamide **281**

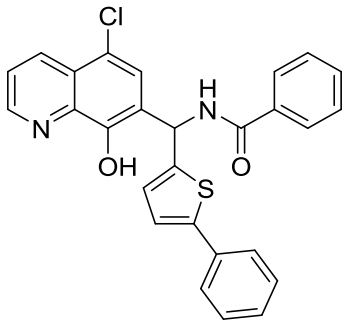

Following general procedure 1, 5-chloro-8-hydroxyquinoline (359 mg, 2.0 mmol), benzamide (242 mg, 2.0 mmol) and 5-phenylthiophene-2-carboxaldehyde (753 mg, 4.0 mmol) gave **281** (702 mg, 75 %) as a white powder.

mp 241 °C; ν_{max}/cm^{-1} 3284 (NH), 1636 (C=O); δ_H (400 MHz, DMSO-d_6) 10.60 (1 H, br. s., N*H*), 9.42 - 9.64 (1 H, m, quinoline-*Ar*), 8.84 - 9.12 (1 H, m, quinoline-*Ar*), 8.39 - 8.58 (1 H, m, quinoline-*Ar*), 8.04 (1 H, s, *Ar*), 7.92 - 8.01 (2 H, m, *Ar*), 7.70 - 7.80 (1 H, m, *Ar*), 7.54 - 7.61 (3 H, m, *Ar*), 7.45 - 7.53 (2 H, m, *Ar*), 7.30 - 7.42 (3 H, m, *Ar*), 7.14 - 7.29 (2 H, m, *Ar*), 6.76 - 6.86 (1 H, m, *Ar*); δ_C (100 MHz, DMSO-d_6) 166.7 (*C*=O), 150.4, 150.1, 146.0, 143.4, 139.6, 134.8, 134.5, 133.4, 132.4, 129.9, 129.2, 128.5, 128.4, 127.4, 127.3, 126.1, 126.0, 125.2, 124.2, 124.0, 119.6, 47.2 (benzyl-*C*); *m/z* (ESI$^+$) 471 ([M+H]$^+$); HRMS (ESI$^+$) $C_{27}H_{19}ClN_2NaO_2S$, ([M+Na]$^+$) requires 493.0748; found 493.0740.

N-((5-Chloro-8-hydroxyquinolin-7-yl)(5-phenylfuran-2-yl)methyl)benzamide **282**

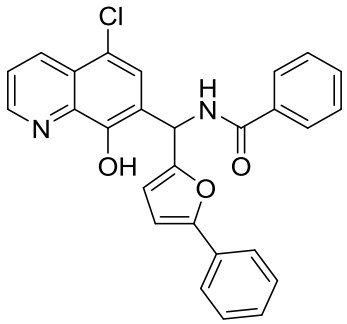

Following general procedure 1, 5-chloro-8-hydroxyquinoline (359 mg, 2.0 mmol), benzamide (242 mg, 2.0 mmol) and 5-phenyl-2-furaldehyde (689 mg, 4.0 mmol) gave **282** (508 mg, 56 %) as a white powder.

mp 238 °C; ν_{max}/cm^{-1} 3290 (NH), 1635 (C=O); δ_H (400 MHz, DMSO-d_6) 10.56 (1 H, br. s., N*H*), 9.39 - 9.53 (1 H, m, quinoline-*Ar*), 8.93 - 9.02 (1 H, m, quinoline-*Ar*), 8.43 - 8.55 (1 H, m, quinoline-*Ar*), 7.91 - 8.01 (3 H, m, *Ar*),

7.69 - 7.78 (1 H, m, *Ar*), 7.61 - 7.68 (2 H, m, *Ar*), 7.53 - 7.59 (1 H, m, *Ar*), 7.45 - 7.52 (2 H, m, *Ar*), 7.33 - 7.43 (2 H, m, *Ar*), 7.19 - 7.30 (1 H, m, *Ar*), 7.07 (1 H, d, *J*=8.5 Hz, benzyl-*H*), 6.83 - 6.92 (1 H, m, *Ar*); δ_C (100 MHz, DMSO-d_6) 166.8 (*C*=O), 154.3, 153.5, 150.7, 150.1, 139.5, 134.9, 133.4, 132.4, 131.1, 129.7, 129.2, 128.5, 128.3, 127.4, 126.1, 124.1, 124.0, 123.6, 119.4, 110.8, 107.4, 45.9 (benzyl-*C*); *m/z* (ESI^+) 455 ($[M+H]^+$); HRMS (ESI^+) $C_{27}H_{19}ClN_2NaO_3$, ($[M+Na]^+$) requires 477.0976; found 477.0961.

N-((5-Chloro-8-hydroxyquinolin-7-yl)(6-(3-nitrophenyl)pyridin-2-yl)methyl)benzamide **283**

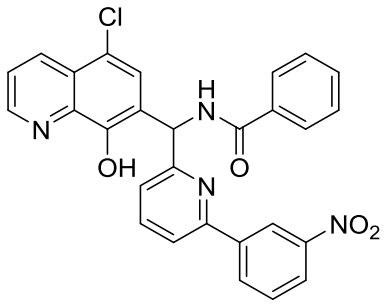

Following general procedure 1, 5-chloro-8-hydroxyquinoline (359 mg, 2.0 mmol), benzamide (242 mg, 2.0 mmol) and 6-(3-nitrophenyl)-2-pyridinecarboxaldehyde (912 mg, 4.0 mmol) gave **283** (584 mg, 71 %) as a white powder.

mp 243 °C; ν_{max}/cm^{-1} 3274 (NH), 1647 (C=O); δ_H (400 MHz, DMSO-d_6) 10.54 (1 H, br. s., N*H*), 9.39 - 9.50 (1 H, m, quinoline-*Ar*), 9.14 - 9.26 (1 H, m, quinoline-*Ar*), 8.85 - 9.06 (1 H, m, quinoline-*Ar*), 8.50 - 8.62 (1 H, m, quinoline-*Ar*), 8.21 - 8.33 (1 H, m, *Ar*), 7.87 - 8.08 (6 H, m, *Ar*), 7.68 - 7.83 (1 H, m, *Ar*), 7.40 - 7.61 (4 H, m, *Ar*), 7.02 - 7.20 (1 H, m, *Ar*); δ_C (100 MHz, DMSO-d_6) 167.0 (*C*=O), 166.8, 160.7, 159.2, 153.5, 153.4, 150.7, 150.0, 149.3, 140.9, 139.6, 139.5, 135.1, 134.7, 133.6, 132.5, 131.3, 129.7, 128.3, 128.0, 126.0, 123.9, 122.3, 120.9, 119.4, 52.8 (benzyl-*C*); *m/z* (ESI^-) 509 ($[M-H]^-$); HRMS (ESI^-) $C_{28}H_{19}ClN_4NaO_4$, ($[M+H]^+$) requires 533.0987; found 533.0979.

N-((5-Chloro-8-hydroxyquinolin-7-yl)(3',5'-dimethoxy-[1,1'-biphenyl]-3-yl)methyl)benzamide **284**

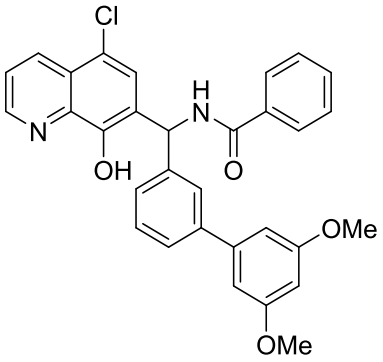

Following general procedure 1, 5-chloro-8-hydroxyquinoline (359 mg, 2.0 mmol), benzamide (242 mg, 2.0 mmol) and **98** (634 mg, 2.6 mmol) gave **284** (513 mg, 49 %) as a white powder.

mp 239 °C; ν_{max}/cm^{-1} 3298 (NH), 1633 (C=O); δ_H (400 MHz, DMSO-d_6) 10.50 (1 H, br. s., N*H*), 9.19 - 9.43 (1 H, m, quinoline-*Ar*), 8.88 - 9.02 (1 H, m, quinoline-*Ar*), 8.31 - 8.62 (1 H, m, quinoline-*Ar*), 7.90 - 8.04 (3 H, m, *Ar*), 7.68 - 7.76 (1 H, m, *Ar*), 7.66 (1 H, s, *Ar*), 7.52 - 7.59 (2 H, m, *Ar*), 7.46 - 7.52 (2 H, m, *Ar*), 7.40 - 7.45 (1 H, m, *Ar*), 7.32 - 7.39 (1 H, m, *Ar*), 7.07 (1 H, d, *J*=9.0 Hz, benzyl-*H*), 6.69 - 6.76 (2 H, m, *Ar*), 6.50 (1 H, s, *Ar*), 3.77 (6 H, s, OC*H*$_3$); δ_C (100 MHz, DMSO-d_6) 167.0 (*C*=O), 161.7 (*C*OCH$_3$),150.4, 150.1, 143.1, 143.1, 141.1, 139.6, 135.2, 133.4, 132.3, 129.9, 129.2, 129.1, 128.5, 127.5, 127.4, 126.5, 126.0, 125.8, 123.9, 119.5, 105.8, 100.0, 56.1 (O*C*H$_3$), 51.2 (benzyl-*C*); *m/z* (EI$^+$) 524 ([M]$^+$); HRMS (EI$^+$) $C_{31}H_{25}ClN_2O_4$, ([M]$^+$) requires 524.1503; found 524.1511.

N-((5-Chloro-8-hydroxyquinolin-7-yl)(3'-methoxy-[1,1'-biphenyl]-3-yl)methyl)benzamide **285**

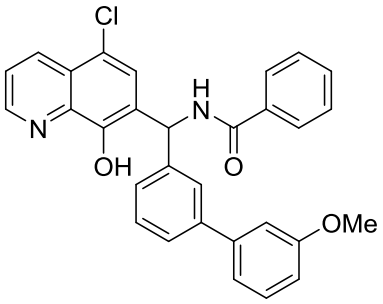

Following general procedure 1, 5-chloro-8-hydroxyquinoline (359 mg, 2.0 mmol), benzamide (242 mg, 2.0 mmol) and **99** (770 mg, 3.6 mmol) gave **285** (497 mg, 50 %) as a white powder.

mp 208 °C; ν_{max}/cm^{-1} 3297 (NH), 1633 (C=O); δ_H (400 MHz, DMSO-d_6) 10.49 (1 H, br. s., N*H*), 9.22 - 9.45 (1 H, m, quinoline-*Ar*), 8.81 - 9.05 (1 H, m, quinoline-*Ar*), 8.31 - 8.54 (1 H, m, quinoline-*Ar*), 7.88 - 7.99 (3 H, m, *Ar*), 7.64 - 7.75 (2 H, m, *Ar*), 7.52 - 7.58 (2 H, m, *Ar*), 7.46 - 7.52 (2 H, m, *Ar*), 7.40 - 7.46 (1 H, m, *Ar*), 7.30 - 7.39 (2 H, m, *Ar*), 7.02 - 7.21 (3 H, m, *Ar*), 6.87 - 6.96 (1 H, m, *Ar*), 3.78 (3 H, s, OC*H*$_3$); δ_C (100 MHz, DMSO-d_6) 167.0 (*C*=O), 160.5 (*C*OCH$_3$),150.4, 150.1, 143.2, 142.5, 141.1, 139.6, 135.2, 133.4, 132.3, 130.9, 129.9, 129.2, 128.5, 127.4, 126.4, 126.0, 125.8, 123.9, 119.9, 119.5, 113.8, 113.2, 55.9 (O*C*H$_3$), 51.2 (benzyl-*C*); *m/z* (EI$^+$) 494 ([M]$^+$); HRMS (EI$^+$) $C_{30}H_{23}ClN_2O_3$, ([M]$^+$) requires 494.1397; found 494.1396.

N-((5-Chloro-8-hydroxyquinolin-7-yl)(3,4-dihydroxyphenyl)methyl)benzamide **286**

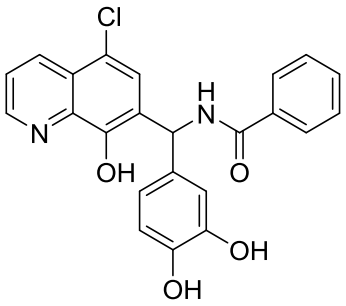

To a solution of **222** (250 mg, 0.5 mmol) in CH_2Cl_2 (2 mL) at 0 °C was added a 1M solution of boron tribromide in CH_2Cl_2 (3 mL, 3 mmol). The reaction mixture was stirred for 30 min at 0 °C, allowed to warm to room temperature, and then stirred at room temperature for 24 h. The reaction mixture was quenched with MeOH (10 mL) and neutralised with a 1M aqueous solution of NaOH. The precipitate was collected by filtration and dried under vacuum to give **286** as an off-white powder (210 mg, 100 %).

mp decomposition > 220 °C; ν_{max}/cm^{-1} 3294 (NH), 1634 (C=O); δ_H (400 MHz, DMSO-d_6) 10.20 (1 H, br. s., N*H*), 9.04 - 9.10 (1 H, m, quinoline-*Ar*), 8.91 - 8.96 (1 H, m, quinoline-*Ar*), 8.43 - 8.49 (1 H, m, quinoline-*Ar*), 7.88 - 7.95 (3 H, m, *Ar*), 7.67 - 7.72 (1 H, m, *Ar*), 7.50 - 7.56 (1 H, m, *Ar*), 7.42 - 7.49 (2 H, m, *Ar*), 6.83 (1 H, d, *J*=8.5 Hz, benzyl-*H*), 6.50 - 6.56 (1 H, m, *Ar*), 6.41 - 6.46 (1 H, m, *Ar*), 6.36 - 6.41 (1 H, m, *Ar*); δ_C (100 MHz, DMSO-d_6) 166.6 (*C*=O), 152.5, 151.1, 149.9, 149.9, 139.5, 135.4, 133.3, 132.0, 131.4, 129.1, 128.4, 127.8, 127.3, 125.5, 123.6, 119.1, 117.1, 107.9, 107.6, 51.1 (benzyl-*C*); *m/z* (ESI$^-$) 419 ([M-H]$^-$); HRMS (FI$^+$) $C_{23}H_{17}ClIN_2O_4$, ([M]$^+$) requires 420.0877; found 420.0883.

N-((5-Chloro-8-hydroxyquinolin-7-yl)(3',5'-dihydroxy-[1,1'-biphenyl]-3-yl)methyl)benzamide **287**

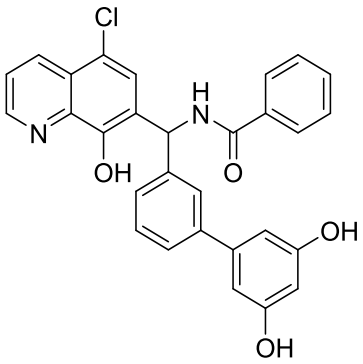

To a solution of **284** (200 mg, 0.38 mmol) in CH_2Cl_2 (8 mL) at 0 °C was added a 1M solution of boron tribromide in CH_2Cl_2 (2.3 mL, 2.3 mmol). The reaction mixture was stirred for 30 min at 0 °C, allowed to warm to room temperature, and then stirred at room temperature for 24 h. The reaction mixture was quenched with MeOH (10 mL) and neutralised with a 1M aqueous solution of NaOH. The solvent was removed under reduced pressure and the residue redissolved in CH_2Cl_2. The organic layer was washed with water, brine, and subsequently dried over anhydrous Na_2SO_4. Purification by flash column chromatography using CH_2Cl_2/MeOH (90:10) gave **287** (143 mg, 76 %) as an orange powder.

mp decomposition > 230 °C; ν_{max}/cm^{-1} 3206 (OH), 1597 (C=O); δ_H (400 MHz, DMSO-d_6) 9.16 - 9.50 (1 H, m, quinoline-*Ar*), 8.83 - 9.14 (1 H, m, quinoline-*Ar*), 8.41 - 8.67 (1 H, m, quinoline-*Ar*), 7.95 (3 H, s, *Ar*), 7.70 - 7.82 (1 H, m, *Ar*), 7.51 - 7.58 (1 H, m, *Ar*), 7.44 - 7.51 (2 H, m, *Ar*), 7.35 - 7.42 (1 H, m, *Ar*), 7.30 - 7.35 (2 H, m, *Ar*), 7.20 - 7.26 (1 H, m, *Ar*), 7.08 (1 H, d, *J*=8.5 Hz, benzyl-*H*), 6.43 - 6.48 (1 H, m, *Ar*), 6.16 - 6.24 (1 H, m, *Ar*); δ_C (100 MHz, DMSO-d_6) 167.0 (*C*=O), 1157.9 (*C*OH),156.0, 150.0, 149.7, 144.1, 142.1, 142.0, 138.9, 135.0, 134.3, 132.3, 129.2, 129.0, 128.8, 128.5, 128.1, 126.4, 126.0, 124.0, 119.7, 110.0, 103.2, 99.8, 50.8 (benzyl-*C*); A molecular ion could not be identified *via* the mass spectrometry techniques of ESI, EI or FI.

N-((5-Chloro-8-hydroxyquinolin-7-yl)(3'-hydroxy-[1,1'-biphenyl]-3-yl)methyl)benzamide **288**

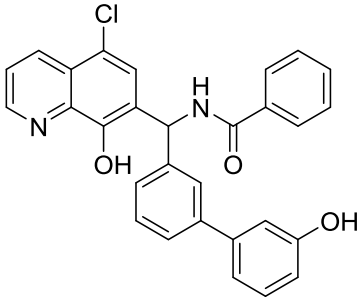

To a solution of **285** (160 mg, 0.31 mmol) in CH_2Cl_2 (10 mL) at 0 °C was added a 1M solution of boron tribromide in CH_2Cl_2 (0.97 mL, 0.97 mmol). The reaction mixture was stirred for 30 min at 0 °C, allowed to warm to room temperature, and then stirred at room temperature for 24 h. The reaction mixture was quenched with MeOH (10 mL) and neutralised with a 1M aqueous solution of NaOH. The solvent was removed under reduced pressure and the residue redissolved in CH_2Cl_2. The organic layer was washed with water, brine, and subsequently dried over anhydrous Na_2SO_4. Purification by flash column chromatography using CH_2Cl_2/MeOH (90:10) gave **288** (84 mg, 55 %) as a yellow powder.

mp decomposition > 180 °C; ν_{max}/cm^{-1} 3206 (NH), 1596 (C=O); δ_H (400 MHz, DMSO-d_6) 9.26 - 9.42 (1 H, m, quinoline-*Ar*), 8.88 - 9.07 (1 H, m, quinoline-*Ar*), 8.46 - 8.64 (1 H, m, quinoline-*Ar*), 7.87 - 8.02 (3 H, m, *Ar*), 7.70 - 7.83 (1 H, m, *Ar*), 7.46 - 7.63 (5 H, m, *Ar*), 7.38 - 7.45 (1 H, m, *Ar*), 7.30 - 7.36 (1 H, m, *Ar*), 7.18 - 7.27 (1 H, m, *Ar*), 7.08 (1 H, d, *J*=8.5 Hz, benzyl-*H*) 6.92 - 7.02 (2 H, m, *Ar*), 6.67 - 6.81 (1 H, m, *Ar*); δ_C (100 MHz, DMSO-d_6) 167.0 (*C*=O), 158.7, 149.8, 149.7, 142.9, 142.4, 141.4, 138.8, 135.1, 134.4, 132.3, 130.8, 129.9, 129.2, 128.5, 127.7, 127.2, 126.7, 126.3, 126.2, 126.0, 124.0, 119.8, 118.3, 115.4, 114.3, 51.1 (benzyl-*C*); *m*/*z* (FI$^+$) 496 ([M]$^+$); HRMS (FI$^+$) $C_{29}H_{21}ClN_2O_4$, ([M]$^+$) requires 496.1190; found 496.1186.

N-((5-Chloro-8-hydroxyquinolin-7-yl)(3-phenylisoxazol-5-yl)methyl)benzamide 289

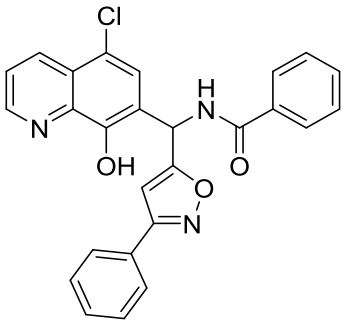

Following general procedure 1, 5-chloro-8-hydroxyquinoline (359 mg, 2.0 mmol), benzamide (242 mg, 2.0 mmol) and 3-phenylisoxazole-5-carboxaldehyde (693 mg, 4.0 mmol) gave **289** (450 mg, 49 %) as a white powder.

mp 260 °C; ν_{max}/cm^{-1} 3290 (NH), 1644 (C=O); δ_H (400 MHz, DMSO-d_6) 10.75 (1 H, br. s., N*H*), 9.53 - 9.76 (1 H, m, quinoline-*Ar*), 8.90 - 9.10 (1 H, m, quinoline-*Ar*), 8.44 - 8.60 (1 H, m, quinoline-*Ar*), 7.95 - 8.02 (2 H, m, *Ar*), 7.93 (1 H, s, *Ar*), 7.83 - 7.91 (2 H, m, *Ar*), 7.73 - 7.80 (1 H, m, *Ar*), 7.55 - 7.64 (1 H, m, *Ar*), 7.42 - 7.54 (5 H, m,

Ar), 7.13 - 7.23 (1 H, m, *Ar*), 6.94 (1 H, s, *Ar*); δ_C (100 MHz, DMSO-d_6) 173.0 (*C*=N), 167.0 (*C*=O),162.8, 151.0, 150.2, 139.6, 134.4, 133.5, 132.6, 131.1, 129.9, 129.2, 128.6, 127.5, 127.1, 126.5, 124.2, 122.1, 119.7, 102.1, 45.0 (benzyl-*C*); *m/z* (EI^+) 455 ($[M]^+$); HRMS (EI^+) $C_{26}H_{18}ClN_3O_3$, ($[M]^+$) requires 455.1037; found 455.0306.

N-([1,1'-Biphenyl]-3-yl(8-hydroxy-5-nitroquinolin-7-yl)methyl)benzamide **290**

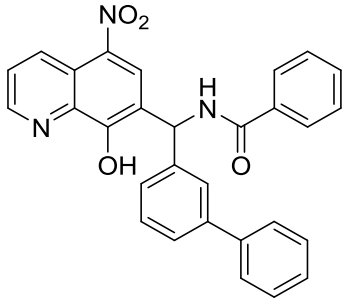

Following general procedure 1, 5-chloro-8-hydroxyquinoline (359 mg, 2.0 mmol), benzamide (242 mg, 2.0 mmol) and biphenyl-3-carboxaldehyde (651 µL, 4.0 mmol) gave **290** (666 mg, 70 %) as a yellow powder.

mp 213 °C; v_{max}/cm^{-1} 3283 (NH), 1633 (C=O); δ_H (400 MHz, DMSO-d_6) 9.40 - 9.62 (1 H, m, quinoline-*Ar*), 9.11 - 9.29 (1 H, m, quinoline-*Ar*), 8.93 - 9.07 (1 H, m, quinoline-*Ar*), 8.88 (1 H, s, quinoline-*Ar*), 7.92 - 8.03 (2 H, m, *Ar*), 7.84 - 7.91 (1 H, m, *Ar*), 7.72 (1 H, s, *Ar*), 7.53 - 7.65 (4 H, m, *Ar*), 7.38 - 7.52 (6 H, m, *Ar*), 7.28 - 7.37 (1 H, m, *Ar*), 7.07 (1 H, d, *J*=8.5 Hz, benzyl-*H*); δ_C (100 MHz, DMSO-d_6) 167.0 (*C*=O),158.7, 149.8, 142.5, 141.4, 140.9, 137.7, 135.1, 135.0, 134.0, 132.3, 130.0, 129.8, 129.2, 128.9, 128.5, 128.4, 127.6, 127.5, 126.6, 126.1, 124.7, 122.6, 51.3 (benzyl-*C*); *m/z* (ESI^+) 476 ($[M+H]^+$); HRMS (ESI^+) $C_{29}H_{21}N_3NaO_4$, ($[M+Na]^+$) requires 498.1424; found 498.1440.

tert-Butyl (8-hydroxyquinolin-5-yl)carbamate **291**

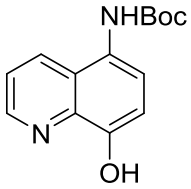

Di-*tert*-butyl dicarbonate (2.4 g, 11 mmol) was added portionwise to a stirring solution of 5-amino-8-hydroxyquinoline dichloride (2.3 g, 10 mmol) and diisopropylethylamine (5.2 mL, 30 mmol) in MeOH (20 mL) at room remperature. Stirring was continued overnight. The white precipitate formed was collected by

filtration, washed with MeOH and water, and dried under reduced pressure to give **291** (1.74 g, 67 %) as a white powder.

mp 188 °C; ν_{max}/cm^{-1} 3229 (NH) 1680 (Boc C=O); δ_H (400 MHz, DMSO-d_6) 9.71 (1 H, s, *Ar*), 9.02 (1 H, br. s., N*H*), 8.75 - 8.90 (1 H, m, *Ar*), 8.19 - 8.40 (1 H, m, *Ar*), 7.48 - 7.65 (1 H, m, *Ar*), 7.20 - 7.44 (1 H, m, *Ar*), 6.90 - 7.15 (1 H, m, *Ar*), 1.46 (9 H, s, C(C*H*$_3$)$_3$); δ_C (100 MHz, DMSO-d_6) 155.4 (*C*=O), 151.9, 148.8, 139.1, 132.9, 125.5, 124.8, 122.3, 111.3, 79.6 (*C*(CH$_3$)$_3$), 29.0 (C(*C*H$_3$)$_3$); *m/z* (ESI$^-$) 259 ([M-H]$^-$); HRMS (ESI$^+$) $C_{14}H_{16}N_2NaO_3$, ([M+Na]$^+$) requires 283.1053; found 283.1053.

tert-Butyl (3-bromophenyl)carbamate **292**

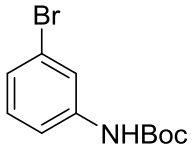

Di-*tert*-butyl dicarbonate (2.18 g, 10 mmol) was added portionwise to a stirring solution of 3-bromoaniline (1088 µL, 10 mmol) in CH_2Cl_2 at room temperature. After 18 h the reaction mixture was poured into ice-cold water and extracted with CH_2Cl_2. The organic layer was washed with brine and dried over anhydrous $MgSO_4$. The solvent was removed under reduced pressure to give **292** (2.72g, 100 %) as a light-pink solid.

mp 78 °C; δ_H (400 MHz, DMSO-d_6) 9.56 (1 H, s, N*H*), 7.76 (1 H, s, *Ar*), 7.35 - 7.41 (1 H, m, *Ar*), 7.16 - 7.23 (1 H, m, *Ar*), 7.10 - 7.15 (1 H, m, *Ar*), 1.47 (9 H, s, C(C*H*$_3$)$_3$); δ_C (100 MHz, DMSO-d_6) 153.4 (*C*=O), 142.1, 131.5, 125.4, 121.1, 117.7, 80.4 (*C*(CH$_3$)$_3$), 28.9 (C(*C*H$_3$)$_3$); *m/z* (ESI$^-$) 270 ([M-H]$^-$).

tert-Butyl (3'-formyl-[1,1'-biphenyl]-3-yl)carbamate **293**

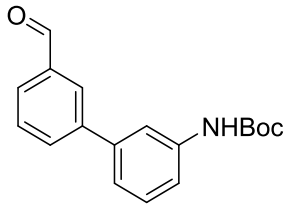

3-Formylphenylboronic acid (900 mg, 6 mmol), **292** (1.36 g, 5 mmol), tetrakis(triphenylphosphine)palladium (0) (171 mg, 1.5 µmol) were mixed in dimethoxyethane (10 mL) inside a sealed vial. A 2 M aqueous solution of sodium carbonate (5 mL) was added, and the vial was purged with N_2 three times. The mixture was stirred

at 100 °C for 2.5 h under microwave irradiation. The reaction mixture was cooled to room temperature and diluted with EtOAc (200 mL). The organic layer was washed with water, a saturated aqueous solution of NH_4Cl, brine, and dried over anhydrous $MgSO_4$. The solvent was removed under reduced pressure. The residue was subjected to flash column chromatography on silica gel using EtOAc/Cyclohexane (20:80) as eluent to give **293** (892 mg, 60 %) as a clear oil.

mp 78 °C; ν_{max}/cm^{-1} 3339 (NH), 1693 (C=O); δ_H (400 MHz, $CDCl_3$) 10.09 (1 H, s, C*H*O), 8.09 (1 H, s, *Ar*), 7.82 - 7.91 (2 H, m, *Ar*), 7.75 (1 H, s, *Ar*), 7.54 - 7.64 (1 H, m, *Ar*), 7.35 - 7.42 (1 H, m, *Ar*), 7.24 - 7.35 (2 H, m, *Ar*), 6.66 (1 H, br. s., N*H*), 1.54 (9 H, s, C(C*H*$_3$)$_3$); δ_C (100 MHz, $CDCl_3$) 192.3 (*C*HO), 152.7, 141.9, 140.6, 139.1, 136.8, 133.2, 129.6, 129.4, 128.6, 128.4, 121.8, 118.0, 117.2, 80.7 (*C*(CH$_3$)$_3$), 28.3 (C(*C*H$_3$)$_3$); *m/z* (ESI$^-$) 296 ([M-H]$^-$); HRMS (ESI$^+$) $C_{18}H_{19}NNaO_3$, ([M+Na]$^+$) requires 320.1257; found 320.1245.

5-Chloro-7-iodoquinolin-8-yl methanesulfonate 294

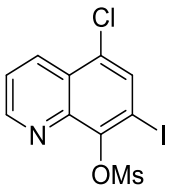

Methanesulfonyl chloride (1 mL, 13 mmol) was added dropwise to a stirring solution of clioquinol (3.1 g, 10 mmol) and triethylamine (2.1 mL) in CH_2Cl_2 at 0 °C. The reaction mixture was warmed to room temperature and stirred for another 12 h before being washed with water, brine, and dried over anhydrous $MgSO_4$ and concentrated under reduced pressure. The crude product was purified by flash column chromatography using EtOAc/Cyclohexane (30:70) as eluent to give **294** (3.06 g, 80 %) as a light-orange powder.

mp 177 °C; ν_{max}/cm^{-1} 1347 (S=O); δ_H (400 MHz, DMSO-d_6) 8.96 - 9.19 (1 H, m, *Ar*), 8.44 - 8.72 (1 H, m, *Ar*), 8.29 (1 H, s, *Ar*), 7.63 - 8.01 (1 H, m, *Ar*), 3.89 (3 H, s. C*H*$_3$); δ_C (100 MHz, DMSO-d_6) 153.2, 148.3, 142.2, 135.9, 134.1, 130.0, 127.2, 124.7, 95.8, 42.2 (*C*H$_3$); *m/z* (ESI$^+$) 406 ([M+Na]$^+$); HRMS (ESI$^+$) $C_{10}H_7ClINNaO_3S$, ([M+Na]$^+$) requires 405.8772; found 405.8767.

5-Morpholinothiophene-2-carbaldehyde **295**

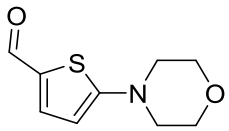

A solution of 5-bromothiophene-2-carboxaldehyde (1.2 mL, 10 mmol) and morpholine (2.6 mL, 30 mmol) in water (10 mL) was heated under reflux overnight. The reaction mixture was cooled to room temperature and extracted with CH_2Cl_2. The organic layer was washed with a saturated aqueous solution of NH_4Cl, brine, and concentrated under reduced pressure. The crude product was purified by flash column chromatography using MeOH/CH_2Cl_2 (5:95) to give **295** (1.22 g, 62 %) as a white powder.

mp 127 °C; ν_{max}/cm^{-1} 1637 (C=O); δ_H (400 MHz, $CDCl_3$) 9.57 (1 H, s, C*H*O), 7.50 (1 H, d, *J*=4.0 Hz, *Ar*), 6.13 (1 H, d, *J*=4.0 Hz, *Ar*), 3.80 - 3.87 (4 H, m, CH_2), 3.27 - 3.35 (4 H, m, CH_2); δ_C (100 MHz, $CDCl_3$) 180.0 (*C*HO), 167.9, 139.7, 128.2, 104.5, 65.9, 49.5; *m*/*z* (ESI$^+$) 199 ([M+H]$^+$); HRMS (ESI$^+$) $C_9H_{12}NO_2S$, ([M+H]$^+$) requires 199.0583; found 199.0587.

5-Chloro-7-iodoquinolin-8-yl trifluoromethanesulfonate **296**

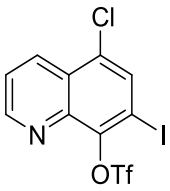

A solution of trifluoromethanesulfonic anhydride (4 mL, 24 mmol) in CH_2Cl_2 (10 mL) was added dropwise to a solution of clioquinol (6.11 g, 20 mmol) and pyridine (3.23 mL, 40 mmol) in CH_2Cl_2 (80 mL) at 0 °C. After complete addition, the mixture was warmed to room temperature and stirred for 1 h. The reaction mixture was then diluted with Et_2O, quenched with 10 % aqueous HCl and washed successively with saturated aqueous $NaHCO_3$ and brine. The solvent was removed under reduced pressure to afford **296** (7.46 g, 85 %) as a white powder.

mp 92 °C; ν_{max}/cm^{-1} 1377 (S=O); δ_H (400 MHz, DMSO-d_6) 8.94 - 9.20 (1 H, m, *Ar*), 8.53 - 8.69 (1 H, m, *Ar*), 8.37 (1 H, s, *Ar*), 7.74 - 7.99 (1 H, m, *Ar*); δ_C (100 MHz, DMSO-d_6) 153.5, 147.6, 140.8, 136.1, 134.2, 131.5, 127.2,

125.3, 92.7; δ_F (377 MHz, DMSO-d_6) -71.9 (CF_3); *m/z* (FI$^+$) 437 ([M]$^+$); HRMS (FI$^+$) $C_{10}H_4ClF_3INO_3S$, ([M]$^+$) requires 436.8597; found 436.8598.

tert-Butyl 5-bromo-1H-imidazole-1-carboxylate 297

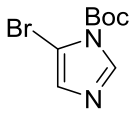

Di-*tert*-butyl dicarbonate (1.31 g, 6 mmol) was added portionwise to a stirring solution of 4-bromo-1-*H*-imidazole (882 mg, 6 mmol) in CH_2Cl_2 (25 mL) at room temperature. After complete addition, the reaction mixture was stirred for 24 h. The solvent was removed under reduced pressure and the crude product was purified by flash column chromatography using EtOAc/Cyclohexane (30:70) as eluent to give **297** (949 mg, 64 %) as a white powder.

mp 107 ^{o}C; δ_H (400 MHz, $CDCl_3$) 7.71 - 7.97 (1 H, m, *Ar*), 7.08 - 7.34 (1 H, m, *Ar*), 1.52 (9 H, s, C(CH_3)$_3$); δ_C (100 MHz, $CDCl_3$) 145.8 (*C*=O), 136.5, 117.3, 116.4, 86.5 (*C*(CH$_3$)$_3$), 27.7 (C(*C*H$_3$)$_3$); *m/z* (ESI$^+$) 269 ([M+Na]$^+$); HRMS (ESI$^+$) $C_8H_{11}BrN_2NaO_2$, ([M+Na]$^+$) requires 268.9896; found 268.9898.

5-Chloro-7-(trimethylsilyl)quinolin-8-yl trifluoromethanesulfonate 298

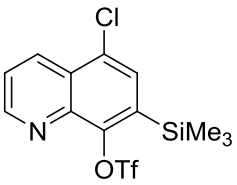

Clioquinol (310 mg, 1 mmol) and hexamethyldisilylamine (HMDS) (227 µL, 1.1 mmol) were stirred in THF (3.3 mL) under reflux for 90 min. The solvent was evaporated under reduced pressure and the residue was subjected to vacuum to remove excess NH_3 and HMDS. The crude product was then dissolved in THF (6 mL) and cooled to -100 °C in a MeOH/liquid N_2 cooling bath. *n*-BuLi (690 µL of 1.6 M in hexanes, 1.1 mmol) was added dropwise and the mixture was then stirred for 20 min. The mixture was then cooled again to -100 °C and trifluoromethanesulfonic anhydride (200 µL, 1.2 mmol) was added dropwise, and the stirring was continued for 20 min. A cold saturated solution of $NaHCO_3$ was added, the phases were separated, and the aqueous layer was extracted with Et_2O. The organic solvent was removed under reduced pressure. The crude

product was purified by flash column chromatography using EtOAc/Cyclohexane (15:85) as eluent to give **298** (260 mg, 68 %) as an off-white powder.

mp 83 °C; ν_{max}/cm^{-1} 1398 (Si=O); δ_H (400 MHz, $CDCl_3$) 8.95 - 9.04 (1 H, m, *Ar*), 8.53 - 8.59 (1 H, m, *Ar*), 7.69 (1 H, s, *Ar*), 7.59 - 7.65 (1 H, m, *Ar*), 0.51 (9 H, s, Si(CH_3)$_3$; δ_C (100 MHz, $CDCl_3$) 150.8, 150.1, 140.2, 134.7, 132.9, 130.8, 130.4, 127.9, 123.3, -0.7 (Si(*C*H_3)$_3$); δ_F (377 MHz, $CDCl_3$) -68.4 (C*F*$_3$); *m/z* (ESI$^+$) 384 ([M+H]$^+$); HRMS (ESI$^+$) $C_{13}H_{13}ClF_3NNaO_3SSi$, ([M+Na]$^+$) requires 405.9918; found 405.9907.

tert-Butyl (5-chloro-2-hydroxyphenyl)carbamate 299

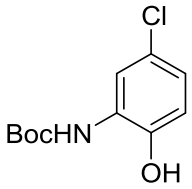

Di-*tert*-butyl dicarbonate (8 g, 36.4 mmol) was added portionwise to a stirring solution of 2-amino-4-chlorophenol (5 g, 34.7 mmol) in 1,4-dioxane (25 mL) at 0 °C. The resulting mixture was stirred at room temperature overnight. The reaction mixture was diluted with CH_2Cl_2 (150 mL) and washed with water, brine, and dried over anhydrous $MgSO_4$. The solvent was evaporated under reduced pressure. The crude product was purified by flash column chromatography using EtOAc/Cyclohexane (20:80) as eluent to give **299** (7.86 g, 93 %) as a light-pink powder.

mp 122 °C; ν_{max}/cm^{-1} 1697 (C=O); δ_H (400 MHz, $CDCl_3$) 7.86 (1 H, br. s., N*H*), 7.24 - 7.31 (1 H, m, *Ar*), 6.93 - 6.99 (1 H, m, *Ar*), 6.82 - 6.89 (1 H, m, *Ar*), 6.75 (1 H, br. s., O*H*), 1.53 (9 H, s, C(CH_3)$_3$); δ_C (100 MHz, $CDCl_3$) 154.5 (*C*=O), 145.5, 126.8, 125.5, 124.8, 120.8, 119.1, 82.4 (*C*(CH$_3$)$_3$), 28.2 (C(*C*H$_3$)$_3$); *m/z* (ESI$^+$) 266 ([M+Na]$^+$); HRMS (ESI$^+$) $C_{11}H_{14}ClNNaO_3$, ([M+Na]$^+$) requires 266.0554; found 266.0545.

3-Methylthiophene-2-carbaldehyde oxime 300

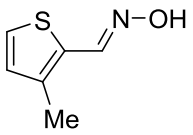

Hydroxylamine hydrochloride (765 mg, 11 mmol) was added over 15 min to a stirring solution of 3-methyl-2-thiophenecarboxaldehyde (1.1 mL, 10 mmol) in EtOH/water (2 mL/1.5 mL). A solution of NaOH (440 mg,

11 mmol) in water (0.5 mL) was added dropwise, and the resulting mixture was stirred for an additional 15 min at room temperature. The reaction mixture was concentrated under reduced pressure to precipitate a solid which was collected by filtration to give **300** (1.34 g, 95 %) as an orange powder.

mp 112 °C; ν_{max}/cm^{-1} 3136 (OH), 1625 (C=N); δ_H (400 MHz, $CDCl_3$) 7.82 (1 H, s, CN*H*), 7.49 (1 H, d, *J*=5.0 Hz, *Ar*), 6.93 (1 H, d, *J*=5.0 Hz, *Ar*), 2.43 (3 H, s, CH_3); δ_C (100 MHz, $CDCl_3$) 141.1 (*C*NH), 139.5, 130.3, 129.2, 124.8, 14.4 (*C*H_3); *m/z* (ESI$^+$) 164 ([M+Na]$^+$); HRMS (ESI$^+$) C_6H_7NNaOS, ([M+Na]$^+$) requires 164.0141; found 164.0145.

Methyl 8-hydroxyquinoline-4-carboxylate 301

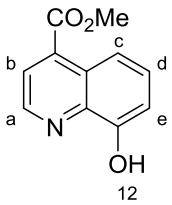

12

24 (146 mg, 0.77 mmol) was dissolved in MeOH (10 mL). The solution was cooled to 0 °C. Thionyl chloride (67 µL, 0.92 mmol) was added dropwise. The reaction mixture was warmed to room temperature and left to stir for 2 h. The solvent was removed under reduced pressure to give **301** (156 mg, 100 %) as a bright-yellow powder.

mp 240 °C; ν_{max}/cm^{-1} 1725 (C=O); δ_H (400 MHz, DMSO-d_6) 9.06 (1 H, d, *J*=5.0 Hz, H_a), 8.07 - 8.14 (2 H, m, $H_{b/e}$), 7.67 (1 H, t, *J*=8.0 Hz), 7.34 (1 H, d, *J*=7.5 Hz, H_c), 3.17 (3 H, s, CH_3); δ_C (100 MHz, DMSO-d_6) 167.0 (*C*=O), 152.0, 146.6, 139.4, 136.1, 129.9, 125.7, 122.4, 115.5, 113.1, 48.6 (*C*H_3); *m/z* (FI$^+$) 188 ([M]$^+$); HRMS (FI$^+$) $C_{11}H_9NO_3$, ([M]$^+$) requires 203.0582; found 203.0585.

(3-Bromophenyl)(phenyl)methanol 302[189]

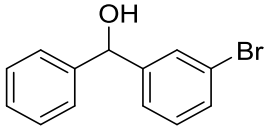

A 3M solution of phenylmagnesium bromide in Et_2O (3 mL, 9 mmol) was slowly added to a stirring solution of 3-bromobenzaldehyde (931 µL, 8 mmol) in Et_2O. After complete addition, the reaction mixture was heated under reflux for 1.5 h, cooled to 0 °C, and quenched by slow addition of a saturated aqueous solution of NH_4Cl. The reaction mixture was then extracted with Et_2O and the organic layer was washed with water,

brine, and dried over anhydrous $MgSO_4$ before the solvent was removed under reduced pressure. The crude product was purified by flash column chromatography using EtOAc/Cyclohexane (10:90) as eluent to give **302** (1.37 g, 58 %) as a clear oil.

δ_H (200 MHz, $CDCl_3$) 7.54 - 7.60 (1 H, m, *Ar*), 7.30 - 7.41 (6 H, m, *Ar*), 7.26 - 7.30 (1 H, m, *Ar*), 7.22 (1 H, d, *J*=7.5 Hz, *Ar*), 5.77 (1 H, d, *J*=3.5 Hz, CH(O*H*)), 2.45 (1 H, d, *J*=3.5 Hz, C*H*(OH)); δ_C (100 MHz, $CDCl_3$) 146.0, 143.2, 130.6, 130.1, 129.5, 128.7, 128.0, 126.6, 125.1, 122.6, 75.6, *C*H(OH)); *m/z* (ESI^-) 261 ($[M-H]^-$);

N-((5-Chloro-8-hydroxyquinolin-7-yl)(3-methylthiophen-2-yl)methyl)cyclobutanecarboxamide 303

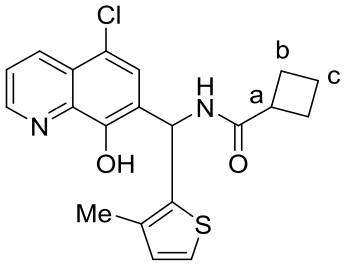

Following general procedure 1, 5-chloro-8-hydroxyquinoline (359 mg, 2.0 mmol), cyclobutanecarboxamide (198 mg, 2.0 mmol) and 3-methyl-2-thiophenecarboxaldehyde (431 µL, 4.0 mmol) gave **303** (308 mg, 40 %) as a light-brown powder.

mp 186 °C; ν_{max}/cm^{-1} 3270 (NH), 1640 (C=O); δ_H (400 MHz, $CDCl_3$) 10.41 (1 H, br. s., N*H*), 8.91 - 9.00 (1 H, m, quinoline-*Ar*), 8.59 - 8.69 (1 H, m, quinoline-*Ar*), 8.40 - 8.54 (1 H, m, quinoline-*Ar*), 7.64 - 7.77 (2 H, m, *Ar*), 7.18 - 7.26 (1 H, m, *Ar*), 6.78 - 6.92 (2 H, m, *Ar*), 3.05 - 3.23 (1 H, m, H_a), 2.11 (3 H, s, CH_3), 1.67 - 2.09 (6 H, m, $H_{b/c}$); δ_C (100 MHz, $CDCl_3$) 173.8 (*C*=O), 150.2, 150.1, 140.3, 139.4, 134.7, 133.4, 131.3, 127.8, 126.8, 125.9, 125.8, 123.8, 119.2, 44.9 (benzyl-*C*), 25.7, 25.2, 18.7, 14.3 (*C*H_3); *m/z* (ESI^-) 386 ($[M-H]^-$); HRMS (ESI^+) $C_{20}H_{19}ClN_2NaO_2S$, ($[M+Na]^+$) requires 409.0748; found 409.0733.

N-((5-Fluoro-8-hydroxyquinolin-7-yl)(3-methylthiophen-2-yl)methyl)benzamide 304

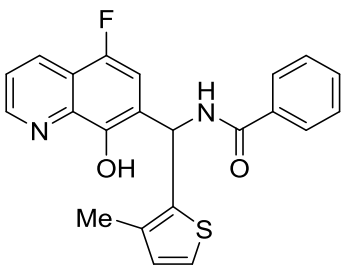

Following general procedure 1, 5-fluoro-8-hydroxyquinoline (326 mg, 2.0 mmol), benzamide (242 mg, 2.0 mmol) and 3-methyl-2-thiophenecarboxaldehyde (431 µL, 4.0 mmol) gave **304** (305 mg, 39 %) as a light-brown powder.

mp 188 °C; ν_{max}/cm^{-1} 3301 (NH), 1639 (C=O); δ_H (400 MHz, DMSO-d_6) 10.14 (1 H, br. s, N*H*), 9.25 - 9.36 (1 H, m, quinoline-*Ar*), 8.88 - 9.01 (1 H, m, quinoline-*Ar*), 8.38 - 8.47 (1 H, m, quinoline-*Ar*), 7.87 - 7.95 (2 H, m, *Ar*), 7.64 - 7.70 (1 H, m, *Ar*), 7.58 - 7.64 (1 H, m, *Ar*), 7.50 - 7.57 (1 H, m, *Ar*), 7.42 - 7.50 (2 H, m, *Ar*), 7.23 - 7.30 (1 H, m, *Ar*), 7.16 - 7.22 (1 H, m, *Ar*, benzyl-*H*), 6.89 (1 H, d, m, *Ar*), 2.17 (3 H, s, C*H*$_3$); δ_C (100 MHz, DMSO-d_6) 166.5 (*C*=O), 150.2, 150.4, 147.4, 140.0, 135.0, 134.9, 132.2, 131.3, 130.0, 129.2, 129.1, 128.5, 124.4, 124.3, 124.0, 123.2, 110.9, 110.7, 45.8 (benzyl-*C*), 14.4 (*C*H$_3$); *m*/*z* (ESI$^-$) 391 ([M-H]$^-$); HRMS (ESI$^+$) $C_{22}H_{17}FN_2NaO_2S$, ([M+Na]$^+$) requires 415.0873; found 415.0887.

N-((5-Bromo-8-hydroxyquinolin-7-yl)(3-methylthiophen-2-yl)methyl)benzamide 305

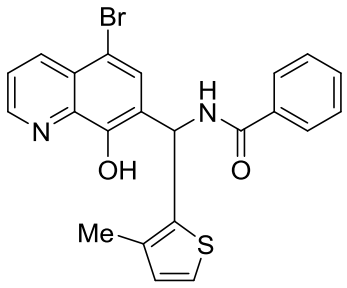

Following general procedure 1, 5-bromo-8-hydroxyquinoline (448 mg, 2.0 mmol), benzamide (242 mg, 2.0 mmol) and 3-methyl-2-thiophenecarboxaldehyde (431 µL, 4.0 mmol) gave **305** (186 mg, 21 %) as an off-white powder.

mp 152 °C; ν_{max}/cm^{-1} 3304 (NH), 1639 (C=O); δ_H (400 MHz, DMSO-d_6) 10.53 (1 H, br. s., N*H*), 9.28 - 9.40 (1 H, m, quinoline-*Ar*), 8.89 - 8.98 (1 H, m, quinoline-*Ar*), 8.34 - 8.50 (1 H, m, quinoline-*Ar*), 8.06 (1 H, s, quinoline-*Ar*), 7.85 - 7.99 (2 H, m, *Ar*), 7.66 - 7.80 (1 H, m, *Ar*), 7.50 - 7.60 (1 H, m, *Ar*), 7.43 - 7.49 (2 H, m, *Ar*), 7.23 - 7.31 (1 H, m, *Ar*), 7.11 - 7.21 (1 H, m, benzyl-*H*), 6.90 (1 H, m, *Ar*), 2.15 (3 H, s, C*H*$_3$); δ_C (100 MHz, $CDCl_3$) 166.5 (*C*=O), 151.1, 150.1, 139.9, 139.7, 135.9, 134.9, 132.3, 131.4, 130.8, 129.1, 128.5, 127.3, 126.2, 124.3, 124.0, 109.1, 45.7 (benzyl-*C*), 14.4 (*C*H$_3$); *m*/*z* (FI) 452 ([M]); HRMS (FI) $C_{22}H_{17}BrN_2O_2S$, ([M]) requires 452.0194; found 452.0199.

N-((5-Chloro-8-hydroxyquinolin-7-yl)(4-phenoxyphenyl)methyl)benzamide **306**

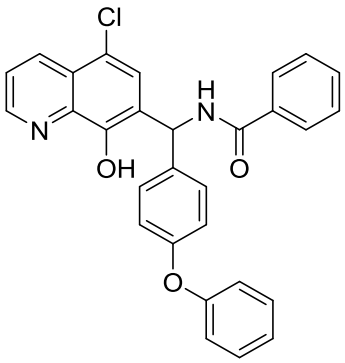

Following general procedure 1, 5-chloro-8-hydroxyquinoline (359 mg, 2.0 mmol), benzamide (242 mg, 2.0 mmol) and 4-phenoxybenzaldehyde (700 µL, 4.0 mmol) gave **306** (573 mg, 60 %) as a white powder.

mp 222 °C; ν_{max}/cm^{-1} 3306 (NH), 1634 (C=O); δ_H (400 MHz, DMSO-d_6) 10.46 (1 H, br. s., N*H*), 9.23 - 9.36 (1 H, m, quinoline-*Ar*), 8.88 - 9.05 (1 H, m, quinoline-*Ar*), 8.40 - 8.57 (1 H, m, quinoline-*Ar*), 7.87 - 8.00 (3 H, m, *Ar*), 7.67 - 7.76 (1 H, m, *Ar*), 7.52 - 7.59 (1 H, m, *Ar*), 7.45 - 7.52 (2 H, m, *Ar*), 7.31 - 7.40 (4 H, m, *Ar*), 7.07 - 7.15 (1 H, m, benzyl-*H*), 6.93 - 7.04 (5 H, m, *Ar*); δ_C (100 MHz, DMSO-d_6) 166.8 (*C*=O), 157.5, 156.4, 150.4, 150.1, 139.5, 137.5, 135.1, 133.4, 132.3, 130.9, 129.8, 129.2, 128.5, 127.5, 126.0, 125.8, 124.3, 123.9, 119.5, 119.4, 50.5 (benzyl-*C*); *m*/*z* (FI) 480 ([M]); HRMS (FI) $C_{29}H_{21}N_2O_3Cl$, ([M]) requires 480.1241; found 480.1248.

N-((5-Chloro-8-hydroxyquinolin-7-yl)(5-ethylthiophen-2-yl)methyl)benzamide **307**

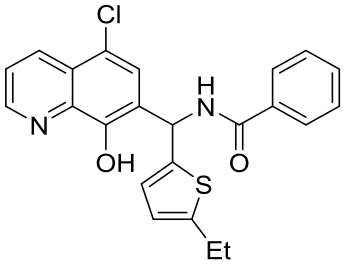

Following general procedure 1, 5-chloro-8-hydroxyquinoline (359 mg, 2.0 mmol), benzamide (242 mg, 2.0 mmol) and 5-ethyl-2-thiophenecarboxaldehyde (500 µL, 4.0 mmol) gave **307** (362 mg, 43 %) as a light-brown powder.

mp 204 °C; ν_{max}/cm^{-1} 3297 (NH), 1634 (C=O); δ_H (400 MHz, DMSO-d_6) 10.50 (1 H, br. s., N*H*), 9.39 - 9.49 (1 H, m, quinoline-*Ar*), 8.93 - 9.02 (1 H, m, quinoline-*Ar*), 8.45 - 8.53 (1 H, m, quinoline-*Ar*), 8.01 (1 H, s, quinoline-*Ar*), 7.90 - 7.96 (2 H, m, *Ar*), 7.69 - 7.78 (1 H, m, *Ar*), 7.52 - 7.59 (1 H, m, *Ar*), 7.43 - 7.52 (2 H, m, *Ar*), 7.12 (1 H,

d, *J*=9.0 Hz, benzyl-*H*), 6.53 - 6.70 (2 H, m, *Ar*), 2.72 (2 H, q, *J*=7.5 Hz, C*H*$_2$) 1.17 (2 H, t, *J*=7.5 Hz, C*H*$_3$); δ_C (100 MHz, DMSO-d_6) 166.6 (*C*=O), 150.3, 150.1, 147.0, 143.5, 139.5, 134.9, 133.4, 132.4, 129.2, 128.5, 127.4, 126.0, 125.7, 125.6, 124.0, 124.0, 119.5, 47.1 (benzyl-*C*), 23.7 (*C*H$_2$), 16.8 (*C*H$_3$); *m/z* (FI) 422 ([M]$^+$); HRMS (FI) $C_{23}H_{19}N_2O_2ClS$, ([M]$^+$) requires 422.0856; found 422.0865.

3-(Bromomethyl)benzaldehyde **308**[190]

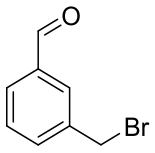

A solution of diisobutylaluminium hydride (1M in hexanes, 36.8 mL, 36.8 mmol) was added dropwise to a stirring solution of α-bromo-*meta*-tolunitrile (6 g, 30.6 mmol) in chlorobenzene (60 mL) at 0 °C over a period of 20 min. The resulting mixture was stirred for one further hour at 0 °C and then diluted with $CHCl_3$ (100 mL). The mixture was shaken with 10 % HCl aq. for about 10 min and then extracted with $CHCl_3$. The combined organic layers were dried over anhydrous $MgSO_4$ and concentrated *in vacuo*. The crude product was purified *via* flash column chromatography (5 % EtOAc, 95 % cyclohexane) to give **308** as an off-white solid (4.55 g, 75 %).

mp 47 °C; δ_H (200 MHz, $CDCl_3$) 10.02 (1 H, s, C*H*O), 7.87 - 7.96 (1 H, m, *Ar*), 7.78 - 7.86 (1 H, m, *Ar*), 7.62 - 7.73 (1 H, m, *Ar*), 7.47 - 7.59 (1 H, m, *Ar*), 4.55 (2 H, s, C*H*$_2$); δ_C (100 MHz, $CDCl_3$) 191.7 (*C*HO), 139.0, 136.9, 134.9, 129.9, 129.8, 129.6, 32.1 (*C*H$_2$); *m/z* (FI) 198 ([M]$^+$); HRMS (FI) C_8H_7OBr, ([M]$^+$) requires 197.9680; found 197.9678.

N-((5-Chloro-8-hydroxyquinolin-7-yl)(4,5-dimethylthiophen-2-yl)methyl)benzamide **309**

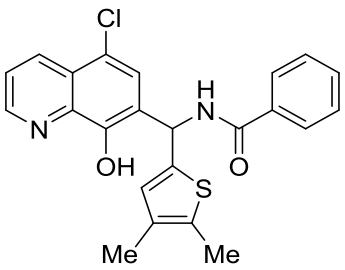

Following general procedure 1, 5-chloro-8-hydroxyquinoline (359 mg, 2.0 mmol), benzamide (242 mg, 2.0 mmol) and 4,5-dimethylthiophene-2-carboxaldehyde (475 µL, 4.0 mmol) gave **309** (273 mg, 32 %) as an off-white powder.

mp 239 °C; ν_{max}/cm^{-1} 3283 (NH), 1637 (C=O); δ_H (400 MHz, DMSO-d_6) 10.47 (1 H, br. s., N*H*), 9.26 - 9.45 (1 H, m, quinoline-*Ar*), 8.91 - 9.05 (1 H, m, quinoline-*Ar*), 8.39 - 8.56 (1 H, m, quinoline-*Ar*), 7.99 (1 H, s, *Ar*), 7.88 - 7.96 (2 H, m, *Ar*), 7.68 - 7.78 (1 H, m, *Ar*), 7.52 - 7.60 (1 H, m, *Ar*), 7.44 - 7.51 (2 H, m, *Ar*), 7.06 (1 H, d, *J*=8.5 Hz, benzyl-*H*), 6.47 (1 H, s) 2.22 (3 H, s, CH_3), 1.98 (3 H, s, CH_3); δ_C (100 MHz, DMSO-d_6) 166.6 (*C*=O), 150.2, 150.1, 141.1, 139.5, 134.9, 133.4, 133.1, 132.3, 129.2, 128.7, 128.5, 127.4, 126.0, 125.6, 123.9, 119.4, 47.0 (benzyl-*C*), 14.2 (*C*H$_3$), 13.5 (*C*H$_3$); *m/z* (ESI$^-$) 421 ([M-H]$^-$); HRMS (ESI$^+$) $C_{23}H_{19}ClN_2NaO_2S$, ([M+Na]$^+$) requires 445.0748; found 445.0737.

N-((5-Chloro-8-hydroxyquinolin-7-yl)(3-methylthiophen-2-yl)methyl)-3-methoxybenzamide 310

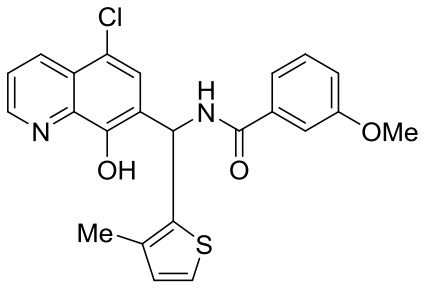

Following general procedure 1, 5-chloro-8-hydroxyquinoline (359 mg, 2.0 mmol), 3-methoxybenzamide (302 mg, 2.0 mmol) and 3-methyl-2-thiophenecarboxaldehyde (431 µL, 4.0 mmol) gave **310** (129 mg, 15 %) as a light-brown powder.

mp 145 °C; ν_{max}/cm^{-1} 3291 (NH), 1640 (C=O); δ_H (400 MHz, DMSO-d_6) 10.51 (1 H, br. s., N*H*), 9.24 - 9.39 (1 H, m, quinoline-*Ar*), 8.91 - 9.02 (1 H, m, quinoline-*Ar*), 8.43 - 8.59 (1 H, m, quinoline-*Ar*), 7.88 (1 H, s, *Ar*), 7.67 - 7.78 (1 H, m, *Ar*), 7.50 - 7.55 (1 H, m, *Ar*), 7.44 - 7.49 (1 H, m, *Ar*), 7.35 - 7.41 (1 H, m, *Ar*), 7.24 - 7.30 (1 H, m, *Ar*), 7.08 - 7.18 (2 H, m, *Ar*), 6.87 - 6.93 (1 H, m, *Ar*), 3.80 (3 H, s, OCH_3), 2.15 (3 H, s, CH_3); δ_C (100 MHz, DMSO-d_6) 166.2 (*C*=O), 160.0, 150.5, 150.1, 139.8, 139.4, 137.6, 136.2, 135.0, 133.4, 131.4, 130.3, 127.3, 126.0, 125.5, 124.0, 120.8, 119.2, 118.0, 113.7, 56.2 (benzyl-*C*), 45.8 (O*C*H$_3$), 14.4 (*C*H$_3$); *m/z* (ESI$^-$) 437 ([M-H]$^-$); HRMS (ESI$^+$) $C_{23}H_{19}ClN_2NaO_3S$, ([M+Na]$^+$) requires 461.0697; found 461.0699.

N-((5-Chloro-8-hydroxyquinolin-7-yl)(3-methylthiophen-2-yl)methyl)-4-nitrobenzamide **311**

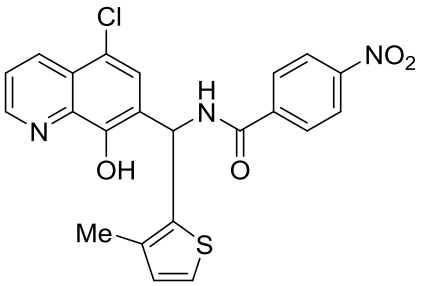

Following general procedure 1, 5-chloro-8-hydroxyquinoline (359 mg, 2.0 mmol), 4-nitrobenzamide (332 mg, 2.0 mmol) and 3-methyl-2-thiophenecarboxaldehyde (431 µL, 4.0 mmol) gave **311** (365 mg, 40 %) as a light-brown powder.

mp 194 °C; ν_{max}/cm^{-1} 3312 (NH), 1643 (C=O); δ_H (400 MHz, DMSO-d_6) 10.57 (1 H, br. s., N*H*), 9.66 - 9.75 (1 H, m, quinoline-*Ar*), 8.93 - 9.03 (1 H, m, quinoline-*Ar*), 8.42 - 8.56 (1 H, m, quinoline-*Ar*), 8.24 - 8.36 (2 H, m, quinoline-*Ar*), 8.12 - 8.18 (2 H, m, *Ar*), 7.86 (1 H, s, *Ar*), 7.68 - 7.78 (1 H, m, *Ar*), 7.26 - 7.34 (1 H, m, *Ar*), 7.12 - 7.20 (1 H, m, *Ar*), 6.88 - 6.95 (1 H, m, *Ar*), 2.16 (3 H, s, C*H*$_3$); δ_C (100 MHz, DMSO-d_6) 165.0 (*C*=O), 150.6, 150.2, 150.0, 140.4, 139.4, 135.2, 133.4, 131.4, 130.0, 129.8, 127.1, 126.1, 125.1, 124.4, 124.2, 124.1, 119.3, 46.0 (benzyl-*C*), 14.4 (*C*H$_3$); *m*/*z* (ESI$^-$) 452 ([M-H]$^-$); HRMS (ESI$^+$) $C_{22}H_{16}ClN_3NaO_4S$, ([M+Na]$^+$) requires 476.0442; found 476.0453.

7-(Benzamido(phenyl)methyl)-8-hydroxyquinoline 1-oxide **312**

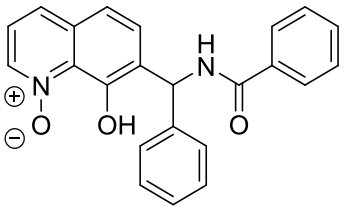

Following general procedure 1, 8-hydroxyquinoline-*N*-oxide (322 mg, 2.0 mmol), benzamide (242 mg, 2.0 mmol) and benzaldehyde (406 µL, 4.0 mmol) gave **312** (274 mg, 37 %) as a light-brown powder.

mp 296 °C; ν_{max}/cm^{-1} 3275 (NH), 1633 (C=O); δ_H (400 MHz, DMSO-d_6) 9.20 - 9.34 (1 H, m, quinoline-*Ar*), 8.48 - 8.64 (1 H, m, quinoline-*Ar*), 8.02 - 8.16 (1 H, m, quinoline-*Ar*), 7.88 - 8.02 (3 H, m, *Ar*), 7.81 (1 H, m, *Ar*), 7.41 - 7.61 (6 H, m, *Ar*), 7.19 - 7.38 (3 H, m, *Ar*), 6.87 (1 H, m, *Ar*); δ_C (100 MHz, DMSO-d_6) 166.5 (*C*=O), 150.8, 141.8,

136.1, 134.8, 132.1, 131.8, 131.6, 130.8, 130.7, 129.9, 127.5, 127.4, 127.0, 122.2, 122.1, 117.6, 117.0, 50.6 (benzyl-*C*); *m/z* (ESI$^+$) 371 ([M+H]$^+$); HRMS (ESI$^+$) $C_{23}H_{18}N_2NaO_3$, ([M+Na]$^+$) requires 393.1210; found 393.1202.

3-Chloro-8-nitroquinoline **313**[191]

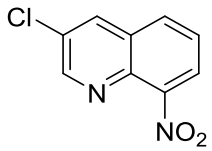

N-Chlorosuccinimide (8.8 g, 66 mmol) was added in small portions to a stirring solution of 8-nitroquinoline (10.4 g, 60 mmol) in acetic acid (120 mL) at 110 °C. The resulting mixture was stirred for 2 h without further heating and subsequently poured onto 500 mL of ice water and stirred for another 30 min. The precipitate was collected by filtration, washed with water, and dried to give **313** (13.4 g, 100 %) as a bright-yellow solid.

mp 124 °C; δ_H (400 MHz, DMSO-d_6) 8.99 - 9.11 (1 H, m) 8.76 - 8.87 (1 H, m) 8.17 - 8.37 (2 H, m) 7.79 - 7.92 (1 H, m); δ_C (100 MHz, DMSO-d_6) 152.0, 148.2, 136.9, 135.3, 132.0, 130.0, 129.3, 127.8, 124.2; *m/z* (FI) 208 ([M]$^+$); HRMS (FI) $C_9H_5N_2O_2Cl$, ([M]$^+$) requires 208.0040; found 208.0043.

3-Bromo-8-nitroquinoline **314**

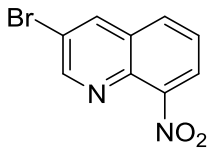

N-Bromosuccinimide (10.4 g, 66 mmol) was added in small portions to a stirring solution of 8-nitroquinoline (10.4 g, 60 mmol) in acetic acid (120 mL) at 110 °C. The resulting mixture was stirred for 2 h without further heating and subsequently poured onto 500 mL of ice water and stirred for another 30 min. The precipitate was collected by filtration, washed with water, and dried to give **314** (14.0 g, 92 %) as an off-white powder.

mp 121 °C; δ_H (400 MHz, DMSO-d_6) 9.09 - 9.13 (1 H, m), 8.93 - 9.00 (1 H, m), 8.31 - 8.36 (1 H, m), 8.22 - 8.29 (1 H, m), 7.79 - 7.88 (1 H, m); δ_C (100 MHz, DMSO-d_6) 153.8, 148.2, 138.5, 137.0, 132.0, 129.9, 127.7, 124.3, 119.2; *m/z* (FI) 252 ([M]$^+$); HRMS (FI) $C_9H_5N_2O_2Br$, ([M]$^+$) requires 251.9534; found 251.9534.

N-((5-Bromo-8-hydroxyquinolin-7-yl)(3-methylthiophen-2-yl)methyl)-2-phenylacetamide **315**

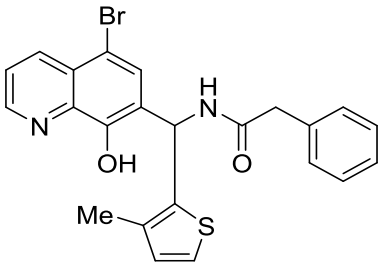

Following general procedure 1, 5-bromo-8-hydroxyquinoline (448 mg, 2.0 mmol), 2-phenylacetamide (270 mg, 2.0 mmol) and 3-methyl-2-thiophenecarboxaldehyde (431 µL, 4.0 mmol) gave **315** (738 mg, 79 %) as a white powder.

mp 187 °C; ν_{max}/cm^{-1} 3222 (NH), 1635 (C=O); δ_H (400 MHz, DMSO-d_6) 10.48 (1 H, br. s., N*H*), 9.07 - 9.17 (1 H, m, quinoline-*Ar*), 8.88 - 8.99 (1 H, m, quinoline-*Ar*), 8.37 - 8.50 (1 H, m, quinoline-*Ar*), 7.92 (1 H, s, quinoline-*Ar*), 7.62 - 7.79 (1 H, m, *Ar*), 7.17 - 7.36 (5 H, m, *Ar*), 6.86 - 6.92 (1 H, m, *Ar*), 6.83 (1 H, d, *J*=8.0 Hz, benzyl-*H*), 3.51 - 3.58 (2 H, m, CH_2), 2.11 (3 H, s, CH_3); δ_C (100 MHz, DMSO-d_6) 169.7 (*C*=O), 150.5, 149.7, 139.4, 139.3, 136.8, 135.5, 134.6, 130.9, 129.6, 129.5, 129.4, 128.7, 126.8, 126.1, 123.9, 123.6, 108.8, 44.8 (benzyl-*C*), 42.5 (*C*H_2), 13.9 (*C*H_3); *m/z* (ESI$^-$) 465 ([M-H]$^-$); HRMS (ESI$^+$) $C_{23}H_{19}BrN_2NaO_2S$, ([M+Na]$^+$) requires 489.0243; found 489.0242.

3-Chloroquinolin-8-amine **316**[191]

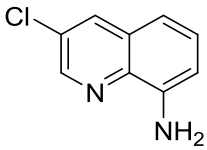

A suspension of **313** (4.2 g, 20 mmol) and sodium dithionite (35 g, 200 mmol) in methanol (50 mL) and H_2O (50 mL) was stirred for 16 h at 50 °C. The solvent was evaporated and the solids redissolved in $CHCl_3$ and H_2O. The organic layer was washed with H_2O and brine and the organic layer was concentrated *in vacuo*. The crude product was purified *via* flash column chromatography (EtOAc 5 % - 20 %, cyclohexane) to give **316** (1.68 g, 47 %) as a yellow solid.

mp 106 °C; δ_H (400 MHz, DMSO-d_6) 8.62 - 8.73 (1 H, m), 8.28 - 8.42 (1 H, m), 7.21 - 7.48 (1 H, m), 6.99 - 7.08 (1 H, m), 6.83 - 6.93 (1 H, m), 6.04 (2 H, br. s, NH_2); δ_C (100 MHz, DMSO-d_6) 146.0, 145.8, 135.8, 134.4, 129.7,

129.5, 128.1, 113.3., 109.7; *m/z* (ESI$^+$) 179 ([M+H]$^+$); HRMS (ESI$^+$) $C_9H_7ClN_2$, ([M+H]$^+$) requires 179.0371; found 179.0168.

3-Bromoquinolin-8-amine **317**

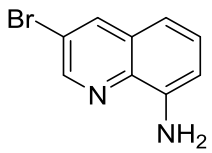

A suspension of **314** (5.1 g, 20 mmol) and sodium dithionite (35 g, 200 mmol) in methanol (50 mL) and H_2O (50 mL) was stirred for 16 h at 50 °C. The solvent was evaporated and the solids redissolved in $CHCl_3$ and H_2O. The organic layer was washed with H_2O and brine and the organic layer was concentrated *in vacuo*. The crude product was purified *via* flash column chromatography (EtOAc 5 % - 20 %, cyclohexane) to give **317** (2.4 g, 53 %) as a yellow solid.

mp 229 °C; δ_H (400 MHz, DMSO-d_6) 8.63 - 8.84 (1 H, m), 8.39 - 8.58 (1 H, m), 7.22 - 7.48 (1 H, m), 6.98 - 7.10 (1 H, m), 6.83 - 6.95 (1 H, m), 6.03 (2 H, br. s, NH_2); δ_C (100 MHz, DMSO-d_6) 147.6, 146.0, 137.6, 135.8, 130.2, 129.6, 117.3, 113.3, 109.8; *m/z* (ESI$^+$) 223 ([M+H]$^+$); HRMS (ESI$^+$) $C_9H_8N_2Br$, ([M+H]$^+$) requires 222.9865; found 222.9861.

5-Chloro-6-nitroquinolin-8-ol **318**

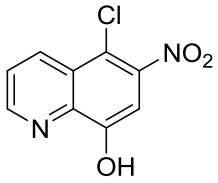

Following general procedure 2, 2-amino-4-chloro-5-nitrophenol (1.89 g, 10 mmol) and acrolein (1 mL, 15 mmol) gave **318** (627 mg, 28 %) as a light-brown powder.

mp 186 °C; ν_{max}/cm^{-1} 3087 (OH); δ_H (400 MHz, DMSO-d_6) 9.02 - 9.18 (1 H, m), 8.59 - 8.83 (1 H, m), 7.78 - 7.98 (1 H, m), 7.63 (1 H, s); δ_C (100 MHz, DMSO-d_6) 154.8, 151.9, 146.9, 140.3, 134.8, 126.5, 125.2, 111.5, 106.8; *m/z* (ESI$^+$) 225 ([M+H]$^+$); HRMS (ESI$^+$) $C_9H_5ClN_2O_3$, ([M+H]$^+$) requires 225.0061; found 225.1019.

N-((6-Chloro-8-hydroxyquinolin-7-yl)(3-methylthiophen-2-yl)methyl)benzamide **319**

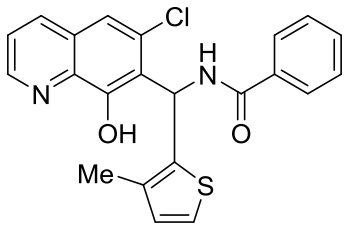

Following general procedure 1, **118** (359 mg, 2 mmol), benzamide (242 mg, 2 mmol) and 3-methyl-2-thiophenecarboxaldehyde (431 µL, 4 mmol) gave **319** (352 mg, 43 %) as a light brown powder after purification *via* flash column chromatography (10 % - 20 % EtOAc, cyclohexane).

mp 160 °C; ν_{max}/cm^{-1} 3058 (NH), 1660 (C=O); δ_H (400 MHz, DMSO-d_6) 8.96 - 9.02 (1 H, m, quinoline-*Ar*), 8.87 - 8.94 (1 H, m, quinoline-*Ar*), 8.27 - 8.40 (1 H, m, quinoline-*Ar*), 7.82 - 7.90 (2 H, m, *Ar*), 7.61 - 7.69 (1 H, m, *Ar*), 7.52 - 7.58 (1 H, m, *Ar*), 7.44 - 7.51 (2 H, m, *Ar*), 7.32 (1 H, d, *J*=8.5 Hz, benzyl-*H*), 7.24 - 7.28 (1 H, m, *Ar*), 6.84 - 6.91 (1 H, m, *Ar*), 2.29 (3 H, s, C*H*$_3$); δ_C (100 MHz, DMSO-d_6) 165.4 (*C*=O), 153.2, 149.4, 137.9, 137.5, 135.9, 135.0, 134.4, 132.1, 132.0, 130.7, 129.0, 128.3, 127.7, 124.1, 123.7, 122.3, 118.0, 47.3 (benzyl-*C*), 14.3 (thiophene-*C*H$_3$); *m/z* (ESI$^-$) 407 ([M-H]$^-$); HRMS (ESI$^+$) $C_{22}H_{17}O_2N_2ClNaS$, ([M+Na]$^+$) requires 431.0592; found 431.0583.

Quinoxalin-5-ol **320**[192]

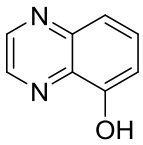

2,3-Diaminophenol (1 g, 8.1 mmol) was dissolved in a mixture of sodium acetate (11 mL, 4 M aq.) and acetic acid (16 mL, 2 M aq.) and heated to 60 °C. In a second flask, a solution of sodium glyoxal bisulfite (2.25 g, 8.5 mmol) in H_2O (60 mL) was heated to 60 °C. The 2,3-diaminophenol solution was then transferred into the sodium glyoxal bisulfite solution with a pipette and stirred for 1 h at 60 °C. After cooling to room temperature, 1N NaOH aq. was used to adjust the pH to ~8. The resulting aqueous solution was then extracted with EtOAc, dried over anhydrous $MgSO_4$ and concentrated *in vacuo*. The crude product was purified *via* flash column chromatography (10 % - 50 % EtOAc, cyclohexane) to give **320** (553 mg, 47 %) as a brown powder.

mp 101 °C; δ_H (400 MHz, methanol-d_4) 8.32 - 8.91 (2 H, m), 7.52 - 7.61 (1 H, m), 7.38 - 7.47 (1 H, m), 7.02 - 7.12 (1 H, m); δ_C (100 MHz, methanol-d_4) 153.4, 145.1, 143.1, 142.8, 133.8, 130.9, 118.5, 111.8; *m/z* (ESI^+) 147 ($[M+H]^+$); HRMS (ESI^-) $C_8H_5ON_2$, ($[M-H]^-$) requires 145.0407; found 145.0405.

Methyl 2-((5-Chloroquinolin-8-yl)oxy)acetate **321**

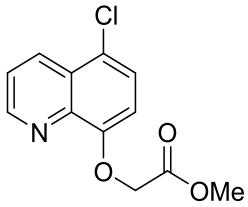

A suspension of 5-chloro-8-hydroxyquinoline (900 mg, 5 mmol), methyl bromoacetate (574 µL, 6 mmol), and potassium carbonate (850 mg, 6 mmol) was stirred in a mixture of acetone (10 mL) and tetrahydrofuran (10 mL) for 16 h under reflux. The solvent was evaporated and the residue redissolved in a mixture of EtOAc and H_2O. The organic layer was extracted with H_2O and brine, dried over anhydrous $MgSO_4$ and concentrated *in vacuo*. The crude product was purified *via* flash column chromatography to give **321** (995 mg, 79 %) as an off-white solid.

mp 105 °C; ν_{max}/cm^{-1} 1771 (C=O); δ_H (400 MHz, DMSO-d_6) 8.92 - 9.05 (1 H, m, quinoline-*Ar*), 8.41 - 8.61 (1 H, m, quinoline-*Ar*), 7.69 - 7.80 (1 H, m, quinoline-*Ar*), 7.67 (1 H, s, quinoline-*Ar*), 7.10 - 7.21 (1 H, m, quinoline-*Ar*), 5.08 (2 H, s, O*C*H_2) 3.73 (3 H, s, *C*H_3); δ_C (100 MHz, DMSO-d_6) 169.4 (*C*=O), 153.3, 150.4, 140.5, 132.7, 127.1, 126.7, 123.6, 122.1, 110.8, 65.9 (O*C*H_2), 52.4 (*C*H_3); *m/z* (ESI^+) 252 ($[M+H]^+$); HRMS (ESI^+) $C_{12}H_{11}O_3NCl$, ($[M+H]^+$) requires 252.0422; found 252.0417.

Methyl 8-(2-Methoxy-2-oxoethoxy)quinoline-5-carboxylate **322**

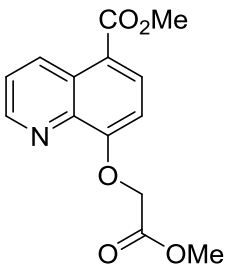

A solution of methyl 8-hydroxyquinoline-5-carboxylate (203 mg, 1 mmol), methyl bromoacetate (115 µL, 1 mmol), and potassium carbonate (170 mg, 1.2 mmol) in a mixture of acetone (2 mL) and THF (2 mL) was

stirred at 100 °C for 2 h under microwave irradiation. The solvent was evaporated under reduced pressure and the residue was redissolved in EtOAc (10 mL) and water (10 mL). The organic layer was washed with brine, dried over anhydrous Na_2SO_4 and concentrated *in vacuo*. The crude reaction product was purified *via* flash column chromatography (0 % - 10 % MeOH, CH_2Cl_2) to give **322** (264 mg, 96 %) as an off-white solid.

mp 151 ^{o}C; ν_{max}/cm^{-1} 1767 (C=O); δ_H (400 MHz, DMSO-d_6) 9.19 - 9.40 (1 H, m, *Ar*), 8.82 - 9.04 (1 H, m, *Ar*), 8.13 - 8.29 (1 H, m, *Ar*), 7.56 - 7.81 (1 H, m, *Ar*), 7.03 - 7.36 (1 H, m, *Ar*), 5.17 (2 H, s, CH_2), 3.92 (3 H, s, CH_3), 3.75 (3 H, s, CH_3); δ_C (100 MHz, DMSO-d_6) 169.1 (*C*=O), 166.5 (*C*=O), 157.7, 149.8, 139.7, 134.1, 132.6, 128.2, 123.8, 118.7, 108.9, 65.8 (*C*H$_2$), 52.6 (O*C*H$_3$), 52.5 (O*C*H$_3$); *m/z* (ESI$^+$) 276 ([M+H]$^+$); HRMS (ESI$^+$) $C_{14}H_{14}O_5N$, ([M+H]$^+$) requires 276.0867; found 276.0863.

4-Cyanoquinolin-8-yl 4-methylbenzenesulfonate 323

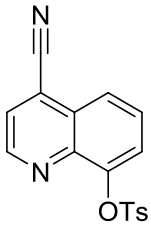

Prior to use, anhydrous dimethylacetamide was sparged with a gentle stream of nitrogen gas for 30 min. A 50 mM solution of sulphuric acid was prepared with 10 mL dimethylacetamide and 26.8 µL of concentrated H_2SO_4 and sparged with N_2 for 10 min. A microwave vial equipped with a magnetic follower was charged with palladium acetate (56 mg, 0.1 mmol) and XPhos (238 mg, 0.5 mmol). The vial was then sealed, subjected to an atmosphere of N_2 and filled with H_2SO_4 (2 mL, 50 mM in dimethyl acetamide). The catalyst mixture is then stirred at 80 °C for 30 min under microwave irradiation.

In parallel, a microwave vial equipped with a magnetic follower was charged with zinc dust (13.1 mg, 0.2 mmol), zinc cyanide (352 mg, 3 mmol) and **125** (1.67 g, 5 mmol). The vial was sealed and subjected to an atmosphere of N_2 and 15 mL of dimethylacetamide were added. Then, the previously prepared catalyst solution was added (1 mL) and the reaction mixture was stirred for 45 min at 160 °C under microwave irradiation. The mixture was then diluted with EtOAc and extracted with H_2O and brine. The combined organic layers were dried over anhydrous $MgSO_4$ and concentrated *in vacuo*. The crude product was purified

via flash column chromatography (15 % - 30 % EtOAc, cyclohexane) to give **323** (1.09 g, 23 %) as an off-white powder.

mp 115 °C; ν_{max}/cm^{-1} 2220 (nitrile); δ_H (400 MHz, $CDCl_3$) 8.81 - 8.93 (1 H, m, *Ar*), 7.98 - 8.12 (1 H, m, *Ar*), 7.71 - 7.84 (2 H, m, *Ar*), 7.60 - 7.69 (3 H, m, *Ar*), 7.16 - 7.25 (2 H, m, *Ar*), 2.36 (3 H, s, C*H*$_3$); δ_C (100 MHz, $CDCl_3$) 149.9, 146.0, 145.5, 141.8, 129.7, 128.9, 128.0, 127.0, 125.7, 124.3, 124.0, 120.8, 118.8, 115.2, 21.7 (*C*H$_3$); *m/z* (ESI$^+$) 325 ([M+H]$^+$); HRMS (ESI$^+$) $C_{17}H_{12}O_3N_2NaS$, ([M+Na]$^+$) requires 347.0461; found 347.0457.

8-Hydroxyquinoline-4-carbonitrile **324**

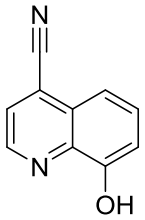

A solution of **324** (343 mg, 1.1 mmol) in sodium hydroxide (1M aq., 1.1 mL), ethanol (6 mL) and H_2O (6 mL) was stirred under reflux for 1 h. The ethanol was removed *in vacuo* and the pH adjusted to 5. The precipitate was filtered and dried to give **324** (87 mg, 46 %) as a bright-yellow solid.

mp 200 °C; ν_{max}/cm^{-1} 2235 (nitrile); δ_H (200 MHz, DMSO-d_6) 8.93 - 9.13 (1 H, m), 8.06 - 8.25 (1 H, m), 7.64 - 7.92 (1 H, m), 7.40 - 7.63 (1 H, m), 7.13 - 7.35 (1 H, m); δ_C (100 MHz, DMSO-d_6) 158.8, 148.1, 138.7, 131.3, 128.6, 126.8, 117.8, 114.4, 114.0; *m/z* (ESI$^+$) 171 ([M+H]$^+$); HRMS (ESI$^+$) $C_{10}H_5ON_2$, ([M-H]$^-$) requires 169.0407; found 169.0406.

N-((5-Chloro-8-hydroxyquinolin-7-yl)(4-ethynylphenyl)methyl)benzamide **325**

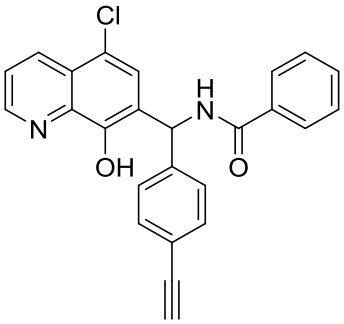

Following general procedure 1, 5-chloro-8-hydroxyquinoline (359 mg, 2.0 mmol), benzamide (242 mg, 2.0 mmol) and 4-ethynylbenzaldehyde (260 mg, 4.0 mmol) gave **325** (430 mg, 52 %) as an off-white powder.

mp 228 °C; ν_{max}/cm^{-1} 3301 (NH), 1630 (C=O); δ_H (400 MHz, DMSO-d_6) 10.53 (1 H, br. s., N*H*), 9.23 - 9.45 (1 H, m, quinoline-*Ar*), 8.90 - 9.08 (1 H, m, quinoline-*Ar*), 8.40 - 8.57 (1 H, m, quinoline-*Ar*), 7.93 - 8.00 (2 H, m, *Ar*), 7.86 (1 H, s, *Ar*), 7.70 - 7.79 (1 H, m, *Ar*), 7.55 - 7.60 (1 H, m, *Ar*), 7.44 - 7.54 (4 H, m, *Ar*), 7.32 - 7.39 (2 H, m, *Ar*), 7.04 (1 H, d, *J*=9.0 Hz, benzyl-*H*), 4.18 (1 H, s, C*H*); δ_C (100 MHz, DMSO-d_6) 166.6 (*C*=O), 150.1, 149.7, 143.0, 139.1, 134.6, 133.0, 132.3, 132.0, 128.8, 128.1, 128.0, 127.1, 125.5, 125.0, 123.6, 130.9, 119.2, 83.8, 81.3, 50.4; *m/z* (ESI$^+$) 413 ([M+H]$^+$); HRMS (ESI$^+$) $C_{25}H_{17}O_2N_2ClNa$, ([M+Na]$^+$) requires 435.0871; found 435.0866.

N-((5-Chloro-8-hydroxyquinolin-7-yl)(3-ethynylphenyl)methyl)benzamide 326

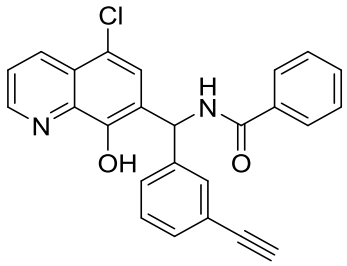

Following general procedure 1, 5-chloro-8-hydroxyquinoline (345 mg, 1.9 mmol), benzamide (233 mg, 1.9 mmol) and 3-ethynylbenzaldehyde (250 mg, 1.92 mmol) gave **326** (220 mg, 27 %) as an off-white powder.

mp 200 °C; ν_{max}/cm^{-1} 3297 (NH), 1637 (C=O); δ_H (400 MHz, DMSO-d_6) 10.55 (1 H, br. s., N*H*), 9.22 - 9.44 (1 H, m, quinoline-*Ar*), 8.92 - 9.05 (1 H, m, quinoline-*Ar*), 8.43 - 8.58 (1 H, m, quinoline-*Ar*), 7.92 - 7.99 (2 H, m, *Ar*), 7.89 (1 H, s, *Ar*), 7.70 - 7.77 (1 H, m, *Ar*), 7.54 - 7.60 (1 H, m, *Ar*), 7.47 - 7.54 (2 H, m, *Ar*), 7.34 - 7.45 (4 H, m, *Ar*), 7.02 (1 H, d, *J*=9.0 Hz, benzyl-*H*), 4.20 (1 H, s, C*H*); δ_C (100 MHz, DMSO-d_6) 166.6 (*C*=O), 150.1, 149.8, 142.7, 139.1, 134.5, 133.0, 132.0, 130.9, 130.6, 129.5, 128.8, 128.6, 128.1, 126.9, 125.5, 125.0, 123.6, 122.2, 119.2, 83.9, 81.5, 50.4; *m/z* (ESI$^+$) 413 ([M+H]$^+$); HRMS (ESI$^+$) $C_{25}H_{17}O_2N_2ClNa$, ([M+Na]$^+$) requires 435.0871; found 435.0867.

8-Hydroxy-2-methylquinoline-5-carboxylic acid 327

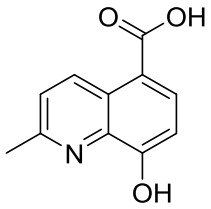

Following general procedure 2, 3-amino-4-hydroxybenzoic acid (3.2 g, 21.5 mmol) and crotonaldehyde (2.7 mL, 32.3 mmol) gave **327** (3.0 g, 69 %) as a light-brown powder.

δ_H (400 MHz, DMSO-d_6) 9.61 - 9.97 (1 H, m), 8.28 - 8.45 (1 H, m), 8.01 (1 H, m), 7.49 - 7.70 (1 H, m), 2.97 (3 H, s, CH_3); δ_C (100 MHz, DMSO-d_6) 167.4 (*C*=O), 157.9, 153.4, 142.6, 134.7, 130.6, 127.3, 126.2, 117.2, 114.4, 21.4 (*C*H_3); *m*/*z* (ESI$^-$) 202 ([M-H]$^-$);

Methyl 8-Hydroxy-2-methylquinoline-5-carboxylate 328

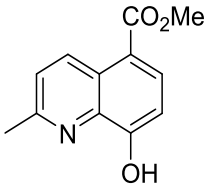

Thionyl chloride (870 µL, 12 mmol) was added dropwise to a stirring suspension of **327** (2.03 g, 10 mmol) in methanol (50 mL) at 0 °C. The resulting mixture was brought to boiling and stirred for 16 h under reflux. After cooling to room temperature, the solvent was removed *in vacuo* to give **328** (2.2 g, 100 %) as a light-brown solid.

mp 228 °C; ν_{max}/cm^{-1} 1702 (C=O); δ_H (200 MHz, DMSO-d_6) 9.44 - 9.80 (1 H, m), 8.22 - 8.45 (1 H, m), 7.80 - 8.08 (1 H, m), 7.39 - 7.63 (1 H, m), 3.91 (3 H, s, OCH_3), 2.93 (3 H, s, CH_3); *m*/*z* (ESI$^+$) 218 ([M+H]$^+$); HRMS (ESI$^+$) $C_{12}H_{12}O_3N$, ([M+H]$^+$) requires 218.0812; found 218.0809.

Chapter IV: Epigenetic Drug Discovery: Prospects in Terms of Technology, Market, and Organisational Capabilities

Introduction

Epigenetics is a relatively young field of biology for which one definition comprises 'heritable genomic changes transmitted in a manner other than by changes in the ATCG DNA sequence' (Figure 54). However, the term epigenetics is now used more loosely for the mechanisms that alter gene expression, especially those at the transcriptional level. Epigenetics is an area of intense scientific interest with current studies ranging from fundamental science to pharmaceutical development. Small molecules targeting epigenetic pathways have been approved for use by the Food and Drug Administration (FDA) for treatment of blood cancers, such as the DNA methyltransferase (DNMT) inhibitor azacitidine **8** and the histone deacetylase (HDAC) inhibitor vorinostat **10** (see Figure 5, Chapter I). This chapter outlines the potential of epigenetics in terms of drug discovery within the technology, market, and organisational capabilities (T-M-O) framework. The Structural Genomics Consortium (SGC) is taken as a model organisation because it is considered as being at the forefront of epigenetics and because it conducts innovative research in a novel way: as an open-innovation consortium between academia and pharmaceutical companies (www.thesgc.com). The approach was to collect data from interviews with several key people in epigenetics working in Oxford. This enabled collection of the most up-to-date insights from experts in the field by identifying key questions and linking them to the most suitable persons to provide answers within the T-M-O framework. The key people interviewed were Dr Graham Wynne, Prof. Christopher Schofield, Dr Akane Kawamura, Dr William LaMarr, Dr Chas Bountra, and Dr Paul Brennan.

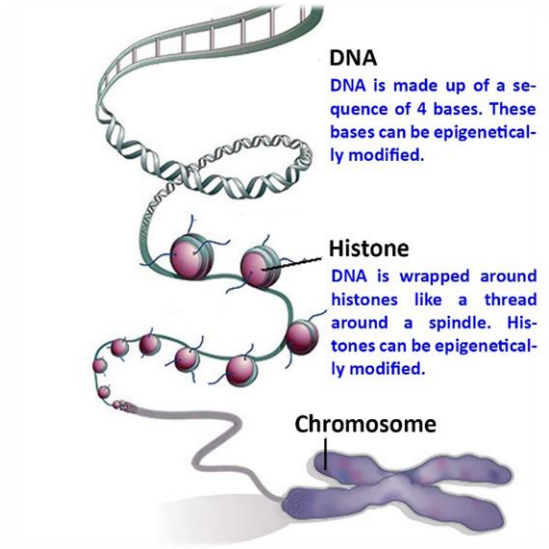

Figure 54: Epigenetic biology is driven by modifications of DNA bases and histone proteins. These modifications can be regarded as contribution to the 'chemistry of genetics' and are involved in human diseases such as cancer, Parkinson's and heart disease.

Epigenetics has the potential to give rise to novel therapies and diagnostic tools in the clinic. Targeting epigenetic mechanisms may result in the next paradigm shift in pharmaceutical development since the targeting of kinases observed some 2-3 decades ago.[193] In fact, the similarities of the early stages between the two sets of targets are numerous. Initially, people did not believe that the targeting of kinases would be a clinically useful strategy in drug discovery. The negative arguments that were put forward included that kinases are too ubiquitous in biology, that they all use adenosine triphosphate (ATP) as a cofactor and hence it would be nearly impossible to generate potent and selective compounds for specific targeting of clinically viable kinases. Today, there are about twenty-five FDA-approved kinase-targeting drugs on the market, the most famous being imatinib (Gleevec), which is primarily used against chronic myelogenous leukemia (CML).[194] Similar arguments were initially raised against targeting epigenetic targets: they are involved ubiquitously in various diseases, there are about 300-400 of them, many of them use the same substrates (e.g. 2-oxoglutarate for many histone demethylases) and their relative interplay is poorly understood. Nevertheless, there are already four FDA-approved drugs on the market which specifically target epigenetic mechanisms, namely DNMT and HDAC inhibitors (Figure 5, Chapter I). What does the future hold?

Technology

A convenient tool for assessing technology life cycles and industry maturity is the so-called S-curve which was developed by Richard D. Foster (Figure 55).[195] These curves usually picture a measure of innovation in a given industry against time, and usually possess a characteristic S-shape. The initiation phase depicts a time where the industry comprises a high degree of uncertainty. Many different people do things differently: although a high degree of innovation, multiple components are scattered across an area and do not directly contribute to a single product. Over time, however, certain aspects of the given industry converge into a single prototype, or a dominant design. The appearance of such a dominant design usually marks the beginning of an exponential growth phase, because every innovation based on the dominant design significantly contributes to the development of the technology in question. At the same time, the appearance of a dominant design enables optimisation between various components, as well as their production and considerations of operational efficiency. Once industry maturity is reached, the measure of innovation reaches a plateau because the degrees of achievable innovation and optimisation are more or less exhausted, and single innovations do not significantly contribute to a complex product anymore. A plot of the Foster curve taking the number of publications on the topic of epigenetics per year as measure of innovation over time reveals that the research into epigenetics has grown exponentially shortly after the millennium change (Figure 55). Two primary points of interest directly emerge from inspection of the curve: the long initiation phase, and the question as to whether a dominant design has already emerged.

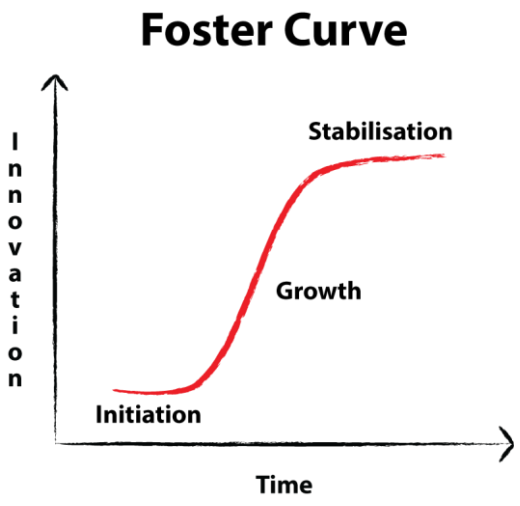

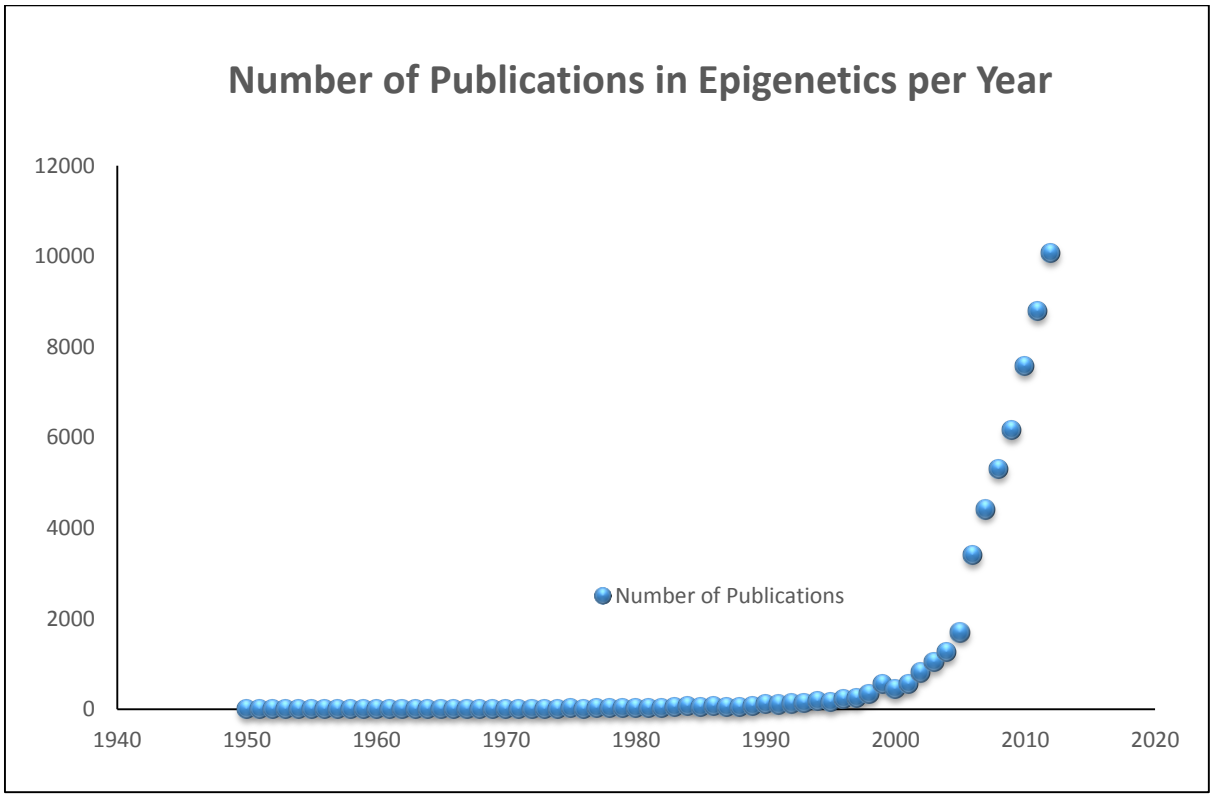

Figure 55: Top (p. 236): A model Foster technology curve highlighting the three stages of initiation, growth, and stabilisation. **Bottom:** A plot of the number of publications in epigenetics against time reveals that this field is now in an exponential growth phase after a relatively long initiation period.

Initiation Phase

The initiation phase for epigenetic research has apparently lasted for about 50 years (Figure 55). This is unusually long compared to many other innovative fields in science and technology, for example automobiles or the internet. Epigenetics is a highly interdisciplinary field requiring the interplay of multiple areas of fundamental sciences, including:

- Mathematics
- Physics
- Computer modelling
- X-ray crystallography
- Chemistry
- Protein production
- Biochemistry
- Biology

- Physiology
- Medicine

In order to ultimately yield clinically useful medicines, each of the individual component fields needs to have reached a certain scientific and technological level to be able to engage in drug discovery. For example, a protein target may need to be characterised, produced in sufficient quantities, and of acceptable purity, before it can be used for crystallisation and subsequent inhibitor design. All these steps are enabling drug discovery, but may require advanced technologies ranging from mathematics through biology. To gain an appreciation of this time scale, it is worthwhile to assess whether epigenetics is disruptive or incremental in terms of how science is done in the individual component fields.

Disruptive or Incremental?

For the successful scientist the explicit general skills in epigenetics research are likely the same as for any other area of biology. In principle, the scientist needs to formulate an adequate hypothesis which may be tested by designing appropriate repeatable experiments which in turn lead to further hypotheses. The concept of epigenetics is being widely investigated as an incremental innovation in terms of explicit scientific methods and knowledge.

In terms of tacit knowledge, the laboratory techniques used in epigenetics are based on techniques found in other areas of science, but adapted to the field of epigenetics. For example, the chemical biology expert Dr Akane Kawamura adapted the AlphaScreen® method, an antibody-based fluorescence technology widely used for *in vitro* screening, such as kinase screening, for the use of screening compounds against histone demethylases.[181] She used a reliable experimental technique from an established area of biology and enabled innovation in epigenetics by optimising the technique specifically for the epigenetic demethylase targets. Dr Kawamura enabled incremental innovation.

Another example is the use of RapidFire™ technology for inhibitor screening. RapidFire™ is a high-throughput-compatible mass spectrometry-based technique particularly suited for histone modifications (Figure 54) because multiple site modifications, a common occurrence in epigenetics, are easily quantified in

comparison with other techniques based, for example, on fluorescence.[182] Similarly to AlphaScreen®, RapidFire™ allows screening of inhibitors against epigenetic targets by using an established technique and adapting it to the needs of epigenetic targets. Screening epigenetic targets with RapidFire™ is the result of incremental innovation.

These two examples illustrate a recurring theme when analysing the individual fundamental sciences necessary for epigenetic drug discovery: an established experimental technique in a given field is taken as a basis and modified to accommodate the needs of epigenetic research. The individual scientific components of epigenetic research are the result of incremental innovation.

Coalescence is Radical

The individual scientific areas that constitute the core of epigenetic research underwent incremental innovation to account for the specific needs of epigenetics. Further inspection reveals that the coalescence of these individual component fields is radical. Many crucial techniques for epigenetic drug discovery, such as recombinant protein production (1970s), the polymerase chain reaction (PCR) (1980s), and high-throughput screening (HTS) technology (1990s) were developed at relatively delayed times to each other.

A further complication of this coalescence is the translation or adaptability of the concept of epigenetics in various fields. Epigenetics is a construct of biology relying on concepts of genes, heritability, and Darwinian evolution. How these biological concepts translate into the language of the physical sciences is somewhat unclear. For example, what is the chemical basis of heritability and evolution? This is a question which may very well be answered some time in the future, but nowadays this area is a matter of vehement debate. It is very difficult to conduct quantitative research in a field if the fundamental concepts in that area are ill-defined. A similar situation is encountered in fields like neuroscience, where molecular mechanisms of a concept such as memory are ill-defined.

Figure 55 suggests that the individual scientific components of epigenetics may not have been sufficiently developed until about the millennium change in order to enable collaboration and original research in epigenetics. This scenario is reminiscent of the evolution in the high-definition (HDTV) field. HDTV sets were

ready for manufacturing since the early 1990s. Nevertheless, the HDTV field could not take off at that stage because complements such as studio production equipment or broadcasting technology were not advanced enough for HDTV to be a success at that time. Similarly, once the concept of epigenetics was translatable into every single area, and the individual experimental techniques were made adequate *via* incremental innovation, the field of epigenetics could finally take off and bring about radical innovation in drug discovery by combining these scientific areas in a specific way. The coalescence of the relevant individual scientific fields which compose epigenetics constitutes radical innovation to potentially bring about a paradigm shift in drug discovery.

Position on the Technology Curve

Given the recent substantial increase in epigenetics publications, the question of the maturity of the field arises. Is there a dominant design in epigenetics?

Prof. Chris Schofield defines epigenetics as 'the chemistry of genetics'. Chemical biology, which analyses the chemical basis of biology, is a very young field in itself. The chemical principles of biology are a worthwhile research field of the future because they are not very well understood at present times. Given chemical biology is not well understood, the chemistry of epigenetics is even less well understood. The technology curve, although past the initiation phase, is hence at a very early stage as well.

Similarly, the various experimental techniques used in epigenetics are still in their developmental stages. Some experimental techniques, such as AlphaScreen® and RapidFire™ screening technologies, are widely used already, but their usefulness is very specific to the protein target in question. For example, the screening technology for epigenetic targets is optimised for the highest signal-to-noise ratio whilst using the minimum amount of reagents required. Demethylase protein targets are perfectly suitable for inhibitor screening with AlphaScreen® or RapidFire™, but other targets may not be suitable because the assays have not been optimised for this purpose and other techniques may need to be used. For example, many assays rely on specialised reagents such as antibodies, which may not yet have been optimised, or even developed.

We may hence conclude that some experimental techniques are predominantly used for a particular purpose (e.g. demethylase screening), but they may not be suitable for other uses or not be adapted so far (e.g. bromodomain inhibitor screening). These techniques are predominantly used, but there is no particular dominant design yet. There is still a significant degree of technological ambiguity.

In conclusion, after a relatively long initiation period, epigenetics is in plain take-off, but has not produced a dominant design yet.

Market

Building a Market for Epigenetic Drug Discovery

There is always a common need, and hence market, for novel or improved treatments and diagnostics. Epigenetics is a particularly promising field for future drug discovery because epigenetic biology has been found to have underlying implications in some of the most challenging disease areas such as cancer and central nervous system (CNS) diseases, like Parkinson's or Alzheimer's, which pose an increasing burden in modern day society. The challenge is how to actively build a market and secure funding for epigenetic research and drug discovery.

Claiming, Demarcating, and Controlling[196]

Claiming: Analogies and Signalling Leadership

Although a scientifically very complex topic, epigenetics and its importance are amenable to analogies and precedents to make it accessible to the general intelligent public and public funding bodies. A common narration to the general public may be as follows.

Epigenetics is a very novel and exciting field in biology and means 'beyond genetics'. Many complex diseases such as cancer are driven by malfunctioning genetics, which relates to your DNA. Recent findings, however, make it clear that genetics is not enough to understand complex diseases such as cancer, and that there are biological drivers which go beyond genetics: epigenetics. Epigenetics does not directly relate to your DNA, but describes how your DNA is organised and regulated. Epigenetics has three main agents: readers, writers, and erasers. Readers read information about what to do with the DNA, writers write information about what to do with the DNA, and erasers can erase this information. Some diseases such as Parkinson's are directly linked to epigenetics but have no clear connection to genetics, whereas cancer has links to both genetics and epigenetics. Four novel epigenetic drugs have already been approved by the FDA. Epigenetic drug discovery hence holds the potential to find both novel and better drugs against challenging diseases.

This story builds on the scientific concepts of genetics that are relatively well-understood and states that genetics is important but not sufficient for tackling disease. It gives an idea about epigenetic processes with

the common activities of 'reading, writing and erasing'. It states that epigenetics holds potential for unmet, or insufficiently met disease areas, and it validates this point by mentioning that the first epigenetic drugs are already on the market. Overall, the above story makes the significance and potential of epigenetic drug discovery relatively clear to the non-expert in the field.

Another way to claim the market is to signal leadership. One of the current main drivers of epigenetic research is the Structural Genomics Consortium (SGC). The SGC is a consortium between both public and private research. To the non-expert, it signals leadership by associating with notable labels from academia and industry such as Oxford, Toronto, the Wellcome Trust, GlaxoSmithKline (GSK), Pfizer, Novartis *et cetera*. This association with big labels enables the SGC to borrow the reputation of any one label and convey credibility and expertise which is important especially at early stages, when the scientific record may not be well-developed yet. Nowadays, the SGC signals leadership by having a very high publication record in high-impact scientific journals and by providing well-characterised tools to conduct epigenetic research. Association with large pharmaceutical companies and the scientific impact convey legitimacy to the consortium.

Demarcating

Unique Selling Propositions (USPs)

Demarcation of the market in preclinical epigenetic drug discovery is a prominent feature of the consortium character of the SGC. The SGC has two major Unique Selling Propositions (USPs):

1. Publication of protein structures.
2. Delivery of chemical probes.

Both USPs are distinct from both purely academic or industrial interests for the following reasons.

1. Soon after a protein is purified and crystallised, its structure is made publicly available on the Protein Data Bank (PDB, http://www.rcsb.org). In a purely academic environment, publication may be significantly delayed due to the requirement for the lengthy process of manuscript drafting and peer review before publication in a scientific journal. In a purely industrial environment, the protein structure would not normally be made

publicly available at this stage because of competition with other pharmaceutical companies and IP protection issues. The benefit of publishing the protein structures as soon as possible in an open-access database is that research related to structural biology may proceed as soon as possible.

2. Chemical probes can be defined as tool compounds which have drug-like properties (they are potent, selective, and cell-permeable small molecules).[197] They are, however, pure tool compounds and may not be viable drug candidates because of unfavourable behaviour in living disease models, for example due to poor pharmacokinetic properties. These compounds do however have significant value for *in vitro* and cellular assays to advance drug target validation. These compounds do hence have substantial academic value to help generate novel molecular biology advancements for publication in high-impact scientific journals and they reduce risk for pharmaceutical companies by enabling in-depth target validation.

Both USPs do therefore, in principle, not interfere with the primary interests of purely academic or industrial areas.

Co-Opting Alliances

The SGC is a consortium between key players in both academia and industry. Currently the SGC is located in two sites: one at the University of Oxford, and one at the University of Toronto. There are more than 200 academic collaborators across the world. Currently, there are 8 partners from the pharmaceutical industry, and two new partners are in the process of joining the SGC. What are the incentives to join the SGC?

The incentive for academic collaborators are scientific publications and reputation. Publication in high-impact scientific journals is a currency and measure of success in the academic world. The SGC can provide the funding, infrastructure, and expertise in epigenetics regarding protein production and crystallisation, *in vitro* and cell assays, and chemical probe development. Any further expertise which is not available in-house, such as supply with diverse sets of chemical libraries, specialised assays, or exploration of novel technologies, may be acquired by identifying and engaging in suitable academic collaborations. The collaborations result in scientific publications between the collaborators and the SGC, which are of direct academic value for all parties involved.

Industrial partnerships are also partly driven by the incentive of scientific publications, for the same reason as for the academic collaborators. In addition to stimulating the publication record, the incentive for industrial partners to join the SGC is a long-term investment into emerging technologies. The investment is a four-year commitment of $8m total, or $2m per year. Six and a half years ago GSK was the sole industrial partner of the epigenetics section of the SGC. The incentive was to produce chemical probes for the advancement of target validation. The SGC would provide the proteins and protein structures, whereas GSK would provide their medicinal chemistry capacities to design and synthesise the probes. The idea was that each institution contributes their area of expertise. Releasing the chemical probes into the scientific community free of charge would generate a lot more science than GSK could generate on their own. There would be no point taking out IP on these molecules because they would be too early in the stages of drug discovery to be viable clinical drug candidates.

Seven other companies joined up to the present date. By investing $8m each they gain access to the common funding of the SGC, e.g. $56m for the 8th company that joined. Furthermore, they gain access to all of the public funding: for example the Wellcome Trust has invested £50m into the SGC at Oxford up to now. Taken together, that is an amount of funding which vastly exceeds any research funding available at any single collaboration in an academic setting.

In addition to the financial investment, the companies also gain access to the very extended network of academic collaborations (about 200 collaborations for now). They gain access to all of the data generated within the SGC, all the laboratory reagents, and all the expertise. There is also the opportunity to send scientists to different laboratories to be trained in a specific technique. So even tacit knowledge is shared, in addition to the explicit knowledge in the form of data produced.

This open-access sharing of data, reagents, and expertise creates trust which facilitates collaboration, accelerates science, and facilitates drug discovery, which then in turn generates more data. This workflow is at the basis of the virtuous cycle proposed in Figure 56.

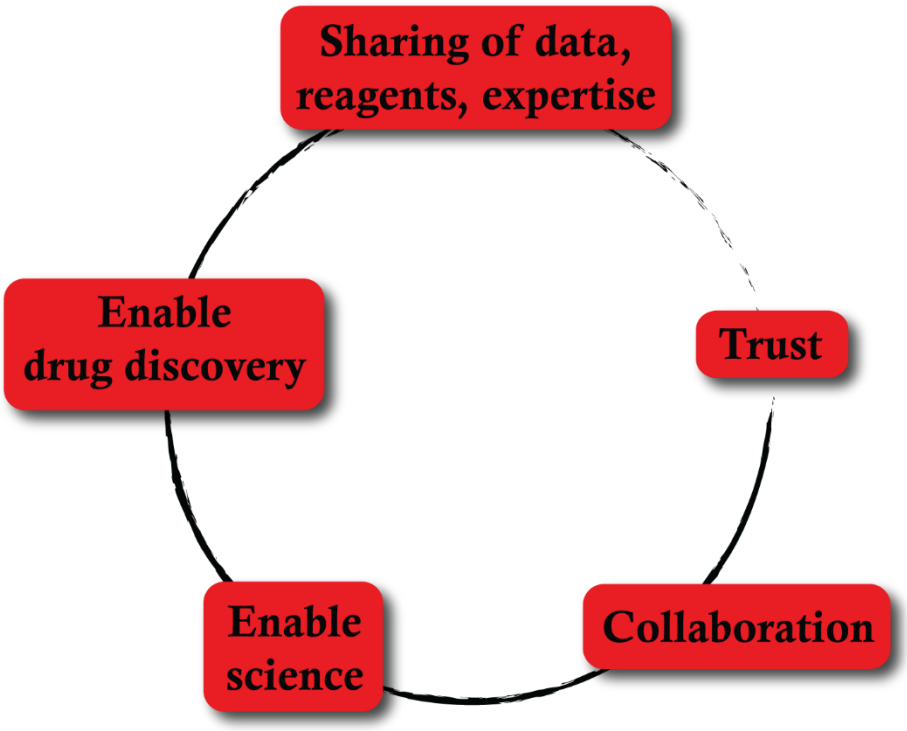

Figure 56: The proposed virtuous cycle of consortium-based epigenetic drug discovery.

To put this into a financial perspective for R&D budget: in 2010 Pfizer, on their own, spent $9b. Compared to this, $2m per year seems like a very good investment given all the above benefits which are unlikely to be generated by Pfizer on their own solely to advance science and drug discovery.

Controlling

The SGC does not control a market by acquisition. In fact, there are no acquisitions at all, but only collaborations. The SGC acts in a platform collaboration which is in line with its primarily intrinsic motivations for success: scientific development, intellectual challenge, and reputation in an open community. The SGC may be assimilated to an integrator platform because it is wedged between external innovators (academic collaborators, industrial partners) and customers (users of their chemical probes, other academic collaborators and industrial partners) (Figure 57). An example of such an integrator platform would be Apple's iTunes which regulates and 'owns' interactions with iDevice users (just like the SGC with users of chemical probes). By doing so, the SGC maintains a relatively high level of control about the standard of the science it produces, the publication record, and the quality of the chemical probes it produces. It also has control about which scientific projects to engage in by actively fostering collaborations and vetoing

participation which it qualifies unsuitable. For example, the SGC was approached by a biotechnology company to set up a new partnership. However, the collaboration was judged unsuitable by the SGC because the biotechnology company, in essence, tried to do exactly the same as the SGC but ultimately wanted to take out IP on their molecules. A biotechnology company with total funding of $50m is not able to invest $8m into a partnership when they only work on 3 or 4 already defined targets and want to generate proprietary molecules. This will clash with the open-access and fundamental science-advancing philosophy of the SGC. The proposal from the company was turned down.

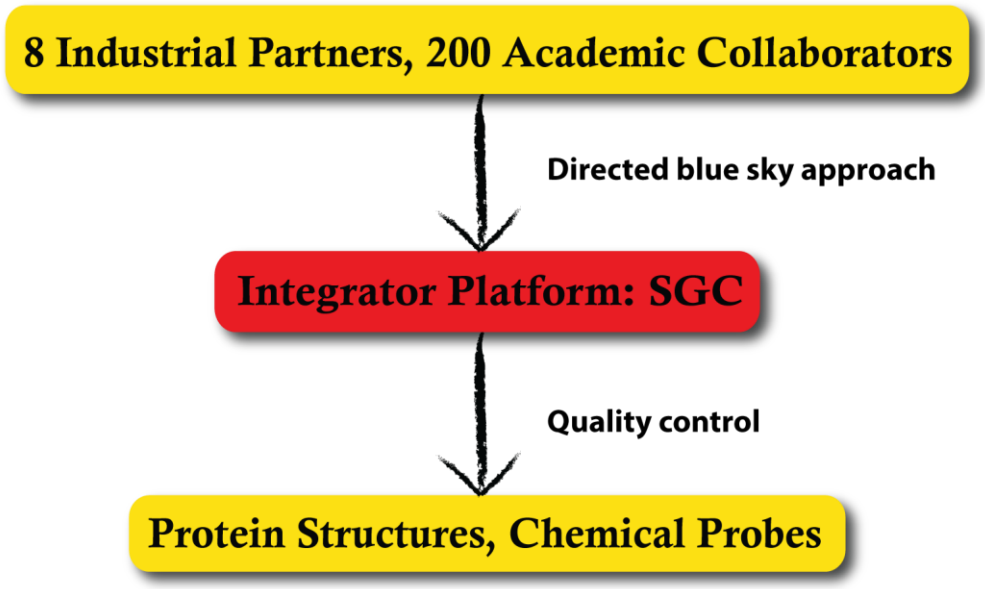

Figure 57: The SGC functions as an integrator platform.

Organisational Capabilities

Knowledge Brokering

Knowledge Brokering in a Consortium

Knowledge brokering at the SGC is a mixture between industrial and academic knowledge brokering.

In the pharmaceutical industry, knowledge brokering is normally directed and very prescriptive. A target or a biological pathway is identified by a scientist or from the literature. Value is added if competitors are on the same track and, obviously, competition is high. This means that the company's objectives may appear to be short-term goal driven and resources will be focused on this short-term goal where scientifically interesting tangents cannot be pursued due to constrains on time and resources. Bench scientists will focus on the project and will not be able to come up with new project ideas.

In academia the knowledge brokering is often a very opportunistic process: a blue-sky approach. Scientists initially decide to work on a particular project. As the work progresses, they will discover unexpected things, they will talk to interested people outside their research organisation, or they may obtain results that may have potential in another field than their current focus. They are free to pursue all these tangents which give rise to new and interesting research projects. Academic scientists pursue a very meandering path.

The SGC situates itself between these two pathways of knowledge brokering: a directed blue-sky approach. Its main focus at the moment is chemical probes. The biological properties of these chemical probes are strictly defined and the SGC focuses on fulfilling these criteria. Nevertheless, many scientifically interesting and useful things are discovered along the chemical probe project, such as polypharmacology (compounds that hit more than one target) that may have a positive disease link. It is perfectly possible to pursue these novel directions even though these may not have been initially defined in the chemical probe project. Similarly, the vast number of collaborations ensures a constant flow of both explicit and tacit knowledge while keeping people updated about new technologies and laboratory techniques. It is hence possible to widen the SGC's resources based on scientific interest and potential, rather than solely strictly defined benchmarks of a molecule.

Structural Holes

Identification of structural holes is a direct consequence of the knowledge brokering process at the SGC. While conducting research, the SGC keeps an open mind towards pursuing novel and interesting projects and developing novel technologies. Usually, if a new project requires expertise which is not available within the site of the SGC, principal investigators will seek to identify a suitable person within the SGC's large network of 200 academic collaborators and 8 industrial partners.

If a suitable person is not within reach inside the network, the principal investigators will approach a person by using their weak ties to approach someone within academia. It is a lot easier to collaborate with academic partners because such collaborations mainly rely on weak ties: it only takes an informal agreement to collaborate and both parties are free to engage in their joint work. The weak ties which link both partners may be former academic links or encounters at scientific conferences, or even just personal friendship. For example, Dr Paul Brennan set up a collaboration with his former mentor, Prof. Steve Ley in Cambridge, to develop the use of flow technology for epigenetic medicinal chemistry. Such collaborations are more difficult, not to say impossible, to establish with industrial partners outside the SGC's network because these collaborations rely on strong ties, extensive formal agreements because of IP and information sharing regulations, and potential industrial collaborators would not be able to engage in side projects solely on the grounds of scientific curiosity.

Process, Management, Organisation, Culture (PMOC)

Process

The process of advancing the epigenetic sciences *via* the application of small molecules is focused around the generation of chemical probes. 'Epigenetic proteins' are expressed, purified, and crystallised before inhibitor design can start in terms of medicinal chemistry. This is done in a collaborative effort by pooling all the resources: in-house, academic collaborators, and industrial partners. Once a compound has been declared a chemical probe, the process is a self-sustaining virtuous cycle: the chemical probes generate scientific results, which increase knowledge about epigenetic biology, which generates more questions to be answered by science, which generate more potential starting points for future probe design, which generate

more chemical probe projects etc. Scientific value is generated at every stage of this virtuous cycle, which in turn fosters knowledge, collaborative effort, and the advancement of epigenetic drug discovery (Figure 56).

Management

The SGC has a hierarchical structure organised in departments which are headed by one principle investigator who manages one research group. In Oxford, for example, the departments include chemical biology, protein crystallography, epigenetics and inflammation, epigenetics and cellular biology. These departments act under internal collaboration and the principal investigators meet regularly to discuss results, strategy, and further directions. The principal investigators are from both academic and industrial backgrounds, and some people even have worked in both academia and industry before joining the SGC. The group leaders from the SGC work for the SGC full time and are not affiliated at the same time with any of the collaborators or industrial partners. The management from the collaborators or industrial partners do consult with the SGC to discuss results and further directions, but they do not assume a management role within the SGC. At Oxford, the SGC is headed by Dr Chas Bountra. The hierarchy within Oxford is hence: head of the SGC, principal investigators, research scientists.

Organisation

The SGC is a consortium between academia and industry. This consortium structure for drug discovery is a novelty by its own: there are no other examples of a similar structure in the past. Both in industry and academia, the way drug discovery in novel fields was done in the past had one major drawback: duplication. Group leaders from specific areas usually read the same literature and attend the same conferences, so they receive the same information at about the same time. They will head off to their laboratories with similar ideas and try to solve similar problems: for example they try to obtain the structure of the same protein at the same time. One group will succeed first to obtain the structure, but they will keep the result to themselves until they publish it in a scientific journal because competition in the field is very high. All the other groups will still try and solve the same problem, unaware that one group has already succeeded. It will take another couple of months until the successful group will have gathered all their data, written a manuscript for submission, and adapted it according to the peer review process until publication occurs. In the end, all the

competing groups will have spent unnecessary amounts of time, money, and effort, unaware of the first group's success. In an industrial setting, this waste of resources may even occur over multiple years because no information is released into the public domain until a clinical candidate has been identified. This waste of resources is even aggravated when considering that 90% of the clinical candidates will fail in one of the clinical trials because the putative drug target was not the right one, or because idiosyncratic toxicities may be observed. Other companies may advance a different clinical candidate, but the target-related failures will still persist. So in addition to a waste of resources, there are ethical drawbacks. Given clinical trials involve patients, duplication of drug discovery may result in unnecessary clinical trials putting people through unnecessary procedures. In addition to this waste of patients, there will also be a waste of careers: academics and group leaders who base their careers on scientific success will see their careers unsuccessful after focusing all their efforts on a dead end.

The consortium-based pre-clinical drug discovery ensures that all the results are shared between each collaborating partner. The collaborative effort will reduce the time to obtain successful results and it will hence be in everybody's interest for somebody to succeed first because the results will be made available to everybody, free of charge. Targets will be validated more extensively before they will be taken on by the pharmaceutical industry, which in turn yields lower rates of attrition and hence a greater chance of developing successful drugs.

Culture

The culture of the SGC may be assimilated with Xerox Parc (www.parc.com). The work is driven by science alone in an 'exploration through exploitation' philosophy. The science undertaken is not driven with a motivation to most likely yield a clinically exploitable result (which may in fact be meaningless at such an early stage in a novel field of biology), but the work undertaken is motivated by factors in order to yield and answer the scientifically most interesting questions. The SGC takes both a disease- and target-agnostic view with respect to which proteins to work on.

The industrial partners also collaborate with the aim of advancing scientific knowledge which ultimately adds value to their target validation process. They are not prescriptive on what targets to work on. In contrary,

they rely on the work of the SGC for target identification. They are, however, selective about which compounds to screen. At later stages, they may prescribe which compound to screen against which targets, which is a consequence of the maturity of the field they will have worked on and they may develop their own ideas about what paths to pursue. In the beginning, however, they keep an open mind.

The extensive collaborative culture and resulting economies of scale within the SGC also foster a 'fail early, fail often' attitude which is prominent in places like Silicon Valley. Although the individual partners and collaborators may be regarded as competitors in a classical sense, they all have an interest to collaborate and share their knowledge and expertise within the SGC so as to maximise scientific progress and avoid duplication. The pooling of money, expertise, and data means that every partner of the SGC will succeed together. It also means that, if projects fail, everybody will fail together. This failure will only occur once, rather than have every individual partner fail on the same hurdle on their own. This approach reduces risk which is an inherent factor of a novel field of drug discovery such as epigenetics.

Conclusions

Overall, some aspects of epigenetics may be a new paradigm shift in drug discovery and associated research. Coupled with the innovation of consortium-based research organisations in drug discovery, these two innovations are likely to hold a promising future for novel therapies and diagnostics, and ultimately for our health and our society.

As outlined above, epigenetic drug discovery is a highly interdisciplinary field. This interdisciplinarity may be in part responsible for the long initiation phase on the technology curve. The field is in full take-off right now but has not yet produced a dominant design. Nevertheless, there are concepts which are predominantly used. A dominant design is likely to emerge in the near future. An example may be mass spectrometry-based screening platforms.

A market for epigenetic drugs may be enabled by a large collaborative alliance of both academia and the pharmaceutical industry, for example the SGC. Given the complexity and early stages of the field, fundamental research is a primary driver for future directions. The SGC acts as an integrator platform and

centralises a large pool of public and private funding, academic and industrial expertise, and a large network for preclinical epigenetic drug discovery (Figure 57). This form of collaborative open-access drug discovery is a novel concept and has not been seen before.

The drug discovery consortium has the potential to maximise availability of both explicit and tacit resources, it fosters sharing of expertise, which minimises duplication and maximises output and trust. This will accelerate both fundamental science and epigenetic drug discovery (Figure 56). A virtuous cycle.

The consortium structure also has potential to move from the preclinical to the clinical field by expanding into clinical trials and, hopefully, see the first drugs approved which emerged from this novel type of drug discovery (see next section: Recommendations).

Recommendations

Based on the T-M-O analysis of the field of epigenetic drug discovery, I have three recommendations.

1. Create an Idea Database

The knowledge brokering and virtuous cycles created by the chemical probes are focused on primary scientific data which is stored in a homogenous form within the SGC. However, novel project ideas are not stored in a uniform way. They may only exist in a principal investigator's mind or maybe in a report or presentation, but they are not uniformly accessible within the organisation in the same way as scientific data. This inevitably leads to potentially fruitful ideas never being pursued or forgotten on the sole basis of inefficient storage. This is a waste of precious resources. I therefore suggest to store ideas in a homogenous way, similarly to raw scientific data. This may have the form of noting down a specific idea, the inspiration for the idea, and the scientific challenge it addresses. People may browse this database and base their research interests around this database to generate novel scientific data. Such a database may also be useful in retrospect, after a project turned out successful. People may recur to this idea database when they tackle a similar project and try and work out what methodology led to the project being successful. A similar model is used at the design company IDEO where people collect ideas under form of prototypes which they present from time to time to their co-workers. This methodology keeps good ideas alive and fosters creativity.

2. Establish a Control Mechanism for IP

The SGC shares data transparently between collaborators and industrial partners without any partner generating any form of proprietary material within the projects at the SGC. Acting as an integrator collaborative platform, the SGC also has control that the open-access philosophy is followed. Nevertheless I think that the *status quo* is amenable to a legally grey area regarding IP. An industrial partner may collaborate in a certain area of their R&D with the SGC and participate in open-access drug discovery for that specific field. Any other research the industrial partner does within their own premises, detached from the SGC, will be proprietary and may be exploited commercially. The interface between the open-access collaboration and the proprietary drug discovery is not well-defined. For example, if research area A is similar to research area B, but A is conducted together with the SGC and B is proprietary, it seems very hard, if not impossible, to control that results from A do not directly feed into B to ultimately generate proprietary molecules by hijacking the large pool of money, knowledge, and expertise of the SGC. There seems to be a need for a control mechanism to ensure correct representation and execution of the values the SGC stands for: fostering collaboration to advance drug discovery.

3. Reach out to Late-Stage Drug Discovery

The SGC is currently focused on early-stage drug discovery, such as target identification, validation, and the generation of chemical probes which may form the basis for lead compounds to become clinical candidates. In only 6.5 years the epigenetics component of the SGC has become a hub for innovation: they produce proteins, assays, and chemical probes and have significant impact on the advancement of the biology of epigenetics. Also, the SGC has become a hub for the pharmaceutical industry because they extended their number of industrial partners from 1 to 8 in just 6.5 years, and they will soon have 10 partners. Although these are very respectable achievements given the short time frame, it should be kept in mind that the ultimate aim of drug discovery, regardless if academic, industrial, or consortium, is to generate clinically useful medicines. The SGC should reach out from pre-clinical drug discovery to late-stage drug discovery. Given their success within the early stages, it seems that open-access clinical trials, as a consortium, should be a logical extension of the current activities. Clinical trials as a consortium will have the same benefits as

pre-clinical drug discovery: pooling money, expertise, and networks to accelerate science and drug discovery by reducing duplication and diluting risk. Reducing duplication in clinical trials will mean making the trials more efficient, which also means that fewer patients will be part of the overall 90% clinical trials that fail. Besides the obvious economic advantage, this will also have a huge ethical advantage because fewer patients will be undergoing failing clinical trials.

Will drug discovery within a consortium be the future of drug discovery? We will have to wait until the SGC is shown to have contributed to the first approved drug on the market.

Chapter V: The Development of an Assay for OGFOD1 Inhibitor Screening

Introduction

The field of ribosomal 2OG oxygenases is relatively unexplored compared to, for example, the histone demethylases, or the HIF prolyl hydroxylases. This area hereby offers a wealth of opportunities for biochemical characterisation and functional studies on this class of 2OG oxygenases. The subject of my work was the human RPS23 ribosomal protein prolyl hydroxylase OGFOD1, which stands for 2OG- and Fe(II)-dependent oxygenase 1.

As outlined in the introduction to this thesis, initial results suggest that OGFOD1 is associated with stop-codon readthrough and translational accuracy.[95,99] On a molecular basis, this effect may be associated with the observation that the hydroxylation site, Pro62, is the amino acid closest to the ribosomal decoding centre in the fully assembled ribosome (see Figure 10, Chapter I). These insights may have the potential to contribute to the development of new treatments for diseases associated with anomalies of stop codon readthrough, such as muscular dystrophy.[198]

Currently available OGFOD1 functional analyses were obtained by means of biological techniques, primarily *via OGFOD1* gene knock-down.[99] Both biochemical and functional OGFOD1 characterisation could be greatly facilitated by using a selective small-molecule tool compound. No such tool compound, however, has been reported to date. In fact, no such tool compound is currently available for any of the reported ribosomal hydroxylases, which exemplifies the novelty of this area of investigation.

Our team of X-ray crystallographers successfully co-crystallised OGFOD1 and obtained an X-ray crystal structure during the course of this thesis, hereby greatly facilitating the process of future inhibitor design (Horita *et al*., manuscript in preparation). The catalytic domain of OGFOD1 is structurally very similar to the catalytic domain of the PHD2 HIF hydroxylase, as discussed in Chapter VI. It was therefore thought that OGFOD1 inhibitor design may benefit from previous insights into inhibitor design for other prolyl hydroxylases, especially PHD2.

The foundation for OGFOD1 inhibitor development consisted of the development of a suitable small-molecule screening platform. Previous work on the prolyl hydroxylases provided a wealth of information for pertinent biochemical techniques, comprising both binding and activity assays.[199] The production and purification of OGFOD1 with sufficient catalytic activity proved challenging in early work; it was therefore considered that binding assays would provide some insights into inhibitor interactions while OGFOD1 activity was investigated.

Binding Assays

Several OGFOD1 protein batches were specifically produced for protein crystallisation by Dr Shoishiro Horita, and yielded X-ray co-crystal structures with NOG **22** and 2,4-PDCA **23**, but these samples failed to display any catalytic activity. On the basis that the proteins fold into their tertiary structure, and were able to bind small-molecule inhibitors, the crystallography samples were considered suitable for the development of binding assays.

Intrinsic Fluorescence Assay

Intrinsic fluorescence assay (IFA) has previously been shown to be a suitable binding assay for assessing the interactions between bound small-molecule inhibitors and PHD2 (Hancock, R., Part II thesis 2011 and Dazzi, M., Part II thesis 2014, Schofield and Flashman groups, unpublished).

In principle, any protein possessing tryptophan, tyrosine, or phenylalanine residues in its amino acid sequence may display intrinsic fluorescence caused by the fluorescence of the individual amino acids. Tryptophan is particularly suitable for IFA owing to its high quantum yield.[200] Tryptophan fluorescence may be quenched by various factors, such as solvent interactions or pH effects.[201] For IFA, the key type of fluorescence quenching is predicted to result from ligand binding interactions.[202] In the case of PHD2, four Trp residues are located within the catalytic domain: Trp258 and Trp389 are located within the active site, and Trp334 and Trp367 outside the active site. It was postulated that the fluorescence of these four Trp residues will primarily be affected upon ligand binding to induce an overall change in the PHD2 intrinsic fluorescence.

The structural similarities between PHD2 and OGFOD1 offered an opportunity to adapt IFA to assess ligand binding interactions with OGFOD1. With OGFOD1, IFA did indeed show dose dependence by titration of Fe(II) into a solution of apo-OGFOD1; the corresponding apparent K_M was found to be 267 µM (Figure 58). This value is, however, unusually high: the corresponding apparent K_M for Fe(II) and PHD2 is 1 µM. Subsequent titrations of either 2OG **1** or NOG **22**, however, showed no IFA dose dependence at all. The OGFOD1 sequence contains a total of ten Trp residues, only one of which, Trp236, is located close to the active site. Upon titration of Fe(II) the overall structure of OGFOD1 may be considerably altered upon going from an apo-state to a metal-bound state, so the overall ordering of all Trp residues may be affected upon Fe(II) binding: hence the apparent IFA dose response. Once the metal is bound, however, the nine Trp residues outside the active site may be only affected to a small extent upon ligand binding. The effect of fluorescence quenching of one single Trp residue, Trp236, may be outweighed by the fluorescence of nine relatively unaffected Trp residues; no considerable effect, if any, is hence perceived. IFA was therefore judged unsuitable for inhibitor binding studies with wild-type OGFOD1. Possible strategies to improve the suitability of IFA for applications to OGFOD1 may be to remove external Trp residues by site-directed mutagenesis to increase the sensitivity of the active-site Trp236, or to express the catalytic domain only for binding studies.

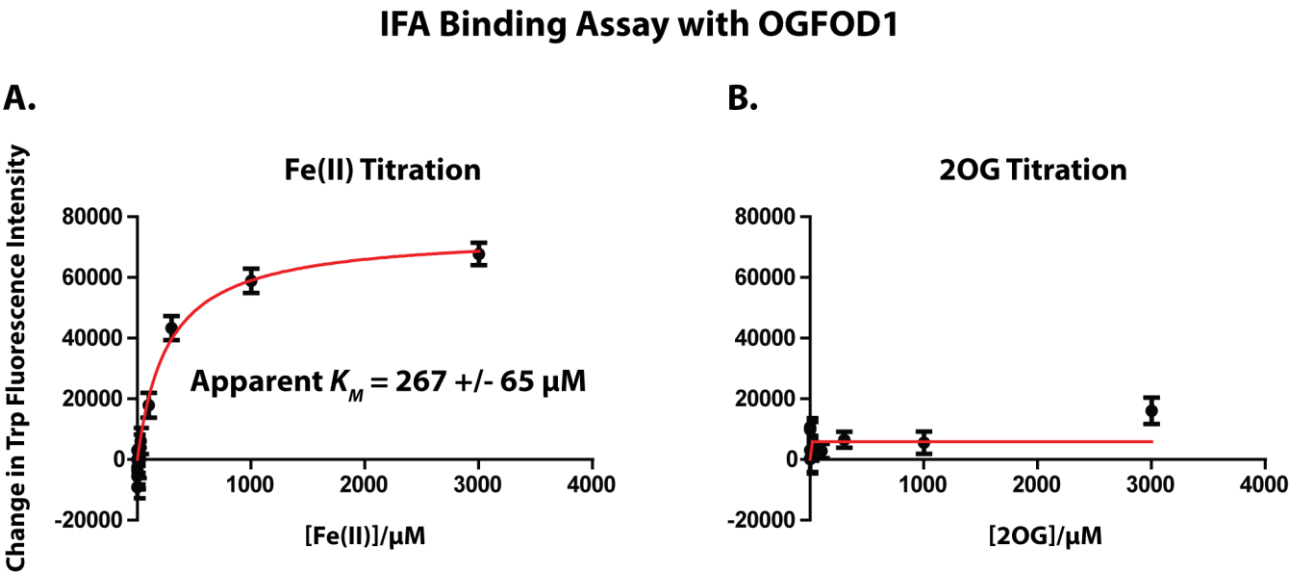

Figure 58: IFA binding assay with OGFOD1. **A.** Measurements were carried out in triplicate using OGFOD1 (10 µM) and $(NH_4)_2Fe(SO_4)_2 \bullet 6H_2O$ (0.01, 0.03, 0.1, 0.3, 1.0, 3.0, 10, 30, 100, 300, 1000, and 3000 µM) in 50 mM HEPES pH 7.5 with incubation for 60 min at room temperature. Data points represent the arithmetic average for each triplicate with the corresponding standard deviation plotted as error bar. **B.** Measurements were carried out in triplicate using OGFOD1 (10 µM), $(NH_4)_2Fe(SO_4)_2 \bullet 6H_2O$ (50 µM) and 2OG (0.01, 0.03, 0.1, 0.3, 1.0, 3.0, 10, 30, 100, 300, 1000, and 3000 µM) in 50 mM HEPES pH 7.5 with incubation for 60 min at room temperature. Data points represent the arithmetic average for each triplicate with the corresponding standard deviation plotted as error bar.

Differential Scanning Fluorimetry

Another potential binding assay for OGFOD1 is differential scanning fluorimetry (DSF), also known as thermal shift (T_m) assay.[203] DSF involves a dye whose fluorescence is quenched in apolar environments. The dye binds non-specifically to the hydrophobic parts of a protein which are gradually exposed upon thermal unfolding by an incremental temperature increase: an increase in fluorescence intensity is observed. The melting temperature, T_m, is the temperature at which the concentrations of folded and unfolded protein are equal: this point occurs at the point of inflection of the resulting sigmoidal-shaped curve. Binding of ligands to a protein usually results in protein stabilisation whose extent parallels an increase in T_m relative to unbound protein. An increase in T_m is therefore an indication of ligand binding to an enzyme of interest.

In a proof-of-principle experiment, the OGFOD1 stabilisation effects of pan-2OG oxygenase inhibitors NOG **22** and 2,4-PDCA **23**, as well as IOX1 **47** and 8HQ **52**, were investigated. Both NOG **22** and 2,4-PDCA **23** induced a ΔT_m of 10 °C, whereas IOX1 **47** revealed a smaller ΔTm of 3 °C. Unsubstituted 8HQ **52** had little effect on ΔT_m (Figure 59). These results reflect what might be expected by inferring from the corresponding binding and activity assays with the PHD2 prolyl hydroxylase: the generic inhibitors NOG **22** and 2,4-PDCA **23** are the strongest stabilisers for OGFOD1, IOX1 **47** is weaker, possibly because it was shown to be somewhat more specific for histone demethylases; unsubstituted 8HQ is generally a weak inhibitor of 2OG oxygenases.[204] It is important to note that, although high T_m shifts can correlate with strong protein stabilisation, negligible T_m shifts do not necessarily correlate with weak ligand binding.[205]

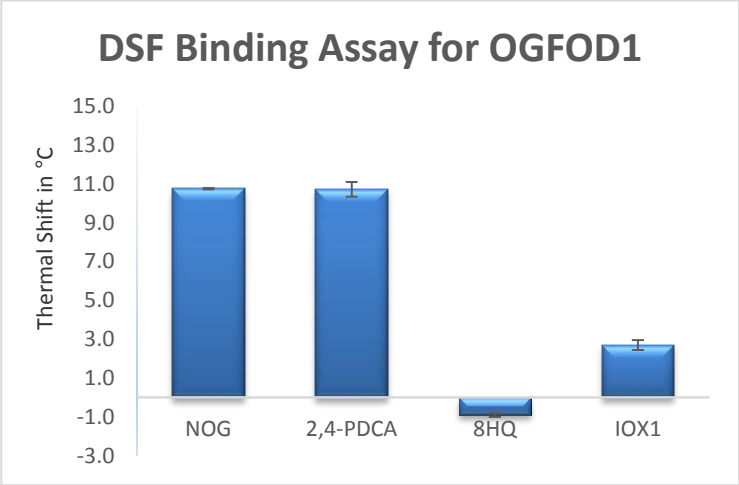

Figure 59: DSF binding assay with OGFOD1. Measurements were carried out in triplicate using OGFOD1 (2 µM), $MnCl_2 \bullet 4H_2O$ (50 µM), inhibitor (200 µM) and Sypro® Orange (1:5000 dilution) in 50 mM HEPES pH 7.5. Data points represent the arithmetic average for each triplicate with the corresponding standard deviation plotted as error bar.

Overall, these preliminary results validated DSF as a method for assessing small-molecule ligands for OGFOD1. The method offers an opportunity for rapid and inexpensive screening of large compound libraries. However, given that small molecule binding does not necessarily correlate with enzyme inhibition, there was still a need for the development of a more direct assay.

OGFOD1 Activity Assays

The preferred method for activity assays is generally considered to be a direct-detection activity assay, because the inherently low propensity for interference reduces the likelihood of either false-positive or false-negative results. Of particular value are mass spectrometry-based methods because they enable direct quantification of the relative amounts of the hydroxylated product and non-hydroxylated substrate. Specifically, matrix-assisted laser desorption ionisation time-of-flight mass spectrometry (MALDI-TOF MS) has proved especially useful in the past for conducting 2OG oxygenase activity assays.[119]

Three different OGFOD1 protein samples, produced from different constructs and purification methods as summarised in the table below, were initially available for activity testing (sample 1 was produced by Dr Armin Thalhammer, sample 2 by Gareth Elliott, sample 3 by Dr Shoishiro Horita).

Sample	Tag	Purification	Calc. MW	Observed MW	Storage
1	*N*-terminal	Ni-affinity column	65283	65283	3 years
2	*C*-terminal	Ni-affinity column	64249	64249	< 1 week
3	*N*-terminal	Ni-affinity column, size exclusion, and ion exchange	65283	65283	< 1 week

Table 7: Overview of initially available OGFOD1 samples for assay development.

As a proof of concept, a general MALDI-TOF MS-based hydroxylation assay protocol was followed to test for OGFOD1 activity (Figure 60). This protocol uses every reaction component in a large excess relative to the enzyme, in combination with extended incubation times, to ensure amounts of substrate hydroxylation sufficient for convenient detection. Only sample 1 caused hydroxylation of the 20mer RPS23 peptide substrate *in vitro*; no hydroxylation was observed with samples 2 or 3.

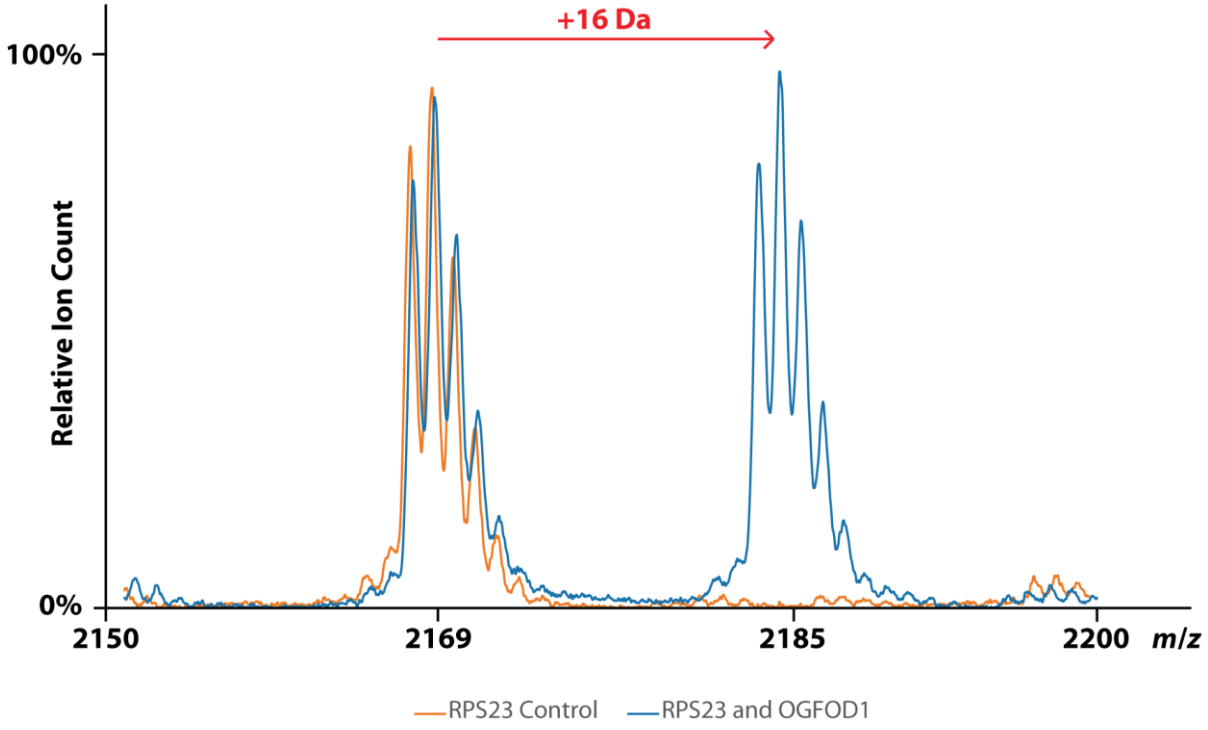

Figure 60: Preliminary MALDI-TOF MS hydroxylation assay with OGFOD1 sample 1. Measurements were carried out in triplicate using OGFOD1 (10 µM), RPS23 (sequence VLEKVGVEAKQPNSAIRKCV-NH_2, 100 µM), 2OG (300 µM), $(NH_4)_2Fe(SO_4)_2 \bullet 6H_2O$ (100 µM), and sodium ascorbate (1 mM) in 50 mM HEPES pH 7.5 with incubation for 60 min at 37 °C.

Analysis by sodium dodecyl sulphate polyacrylamide gel electrophoresis (SDS-PAGE) of all three samples did not reveal any significant differences between the three batches. All presented a major protein band around 65 kDa which corresponds to the molecular weight of His-tagged OGFOD1 protein, and a minor band around 55 kDa, corresponding to the molecular weight of OGFOD1 after cleavage of the His-tag (Figure 61 A). During

SDS page sample preparation, however, precipitation occurred for sample 1. This precipitate was removed by filtration prior to analysis.

It was postulated that the precipitate might be co-purified RNA which might be required for OGFOD1 activity, or alternatively might inhibit OGFOD1 activity. This theory seemed viable given that OGFOD1 is a ribosomal hydroxylase and hence would be found in an environment of high RNA concentration. Nucleic acid quantitation, based on the relative absorption of a sample at 260 and 280 nM, did not, however, indicate significant differences between the 3 samples (Figure 61 B). As nucleic acid quantitation is a good indication for protein contamination of nucleic acid samples, but not the reverse, the samples were subjected to agarose gel electrophoresis. The agarose gel did not reveal the presence of any nucleic acids in any of the three samples (Figure 61 C). The precipitate is thus likely to result from factors other than nucleic acid contamination.

A.

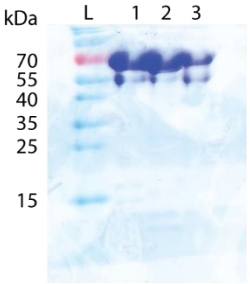

B.

Sample	260/280
1	0.53
2	0.54
3	0.57

C.

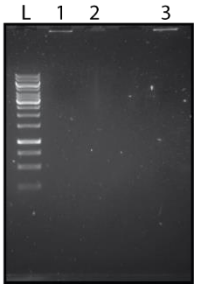

Figure 61: A. SDS-PAGE analysis of three different samples of OGFOD1: 1, 2, and 3. L represents the SeeBlue Plus2 Pre-Stained Standard (Invitrogen) molecular weight marker. All three samples migrate near the predicted molecular weight of 65 kDa. **B.** Nucleic acid quantitation giving the relative ratios of the sample absorptions at 260 nM and 280 nM. The measured absorption ratios do not indicate the presence of co-purified nucleic acids. **C.** Agarose gel electrophoresis analysis of three different batches of OGFOD1: 1, 2, and 3. L represents a 2-log DNA Ladder 0.1-10 kb (Invitrogen). The absence of fluorescence in lanes 1, 2, and 3 indicates the absence of co-purified nucleic acids.

Mass spectrometric analysis of the three samples revealed 2 different masses: the molecular weights of samples 1 and 3 were identical with a molecular weight of 65283 Da, whereas 2 had a different molecular weight of 64249 Da. The molecular weights of samples 1 and 3 were assigned to constructs encoding *N*-terminal His-tagged proteins, whereas the molecular weight of sample 2 corresponded to the *C*-terminal His-tagged protein. Sample 1 contained a further signal at 65458 Da which was assigned to post-translationally glycosylated *N*-terminal His-tagged OGFOD1, a modification which commonly occurs during recombinant protein expression in *E. Coli*.[206]

Sample 3 was highly pure, triply purified protein produced for protein crystallisation experiments: it was subjected to a succession of Nickel-affinity, then size exclusion, then MonoQ ion exchange columns. Samples 1 and 2 were purified in one step, using a Ni-affinity column only. Enzyme activity can be affected by both protein construct and method of purification. A new protein purification was therefore carried out; protein samples were removed and checked for activity after each purification step. A clear decrease in activity was observed after each column: the nickel affinity column-only purified OGFOD1 yielded about 60% hydroxylation under the trial conditions, whereas additional purification *via* a MonoQ basic exchange column gave protein which enabled hydroxylation to only about 30%. It was hence decided to purify OGFOD1 using a Ni-affinity column without further purification for activity assays. Studies on the effect of various additives on OGFOD1 activity, such as sodium chloride (NaCl), dithithreitol (DTT), *tris*(2-carboxyethyl)phosphine (TCEP), or glycerol, had no considerable effect on activity. In fact, activity seemed to somewhat decrease at high NaCl concentration and with addition of glycerol, whereas DTT and TCEP had no effect at the tested concentrations (Figure 62).

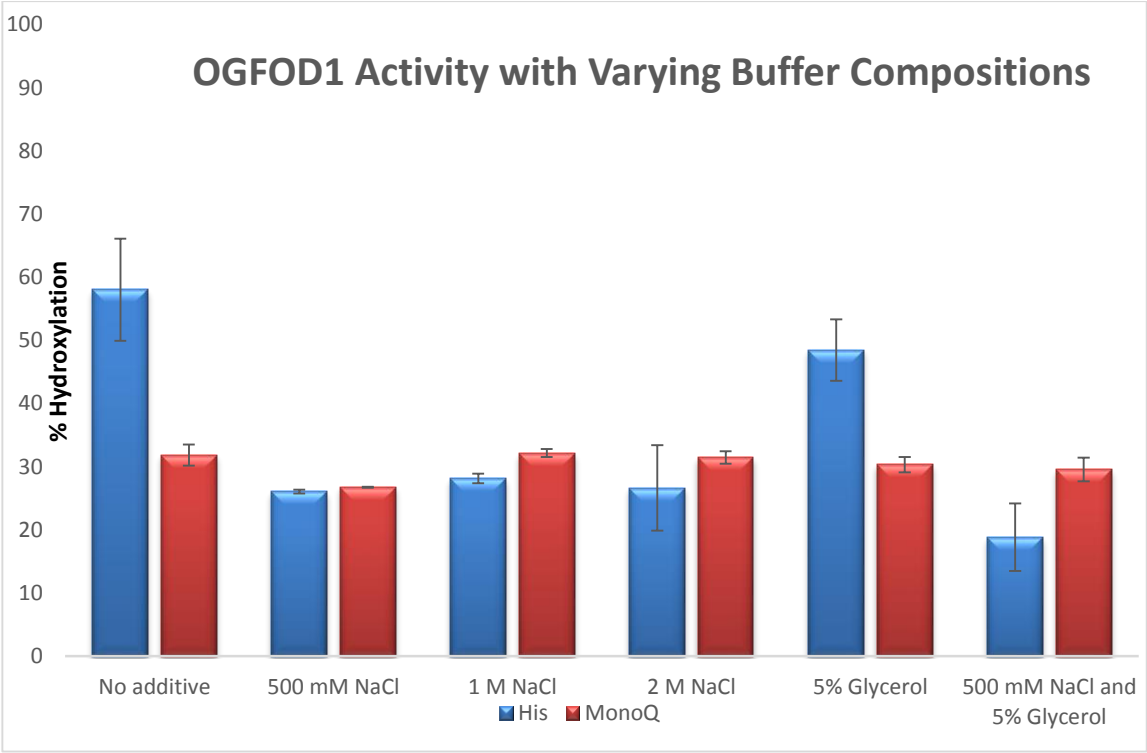

Figure 62: Comparison of OGFOD1 activity after purification with Ni-affinity column only (His) and additional MonoQ ion exchange column and various buffer additives. Measurements were carried out in triplicate using OGFOD1 (10 µM), RPS23 (sequence VLEKVGVEAKQPNSAIRKCV-NH_2, 100 µM), 2OG (300 µM), $(NH_4)_2Fe(SO_4)_2 \bullet 6H_2O$ (100 µM), and sodium ascorbate (1 mM) in 50 mM HEPES pH 7.5 with incubation for 60 min at 37 °C. Data points represent the arithmetic average for each triplicate with the corresponding standard deviation plotted as error bar.

Another complication arose from the RPS23 20mer substrate peptide. Initial hydroxylation experiments were conducted with peptide synthesised in-house. A new batch of the same 20mer peptide was ordered from a commercial supplier. The new commercial batch did not undergo hydroxylation, even with the OGFOD1 sample 3 that hydroxylated the peptide produced in-house. Both peptides were confirmed to have identical sequences by MS-MS analysis: the only difference was that the in-house produced peptide was a *C*-terminal amide, whereas the commercially produced peptide was a *C*-terminal acid. The observation that switching from *C*-terminal amide to acid may turn a peptide from substrate into no substrate was hitherto unnoticed for *in vitro* activity assays for 2OG oxygenases. These results led to a more careful consideration of the carbon termini of peptides for activity studies.

Subsequent OGFOD1 hydroxylation activity studies led to repeatable production (*N*-terminal construct) and purification (Ni-affinity column only) of OGFOD1 for hydroxylation of *C*-terminal amide RPS23 20mer peptide.

Activity Assay by MALDI-TOF MS

The systematic optimisation, and documentation, of OGFOD1 production and purification conditions enabled detection of RPS23 20mer substrate hydroxylation *in vitro*: this provided the basis for OGFOD1 activity assay development.

Current PHD2 prolyl hydroxylase activity assays include AlphaScreen® and MALDI-TOF MS-based methods.[119,181] AlphaScreen® is a fluorescence-based assay using antibody-mediated indirect detection of hydroxylated peptide, whereas MALDI-TOF MS uses direct detection of hydroxylated peptide. Furthermore, the AlphaScreen® assay requires production and optimisation of assay reagents, such as biotinylated peptide substrate, the corresponding detection antibody, and reagent-coated beads. These additional factors represent further hurdles for assay optimisation. Being a direct detection method without the need for handling and optimisation of surrogate assay reagents, MALDI-TOF MS was the method of choice for the development of an OGFOD1 activity assay.

The first step was to determine the linear range of enzyme reaction by performing a time course experiment, with all reagents in excess. The linear reaction range was found to last for about 20 min after initiation of

reaction (Figure 63). Any subsequent reactions were therefore quenched 15 min or less after reaction initiation.

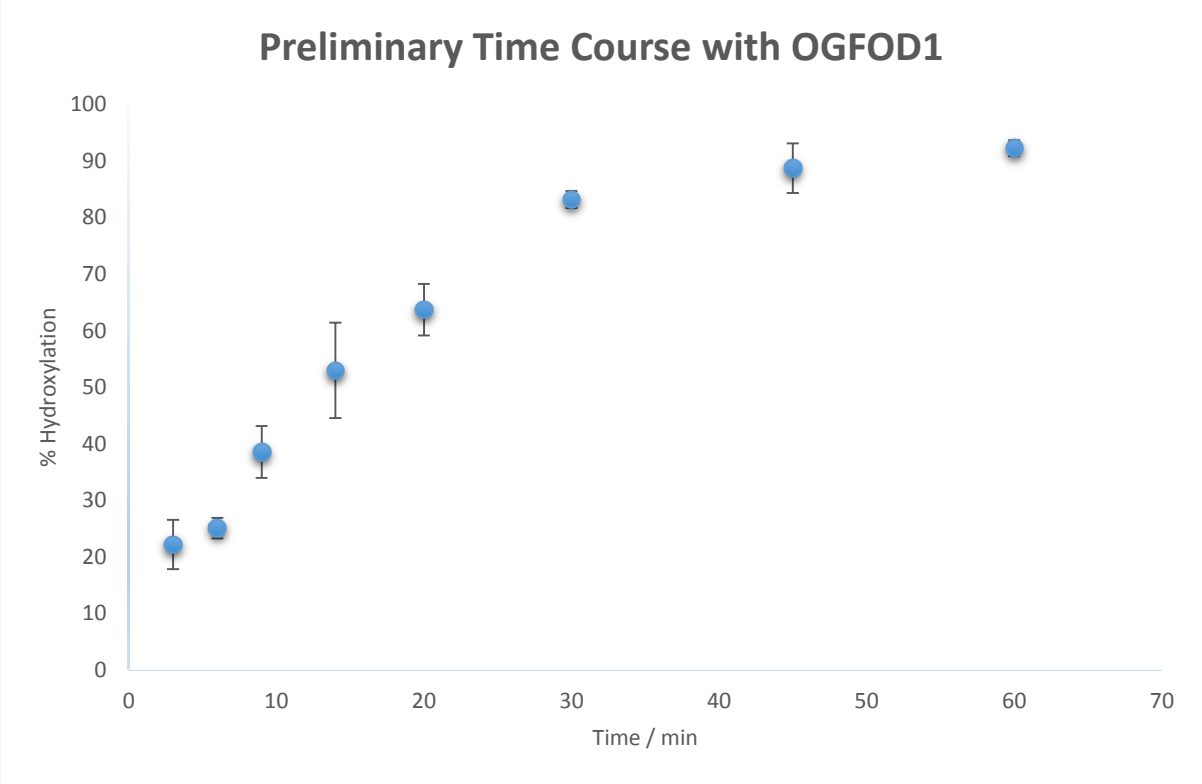

Figure 63: Preliminary MALDI-TOF MS hydroxylation time course with OGFOD1. Measurements were carried out in triplicate using OGFOD1 (10 µM), RPS23 (sequence VLEKVGVEAKQPNSAIRKCV-NH_2, 100 µM), 2OG (300 µM), $(NH_4)_2Fe(SO_4)_2 \bullet 6H_2O$ (100 µM), and sodium ascorbate (1 mM) in 50 mM HEPES pH 7.5 with incubation at 37 °C. Data points represent the arithmetic average for each triplicate with the corresponding standard deviation plotted as error bar.

Initial trial reactions for assay optimisation focused on reducing the final enzyme concentration whilst achieving reaction conversion of at least 25 % within the linear range. Together, these conditions ensure maximisation of assay sensitivity, both from kinetic and signal-to-noise considerations, while minimising the enzyme consumption per reaction. These boundary conditions also called for optimisation of the enzyme-to-substrate ratio in order to account for the intrinsic sensitivity, and signal-to-noise ratio, of MALDI-TOF MS. Various peptide-to-enzyme ratios were investigated: the most favourable reaction conditions with respect to enzyme use minimisation, hydroxylation turnover, and signal-to-noise ratio comprised 1 µM OGFOD1 and 25 µM RPS23 peptide substrate (Figure 64). A final time course with these enzyme and peptide concentrations validated this choice and confirmed a linear reaction rate of 20 min after reaction initiation.

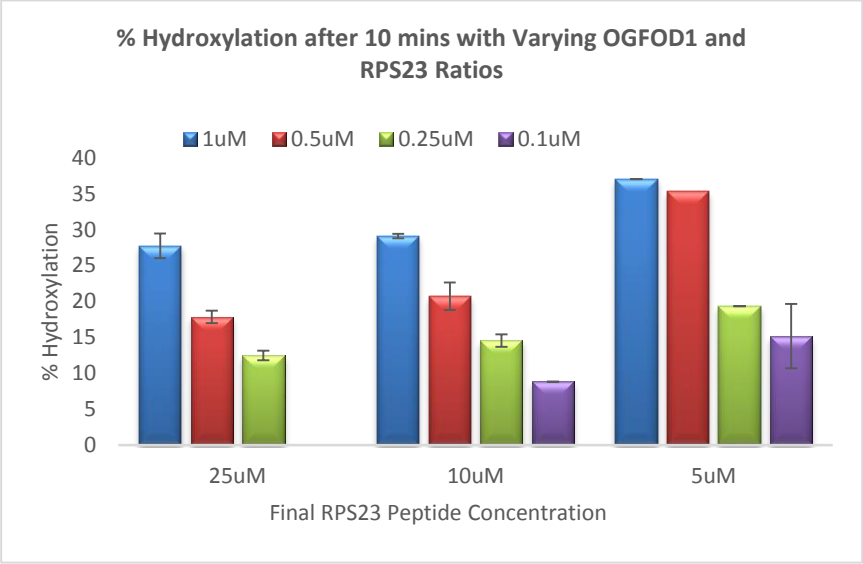

Figure 64: Trial MALDI-TOF MS hydroxylation assay with varying OGFOD1 and RPS23 20mer peptide concentrations. Measurements were carried out in triplicate using OGFOD1 (1.0 (blue), 0.5 (red), 0.25 (green), and 0.1 µM (purple)), RPS23 (sequence VLEKVGVEAKQPNSAIRKCV-NH_2, 25, 10, and 5.0 µM), 2OG (300 µM), $(NH_4)_2Fe(SO_4)_2 \bullet 6H_2O$ (100 µM), and sodium ascorbate (1 mM) in 50 mM HEPES pH 7.5 with incubation for 15 min at 37 °C. Data points represent the arithmetic average for each triplicate with the corresponding standard deviation plotted as error bar.

With every cofactor in excess relative to OGFOD1, including 2OG, Fe(II), and ascorbate, it was sought to optimise for the final concentration of each individual component by investigating the dose dependence for each reaction component on the rate of hydroxylation. These experiments enabled the simultaneous determination of both (apparent) K_m values and minimal cofactor/cosubstrate concentrations for maximal reaction rate. The apparent K_M value for Fe(II), and the K_m value for 2OG were found to be 1.6 µM and 21.8 µM respectively, with the corresponding saturation concentrations at about 10 µM and 100 µM (Figure 65). The order of magnitude of these numbers is in line with the corresponding data found for other 2OG oxygenases, such as PHD2.[45] These data further support that the apparent K_m value for Fe(II) of 267 µM found *via* IFA is not relevant to OGFOD1 enzyme kinetics.

Some, but not all, 2OG oxygenases depend on the presence of ascorbate for their respective reactions to proceed.[207] Despite the role of ascorbate not being clear, it is postulated that ascorbate, a reducing agent, plays a role in promoting reduction of the oxidised active-site Fe(III) back into Fe(II) after substrate hydroxylation. OGFOD1 was shown to display a clear dose response for ascorbate, with the respective apparent K_m and saturation concentration being 23.2 µM and about 100 µM respectively (Figure 65).

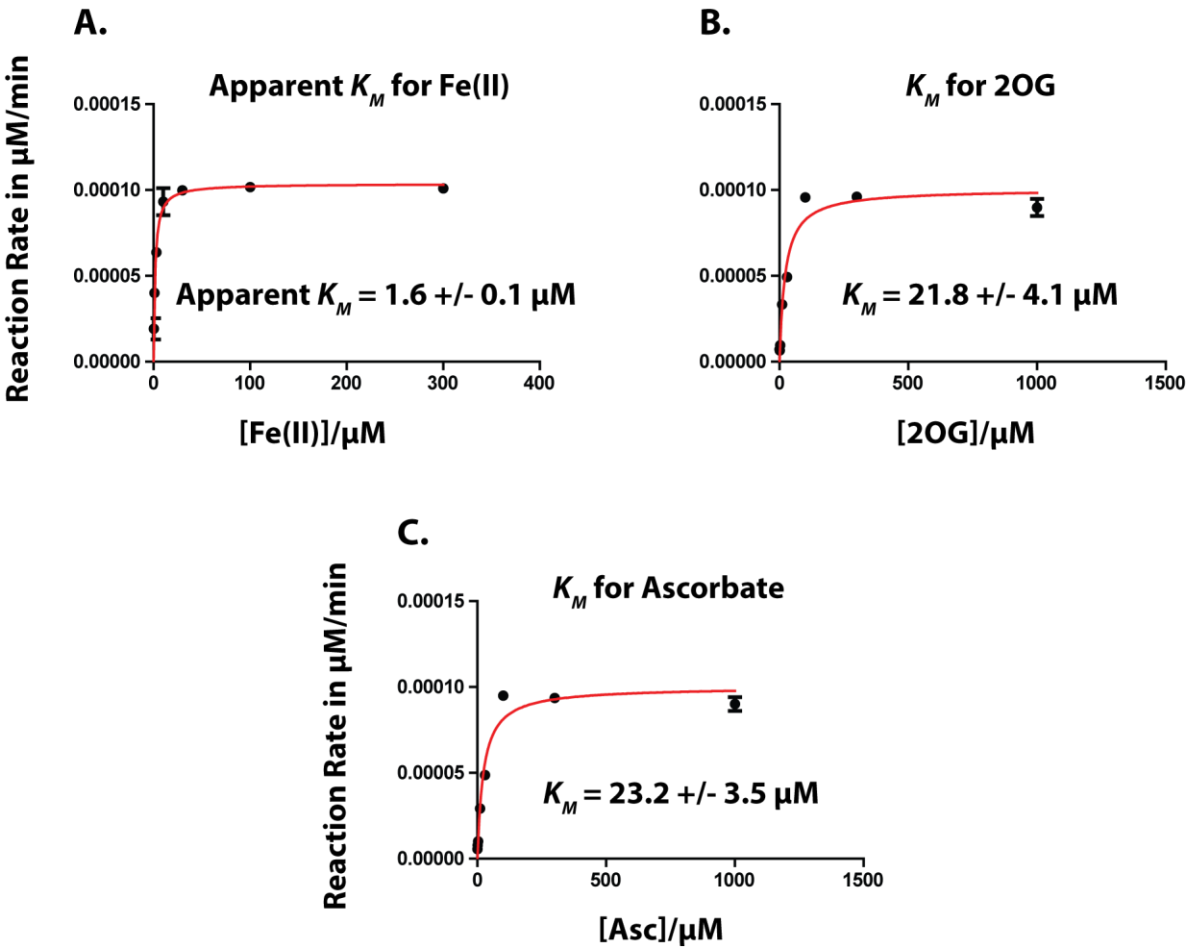

Figure 65: Determination of cofactor and sobsubstrate (apparent) K_M values by the MALDI-TOF MS hydroxylation assay. Measurements were carried out in triplicate using OGFOD1 (1.0 µM), RPS23 (sequence VLEKVGVEAKQPNSAIRKCV-NH_2, 25 µM), and the specified cofactor concentrations in 50 mM HEPES pH 7.5 with incubation for 15 min at 37 °C. Data points represent the arithmetic average for each triplicate with the corresponding standard deviation plotted as error bar. **A.** Determination of apparent K_M for Fe(II). 2OG (300 µM), sodium ascorbate (1 mM), and $(NH_4)_2Fe(SO_4)_2 \bullet 6H_2O$ (300, 100, 30, 10, 3, 1, and 0.3 µM). **B.** Determination of K_M for 2OG. $(NH_4)_2Fe(SO_4)_2 \bullet 6H_2O$ (50 µM), sodium ascorbate (1 mM), and 2OG (1000, 300, 100, 30, 10, 3, 1, and 0.3 µM). **C.** Determination of K_M for ascorbate. $(NH_4)_2Fe(SO_4)_2 \bullet 6H_2O$ (50 µM), 2OG (100 µM), and sodium ascorbate (1000, 300, 100, 30, 10, 3, 1, and 0.3 µM).

Determination of the K_m for the RPS23 20mer substrate yielded a value of 159 µM, and the corresponding graph suggests maximal reaction rate is achieved around 200 µM peptide (Figure 66).

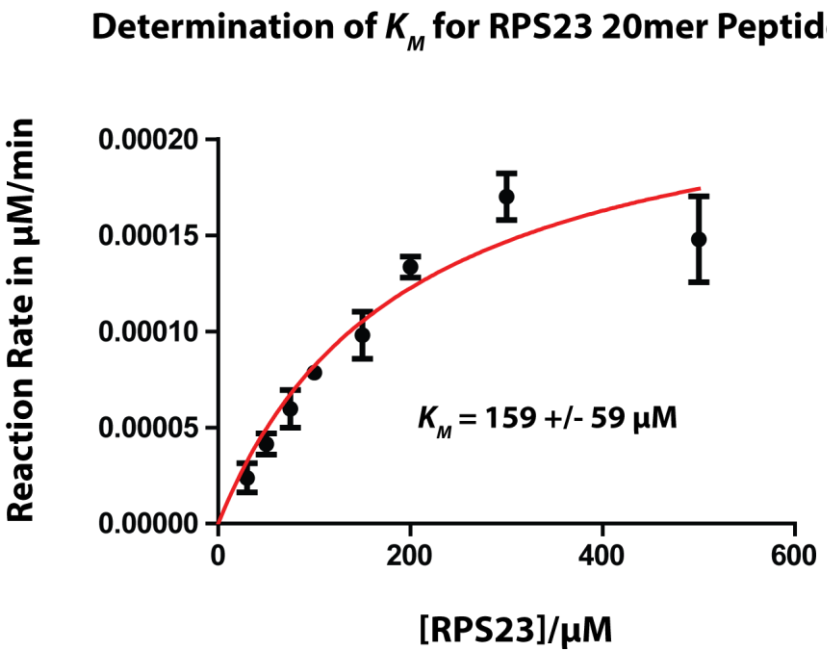

Figure 66: Determination of K_m for RPS23 20mer peptide substrate. Measurements were carried out in triplicate using OGFOD1 (1 µM), 2OG (100 µM), $(NH_4)_2Fe(SO_4)_2 \bullet 6H_2O$ (50 µM), and sodium ascorbate (100 µM), and RPS23 (sequence VLEKVGVEAKQPNSAIRKCV-NH_2, 500, 300, 200, 150, 100, 75, 50, 30 µM) in 50 mM HEPES pH 7.5 with incubation for 15 min at 37 °C. Data points represent the arithmetic average for each triplicate with the corresponding standard deviation plotted as error bar.

Use of 200 µM final peptide, together with 1 µM OGFOD1, however, did not result in sufficient turnover (> 25 %) for reliable quantification of reaction kinetics. This complication, which is an intrinsic sensitivity drawback of MALDI-TOF MS, has also been identified for MALDI-TOF MS-based assays for PHD2.[208] Inspection of the initial trial reactions with varying peptide-to-enzyme ratios (Figure 64), as well as the corresponding PHD2 assay led to the decision to use a final OGFOD1 concentration of 1 µM and to arbitrarily fix the final RPS23 20mer peptide concentration at 25 µM, below the saturating concentration, as a trade-off between assay sensitivity and optimal peptide concentration. Given all other cofactors are used at their respective saturation concentration, and the same assay will be used for all subsequent studies within this context, all the values obtained will be comparable between themselves. In summary, the final MALDI-TOF MS *in vitro* hydroxylation assay conditions were partially optimised as follows (Table 8):

Final Concentration	Initial Conditions	Optimised Conditions
OGFOD1	10 µM	1 µM
RPS23 20mer	100 µM	25 µM
2OG	300 µM	100 µM (25 µM)*
Fe(II)	100 µM	50 µM (10 µM)**
Ascorbate	1000 µM	100 µM
Reaction Time	60 min	15 min

Table 8: Summary of optimisation of MALDI-TOF MS hydroxylation assay for OGFOD1 activity. * The 2OG concentration for inhibitor studies was adjusted to the 2OG K_m value of 25 µM in order to enable competition between inhibitor and co-factor. ** The saturating concentration for Fe(II) was found to be around 10 µM. Nevertheless, 50 µM were used in practice to parallel the corresponding PHD2 MALDI-TOF MS inhibitor assay.

The partially optimised *in vitro* hydroxylation conditions were subsequently used for inhibitor screening and IC_{50} determinations. As the final OGFOD1 concentration is 1 µM, inhibitors tending towards single-digit micromolar IC_{50} values approach the limits of assay sensitivity, and the highest measurable potency, by definition, will be an IC_{50} of 0.5 µM, assuming 100 % enzyme activity. Assay handling was directly adapted from histone demethylase *in vitro* assay handling. Two master solutions were prepared in HEPES buffer (50 mM, pH 7.5): one containing enzyme only, the other containing cofactors and substrate. Inhibitor stock solutions were incubated at 37°C with the enzyme solution for 5 min before the hydroxylation reaction was initiated by adding the cofactor/substrate master solution. As a proof of principle, dose response curves were obtained for both NOG **22** and 2,4-PDCA **24**: the determined IC_{50} values were 0.8 µM and 0.5 µM respectively (Figure 67).

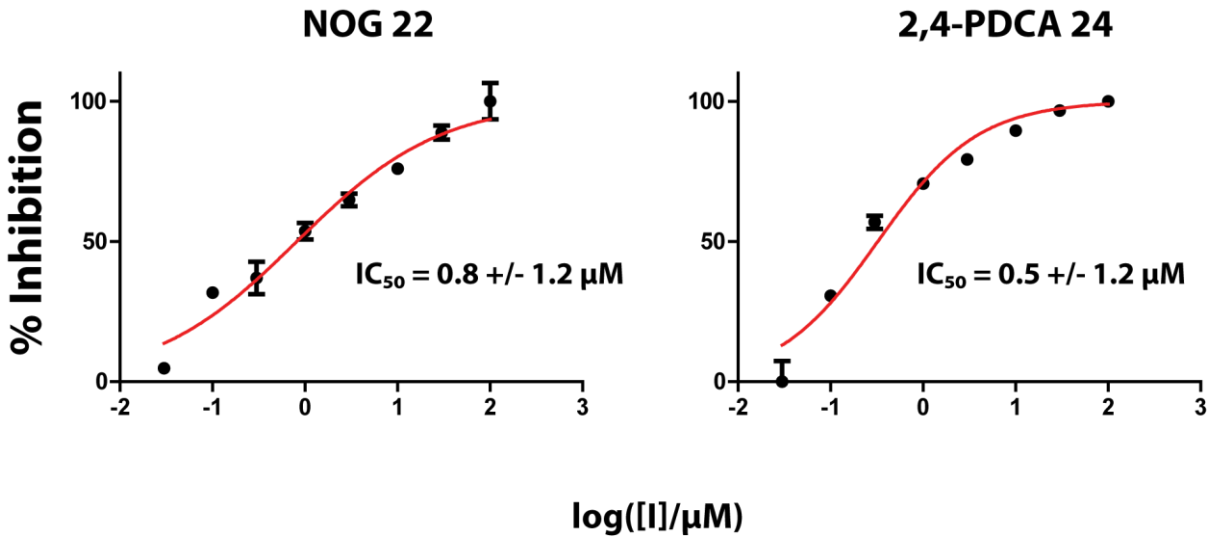

Figure 67: Determination of IC_{50} values for NOG **22** and 2,4-PDCA **24** against OGFOD1. Measurements were carried out in triplicate using OGFOD1 (1 µM), 2OG (25 µM), $(NH_4)_2Fe(SO_4)_2 \bullet 6H_2O$ (50 µM), sodium ascorbate (100 µM), and RPS23 (sequence VLEKVGVEAKQPNSAIRKCV-NH_2, 25 µM), and inhibitor (100, 30, 10, 3.0, 1.0, 0.3, 0.1, and 0.03 µM) in 50 mM HEPES pH 7.5 with incubation for 15 min at 37 °C. Data points represent the arithmetic average for each triplicate with the corresponding standard deviation plotted as error bar.

RapidFire™ Activity Assay

The MALDI-TOF MS *in vitro* assay was perfectly suitable for initial OGFOD1 inhibitor testing, incorporating all advantages of mass spectrometry-based assays: label-free detection, quantitative analysis, (near)-native reaction substrates and products (as opposed to the need for radioactivity, surrogate analytes, and indirect or secondary components), and the advantage of functional biochemical, rather than target binding, assays.[182] The major disadvantages of MALDI-TOF MS, however, are sample preparation and data acquisition: each reaction needs to be individually spotted onto the MALDI sample plate and then mixed with the α-cyano-4-hydroxycinnamic acid (CHCA) matrix solution. Data acquisition is also relatively cumbersome because acquisition parameters usually need to be adjusted individually for every sample (in principle, the laser needs to be focused for every sample in order to optimise signal-to-noise ratio and obtain high-quality data; automation failed to provide reliable results). MALDI-TOF MS is therefore suitable for low throughput, but not medium- to high-throughput applications. Another drawback of the MALDI-TOF MS-based assay is the end-point nature of the assay. In general, continuous reading platforms are more convenient to use, especially for reaction monitoring and kinetic studies.

The RapidFire™ technology (Agilent), in analogy with LC-MS methods, combines the advantages of MS-based methods with plate-reader technology.[182] The time-limiting step of LC, such as sample run time and the general need for protein removal before sample run, is however overcome by use of integrated, automated, micro-scale solid-phase extraction (µSPE), leading to cycle times of only 6-10 s per sample. This technology is compatible with many biological matrices, such as cell culture supernatant, tissue extracts and plasma, whole blood, and urine. Reactions can hence be run in a plate format, with continuous sample extraction and analysis, without the need for prior sample preparation, such as protein removal.

In an effort to investigate whether the moderate assay sensitivity of MALDI-TOF MS is inherent to the MS sensitivity, and whether it can therefore be improved by using more sensitive equipment, the assay conditions from the MALDI-TOF MS-based assay were directly applied to RapidFire™: the final enzyme concentration, however, was reduced to 300 nM. No satisfactory time course could, however, be obtained. Increasing the OGFOD1 concentration to 600 nM in the next instance did then give rise to a time course

consistent with the time course obtained with MALDI-TOF MS (Figure 68). The linear reaction rate was observed over 20 min. The observed substrate conversion after 20 min was about 17 %, which is in line with the corresponding conversion at 1 µM final enzyme concentration. In fact, according to basic enzyme reaction kinetics, the rate of reaction is directly proportional to the final enzyme concentration.

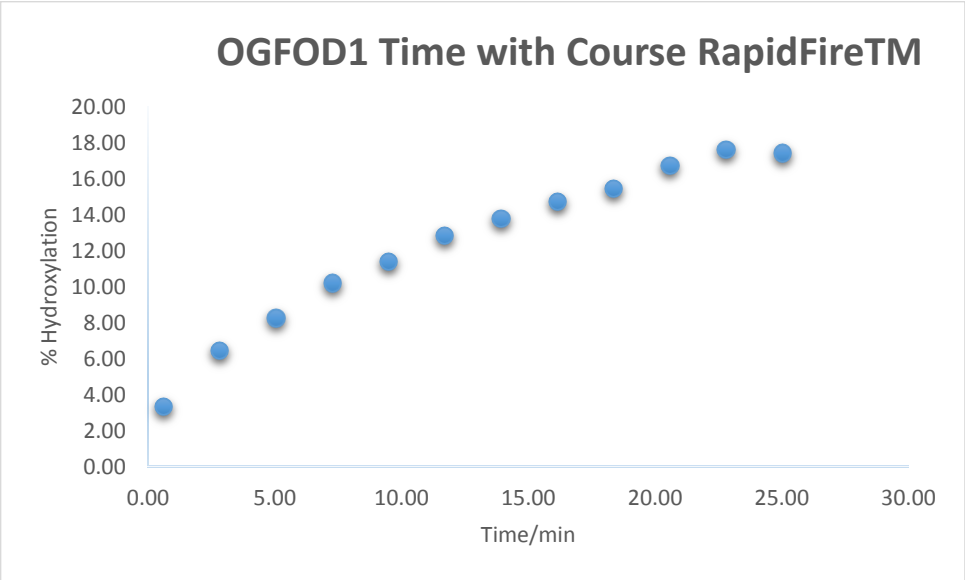

Figure 68: Preliminary RapidFire™ time course with OGFOD1. Measurements were carried out as a singleton using OGFOD1 (600 nM), RPS23 (sequence VLEKVGVEAKQPNSAIRKCV-NH_2, 10 µM), 2OG (50 µM), $(NH_4)_2Fe(SO_4)_2 \bullet 6H_2O$ (50 µM), and sodium ascorbate (100 µM) in 50 mM HEPES pH 7.5 with incubation at room temperature.

Based on this preliminary test, it can be concluded that the MALDI-TOF MS assay conditions can be directly transferred to the RapidFire™ assay platform. This was to be anticipated because the hydroxylation reaction conditions are exactly the same in both instances, merely the method of detection changes. The *in vitro* OGFOD1 activity assay can hence be performed with continuous reading, and at high throughput, by changing the assay platform from MALDI-TOF MS to RapidFire™. Comparison of both assays also led to the conclusion that the method of MS-based detection, i.e. MALDI-TOF *versus* RapidFire™, does not change assay sensitivity. In order to improve assay sensitivity, i.e. achieve at least about 25 % substrate conversion within the linear range of reaction rate, a more catalytically active OGFOD1 protein will be required (possibly *via* further optimisation of expression and purification conditions), or a better *in vitro* substrate (possibly an optimised peptide length/sequence, or a cyclic peptide); or both factors at the same time. Nevertheless, the *status quo* of the optimised MALDI-TOF MS-based activity assay was judged suitable for early-stage OGFOD1 inhibitor development.

Peptide Hydroxylation Trials

Co-immunoprecipitation studies identified a variety of potential OGFOD1 binding partners (Dr Matthew Cockman, unpublished). It was therefore of interest to investigate whether any of these potential binding partners might act as OGFOD1 substrates and be hydroxylated. The potential substrate candidates of interest were Haem-Regulated Initiation Factor 2α Kinase (HRI), THAP domain-containing protein 1 (THAP1), Huntingtin-Associated Protein 1 (HAP1), and Transcriptional Activator Protein Pur-Beta (PURB). Clustal sequence alignment studies with RPS23 were conducted. The homologous sequence was then truncated to a 20mer peptide sequence containing the proline residue corresponding to Pro62 of RPS23 at about mid-sequence. The resulting sequences, as well as the corresponding positive control RPS23 (and RPS23 C-A mutant), were synthesised by MultiPep peptide synthesis (Table 9).

Sequence	Origin
VLEKVGVEAKQPNSAIRKCV	RPS23
VLEKVGVEAKQPNSAIRKAV	RPS23 C Mutant
TGLRTGQLPESLRKRAPVQA	HRI
AQTAQLQPNLVSASAAVLLT	THAP11, P147
VLLTLQATVDSSQAPGSVQP	THAP11
VGRRPGVSGPERAAFIRELE	HAP1
GGGGFGAGPGPGGLQSGQTI	PURB, 173 and 175
DDELAGGPGGGAGGPGGGLY	PURB, 216 and 223

Table 9: 20-mer peptide sequences for OGFOD1 hydroxylation trials.

THAP11 and THAP11 P147 were rather insoluble and the results may not be entirely reliable. The peptides were initially incubated in equimolar ratio with OGFOD1 for 3 h: none of the peptides, except for both positive control RPS23 and RPS23 C-A mutant, were hydroxylated. Future studies could be to investigate various positions in the peptide of the proline residue to be hydroxylated, with various peptide lengths. If possible, whole-protein hydroxylation studies may be undertaken. Alternatively, it may be worthwhile to investigate whether any of the above peptides act as OGFOD1 inhibitors.

Summary

The work in this chapter was primarily aimed at developing *in vitro* assay platforms suitable for OGFOD1 inhibitor screening.

The differential scanning fluorimetry (DSF) binding assay was validated and judged suitable for OGFOD1 inhibitor studies. An alternative binding assay used for PHD2 inhibitor screening, called intrinsic fluorescence assay (IFA), was found to be unsuitable for applications with full-length OGFOD1 protein.

The development of an OGFOD1 activity assay was initially impeded because OGFOD1 catalytic activity was relatively low. The optimisation, and documentation, of OGFOD1 purification conditions, as well as assay components, was therefore undertaken to identify parameters responsible for OGFOD1 catalytic activity.

After the successful determination of parameters for the production of catalytically active OGFOD1, a MALDI-TOF MS activity assay was developed for the assessment of small-molecule inhibitors for OGFOD1. Kinetic experiments led to partial optimisation of assay conditions suitable for initial inhibitor development.

Chapter VI: Inhibitor Development for OGFOD1

Structural Considerations

An X-ray co-crystal structure of OGFOD1 in complex with NOG **22** was recently obtained (Horita *et al.*, unpublished). Both the OGFOD1 active site, and the substrate binding pocket, are structurally very similar to the active site and substrate binding pocket of PHD2. Overlay of the structures of OGFOD1 and PHD2 in complex with NOG **22** exemplify the very similar, if not identical, binding mode of this generic inhibitor. The metal-chelating moiety binds to the active site Fe(II) in a bidentate manner, while the carboxylate interacts with the enzyme active site tyrosine and arginine residues (Tyr169 and Arg230 for OGFOD1, Tyr329 and Arg383 for PHD2) in a salt bridge interaction (Figure 69). The structural similarities between these prolyl hydroxylases imply that the biggest challenge for OGFOD1 inhibitor design is likely to achieve selectivity over PHD2.

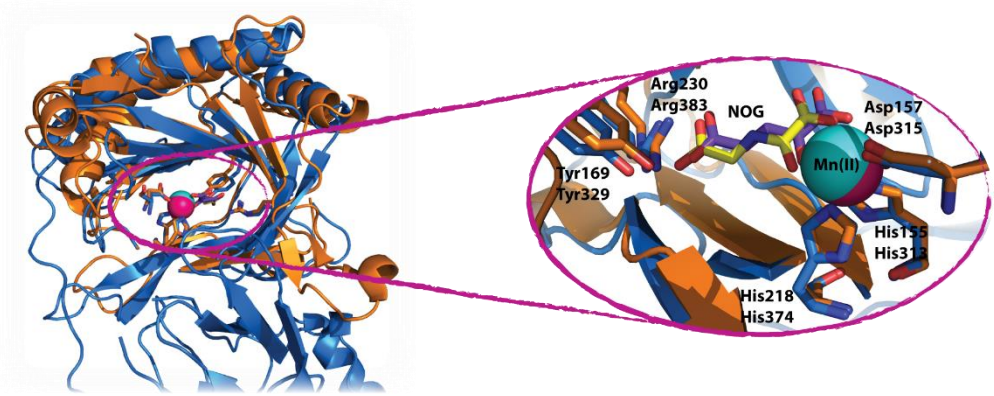

Figure 69: View from an overlay of X-ray crystal structures of the catalytic domains of the OGFOD1 (blue) and PHD2 (orange) (PDB ID: 4BQY) prolyl hydroxylases. Inspection of the catalytic sites reveals near-identical binding modes of the generic 2OG oxygenase inhibitor NOG **22**. The highlighted amino acid residues with the lowest number of each pair relate to OGFOD1, the ones with the highest number relate to PHD2.

Inspection of individual amino acids within the OGFOD1 and PHD2 active sites and substrate binding pockets reveals seven differences in the residues in the direct vicinity of the active site (Figure 70). These were judged to offer potential handles for achieving selectivity of future inhibitors.

OGFOD1	PHD2	Nature of Difference
Leu152	Tyr310	Polar *vs.* apolar
Phe98	Asp254	Polar *vs.* apolar
Lys91	No equivalent	Sterics
Arg162	No equivalent	Sterics
Gln100	Ile256	Polar vs apolar
Tyr96	Tyr310	Shifted by some distance
No equivalent	Met299	Sterics

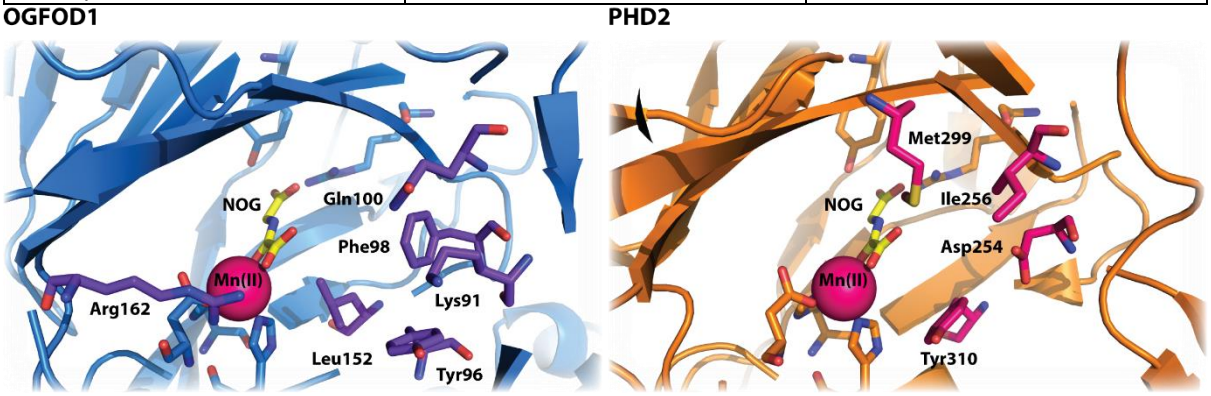

Figure 70: View from an overlay of X-ray crystal structures of the catalytic domains of the OGFOD1 (blue) and PHD2 (orange) (PDB ID: 4BQY) prolyl hydroxylases. The highlighted residues correspond to the residues listed in the above table and are unique to the respective enzyme.

Strategy for OGFOD1 Inhibitor Design

The high degree of structural similarity between OGFOD1 and PHD2 offered a viable starting point for OGFOD1 inhibitor design. Despite the challenge of achieving selectivity, there is wealth of information about current PHD2 inhibitors (see Figure 15, Chapter I). Notably, some inhibitors are in various stages of drug development, including in patient clinical trials. By definition, these inhibitors have therefore been optimised not only in terms of potency and selectivity, but also in terms of administration, distribution, metabolism, excretion, and toxicity (ADMET). It was therefore postulated that the highest value for initial screening could be achieved by compiling a focused library based on known PHD2 inhibitors of pharmaceutical relevance. This methodology would, ideally, maximise the likelihood of finding hit compounds against OGFOD1 (given the high structural similarity with PHD2) while maintaining ADMET properties based on a chemotype already optimised for clinical use. The challenge of selectivity may then be addressed by considerations of the above structural differences. Exploiting the structural similarities between OGFOD1 and PHD2 was therefore considered to be of significantly higher value than other approaches based on, for example, high-throughput screening, or focused libraries centred around 2OG mimetics.

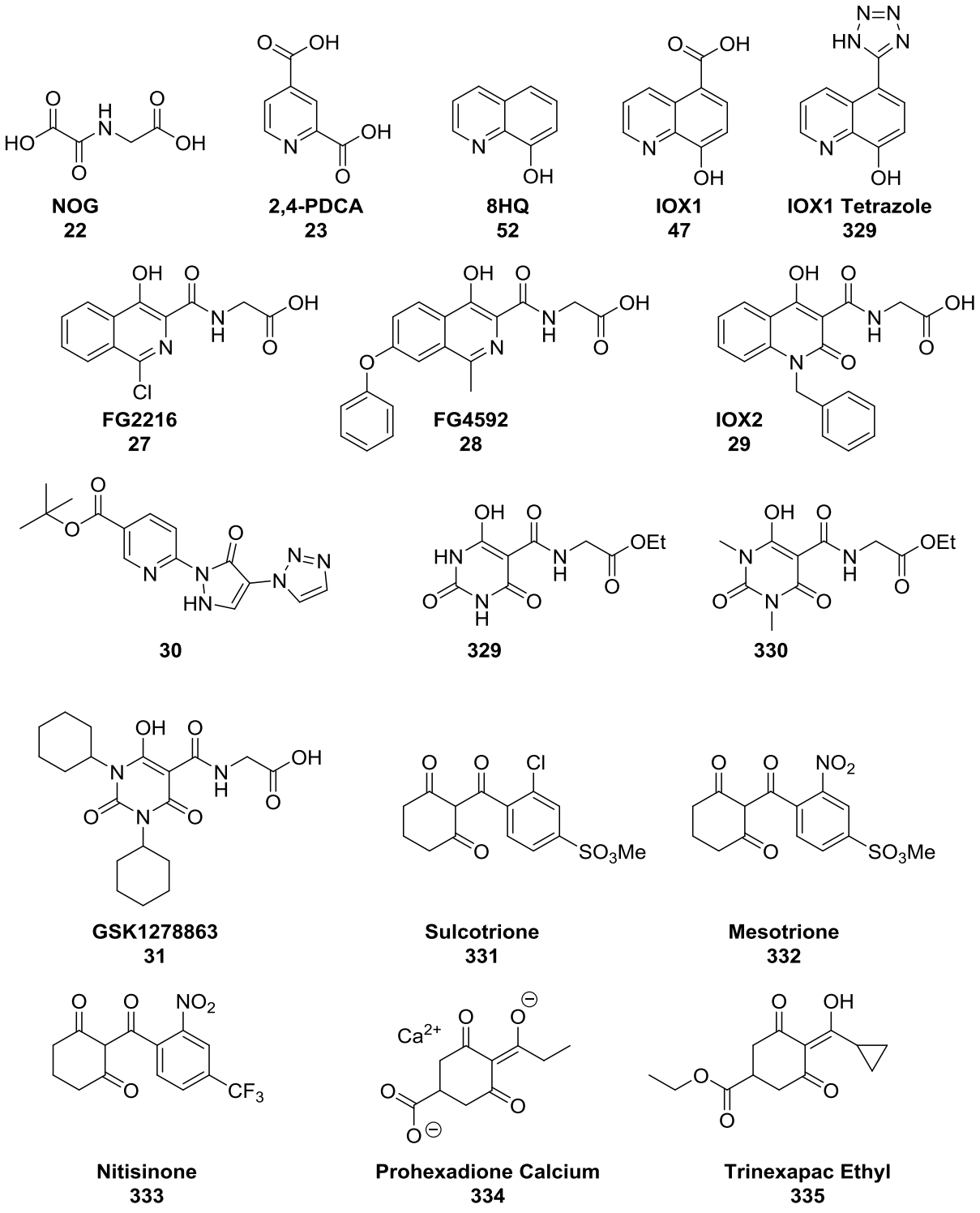

Figure 71: Initial screening library consisting of known, biologically characterised, inhibitors for 2OG oxygenases.

The initial library consisted of the known PHD2 inhibitors depicted in Figure 71. The library was extended to include 4-hydroxyphenylpyruvate dioxygenase (HPPD) inhibitor nitisinone **333** and the related plant growth inhibitors sulcotrione **331**, mesotrione **332**, prohexadione calcium **334**, and trinexapac ethyl **335** because these inhibitors are based on the same triketone chemotype as GSK1278863 **31** and are used in the clinic as well as agriculture.[127,208-214] These inhibitors were screened by both differential scanning fluorimetry (DSF)

and matrix-assisted laser desorption ionisation time-of-flight mass spectrometry (MALDI-TOF MS) against OGFOD1 and PHD2.[119,203]

Each PHD2 inhibitor considerably stabilised OGFOD1 (Figure 72). This observation is in line with the high structural similarity between both enzymes. Most PHD2 inhibitors seemed to stabilise OGFOD1 to a somewhat lesser extent than PHD2. Whether this observation was an indication of selectivity might be debatable given the assay was performed on full-length OGFOD1, but catalytic domain-only PHD2. Further, OGFOD1 contains an unstructured acidic loop region which might result in an overall lower thermal stability compared to PHD2. Nevertheless, the triketone HPPD and plant growth inhibitors **331** - **335** had little stabilisation effect on PHD2 relative to the known potent PHD2 inhibitors **27** - **31**, while the relative stabilising effect of these molecules on OGFOD1, compared to the stabilising effect of PHD2 inhibitors, was greater. In fact, trinexapac ethyl **335** appeared to stabilise OGFOD1 to a similar extent to NOG **22** or 2,4-PDCA **23**.

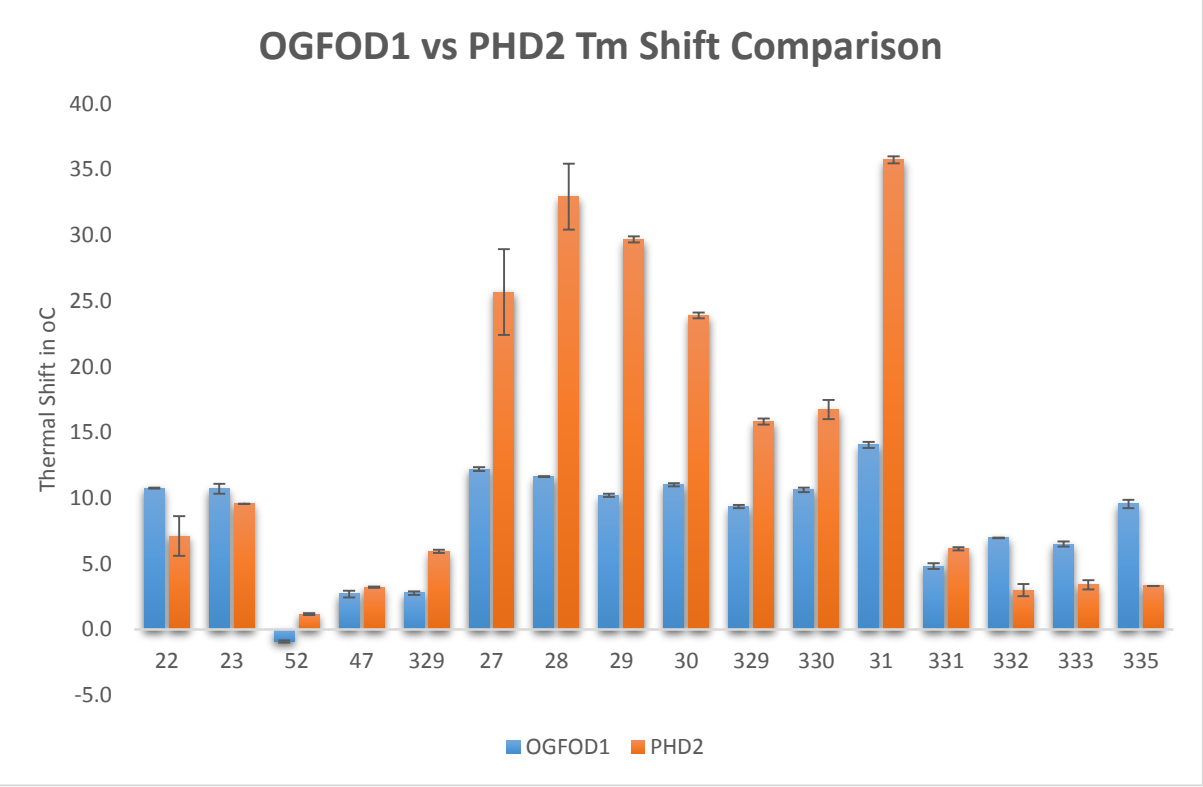

Figure 72: DSF binding assay with OGFOD1. Measurements were carried out in triplicate using OGFOD1 (2 µM), $MnCl_2 \bullet 4H_2O$ (50 µM), inhibitor (200 µM) and Sypro® Orange (1:5000 dilution) in 50 mM HEPES pH 7.5. Data points represent the arithmetic average for each triplicate with the corresponding standard deviation plotted as error bar.

The single concentration MALDI-TOF MS-based activity screening results paralleled the results from the DSF assay (Figure 73). All the PHD2 inhibitors were also potent inhibitors of OGFOD1. However, the triketone

HPPD and plant growth inhibitors **331** - **335** displayed moderate inhibition against OGFOD1, while having no measurable effect on PHD2 activity. Subsequently, dose response curves for the PHD2 inhibitors, as well as mesotrione **332**, prohexadione calcium **334**, and trinexapac ethyl **335** were obtained against OGFOD1. FG2216 **27**, FG4592 **28**, IOX2 **29**, and **30** all displayed sub-micromolar IC_{50} values, whereas the series based around **31** was somewhat less potent in the single-digit micromolar IC_{50} range. Mesotrione **332**, prohexadione **334**, and trinexapac ethyl **335** displayed IC_{50} values in the mid double-digit micromolar range (Figure 74).

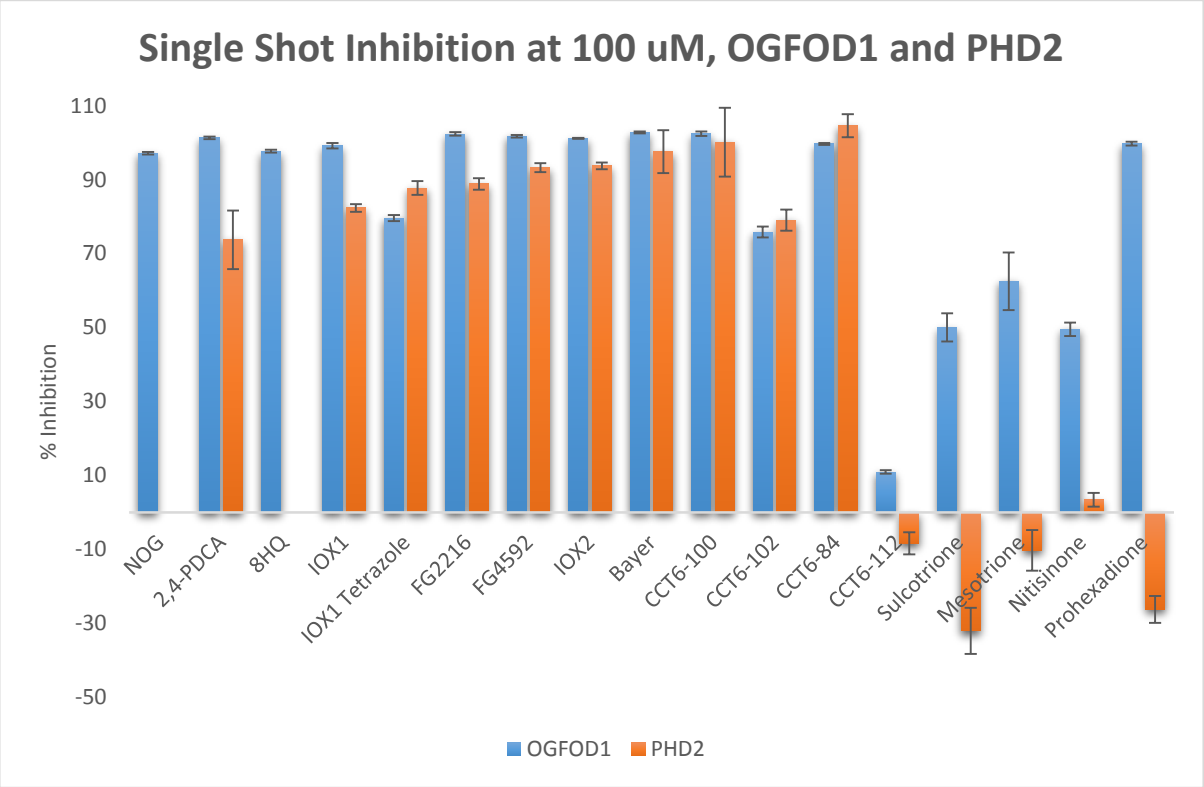

Figure 73: Single concentration inhibition of OGFOD1 by MALDI-TOF MS hydroxylation assay. Measurements were carried out in triplicate using OGFOD1 (1 µM), 2OG (25 µM), $(NH_4)_2Fe(SO_4)_2 \bullet 6H_2O$ (50 µM), sodium ascorbate (100 µM), RPS23 (sequence VLEKVGVEAKQPNSAIRKCV-NH_2, 25 µM), and the specified inhibitor (100 µM) in 50 mM HEPES pH 7.5 with incubation for 15 min at 37 °C. Data points represent the arithmetic average for each triplicate with the corresponding standard deviation plotted as error bar.

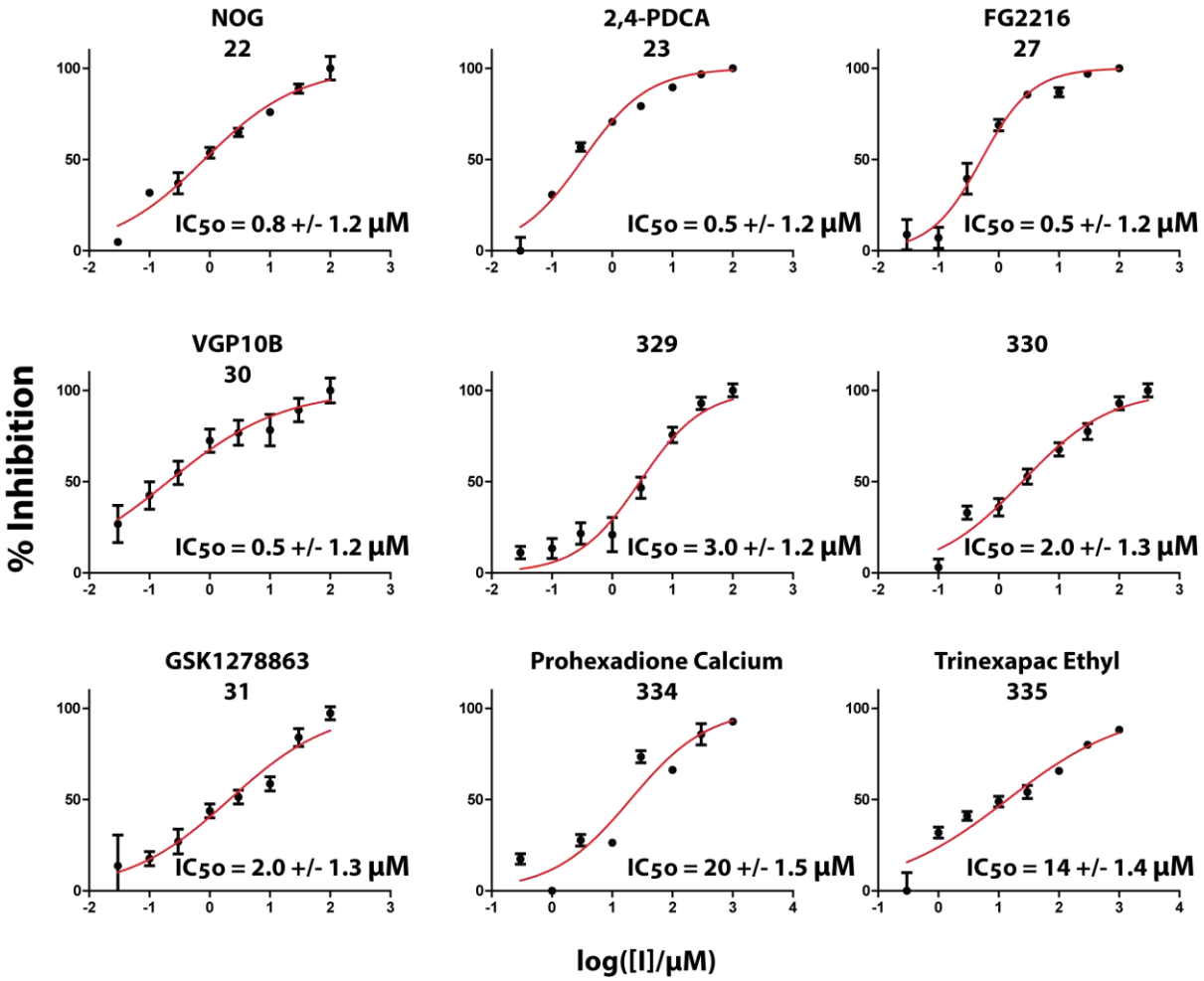

Figure 74: Determination of IC_{50} values against OGFOD1. Measurements were carried out in triplicate using OGFOD1 (1 µM), 2OG (25 µM), $(NH_4)_2Fe(SO_4)_2 \bullet 6H_2O$ (50 µM), sodium ascorbate (100 µM), RPS23 (sequence VLEKVGVEAKQPNSAIRKCV, 25 µM), and inhibitor (8-point titration, 1000, 300, 100, 30, 10, 3.0, 1.0, 0.3, 0.1, and 0.03 µM) in 50 mM HEPES pH 7.5 with incubation for 15 min at 37 °C. Data points represent the arithmetic average for each triplicate with the corresponding standard deviation plotted as error bar.

Molecular Modelling

GSK1278863 **31** and sulcotrione **331** were manually docked into the active sites of both OGFOD1 and PHD2 based on considerations of metal-chelating properties, salt bridge interaction, and overlay with FG2216 **27**. It is likely that both **31** and **331** engage in Fe(II) chelation using their 1,3-diketone motif, possibly *via* the corresponding enolate form. The glycine-type side chain of GSK1278863 **31** was positioned to interact in a salt bridge interaction with Arg230 of OGFOD1, in analogy with co-crystal structures with other PHD2 inhibitors, such as FG2216 **27** (Figure 75).

The structure of **31** explores two planes perpendicular to each other: one plane, P_x, containing the core structure with the Fe(II) and salt bridge interaction motif, the other plane, P_y, spanning the cyclohexyl side chains. These side chains are conveniently positioned to, in principle, engage in interactions with the residues

which are exclusive to the OGFOD1 active site (Figure 70). In contrast, compounds based on the isoquinoline chemotype primarily span one single plane P_x: they are completely flat, and therefore have less potential to offer synthetic handles to interact with the different key residues which delineate the OGFOD1 from the PHD2 active site.

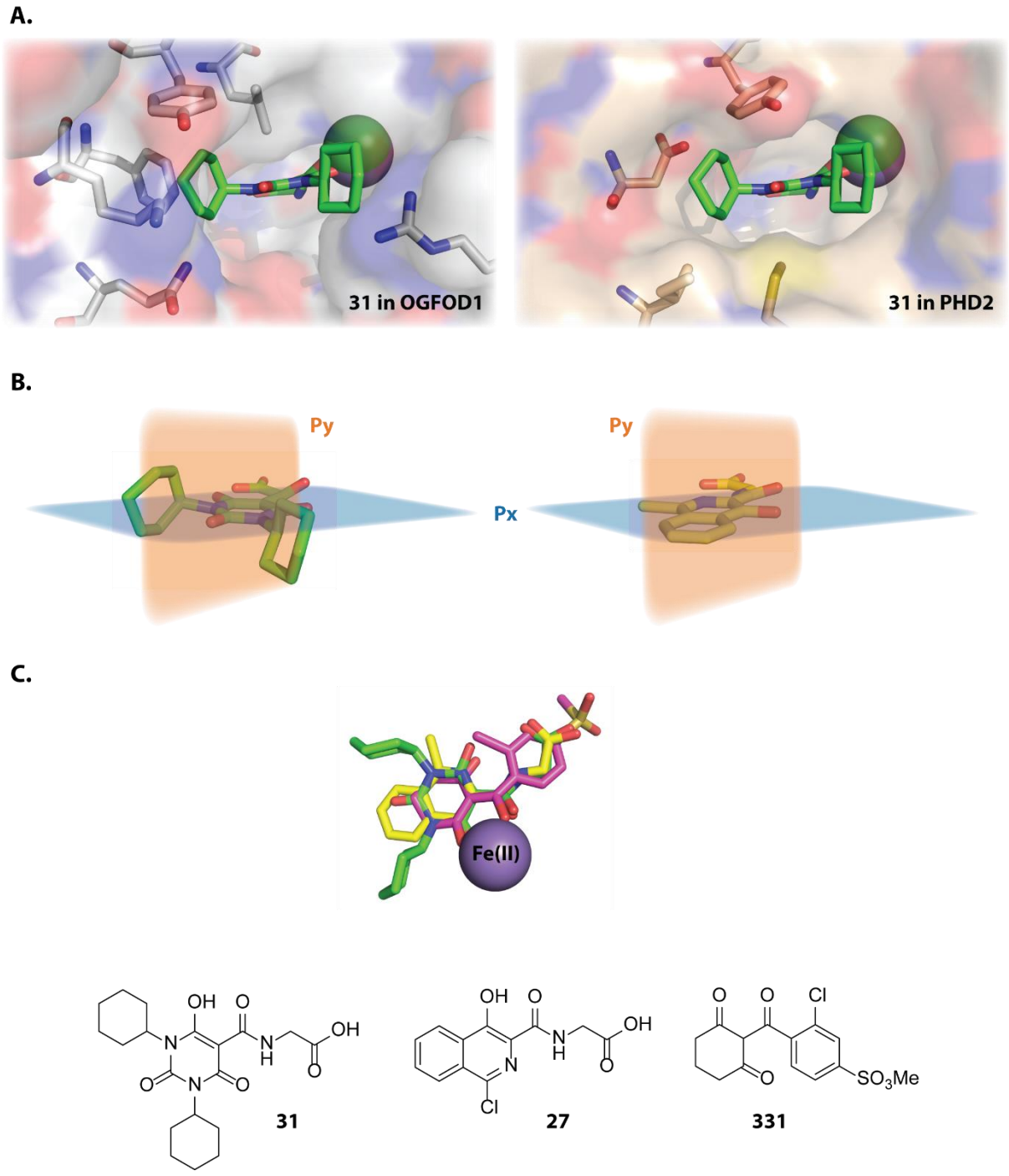

Figure 75: A. *In silico* binding model of **31** in OGFOD1 and PHD2. The triketone moiety binds the active site metal, whereas the cyclohexyl substituents lean onto the substrate binding pocket. The PHD2 entrance channel appears to be wider than the corresponding OGFOD1 pocket. **B. 31** occupies two planes Px (blue) and Py (orange) with the triketone motif being in plane Px and the cyclohexyl substituents reaching into plane Py. FG2216 **27** only occupies one single plane Px. **C.** Overlay of **31** (green), FG2216 **27** (yellow), and sulcotrione **331** (fuchsia). The metal-binding chelating motifs do coincide for all three inhibitors. The *N*-substituents of the **31** scaffold offer an opportunity to reach into space other than the metal-binding plane.

Lead Compound Generation

In an effort to achieve selectivity for OGFOD1 while ensuring good potency, the structural properties of the PHD2 inhibitors and the plant growth inhibitors were inspected. According to the DSF assay, it seemed like the plant growth inhibitors might stabilise OGFOD1 to a greater extent than PHD2; the known PHD2 inhibitors stabilised PHD2 to a greater extent than OGFOD1. Every tested PHD2 inhibitor possesses a glycine-like carboxylic acid side chain for salt bridge interaction with Arg383 in PHD2, whereas the plant growth inhibitors do not possess such a carboxylic acid side chain. By consideration of the *in silico* model, it was initially thought that the methyl sulfonate in sulcotrione **331**, or the nitro group of mesotrione **332** and nitisinone **333**, might mimic the corresponding carboxylic acid side chain. Another difference between the **31**-based compounds and the triketone HPPD and plant growth inhibitors **331** - **335** is the barbiturate cyclic core as opposed to the cyclohexane 1,3-dione core structure. From a structural point of view, the barbituric acid ring is relatively flat because of the bis-amide functionality, as opposed to the skewed cyclohexane 1,3-dione functionality (this applies to both tautomers of the enolisable moiety). Both structural features, carboxylate or absence thereof, as well as barbiturate *versus* cyclohexane 1,3-dione core motif, hence present potential synthetic handles for achieving selectivity for OGFOD1 against PHD2 (Figure 75).

Exploration of the Core Structure

In order to optimise the core structure of the metal-chelating moiety, a variety of di- and triketone motifs were explored. The fragment library consisted of malonate **336** and 2-acetylcyclohexanone **337** for representing 1,3-diketones, triacetylmethane **338** and the substituted 1,3-cyclohexanedione molecules **339 – 341** as representatives for the triketones, the aromatic 2',6'-dihydroxyacetophene **342**, and barbituric acid **343** (Figure 76).

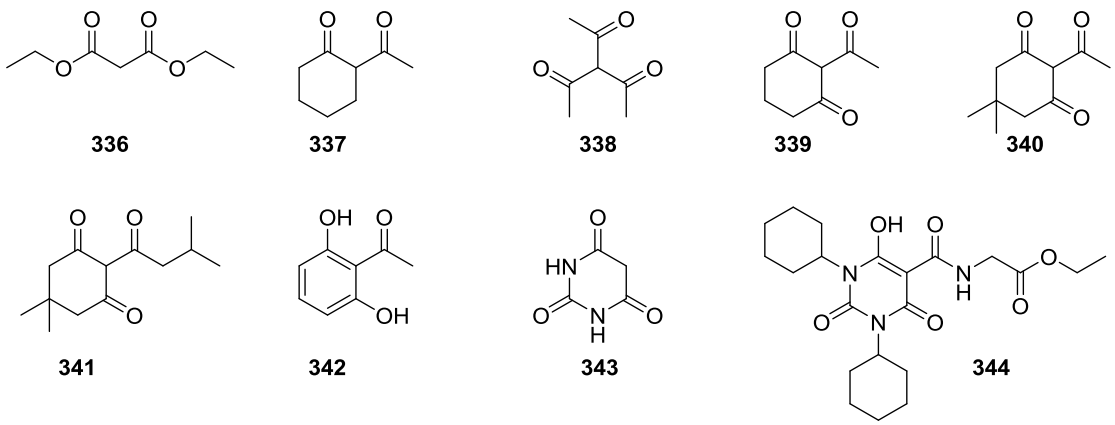

Figure 76: Structural motifs relating to **31** and the triketone HPPD and plant growth inhibitors.

Single point MALDI-TOF MS revealed that OGFOD1 inhibition paralleled the propensity for enolisation (Figure 77). Diketones such as diethyl malonate **336** and 2-acetylcyclohexanone **337** were poor inhibitors, whereas the corresponding triketones, triacetylmethane **338** and 2-acetyl-1,3-cyclohexanediones **339** - **341**, were relatively better inhibitors. The aromatic 2',6'-dihydroxyacetophene **342** was a comparatively poor inhibitor.

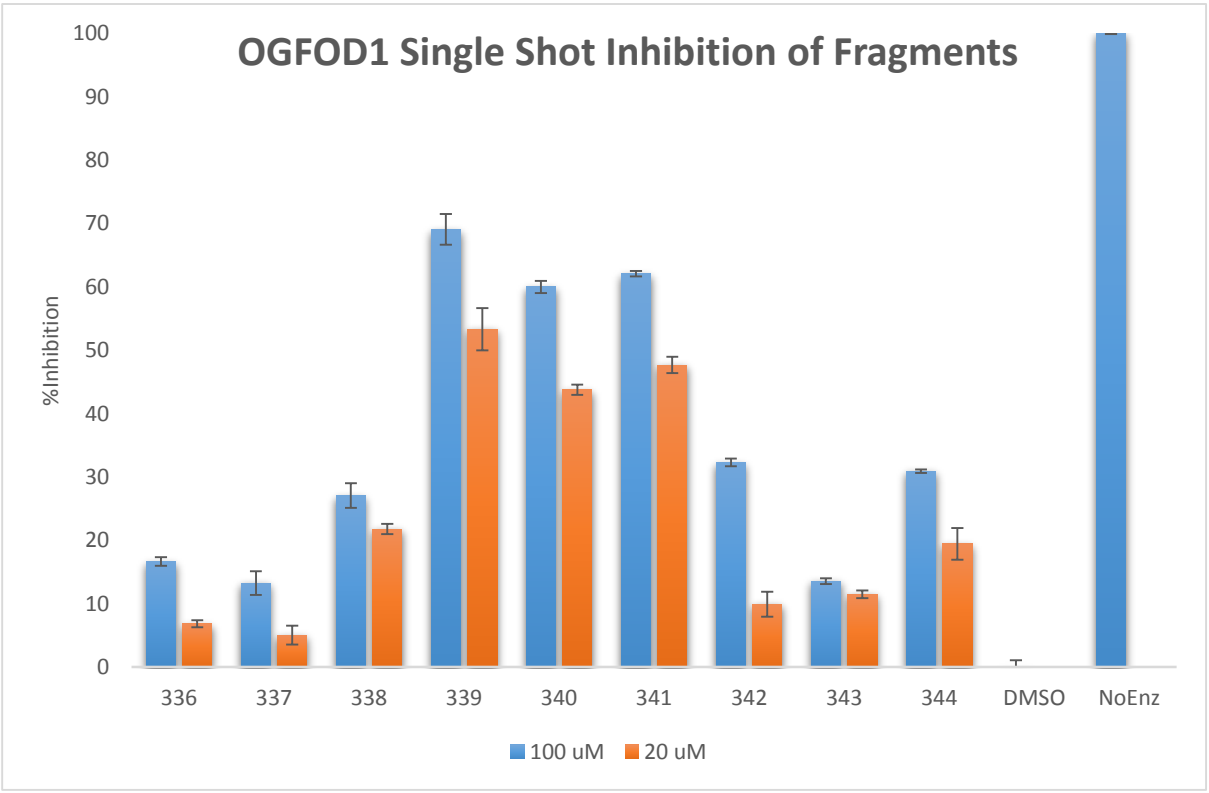

Figure 77: Single point inhibition of OGFOD1 by MALDI-TOF MS hydroxylation assay. Measurements were carried out in triplicate using OGFOD1 (1 µM), 2OG (25 µM), $(NH_4)_2Fe(SO_4)_2 \bullet 6H_2O$ (50 µM), sodium ascorbate (100 µM), RPS23 (sequence VLEKVGVEAKQPNSAIRKCV-NH_2, 25 µM), and inhibitor (100, 20 µM) in 50 mM HEPES pH 7.5 with incubation for 15 min at 37 °C. Data points represent the arithmetic average for each triplicate with the corresponding standard deviation plotted as error bar.

The most potent triketone motif was based on barbituric acid in the form of acetylbarbiturates **345** – **347** (Figure 78). This scaffold also possesses the most acidic proton for enolisation. Not only is the enolisation

driven by the presence of three ketones for conjugate base stabilisation, but also concomitant aromatisation of the barbiturate core upon deprotonation. The 1,3-dimethylbarbituric acid core of **347** further improved both potency and solubility of the inhibitor: subsequent inhibitors were therefore based on the 1,3-dimethylbarbituric acid core structure. It is likely that propensity for enolisation directly parallels metal chelating properties. The more enolisable molecules may hence benefit from a stronger Fe(II) binding contribution which may explain the relatively high potency of these compounds. A core based on thiobarbituric acid, as in **346**, did not reveal any improvements over barbituric acid. Given the higher lipophilicity of thiobarbituric acid compared to barbituric acid, and the commercial unavailability of the corresponding 1,3-dimethyl thiobarbiturate analogue, a series of thiobarbiturates was not explored. After optimisation of the metal-binding core structure, the focus shifted towards optimisation of the side chains at position 5.

Optimisation of Side Chains

Compound **349** was synthesised in an effort to merge the structural features of **330** and the HPPD/plant growth inhibitors **331** - **335**, namely a 1,3-dimethyl barbituric acid core motif from previous optimisation, and an aromatic α-carbon substituent, as opposed to the prevalent glycine-like side chains in commonly used PHD2 inhibitors. Manual docking with sulcotrione **331** suggested that the aromatic substituent might reach inside the active site binding pocket with the methyl sulfonate mimicking the carboxylate of the commonly used PHD2 inhibitors (Figure 75). The initial inhibitors encompassed acetyl **347**, phenyl **349**, benzyl **350**, and hydrocinnamoyl **351** substituents (Figures 78 and 79).

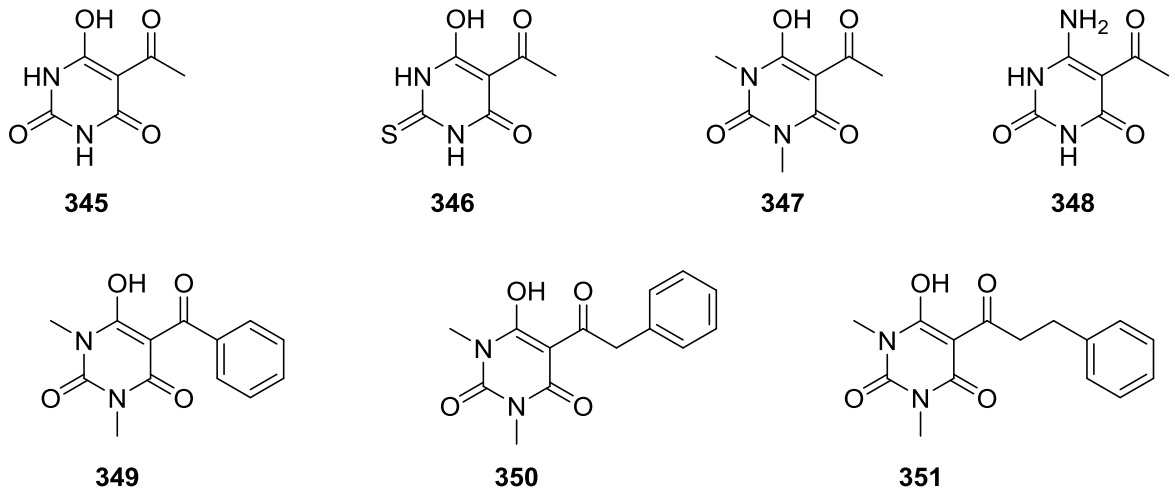

Figure 78: Structures of initial series of triketone barbiturate-based inhibitors.

The resulting compounds were potent against OGFOD1, with a notable increase by one order of magnitude upon extending the carbon chain length from **349** (IC_{50} = 30 µM) to **350** (IC_{50} = 2 µM), and from **350** to **351** (IC_{50} = 0.7 µM) (Figure 80). These compounds displayed no inhibition, at all, at 100 µM final concentration against PHD2.

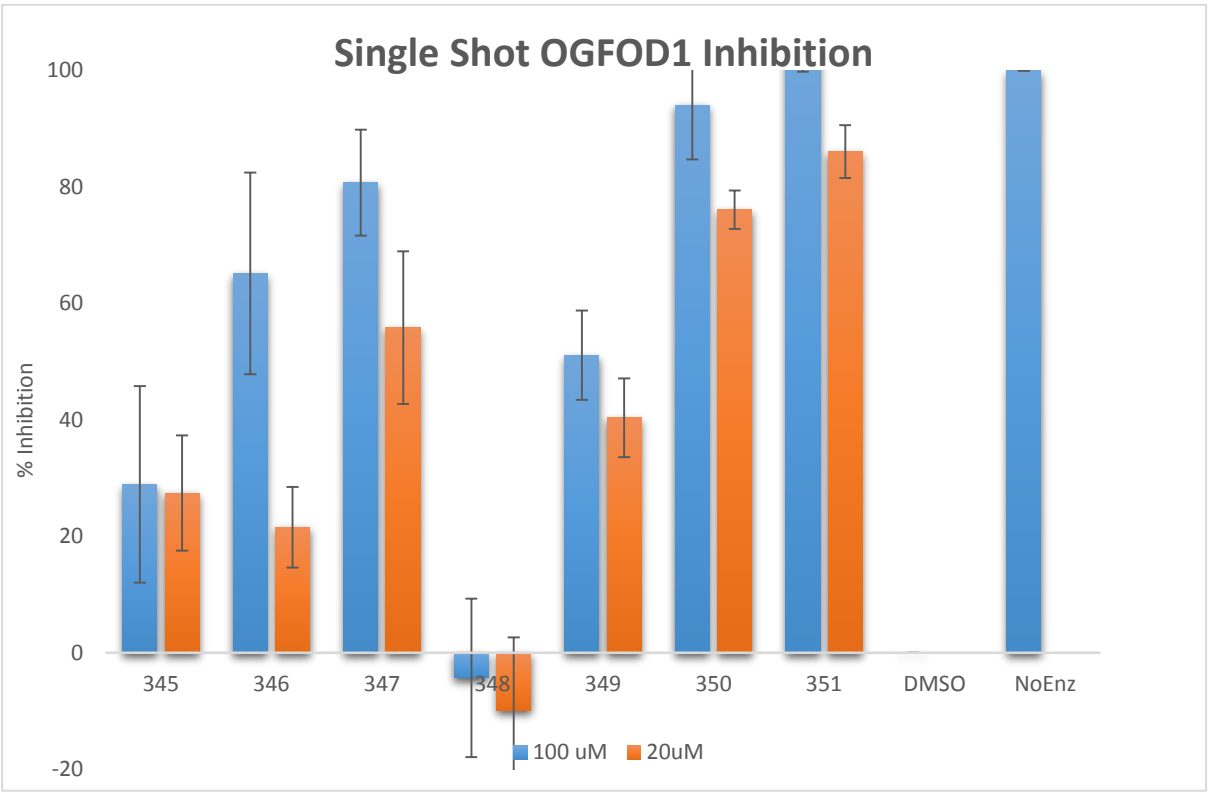

Figure 79: Single point inhibition of OGFOD1 by MALDI-TOF MS hydroxylation assay. Measurements were carried out in triplicate using OGFOD1 (1 µM), 2OG (25 µM), $(NH_4)_2Fe(SO_4)_2 \bullet 6H_2O$ (50 µM), sodium ascorbate (100 µM), RPS23 (sequence VLEKVGVEAKQPNSAIRKCV-NH_2, 25 µM), and inhibitor (100, 20 µM) in 50 mM HEPES pH 7.5 with incubation for 15 min at 37 °C. Data points represent the arithmetic average for each triplicate with the corresponding standard deviation plotted as error bar.

These results suggest that it is likely that the carboxylate side chain at position 5 of **31** offers a selectivity handle for OGFOD1 against PHD2. Given the glycine carboxylate motif occurs in every commonly used PHD2 inhibitor, e.g. **27** - **31**, the salt bridge interaction with Arg384 inside the PHD2 active site appears crucial for potency against PHD2. This salt bridge interaction with the corresponding Arg230 inside OGFOD1 is of lesser importance for achieving potency against OGFOD1; in fact **351** is more potent than **330**.

Molecular modelling reveals that it is unlikely that the aromatic side chains of either **350** or **351** point towards the OGFOD1 2OG binding site because of steric constraints. It is more likely that the side chains point towards the substrate binding site; **349** may orient either way from a 3D space point of view in analogy to sulcotrione. The manual docking suggests that **351** may allow its side chain to snugly fit itself onto the surface of the substrate binding pocket, whereas the side chain torsion angles of **350** are less favourable to achieve a similar binding mode. In addition, **351** may engage in a π-cation interaction with Arg162, a residue which is absent in PHD2 (Figure 80).

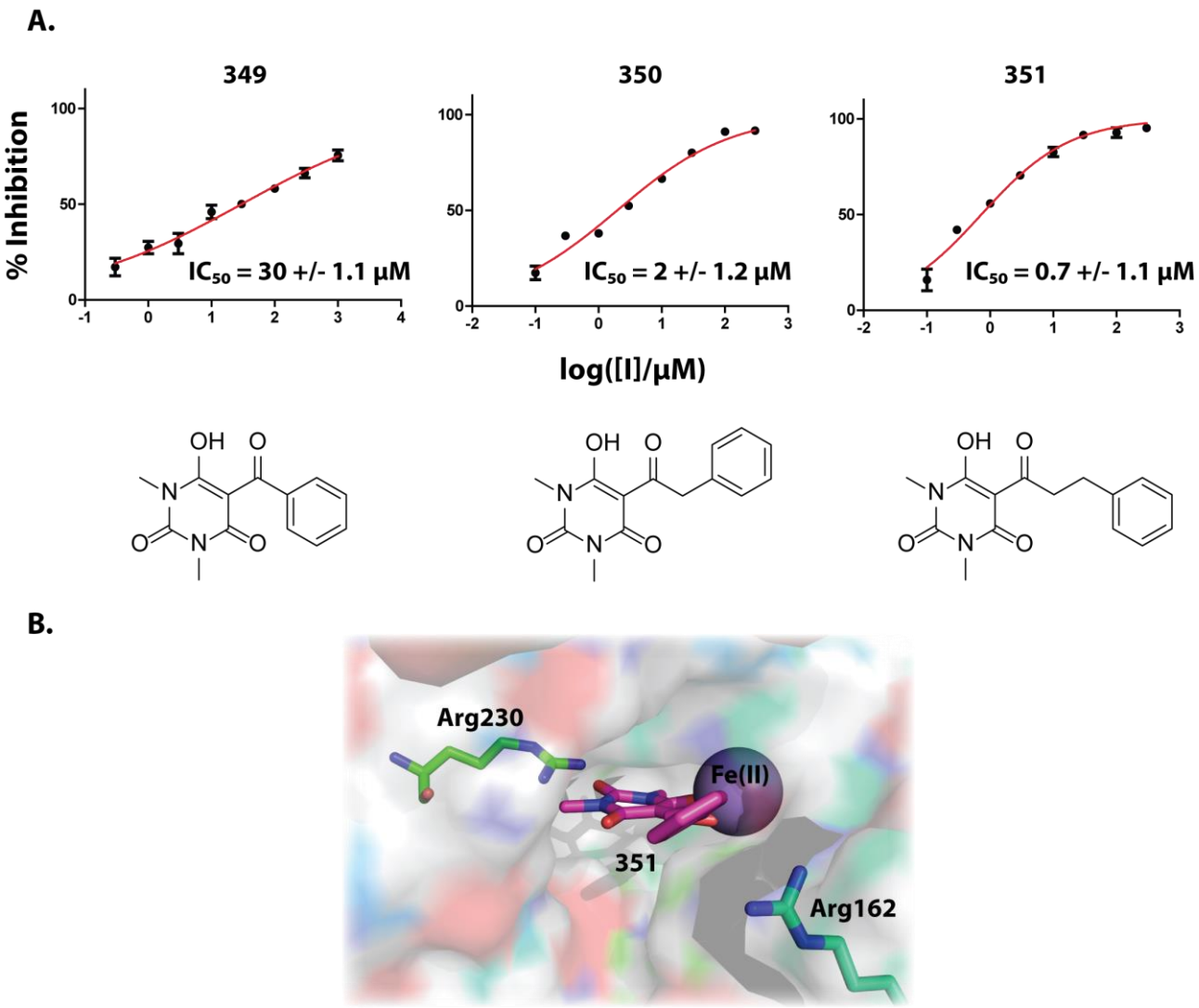

Figure 80: A. Determination of IC_{50} values against OGFOD1. Measurements were carried out in triplicate using OGFOD1 (1 µM), 2OG (25 µM), $(NH_4)_2Fe(SO_4)_2 \bullet 6H_2O$ (50 µM), sodium ascorbate (100 µM), RPS23 (sequence VLEKVGVEAKQPNSAIRKCV-NH_2, 25 µM), and inhibitor (300, 100, 30, 10, 3.0, 1.0, 0.3 and 0.1 µM) in 50 mM HEPES pH 7.5 with incubation for 15 min at 37 °C. Data points represent the arithmetic average for each triplicate with the corresponding standard deviation plotted as error bar. **B.** *In silico* docking model of **351** inside the OGFOD1 active site. The 2-oxo group is likely to engage in hydrogen bonding with Arg230, whereas the phenyl ring may engage in a π stacking interaction with Arg162, a residue which has no counterpart in PHD2.

A further series of compounds was synthesised based around the **351** hydrocinnamoyl side chain in order to further explore SAR. The relatively high potency of **351** in the range of the assay detection limit, with an IC_{50} of 0.7 µM under the given assay conditions employing a final OGFOD1 concentration of 1 µM, however, predisposes the potencies of subsequent compounds to also fall within the assay detection limit. Although a general indicator of potency, absolute IC_{50} values are therefore likely to be only of limited value in order to compare different high-potency compounds amongst themselves.

The primary focus of the subsequent series was on the hydrocinnamoyl substituents of the side chain. These included various aromatic rings with differing substitution patterns, heterocycles, bicyclic, and saturated

rings of different sizes. In addition, amide substitution, as well as α- and β-substitution were explored (Figure 82). Most compounds displayed high potency against OGFOD1; in fact the single point assay which was routinely performed at 100 μM and 20 μM final inhibitor concentration did not discriminate between the various inhibitors: the single point assay had to be repeated at 5 μM and 1 μM final concentrations to reveal some variation between the inhibitors (Figure 81).

Little variation was apparent for differing aromatic substitution patterns, varying aromatic, heterocyclic, bicylic, and saturated rings. Changing the nature of the side chain link from aliphatic chain to amide had little effect, as well as extending the carbon chain length beyond two carbons between the carbonyl and the substituent. The 2-thiophenyl-substituted **363** appeared to be one of the most potent compounds, within variation of the assay detection limit. The associated IC_{50} was found to be 0.5 μM: the theoretical absolute lowest detectable IC_{50} value as the OGFOD1 concentration of the adopted MALDI-TOF MS-based assay is 1 μM. The only compound which was notably less potent than the other compounds of the series was α-methyl-substituted **366**.

The *in silico* manual docking model indicates that α-methyl substitution of **366** may be sterically unfavourable because it distorts the alignment of the aromatic group to the surface of the substrate binding pocket. On the other hand, β-methyl substitution is relatively well tolerated because the methyl group may fit into a small pocket without distorting the alignment of the inhibitor to the enzyme surface. The manual docking model also indicates that the (apparent) higher potency of **363** compared to **351** may arise from the increased electron density of the thiophenyl ring compared to simple phenyl: this increased electron density may render the postulated π-stacking interaction with Arg162 relatively more favourable. **363** was subsequently selected as a lead compound.

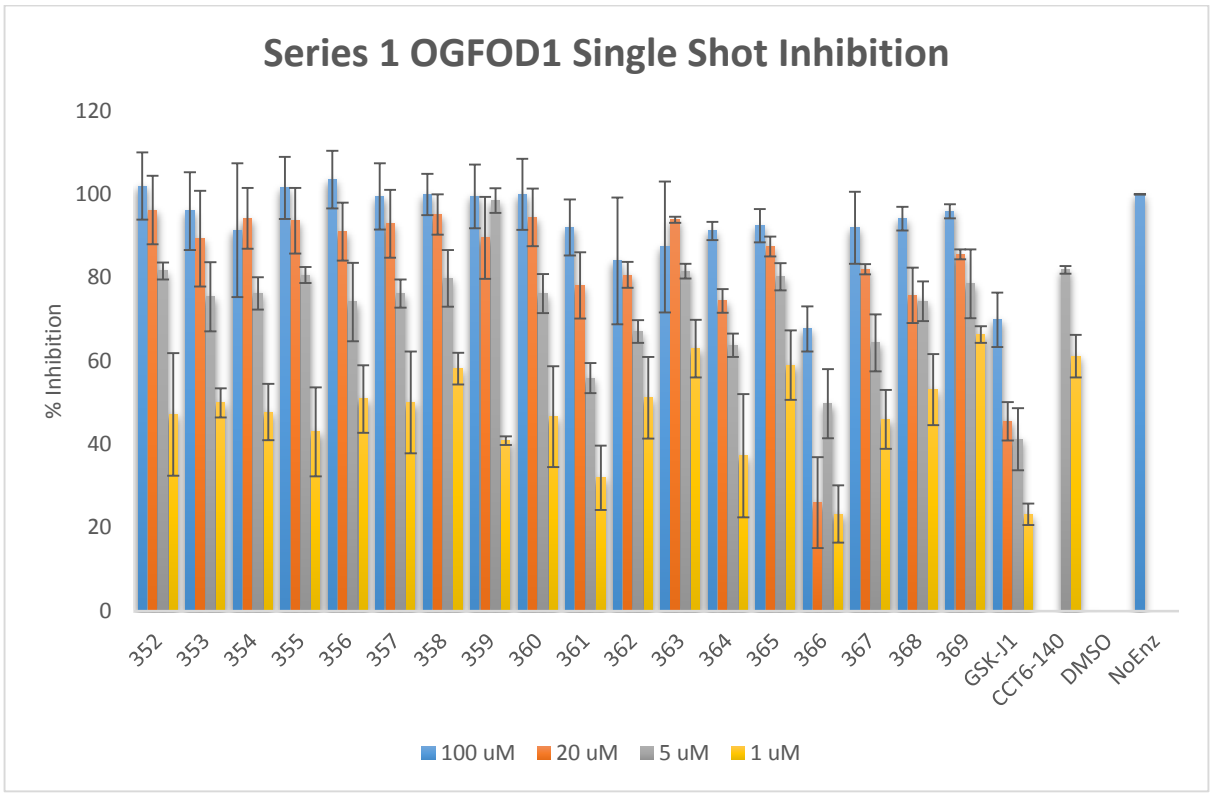

Figure 81: Single point inhibition of OGFOD1 by MALDI-TOF MS hydroxylation assay. Measurements were carried out in triplicate using OGFOD1 (1 µM), 2OG (25 µM), $(NH_4)_2Fe(SO_4)_2 \bullet 6H_2O$ (50 µM), sodium ascorbate (100 µM), RPS23 (sequence VLEKVGVEAKQPNSAIRKCV-NH_2, 25 µM), and inhibitor (100, 20, 5.0 and 1.0 µM) in 50 mM HEPES pH 7.5 with incubation for 15 min at 37 °C. Data points represent the arithmetic average for each triplicate with the corresponding standard deviation plotted as error bar.

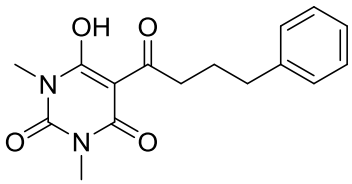

352

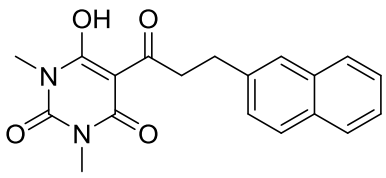

353

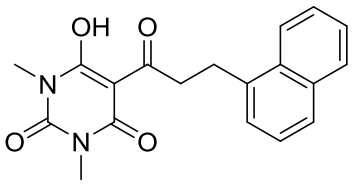

354

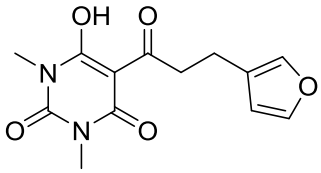

355

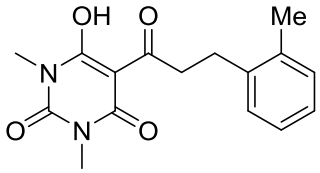

356

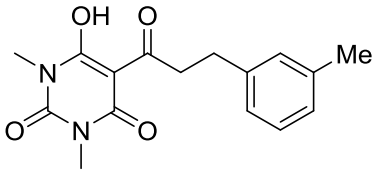

357

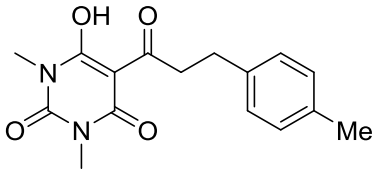

358

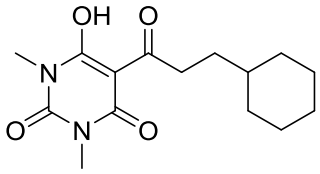

359

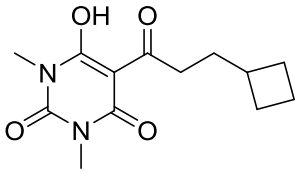

360

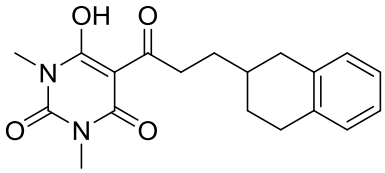

361

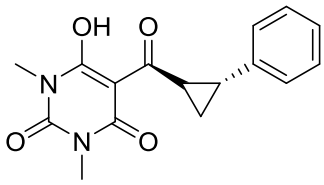

362

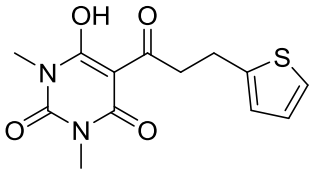

363

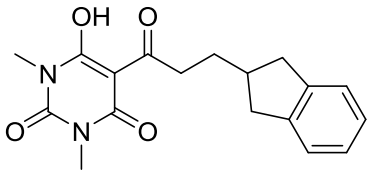

364

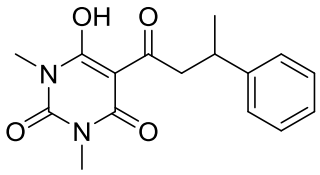

365

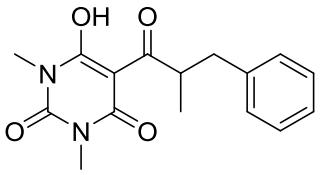

366

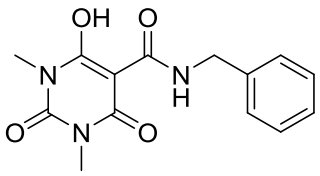

367

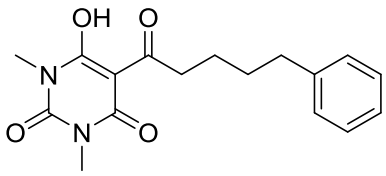

368

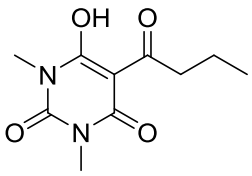

369

Figure 82: Structures of the inhibitors based around **351**.

Synthesis of Potent OGFOD1 Inhibitors

The general strategy for the synthesis of the target compounds involves condensation between the required barbituric acid and the activated carboxylic acid of interest. The reactivity of barbituric acid resembles aldol-type chemistry. For example, the synthesis of acetyl-substituted **345**, **346**, and **347** involved reflux of barbituric acid, 1,3-dimethylbarbituric acid, or thiobarbituric acid in acetic anhydride in the presence of a drop of catalytic sulphuric acid.[215] The analogous reaction was performed with the aminobarbituric acid **373** to give the imine analogue **348**.

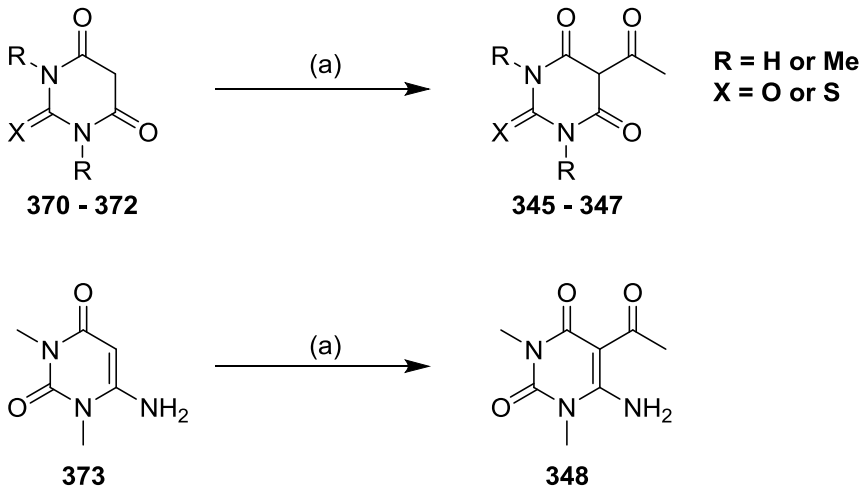

Scheme 36: Acetylation of barbituric acid derivatives. Reagents and conditions: (a) Acetic anhydride, H_2SO_4 (cat.), reflux, 1 h.

Only barbituric acid itself, 1,3-dimethylbarbituric acid, and thiobarbituric acid were commercially available. One method for the synthesis of barbituric acids involves condensation of the required urea with activated malonic acid.[216] A convenient synthetic procedure is exemplified by the synthesis of **375** where 1,3-diethylurea **374** and malonic acid are stirred in a 1:1 mixture of acetic acid and acetic anhydride. Malonic acid is activated *in situ* by reaction with acetic anhydride before reaction with 1,3-diethylurea to form **375**. An analogous approach is used for the synthesis of 1,3-dimethylaminobarbituric acid **373** where 1,3-dimethylurea **376** is condensed with cyanoacetic acid **377**, instead of malonic acid (Scheme 37).

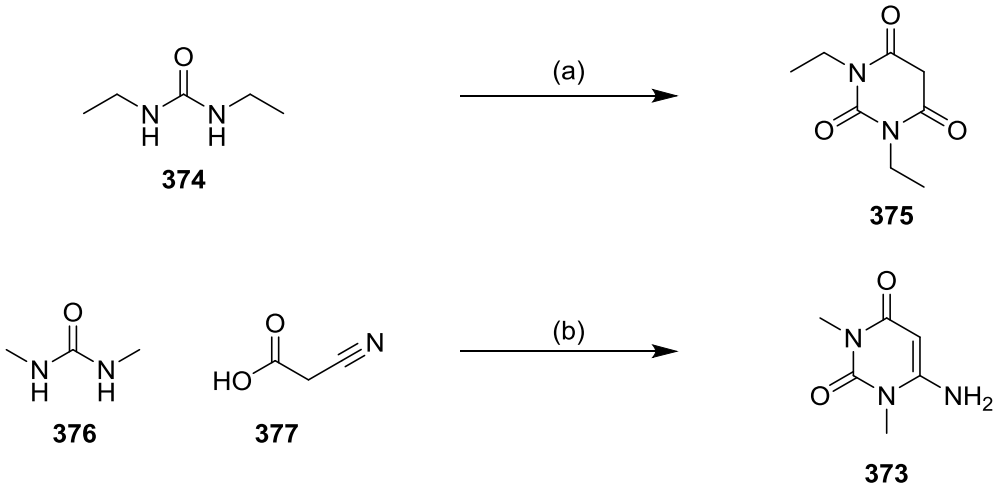

Scheme 37: Synthesis of barbituric acid cores. Reagents and conditions: (a) Malonic acid, acetic anhydride, acetic acid, 60 °C, 6 h. (b) Acetic anhydride, 70 °C, 16 h.

A rather unusual, but analogous to the previous, approach was used for the synthesis of 1,3-diisopropylbarbituric and 1,3-dicyclohexylbarbituric acids **380** and **381**. These compounds were synthesised by condensing malonic acid with the diisopropyl **378** and dicyclohexyl carbodiimide **379** (DIC and DCC) coupling reagents respectively . The carbodiimide reagents act as coupling reagents and provide a source for *N*-substituted ureas at the same time (Scheme 38).

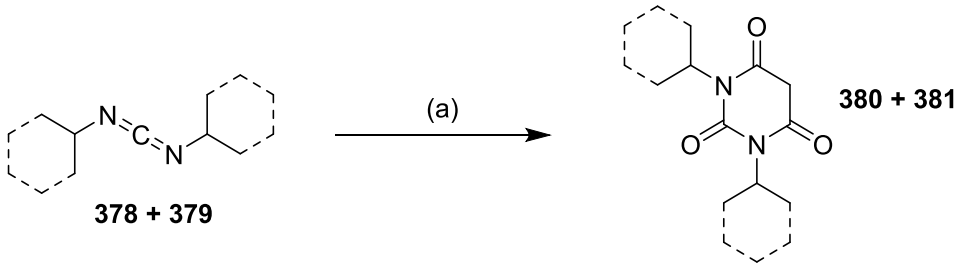

Scheme 38: Synthesis of barbituric acid derivatives from carbodiimides. Reagents and conditions: (a) Malonic acid, THF, 0 °C to RT, 3 h.

A convenient procedure for the synthesis of non-acetyl-substituted barbiturates was *via* condensation with the corresponding acid chloride.[217] The commercially available benzyl chloride **382**, phenylacetyl chloride **383**, and hydrocinnamoyl chloride **384** were condensed with 1,3-dimethylbarbituric acid in pyridine at room temperature to give **349**, **350**, and **351** respectively (Scheme 39).

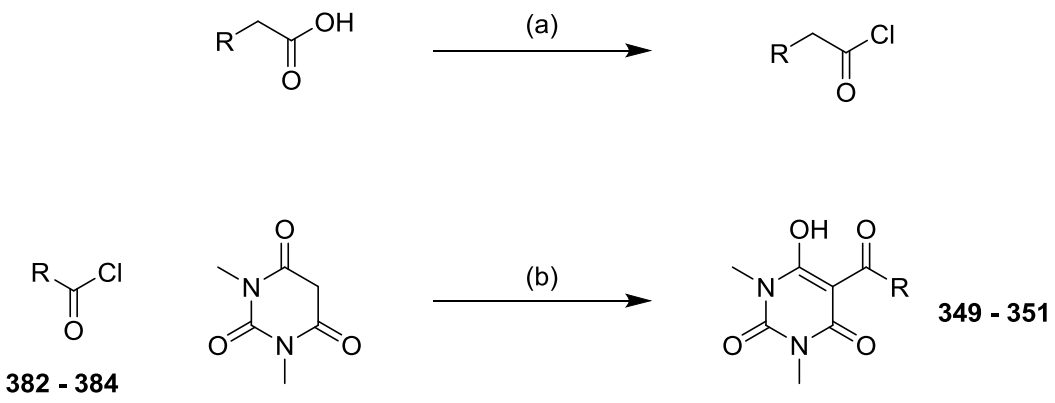

Scheme 39: Reagents and conditions: (a) Oxalyl chloride, DMF (cat.), CH_2Cl_2, RT, 2 h. (b) Pyridine, RT, 2 h.

The majority of substituents of interest were commercially available as the corresponding free carboxylic acids, not the acid chlorides. It was therefore of interest to optimise methodology to allow for parallel, one-pot synthetic procedures to improve operational efficiency. All reactions were performed in disposable glass vials arranged in a 24-vial rack suitable for use inside the Radleigh's Blowdown Evaporator System. The required acid chlorides were synthesised by stirring the carboxylic acid of interest with an excess of oxalyl chloride in dichloromethane at room temperature for three hours. The solvent and excess oxalyl chloride were then evaporated in parallel by subjecting the reaction mixtures to a constant flow of nitrogen gas. A solution of 1,3-dimethylbarbituric acid in pyridine was then slowly added to each reaction vial and the mixture was then stirred at room temperature for two hours. In order to remove the pyridine solvent *via* extraction, a solution of methanol, water, and concentrated hydrochloric acid was then slowly added to the reaction mixture which was subsequently stirred for 30 min. Some of the target compounds precipitated from this mixture and were collected by filtration, washed with water and dried. The majority of compounds, however, did not form precipitates. These reaction mixtures were diluted with dichloromethane and vigorously shaken before the organic layer was collected via Biotage Phase Separator cartridges. Subsequent evaporation of the solvent and purification *via* flash column chromatography yielded the target compounds in high purity.

Pharmacokinetic Characterisation *In Vitro*

An early-stage characterisation of metabolic stability of the lead compound **363**, and the early analogue **351**, was undertaken to verify whether the methodology of basing their chemotype on the chemotype of

pharmaceutically useful entities would make these compounds more likely to be drug-like. Turbidimetric aqueous solubility and S9 liver microsome stability were therefore performed *in vitro*. Both compounds displayed good aqeous solubility with solubilities > 100 µM in water. **351** displayed a half-life of 146 min in S9 microsomes, and **363** a half life of 90 min (experiments performed by Cyprotex).

Another point of interest for these particular compounds was their potential to penetrate the blood brain barrier (BBB). This interest arised from the observation that these compounds are based on the barbiturate core structure: barbiturates are well-known psychoactive compounds.[218] Derivatisation of the corresponding side chains did not substantially alter the number of hydrogen bond donors or acceptors. It was therefore postulated that these compounds may have good potential for BBB crossing.

Initial *in silico* calculations with an online BBB permeability prediction tool (www.cbligand.org) did indeed predict good BBB penetration for both **351** and **363**. An MDCK-MDR1 *in vitro* efflux assay was then used as an *in vitro* predictor for BBB penetration: both compounds are indeed expected to display good BBB penetration by consideration of the MDCK-MDR1 assay (performed by Cyprotex).

Being in possession of BBB-permeable compounds at initial stages is an opportunity to tune *in vivo* distribution considering it is a lot more challenging to turn a BBB-impermeable compound into a BBB-permeable one than *vice versa*. Small changes to the structure of **363** are likely to turn the compound into a BBB-impermeable compound; it may even be possible to alter compound concentration ratios of brain relative to body, while maintaining very similar on-target effects. For example, the amide-linked compound **367** is predicted by the *in silico* BBB permeability predictor tool to be BBB-impermeable. BBB permeability is known to be very sensitive to the number of hydrogen bond donors and acceptors in a molecule.[219] According to the *in silico* model, one amide can undermine BBB permeability: this compound displayed the same OGFOD1 *in vitro* profile than **363**. Small chemical changes can induce a large biological change.

Summary

The successful development of an assay for the assessment of OGFOD1 catalytic activity, as well as the acquisition of a high-resolution OGFOD1 X-ray co-crystal structure, were at the basis for OGFOD1 inhibitor development.

The high degree of similarity between the OGFOD1 and PHD2 active sites was exploited for early-stage chemotype optimisation for OGFOD1 inhibition. Specifically, an initial library was based on clinical candidates for PHD2 inhibition, as well as related agrochemicals, because these molecules are optimised not only in terms of potency and selectivity, but also in terms of ADMET properties. Every clinical-candidate PHD2 inhibitor was in fact found to be a potent inhibitor of OGFOD1. These results raise the possibility that the clinical candidates may also inhibit other human 2OG oxygenases, such as the procollagen hydroxylases. These observations may need to be addressed with respect to future clinical trials in order to assess the molecules more accurately *in vivo*.

Systematic studies into the metal-binding properties of the initial library yielded a chemotype based on triketone barbiturates because of the opportunity to extend side chains toward OGFOD1-specific amino acid residues which are not present in PHD2. At the same time, it was found that the glycine-like side chain ubiquitously present in PHD2 inhibitors is crucial for PHD2 inhibition, but not necessarily for OGFOD1 inhibition. This finding offered a 'selectivity handle' against PHD2.

Merging the triketone barbiturate scaffold of clinical candidate GSK1278863 **31** with the side chains of agrochemicals, and subsequent optimisation, yielded sub-micromolar OGFOD1 inhibitor **363**. This initial lead compound does not inhibit PHD2 at 100 µM final concentration. The latest OGFOD1 inhibitors display potencies within the assay detection limit. Further inhibitor development will require prior development of a more sensitive OGFOD1 inhibitor assay. Current results suggest this may be achieved either *via* use of an improved substrate peptide, e.g. a cyclic peptide or an optimised length/sequence, or *via* optimisation of OGFOD1 expression and purification conditions, e.g. by expressing the catalytic domain only.

Given the chemotype of lead **363**, it is possible that this inhibitor will cross the blood brain barrier. Surrogate *in vitro* assay studies validated this hypothesis. Overall, the strategy of basing **363** on clinically validated chemotypes holds substantial potential toward the properties of this compound for use inside living systems.

Overall, the work has resulted in the first example of inhibitors targeting a specific subfamily of human prolyl hydroxylases.

Compound Characterisation

General Procedure 3 for 5-Substitution of Barbituric Acids

The requisite carboxylic acid (1 eq.) was stirred with oxalyl chloride (762 µL, 9 mmol) and DMF (cat., 1 drop) in CH_2Cl_2 (2 mL) for 2 h at room temperature. The solvent and excess oxalyl chloride were subsequently evaporated using a gentle stream of N_2. Then, a solution of 1,3-dimethylbarbituric acid (1 eq.) in pyridine (2 mL) was slowly added to the residue and the resulting reaction mixture was stirred for 2 h at room temperature. The mixture was then slowly transferred into a stirring mixture of methanol (2 mL), H_2O (1.7 mL), and concentrated HCl aq. (5 mL) and stirring was continued for another 1 h at room temperature. If precipitation occurred, the solids were collected by filtration, washed with dilute HCl (10 % conc. HCl, 90 % H_2O), and dried under vacuum. Otherwise, CH_2Cl_2 (15 mL) was added, the mixture was shaken, and the organic layer was collected by passing the mixture through a phase separator cartridge. The organic layer was dried over anhydrous $MgSO_4$ and concentrated *in vacuo*. The crude product was then purified *via* flash column chromatography (20 % - 50 % EtOAc, cyclohexane) to give the corresponding triketone product.

(1,3-Dicyclohexyl-6-hydroxy-2,4-dioxo-1,2,3,4-tetrahydropyrimidine-5-carbonyl)glycine **31**[209]

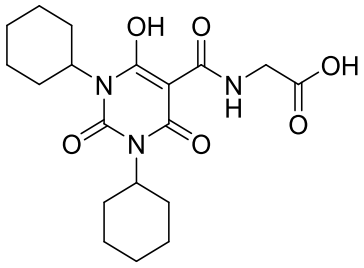

A suspension of **344** (532 mg, 1.3 mmol) in EtOH (1.5 mL) was treated dropwise with NaOH (6 M in H_2O, 250 µL) and stirred for 3 h at room temperature. The reaction mixture was then acidified by slow addition of HCl (6 M in H_2O, 300 µL) and diluted with H_2O (1 mL). The precipitate was collected by filtration. The crude solid was then slurried in H_2O, heated to 35 °C, and stirred vigorously for 1 h, filtered, and dried. The solid material was purified *via* recrystallisation from hot glacial acetic acid (1.5 mL). Subsequent purification *via* flash column chromatography (15 % - 40 % EtOAc, cyclohexane, 0.1 % AcOH) gave **31** (332 mg, 67 %) as a white solid.

mp 262 °C; ν_{max}/cm^{-1} 1717 (C=O), 1662 (C=O); δ_H (400 MHz, DMSO-d_6) 4.49 - 4.76 (2 H, m, NC*H*), 4.12 (2 H, d, *J*=5.5 Hz, NHCH_2), 2.13 - 2.37 (4 H, m), 1.71 - 1.86 (4 H, m), 1.50 - 1.68 (6 H, m), 1.41 (2 H, s), 1.19 - 1.35 (4 H, m), 1.03 - 1.18 (2 H, m); δ_C (100 MHz, DMSO-d_6) 171.2 (*C*=O), 170.3 (*C*=O), 42.0, 29.1, 26.8, 26.5, 25.5; *m*/*z* (ESI$^-$) 392 ([M-H]$^-$); HRMS (ESI$^-$) $C_{19}H_{26}O_6N_3$, ([M-H]$^-$) requires 392.1816; found 392.1833.

Ethyl (6-Hydroxy-2,4-dioxo-1,2,3,4-tetrahydropyrimidine-5-carbonyl)glycinate 329

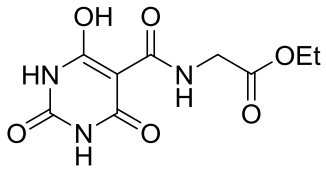

Ethyl isocyanatoacetate (560 µL, 5 mmol) was slowly added to a stirring solution of barbituric acid (512 mg, 4 mmol) in diisopropylethylamine (2mL), CH_2Cl_2 (3 mL) and DMF (5 mL) at room temperature. The resulting solution was stirred at room temperature for 16 h after which the solvent was evaporated under reduced pressure. The residue was redissolved in a mixture of EtOH (5 mL) and NaOH (1 M in H_2O) and the resulting mixture was stirred at room temperature for 60 min. The pH was adjusted to 7 with HCl (1 M in H_2O) and the resulting solid was collected by filtration, washed with H_2O, and dried under vacuum to give **329** (812 mg, 79 %) as a white powder.

mp >250 °C; ν_{max}/cm^{-1} 1718 (C=O), 1650 (C=O), 1620 (C=O); δ_H (400 MHz, DMSO-d_6) 3.96 - 4.19 (4 H, m, OCH_2CH$_3$ and NCH_2), 1.21 (1 H, t, *J*=7.0 Hz, OCH$_2$CH_3); δ_C (100 MHz, DMSO-d_6) 170.4 (*C*=O), 169.6 (*C*=O), 150.2, 61.0 (O*C*H$_2$CH$_3$), 41.1 (N*C*H$_2$), 29.9 (N*C*H$_3$), 14.6 (OCH$_2$*C*H$_3$); *m*/*z* (ESI$^-$) 256 ([M-H]$^-$); HRMS (ESI$^-$) $C_9H_{11}O_6N_3$, ([M-H]$^-$) requires 256.0575; found 256.0580.

Ethyl (6-Hydroxy-1,3-dimethyl-2,4-dioxo-1,2,3,4-tetrahydropyrimidine-5-carbonyl)glycinate 330

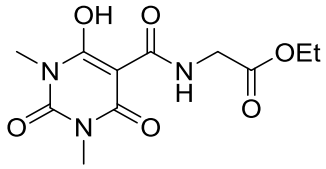

Ethyl isocyanatoacetate (560 µL, 5 mmol) was slowly added to a stirring solution of 1,3-dimethylbarbituric acid (624 mg, 4 mmol) in diisopropylethylamine (2mL), CH_2Cl_2 (3 mL) and DMF (5 mL) at room temperature. The resulting solution was stirred at room temperature for 16 h after which the solvent was evaporated

under reduced pressure. The residue was redissolved in a mixture of EtOH (5 mL) and NaOH (1 M in H_2O) and the resulting mixture was stirred at room temperature for 60 min. The pH was adjusted to 7 with HCl (1 M in H_2O) and the resulting solid was collected by filtration, washed with H_2O, and dried under *vacuum* to give **330** (821 mg, 72 %) as a white powder.

mp > 250 °C; ν_{max}/cm^{-1} 1756 (C=O), 1737 (C=O), 1724 (C=O), 1671 (C=O); δ_H (400 MHz, DMSO-d_6) 4.12 (2 H, q, *J*=7.0 Hz, OCH_2CH$_3$), 4.07 (2 H, d, *J*=5.5 Hz, NHCH_2), 3.16 (6 H, s, NCH_3), 1.21 (3 H, t, *J*=7.0 Hz, OCH$_2$CH_3); δ_C (100 MHz, DMSO-d_6) 170.4 (*C*=O), 169.6 (*C*=O), 151.3, 61.0 (O*C*H$_2$CH$_3$), 41.3 (N*C*H$_2$), 27.7 (N*C*H$_3$), 14.6 (OCH$_2$*C*H$_3$); *m*/*z* (ESI$^-$) 284 ([M-H]$^-$); HRMS (ESI$^-$) $C_{11}H_{14}O_6N_3$, ([M-H]$^-$) requires 284.0877; found 284.0889.

Ethyl (1,3-Dicyclohexyl-6-hydroxy-2,4-dioxo-1,2,3,4-tetrahydropyrimidine-5-carbonyl)glycinate 344

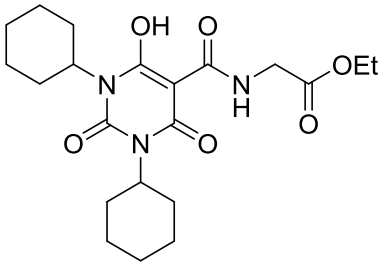

Ethyl isocyanatoacetate (460 µL, 3.7 mmol) was slowly added to a stirring solution of **381** (1.09 g, 3.7 mmol) and diisopropylethylamine (1.3 mL) in CH_2Cl_2 (15 mL) at room temperature. The resulting solution was stirred at room temperature for 16 h. The resulting reaction mixture was extracted with HCl (6 M in H_2O, 5 mL) and the organic layer was dried over anhydrous Na_2SO_4 and concentrated *in vacuo*. The resulting solid was slurried in cyclohexane (5 mL) and heated to reflux. The mixture was allowed to cool to room temperature, the precipitate was collected by filtration and purified *via* flash column chromatography (10 % - 40 % EtOAc, cyclohexane) to give **344** (840 mg, 54 %) as a white powder.

mp 163 °C; ν_{max}/cm^{-1} 1750 (C=O), 1676 (C=O), 1627 (C=O); δ_H (400 MHz, $CDCl_3$) 4.53 - 4.81 (2 H, m, NC*H*), 4.19 (2 H, q, *J*=7.0 Hz, OCH_2), 4.08 (2 H, d, *J*=5.5 Hz, NHCH_2), 2.14 - 2.41 (4 H, m), 1.68 - 1.84 (4 H, m), 1.49 - 1.67 (6 H, m), 1.02 - 1.40 (9 H, m); δ_C (100 MHz, $CDCl_3$) 171.8 (*C*=O), 168.4 (*C*=O), 61.9, 41.5, 29.2, 29.0, 26.5, 26.4, 25.3, 25.2, 14.2; *m*/*z* (ESI$^-$) 429 ([M-H]$^-$); HRMS (ESI$^-$) $C_{21}H_{30}O_6N_3$, ([M-H]$^-$) requires 420.2129; found 420.2140.

5-Acetyl-6-hydroxypyrimidine-2,4(1H,3H)-dione **345**[215]

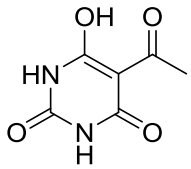

Barbituric acid (1.3 g, 10 mmol) was heated at reflux in acetic anhydride (30 mL) in the presence of 3 drops of sulphuric acid for 60 min. The reaction mixture was concentrated to a total volume of about 15 mL under reduced pressure and then cooled in an ice bath. The resulting precipitate was collected by filtration and washed with hot water and acetone before being dried under reduced pressure to give **345** (872 mg, 51 %) as a light-brown powder.

mp 309 °C; ν_{max}/cm^{-1} 1735 (ketone C=O), 1627 (amide C=O); δ_H (400 MHz, DMSO-d_6) 11.80 (1 H, br. s., N*H*), 11.07 (1 H, br. s., N*H*), 2.59 (3 H, s, CH_3); δ_C (100 MHz, DMSO-d_6) 195.4 (*C*=O), 172.2 (*C*=O), 162.8 (*C*=O),149.5 (*C*=O), 95.9 (C_5), 24.3 (*C*H$_3$); *m*/*z* (ESI$^-$) 169 ([M-H]$^-$); HRMS (ESI$^-$) $C_6H_5O_4N_2$, ([M-H]$^-$) requires 169.0255; found 169.0253.

5-Acetyl-6-hydroxy-2-thioxo-2,3-dihydropyrimidin-4(1*H*)-one **346**

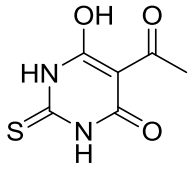

Thiobarbituric acid (1.4 g, 10 mmol) was heated at reflux in acetic anhydride (30 mL) in the presence of 3 drops of sulphuric acid for 60 min. The reaction mixture was concentrated to a total volume of about 15 mL under reduced pressure and then cooled in an ice bath. The resulting precipitate was collected by filtration and washed with hot water and acetone before being dried under reduced pressure to give **347** (560 mg, 30 %) as a dark-brown powder.

mp decomposition > 200 °C; ν_{max}/cm^{-1} 1722 (ketone C=O), 1655 (amide C=O); δ_H (400 MHz, DMSO-d_6) 2.60 (3 H, s, CH_3); δ_C (100 MHz, DMSO-d_6) 197.0 (*C*=O), 177.2 (*C*=O), 97.6 (C_5), 24.8 (*C*H$_3$); *m*/*z* (FI) 186 ([M]$^+$); HRMS (FI) $C_6H_6N_2O_3S$, ([M]$^+$) requires 186.0099; found 186.0094.

5-Acetyl-6-hydroxy-1,3-dimethylpyrimidine-2,4(1*H*,3*H*)-dione **347**

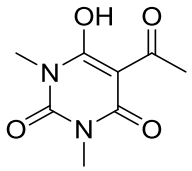

1,3-Dimethylbarbituric acid (1.6 g, 10 mmol) was heated at reflux in acetic anhydride (30 mL) in the presence of 3 drops of sulphuric acid for 60 min. The reaction mixture was concentrated to a total volume of about 15 mL under reduced pressure and then cooled in an ice bath. The resulting precipitate was collected by filtration and washed with hot water and acetone before being dried under reduced pressure to give **347** (1.68 g, 85 %) an off-white powder.

mp 104 °C; ν_{max}/cm^{-1} 1722 (ketone C=O), 1655 (amide C=O); δ_H (400 MHz, DMSO-d_6) 3.19 (6 H, s, NCH_3), 2.64 (3 H, s, CH_3); δ_C (100 MHz, DMSO-d_6) 195.0 (*C*=O), 150.5 (*C*=O), 96.4 (C_5), 28.1 (N*C*H$_3$), 24.5 (*C*H$_3$); *m*/*z* (FI) 198 ([M]$^+$); HRMS (FI) $C_8H_{10}N_2O_4$, ([M]$^+$) requires 198.0641; found 198.0643.

5-Acetyl-6-amino-1,3-dimethylpyrimidine-2,4(1*H*,3*H*)-dione **348**

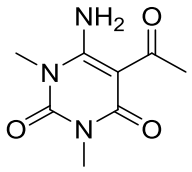

373 (1.6 g, 10 mmol) was heated at reflux in acetic anhydride (30 mL) in the presence of 3 drops of sulphuric acid for 60 min. The reaction mixture was concentrated to a total volume of about 15 mL under reduced pressure and then cooled in an ice bath. The resulting precipitate was collected by filtration and washed with hot water and acetone before being dried under reduced pressure to give **348** (614 mg, 31 %) as a light-brown powder.

mp 265 °C; ν_{max}/cm^{-1} 1701 (ketone C=O), 1660 (C=O); δ_H (400 MHz, pyridine-d_5) 5.14 (6 H, s, NCH_3), 4.93 (3 H, s, COCH_3); δ_C (100 MHz, pyridine-d_5) 161.0 (*C*=O), 160.9 (*C*=O), 152.9, 105.5 (C_5), 29.9 (N*C*H$_3$), 28.2 (N*C*H$_3$), 18.2 (CO*C*H$_3$); No mass spectrum could be obtained.

5-Benzoyl-6-hydroxy-1,3-dimethylpyrimidine-2,4(1*H*,3*H*)-dione **349**[217]

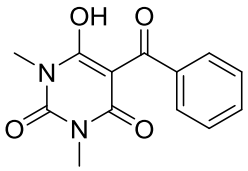

Benzoyl chloride (1.2 mL, 10 mmol) was slowly added to a stirring solution of 1,3-dimethylbarbituric acid (1.6 g, 10 mmol) in pyridine (6 mL) at room temperature. The resulting reaction mixture was stirred for an additional 2 h at room temperature before being slowly added to a stirring mixture of methanol (6 mL), H_2O (5 mL), and concentrated HCl aq. (15 mL). The resulting suspension was stirred for an additional 30 min at room temperature and then for 1 h at 0 °C. The precipitate was collected by filtration, washed with dilute HCl (10 % conc. HCl, 90 % H_2O), and dried under vacuum. The crude product was purified *via* flash column chromatography (20 % - 50 % EtOAc, cyclohexane) to give **349** (334 mg, 13 %) as a light-yellow powder.

mp 105 °C; ν_{max}/cm^{-1} 1719 (ketone C=O), 1670 (amide C=O); δ_H (400 MHz, DMSO-d_6) 7.84 - 8.06 (2 H, m, *Ar*), 7.28 - 7.75 (3 H, m, *Ar*), 3.19 (6 H, s, NCH_3); δ_C (100 MHz, DMSO-d_6) 189.8 (*C*=O), 167.8.5 (*C*=O), 150.7, 133.3, 129.7, 129.0, 128.8, 128.1, 96.2 (C_5), 28.2 (N*C*H$_3$); *m/z* (ESI$^-$) 259 ([M-H]$^-$); HRMS (ESI$^-$) $C_{13}H_{11}O_4N_2$, ([M-H]$^-$) requires 259.0724; found 259.0723.

6-Hydroxy-1,3-dimethyl-5-(2-phenylacetyl)pyrimidine-2,4(1H,3H)-dione **350**

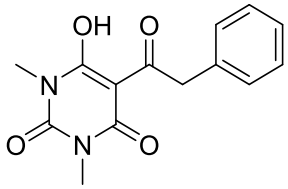

Phenylacetyl chloride (1.2 mL, 10 mmol) was slowly added to a stirring solution of 1,3-dimethylbarbituric acid (1.6 g, 10 mmol) in pyridine (6 mL) at room temperature. The resulting reaction mixture was stirred for an additional 2 h at room temperature before being slowly added to a stirring mixture of methanol (6 mL), H_2O (5 mL), and concentrated HCl aq. (15 mL). The resulting suspension was stirred for an additional 30 min at room temperature and then for 1 h at 0 °C. The precipitate was collected by filtration, washed with dilute HCl (10 % conc. HCl, 90 % H_2O), and dried under vacuum. The crude product was purified *via* flash column chromatography (20 % - 50 % EtOAc, cyclohexane) to give **350** (1.67 mg, 61 %) as a light-brown powder.

mp 90 °C; ν_{max}/cm^{-1} 1720 (C=O), 1659 (C=O); δ_H (400 MHz, DMSO-d_6) 7.23 - 7.38 (5 H, m, *Ar*), 4.49 (2 H, s, CH_2), 3.21 (6 H, s, NCH_3); δ_C (100 MHz, DMSO-d_6) 195.0 (*C*=O), 150.4 (*C*=O), 135.4, 129.9, 128.9, 127.4, 127.0, 96.2 (C_5), 41.3 (CH_2), 28.2 (NCH_3); *m/z* (ESI$^-$) 273 ([M-H]$^-$); HRMS (ESI$^-$) $C_{14}H_{14}O_4N_2$, ([M-H]$^-$) requires 273.0870; found 277.0882.

6-Hydroxy-1,3-dimethyl-5-(3-phenylpropanoyl)pyrimidine-2,4(1*H*,3*H*)-dione **351**

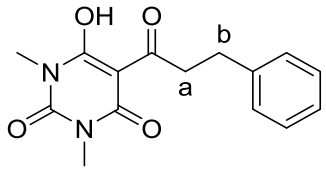

Hydrocinnamoyl chloride (1.5 mL, 10 mmol) was slowly added to a stirring solution of 1,3-dimethylbarbituric acid (1.6 g, 10 mmol) in pyridine (6 mL) at room temperature. The resulting reaction mixture was stirred for an additional 2 h at room temperature before being slowly added to a stirring mixture of methanol (6 mL), H_2O (5 mL), and concentrated HCl aq. (15 mL). The resulting suspension was stirred for an additional 30 min at room temperature and then for 1 h at 0 °C. The precipitate was collected by filtration, washed with dilute HCl (10 % conc. HCl, 90 % H_2O), and dried under vacuum. The crude product was purified *via* flash column chromatography (20 % - 50 % EtOAc, cyclohexane) to give **351** (2.07 g, 72 %) as a light-brown powder.

mp 91 °C; ν_{max}/cm^{-1} 1719 (ketone C=O), 1664 (amide C=O); δ_H (400 MHz, DMSO-d_6) 7.26 - 7.37 (4 H, m, *Ar*), 7.15 - 7.25 (1 H, m, *Ar*), 3.34 - 3.42 (2 H, m, H_a), 3.21 (6 H, s, NCH_3), 2.87 - 2.98 (2 H, m, H_b); δ_C (100 MHz, DMSO-d_6) 197.1 (*C*=O), 150.4 (*C*=O), 140.9, 128.9, 128.8, 126.7, 95.9 (C_5), 38.4 (C_a), 31.3 (C_b), 28.2 (NCH_3); *m/z* (ESI$^-$) 277 ([M-H]$^-$); HRMS (ESI$^-$) $C_{13}H_{13}O_5N_2$, ([M-H]$^-$) requires 277.0830; found 277.0838.

6-Hydroxy-1,3-dimethyl-5-(4-phenylbutanoyl)pyrimidine-2,4(1*H*,3*H*)-dione **352**

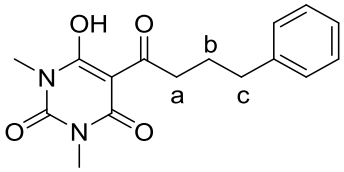

Following general procedure 3, 3-phenylbutyric acid (293 mg, 3 mmol) and 1,3-dimethylbarbituric acid (468 mg, 3 mmol) gave **352** (444 mg, 49 %) as an off-white solid.

mp 68 °C; ν_{max}/cm^{-1} 1716 (ketone C=O), 1648 (amide C=O); δ_H (400 MHz, DMSO-d_6) 7.14 - 7.35 (5 H, m, *Ar*), 3.19 (6 H, s, NCH_3), 3.06 - 3.15 (2 H, m, H_a), 2.68 (2 H, t, *J*=7.5 Hz, H_c), 1.93 (2 H, quin, *J*=7.5 Hz, H_c); δ_C (100 MHz, DMSO-d_6) 197.9 (*C*=O), 150.4 (*C*=O), 141.8, 128.8, 1264., 96.0 (C_5), 35.9 (C_a), 35.2 (C_c), 28.1 (N*C*H$_3$), 27.3 (C_b); *m/z* (ESI$^-$) 301 ([M-H]$^-$); HRMS (ESI$^-$) $C_{16}H_{17}O_4N_2$, ([M-H]$^-$) requires 301.1194; found 301.1200.

6-Hydroxy-1,3-dimethyl-5-(3-(naphthalen-2-yl)propanoyl)pyrimidine-2,4(1*H*,3*H*)-dione **353**

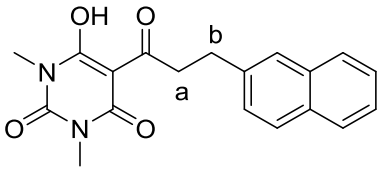

Following general procedure 3, 3-(naphthalene-2-yl)propanoic acid (244 mg, 1.2 mmol) and 1,3-dimethylbarbituric acid (190 mg, 1.2 mmol) gave **353** (176 mg, 43 %) as an off-white powder.

mp 157 °C; ν_{max}/cm^{-1} 1721 (C=O), 1699 (C=O); δ_H (400 MHz, pyridine-d_5) 9.32 - 9.40 (3 H, m, *Ar*), 9.08 - 9.12 (1 H, m, *Ar*), 8.87 - 9.01 (3 H, m, *Ar*), 5.13 - 5.23 (2 H, m, H_a), 4.84 (6 H, s, NCH_3), 4.71 - 4.81 (2 H, m, H_b); δ_C (100 MHz, DMSO-d_6) 197.3 (*C*=O), 134.0, 132.5, 128.3, 127.9, 127.8, 127.6, 126.9, 126.3, 125.6, 122.9, 95.9 (C_5), 39.3 (C_a), 31.9 (C_b), 27.6 (N*C*H$_3$); *m/z* (ESI$^-$) 337 ([M-H]$^-$); HRMS (ESI$^-$) $C_{19}H_{17}O_4N_2$, ([M-H]$^-$) requires 337.1194; found 337.1203.

6-Hydroxy-1,3-dimethyl-5-(3-(naphthalen-1-yl)propanoyl)pyrimidine-2,4(1*H*,3*H*)-dione **354**

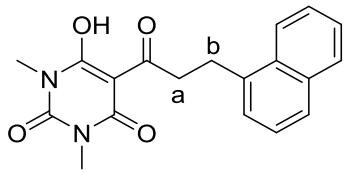

Following general procedure 3, 3-(1-naphthyl)propanoic acid (600 mg, 3 mmol) and 1,3-dimethylbarbituric acid (468 mg, 3 mmol) gave **354** (506 mg, 50 %) as a yellow powder.

mp 179 °C; ν_{max}/cm^{-1} 1717 (C=O), 1699 (C=O); δ_H (400 MHz,pyridine-d_5) 9.39 - 9.48 (1 H, m, *Ar*), 9.25 - 9.34 (1 H, m, *Ar*), 8.97 - 9.05 (3 H, m, *Ar*), 8.88 - 8.96 (2 H, m, *Ar*), 5.17 - 5.25 (2 H, m, H_a), 5.04 - 5.16 (2 H, m, H_b), 4.84 (6 H, s, NCH_3); δ_C (100 MHz, DMSO-d_6) 198.4 (*C*=O), 138.5, 136.9, 136.0, 135.4, 133.3, 130.2, 128.5, 127.7, 127.6, 127.1, 97.1 (C_5), 39.8 (C_a), 30.1 (C_b), 28.8 (N*C*H$_3$); *m/z* (ESI$^-$) 337 ([M-H]$^-$); HRMS (ESI$^-$) $C_{19}H_{17}O_4N_2$, ([M-H]$^-$) requires 337.1194; found 337.1204.

5-(3-(Furan-3-yl)propanoyl)-6-hydroxy-1,3-dimethylpyrimidine-2,4(1*H*,3*H*)-dione **355**

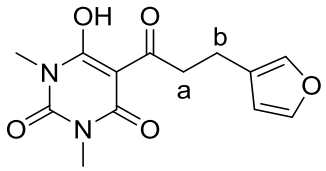

Following general procedure 3, 3-(furan-3-yl)propanoic acid (240 mg, 1.7 mmol) and 1,3-dimethylbarbituric acid (267 mg, 1.7 mmol) gave **355** (11 mg, 2 %) as a light-pink oil.

ν_{max}/cm^{-1} 3422 (OH), 1653 (C=O); δ_H (400 MHz, DMSO-d_6) 7.56 - 7.61 (1 H, m, *Ar*), 7.46 - 7.53 (1 H, m, *Ar*), 6.41 - 6.47 (1 H, m, *Ar*), 3.31 - 3.41 (2 H, m, H_a), 3.21 (6 H, s, NCH_3), 2.67 - 2.81 (2 H, m, H_b); δ_C (100 MHz, DMSO-d_6) 150.4, 143.7, 139.7, 128.9, 111.6, 96.0, 36.9, 28.2(NCH_3); *m*/*z* (ESI$^-$) 277 ([M-H]$^-$); HRMS (ESI$^-$) $C_{13}H_{13}N_2O_5$, ([M-H]$^-$) requires 277.0830; found 277.0837.

6-Hydroxy-1,3-dimethyl-5-(3-(o-tolyl)propanoyl)pyrimidine-2,4(1*H*,3*H*)-dione **356**

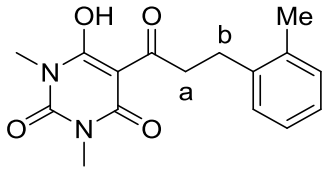

Following general procedure 3, 2-methylhydrocinnamic acid (492 mg, 3 mmol) and 1,3-dimethylbarbituric acid (468 mg, 3 mmol) gave **356** (466 mg, 51 %) as a white solid.

mp 125 °C; ν_{max}/cm^{-1} 1717 (ketone C=O), 1662 (amide C=O); δ_H (400 MHz, DMSO-d_6) 7.05 - 7.28 (4 H, m, *Ar*), 3.28 - 3.39 (2 H, m, H_a), 3.21 (6 H, s, NCH_3) 2.80 - 3.00 (2 H, m, H_a), 2.32 (3 H, s, CH_3); δ_C (100 MHz, DMSO-d_6) 197.0 (*C*=O), 150.4, 138.9, 136.2, 130.5, 129.0, 126.8, 126.5, 96.0 (C_5), 37.0 (C_a), 28.9 (C_b), 28.2 (NCH_3), 19.3 (CH_3); *m*/*z* (ESI$^-$) 301 ([M-H]$^-$); HRMS (ESI$^-$) $C_{16}H_{17}O_4N_2$, ([M-H]$^-$) requires 301.1194; found 301.1192.

6-Hydroxy-1,3-dimethyl-5-(3-(*m*-tolyl)propanoyl)pyrimidine-2,4(1*H*,3*H*)-dione **357**

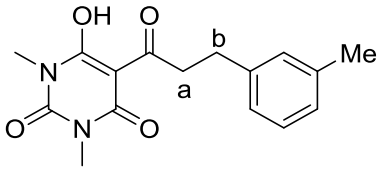

Following general procedure 3, 3-methylhydrocinnamic acid (492 mg, 3 mmol) and 1,3-dimethylbarbituric acid (468 mg, 3 mmol) gave **357** (506 mg, 56 %) as a white powder.

mp 131 °C; ν_{max}/cm^{-1} 1717 (C=O), 1661 (C=O); δ_H (400 MHz, pyridine-d_5) 7.15 - 7.25 (4 H, m, *Ar*), 3.52 - 3.61 (2 H, m, H_a), 3.31 (6 H, s, NCH_3), 2.97 - 3.13 (2 H, m, H_b), 2.21 (3 H, s, CH_3); δ_C (100 MHz, pyridine-d_5) 197.4 (*C*=O), 150.3 (*C*=O), 141.1, 138.0, 129.5, 128.6, 127.1, 125.8, 95.8 (C_5), 39.3 (C_a), 31.6 (C_b), 27.6 (N*C*H$_3$), 21.1 (*C*H$_3$); *m*/*z* (ESI$^-$) 301 ([M-H]$^-$); HRMS (ESI$^-$) $C_{16}H_{17}O_4N_2$, ([M-H]$^-$) requires 301.1194; found 301.1200.

6-Hydroxy-1,3-dimethyl-5-(3-(*p*-tolyl)propanoyl)pyrimidine-2,4(1*H*,3*H*)-dione **358**

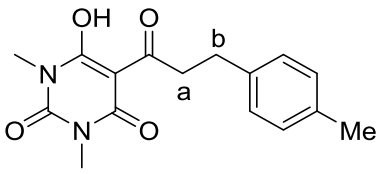

Following general procedure 3, 4-methylhydrocinnamic acid (492 mg, 3 mmol) and 1,3-dimethylbarbituric acid (468 mg, 3 mmol) gave **358** (565 mg, 62 %) as a white solid.

mp 140 °C; ν_{max}/cm^{-1} 1720 (ketone C=O), 1699 (amide C=O); δ_H (400 MHz, DMSO-d_6) 7.03 - 7.23 (4 H, m, *Ar*), 3.32 - 3.39 (2 H, m, H_a), 3.21 (6 H, s, NCH_3), 2.84 - 2.93 (2 H, m, H_b), 2.28 (3 H, s, CH_3); δ_C (100 MHz, DMSO-d_6) 150.4, 137.8, 135.6, 129.4, 129.3, 128.6, 128.5, 96.0 (C_5), 38.4 (C_a), 31.0 (C_b), 28.2 (N*C*H$_3$), 21.1 (*C*H$_3$); *m*/*z* (ESI$^-$) 301 ([M-H]$^-$); HRMS (ESI$^-$) $C_{16}H_{17}O_4N_2$, ([M-H]$^-$) requires 301.1194; found 301.1200.

5-(3-Cyclohexylpropanoyl)-6-hydroxy-1,3-dimethylpyrimidine-2,4(1*H*,3*H*)-dione **359**

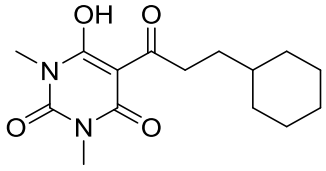

Following general procedure 3, cyclohexanepropionic acid (468 µL, 3 mmol) and 1,3-dimethylbarbituric acid (468 mg, 3 mmol) gave **359** (444 mg, 61 %) as a white solid.

mp 58 °C; ν_{max}/cm^{-1} 1720 (ketone C=O), 1670 (amide C=O); δ_H (400 MHz, DMSO-d_6) (6 H, s, NCH_3), 3.02 - 3.12 (2 H, m, H_a), 1.57 - 1.79 (6 H, m), 1.45 - 1.55 (2 H, m, H_b), 1.06 - 1.26 (3 H, m), 0.91 (2 H, m); δ_C (100 MHz,

DMSO-d_6) 198.6, 150.4, 95.8 (C_5), 37.5, 33.9, 33.3, 33.0, 28.1, 26.5, 26.2 (NCH_3); *m/z* (ESI$^-$) 293 ([M-H]$^-$); HRMS (ESI$^-$) $C_{15}H_{21}O_4N_2$, ([M-H]$^-$) requires 293.1507; found 293.1511.

5-(3-Cyclobutylpropanoyl)-6-hydroxy-1,3-dimethylpyrimidine-2,4(1*H*,3*H*)-dione **360**

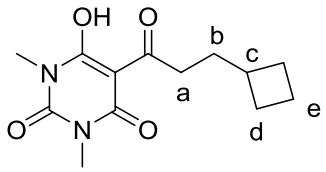

Following general procedure 3, 3-cyclobutylpropanoic acid (250 mg, 2 mmol) and 1,3-dimethylbarbituric acid (312 mg, 2 mmol) gave **360** (135 mg, 17 %) as a light-yellow oil.

ν_{max}/cm^{-1} 1723 (ketone C=O), 1668 (amide C=O); δ_H (400 MHz, DMSO-d_6) 3.20 (6 H, s, NCH_3), 2.87 - 3.06 (2 H, m, H_a), 2.32 (1 H, quin, *J*=8.0 Hz, H_c), 1.95 - 2.09 (2 H, m, H_b), 1.75 - 1.91 (2 H, m, H_e), 1.53 - 1.74 (4 H, m, H_d); δ_C (100 MHz, DMSO-d_6) 198.2, 150.4, 95.8 (C_5), 35.6, 34.2, 32.9, 28.1, 27.9, 18.2; *m/z* (ESI$^-$) 265 ([M-H]$^-$); HRMS (ESI$^-$) $C_{13}H_{17}O_4N_2$, ([M-H]$^-$) requires 265.1194; found 265.1192.

6-Hydroxy-1,3-dimethyl-5-(3-(1,2,3,4-tetrahydronaphthalen-2-yl)propanoyl)pyrimidine-2,4(1*H*,3*H*)-dione **361**

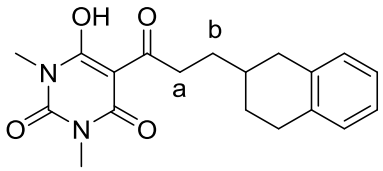

Following general procedure 3, 1,2,3,4-tetrahydro-2-naphthoic acid (528 mg, 3 mmol) and 1,3-dimethylbarbituric acid (468 mg, 3 mmol) gave **361** (485 mg, 47 %) as an off-white solid.

mp 121 °C; ν_{max}/cm^{-1} 1721 (ketone C=O), 1655 (amide C=O); δ_H (400 MHz, DMSO-d_6) 6.96 - 7.19 (4 H, m, *Ar*), 3.21 (6 H, s, NCH_3), 2.90 - 2.99 (2 H, m, H_a), 2.72 - 2.89 (4 H, m), 2.01 - 2.17 (2 H, m, H_b), 1.65 - 1.90 (2 H, m); δ_C (100 MHz, DMSO-d_6) 200.5, 176.7, 150.3, 135.9, 135.3, 129.3, 129.2, 126.3, 126.1, 95.3 (C_5), 31.7, 31.6, 28.8, 28.2 (NCH_3), 26.8, 26.4, 25.9; A mass spectrum could not be obtained *via* ESI or FI.

6-Hydroxy-1,3-dimethyl-5-((1S,2R)-2-phenylcyclopropane-1-carbonyl)pyrimidine-2,4(1H,3H)-dione **362**

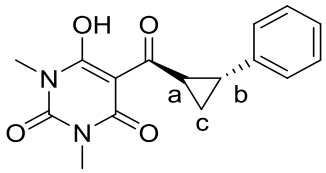

Following general procedure 3, *trans*-2-phenylcyclopropane-1-carboxylic acid (486 mg, 3 mmol) and 1,3-dimethylbarbituric acid (468 mg, 3 mmol) gave **362** (419 mg, 47 %) as a white solid.

mp 111 °C; ν_{max}/cm^{-1} 1716 (ketone C=O), 1672 (amide C=O); δ_H (400 MHz, DMSO-d_6) 7.07 - 7.44 (5 H, m, *Ar*), 3.18 (6 H, s, NCH_3), 2.75 - 2.96 (1 H, m, H_a), 1.91 - 2.05 (1 H, m, H_b), 1.75 - 1.89 (2 H, m, H_c); δ_C (100 MHz, DMSO-d_6) 150.3, 140.2, 129.0, 128.8, 127.2, 126.6, 126.4, 95.9 (C_5), 31.8, 28.2, 27.3, 20.7; *m/z* (ESI$^-$) 299 ([M-H]$^-$); HRMS (ESI$^-$) $C_{16}H_{15}O_4N_2$, ([M-H]$^-$) requires 299.1037; found 299.1041.

6-Hydroxy-1,3-dimethyl-5-(3-(thiophen-2-yl)propanoyl)pyrimidine-2,4(1*H*,3*H*)-dione **363**

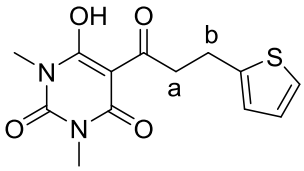

Following general procedure 3, 2-thiophenepropionic acid (468 mg, 3 mmol) and 1,3-dimethylbarbituric acid (468 mg, 3 mmol) gave **363** (371 mg, 42 %) as a light-yellow solid.

mp 91 °C; ν_{max}/cm^{-1} 1716 (ketone C=O), 1661 (amide C=O); δ_H (400 MHz, DMSO-d_6) 7.23 - 7.42 (1 H, m, *Ar*), 6.84 - 7.05 (2 H, m, *Ar*), 3.37 - 3.56 (2 H, m, H_a), 3.21 (6 H, s, NCH_3), 3.14 - 3.19 (2 H, m, H_b); δ_C (100 MHz, DMSO-d_6) 196.4, 150.4, 143.2, 127.4, 125.5, 124.6, 96.0 (C_5), 38.5 (C_a), 28.2 (NCH_3), 25.3 (C_b); *m/z* (ESI$^-$) 293 ([M-H]$^-$); HRMS (ESI$^-$) $C_{13}H_{13}O_4N_2S$, ([M-H]$^-$) requires 293.0602; found 293.0602.

5-(2,3-Dihydro-1*H*-indene-2-carbonyl)-6-hydroxy-1,3-dimethylpyrimidine-2,4(1*H*,3*H*)-dione **364**

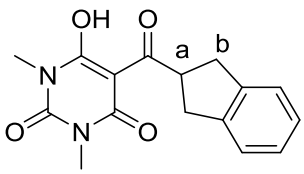

Following general procedure 3, indan-2-carboxylic acid (486 mg, 3 mmol) and 1,3-dimethylbarbituric acid (468 mg, 3 mmol) gave **364** (454 mg, 50 %) as an off-white solid.

mp 120 °C; ν_{max}/cm^{-1} 1718 (ketone C=O), 1663 (amide C=O); δ_H (400 MHz, DMSO-d_6) 7.02 - 7.44 (4 H, m, *Ar*), 4.69 - 4.99 (1 H, m, H_a), 3.22 (6 H, s, NCH_3), 3.10 - 3.33 (4 H, m, H_b); δ_C (100 MHz, DMSO-d_6) 199.6, 150.3, 141.8, 127.0, 124.7, 95.3 (C_5), 43.8 (C_a), 36.4 (C_b), 28.2 (NCH$_3$); *m*/*z* (ESI$^-$) 299 ([M-H]$^-$); HRMS (ESI$^-$) $C_{16}H_{15}O_4N_2$, ([M-H]$^-$) requires 299.1037; found 299.1043.

6-Hydroxy-1,3-dimethyl-5-(3-phenylbutanoyl)pyrimidine-2,4(1*H*,3*H*)-dione **365**

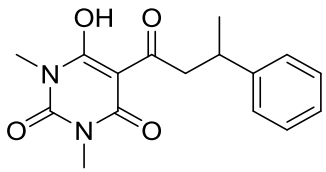

Following general procedure 3, 3-phenylbutyric acid (492 mg, 3 mmol) and 1,3-dimethylbarbituric acid (468 mg, 3 mmol) gave **365** (316 mg, 35 %) as an off-white wax.

mp 100 °C; ν_{max}/cm^{-1} 1706 (ketone C=O), 1655 (amide C=O); δ_H (400 MHz, DMSO-d_6) 7.24 - 7.33 (5 H, m, *Ar*), 3.39 - 3.47 (1 H, m, C*H*), 3.26 - 3.37 (2 H, m, CH_2), 3.20 (6 H, s, NCH_3), 1.25 - 1.33 (3 H, m, CH_3); δ_C (100 MHz, DMSO-d_6) 196.7, 150.4, 146.1, 128.8, 127.2, 126.8, 96.5 (C_5), 44.3 (*C*H), 37.1 (*C*H$_2$), 28.2 (N*C*H$_3$), 22.1 (*C*H$_3$); *m*/*z* (ESI$^-$) 301 ([M-H]$^-$); HRMS (ESI$^-$) $C_{16}H_{17}O_4N_2$, ([M-H]$^-$) requires 301.1194; found 301.1200.

6-Hydroxy-1,3-dimethyl-5-(2-methyl-3-phenylpropanoyl)pyrimidine-2,4(1*H*,3*H*)-dione **366**

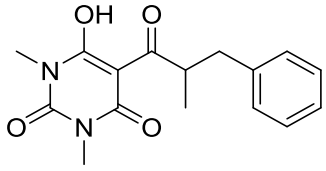

Following general procedure 3, α-methylhydrocinnamic acid (492 mg, 3 mmol) and 1,3-dimethylbarbituric acid (468 mg, 3 mmol) gave **366** (378 mg, 42 %) as an off-white wax.

ν_{max}/cm^{-1} 1720 (ketone C=O), 1654 (amide C=O); δ_H (400 MHz, DMSO-d_6) 7.04 - 7.42 (5 H, m, *Ar*), 3.21 (6 H, s, NCH_3), 2.95 - 3.11 (1 H, m, C*H*), 2.54 - 2.77 (2 H, m, CH_2), 1.10 (3 H, d, *J*=7.0 Hz, CH_3); δ_C (100 MHz, DMSO-d_6)

177.3, 150.3, 140.1, 139.7, 129.4, 128.7, 126.5, 95.3 (C_5), 41.1 (*C*H), 28.2 (N*C*H$_3$), 17.1, 17.0; *m/z* (ESI$^-$) 301 ([M-H]$^-$); HRMS (ESI$^-$) $C_{16}H_{17}O_4N_2$, ([M-H]$^-$) requires 301.1194; found 301.1197.

N-Benzyl-6-hydroxy-1,3-dimethyl-2,4-dioxo-1,2,3,4-tetrahydropyrimidine-5-carboxamide **367**

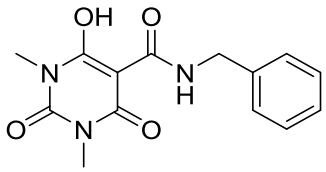

A solution of benzyl isocyanate (605 µL, 5 mmol) in CH_2Cl_2 (5 mL) was added dropwise to a stirring solution of 1,3-dimethylbarbituric acid (780 mg, 5 mmol) and diisopropylethylamine (1.74 mL, 10 mmol) in CH_2Cl_2 (15 mL). The resulting reaction mixture was stirred for 16 h at room temperature before HCl (6 N aq., 5 mL) was added dropwise. The organic layer was separated, dried over anhydrous $MgSO_4$, and concentrated *in vacuo*. The crude product was purified *via* flash column chromatography (20 % - 50 % EtOAc, cyclohexane) to give **367** (1.09 g, 75 %) as an off-white powder.

mp 103 °C; ν_{max}/cm^{-1} 1697 (ketone C=O), 1638 (amide C=O); δ_H (400 MHz, DMSO-d_6) 7.08 - 7.63 (5 H, m, *Ar*), 4.60 (2 H, d, *J*=6.0 Hz, C*H*$_2$), 3.18 (6 H, s, NC*H*$_3$); δ_C (100 MHz, DMSO-d_6) 170.6, 150.4, 137.9, 129.1, 127.9, 79.8 (C_5), 43.5 (*C*H$_2$), 27.8 (N*C*H$_3$); *m/z* (ESI$^-$) 288 ([M-H]$^-$); HRMS (ESI$^-$) $C_{14}H_{10}O_4N_3$, ([M-H]$^-$) requires 288.0990; found 288.0994.

6-Hydroxy-1,3-dimethyl-5-(5-phenylpentanoyl)pyrimidine-2,4(1*H*,3*H*)-dione **368**

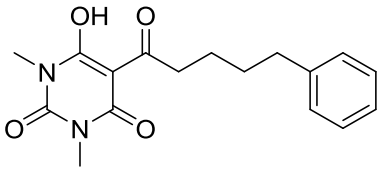

Follwing general procedure 3, 5-phenylvaleric acid (534 mg, 3 mmol) and 1,3-dimethylbarbituric acid (468 mg, 3 mmol) gave **368** (519 mg, 55 %) as a light-yellow oil.

ν_{max}/cm^{-1} 1722 (ketone C=O), 1667 (amide C=O); δ_H (400 MHz, DMSO-d_6) 7.03 - 7.44 (5 H, m, *Ar*), 3.19 (6 H, s, NC*H*$_3$), 3.07 - 3.15 (2 H, m), 2.57 - 2.67 (2 H, m), 1.59 - 1.72 (4 H, m); δ_C (100 MHz, DMSO-d_6) 150.4, 142.3, 128.8, 126.2, 95.9 (C_5), 36.0, 35.2, 31.1, 28.1 (N*C*H$_3$), 25.5; *m/z* (ESI$^-$) 315 ([M-H]$^-$); HRMS (ESI$^-$) $C_{17}H_{19}O_4N_2$, ([M-H]$^-$) requires 315.1350; found 315.1356.

5-Butyryl-6-hydroxy-1,3-dimethylpyrimidine-2,4(1*H*,3*H*)-dione **369**

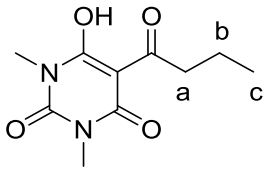

Butyryl chloride (309 µL, 3 mmol) was slowly added to a solution of 1,3-dimethylbarbituric acid (468 mg, 3 mmol) in pyridine (2 mL) and the resulting reaction mixture was stirred for 2 h at room temperature. The mixture was then slowly transferred into a stirring mixture of methanol (2 mL), H_2O (1.7 mL), and concentrated HCl aq. (5 mL) and stirring was continued for another 1 h at room temperature. CH_2Cl_2 (15 mL) was added, the mixture was shaken, and the organic layer was collected by passing the mixture through a phase separator cartridge. The organic layer was dried over anhydrous $MgSO_4$ and concentrated *in vacuo*. The crude product was then purified *via* flash column chromatography (20 % - 50 % EtOAc, cyclohexane) to give **369** (448 mg, 66 %) as a light-yellow oil.

ν_{max}/cm^{-1} 1722 (ketone C=O), 1667 (amide C=O); δ_H (400 MHz, DMSO-d_6) 3.20 (6 H, s, NCH_3), 3.00 - 3.10 (2 H, m, H_a), 1.65 (2 H, sxt, J=7.5 Hz, H_b), 0.97 (3 H, t, J=7.5 Hz, H_c); δ_C (100 MHz, DMSO-d_6) 198.1, 150.4, 95.9 (C_5), 38.1 (C_a), 28.1 (NCH_3), 19.3 (C_b), 14.2 (C_c); *m*/*z* (FI) 226 ([M]$^+$); HRMS (FI) $C_{10}H_{14}N_2O_4$, ([M]$^+$) requires 226.0954; found 226.0957.

6-Amino-1,3-dimethylpyrimidine-2,4(1*H*,3*H*)-dione **373**[220]

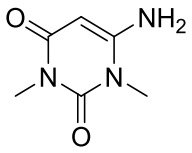

A solution of *N*,*N*'-dimethylurea (3.52 g, 40 mmol) and cyanoacetic acid (3.74 g, 44 mmol) in acetic anhydride (30 mL) was stirred at 70 °C for 16 h. The solvent was evaporated *in vacuo* and the resulting oily residue was diluted with NaOH (5 M in H_2O, 15 mL). The precipitate was collected by filtration, washed with cold H_2O, and purified by recrystallisation from a 1:1 mixture of MeOH and H_2O to give **373** (3.5 g, 57 %) as a white powder.

δ_H (400 MHz, DMSO-d_6) 4.71 (1 H, s, C*H*), 3.24 (3 H, s, NCH_3), 3.07 (3 H, s, NCH_3); δ_C (100 MHz, DMSO-d_6) 162.0, 155.4, 152.1, 75.4, 29.7, 27.5; *m*/*z* (ESI$^-$) 154 ([M-H]$^-$).

1,3-Diethylpyrimidine-2,4,6(1*H*,3*H*,5*H*)-trione **375**[221]

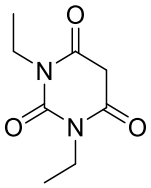

A stirring solution of malonic acid (5 g, 48 mmol) and 1,3-diethylurea (5 g, 48 mmol) in acetic acid (10 mL) was heated to 60 °C. Acetic anhydride (10 mL) was added to the reaction mixture which was stirred for another 6 h at 60 °C. Then, H_2O is (5 mL) is slowly added, and the mixture was stirred at 70 °C for 30 min. After cooling to room temperature, the reaction volume was reduced and the precipitate was collected by filtration, washed with H_2O, and dried to give **375** (5.73 g, 65 %) as a white powder.

δ_H (400 MHz, DMSO-d_6) 3.77 (4 H, q, *J*=7.0 Hz, CH_2), 3.71 (2 H, s, C$^5H_2$), 1.10 (6 H, t, *J*=7.0 Hz, CH_3); δ_C (100 MHz, DMSO-d_6) 166.0, 151.9, 36.5 (*C*H_2), 13.4 (*C*H_3); *m*/*z* (ESI$^-$) 183 ([M-H]$^-$).

1,3-Diisopropylpyrimidine-2,4,6(1*H*,3*H*,5*H*)-trione **380**[222]

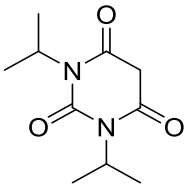

A solution of *N*,*N*'-diisopropylcarbodiimide (3.1 mL, 20 mmol) in THF (10 mL) was slowly added to a solution of malonic acid (1.04 g, 10 mmol) in THF (10 mL) at 0 °C. The resulting reaction mixture was warmed to room temperature and stirred for 2 h. The precipitate was collected by filtration and immediately slurried in ethanol (20 mL) and heated to reflux. The mixture was then allowed to cool to room temperature and the precipitate was filtered, washed with cold ethanol, and dried to give **378** (1.45 g, 68 %) as a white powder.

δ_H (400 MHz, DMSO-d_6) 5.50 (2 H, d, *J*=7.5 Hz, C$^5H_2$), 3.58 - 3.71 (2 H, m, C*H*(CH_3)$_2$), 1.01 (12 H, d, *J*=6.5 Hz, CH(CH_3)$_2$; δ_C (100 MHz, DMSO-d_6) 157.3, 41.1 (*C*H(CH$_3$)$_2$), 23.8 (CH(*C*H$_3$)$_2$); *m*/*z* (ESI$^-$) 211 ([M-H]$^-$);

1,3-Dicyclohexylpyrimidine-2,4,6(1*H*,3*H*,5*H*)-trione **381**

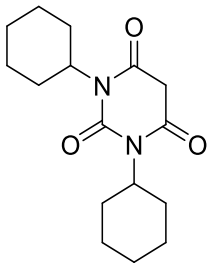

A solution of *N*,*N*'-dicyclohexylcarbodiimide (2.54 g, 12.3 mmol) in THF (10 mL) was slowly added to a solution of malonic acid (641 mg, 6.2 mmol) in THF (10 mL) at 0 °C. The resulting reaction mixture was warmed to room temperature and stirred for 2 h. The precipitate was collected by filtration and immediately slurried in ethanol (20 mL) and heated to reflux. The mixture was then allowed to cool to room temperature and the precipitate was filtered, washed with cold ethanol, and dried to give **379** (1.3 g, 72 %) as a white powder.

mp 203 °C; ν_{max}/cm^{-1} 1743 (C=O), 1691 (C=O), 1672 (C=O); δ_H (400 MHz, DMSO-d_6) 4.34 - 4.54 (2 H, m, NC*H*), 3.70 (2 H, s, C$^5H_2$), 2.00 - 2.29 (4 H, m), 1.70 - 1.86 (4 H, m), 1.48 - 1.68 (6 H, m), 1.19 - 1.38 (4 H, m), 1.03 - 1.18 (2 H, m); δ_C (100 MHz, DMSO-d_6) 166.5, 152.0, 54.2, 41.7, 29.1, 26.4, 25.3; *m*/*z* (ESI$^-$) 291 ([M-H]$^-$); HRMS (ESI$^-$) $C_{16}H_{23}O_3N_2$, ([M-H]$^-$) requires 291.1703; found 291.1716.

6-Hydroxy-1,3-dimethyl-5-palmitoylpyrimidine-2,4(1*H*,3*H*)-dione **382**

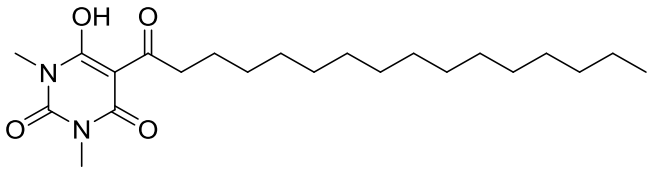

Palmitoyl chloride (911 µL, 3 mmol) was slowly added to a stirring solution of 1,3-dimethylbarbituric acid (468 mg, 3 mmol) in pyridine (1 mL) at room temperature. The resulting reaction mixture was stirred for an additional 2 h at room temperature before being slowly added to a stirring mixture of methanol (6 mL), H_2O (5 mL), and concentrated HCl aq. (15 mL). The resulting suspension was stirred for an additional 30 min at room temperature and then for 1 h at 0 °C. The precipitate was collected by filtration, washed with dilute HCl (10 % conc. HCl, 90 % H_2O), and dried under vacuum to give **382** (490 mg, 41 %) as an off-white powder.

mp 67 °C; ν_{max}/cm^{-1} 1720 (C=O), 1700 (C=O); δ_H (400 MHz, pyridine-d_5) 4.83 (6 H, s, NCH_3), 4.71 - 4.79 (2 H, m), 3.16 - 3.38 (2 H, m), 2.86 - 3.00 (2 H, m), 2.67 - 2.83 (22 H, m), 2.27 - 2.43 (3 H, m, CH_3); δ_C (100 MHz,

pyridine-d_5) 199.9 (*C*=O), 177.0 (*C*=O), 96.9 (C_5), 38.0, 35.9, 33.1, 30.9, 30.9, 30.8, 30.8, 30.7, 30.6, 30.6, 28.7, 27.2, 26.6, 23.9, 15.2; *m/z* (ESI$^-$) 393 ([M-H]$^-$); HRMS (ESI$^-$) $C_{22}H_{37}O_4N_2$, ([M-H]$^-$) requires 393.2759; found 393.2775.

6-Hydroxy-1,3-dimethyl-5-(2-phenoxyacetyl)pyrimidine-2,4(1*H*,3*H*)-dione **383**

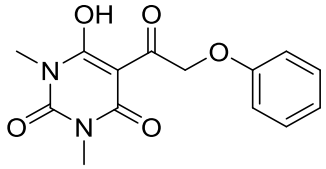

Phenoxyacetyl chloride (414 µL, 3 mmol) was slowly added to a stirring solution of 1,3-dimethylbarbituric acid (468 mg, 3 mmol) in pyridine (1 mL) at room temperature. The resulting reaction mixture was stirred for an additional 2 h at room temperature before being slowly added to a stirring mixture of methanol (6 mL), H_2O (5 mL), and concentrated HCl aq. (15 mL). The resulting suspension was stirred for an additional 30 min at room temperature and then for 1 h at 0 °C. The precipitate was collected by filtration, washed with dilute HCl (10 % conc. HCl, 90 % H_2O), and dried under vacuum to give **383** (347 mg, 40 %) as an off-white powder.

mp 192 °C; ν_{max}/cm^{-1} 1714 (C=O), 1654 (C=O); δ_H (400 MHz, pyridine-d_5) 8.76 - 8.83 (2 H, m, *Ar*), 8.72 - 8.75 (2 H, m, *Ar*), 8.38 - 8.45 (1 H, m, *Ar*), 7.40 (2 H, s, C*H*$_2$), 4.98 (6 H, s, NC*H*$_3$); δ_C (100 MHz, DMSO-d_6) 193.4 (*C*=O), 166.0 (*C*=O), 161.2, 153.3, 130.7, 121.4, 116.3, 116.1, 96.4 (C_5), 74.4 (*C*H$_2$), 29.1 (N*C*H$_3$), 28.5 (N*C*H$_3$); *m/z* (ESI$^-$) 289 ([M-H]$^-$); HRMS (ESI$^-$) $C_{14}H_{13}O_5N_2$, ([M-H]$^-$) requires 289.0830; found 289.0834.

5-(3-(Furan-2-yl)propanoyl)-6-hydroxy-1,3-dimethylpyrimidine-2,4(1*H*,3*H*)-dione **384**

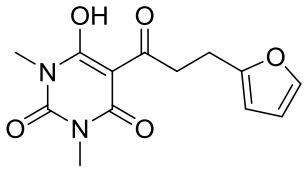

Following general procedure 3, 3-2(furyl)propionic acid (420 mg, 3 mmol) and 1,3-dimethylbarbituric acid (468 mg, 3 mmol) gave **384** (5 mg, 1 %) as a light-orange solid.

Given the low yield, only LC-MS data was acquired. *m/z* (ESI$^+$) 279 ([M+H]$^+$).

5-(3-Cyclopentylpropanoyl)-1,3-diethyl-6-hydroxypyrimidine-2,4(1*H*,3*H*)-dione **385**

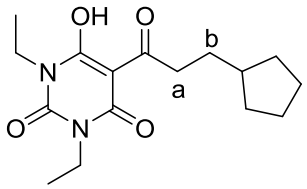

Cyclopentanepropionyl chloride (460 µL, 3 mmol) was slowly added to a solution of **375** (552 mg, 3 mmol) in pyridine (2 mL) and the resulting reaction mixture was stirred for 2 h at room temperature. The mixture was then slowly transferred into a stirring mixture of methanol (2 mL), H_2O (1.7 mL), and concentrated HCl aq. (5 mL) and stirring was continued for another 1 h at room temperature. CH_2Cl_2 (15 mL) was added, the mixture was shaken, and the organic layer was collected by passing the mixture through a phase separator cartridge. The organic layer was dried over anhydrous $MgSO_4$ and concentrated *in vacuo*. The crude product was then purified *via* flash column chromatography (20 % - 50 % EtOAc, cyclohexane) to give **385** (536 mg, 58 %) as a light-yellow oil.

ν_{max}/cm^{-1} 1720 (ketone C=O), 1667 (amide C=O); δ_H (400 MHz, DMSO-d_6) 3.76 - 3.93 (4 H, m, NCH_2), 3.01 - 3.20 (2 H, m, H_a), 1.68 - 1.91 (3 H, m), 1.41 - 1.66 (6 H, m), 1.01 - 1.23 (8 H, m); δ_C (100 MHz, DMSO-d_6) 198.7, 149.5, 95.8 (C_5), 35.7, 32.4, 32.1, 25.2, 25.1, 13.4; *m/z* (ESI$^-$) 307 ([M-H]$^-$); HRMS (ESI$^-$) $C_{16}H_{23}O_4N_2$, ([M-H]$^-$) requires 307.1663; found 307.1667.

1,3-Dicyclohexyl-5-(3-cyclopentylpropanoyl)-6-hydroxypyrimidine-2,4(1*H*,3*H*)-dione **386**

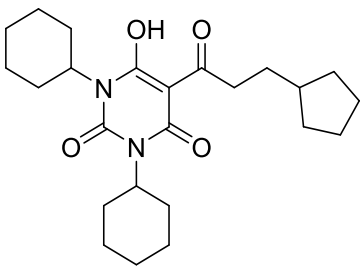

Cyclopentanepropionyl chloride (460 µL, 3 mmol) was slowly added to a solution of **381** (876 mg, 3 mmol) in pyridine (6 mL) and the resulting reaction mixture was stirred for 2 h at room temperature. The mixture was then slowly transferred into a stirring mixture of methanol (2 mL), H_2O (1.7 mL), and concentrated HCl aq. (5 mL) and stirring was continued for another 1 h at room temperature. CH_2Cl_2 (15 mL) was added, the mixture was shaken, and the organic layer was collected by passing the mixture through a phase separator cartridge.

The organic layer was dried over anhydrous $MgSO_4$ and concentrated *in vacuo*. The crude product was then purified *via* flash column chromatography (20 % - 50 % EtOAc, cyclohexane) to give **386** (763 mg, 61 %) as a light-yellow oil.

ν_{max}/cm^{-1} 1741 (ketone C=O), 1668 (amide C=O); δ_H (400 MHz, DMSO-d_6) 4.45 - 4.73 (2 H, m, NC*H*), 2.97 - 3.13 (2 H, m, COCH_2), 2.12 - 2.37 (5 H, m), 1.44 - 1.92 (22 H, m), 0.98 - 1.36 (4 H, m); δ_C (100 MHz, pyridine-d_5) 199.2 (*C*=O), 96.1 (C_5), 54.4, 40.1, 36.6, 32.4, 32.1, 29.1, 26.5, 25.5, 25.2; *m*/*z* (ESI$^-$) 415 ([M-H]$^-$); HRMS (ESI$^-$) $C_{24}H_{35}O_4N_2$, ([M-H]$^-$) requires 415.2602; found 415.2623.

5-(3-Cyclopentylpropanoyl)-6-hydroxy-1,3-dimethylpyrimidine-2,4(1*H*,3*H*)-dione 387

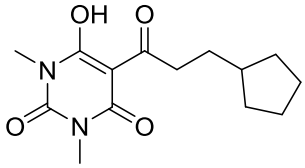

Cyclopentanepropionyl chloride (460 µL, 3 mmol) was slowly added to a solution of 1,3-dimethylbarbituric acid (312 mg, 3 mmol) in pyridine (2 mL) and the resulting reaction mixture was stirred for 2 h at room temperature. The mixture was then slowly transferred into a stirring mixture of methanol (2 mL), H_2O (1.7 mL), and concentrated HCl aq. (5 mL) and stirring was continued for another 1 h at room temperature. CH_2Cl_2 (15 mL) was added, the mixture was shaken, and the organic layer was collected by passing the mixture through a phase separator cartridge. The organic layer was dried over anhydrous $MgSO_4$ and concentrated *in vacuo*. The crude product was then purified *via* flash column chromatography (20 % - 50 % EtOAc, cyclohexane) to give **387** (361 mg, 42 %) as a light-yellow oil.

ν_{max}/cm^{-1} 1724 (ketone C=O), 1669 (amide C=O); δ_H (400 MHz, DMSO-d_6) 3.19 (6 H, s, NCH_3), 3.01 - 3.13 (2 H, m, COCH_2), 1.68 - 1.90 (4 H, m), 1.40 - 1.66 (6 H, m); δ_C (100 MHz, DMSO-d_6) 198.7, 150.4, 95.8 (C_5), 35.6, 32.4, 32.2, 28.1 (NCH_3), 25.2; *m*/*z* (ESI$^-$) 279 ([M-H]$^-$); HRMS (ESI$^-$) $C_{14}H_{19}O_4N_2$, ([M-H]$^-$) requires 279.1350; found 279.1351.

6-Hydroxy-5-(3-(2-methoxyphenyl)propanoyl)-1,3-dimethylpyrimidine-2,4(1*H*,3*H*)-dione **388**

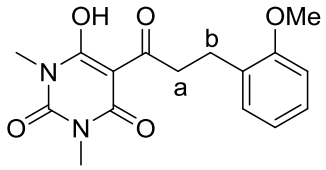

Following general procedure 3, 3-(2-methoxyphenyl)propionic acid (540 mg, 3 mmol) and 1,3-dimethylbarbituric acid (468 mg, 3 mmol) gave **388** (544 mg, 57 %) as an off-white solid.

mp 144 °C; ν_{max}/cm^{-1} 1708 (ketone C=O), 1654 (amide C=O); δ_H (400 MHz, pyridine-d_5) 7.35 - 7.42 (1 H, m, *Ar*), 7.21 - 7.28 (1 H, m, *Ar*), 6.92 - 7.01 (1 H, m, *Ar*), 6.86 - 6.92 (1 H, m, *Ar*), 3.68 (3 H, s, OCH_3), 3.59 - 3.66 (2 H, m, H_a), 3.30 (6 H, s, NCH_3), 3.14 - 3.25 (2 H, m, H_b); δ_C (100 MHz, pyridine-d_5) 198.0 (*C*=O), 157.7 (*C*=O), 130.1, 129.1, 127.9, 120.7, 110.7, 95.8 (C_5), 55.0 (OCH$_3$), 37.3 (C_a), 27.5 (NCH$_3$), 26.3 (C_b); *m*/*z* (ESI$^-$) 317 ([M-H]$^-$); HRMS (ESI$^-$) $C_{16}H_{17}O_5N_2$, ([M-H]$^-$) requires 317.1143; found 317.1148.

6-Hydroxy-5-(3-(3-methoxyphenyl)propanoyl)-1,3-dimethylpyrimidine-2,4(1*H*,3*H*)-dione **389**

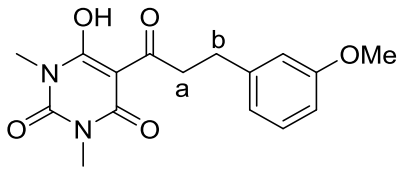

Following general procedure 3, 3-(3-methoxyphenyl)propionic acid (540 mg, 3 mmol) and 1,3-dimethylbarbituric acid (468 mg, 3 mmol) gave **389** (649 mg, 68 %) as an off-white solid.

mp 118 °C; ν_{max}/cm^{-1} 1717 (ketone C=O), 1660 (amide C=O); δ_H (400 MHz, DMSO-d_6) 7.14 - 7.30 (1 H, m, *Ar*), 6.83 - 6.91 (2 H, m, *Ar*), 6.73 - 6.81 (1 H, m, *Ar*), 3.75 (3 H, s, OCH_3), 3.31 - 3.45 (2 H, m, H_a), 3.21 (6 H, s, NCH_3), 2.81 - 2.98 (2 H, m, H_b); δ_C (100 MHz, DMSO-d_6) 197.1 (*C*=O), 159.8, 150.4, 132.5, 129.9, 121.0, 114.5, 112.0, 95.9 (C_5), 55.4 (OCH$_3$), 38.2 (C_a), 31.3 (C_b), 28.2 (NCH$_3$); *m*/*z* (ESI$^-$) 317 ([M-H]$^-$); HRMS (ESI$^-$) $C_{16}H_{17}O_5N_2$, ([M-H]$^-$) requires 317.1143; found 317.1148.

6-Hydroxy-5-(3-(4-methoxyphenyl)propanoyl)-1,3-dimethylpyrimidine-2,4(1*H*,3*H*)-dione **390**

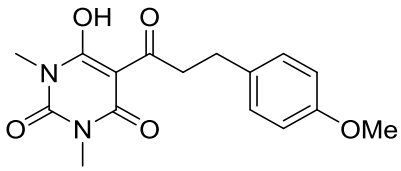

Following general procedure 3, 3-(4-methoxyphenyl)propionic acid (540 mg, 3 mmol) and 1,3-dimethylbarbituric acid (468 mg, 3 mmol) gave **390** (582 mg, 61 %) as an off-white solid.

mp 148 °C; ν_{max}/cm^{-1} 1710 (ketone C=O), 1656 (amide C=O); δ_H (400 MHz, pyridine-d_5) 7.27 - 7.40 (2 H, m, *Ar*), 6.86 - 7.05 (2 H, m, *Ar*), 3.65 (3 H, s, OCH_3), 3.53 - 3.59 (2 H, m, H_a), 3.32 (6 H, s, NCH_3), 3.00 - 3.09 (2 H, m, H_b); δ_C (100 MHz, pyridine-d_5) 197.5 (*C*=O), 158.8 (*C*=O), 133.1, 129.7, 114.2, 95.8 (C_5), 54.9 (OCH_3), 39.4 (C_a), 30.9 (NCH_3), 27.6 (C_b); *m/z* (ESI$^-$) 317 ([M-H]$^-$); HRMS (ESI$^-$) $C_{16}H_{17}O_5N_2$, ([M-H]$^-$) requires 317.1143; found 317.1149.

5-(3-Cyclopropylpropanoyl)-6-hydroxy-1,3-dimethylpyrimidine-2,4(1*H*,3*H*)-dione 391

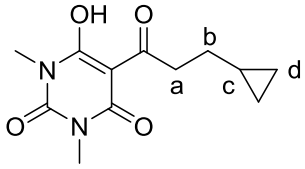

Following general procedure 3, 3-cyclopropylpropionic acid (250 mg, 2.2 mmol) and 1,3-dimethylbarbituric acid (342 mg, 2.2 mmol) gave **391** (227 mg, 41 %) a light-yellow oil.

ν_{max}/cm^{-1} 1722 (ketone C=O), 1666 (amide C=O); δ_H (400 MHz, DMSO-d_6) 2.99 - 3.16 (8 H, m, NCH_3 and H_a), 1.33 - 1.55 (2 H, m, H_b), 0.59 - 0.76 (1 H, m, H_c), 0.26 - 0.40 (2 H, m, H_d), -0.09 - 0.07 (2 H, m, H_d); δ_C (100 MHz, DMSO-d_6) 198.0, (*C*=O), 150.4, 95.0 (C_5), 38.7 (C_a), 30.9 (C_b), 28.1 (NCH_3), 11.9 (C_c), 5.0 (C_d); *m/z* (ESI$^-$) 251 ([M-H]$^-$); HRMS (ESI$^-$) $C_{12}H_{15}O_4N_2$, ([M-H]$^-$) requires 251.1037; found 251.1036.

6-Hydroxy-1,3-dimethyl-5-(3-(thiophen-3-yl)propanoyl)pyrimidine-2,4(1*H*,3*H*)-dione 392

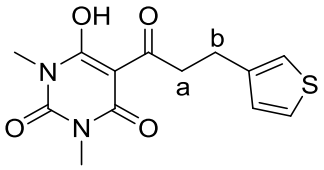

Following general procedure 3, 3-(thiophene-3-yl)propanoic acid (250 mg, 1.6 mmol) and 1,3-dimethylbarbituric acid (250 mg, 1.6 mmol) gave **392** (230 mg, 49 %) as a light-brown solid.

mp 82 °C; ν_{max}/cm^{-1} 1716 (ketone C=O), 1659 (amide C=O); δ_H (400 MHz, DMSO-d_6) 7.41 - 7.54 (1 H, m, *Ar*), 7.16 - 7.32 (1 H, m, *Ar*), 6.98 - 7.12 (1 H, m, *Ar*), 3.34 - 3.49 (2 H, m, H_a), 3.21 (6 H, s, NCH_3), 2.85 - 3.06 (2 H,

m, H_b); δ_C (100 MHz, DMSO-d_6) 197.1, (*C*=O), 150.4, 141.1, 128.7, 126.5, 121.5, 96.0 (C_5), 37.4 (C_a), 28.2 (N*C*H$_3$), 25.8 (C_b); *m/z* (ESI$^-$) 293 ([M-H]$^-$); HRMS (ESI$^-$) $C_{13}H_{13}O_4N_2S$, ([M-H]$^-$) requires 293.0602; found 293.0600.

6-Hydroxy-1,3-dimethyl-5-(2-methyl-3-(thiophen-3-yl)propanoyl)pyrimidine-2,4(1*H*,3*H*)-dione **393**

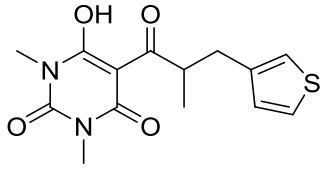

Following general procedure 3, 2-methyl-3-thiophen-2-yl-propanoic acid (250 mg, 1.5 mmol) and 1,3-dimethylbarbituric acid (229 mg, 1.5 mmol) gave **393** (240 mg, 53 %) as an off-white solid.

mp 103 °C; ν_{max}/cm^{-1} 1721 (ketone C=O), 1652 (amide C=O); δ_H (400 MHz, DMSO-d_6) 7.24 - 7.41 (1 H, m, *Ar*), 6.90 - 6.97 (1 H, m, *Ar*), 6.86 - 6.90 (1 H, m, *Ar*), 4.47 (1 H, q, *J*=7.0 Hz, C*H*), 3.13 - 3.29 (8 H, m, C*H*$_2$ and NC*H*$_3$), 1.18 (3 H, d, *J*=7.0 Hz, C*H*$_3$); δ_C (100 MHz, DMSO-d_6) 200.5, (*C*=O), 150.3, 142.0, 127.4, 126.3, 124.9, 96.5 (C_5), 39.4 (*C*H), 33.0 (*C*H$_2$), 28.2 (N*C*H$_3$), 17.4 (*C*H$_3$); *m/z* (ESI$^-$) 307 ([M-H]$^-$); HRMS (ESI$^-$) $C_{14}H_{15}O_4N_2S$, ([M-H]$^-$) requires 307.0758; found 307.0762.

6-Hydroxy-1,3-dimethyl-5-(3-methyl-3-(thiophen-3-yl)butanoyl)pyrimidine-2,4(1H,3H)-dione **394**

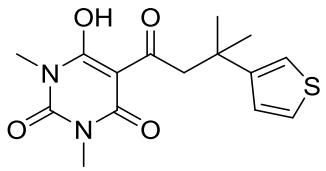

Following general procedure 3, 3-methyl-3-(thiophen-2-yl)butanoic acid (250 mg, 1.4 mmol) and 1,3-dimethylbarbituric acid (212 mg, 1.4 mmol) gave 394 (176 mg, 39 %) as a light-yellow oil.

ν_{max}/cm^{-1} 1722 (ketone C=O), 1664 (amide C=O); δ_H (400 MHz, DMSO-d_6) 7.23 - 7.39 (1 H, m, *Ar*), 6.86 - 7.03 (2 H, m, *Ar*), 3.52 - 3.69 (2 H, m, C*H*$_2$), 3.19 (6 H, s, NC*H*$_3$), 1.48 (6 H, s, C*H*); δ_C (100 MHz, DMSO-d_6) 195.3, (*C*=O), 150.2, 127.1, 123.7, 123.1, 97.6 (C_5), 47.9 (*C*H$_2$), 38.6, 30.4 (*C*H$_3$), 28.2 (N*C*H$_3$); *m/z* (ESI$^-$) 321 ([M-H]$^-$); HRMS (ESI$^-$) $C_{15}H_{17}O_4N_2S$, ([M-H]$^-$) requires 321.0915; found 321.0920.

Chapter VII: Summary and Future Work

Two tool compounds, **193** for the subfamily of KDM4 histone demethylases, and **363** for the ribosomal oxygenase OGFOD1, were generated during the course of this thesis. The fields of histone demethylases and ribosomal oxygenases are both very young, although at different stages of development. The KDM field is relatively more advanced from a chemical biology perspective, with a wide range of techniques already available for protein production and inhibitor screening. **193**, and the corresponding negative control **224**, could therefore be used for functional studies immediately after *in vitro* characterisation. The field of ribosomal oxygenases only emerged during the course of this thesis, and therefore the nature of work involved for tool compound development was very different. The work for the development of **363** was focused around *in vitro* considerations, whereas **193** has already been of benefit in a cellular context. If one assumes the process for tool compound development to be relatively linear, with distinct stages of 'assay platform development', 'compound development', 'cell studies', and '*in vivo*' studies, we can get an appreciation of the relative stages of development of both tool compounds **193** and **363**. **193** is currently at the stage of 'cell studies', whereas **363** is at the stage of '*in vitro*' studies. A more specific summary for each project is given below (Figure **83**).

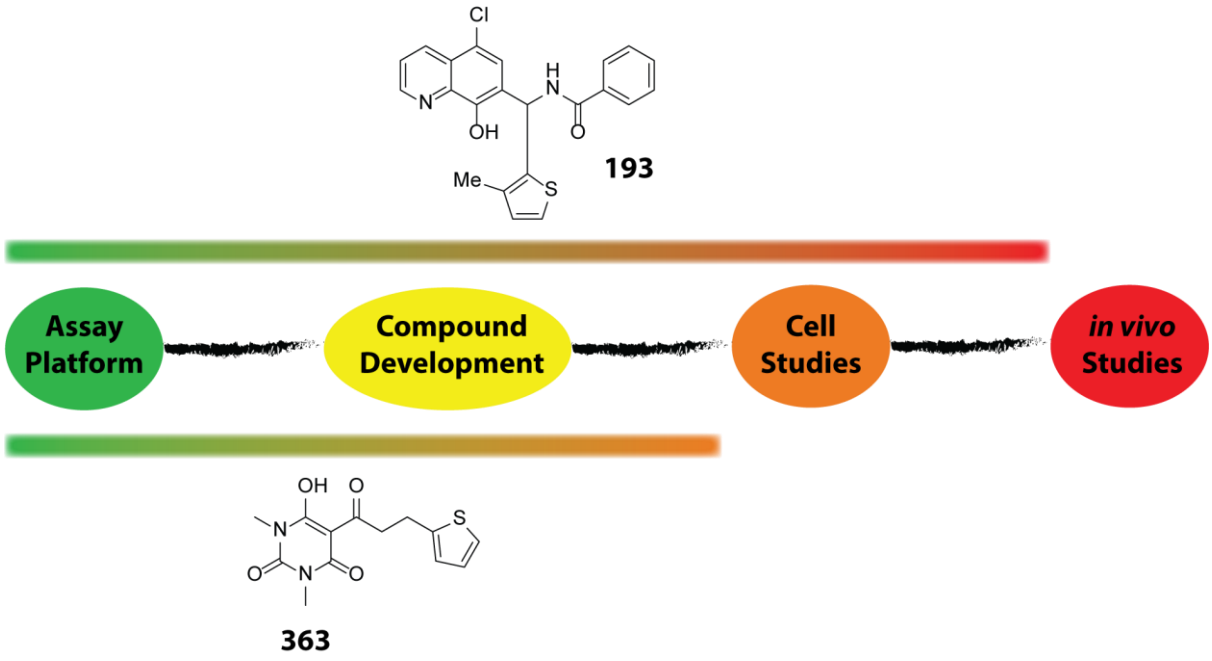

Figure 83: Relative stages of development of tool compounds **193** and **363**.

Tool Compound 193 for the KDM4 Histone Demethylases

In Chapters II and III, an open-skies approach was adopted for the development of the KDM4 tool compound **193** (Figure 84). Based on *in silico*, *in vitro*, and cellular precedents, 8HQ was judged to be an attractive generic inhibitor template to which side chains can be attached to synthesise 2OG oxgygenase-selective small molecules. A one-pot three-component synthetic methodology was developed for rapid access to a diverse range of 7-substituted 8HQs, alongside the required methodologies associated with the synthesis of the corresponding starting materials. Systematic generation of focused libraries alongside concomitant *in vitro* screening led to emerging structure-activity and structure-selectivity relationships which were also at the basis of an *in silico* docking model to guide future synthesis. In particular, the combination of 5-chloro substitution of the 8HQ core, as well as *meta*-substitution of the aldehyde-derived moiety, led to inhibitors selective for the KDM4 over the KDM5 subfamily.

The particular value of 7-substituted 8HQs is their activity in cells: the EC_{50} values in cells are generally of the same order of magnitude than the corresponding *in vitro* IC_{50} values. A combination of *in vitro* potency and selectivity, as well as cell activity considerations led to the selection of **193** as a tool compound. A negative control, **224**, was synthesised by methylation of the 8HQ phenol, hereby preventing Fe(II) binding inside the enzyme active site and rendering the compound inactive, as demonstrated *in vitro* and in cells.

Treatment of HeLa and MCF7 cells with **193** led to stabilisation of the H3K9me3 mark, both in systems with overexpressed KDM4A, as well as endogenous KDM levels. At high concentration the compound inhibits cell proliferation in these cell lines. The observation that KDM4 overexpression is related to several cancers, including lung, led to assessment of **193** in patient-matched lung cell lines: one derived from cancer, one from healthy lung, of the same patient. **193** selectively reduced viability of the tumour cells, but not the normal cells.

Analysis of the effect of **193** on whole histones revealed that the pattern of post-translational modifications is altered for H3 of treated relative to untreated cells. No effect was observed for H2A, H2B, or H4. This result is in line with current evidence that the KDM4 subfamily selectively acts on H3K9 and H3K36.

Recent findings also reveal that **193** stabilises HIF to a similar extent to the potent PHD2 inhibitor FG4592 **28**. **193**, however, seems to operate *via* a mechanism independent of PHD2 inhibition, as suggested by PHD2 inhibition and binding studies.

Ongoing, and future work, will be mediated *via* distribution of **193**, and maybe improved variants, to collaborators for functional elucidation of the KDM4 subfamily in cells, and ultimately *in vivo*. Given the success of the template-based approach, it is worthwhile to explore this approach for the generation of inhibitors for other 2OG oxygenases and/or other enzyme superfamilies. Follow-up work would also be conducted in the areas of dual inhibitors and affinity purification based on 7-substituted 8HQs.

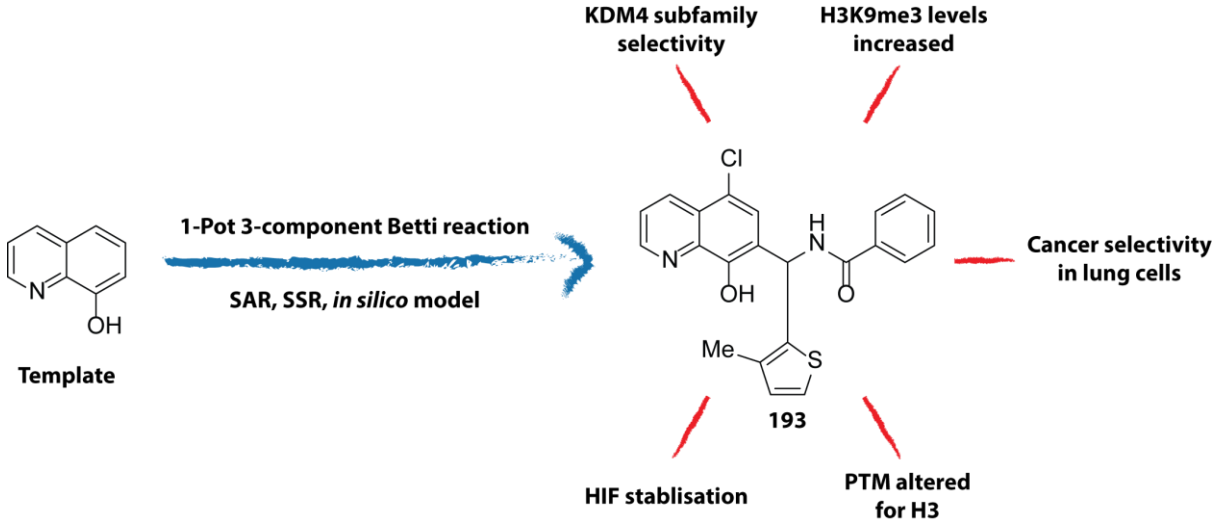

Figure 84: Summarising overview for the development of the KDM4 subfamily tool compound **193**. 8HQ was used as a template to generate 8HQ-based **193** *via* considerations of synthetic strategies for library generation, SAR, SSR, and *in silico* models. **193** was then used for functional investigations relating to the H3K9me3 histone mark.

Tool Compound 363 for the Ribosomal Prolyl Hydroxylase OGFOD1

The first step for OGFOD1 inhibitor development was the identification and subsequent development of a suitable *in vitro* screening platform, as described in Chapter V. Differential scanning fluorimetry (DSF) proved suitable for binding studies. Intrinsic fluorescence assay (IFA), however, is not suitable for small-molecule binding studies with full-length OGFOD1.

Optimisation, and documentation, of OGFOD1 expression and purification conditions was undertaken to reproducibly yield catalytically active OGFOD1. Subsequent determination of the requisite kinetic parameters, such as linear range of catalytic turnover, as well as (apparent) K_M values and saturation

concentrations for the cofactors and cosubstrates, was at the basis for the development of a MALDI-TOF MS-based OGFOD1 activity assay. The associated assay conditions were directly transferrable into RapidFire™ assay technology.

The hydroxylation assay enabled subsequent inhibitor development. In Chapter VI, an initial focused library was based on small molecules which are either (former) clinical candidates, or currently used agrochemicals, against structurally related enzymes. This selection was thought to furnish chemotypes which are likely to inhibit OGFOD1, while already being optimised for ADMET properties for future use *in vivo*. In fact, all of the PHD2 inhibitors were also potent inhibitors of OGFOD1. This insight may need to be addressed for future evaluation of these compounds as clinical candidates, for example with regards to monitoring off-target effects. Monitoring (surrogate) effects related to ribosome modifications may not seem obvious when assessing compounds primarily affecting the transcriptional machinery *via* the HIF pathway. Appropriate monitoring of phenotypes related to, for example, stop codon readthrough should therefore be taken into account in the future when assessing PHD2 inhibitors.

The triketone chemotype was selected based on *in vitro* potency considerations, as well as *in silico* docking considerations because this particular chemotype offered an opportunity to reach toward OGFOD1-specific residues which are not present in PHD2. Screening of various core structures then identified the barbiturate core as most likely to furnish potent inhibitors.

It was then discovered that the glycine-type side chain, omnipresent in PHD2 inhibitors, is not necessarily required for potency against OGFOD1 in combination with the triketone core structure. Subsequent exploration of various side chains revealed that a hydrocinnamoyl-based side chain, in combination with the triketone barbiturate core, led to potent inhibitors for OGFOD1 which are selective against PHD2. **363** was selected as a lead compound because it seemed to be the most potent compound in the current library. However, the potency of these molecules lies within the assay detection limit, leading to a current high-potency plateau because the compounds appear to be indistinguishable from each other (Figure 85).

Given that the current OGFOD1 inhibitors are based on clinically relevant compounds, and barbiturates are well-known molecules used for CNS applications, it was worthwhile to test for some drug-like properties, as

well as the ability of these compounds to cross the blood-brain barrier.[218] Indeed, aqueous solubility, stability in S9 liver microsomes, and a surrogate assay for BBB permeability prediction indicated that **363** has the potential to be a useful compound *in vivo*, and may be able to cross the BBB. If BBB permeability is not desired, it should be relatively easy to change the physical properties to prevent BBB crossing. Turning a BBB-impermeable compound into a permeable one, conversely, is assumed to be relatively more challenging.

Future work will require optimisation of the sensitivity, i.e. reduce the enzyme concentration, of the *in vitro* assay in order to assess high-potency compounds. This may be achieved by increasing OGFOD1 catalytic activity (e.g. by expressing the catalytic domain only) or by finding a better *in vitro* substrate (e.g. by using a cyclic peptide). In addition, there is a need to develop a cell-based assay for OGFOD1. Possibilities include the generation of a specific antibody for hydroxylated RPS23, or adapting the stop-codon readthrough assay currently in use for the Tpa1p yeast homologue for applications with OGFOD1.[95]

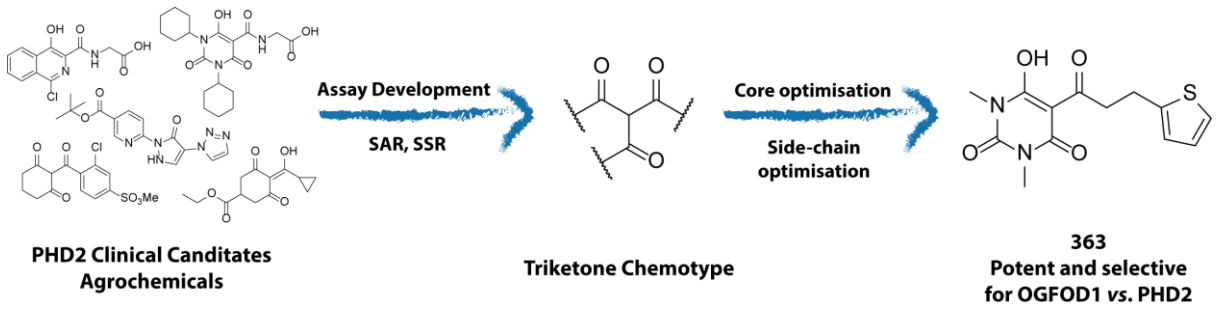

Figure 85: Summarising overview for the development of the OGFOD1 tool compound **363**. Assay development and subsequent screening of a focused library based on clinical candidates for PHD2 and related agrochemicals suggested a triketone chemotype for adding most value to the development of OGFOD1-selective small molecules. Investigations into core and side chain optimisation yielded lead compound **363** with a 1,3-dimethyl barbiturate core and a hydrocinnamoyl-derived side chain. This compound is potent for OGFOD1 and selective against PHD2.

Epigenetic Drug Discovery and Open Innovation

From the analysis in Chapter IV, it appears that the field of epigenetics has the potential to bring about a paradigm shift in some aspects of drug discovery. Epigenetics required an unusually long initiation phase, but has experienced exponential growth in the last years. This initiation phase is likely to be at a very early stage, and the growth rate is predicted to increase in the near future.

The very interdisciplinary nature of the epigenetic field is likely to optimally benefit from an open-innovation collaborative platform in a consortium. Fundamental research is essential for the advancement of

technologies related to epigenetics, especially with respect to the generation of a future dominant design for optimal advancement of the field. In particular, the development of chemical probes can generate multiple virtuous cycles for the generation of both science and technology.

General Conclusions

Both fundamental research, as well as technology-driven projects, can substantially benefit from small-molecule compounds which are potent, cell-permeable, and selective for particular (sets of) enzymes for the elucidation of biological pathways. Two such compounds, **193** and **363**, were generated during the course of work described within this thesis. Given the relatively young nature of the fields of both KDMs and ribosomal 2OG oxygenases, one hopes that the distribution, and use, of these compounds will contribute to the functional understanding of these enzymes to ultimately lead to applications for the benefit of our society. Compared to many other 2OG oxygenase inhibitors, commonly based on analogues of the cosubstrate 2OG **1**, **193** and **363** do not possess acidic side chains. Thus, these compounds enable further work that may lead to new cell-active 2OG oxygenase inhibitors with improved *in vivo* properties. Ideally, these compounds should be made available for collaborative studies. With this respect, it may be worthwhile to re-evaluate the recent trend of intensive intellectual property gathering within academic institutions, which may seem beneficial for the generation of spin-out companies. However, this practice hinders the advancement of fundamental research, by reducing the visibility of novel findings and fostering competition, rather than collaboration. **193** and **363** shall actively be used and not disappear within this thesis after putting it on the shelf, like a genie in a bottle (Figure 86).

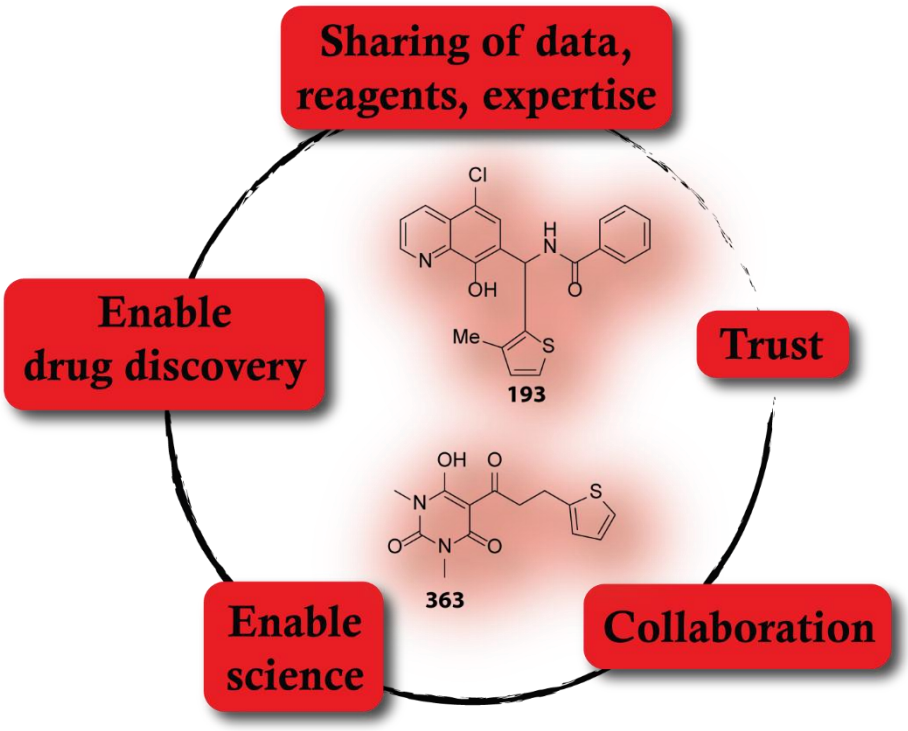

Figure 86: KDM4 and OGFOD1 tool compounds for open-innovation drug discovery. In summary, the tool compounds **193** and **363** developed during the course of this thesis should be used in a collaborative effort to enable functional elucidation of 2OG oxygenases to ultimately pave the way for the development of pharmaceutically useful entities for the (improvement of) treatment and/or diagnosis of disease.

Chapter VIII: Materials and Methods

Chemical Synthesis

All reactions involving moisture-sensitive reagents were carried out under a nitrogen atmosphere using standard vacuum line techniques and flame-dried glassware. Solvents were dried according to the procedure outlined by Grubbs and co-workers.[223] Water was purified by an Elix® UV-10 system. All other solvents and reagents were used as supplied (analytical or HPLC grade). For workups, anhydrous $MgSO_4$ was used as drying agent. Thin layer chromatography was performed on aluminium plates coated with 60 F254 silica. Plates were visualised using UV light (254 nm), or 1% aq. $KMnO_4$. Flash column chromatography was performed on Kieselgel 60 silica on a glass column, or on a Biotage SP4 flash column chromatography platform. Melting points were recorded on a Gallenkamp Hot Stage apparatus. IR spectra were recorded using a Bruker Tensor 27 FT-IR spectrometer as thin films. Selected characteristic peaks are reported in cm^{-1}. NMR spectra were recorded using Bruker Avance spectrometers in the deuterated solvent stated. The field was locked by external referencing to the relevant residual proton resonance. Chemical shifts (δ) are reported in ppm and coupling constants (J) in Hz. Low-resolution mass spectra were recorded on either a VG MassLab 20-250 or a Micromass Platform 1 spectrometer. Accurate mass measurements were run using either a Bruker MicroTOF internally calibrated with polyalanine, or a Micromass GCT instrument fitted with a Scientific Glass Instruments BPX5 column (15 m $\times$ 0.25 mm) using amyl acetate as a lock mass, by the mass spectrometry service of the Chemistry Research Laboratory, University of Oxford, UK.

General Experimental

All chemicals were from Sigma-Aldrich unless otherwise stated. Water was purified using a Millipore Elix® 10 system and then passed through a 0.22 µm filter by a Millipore MilliQ system. Throughout, standard sterile practices were followed. Equipment and media were sterilised by autoclaving for 20 minutes at 121 °C. For heat-sensitive solutions, sterilisation was performed using a 0.22 µm filter.

Except for Fe(II), all stock solutions were prepared in assay buffer (50 mM, pH 7.5). Fe(II) stocks were prepared by dissolving Fe(II) ammonium sulphate in 20 mM hydrochloric acid and further diluting in MilliQ water. 2OG was used as the disodium salt; ascorbate was used as the sodium salt throughout.

Binding Assays

Intrinsic Fluorescence Assay

Fe(II) stocks were prepared by dissolving $(NH_4)_2Fe(SO_4)_2 \bullet 6H_2O$ in 20 mM hydrochloric acid and further diluting in MilliQ water. Metal binding was assessed by conducting the assay in 50 mM HEPES buffer, with enzyme (10 µM) and varying Fe(II) concentrations being incubated at room temperature for 1 h. 2OG binding was assessed by conducting the assay in 50 mM HEPES buffer, with enzyme (10 µM), Fe(II) (50 µM), and varying 2OG concentrations being incubated at room temperature for 1 h. The samples were then excited at 280 nm, and fluorescence emission was measured at 350 nm using a PHERAstar FS Fluorescence plate reader.

Differential Scanning Fluorimetry assay

Temperature-dependent protein denaturation was assessed using a fluorescence-based thermal shift assay (Thermofluor).[203] Assays were conducted in 50 mM HEPES buffer, with enzyme (2 µM), inhibitor (200 µM), $MnCl_2 \bullet 4H_2O$, and Sypro® Orange (1:5000 dilution). Incubations were performed in a white 96-well RT-PCR plate and subjected to thermal cycling in an Opticon thermal cycler (MJ Research Inc.) using a standard protocol provided by the supplier. Datasets were processed using OpticonMONITOR Analysis Software and analysed using customised scripts (developed by Dr Frank Niesen, Structural Genomics Consortium, Oxford) in Microsoft Excel. Curve fitting was performed in GraphPad Prism.

Non-Denaturing ESI-MS studies[112]

PHD2 was desalted using a Bio-Spin 6 Column (Bio-Rad, Hemel Hempstead, U.K.) in 15 mM ammonium acetate (pH 7.5). The stock solution was diluted with the same buffer to a final concentration of 100 µM. Compounds at a 60 mM stock concentration in DMSO were further diluted in ammonium acetate to a concentration of 100 µM. $MnSO_4$ and 2OG were dissolved in MilliQ water at a concentration of 100 mM. This was then diluted with MilliQ water to give a final working concentration of 100 µM. The protein was mixed

with Mn(II), compounds, and 2OG to give final concentrations of 15 µM PHD2, 15 µM Mn(II), and 15 µM compound and 15 µM 2OG. ESI-MS analysis was performed immediately without incubation.

Mass spectrometric data were acquired using a Q-TOF mass spectrometer (Q-TOF micro, Micromass, Altrincham, U.K.) interfaced with a NanoMate (Advion Biosciences, Ithaca, NY) with a chip voltage of 1.70 kV and a delivery pressure 0.5 psi. The sample cone voltage was typically 30 V with a source temperature of 60 °C and with an acquisition/scan time of 1 s/1 s.

Calibration and sample acquisition were performed in the positive ion mode in the range of 2000-3700 m/z. The pressure at the interface between the atmospheric source and the high vacuum region was fixed at 6.30 mbar. External instrument calibration was achieved using a 2:1 mixture of myglobin/trypsinogen. Data were processed with the MassLynx 4.0 (Waters).

Activity assays

MALDI-TOF MS assays

OGFOD1 activity assays

OGFOD1 used for biochemical assays was stored at -80 °C in 50 mM HEPES (pH 7.5), 150 mM NaCl, 1 mM DTT and 5% (*w*/*v*) glycerol after HisTrap HP column purification. Activity assays were performed by determining the extent of hydroxylation of a 20mer fragment of RPS23 containing amino acid residues 51-70 (H_2N-VLEKVGVEAKQPNSAIRKCV-$CONH_2$) by matrix-assisted laser desorption/ionisation time-of-flight mass spectrometry (MALDI-TOF MS) using a Waters® Micromass® MALDI micro MX™ mass spectrometer and MassLynx™ 4.1 as previously described.[119] The optimised hydroxylation assay involved incubation of OGFOD1 (1 µM) with inhibitor (1 % *v*/*v* in DMSO) in the presence of Fe(II) (50 µM), 2OG (25 µM), ascorbate (100 µM) and $RPS23_{51-70}$ (25 µM) in HEPES (50 mM, pH 7.5) at 37 °C for 15 min. Reactions were quenched with formic acid (1 % *v*/*v*). Samples were prepared by mixing reaction mixture (1 µL) with α-cyano-4-hydrocinnamic acid (CHCA) solution (water: acetonitrile 1:1) (1 µL). Dose-response was assessed in 8-point triplicates. Data was analysed with GraphPad Prism® 5.04.

PHD2 activity assays

The PHD2 mass spectrometry-based activity assay was performed by determining the extent of hydroxylation of HIF-1αCODD peptide substrate (HIF-1α residues 556-574) by matrix-assisted laser desorption/ionization time-of-flight mass spectrometry (MALDI-TOF MS) using a Waters® Micromass® MALDI micro MX™ mass spectrometer and MassLynx™ 4.1 as previously described.[119] The optimised hydroxylation assay involved incubation of PHD2 (1 µM) with inhibitor (1 % *v*/*v* in DMSO) in the presence of Fe(II) (10 µM), 2OG (60 µM), ascorbate (100 µM) and HIF-1αCODD $_{556\text{-}574}$ (50 µM) in HEPES (50 mM, pH 7.5) at 37 °C for 15 min. Reactions were quenched with formic acid (1 % *v*/*v*). Samples were prepared by mixing reaction mixture (1 µL) with α-cyano-4-hydrocinnamic acid (CHCA) solution (water: acetonitrile 1:1) (1 µL). Dose-response was assessed in 8-point triplicates. Data were analysed using GraphPad Prism® 5.04.

For inhibition assays, enzymes were pre-incubated with inhibitor for 5 min before initiation of the reaction with all other reagents. Data were normalised to both a no enzyme negative control and a no inhibitor positive control.

AlphaScreen® activity assays

Assays were initiated by mixing of two stocks. One contained enzyme and $(NH_4)_2Fe(SO_4)_2$, the other contained all other reagents. Buffer was supplemented with 0.1 % w/v BSA and 0.01 % v/v Tween-20 to a final volume of 10 µL in 384-well white Proxiplates (Perkin Elmer). Reactions were quenched with 5 µL 30 mM EDTA and 5 µL ALPHA screen donor and acceptor beads (Protein A donor beads, streptavidin acceptor beads, pre-incubated with the required antibody, final bead concentration 0.02 mg.mL^{-1}) added (Perkin Elmer). The sample was left in the dark for 1 hour before analysis using an EnVision™ 2104 Multilabel Reader (Perkin Elmer). For inhibition assays, enzyme and inhibitor were pre-incubated together in buffer for 15 min before initiation of the reaction with all other reagents. Where necessary for inhibitor solubilisation, 1 % DMSO was included in the assay buffer. Data were normalised to a no-enzyme control.[181]

KDM4C RapidFire™ Mass Spectrometry (RF-MS) assay

Inhibition of KDM4C activity was assessed by RapidFire™ MS.[182] Inhibition assays were performed in a 384-well plate format using polypropylene V-bottom plates (Greiner Bio One). 2-(*N*-Morpholino) ethanesulphonic

acid (MES buffer) was from Thermo Fisher Scientific. The KDM4C H3-K9 trimethyl peptide substrate: ARTAQTARK(me3)STGGIA was synthesized by Peptide Protein Research Ltd (Hampshire, UK).

Every reaction was performed in assay buffer (50 mM MES pH7.0). 25.0 µl of assay buffer containing 2X KDM4C enzyme (300 nM) was transferred into each well of a 384-well polypropylene microplate. Titrations of compounds (0.1 µl) were transferred to each well and the enzyme incubated with compound for 15 minutes. 25 µl of a 2X substrate mix consisting of FAS (20 µM), L-AA (200 µM), 2OG (20 µM) and peptide (20 µM) was dispensed into each well and the enzyme reaction progressed for 50 minutes. The enzyme reaction was stopped by addition of 5 µl of 10% formic acid and transferred to a RapidFire™ RF360 high-throughput sampling robot connected to an Agilent 6530 Accurate-Mass Quadrupole Time-of-Flight (Q-TOF) mass spectrometer operated in positive ion mode (Agilent, Wakefield, MA USA). RapidFire™ technology uses a solid phase extraction (µSPE) cartridge to remove buffer salts from samples before analysis by mass spectrometry and has been successfully applied to screening demethylase targets. A cycle of sample loading, aqueous wash and organic elution onto a mass spectrometer is typically performed in less than 15 sec.

Samples were aspirated under vacuum for 400 ms, loaded onto a C4 SPE cartridge and buffer salts were removed by washing the cartridge with 0.1 % formic acid in water at a flow rate of 1.5 ml / min for 4.5 sec. Following the aqueous wash peptides were eluted onto the mass spectrometer with 85 % acetonitrile, 15 % deionised water containing 0.1 % formic acid at a flow rate of 1.25 ml / min for 4.5 seconds. The cartridge was re-equilibrated with water for 500 ms.

Ion chromatogram data was extracted for the +3 charge state for the dimethyl substrate and the monomethyl product and peak area data for extracted ion chromatograms were integrated using RapidFire™ Integrator software (Agilent, Wakefield, MA, USA). % conversion of dimethyl substrate to monomethyl product was calculated using the equation:

$$\%\text{Conversion} = 100\text{xDimethyl}/(\text{Dimethyl}+\text{Trimethyl})$$

IC_{50} data were determined from nonlinear regression curve fit using GraphPad Prism 5.

Peptide synthesis

Peptides were either purchased from GLS Biochem at >95 % purity or synthesised in-house by solid phase peptide synthesis (SPPS) from their *C*-termini using a CS-Bio CS336S or CS336X automated peptide synthesiser, using polystyrene crosslinked with divinylbenzene aminomethylated (PL-AMS) resin and a Rink amide linker (4-(2',4'-dimethoxyphenyl-Fmoc-aminomethyl)-phenoxyacetamido-norleucyl-MBHA resin). Amino acids were purchased from Novabiochem or CS Bio and were used in large excess (10 eq.) except in the case of expensive modified amino acids (such as methylated arginyl-residues) where, for cost efficiency, lower excesses were used (3-5 eq.), and the coupling time doubled to six hours. N^{α}-FMOC-protected amino acids were activated using diisopropylcarbodiimide and hydroxybenzotriazole (AGTC Bioproducts) before addition to the resin. Resin and amino acids were incubated with shaking for 3 hours before the solution-phase reagents were drained and the N^{α}-Fmoc removed by treating the resin with 20 % piperidine (Merck Chemicals) in DMF (Rathburn Chemicals). The process was then repeated with the other amino acids. Final cleavage of the peptides from the resin was achieved by incubation for three hours with trifluoroacetic acid (TFA):triethylsilane (97.5:2.5), which also removed the side-chain protecting groups. The peptide was precipitated with diethyl ether from the cleavage mixture and the resultant solid dissolved in MilliQ water and lyophilised overnight. Peptides were purified by HPLC and the mass and purity confirmed by MALDI-TOF MS.

Lyophilisation

Samples were frozen at -80 °C before being lyophilised at RT and 4 mBar using a Micro Modulyo freeze drier. Samples remained on the machine until only a powder remained.

SDS-PAGE gel electrophoresis

Reagent	Resolving gel (18 % / 15 % / 12 %)	Stacking gel
Tris-HCl (1 M, pH 7.5)	1.25 mL	-
Tris-HCl (0.5 M, pH 6.8)	-	0.63 mL
Milli-Q water	0.65 mL / 1.15 mL / 1.65 mL	1.57 mL
30 % (w/v) acrylamide / 1.034 % (w/v) bis-acrylamide stock	3 mL / 2.5 mL / 2 mL	0.25 mL
SDS (10% (*w*/*v*))	50 µL	25 µL
10% (*w*/*v*) APS	50 µL	25 µL
TEMED	4 µL	2.5 µL

TEMED and APS were added just prior to gel casting. Resolving gel % was determined based on the size of the proteins to be separated.

10 × SDS-PAGE running buffer (1 L)

Reagent	Amount /g
Tris-HCl	30
Glycine	144
SDS	10

SDS-PAGE gel destain

Reagent	Amount
Acetic acid	10% (*w*/*v*)
Methanol	30% (*w*/*v*)

SDS-PAGE gel stain

As for gel destain with addition of 0.25% (*w*/*v*) Coomassie® brilliant blue R

SDS-PAGE sample loading buffer (100 mL):

Reagent	Amount
Tris-HCl (0.5 M, pH 6.8)	10 mL
Bromophenol blue (0.2% (*w*/*v*))	0.2 g
SDS (10% (*w*/*v*))	20 mL
Glycerol	12 mL
β-mercaptoethanol	5 mL

Method

Samples were heated for 5 min at 100 °C before use. Polyacrylamide gels were run under denaturing conditions for 40-60 min at RT, 180 V using a Bio-Rad Mini-PROTEAN II system. Gels were stained with SDS-PAGE gel stain for 20 min and then destained with SDS-PAGE destain overnight.

Agarose gel electrophoresis

50 x TAE (100 mL)

Reagent	Amount
Tris-HCl	24.2 g
Glacial acetic acid	5.71 mL
EDTA	1.86 g

5 x DNA sample loading buffer (5 mL)

Reagent	Amount
TAE (1 ×)	1.5 mL
Glycerol	3.5 mL
Bromophenol blue (0.25% (*w*/*v*))	12.5 mg

Method

1 % agarose gels were used for DNA visualisation. They were formed by heating 0.4 g agarose (Bioline) in 40 mL TAE buffer until dissolved, using a SuperWave 750 microwave (Tecnolec). This was allowed to cool to around 60 °C, before addition of 4 µl SYBR Safe™ DNA gel stain (Invitrogen). Gels were cast in an H2-SET gel tray (Anachem) to a depth of 0.7 cm with a comb inserted at one end of the gel to enable sample loading and allowed to cool at room temperature for the gel to set. Gels were run on a Bio-Rad system at a constant potential of 120 V for approximately 35 min. Bands were visualised by UV light illumination using a Gel Logic 200 imaging system (Kodak) and a 535 nm emission filter. Samples were run against a 2-log DNA Ladder 0.1-10 kb (Invitrogen) allowing molecular weight determination.

Mammalian cell culture

Reagents

All procedures were carried out in a Class II Biological Safety Cabinet (Nuaire Nu 437-400E). *H. Sapiens* HEK 293T, HeLa and MCF7 cells were grown in Dulbecco's Modified Eagle's Medium (DMEM, Lonza) supplemented with glutamax and 10 % fetal bovine serum (FBS) in a Binder BD 53 incubator with a humidified 5 % CO_2 atmosphere at 37 °C unless otherwise described.

Vessel	Surface area /cm²	No. cells at 100 % confluence	Media volume /mL
96 well plate	0.3	2.8×10^4	0.1
25 cm^2 flask (T25)	25	2.5×10^6	5
10 cm diameter Petri dish	55	5.5×10^6	10
15 cm diameter Petri dish	148	1.48×10^7	20

Cell passaging

Strongly adherent HeLa cells and MCF7 cells were washed with PBS, then hydrolysed from the plate using 0.2 $mg.mL^{-1}$ Trypsin (Lonza) at 37 °C until cells were released from the surface of the plate. The reaction was quenched by addition of fresh media. Cells were fully resuspended by pipetting and the appropriate volume added to new plates containing pre-warmed media.

Semi-adherent 293T were washed with PBS and then removed from the plate surface by pipetting in PBS to form a suspension. An appropriate volume of cells were added to new plates containing prewarmed media.

Cell Storage

Cells were frozen in DMEM containing 20 % FBS and 10 % DMSO and stored in a -80 °C freezer for short term storage (less than 1 year) and in a liquid nitrogen dewar for longer term storage.

Viability analysis

Antiproliferative activities of compounds were determined by the MTT (3-[4,5-dimethylthiazol-2-yl]-2,5-diphenyl tetrazolium bromide) assay (Promega). HeLa cells were seeded into 96-well plates (2000 cells/well) and cultured at 37 °C for 24 h to achieve 70 % confluency. Subsequently, the medium was replaced with DMEM medium containing the tested compounds in different concentrations of 1-300 µM in 1 % DMSO. Staurosporine in 0.03-10 µM final concentration was used as a control for cytotoxicity. After 24 h of treatment, the medium was replaced with CellTiter 96® Aqueous One Solution Reagent (Promega) and incubated for 4 h. IC_{50} values were calculated in Prism 6 software after normalisation against corresponding 1 % DMSO treated cells and 1 % DMSO in media (no cells) controls.

Transfection

Cells were transiently transfected with plasmid DNA using linear PEI (1 $mg.mL^{-1}$ poly(ethylenimine), pH 7.2) or Lipofectamine® 2000. Transfection was carried out with cells at ~50 % confluency as judged using a Motic

AE20 (Ted Pella) microscope. In both cases, 2 hours prior to transfection media were exchanged for fresh media. DNA for transfection and transfection reagent were separately diluted in OptiMEM® and incubated at room temperature for 5 min. The two reagents were then mixed and left at room temperature for 10 min before adding dropwise to the cells. 0.1 µg plasmid DNA was used for transfections in 96 well plates and 20 µg DNA for transfections in 15 cm dishes. Linear PEI was used at a ratio of 12:1 *w*/*w* and for transfections in 96-well plates 0.2 µL Lipofectamine® 2000 was used.

Immunofluoresence

8000 cells per well were plated into 96-well plates one day prior to transfection. For experiments at endogenous enzyme expression levels, 5000 cells per well were seeded into 96 well plates one day prior to compound dosing. Both media and inhibitor were replaced every 24 h in case of multiple-day experiments. Transfection was carried out as described above. After 24 hours, cells were washed with PBS and then fixed with 4 % formaldehyde in PBS for 15 min at room temperature. Formaldehyde was produced by heating paraformaldehyde at 60 °C in water until it dissolved. After 15 min the formaldehyde was removed and the cells washed twice with PBS. Cells were permeabilised by incubation for 6 - 8 min at room temperature with 0.2 % Triton-X100. The Triton-X100 was removed and the cells washed three times with PBS before being blocked for 30 min at room temperature with 5 % FBS in PBS. Primary antibodies were made up to the appropriate dilution in blocking buffer and added to the cells before incubation for 1 hr at room temperature. After incubation, cells were washed with PBS (3 × 10 min). Secondary antibodies were added, again at the appropriate dilution in blocking buffer, for 1 hr at room temperature in the dark. Cells were washed with PBS (3 × 10 min) and stained with DAPI (0.2 µg.mL^{-1}) before visualisation. Cells were visualised using a Zeiss Axioobserver epifluorescence microscope with a 20 × objective.

Fluorophore	Excitation wavelength /nm	λ_{max} absorption /nm	λ_{max} emission /nm
DAPI	445	358	461
AlexaFluor 488	525	496	519
AlexaFluor 594	543	590	617

Global Histone Analysis

Histone Extraction - acid extraction method

Prepared cell (HEK293T or HeLa) pellets were re-suspended in cooled hypotonic lysis buffer (10 mM Tris-HCl pH 8.0, 1 mM KCl, 1.5 mM $MgCl_2$, 1mM dithiothreitol (DDT) and 1 mM phenylmethanesulfonylfluoride (PMSF), supplemented with 1x protease and phosphatase inhibitor and then incubated on a rotor at 4 ^{0}C for 30 minutes. The nuclei were pelleted by centrifugation at 10,000g for 10 min at 4 ^{0}C, and then the supernatant was removed. Pellets were resuspended in 400 µl 0.4 M ice-cold HCl. The sample was then centrifuged at 16,000 g for 10 min at 4 ^{0}C and the supernatant containing histones was transferred into a fresh tube. Subsequently, three different methods were used to purify the histones as below.

Acetone precipitation: Following the above acid extraction method, approximately 400 µl of supernatant were added to the 15 mL falcon tube with 4 mL of acetone and then placed at -20 ^{0}C overnight for precipitation. The sample was centrifuged for 10 min at 2,500 g and at 4 ^{0}C. The supernatant was carefully discarded and the pellet was transferred into the fresh 1.5 ml tube. Three washes with ice-cold acetone were carried out by centrifugation at 16,000 g for 5 min and at 4 ^{0}C. The pellet was dried at room temperature. The appropriate volume of 0.1 % folic acid or H_2O (typically 100 µL) was added to dissolve the final pellet and the solution was stored at -20 ^{0}C.

Liquid chromatography–mass spectrometry (LC-MS) for histone analysis

Samples of histones, extracted as described above, were separated by reversed phase ultra-performance liquid chromatography (RP-UPLC) and analysed by electrospray ionisation time-of-flight mass spectrometry (ESI-TOF MS). The instrument of Waters Acquity UPLC system connected directly to Waters LCT ESI-TOF MS was used. UPLC separation was carried out at a flow of 0.25 mL/min on a Waters BEH C4 reversed phase column (2.1 x 150 mm, 1.7µm particle size, 300 Å pore size) at 40 ^{0}C. The column was equilibrated with solvent A (0.5 % formic acid in H_2O water) and solvent B (0.5 % formic acid in acetonitrile). 5 µL of the histone sample were injected onto the column and histones were eluted by using a gradient from solvent A to solvent B. The MS parameters settings were as follows: polarity mode: ES+; capillary voltage: 3,000 V; sample cone voltage: 35 V; extraction cone voltage: 2.5V; desolvation temperature: 250 ^{0}C; cone gas flow rate: 10 L/hour;

desolvation gas flow (N2): 500 L/hour. The mass range were covered from 100 to 2000 *m/z* using MassLynx 4.1 software (Waters) and histones molecular weight and distribution were acquired using Maxent 1 with mass accuracy 70 ppm and continnum mode at the rate of 1 spectrum/s. Masses were confirmed using manual component analysis. Leu-Enkephalin was used as lock spray reagent for calibration of the mass spectrometer at the monoisotopic mass of 556.277 $[M+H]^+$.

ADMET *in vitro* Predictors

Turbidimetric solubility

Aqueous solubility was measured using a high-throughput turbidimetric assay. Initially, a stock DMSO solution was diluted in DMSO to produce a range of concentrations. These were then added to buffer, typically phosphate buffered saline at pH 7.4 (final test compound concentrations = 1 µM, 3 µM, 10 µM, 30 µM, 100 µM, final DMSO concentration = 1 %, 7 replicates per concentration) and incubated for 2 h at 37 °C. At the end of the incubation period, the absorbance at 620 nm was read for each concentration and each replicate.[224]

S9 Liver Microsome Stability

The liver is the main organ of drug metabolism in the body. Subcellular fractions are useful *in vitro* models of hepatic clearance as they contain many of the drug metabolising enzymes found in the liver. The two main subcellular fractions used for drug metabolism studies are microsomes and S9 fraction (post-mitochondrial supernatant fraction). Both are easy to prepare and can be stored for long periods of time. They are easily adaptable to high throughput screens which enable large numbers of compounds to be screened rapidly and inexpensively. S9 fraction consists of both microsomal and cytosolic enzymes, and so contains a wide variety of both Phase I and Phase II enzymes. It can be supplemented with cofactors such as UDPGA and PAPS to investigate Phase II metabolic pathways.

The S9 fraction is incubated with the test compound at 37 °C in the presence of the co-factor(s) which initiate the reaction. The reaction is terminated by the addition of methanol-containing internal standard. Following

centrifugation, the supernatant is analysed using LC-MS/MS. The disappearance of test compound is monitored over a 45 minute time period.[225]

MDCK-MDR1 Efflux Assay[226]

Test Compound Concentration	10 µM (different concentrations available)
Direction	Apical to Basolateral and/or Basolateral to Apical
Number of Replicates	2
Incubation Time	60 min
Growth Period	4 days
Compound Requirements	100 µL of 10 mM solution
Analysis Method	LC-MS/MS quantification
Integrity Marker	Lucifer Yellow
Data Delivery	Papp Efflux Ratio of Bidirectional Assessment

Appendix A: Key for the Conversion of Thesis Number into Internal Reference

Thesis Number to Internal Reference Correlation

Number in Thesis	CCT Code
24	3-164
31	6-84
48	1-194
49	5-198
50	1-24
61	1-92
63	1-66
64	1-68
65	1-62
66	1-82
67	1-80
68	1-100
69	1-94
70	1-104
71	2-54
72	2-56
73	2-58
74	2-68
75	2-34
76	2-52
77	4-24
78	3-28
79	2-44
80	2-42
81	2-36
82	2-46
83	2-50
84	2-48
86	6-76
87	6-72
88	6-70
89	6-68
90	6-66
91	6-64
93	6-56
94	6-92
97	4-48
98	3-24

99	3-26
105	4-66
110	4-146
111	4-152
112	4-150
113	4-118
114	4-126
115	4-120
116	4-122
117	4-124
118	4-128
119	4-134
120	4-156
123	2-138
124	2-140
125	2-162
126	5-94
127	4-114
129	3-162
130	2-130
131	1-168
133	3-112
134	5BrOMe
135	3-56
146	5-100
147	5-82
148	5-114
149	5-102
150	5-118
151	5-126
152	5-142
153	5-148
155	2-160
156	2-168
157	2-166
159	2-84
160	2-112
161	2-96
162	2-32
163	2-100
164	2-104
165	2-108
166	2-106
167	2-114
168	2-86
174	1-122
176	2-80

178	3-84
180	3-86
182	2-120
183	2-124
184	5-26
187	1-136
188	1-134
189	1-102
190	2-38
191	2-40
192	2-110
193	2-66
194	2-132
195	2-134
196	2-136
197	2-118
198	2-122
199	3-200
200	4-26
201	3-198
202	4-92
203	4-106
204	4-108
205	2-200
206	2-206
207	5-44
208	5-48
209	5-38
210	5-42
211	4-102
212	3-168
213	3-120
214	4-180
215	4-162
216	4-164
217	4-166
218	4-174
219	4-170
220	4-182
221	5-130
222	2-20
223	2-88
224	4-112
225	2-156
226	1-60
227	1-70
228	1-72

229	1-86
230	1-106
231	1-128
232	1-130
233	1-132
234	1-138
235	1-140
236	1-142
237	1-150
238	1-152
239	1-154
240	1-156
241	1-160
242	1-162
243	1-164
244	1-166
245	1-170
246	1-172
247	1-174
248	1-178
249	1-180
250	1-182
251	1-186
252	1-188
253	1-190
254	1-192
255	1-206
256	2-22
257	2-24
258	2-26
259	2-28
260	2-30
261	2-64
262	2-70
263	2-82
264	2-102
265	2-144
266	2-146
267	2-148
268	2-150
269	2-152
270	2-158
271	2-170
272	2-172
273	2-190
274	2-198
275	2-202

276	2-204
277	3-30
278	3-32
279	3-34
280	3-36
281	3-38
282	3-40
283	3-42
284	3-48
285	3-50
286	3-54
287	3-58
288	3-60
289	3-62
290	3-64
291	3-72
292	3-88
293	3-94
294	3-102
295	3-114
296	3-122
297	3-126
298	3-130
299	3-134
300	3-138
301	3-174
302	3-180
303	3-186
304	3-190
305	3-196
306	3-202
307	3-204
308	3-206
309	4-22
310	4-34
311	4-36
312	4-88
313	4-94
314	4-96
315	4-104
316	4-130
317	4-132
318	4-136
319	4-176
320	5-36
321	5-58
322	5-76

323	5-132
324	5-144
325	6-42
326	6-44
327	6-86
328	6-94
329	6-100
330	6-102
344	6-82
345	6-128
346	6-130
347	6-132
348	6-134
349	6-136
350	6-138
351	6-40
352	6-154
353	6-156
354	6-158
355	6-160
356	6-162
357	6-164
358	6-166
359	6-168
360	6-170
361	6-172
362	6-174
363	6-176
364	6-178
365	6-182
366	6-184
367	6-186
368	6-190
369	6-192
373	6-108
375	6-196
380	6-198
381	6-80
382	6-144
383	6-150
384	6-188
385	6-200
386	6-204
387	6-206
388	7-22
389	7-24
390	7-26

391	7-32
392	7-34
393	7-36
394	7-38

Appendix B: 8HQ Screening Data

References

1 Flashman, E. & Schofield, C. J. The most versatile of all reactive intermediates? *Nature chemical biology* **3**, 86-87, doi:10.1038/nchembio0207-86 (2007).

2 Clifton, I. J. *et al.* Structural studies on 2-oxoglutarate oxygenases and related double-stranded beta-helix fold proteins. *Journal of Inorganic Biochemistry* **100**, 644-669, doi:10.1016/j.jinorgbio.2006.01.024 (2006).

3 McDonough, M. A., Loenarz, C., Chowdhury, R., Clifton, I. J. & Schofield, C. J. Structural studies on human 2-oxoglutarate dependent oxygenases. *Current Opinion in Structural Biology* **20**, 659-672, doi:10.1016/j.sbi.2010.08.006 (2010).

4 Bleijlevens, B. *et al.* Dynamic states of the DNA repair enzyme AlkB regulate product release. *EMBO Rep* **9**, 872-877, doi:10.1038/embor.2008.120 (2008).

5 Roach, P. L. *et al.* Structure of isopenicillin N synthase complexed with substrate and the mechanism of penicillin formation. *Nature* **387**, 827-830 (1997).

6 Kivirikko, K. I. & Myllyharju, J. Prolyl 4-hydroxylases and their protein disulfide isomerase subunit. *Matrix Biology* **16**, 357-368, doi:10.1016/s0945-053x(98)90009-9 (1998).

7 Klose, R. J., Kallin, E. M. & Zhang, Y. JmjC-domain-containing proteins and histone demethylation. *Nat Rev Genet* **7**, 715-727, doi:http://www.nature.com/nrg/journal/v7/n9/suppinfo/nrg1945_S1.html (2006).

8 Horton, J. R. *et al.* Enzymatic and structural insights for substrate specificity of a family of jumonji histone lysine demethylases. *Nat. Struct. Mol. Biol.* **17**, 38-43, doi:10.1038/nsmb.1753 (2010).

9 Yue, W. W. *et al.* Crystal structure of the PHF8 Jumonji domain, an N-epsilon-methyl lysine demethylase. *FEBS letters* **584**, 825-830, doi:10.1016/j.febslet.2009.12.055 (2010).

10 Agger, K., Christensen, J., Cloos, P. A. C. & Helin, K. The emerging functions of histone demethylases. *Current Opinion in Genetics & Development* **18**, 159-168, doi:10.1016/j.gde.2007.12.003 (2008).

11 Ng, S. S. *et al.* Crystal structures of histone demethylase JMJD2A reveal basis for substrate specificity. *Nature* **448**, 87-91, doi:10.1038/nature05971 (2007).

12 Sekirnik, R. *et al.* Inhibition of the histone lysine demethylase JMJD2A by ejection of structural Zn(ii). *Chemical Communications*, 6376-6378, doi:10.1039/B916357C (2009).

13 Valegard, K. *et al.* Structure of a cephalosporin synthase. *Nature* **394**, 805-809 (1998).

14 Costas, M., Mehn, M. P., Jensen, M. P. & Que, L. Dioxygen activation at mononuclear nonheme iron active sites: Enzymes, models, and intermediates. *Chemical Reviews* **104**, 939-986, doi:10.1021/cr020628n (2004).

15 McNeill, L. A. *et al.* Hypoxia-inducible factor prolyl hydroxylase 2 has a high affinity for ferrous iron and 2-oxoglutarate. *Molecular Biosystems* **1**, 321-324, doi:10.1039/b511249b (2005).

16 Hausinger, R. P. Fe(II)/alpha-ketoglutarate-dependent hydroxylases and related enzymes. *Critical Reviews in Biochemistry and Molecular Biology* **39**, 21-68, doi:10.1080/10409230490440541 (2004).

17 Price, J. C., Barr, E. W., Glass, T. E., Krebs, C. & Bollinger, J. M. Evidence for hydrogen abstraction from C1 of taurine by the high-spin Fe(IV) intermediate detected during oxygen activation by taurine :alpha-ketoglutarate dioxygenase (TauD). *Journal of the American Chemical Society* **125**, 13008-13009, doi:10.1021/ja037400h (2003).

18 Majamaa, K., Hanauskeabel, H. M., Gunzler, V. & Kivirikko, K. I. THE 2-OXOGLUTARATE BINDING-SITE OF PROLYL 4-HYDROXYLASE - IDENTIFICATION OF DISTINCT SUBSITES AND EVIDENCE FOR 2-OXOGLUTARATE DECARBOXYLATION IN A LIGAND REACTION AT THE ENZYME-BOUND FERROUS ION. *European Journal of Biochemistry* **138**, 239-245, doi:10.1111/j.1432-1033.1984.tb07907.x (1984).

19 Price, J. C., Barr, E. W., Tirupati, B., Bollinger, J. M. & Krebs, C. The first direct characterization of a high-valent iron intermediate in the reaction of an alpha-ketoglutarate-dependent dioxygenase: A high-spin Fe(IV) complex in taurine/alpha-ketoglutarate dioxygenase (TauD) from Escherichia coli. *Biochemistry* **42**, 7497-7508, doi:10.1021/bi030011f (2003).

20 Sinnecker, S. *et al.* Spectroscopic and computational evaluation of the structure of the high-spin Fe(IV)-oxo intermediates in taurine: alpha-Ketoglutarate dioxygenase from Escherichia coli and its

His99Ala ligand variant. *Journal of the American Chemical Society* **129**, 6168-6179, doi:10.1021/ja067899q (2007).

21 Proshlyakov, D. A., Henshaw, T. F., Monterosso, G. R., Ryle, M. J. & Hausinger, R. P. Direct detection of oxygen intermediates in the non-heme Fe enzyme taurine/alpha-ketoglutarate dioxygenase. *Journal of the American Chemical Society* **126**, 1022-1023, doi:10.1021/ja039113j (2004).

22 Hanauskeabel, H. M. & Gunzler, V. A STEREOCHEMICAL CONCEPT FOR THE CATALYTIC MECHANISM OF PROLYLHYDROXYLASE - APPLICABILITY TO CLASSIFICATION AND DESIGN OF INHIBITORS. *Journal of Theoretical Biology* **94**, 421-455, doi:10.1016/0022-5193(82)90320-4 (1982).

23 Flashman, E. *et al.* Evidence for the slow reaction of hypoxia-inducible factor prolyl hydroxylase 2 with oxygen. *Febs Journal* **277**, 4089-4099, doi:10.1111/j.1742-4658.2010.07804.x (2010).

24 Price, J. C., Barr, E. W., Hoffart, L. M., Krebs, C. & Bollinger, J. M. Kinetic Dissection of the Catalytic Mechanism of Taurine:α-Ketoglutarate Dioxygenase (TauD) from Escherichia coli†. *Biochemistry* **44**, 8138-8147, doi:10.1021/bi050227c (2005).

25 Majamaa, K., Sasaki, T. & Uitto, J. INHIBITION OF PROLYL HYDROXYLATION DURING COLLAGEN BIOSYNTHESIS IN HUMAN-SKIN FIBROBLAST-CULTURES BY ETHYL 3,4-DIHYDROXYBENZOATE. *Journal of Investigative Dermatology* **89**, 405-409, doi:10.1111/1523-1747.ep12471775 (1987).

26 Franklin, T. J. & Hitchen, M. INHIBITION OF COLLAGEN HYDROXYLATION BY 2,7,8-TRIHYDROXYANTHRAQUINONE IN EMBRYONIC-CHICK TENDON CELLS. *Biochemical Journal* **261**, 127-130 (1989).

27 Jenkins, C. L. & Raines, R. T. Insights on the conformational stability of collagen. *Natural Product Reports* **19**, 49-59, doi:10.1039/a903001h (2002).

28 Vranka, J. A., Sakai, L. Y. & Bachinger, H. P. Prolyl 3-hydroxylase 1, enzyme characterization and identification of a novel family of enzymes. *Journal of Biological Chemistry* **279**, 23615-23621, doi:10.1074/jbc.M312807200 (2004).

29 Myllyharju, J. & Kivirikko, K. I. Collagens, modifying enzymes and their mutations in humans, flies and worms. *Trends in Genetics* **20**, 33-43, doi:10.1016/j.tig.2003.11.004 (2004).

30 Vaz, F. M. & Wanders, R. J. A. Carnitine biosynthesis in mammals. *Biochemical Journal* **361**, 417-429, doi:10.1042/0264-6021:3610417 (2002).

31 Schofield, C. J. & McDonough, M. A. Structural and mechanistic studies on the peroxisomal oxygenase phytanoyl-CoA 2-hydroxylase (PhyH). *Biochemical Society Transactions* **35**, 870-875, doi:10.1042/bst0350870 (2007).

32 Englard, S., Blanchard, J. S. & Midelfort, C. F. GAMMA-BUTYROBETAINE HYDROXYLASE - STEREOCHEMICAL COURSE OF THE HYDROXYLATION REACTION. *Biochemistry* **24**, 1110-1116, doi:10.1021/bi00326a007 (1985).

33 Hulse, J. D., Ellis, S. R. & Henderson, L. M. CARNITINE BIOSYNTHESIS - BETA-HYDROXYLATION OF TRIMETHYLLYSINE BY AN ALPHA-KETOGLUTARATE DEPENDENT MITOCHONDRIAL DIOXYGENASE. *Journal of Biological Chemistry* **253**, 1654-1659 (1978).

34 Lindstedt, G., Lindstedt, S. & Nordin, I. PURIFICATION AND PROPERTIES OF GAMMA-BUTYROBETAINE HYDROXYLASE FROM PSEUDOMONAS-SP-AK-1. *Biochemistry* **16**, 2181-2188, doi:10.1021/bi00629a022 (1977).

35 Lindsted.G. HYDROXYLATION OF GAMMA-BUTYROBETAINE TO CARNITINE IN RAT LIVER. *Biochemistry* **6**, 1271-&, doi:10.1021/bi00857a007 (1967).

36 Dambrova, M., Liepinsh, E. & Kalvinsh, I. Mildronate: Cardioprotective action through carnitine-lowering effect. *Trends in Cardiovascular Medicine* **12**, 275-279, doi:10.1016/s1050-1738(02)00175-5 (2002).

37 Simkhovich, B. Z. *et al.* 3-(2,2,2-TRIMETHYLHYDRAZINIUM)PROPIONATE (THP) - A NOVEL GAMMA-BUTYROBETAINE HYDROXYLASE INHIBITOR WITH CARDIOPROTECTIVE PROPERTIES. *Biochemical Pharmacology* **37**, 195-202, doi:10.1016/0006-2952(88)90717-4 (1988).

38 Wanders, R. J. A., Komen, J. & Ferdinandusse, S. Phytanic acid metabolism in health and disease. *Biochimica Et Biophysica Acta-Molecular and Cell Biology of Lipids* **1811**, 498-507, doi:10.1016/j.bbalip.2011.06.006 (2011).

39 Cerretelli, P. & Gelfi, C. Energy metabolism in hypoxia: reinterpreting some features of muscle physiology on molecular grounds. *European Journal of Applied Physiology* **111**, 421-432, doi:10.1007/s00421-010-1399-5 (2011).

40 Semenza, G. L. Oxygen Sensing, Hypoxia-Inducible Factors, and Disease Pathophysiology. *Annual Review of Pathology: Mechanisms of Disease* **9**, 47-71, doi:doi:10.1146/annurev-pathol-012513-104720 (2014).

41 Fraisl, P., Aragones, J. & Carmeliet, P. Inhibition of oxygen sensors as a therapeutic strategy for ischaemic and inflammatory disease. *Nature reviews. Drug discovery* **8**, 139-152, doi:10.1038/nrd2761 (2009).

42 Semenza, G. L. Targeting HIF-1 for cancer therapy. *Nature Reviews Cancer* **3**, 721-732, doi:10.1038/nrc1187 (2003).

43 Wang, G. L., Jiang, B. H., Rue, E. A. & Semenza, G. L. HYPOXIA-INDUCIBLE FACTOR-1 IS A BASIC-HELIX-LOOP-HELIX-PAS HETERODIMER REGULATED BY CELLULAR O-2 TENSION. *Proceedings of the National Academy of Sciences of the United States of America* **92**, 5510-5514, doi:10.1073/pnas.92.12.5510 (1995).

44 Semenza, G. L. Defining the role of hypoxia-inducible factor 1 in cancer biology and therapeutics. *Oncogene* **29**, 625-634, doi:10.1038/onc.2009.441 (2010).

45 Ehrismann, D. *et al.* Studies on the activity of the hypoxia-inducible-factor hydroxylases using an oxygen consumption assay. *Biochemical Journal* **401**, 227-234, doi:10.1042/bj20061151 (2007).

46 Koivunen, P. *et al.* An endoplasmic reticulum transmembrane prolyl 4-hydroxylase is induced by hypoxia and acts on hypoxia-inducible factor alpha. *Journal of Biological Chemistry* **282**, 30544-30552, doi:10.1074/jbc.M704988200 (2007).

47 Klotzsche-von Ameln, A. *et al.* PHD4 Stimulates Tumor Angiogenesis in Osteosarcoma Cells via TGF-alpha. *Molecular Cancer Research* **11**, 1337-1348, doi:10.1158/1541-7786.mcr-13-0201 (2013).

48 Coleman, M. L. *et al.* Asparaginyl hydroxylation of the notch ankyrin repeat domain by factor inhibiting hypoxia-inducible factor. *Journal of Biological Chemistry* **282**, 24027-24038, doi:10.1074/jbc.M704102200 (2007).

49 Dinchuk, J. E. *et al.* Absence of post-translational aspartyl beta-hydroxylation of epidermal growth factor domains in mice leads to developmental defects and an increased incidence of intestinal neoplasia. *Journal of Biological Chemistry* **277**, 12970-12977, doi:10.1074/jbc.M110389200 (2002).

50 Thinnes, C. C. *et al.* Targeting histone lysine demethylases — Progress, challenges, and the future. *Biochimica et Biophysica Acta (BBA) - Gene Regulatory Mechanisms*, doi:http://dx.doi.org/10.1016/j.bbagrm.2014.05.009.

51 Kooistra, S. M. & Helin, K. Molecular mechanisms and potential functions of histone demethylases. *Nat Rev Mol Cell Biol* **13**, 297-311 (2012).

52 Hojfeldt, J. W., Agger, K. & Helin, K. Histone lysine demethylases as targets for anticancer therapy. *Nat Rev Drug Discov* **12**, 917-930, doi:10.1038/nrd4154 (2013).

53 Suganuma, T. & Workman, J. L. Signals and combinatorial functions of histone modifications. *Annu Rev Biochem* **80**, 473-499 (2011).

54 Zentner, G. E. & Henikoff, S. Regulation of nucleosome dynamics by histone modifications. *Nat Struct Mol Biol* **20**, 259-266 (2013).

55 Berdasco, M. & Esteller, M. Aberrant epigenetic landscape in cancer: how cellular identity goes awry. *Dev Cell* **19**, 698-711 (2010).

56 Portela, A. & Esteller, M. Epigenetic modifications and human disease. *Nat Biotech* **28**, 1057-1068 (2010).

57 Greer, E. L. & Shi, Y. Histone methylation: a dynamic mark in health, disease and inheritance. *Nat Rev Genet* **13**, 343-357, doi:http://www.nature.com/nrg/journal/v13/n5/suppinfo/nrg3173_S1.html (2012).

58 Waldmann, T. & Schneider, R. Targeting histone modifications — epigenetics in cancer. *Current Opinion in Cell Biology* **25**, 184-189, doi:http://dx.doi.org/10.1016/j.ceb.2013.01.001 (2013).

59 Rotili, D. & Mai, A. Targeting Histone Demethylases: A New Avenue for the Fight against Cancer. *Genes & cancer* **2**, 663-679, doi:10.1177/1947601911417976 (2011).

60 Xu, W. S., Parmigiani, R. B. & Marks, P. A. Histone deacetylase inhibitors: molecular mechanisms of action. *Oncogene* **26**, 5541-5552, doi:10.1038/sj.onc.1210620 (2007).

61 Gravina, G. L. *et al.* Biological rationale for the use of DNA methyltransferase inhibitors as new strategy for modulation of tumor response to chemotherapy and radiation. *Molecular Cancer* **9**, doi:10.1186/1476-4598-9-305 (2010).

62 Khoury, G. A., Baliban, R. C. & Floudas, C. A. Proteome-wide post-translational modification statistics: frequency analysis and curation of the swiss-prot database. *Scientific Reports* **1**, doi:10.1038/srep00090 (2011).

63 Walsh, C. T., Garneau-Tsodikova, S. & Gatto, G. J. Protein posttranslational modifications: The chemistry of proteome diversifications. *Angewandte Chemie-International Edition* **44**, 7342-7372, doi:10.1002/anie.200501023 (2005).

64 Walport, L. J., Hopkinson, R. J. & Schofield, C. J. Mechanisms of human histone and nucleic acid demethylases. *Curr. Opin. Chem. Biol.* **16**, 525-534, doi:http://dx.doi.org/10.1016/j.cbpa.2012.09.015 (2012).

65 Anand, R. & Marmorstein, R. Structure and mechanism of lysine-specific demethylase enzymes. *Journal of Biological Chemistry* **282**, 35425-35429, doi:10.1074/jbc.R700027200 (2007).

66 Walport, L. J., Hopkinson, R. J. & Schofield, C. J. Mechanisms of human histone and nucleic acid demethylases. *Curr. Opin. Chem. Biol.* **16**, 525-534, doi:10.1016/j.cbpa.2012.09.015 (2012).

67 Shi, Y. *et al.* Histone demethylation mediated by the nuclear amine oxidase homolog LSD1. *Cell* **119**, 941-953 (2004).

68 Harris, W. J. *et al.* The histone demethylase KDM1A sustains the oncogenic potential of MLL-AF9 leukemia stem cells. *Cancer Cell* **21**, 473-487, doi:10.1016/j.ccr.2012.03.014 (2012).

69 Hoffmann, I. *et al.* The role of histone demethylases in cancer therapy. *Molecular Oncology* **6**, 683-703, doi:http://dx.doi.org/10.1016/j.molonc.2012.07.004 (2012).

70 Thalhammer, A., Aik, W., Bagg, E. A. L. & Schofield, C. J. The potential of 2-oxoglutarate oxygenases acting on nucleic acids as therapeutic targets. *Drug Discovery Today: Therapeutic Strategies* **9**, e91-e100, doi:http://dx.doi.org/10.1016/j.ddstr.2012.02.002 (2012).

71 Geurink, P. P., Prely, L. M., van der Marel, G. A., Bischoff, R. & Overkleeft, H. S. in *Activity-Based Protein Profiling* Vol. 324 *Topics in Current Chemistry* (ed S. A. Sieber) 85-113 (2012).

72 Tahiliani, M. *et al.* The histone H3K4 demethylase SMCX links REST target genes to X-linked mental retardation. *Nature* **447**, 601-+, doi:10.1038/nature05823 (2007).

73 Castermans, D. *et al.* Identification and characterization of the TRIP8 and REEP3 genes on chromosome 10q21.3 as novel candidate genes for autism. *European Journal of Human Genetics* **15**, 422-431, doi:10.1038/sj.ejhg.5201785 (2007).

74 Laumonnier, F. *et al.* Mutations in PHF8 are associated with X linked mental retardation and cleft lip/cleft palate. *Journal of Medical Genetics* **42**, 780-786, doi:10.1136/jmg.2004.029439 (2005).

75 Qiu, J. *et al.* The X-linked mental retardation gene PHF8 is a histone demethylase involved in neuronal differentiation. *Cell Research* **20**, 908-918, doi:10.1038/cr.2010.81 (2010).

76 Sedgwick, B., Bates, P. A., Paik, J., Jacobs, S. C. & Lindahl, T. Repair of alkylated DNA: Recent advances. *DNA Repair* **6**, 429-442, doi:http://dx.doi.org/10.1016/j.dnarep.2006.10.005 (2007).

77 Falnes, P. O., Bjoras, M., Aas, P. A., Sundheim, O. & Seeberg, E. Substrate specificities of bacterial and human AlkB proteins. *Nucleic Acids Research* **32**, 3456-3461, doi:10.1093/nar/gkh655 (2004).

78 Chen, B., Liu, H., Sun, X. & Yang, C.-G. Mechanistic insight into the recognition of single-stranded and double-stranded DNA substrates by ABH2 and ABH3. *Molecular BioSystems* **6**, 2143-2149, doi:10.1039/c005148a (2010).

79 Aas, P. A. *et al.* Human and bacterial oxidative demethylases repair alkylation damage in both RNA and DNA. *Nature* **421**, 859-863 (2003).

80 Gerken, T. *et al.* The obesity-associated FTO gene encodes a 2-oxoglutarate-dependent nucleic acid demethylase. *Science* **318**, 1469-1472, doi:10.1126/science.1151710 (2007).

81 Aik, W. *et al.* Structural Basis for Inhibition of the Fat Mass and Obesity Associated Protein (FTO). *Journal of Medicinal Chemistry* **56**, 3680-3688, doi:10.1021/jm400193d (2013).

82 Schmeing, T. M. & Ramakrishnan, V. What recent ribosome structures have revealed about the mechanism of translation. *Nature* **461**, 1234-1242, doi:10.1038/nature08403 (2009).

83 Gilbert, W. V. Functional specialization of ribosomes? *Trends in Biochemical Sciences* **36**, 127-132, doi:10.1016/j.tibs.2010.12.002 (2011).

84 Nesterchuk, M. V., Sergiev, P. V. & Dontsova, O. A. Posttranslational Modifications of Ribosomal Proteins in Escherichia coli. *Acta Naturae* **3**, 22-33 (2011).

85 Ruvinsky, I. & Meyuhas, O. Ribosomal protein S6 phosphorylation: from protein synthesis to cell size. *Trends in Biochemical Sciences* **31**, 342-348, doi:10.1016/j.tibs.2006.04.003 (2006).

86 Liang, X.-H., Liu, Q. & Fournier, M. J. Loss of rRNA modifications in the decoding center of the ribosome impairs translation and strongly delays pre-rRNA processing. *Rna-a Publication of the Rna Society* **15**, 1716-1728, doi:10.1261/rna.1724409 (2009).

87 Mauro, V. P. & Edelman, G. M. The ribosome filter hypothesis. *Proceedings of the National Academy of Sciences of the United States of America* **99**, 12031-12036, doi:10.1073/pnas.192442499 (2002).

88 Mauro, V. P. & Edelman, G. M. The ribosome filter redux. *Cell Cycle* **6**, 2246-2251 (2007).

89 Ge, W. *et al.* Oxygenase-catalyzed ribosome hydroxylation occurs in prokaryotes and humans. *Nature Chemical Biology* **8**, 960-962, doi:10.1038/nchembio.1093 (2012).

90 Suzuki, C. *et al.* Identification of Myc-associated protein with JmjC domain as a novel therapeutic target oncogene for lung cancer. *Molecular Cancer Therapeutics* **6**, 542-551, doi:10.1158/1535-7163.mct-06-0659 (2007).

91 Teye, K. *et al.* Increased expression of a Myc target gene Mina53 in human colon cancer. *American Journal of Pathology* **164**, 205-216, doi:10.1016/s0002-9440(10)63111-2 (2004).

92 Tsuneoka, M., Koda, Y., Soejima, M., Teye, K. & Kimura, H. A novel Myc target gene, mina53, that is involved in cell proliferation. *Journal of Biological Chemistry* **277**, 35450-35459, doi:10.1074/jbc.M204458200 (2002).

93 Zhang, Y. D. *et al.* The human mineral dust-induced gene, mdig, is a cell growth regulating gene associated with lung cancer. *Oncogene* **24**, 4873-4882, doi:10.1038/sj.onc.1208668 (2005).

94 Katz, M. J. *et al.* Sudestada1, a Drosophila ribosomal prolyl-hydroxylase required for mRNA translation, cell homeostasis, and organ growth. *Proceedings of the National Academy of Sciences* **111**, 4025-4030, doi:10.1073/pnas.1314485111 (2014).

95 Loenarz, C. *et al.* Hydroxylation of the eukaryotic ribosomal decoding center affects translational accuracy. *Proceedings of the National Academy of Sciences* **111**, 4019-4024, doi:10.1073/pnas.1311750111 (2014).

96 Gorini, L. & Kataja, E. STREPTOMYCIN-INDUCED OVERSUPPRESSION IN E COLI. *Proceedings of the National Academy of Sciences of the United States of America* **51**, 995-&, doi:10.1073/pnas.51.6.995 (1964).

97 Triman, K. L. in *Advances in Genetics* Vol. 58 *Advances in Genetics* (eds J. C. Hall, J. C. Dunlap, T. Friedmann, & V. VanHeyningen) 89-119 (2007).

98 Alksne, L. E., Anthony, R. A., Liebman, S. W. & Warner, J. R. AN ACCURACY CENTER IN THE RIBOSOME CONSERVED OVER 2 BILLION YEARS. *Proceedings of the National Academy of Sciences of the United States of America* **90**, 9538-9541, doi:10.1073/pnas.90.20.9538 (1993).

99 Singleton, R. S. *et al.* OGFOD1 catalyzes prolyl hydroxylation of RPS23 and is involved in translation control and stress granule formation. *Proceedings of the National Academy of Sciences* **111**, 4031-4036, doi:10.1073/pnas.1314482111 (2014).

100 Klusa, V. *et al.* Mildronate and its Neuroregulatory Mechanisms: Targeting the Mitochondria, Neuroinflammation, and Protein Expression. *Medicina-Lithuania* **49**, 301-309 (2013).

101 Hirsila, M. *et al.* Effect of desferrioxamine and metals on the hydroxylases in the oxygen sensing pathway. *Faseb Journal* **19**, 1308-+, doi:10.1096/fj.04-3399fje (2005).

102 Chen, H. & Costa, M. Iron- and 2-oxoglutarate-dependent Dioxygenases: an emerging group of molecular targets for nickel toxicity and carcinogenicity. *Biometals* **22**, 191-196, doi:10.1007/s10534-008-9190-3 (2009).

103 Chen, H. B., Ke, Q. D., Kluz, T., Yan, Y. & Costa, M. Nickel ions increase histone H3 lysine 9 dimethylation and induce transgene silencing. *Molecular and Cellular Biology* **26**, 3728-3737, doi:10.1128/mcb.26.10.3728-3737.2006 (2006).

104 Kivirikko, K. I. & Pihlajaniemi, T. Collagen hydroxylases and the protein disulfide isomerase subunit of prolyl 4-hydroxylases. *Advances in Enzymology, Vol 72* **72**, 325-+ (1998).

105 Chen, H. *et al.* Nickel Ions Inhibit Histone Demethylase JMJD1A and DNA Repair Enzyme ABH2 by Replacing the Ferrous Iron in the Catalytic Centers. *Journal of Biological Chemistry* **285**, 7374-7383, doi:10.1074/jbc.M109.058503 (2010).

106 Sekirnik, R., Rose, N. R., Mecinovic, J. & Schofield, C. J. 2-Oxoglutarate oxygenases are inhibited by a range of transition metals. *Metallomics* **2**, 397-399, doi:10.1039/C004952B (2010).

107 Mecinovic, J. *et al.* ESI-MS studies on prolyl hydroxylase domain 2 reveal a new metal binding site. *Chemmedchem* **3**, 569-572, doi:10.1002/cmdc.200700233 (2008).

108 Arita, A. & Costa, M. Epigenetics in metal carcinogenesis: nickel, arsenic, chromium and cadmium. *Metallomics* **1**, 222-228, doi:10.1039/b903049b (2009).

109 Salnikow, K. *et al.* Depletion of intracellular ascorbate by the carcinogenic metals nickel and cobalt results in the induction of hypoxic stress. *Journal of Biological Chemistry* **279**, 40337-40344, doi:10.1074/jbc.M403057200 (2004).

110 Fisher, J. W. ERYTHROPOIETIN - PHARMACOLOGY, BIOGENESIS AND CONTROL OF PRODUCTION. *Pharmacological Reviews* **24**, 459-& (1972).

111 Muhammad, N. & Guo, Z. Metal-based anticancer chemotherapeutic agents. *Curr. Opin. Chem. Biol.* **19**, 144-153, doi:10.1016/j.cbpa.2014.02.003 (2014).

112 Hewitson, K. S. *et al.* Structural and mechanistic studies on the inhibition of the hypoxia-inducible transcription factor hydroxylases by tricarboxylic acid cycle intermediates. *Journal of Biological Chemistry* **282**, 3293-3301, doi:10.1074/jbc.M608337200 (2007).

113 Dang, L. *et al.* Cancer-associated IDH1 mutations produce 2-hydroxyglutarate. *Nature* **462**, 739-744, doi:http://www.nature.com/nature/journal/v462/n7274/suppinfo/nature08617_S1.html (2009).

114 Opocher, G. & Schiavi, F. Functional Consequences of Succinate Dehydrogenase Mutations. *Endocrine Practice* **17**, 64-71, doi:10.4158/EP11070.RA (2011).

115 Losman, J.-A. *et al.* (R)-2-Hydroxyglutarate Is Sufficient to Promote Leukemogenesis and Its Effects Are Reversible. *Science* **339**, 1621-1625, doi:10.1126/science.1231677 (2013).

116 Zhao, S. *et al.* Glioma-derived mutations in IDH1 dominantly inhibit IDH1 catalytic activity and induce HIF-1alpha. *Science* **324**, 261-265, doi:10.1126/science.1170944 (2009).

117 Xiao, M. *et al.* Inhibition of alpha-KG-dependent histone and DNA demethylases by fumarate and succinate that are accumulated in mutations of FH and SDH tumor suppressors. *Genes Dev* **26**, 1326-1338, doi:10.1101/gad.191056.112 (2012).

118 Rose, N. R. *et al.* Inhibitor Scaffolds for 2-Oxoglutarate-Dependent Histone Lysine Demethylases. *J. Med. Chem.* **51**, 7053-7056, doi:10.1021/jm800936s (2008).

119 Chowdhury, R. *et al.* The oncometabolite 2-hydroxyglutarate inhibits histone lysine demethylases. *EMBO Rep* **12**, 463-469, doi:10.1038/embor.2011.43 (2011).

120 Xu, W. *et al.* Oncometabolite 2-hydroxyglutarate is a competitive inhibitor of alpha-ketoglutarate-dependent dioxygenases. *Cancer Cell* **19**, 17-30, doi:10.1016/j.ccr.2010.12.014 (2011).

121 MacKenzie, E. D. *et al.* Cell-permeating alpha-ketoglutarate derivatives alleviate pseudohypoxia in succinate dehydrogenase-deficient cells. *Molecular and Cellular Biology* **27**, 3282-3289, doi:10.1128/mcb.01927-06 (2007).

122 Wilson, W. J. & Poellinger, L. The dietary flavonoid quercetin modulates HIF-1 alpha activity in endothelial cells. *Biochemical and Biophysical Research Communications* **293**, 446-450, doi:10.1016/s0006-291x(02)00244-9 (2002).

123 Zhou, Y. D. *et al.* Hypoxia-inducible factor-1 activation by (-)-epicatechin gallate: Potential adverse effects of cancer chemoprevention with high-dose green tea extracts. *Journal of Natural Products* **67**, 2063-2069, doi:10.1021/np040140c (2004).

124 Sakurai, M. *et al.* A miniaturized screen for inhibitors of Jumonji histone demethylases. *Molecular BioSystems* **6**, 357-364, doi:10.1039/B912993F (2010).

125 Nielsen, A. L. *et al.* Identification of catechols as histone-lysine demethylase inhibitors. *FEBS letters* **586**, 1190-1194, doi:10.1016/j.febslet.2012.03.001 (2012).

126 Sayegh, J. *et al.* Identification of Small Molecule Inhibitors of Jumonji AT-rich Interactive Domain 1B (JARID1B) Histone Demethylase by a Sensitive High Throughput Screen. *J. Biol. Chem.* **288**, 9408-9417, doi:10.1074/jbc.M112.419861 (2013).

127 Rose, N. R., McDonough, M. A., King, O. N. F., Kawamura, A. & Schofield, C. J. Inhibition of 2-oxoglutarate dependent oxygenases. *Chemical Society Reviews* **40**, 4364-4397, doi:10.1039/C0CS00203H (2011).

128 Hopkinson, R. J. *et al.* 5-Carboxy-8-hydroxyquinoline is a broad spectrum 2-oxoglutarate oxygenase inhibitor which causes iron translocation. *Chemical Science* **4**, 3110-3117, doi:10.1039/C3SC51122G (2013).

129 Cunliffe, C. J., Franklin, T. J., Hales, N. J. & Hill, G. B. Novel inhibitors of prolyl 4-hydroxylase. 3. Inhibition by the substrate analog N-oxaloglycine and its derivatives. *Journal of Medicinal Chemistry* **35**, 2652-2658, doi:10.1021/jm00092a016 (1992).

130 Mole, D. R. *et al.* 2-oxoglutarate analogue inhibitors of HIF prolyl hydroxylase. *Bioorg Med Chem Lett* **13**, 2677-2680 (2003).

131 Rankin, Erinn B. *et al.* The HIF Signaling Pathway in Osteoblasts Directly Modulates Erythropoiesis through the Production of EPO. *Cell* **149**, 63-74, doi:http://dx.doi.org/10.1016/j.cell.2012.01.051 (2012).

132 Mackeen, M. M. *et al.* Small-Molecule-Based Inhibition of Histone Demethylation in Cells Assessed by Quantitative Mass Spectrometry. *Journal of Proteome Research* **9**, 4082-4092, doi:10.1021/pr100269b (2010).

133 Clement, P. M. J., Hanauske-Abel, H. M., Wolff, E. C., Kleinman, H. K. & Park, M. H. The antifungal drug ciclopirox inhibits deoxyhypusine and proline hydroxylation, endothelial cell growth and angiogenesis in vitro. *International Journal of Cancer* **100**, 491-498, doi:10.1002/ijc.10515 (2002).

134 Schlemminger, I. *et al.* Analogues of dealanylalahopcin are inhibitors of human HIF prolyl hydroxylases. *Bioorganic & Medicinal Chemistry Letters* **13**, 1451-1454, doi:10.1016/s0960-894x(03)00149-5 (2003).

135 Dao, J. H. *et al.* Kinetic characterization and identification of a novel inhibitor of hypoxia-inducible factor prolyl hydroxylase 2 using a time-resolved fluorescence resonance energy transfer-based assay technology. *Analytical Biochemistry* **384**, 213-223, doi:10.1016/j.ab.2008.09.052 (2009).

136 King, O. N. F. *et al.* Quantitative High-Throughput Screening Identifies 8-Hydroxyquinolines as Cell-Active Histone Demethylase Inhibitors. *PLoS One* **5**, e15535, doi:10.1371/journal.pone.0015535 (2010).

137 Hewitson, K. S. & Schofield, C. J. The HIF pathway as a therapeutic target. *Drug discovery today* **9**, 704-711, doi:10.1016/S1359-6446(04)03202-7 (2004).

138 Ino, H., Caltabiano, S., Sakamoto, T., Imai, Y. & Hirama, T. ETHNIC COMPARISON of the PK of a NOVEL HYPOXIA-INDUCIBLE FACTOR PROLYL HYDROXLYASE INHIBITOR (GSK1278863) in HEALTHY JAPANESE and CAUCASIAN SUBJECTS. *American Journal of Kidney Diseases* **61**, A47-A47 (2013).

139 Kruidenier, L. *et al.* A selective jumonji H3K27 demethylase inhibitor modulates the proinflammatory macrophage response. *Nature* **488**, 404-408, doi:http://www.nature.com/nature/journal/v488/n7411/abs/nature11262.html#supplementary-information (2012).

140 Lohse, B. *et al.* Targeting histone lysine demethylases by truncating the histone 3 tail to obtain selective substrate-based inhibitors. *Angew Chem Int Ed Engl* **50**, 9100-9103, doi:10.1002/anie.201101849 (2011).

141 Woon, E. C. Y. *et al.* Linking of 2-Oxoglutarate and Substrate Binding Sites Enables Potent and Highly Selective Inhibition of JmjC Histone Demethylases. *Angew. Chem., Int. Ed.* **51**, 1631-1634, S1631/1631-S1631/1632, doi:10.1002/anie.201107833 (2012).

142 Luo, X. *et al.* A Selective Inhibitor and Probe of the Cellular Functions of Jumonji C Domain-Containing Histone Demethylases. *Journal of the American Chemical Society* **133**, 9451-9456, doi:10.1021/ja201597b (2011).

143 Upadhyay, A. K. *et al.* An analog of BIX-01294 selectively inhibits a family of histone H3 lysine 9 Jumonji demethylases. *J Mol Biol* **416**, 319-327, doi:10.1016/j.jmb.2011.12.036 (2012).

144 Brown, R. G. S., Kawaide, H., Yang, Y.-Y., Rademacher, W. & Kamiya, Y. Daminozide and prohexadione have similar modes of action as inhibitors of the late stages of gibberellin metabolism. *Physiologia Plantarum* **101**, 309-313, doi:10.1111/j.1399-3054.1997.tb01001.x (1997).

145 Rose, N. R. *et al.* Plant Growth Regulator Daminozide Is a Selective Inhibitor of Human KDM2/7 Histone Demethylases. *J. Med. Chem.* **55**, 6639-6643, doi:10.1021/jm300677j (2012).

146 Lienard, B. M. *et al.* Evaluation of aspirin metabolites as inhibitors of hypoxia-inducible factor hydroxylases. *Chemical Communications*, 6393-6395, doi:10.1039/b814440k (2008).

147 Gargiulo, G., Capodanno, D., Longo, G., Capranzano, P. & Tamburino, C. Updates on NSAIDs in patients with and without coronary artery disease: pitfalls, interactions and cardiovascular outcomes. *Expert Review of Anti-Infective Therapy* **12**, 1185-1203, doi:10.1586/14779072.2014.964687 (2014).

148 Karuppagounder, S. S. & Ratan, R. R. Hypoxia-inducible factor prolyl hydroxylase inhibition: robust new target or another big bust for stroke therapeutics? *Journal of Cerebral Blood Flow and Metabolism* **32**, 1347-1361, doi:10.1038/jcbfm.2012.28 (2012).

149 Wissmann, M. *et al.* Cooperative demethylation by JMJD2C and LSD1 promotes androgen receptor-dependent gene expression. *Nat Cell Biol* **9**, 347-353, doi:10.1038/ncb1546 (2007).

150 Rotili, D. *et al.* Pan-Histone Demethylase Inhibitors Simultaneously Targeting Jumonji C and Lysine-Specific Demethylases Display High Anticancer Activities. *Journal of Medicinal Chemistry*, doi:10.1021/jm4012802 (2013).

151 Labbe, R. M., Holowatyj, A. & Yang, Z.-Q. Histone lysine demethylase (KDM) subfamily 4: structures, functions and therapeutic potential. *American journal of translational research* **6**, 1-15 (2013).

152 Young, L. C. & Hendzel, M. J. The oncogenic potential of Jumonji D2 (JMJD2/KDM4) histone demethylase overexpression. *Biochemistry and Cell Biology-Biochimie Et Biologie Cellulaire* **91**, 369-377, doi:10.1139/bcb-2012-0054 (2013).

153 Black, J. C. *et al.* Conserved Antagonism between JMJD2A/KDM4A and HP1γ during Cell Cycle Progression. *Molecular Cell* **40**, 736-748, doi:http://dx.doi.org/10.1016/j.molcel.2010.11.008 (2010).

154 Khoury-Haddad, H. *et al.* PARP1-dependent recruitment of KDM4D histone demethylase to DNA damage sites promotes double-strand break repair. *Proceedings of the National Academy of Sciences* **111**, E728-E737, doi:10.1073/pnas.1317585111 (2014).

155 Young, L. C., McDonald, D. W. & Hendzel, M. J. Kdm4b Histone Demethylase Is a DNA Damage Response Protein and Confers a Survival Advantage following gamma-Irradiation. *Journal of Biological Chemistry* **288**, 21376-21388, doi:10.1074/jbc.M113.491514 (2013).

156 Berry, W. L. & Janknecht, R. KDM4/JMJD2 Histone Demethylases: Epigenetic Regulators in Cancer Cells. *Cancer Research* **73**, 2936-2942, doi:10.1158/0008-5472.can-12-4300 (2013).

157 Klose, R. J. *et al.* The transcriptional repressor JHDM3A demethylates trimethyl histone H3 lysine 9 and lysine 36. *Nature* **442**, 312-316, doi:10.1038/nature04853 (2006).

158 Trojer, P. *et al.* Dynamic Histone H1 Isotype 4 Methylation and Demethylation by Histone Lysine Methyltransferase G9a/KMT1C and the Jumonji Domain-containing JMJD2/KDM4 Proteins. *Journal of Biological Chemistry* **284**, 8395-8405, doi:10.1074/jbc.M807818200 (2009).

159 Frye, S. V. The art of the chemical probe. *Nat Chem Biol* **6**, 159-161 (2010).

160 Smirnova, N. A. *et al.* Utilization of an In Vivo Reporter for High Throughput Identification of Branched Small Molecule Regulators of Hypoxic Adaptation. *Chemistry & Biology* **17**, 380-391, doi:10.1016/j.chembiol.2010.03.008 (2010).

161 Arend, M., Westermann, B. & Risch, N. Modern variants of the Mannich reaction. *Angewandte Chemie-International Edition* **37**, 1044-1070, doi:10.1002/(sici)1521-3773(19980504)37:8<1044::aid-anie1044>3.0.co;2-e (1998).

162 Szatmari, I. & Fueloep, F. Microwave-Assisted One-Pot Synthesis of (Aminoalkyl)naphthols and (Aminoalkyl)quinolinols by Using Ammonium Carbamate or Ammonium Hydrogen Carbonate as Solid Ammonia Source. *Synthesis-Stuttgart*, 775-778, doi:10.1055/s-0028-1083347 (2009).

163 Kenyon, V. *et al.* Discovery of Potent and Selective Inhibitors of Human Platelet-Type 12-Lipoxygenase. *Journal of Medicinal Chemistry* **54**, 5485-5497, doi:10.1021/jm2005089 (2011).

164 Cardellicchio, C., Capozzi, M. A. M. & Naso, F. The Betti base: the awakening of a sleeping beauty. *Tetrahedron: Asymmetry* **21**, 507-517, doi:10.1016/j.tetasy.2010.03.020 (2010).

165 Pace, R. D. & Regmi, Y. The Finkelstein reaction: Quantitative reaction kinetics of an S(N)2 reaction using nonaqueous conductivity. *Journal of Chemical Education* **83**, 1344-1348 (2006).

166 Zheng, H., Fridkin, M. & Youdim, M. From single target to multitarget/network therapeutics in Alzheimer's therapy. *Pharmaceuticals (Basel, Switzerland)* **7**, 113-135, doi:10.3390/ph7020113 (2014).

167 Hay, D. A. *et al.* Discovery and Optimization of Small-Molecule Ligands for the CBP/p300 Bromodomains. *Journal of the American Chemical Society* **136**, 9308-9319, doi:10.1021/ja412434f (2014).

168 Legrain, P. & Rain, J. C. Twenty years of protein interaction studies for biological function deciphering. *J. Proteomics* **107**, 93-97, doi:10.1016/j.jprot.2014.03.038 (2014).

169 Manabe, Y. Recent Advance in Copper-Free Click Chemistry Using Cyclooctynes, and Applications for Living Systems. *Journal of Synthetic Organic Chemistry Japan* **70**, 754-755 (2012).

170 Schiller, R. *et al.* A Cell-Permeable Ester Derivative of the JmjC Histone Demethylase Inhibitor IOX1. *Chemmedchem* **9**, 566-571, doi:10.1002/cmdc.201300428 (2014).

171 Heiskanen, J. P. *et al.* Synthesis of 4-Alkoxy-8-hydroxyquinolines. *ChemInform* **38**, no-no, doi:10.1002/chin.200724122 (2007).

172 Omar, W. A. E., Heiskanen, J. P. & Hormi, O. E. O. Synthesis of 8-hydroxyquinolines with amino and thioalkyl functionalities at position 4. *Journal of Heterocyclic Chemistry* **45**, 593-595, doi:10.1002/jhet.5570450247 (2008).

173 Fuson, R. C. Quinoline and the centroid formula. *J. Am. Chem. Soc.* **47**, 2018-2021 (1925).

174 Zuo, L., Yao, S., Wang, W. & Duan, W. An efficient method for demethylation of aryl methyl ethers. *Tetrahedron Letters* **49**, 4054-4056, doi:10.1016/j.tetlet.2008.04.070 (2008).

175 Kingston, J. V. & Verkade, J. G. Synthesis and Characterization of R2PNP(iBuNCH2CH2)3N: A New Bulky Electron-Rich Phosphine for Efficient Pd-Assisted Suzuki−Miyaura Cross-Coupling Reactions. *The Journal of Organic Chemistry* **72**, 2816-2822, doi:10.1021/jo062452l (2007).

176 Shevlin, M. Sulfate additives generate robust and highly active palladium catalysts for the cyanation of aryl chlorides. *Tetrahedron Letters* **51**, 4833-4836, doi:10.1016/j.tetlet.2010.07.045 (2010).

177 Sharifi, A., Mohsenzadeh, F., Mojtahedi, M. M., Saidi, M. R. & Balalaie, S. Microwave-promoted transformation of nitriles to amides with aqueous sodium perborate. *Synth. Commun.* **31**, 431-434, doi:10.1081/scc-100000535 (2001).

178 Guerinot, A., Reymond, S. & Cossy, J. Ritter Reaction: Recent Catalytic Developments. *European Journal of Organic Chemistry*, 19-28, doi:10.1002/ejoc.201101018 (2012).

179 Maffioli, S. I., Marzorati, E. & Marazzi, A. Mild and reversible dehydration of primary amides with PdCl2 in aqueous acetonitrile. *Organic Letters* **7**, 5237-5239, doi:10.1021/ol052100l (2005).

180 King, O. N. F. *et al.* Quantitative high-throughput screening identifies 8-hydroxyquinolines as cell-active histone demethylase inhibitors. *PLoS One* **5**, No pp. given, doi:10.1371/journal.pone.0015535 (2010).

181 Kawamura, A. *et al.* Development of homogeneous luminescence assays for histone demethylase catalysis and binding. *Analytical Biochemistry* **404**, 86-93, doi:10.1016/j.ab.2010.04.030 (2010).

182 Hutchinson, S. E. *et al.* Enabling Lead Discovery for Histone Lysine Demethylases by High-Throughput RapidFire Mass Spectrometry. *Journal of Biomolecular Screening* **17**, 39-48, doi:10.1177/1087057111416660 (2012).

183 Herold, J. M. *et al.* Small-Molecule Ligands of Methyl-Lysine Binding Proteins. *Journal of Medicinal Chemistry* **54**, 2504-2511, doi:10.1021/jm200045v (2011).

184 Cory, A. H., Owen, T. C., Barltrop, J. A. & Cory, J. G. USE OF AN AQUEOUS SOLUBLE TETRAZOLIUM FORMAZAN ASSAY FOR CELL-GROWTH ASSAYS IN CULTURE. *Cancer Communications* **3**, 207-212 (1991).

185 Wang, L. *et al.* A small molecule modulates Jumonji histone demethylase activity and selectively inhibits cancer growth. *Nat Commun* **4**, doi:10.1038/ncomms3035 (2013).

186 Smirnova, N. A. *et al.* Utilization of an In Vivo Reporter for High Throughput Identification of Branched Small Molecule Regulators of Hypoxic Adaptation. *Chemistry & Biology* **17**, 380-391, doi:10.1016/j.chembiol.2010.03.008 (2010).

187 Chamoin, S., Houldsworth, S., Kruse, C. G., Iwema Bakker, W. & Snieckus, V. The Suzuki-Miyaura cross coupling reactions on solid support. Link to solution phase directed ortho metalation. The Leznoff acetal linker approach to biaryl and heterobiaryl aldehydes. *Tetrahedron Letters* **39**, 4179-4182, doi:http://dx.doi.org/10.1016/S0040-4039(98)00779-5 (1998).

188 Heiskanen, J. P. & Hormi, O. E. O. 4-Aryl-8-hydroxyquinolines from 4-chloro-8-tosyloxyquinoline using a Suzuki-Miyaura cross-coupling approach. *Tetrahedron* **65**, 518-524, doi:10.1016/j.tet.2008.10.097 (2009).

189 Matsuda, K. *et al.* Design, Synthesis, and Characterization of Three Kinds of π-Cross-Conjugated Hexacarbenes with High-Spin (S = 6) Ground States. *J. Am. Chem. Soc.* **117**, 5550-5560, doi:10.1021/ja00125a017 (1995).

190 Bookser, B. C. & Bruice, T. C. Syntheses of quadruply two- and three-atom, aza-bridged, cofacial bis(5,10,15,20-tetraphenylporphyrins). *J. Am. Chem. Soc.* **113**, 4208-4218, doi:10.1021/ja00011a024 (1991).

191 Gershon, H. & Clarke, D. D. Improved syntheses of some monochloro- and monobromo-8-quinolinols. *Monatshefte für Chemie / Chemical Monthly* **122**, 935-941, doi:10.1007/bf00823423 (1991).

192 Keinan, S. *et al.* Computational design, synthesis and biological evaluation of para-quinone-based inhibitors for redox regulation of the dual-specificity phosphatase Cdc25B. *Organic & Biomolecular Chemistry* **6**, 3256-3263 (2008).

193 Cohen, P. & Alessi, D. R. Kinase Drug Discovery – What's Next in the Field? *ACS Chemical Biology* **8**, 96-104, doi:10.1021/cb300610s (2012).

194 Capdeville, R., Buchdunger, E., Zimmermann, J. & Matter, A. Glivec (STI571, imatinib), a rationally developed, targeted anticancer drug. *Nature reviews. Drug discovery* **1**, 493-502 (2002).

195 Christensen, C. M. & Rosenbloom, R. S. Explaining the attacker's advantage: Technological paradigms, organizational dynamics, and the value network. *Research Policy* **24**, 233-257, doi:http://dx.doi.org/10.1016/0048-7333(93)00764-K (1995).

196 Santos, F. M. & Eisenhardt, K. M. CONSTRUCTING MARKETS AND SHAPING BOUNDARIES: ENTREPRENEURIAL POWER IN NASCENT FIELDS. *Academy of Management Journal* **52**, 643-671 (2009).

197 Frye, S. V. The art of the chemical probe. *Nature Chemical Biology* **6**, 159-161 (2010).

198 Keeling, K. M., Xue, X., Gunn, G. & Bedwell, D. M. Therapeutics based on stop codon readthrough. *Annual review of genomics and human genetics* **15**, 371-394, doi:10.1146/annurev-genom-091212-153527 (2014).

199 Rose, N. R., McDonough, M. A., King, O. N., Kawamura, A. & Schofield, C. J. Inhibition of 2-oxoglutarate dependent oxygenases. *Chemical Society reviews* **40**, 4364-4397, doi:10.1039/c0cs00203h (2011).

200 Chen, R. F. Fluorescence Quantum Yields of Tryptophan and Tyrosine. *Analytical Letters* **1**, 35-42, doi:10.1080/00032716708051097 (1967).

201 in *Principles of Fluorescence Spectroscopy* (ed JosephR Lakowicz) Ch. 8, 277-330 (Springer US, 2006).

202 van de Weert, M. & Stella, L. Fluorescence quenching and ligand binding: A critical discussion of a popular methodology. *Journal of Molecular Structure* **998**, 144-150, doi:http://dx.doi.org/10.1016/j.molstruc.2011.05.023 (2011).

203 Niesen, F. H., Berglund, H. & Vedadi, M. The use of differential scanning fluorimetry to detect ligand interactions that promote protein stability. *Nat. Protocols* **2**, 2212-2221 (2007).

204 Hopkinson, R. J. *et al.* Is JmjC Oxygenase Catalysis Limited to Demethylation? *Angewandte Chemie International Edition* **52**, 7709-7713, doi:10.1002/anie.201303282 (2013).

205 Simeonov, A. Recent developments in the use of differential scanning fluorometry in protein and small molecule discovery and characterization. *Expert Opinion on Drug Discovery* **8**, 1071-1082, doi:10.1517/17460441.2013.806479 (2013).

206 Geoghegan, K. F. *et al.* Spontaneous alpha-N-6-phosphogluconoylation of a "His tag" in Escherichia coli: The cause of extra mass of 258 or 178 Da in fusion proteins. *Analytical Biochemistry* **267**, 169-184, doi:10.1006/abio.1998.2990 (1999).

207 Hewitson, K. S., Granatino, N., Welford, R. W. D., McDonough, M. A. & Schofield, C. J. Oxidation by 2-oxoglutarate oxygenases: non-haem iron systems in catalysis and signalling. *Philosophical Transactions of the Royal Society a-Mathematical Physical and Engineering Sciences* **363**, 807-828, doi:10.1098/rsta.2004.1540 (2005).

208 Chowdhury, R. *et al.* Selective Small Molecule Probes for the Hypoxia Inducible Factor (HIF) Prolyl Hydroxylases. *ACS Chemical Biology* **8**, 1488-1496, doi:10.1021/cb400088q (2013).

209 Johnson, B. M., Stier, B. A. & Caltabiano, S. Effect of food and gemfibrozil on the pharmacokinetics of the novel prolyl hydroxylase inhibitor GSK1278863. *Clinical Pharmacology in Drug Development* **3**, 109-117, doi:10.1002/cpdd.83 (2014).

210 Provenzano, R. *et al.* FG2216, a novel oral HIF-PHI stimulates erythropoiesis and increases hemoglobin concentration in patients with non-dialysis CKD. *American Journal of Kidney Diseases* **51**, A80-A80 (2008).

211 Jovic, M. *et al.* Degradation of triketone herbicides, mesotrione and sulcotrione, using advanced oxidation processes. *Journal of Hazardous Materials* **260**, 1092-1099, doi:10.1016/j.jhazmat.2013.06.073 (2013).

212 Kavalier, A. R. *et al.* Targeted analysis of polyphenol metabolism during development of hop (Humulus lupulus L) cones following treatment with prohexadione-calcium. *Food Chemistry* **145**, 254-263, doi:10.1016/Lfoodchem.2013.08.023 (2014).

213 Menchyk, N. *et al.* Nitrogen and Trinexapac-ethyl Applications for Managing 'Diamond' Zoysiagrass Putting Greens in the Transition Zone, U.S. *Hortscience* **49**, 1076-1080 (2014).
214 Lock, E., Ranganath, L. R. & Timmis, O. The role of nitisinone in tyrosine pathway disorders. *Current rheumatology reports* **16**, 457-457, doi:10.1007/s11926-014-0457-0 (2014).
215 Jursic, B. S. & Neumann, D. M. Preparation of 5-formyl- and 5-acetylbarbituric acids, including the corresponding Schiff bases and phenylhydrazones. *Tetrahedron Letters* **42**, 8435-8439, doi:http://dx.doi.org/10.1016/S0040-4039(01)01830-5 (2001).
216 Temprado, M. *et al.* Thermophysical Study of Several Barbituric Acid Derivatives by Differential Scanning Calorimetry (DSC). *Journal of Chemical and Engineering Data* **56**, 263-268, doi:10.1021/je1008944 (2011).
217 Jursic, B. S., Neumann, D. M., Bowdy, K. L. & Stevens, E. D. Simple, efficient, high yield syntheses of substituted and unsubstituted 5-benzoylbarbituric acids, and their corresponding schiff base phenylhydrazones. *Journal of Heterocyclic Chemistry* **41**, 233-246, doi:10.1002/jhet.5570410214 (2004).
218 Morgan, W. M. *BARBITURATES CNS BIOCHEMISTRY*. (1991).
219 Pardridge, W. M. The Blood-Brain Barrier: Bottleneck in Brain Drug Development. *NeuroRX* **2**, 3-14, doi:http://dx.doi.org/10.1602/neurorx.2.1.3 (2005).
220 Hu, S. *et al.* Design, Synthesis and Inhibitory Activities of 8-(Substituted styrol-formamido)phenyl-xanthine Derivatives on Monoamine Oxidase B. *Chemical and Pharmaceutical Bulletin* **60**, 385-390, doi:10.1248/cpb.60.385 (2012).
221 Temprado, M. *et al.* Thermophysical Study of Several Barbituric Acid Derivatives by Differential Scanning Calorimetry (DSC). *Journal of Chemical & Engineering Data* **56**, 263-268, doi:10.1021/je1008944 (2010).
222 Klikar, M. *et al.* N,N[prime or minute]-Dibutylbarbituric acid as an acceptor moiety in push-pull chromophores. *New Journal of Chemistry* **37**, 4230-4240, doi:10.1039/c3nj00683b (2013).
223 Pangborn, A. B., Giardello, M. A., Grubbs, R. H., Rosen, R. K. & Timmers, F. J. Safe and Convenient Procedure for Solvent Purification. *Organometallics* **15**, 1518-1520, doi:10.1021/om9503712 (1996).
224 Di, L. & Kerns, E. H. Application of pharmaceutical profiling assays for optimization of drug-like properties. *Current Opinion in Drug Discovery & Development* **8**, 495-504 (2005).
225 Plant, N. Strategies for using in vitro screens in drug metabolism. *Drug Discovery Today* **9**, 328-336, doi:10.1016/s1359-6446(03)03019-8 (2004).
226 Wang, Q. et al. Evaluation of the MDR-MDCK cell line as a permeability screen for the blood-brain barrier. International Journal of Pharmaceutics 288, 349-359, doi:10.1016/j.ijpharm.2004.10.007 (2005).